

# NISTIR 8271 DRAFT SUPPLEMENT

## Face Recognition Vendor Test (FRVT) Part 2: Identification

Patrick Grother  
Mei Ngan  
Kayee Hanaoka  
*Information Access Division  
Information Technology Laboratory*

This document is a draft supplement of [NIST Interagency Report 8271](#)

2022/06/13



# NISTIR 8271 DRAFT SUPPLEMENT

## Face Recognition Vendor Test (FRVT) Part 2: Identification

Patrick Grother  
Mei Ngan  
Kayee Hanaoka  
*Information Access Division  
Information Technology Laboratory*

This document is a draft supplement of [NIST Interagency Report 8271](#)

February 2022



U.S. Department of Commerce  
*Gina M. Raimondo, Secretary*

National Institute of Standards and Technology  
*Laurie E. Locascio, NIST Director and Undersecretary of Commerce for Standards and Technology*

## RELEASE NOTES

**2022-06-08:** The 1:N track of the FRVT remains open.

- ▷ This document is the seventeenth draft update to [NIST Interagency Report 8271](#). It includes results for algorithms submitted by three first-time participants: Digidata, DiluSense Technology, and Vietnam Posts and Telecommunications Group.
- ▷ The document also includes results for algorithms from five returning developers: Canon Inc, Imagus Technology, Neurotechnology, Thales, and Samsung S1.

**2022-04-28:** The 1:N track of the FRVT remains open.

- ▷ This document is the sixteenth draft update to [NIST Interagency Report 8271](#). It includes results for algorithms submitted by one first-time participants: Hangzhou Allu Network Information Technology.
- ▷ The document also includes results for algorithms from three returning developers: HyperVerge Inc, Qnap Security, and Realnetworks Inc.
- ▷ The [1:N results page](#) has been updated.

**2022-03-30:** The 1:N track of the FRVT remains open.

- ▷ This document is the sixteenth draft update to [NIST Interagency Report 8271](#). It includes results for algorithms submitted by two first-time participants: Intellivision, and Pangiam.
- ▷ The document also includes results for algorithms from three returning developers: Fujitsu Research and Development Center, Idemia, and Gorilla Technology.
- ▷ The [1:N results page](#) has been updated.

**2022-02-23:** The 1:N track of the FRVT remains open.

- ▷ This document is the fifteenth draft update to [NIST Interagency Report 8271](#). It includes results for algorithms submitted by four first-time participants: Cloudwalk - Moontime Smart Technology, Decatur Industries Inc, NotionTag Technologies Private Limited, and Reveal Media Ltd.
- ▷ The document also includes results for algorithms from three returning developers: Cognitec Systems GmbH, Sensetime Group, and Viettel Group
- ▷ The [1:N results page](#) has been updated.

**2022-01-20:** The 1:N track of the FRVT remains open.

- ▷ This document is the fourteenth draft update to [NIST Interagency Report 8271](#). It includes results for algorithms recently submitted by two first-time participants: Daon and SQIsoft.
- ▷ The document also includes results for algorithms from five returning developers: Cyberlink Corp, NEC, Neurotechnology, Paravision, and Rank One Computing.
- ▷ The [1:N results page](#) has been updated.

**2021-12-16:** The 1:N track of the FRVT remains open.

- ▷ This document is the thirteenth draft update to [NIST Interagency Report 8271](#). It includes results for algorithms from six returning developers: Dahua Technology, Imagus Technology, Line Corporation, N-Tech Lab, Qnap Security, and Realnetworks Inc.
- ▷ The [1:N results page](#) has been updated.

**2021-11-22:** The 1:N track of the FRVT remains open.

- ▷ This document is the twelfth draft update to [NIST Interagency Report 8271](#). It includes results for algorithms recently submitted by three first-time participants Clearview AI, Griaule, and Mantra Softech India.
- ▷ This document and the [1:N results page](#) also include results for algorithms from six returning developers: Acer Incorporated, Canon, Dermalog, Samsung S1, VisionLabs, and Veridas Digital Authentication.

**2021-10-28:** The 1:N track of the FRVT remains open.

- ▷ This document is the eleventh draft update to [NIST Interagency Report 8271](#). It includes results for algorithms recently submitted by three first-time participants (20Face, Fujitsu Research and Development Center, and Vision-Box), and five returning participants (Alchera, Gorilla Technology, Tevian, Thales-Cogent, and Visidon). Visidon
- ▷ Both the main [1:N results page](#) and the small-gallery [paperless travel page](#) have been updated.

**2021-09-21:** The 1:N track of the FRVT remains open. Three news items:

- ▷ This document is the tenth draft update to [NIST Interagency Report 8271](#). It includes results for algorithms recently submitted by six first-time developers: Cubox, Fincore, HyperVerge, Qnap Security, Staqu Technologies, and Tripleize (Aize, 3-ize).
- ▷ It includes results also for four returning developers: Cognitec Systems, Incode Technologies, Innovatrics, Neurotechnology, and Rank One Computing.

**2021-08-02:** The 1:N track of the FRVT remains open. Three news items:

- ▷ This document is the ninth draft update to [NIST Interagency Report 8271](#). It includes results for algorithms recently submitted by eight participants: Cyberlink Corp, NEC Corp, N-Tech Lab, Realnetworks Inc., Sensetime Group, Veridas Digital, Viettel Group, and Vigilant Solutions.
- ▷ Algorithms submitted since July 24 will be included in the next update scheduled for September 9, 2021.
- ▷ A new report, NIST Interagency Report 8381 - FRVT Part 7: Identification for Paperless Travel and Immigration, has been released [[PDF](#), [webpage](#)]. It documents the use of FRVT 1:N algorithms in positive access control and immigration status update travel applications where the enrolled population size is as low as 420 people for aircraft boarding, and 42 000 for an airport security line. These population sizes are much smaller than those used in the main [1:N evaluation](#). Going forward, we will update the report and webpage with results for new algorithms.

**2021-07-07:** The 1:N track of the FRVT remains open. One update:

- ▷ This document is the eighth draft update to [NIST Interagency Report 8271](#). It include results for an algorithm from one participant: Kakao Enterprises.

**2021-06-22:** The 1:N track of the FRVT remains open. Three updates:

- ▷ This is the seventh draft of the update to [NIST Interagency Report 8271](#). It includes results for algorithms from three new participants: Line Corporation, Rendip, and Samsung S1 Corp.
- ▷ We have also added results for algorithms from five returning developers: Imagus Technology, Kneron, Tevian, Visidon, and Xforward AI Technology.
- ▷ The algorithm-specific report cards (examples: [1](#), [2](#), and [3](#)) now include figures showing how low threshold values can be used to reduce candidate list lengths for human review, while (usually) elevating miss rates (FNIR) only modestly. The reports also feature some minor additions and clarifications.

**2021-03-26:** The 1:N track of the FRVT remains open. Three updates:

- ▷ This is the sixth draft of the update to [NIST Interagency Report 8271](#). It includes results for algorithms from three returning developers: Neurotechnology, Guangzhou Pixel Solutions, and Tech5 SA.
- ▷ We have added results on the webpage and in the report for a new ageing dataset in which border crossing photos are searched against a gallery of border crossing photos collected between 10 and 15 years prior to the mated search photos. See section 2 for a description of the images. Table 1 has a new entry describing the experiment.
- ▷ We will mostly discontinue running the mugshot ageing test, reserving it for algorithms that show high accuracy on the new border-crossing set.

**2021-03-26:** Regarding the fifth draft of the update to [NIST Interagency Report 8271](#):

- ▷ In addition have added results for first algorithms from two new participants: Viettel Group and Veridas Digital Authentication Solutions.
- ▷ We have added results for algorithms from two returning developers: Idemia and Cognitec Systems.
- ▷ In addition to the report, the [results page](#) and its hyperlinked [report cards](#) have been updated.

**2021-02-08:** Regarding the fourth draft of the update to [NIST Interagency Report 8271](#):

- ▷ We have added results for eight algorithms submitted by eight developers: Cyberlink, Dermalog, Imagus, Paravision, Sensetime, Trueface, Vigilant Solutions, and X-Forward AI. With the exception of Trueface, all of these developers have participated previously.
- ▷ We anticipate updating this report again in the first week of March 2021.
- ▷ The main [results page](#) has been revised with tabs for the investigative and lights-out identification tables, and a new tab dedicated to speed and resource consumption.
- ▷ The report cards (example [here](#)) hyperlinked from the [results page](#) have been revised to improve content and format.

**2020-12-14:** Regarding third draft of the update to [NIST Interagency Report 8271](#):

- ▷ We have added results for fifteen algorithms submitted by thirteen developers. The four first-time participants are: Acer, Akurat Satu Indonesia, Canon, and Xforward AI Technology. The ten returning developers are: AllGoVision, Cyberlink Corp, Dahua Technology, Deepglint, Guangzhou Pixel Solutions, IIT Vision, Innovatrics, Rank One Computing, Scanovate, Sensetime Group, Synesis, and VisionLabs.
- ▷ We have added two new datasets to the evaluation: First a set of “visa-border” photos, representing search of an airport immigration lane photo against a database of closely ISO standard portraits; second a “visa-kiosk” set representing search of a photo collected in a registered traveller kiosk against the same ISO portrait gallery. The images are described in section 2.1.
- ▷ As in previous reports, we include results for searching mugshots against a mugshot gallery containing a single image of each of 12 million people. However we have suspending running searches against a gallery in which multiple lifetime photos per person are present, because this is computationally expensive. We retain a  $N = 3$  million search test dedicated to ageing in which mugshots taken up to 18 years after the first photograph are searched - see Table 7.
- ▷ Tables containing computational resource information, Table 2 . . . , now include duration of the finalization step, in which search algorithms can, at their option, build fast-search data structures.
- ▷ We have linked revised per-algorithm PDF report cards from the main [results page](#).
- ▷ We have regenerated all figures and tables to drop algorithms submitted before June 2018. Results for prior algorithms appear in [archived editions](#) of this report.
- ▷ Going forward, we anticipate producing more frequent updates to this report. Developers may submit one algorithm to this evaluation every four calendar months.

**2020-03-24:** Regarding the second draft of the update to [NIST Interagency Report 8271](#):

- ▷ Adds results for three algorithms from three developers, Dermalog, Innovatrics, and Synesis.
- ▷ Adds Table 7 on ageing showing the increase in false negative rates with time elapsed between two photos. Some of the results were contained in graphs in prior editions of this report, but the table adds results for some newly submitted algorithms.
- ▷ Adjusts frontal mugshot results (for recent and lifetime consolidated galleries) to include the effect of removing some images that should not have been included in image test sets. These images were mostly profile views, images of tattoos containing faces, images of faces on tee shirts, and images of photographs on walls behind the intended subject. This affects many tables and reduces false negative identification rates for all algorithms. The reduction is larger for “recent” enrollments than for “lifetime consolidated” ones with the consequence that accuracy on recent images is now superior.

**2020-02-26:** Regarding the first draft of the update to [NIST Interagency Report 8271](#):

- ▷ Adds results for 38 algorithms from 31 different developers, eleven of whom are entirely new to the 1:N track of FRVT. These are Allgovision, Cyberlink, Deepsea Tencent, Farbar F8, Imperial College London, Intsys MSU, Kedacom, Kneron, Pixelall, and Scanovate.

## DISCLAIMER

Specific hardware and software products identified in this report were used in order to perform the evaluations described in this document. In no case does identification of any commercial product, trade name, or vendor, imply recommendation or endorsement by the National Institute of Standards and Technology, nor does it imply that the products and equipment identified are necessarily the best available for the purpose.

## INSTITUTIONAL REVIEW BOARD

The National Institute of Standards and Technology's Research Protections Office reviewed the protocol for this project and determined it is not human subjects research as defined in Department of Commerce Regulations, 15 CFR 27, also known as the Common Rule for the Protection of Human Subjects (45 CFR 46, Subpart A).

## ACKNOWLEDGMENTS

The authors are grateful for the support and collaboration of the the Department of Homeland Security's Science & Technology Directorate (S&T), Office of Biometric Identity Management (OBIM), and Customs and Border Protection (CBP).

Additionally, the authors are grateful to staff in the NIST Biometrics Research Laboratory for infrastructure supporting rapid evaluation of algorithms.

## Executive Summary

This document is a draft revision of the September 2019 report [NIST Interagency Report 8271](#). That report gave extensive documentation of face recognition applied to mugshots. This report extends that by adding more two more challenging datasets containing images with serious departures from canonical frontal image standards. The report also adds results for algorithms submitted to NIST since in 2019 and 2020. The algorithms, which implement one-to-many identification of faces appearing in two-dimensional images, are prototypes from the research and development laboratories of mostly commercial suppliers, and are submitted to NIST as compiled black-box libraries implementing a NIST-specified C++ test interface. The report therefore does not describe how algorithms operate. The report lists accuracy results alongside developer names and will therefore be useful for comparison of face recognition algorithms and assessment of absolute capability. The report is accompanied by a [webpage](#) with sortable results.

The evaluation uses six datasets: frontal mugshots, profile view mugshots, desktop webcam photos, visa-like immigration application photos, immigration lane photos, and registered traveler kiosk photos. These datasets are sequestered at NIST, meaning that developers do not have access to them for training or testing. This aspect is important because face recognition algorithms are very often deployed without the developer having access to the customers image data. A possible exception to this would be in a cloud-based application where the operational image data is uploaded to a cloud operated by a face recognition developer.

The major result in NIST IR 8271 was that massive gains in accuracy have been achieved in the years 2013 to 2018 and these far exceed improvements made in the prior period, 2010 to 2013. While the industry gains were broad - at least 30 developers' algorithms outperformed the most accurate algorithm from late 2013, there remains a wide range of capability. While this report shows accuracy gains only over the period 2018-2020, the most accurate algorithm reported here is substantially more accurate than anything reported in NIST IR 8271. This is evidence that face recognition development continues apace, and that FRVT reports are but a snapshot of contemporary capability.

From discussion with developers, the accuracy gains stem from the adoption of deep convolutional neural networks. As such, face recognition has undergone an industrial revolution, with algorithms increasingly tolerant of poorly illuminated and other low quality images, and poorly posed subjects. One related result is that a few algorithms correctly match side-view photographs to galleries of frontal photos, with search accuracy approaching that of the best c. 2010 algorithms operating on purely frontal images. The capability to recognize under a 90-degree change in viewpoint - pose invariance - has been a long-sought milestone in face recognition research.

With good quality portrait photos, the most accurate algorithms will find matching entries, when present, in galleries containing 12 million individuals, with rank one miss rates of approaching 0.1%. The remaining errors are in large part attributable to long-run ageing, facial injury and poor image quality. Given this impressive achievement - close to perfect recognition - an advocate might claim that cooperative face recognition is a solved problem, a statement that can be refuted with the following context and caveats:

- ▷ **Mugshots vs. less constrained captures:** The low error rates reported here are attained using mostly excellent cooperative live-capture mugshot images collected with an attendant present. Recognition in other circumstances, particularly those without a dedicated photographic environment and human or automated quality control checks, will lead to declines in accuracy. This is documented here for side-view images, poorer quality webcam images, and, particularly, for newly introduced ATM-style kiosk photos that were not originally intended for automated face recognition. In this case, recognition error rates are much higher, often in excess of 20% even with the more accurate algorithms which variously remain intolerant of face cropping (at image edge) and of large downward head pitch.
- ▷ **Algorithm accuracy spectrum:** Recognition accuracy is very strongly dependent on the algorithm and, more

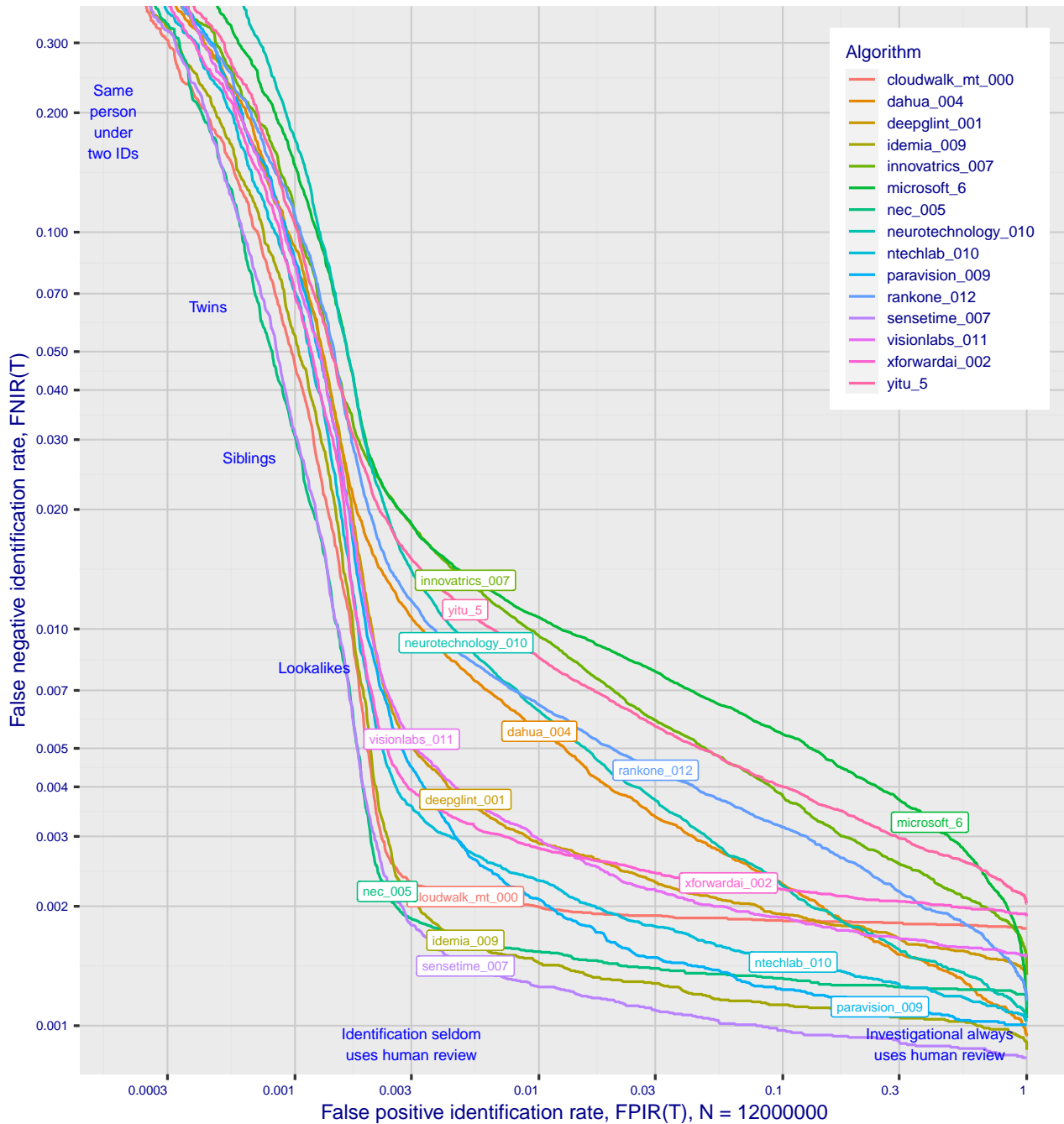


Figure 1: Identification miss rates across the false positive range.  $N = 12$  million individuals are enrolled with one recent image.

generally, on the developer of the algorithm. False negative error rates in a particular scenario range from a few tenths of one percent to beyond fifty percent. This is tabulated exhaustively later: For example Table 11 shows accuracy across datasets. Figure 1 here compares algorithms on mugshot searches in a consolidated gallery of 12 million subjects and 12 million photos. Many algorithms do not achieve the low error rates noted above, and while many of those may still be useful and valuable to end-users, only the most accurate excel on poor quality images and those collected long after the initial enrollment sample.

- ▷ **Versioning:** While results for up to ten algorithms from each developer are reported here, the intra-provider

accuracy variations are usually smaller than the inter-provider variations. That said different versions give an order of magnitude fewer misses. Some developers demonstrate speed-accuracy tradeoffs<sup>1</sup>. See Figs. 18, 19.

- ▷ **Low similarity scores:** In thousands of mugshot cases the correct gallery image is returned at rank 1 but its similarity score is nevertheless low, below some operationally required score threshold. This is not so important when face recognition is used for “lead generation” in investigational applications because human reviewers are specifically required to review potentially long candidate lists and the threshold is effectively 0. In applications where search volumes are higher and labor is not available to review the results from searches, a higher threshold must be applied. This reduces the length of candidate lists and false positive identification rates at the expense of increased false negative miss rates. The tradeoff between the two error rates is reported extensively later.
- ▷ **Population size:** As the number of enrolled subjects grows, some mates are displaced from rank one, decreasing accuracy. As tabulated later for N up to 12 million, false negative rates generally rise slowly with population size. This enables use of face recognition in very large populations. However in most positive and negative identification applications<sup>2</sup>, a score threshold is set to limit the rate at which non-mate searches produce false positives. This has the consequence that some mated searches will report the mate below threshold, i.e. a miss, even if it is at rank 1. The utility of this is that many non-mated searches will return no candidate identities at all. As the error-tradeoff characteristic shows, investigational miss rates on the right side are very low but then rise steadily (in the center region) as threshold is increased to support “lights-out” applications, and ultimately rise quickly (left side) as discussed below. Thus, if we demand that just one in one thousand non-mate searches produce any false positives, the most accurate algorithms there (Sensetime-004 and NEC-3) would fail on between 3 and 5% of mated searches. Even though the graph shows results for the most accurate algorithms, all but two would fail to find the mate in more than 8% of mated searches. While the two most accurate algorithms produce a relatively flat error tradeoff until the threshold is raised to limit false positives to about 1 in 400 non-mated searches<sup>3</sup>.

Thereafter, as the threshold is raised to further reduce false positives, miss rates rise rapidly. This means that low false positive identification rates are inaccessible with these algorithms, a result that does not apply for ten-finger identification algorithms. The rapid rise occurs because the lower mate scores are mixed with very high non-mate scores, the low scores from poor image quality and ageing, the high non-mates from the presence of lookalikes persons (doppelgangers), twins (discussed next) and, ultimately, the presence of a few unconsolidated subjects i.e. persons present under multiple IDs.

- ▷ **False negatives from ageing:** A large source of error in long-run applications where subjects are not re-enrolled on a set schedule is ageing. Changes in facial appearance increase with the time elapsed between photographs. These will depress similarity scores and eventually cause false negatives. All faces age and while this usually proceeds in a graceful and progressive manner, drug use can accelerate this [28]. Elective surgery may be effective in delaying it although this has not been formally quantified with face recognition. As ageing is essentially unavoidable, it can only be mitigated by scheduled re-capture, as in passport re-issuance. To quantify ageing effects, we used the more accurate algorithms to enroll the earliest image of 3.1 million adults and then search

<sup>1</sup>For example, NEC-0 prepares templates much faster than NEC-2 but gives twenty times more misses. Dermalog-5 executes a template search much more quickly than Dermalog-6 but is also much less accurate.

<sup>2</sup>In a positive identification application such as a registered traveler system, a user is making an implicit claim to be enrolled in the system - most users will be. In a negative application, such as with deportees, the implicit claim is that the subject is not enrolled - most will not be.

<sup>3</sup>The gallery size here is 12 million people, one image per person. Given 331 201 non-mated searches, an exhaustive implementation of one-too-many search would execute almost 4 trillion comparisons. At a false positive identification rate of 0.0025 the number of false positives is, to first order, 828 corresponding to single-comparison false match rate of  $828 / 4 \text{ trillion} = 2.1 \times 10^{-10}$  i.e. about 1 in 5 billion. Strictly this FMR computation is meaningful only for algorithms that implement 1:N search using N 1:1 comparisons, which is not always the case.

with 10.3 million newer photos taken up to 18 years after the initial enrollment photo. Figure 2 puts ageing into context by contrasting it with the increase in false negatives that occurs when the number of individuals in an enrollment database becomes larger and the chance of a false positive increases such that higher thresholds may become necessary<sup>4</sup>.

The Figure shows, from top to bottom, increases in false negative identification rates (FNIR) with the algorithm being tested. This applies to increases due to  $N$  on the left side, and increases due to ageing on the right side. The relative spacing of the dots shows that for all algorithms the dependency of FNIR on  $N$  (up to 12 million) is considerably less than on  $\Delta T$  (up to 18 years).

In the inset table, accuracy is seen to degrade progressively with time, as mate scores decline and non-mates displace mates from rank 1 position. More accurate algorithms tend to be less sensitive to ageing. The more accurate algorithms give fewer errors after 18 years of ageing than middle tier algorithms give after four. Note also we do not quantify an ageing rate - more formal methods [2] borrowed from the longitudinal analysis literature have been published for doing so (given suitable repeated measures data). See Figures 60, 84 and 96.

---

<sup>4</sup>Some algorithms implement strategies to automatically adjust scores to account for increased population size. This relieves the system owner of having to increase thresholds as  $N$  increases.

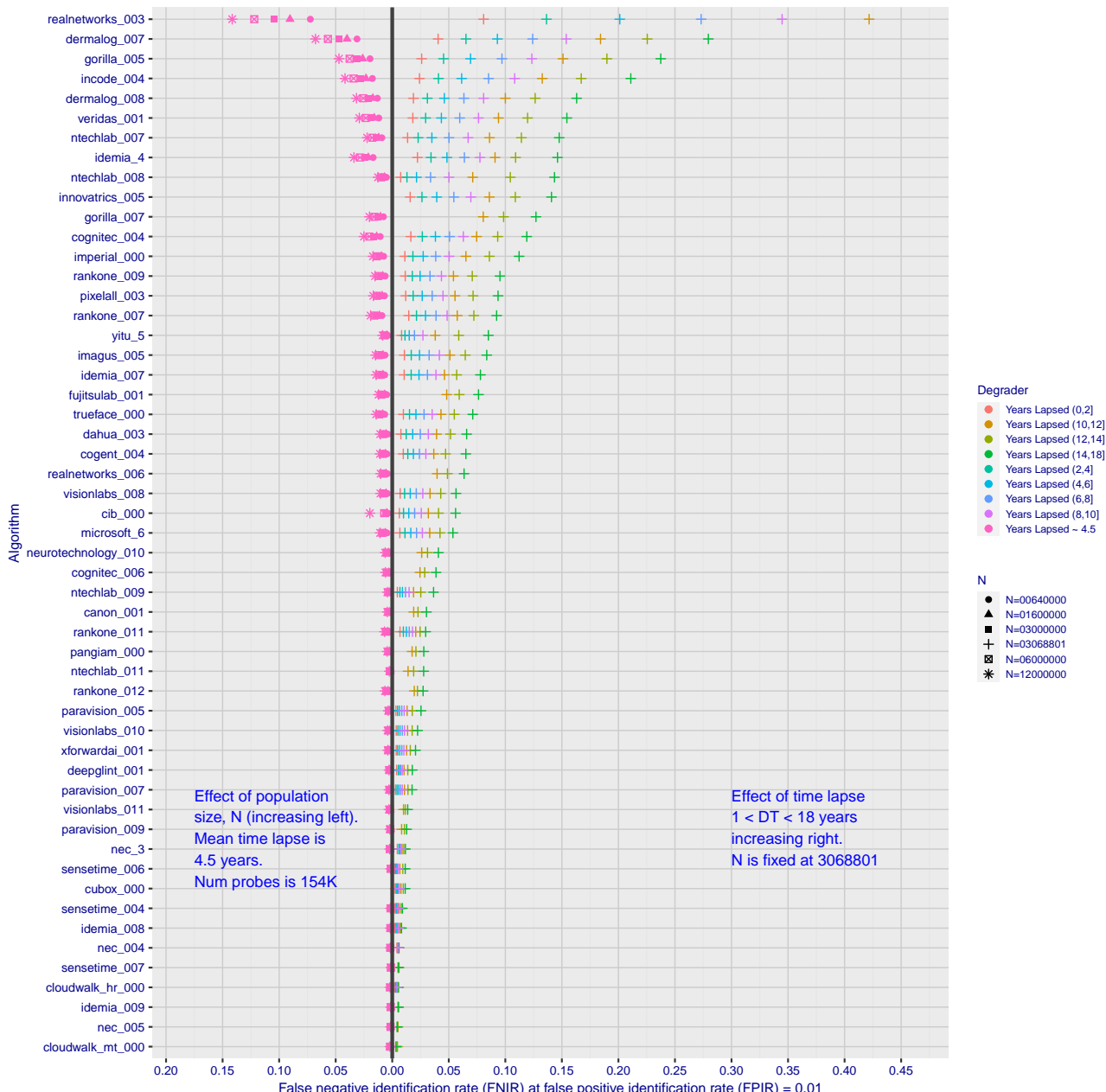


Figure 2: Identification miss rates as a function of enrolled population size,  $N$ , and time-lapse,  $\Delta T$ .

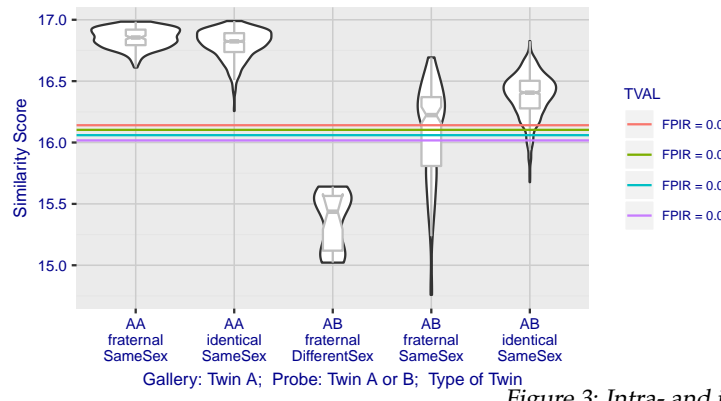


Figure 3: Intra- and inter-twin scores

▷ **False positives from twins:** By enrolling 640 000 mugshots, adding photos of one twin, and then searching photos of those subjects and their twin the inset figure shows, for one typical algorithm, the similarity is generally greater when searching twins against themselves (A) than when searching twins against their sibling (B) but very often still above even stringent thresholds i.e. those corresponding to one in one thousand searches producing a false positive. Thus twins will very often produce a high-scoring non-match on a candidate list and a false alarm in an online identification system. The plot of Fig. 3 shows that fraternal twins are sometimes correctly rejected at those thresholds - including most different sex twins (at center). Figure ?? shows substantially similar behavior for all algorithms tested. In an investigative search, a twin would typically appear at rank 1, or rank 2 if their sibling happened to also be the gallery. Twins (and triplets etc.) constituted 3.3% of all live births [17] in recent years<sup>5</sup>, and because that number is higher today than when the individuals in current adult databases were born, the false positives that arise from twins are now, and will increasingly be, an operational problem. Relative to the United States, twins are born with considerable regional variation. For example they are much less common in East Asia, and much more common in Sub-Saharan Africa [21].

The presence of twins in the mugshot database is inevitable given its size, around 12.3 million people. As this is not an insignificant sample of the domestic United States population, people with other familial ties will be present also. The data was collected over an extended period and because location information is not available, we are unable to estimate the proportion of the domestic population that is present in the dataset. However, if we assume twins are neither more or less disposed to arrest than the general population, we can estimate that hundreds of thousands of individuals in the dataset are twins. This will affect false positive rates because we randomly set aside 331 201 individuals for nonmate searches, and some proportion of those will be twins with siblings in the gallery.

▷ **Database integrity:** An operational error rate should be added to all false negative rates in this report reflecting the proportion of images in a real database that are un-matchable. Such anomalies arise from images that: do not contain a face; include multiple persons; cannot be decoded; are rotated by 90° or 180°; depict a face on clothing; and others introduced by a long tail of various clerical errors. While the mugshot trials in this report have been constructed to minimize such effects, they are a real problem in actual operations.

This report is being updated continuously as new algorithms are submitted to FRVT, and run on new datasets. Participation in the [one-to-many identification track](#) is independent of participation in the [one-to-one verification track](#) of FRVT.

<sup>5</sup>See the CDC's National Vital Statistics Report for 2017: [https://www.cdc.gov/nchs/data/nvsr/nvsr67/nvsr67\\_08-508.pdf](https://www.cdc.gov/nchs/data/nvsr/nvsr67/nvsr67_08-508.pdf)

## Scope and Context

**Audience:** This report is intended for developers, integrators, end users, policy makers and others who have some familiarity with biometrics applications. The methods and metrics documented here will be of interest to organizations engaged in tests of face recognition algorithms. Some of these have been incorporated in the ISO/IEC 19795 Part 1 Biometric Testing and Reporting Framework standard, now nearing publication.

**Prior benchmarks:** Automated face recognition accuracy has improved massively in the two decades since initial commercialization of the various technologies. NIST has tracked that improvement through its conduct of regular independent, free, open, and public evaluations. These have fostered improvements in the state of the art. This report serves as an update to the [NIST Interagency Report 8271](#) on performance of face identification algorithms, published in September 2019.

**Demographics:** In December 2019, NIST published a first report on demographic dependencies in face recognition, [NIST Interagency Report 8280](#) that documented age, sex and race differentials in one-to-one and one-to-many false positive and false negative rates.

**Scope:** NIST IR 8271 documented recognition results for four databases containing in excess of 30.2 million still photographs of 14.4 million individuals. That constituted the largest public and independent evaluation of face recognition ever conducted. It includes results for accuracy, speed, investigative vs. identification applications, scalability to large populations, use of multiple images per person, images of cooperative and non-cooperative subjects.

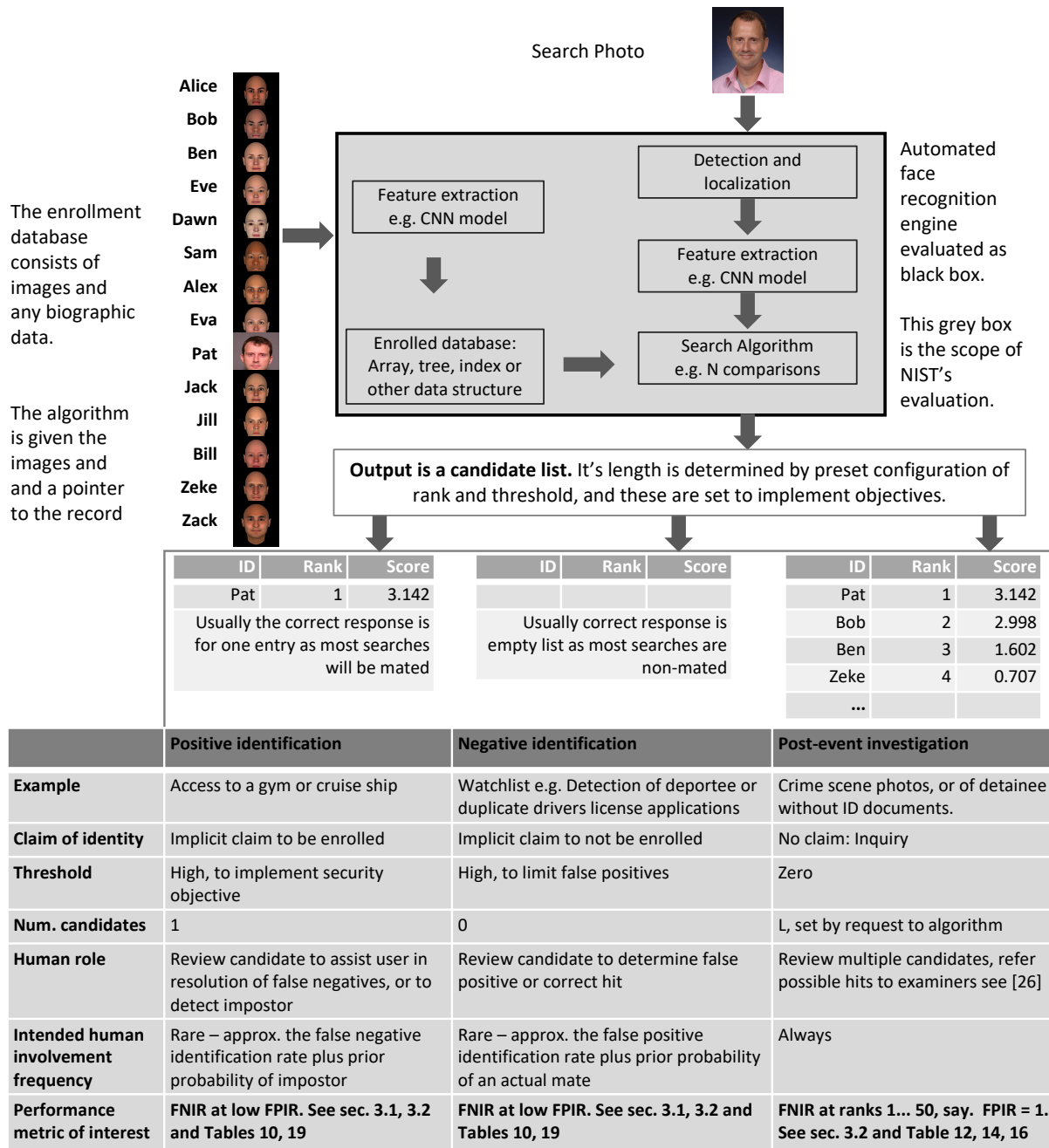
The report also includes results for ageing, recognition of twins, and recognition of profile-view images against frontal galleries. It otherwise does not address causes of recognition failure, neither image-specific problems nor subject-specific factors including demographics. Separate reports on demographic dependencies in face recognition will be published in the future. Additionally out of scope are: performance of live [human-in-the-loop transactional systems](#) like automated border control gates; human recognition accuracy as used in forensic applications; and recognition of persons in video sequences (which NIST evaluated separately [9]). Some of those applications share core matching technologies that *are* tested in this report.

**Images:** Five kinds of images are employed; these are either compared with images of the same kind, or against others from different capture environments as follows. The primary dataset is a set of law enforcement mugshot images (Fig. 5) which are enrolled and then searched with three kinds of images: other mugshots (i.e. within-domain); profile-view photographs (90 degree cross-view); and lower quality webcam images (Fig. 6) collected in similar detention operations (cross-domain). Additionally we compare high quality visa-like photos collected in immigration offices, with: medium quality border crossing images collected in primary immigration lanes; poor quality images collected in ATM-like registered traveller kiosks.

**Participation and industry coverage:** The report includes performance figures for prototype algorithms from the research laboratories of commercial developers and a few universities. This represents a substantial majority of the face recognition industry, but only a tiny minority of the academic community. Participation was open worldwide. While there is no charge for participation, developers incur some software engineering expense in implementing their algorithms behind the NIST application programming interface (API). The test is a black-box test where the function of the algorithm, and the intellectual property associated with it, is hidden inside pre-compiled libraries.

**Recent technology development:** Most face recognition research with deep convolutional neural networks (CNNs) has been aimed at achieving invariance to pose, illumination and expression variations that characterize photojournalism and social media images. The initial research [18, 22] employed large numbers of images of relatively few ( $\sim 10^4$ ) individuals to learn invariance. Inevitably much larger populations ( $\sim 10^7$ ) were employed for training [11, 20] but the benchmark, Labeled Faces in the Wild with (essentially) an equal error rate metric [12], represents an easy task,

one-to-one verification at very high false match rates. While a larger scale identification benchmark duly followed, Megaface [15], its primary metric, rank one hit rate, contrasts with the high threshold discrimination task required in most large-population applications of face recognition, namely credential de-duplication, and background checks. There, identification in galleries containing up to  $10^8$  individuals must be performed using a) very few images per individual and b) stringent thresholds to afford very low false positive identification rates. This track of FRVT was launched to measure the capability of the new technologies, including in these two cases. FRVT has included open-set identification tests since 2002, reporting both false negative and positive identification rates [7].



**Performance metrics for applications:** This report documents the performance of one-to-many face recognition algorithms. The word "performance" here refers to recognition accuracy and computational resource usage, as measured

by executing those algorithms on massive sequestered datasets.

This report includes extensive tabulation of recognition error rates germane to the main use-cases for face search technology. The Figure below, inspired by the Figure 1 in [23] differentiates different applications of the technolgy. The last row directs readers to the main tables relevant to those applications, respectively threshold-based and rank-based metrics that are special cases of the metrics given in section 3. The terms negative identification and positive identification are taken from the ISO/IEC 2382-37:2017 standardized biometrics vocabulary.

The algorithms are specifically configured for these applications by setting thresholds and candidate list lengths. Both rank-based metrics and threshold-based metrics include tradeoffs. In investigation, overall accuracy will be reduced if labor is only available to review a few candidates from the automated system. Note that when a fixed number of candidates are returned, the false positive identification rate of the automated face recognition engine will be 100%, because a probe image of anyone not enrolled will still return candidates. In identification applications where false positives must be limited to satisfy reviewer labor availability or a security objective, higher false negative rates are implied. This report includes extensive quantification of this threshold-based tradeoff.

See Sec. 3

**Template diversity:** The FRVT is designed to evaluate black-box technologies with the consequence that the templates that hold features extracted from face images are entirely proprietary opaque binary data that embed considerable intellectual property of the developer. Despite migration to CNN-based technologies there is no consensus on the optimal feature vector dimension. This is evidenced by template sizes ranging from below 100 bytes to more than four kilobytes. This diversity of approaches, suggests there is no prospect of a standard template something that would require a common feature set to be extracted from faces. Interoperability in automated face recognition remains solidly based on images and documentary standards for those, in particular the ICAO portrait [27] specification deriving from the ISO/IEC 19794-5 Token frontal [24] standard, which are similar to certain ANSI/NIST Type 10 [26] formats.

**Training:** The algorithms submitted to NIST have been developed using image datasets that developers do not disclose. The development will often include application of machine learning techniques and will additionally involve iterative training and testing cycles. NIST itself does not perform any training and does not refine or alter the algorithm in any way. Thus the model, data files, and libraries that define an algorithm are fixed for the duration of the tests. This reflects typical operational reality where recognition software, once installed, is fixed and constant until upgraded. This situation persists because on-site training of algorithms on customer data is atypical essentially because training is not a turnkey process.

**Automated search and human review:** Virtually all applications using automated face search require human review of the outputs at some frequency: Always for investigational applications; rarely in positive identification applications, after rejection (false or otherwise); and rarely in negative identification applications, after an alarm (false or otherwise). The human role is usually to compare a reference image with the query image or the live-subject if present, to render either a definitive decision on “exclusion” (different subjects), or “identification” (same subject), or a declaration that one or both images have “no value” and that no decision can be made. Note that automated face recognition algorithms are not built to do exclusion - low scores from a face comparison arise from different faces *and* poor quality images of the same face.

Human reviewers make recognition errors [5, 19, 25] and are sensitive to image acquisition and quality. Accurate human review is supported by high resolution - as specified in the Type 50, 51 acquisition profiles of the ANSI/NIST Type 10 record [26], and by multiple non-frontal views as specified in the same standard. These often afford views of the ear. Organizations involved in image collection should consider supporting human adjudication by collecting high-resolution frontal and non-frontal views, preparing low resolution versions for automated face recognition [24], and retaining both for any subsequent resolution of candidate matches. Along these lines, the ISO/IEC Joint Technical

Committee 1 subcommittee 37 on biometrics has just initiated projects on image quality assessment and face-aware capture.

## Release Notes

**FRVT Activities:** Since February 2017, NIST has been evaluating one-to-one verification algorithms on an ongoing basis. NIST then restarted FRVT's one-to-many track in February 2018, inviting participants to send up to prototype algorithms. Both tracks allows developers to submit updated algorithms to NIST at any time but no more frequently than four calendar months. This more closely aligns development and evaluation schedules. Results are posted to the web within a few weeks of submission. Details and full report are linked from the [Ongoing FRVT site](#).

**FRVT Reports:** The results of the FRVT appear in the series NIST Interagency Reports tabulated below. The reports were developed separately and released on different schedules. In prior years NIST has mostly reported FRVT results as a single report; this had the disadvantage that results from completed sub-studies were not published until all other studies were complete.

Date	Link	Title	No.
2014-03-20	<a href="#">PDF</a>	FRVT Performance of Automated Age Estimation Algorithms	7995
2015-04-20	<a href="#">PDF</a>	Face Recognition Vendor Test (FRVT) Performance of Automated Gender Classification Algorithms	8052
2014-05-21	<a href="#">PDF</a>	FRVT Performance of face identification algorithms	8009
2017-03-07	<a href="#">PDF</a>	Face In Video Evaluation (FIVE) Face Recognition of Non-Cooperative Subjects	8173
2017-11-23	<a href="#">PDF</a>	The 2017 IARPA Face Recognition Prize Challenge (FRPC)	8197
2018-11-27	<a href="#">PDF</a>	Face Recognition Vendor Test - Part 2: Identification	8271
2019-09-11	<a href="#">PDF</a>	Face Recognition Vendor Test - Part 2: Identification	8271
2019-12-11	<a href="#">PDF</a>	Face Recognition Vendor Test - Part 3: Demographic Effects	8280
2020-01-03	<a href="#">WWW</a>	Face Recognition Vendor Test (FRVT) - Part 1 Verification	Draft

Details appear on pages linked from <https://www.nist.gov/programs-projects/face-projects>.

**Appendices:** This report is accompanied by appendices which present exhaustive results on a per-algorithm basis. These are machine-generated and are included because the authors believe that visualization of such data is broadly informative and vital to understanding the context of the report.

**Typesetting:** Virtually all of the tabulated content in this report was produced automatically. This involved the use of scripting tools to generate directly type-settable L<sup>A</sup>T<sub>E</sub>X content. This improves timeliness, flexibility, maintainability, and reduces transcription errors.

**Graphics:** Many of the Figures in this report were produced using the **ggplot2** package running under **R**, the capabilities of which extend beyond those evident in this document.

# Contents

<b>Release Notes</b>	<b>1</b>
<b>Disclaimer</b>	<b>5</b>
<b>Institutional Review Board</b>	<b>5</b>
<b>Acknowledgments</b>	<b>5</b>
<b>Executive Summary</b>	<b>6</b>
<b>Scope and Context</b>	<b>12</b>
<b>Release Notes</b>	<b>16</b>
<b>1 Introduction</b>	<b>18</b>
<b>2 Evaluation datasets</b>	<b>19</b>
<b>3 Performance metrics</b>	<b>25</b>
<b>4 Results</b>	<b>41</b>
<b>Appendices</b>	<b>80</b>
<b>A Accuracy on large-population FRVT 2018 mugshots</b>	<b>80</b>
<b>B Effect of time-lapse: Accuracy after face ageing</b>	<b>125</b>
<b>C Effect of enrolling multiple images</b>	<b>188</b>
<b>D Accuracy with poor quality webcam images</b>	<b>195</b>
<b>E Accuracy for profile-view to frontal recognition</b>	<b>205</b>
<b>F Search duration</b>	<b>209</b>
<b>G Gallery Insertion Timing</b>	<b>219</b>

# 1 Introduction

One-to-many identification represents the largest market for face recognition technology. Algorithms are used across the world in a diverse range of biometric applications: detection of duplicates in databases, detection of fraudulent applications for credentials such as passports and driving licenses, token-less access control, surveillance, social media tagging, lookalike discovery, criminal investigation, and forensic clustering.

This report contains a breadth of performance measurements relevant to many applications. Performance here refers to accuracy and resource consumption. In most applications, the core accuracy of a facial recognition algorithm is the most important performance variable. Resource consumption will be important also as it drives the amount of hardware, power, and cooling necessary to accommodate high volume workflows. Algorithms consume processing time, they require computer memory, and their static template data requires storage space. This report documents these variables.

## 1.1 Open-set searches

FRVT tested open-set identification algorithms. Real-world applications are almost always “open-set”, meaning that some searches have an enrolled mate, but some do not. For example, some subjects have truly not been issued a visa or drivers license before; some law enforcement searches are from first-time arrestees<sup>6</sup>. In an “open-set” application, algorithms make no prior assumption about whether or not to return a high-scoring result, and for a mated search, the ideal behaviour is that the search produces the correct mate at high score and first rank. For a non-mate search, the ideal behavior is that the search produces zero high-scoring candidates.

Many academic benchmarks execute only closed-set searches. The proportion of mates found in the rank one position is the default accuracy metric. This hit rate metric ignores the score with which a mate is found; weak hits count as much as strong hits. This ignores the real-world imperative that in many applications it is necessary to elevate a threshold to reduce the number of false positives.

---

<sup>6</sup>Operationally closed-set applications are rare because it is usually not the case that all searches have an enrolled mate. One counter-example, however, is a cruise ship in which all passengers are enrolled and all searches should produce exactly one identity. Another example is forensic identification of dental records from an aircraft crash.

## 2 Evaluation datasets

This report documents accuracy for four kinds of images - mugshots, webcam, profiles and wild - as described in the following sections.

### 2.1 Immigration-related images

This report includes benchmark tests sharing a common enrollment of high quality frontal portrait images collected while subject make applications for various immigration benefits. We then search that with two kinds of images, webcam images collected during in-bound immigration and also images collected from registered travelers using a ATM-style kiosk. These are described below and depicted in Figure 4.



Figure 4: Example photos.

- ▷ **Application reference photos:** The images are collected in an attended interview setting using dedicated capture equipment and lighting. The images, at size 300x300 pixels, are smaller than normally indicated by ISO. The images are all high-quality frontal portraits collected in immigration offices and with a white background. As such, potential quality related drivers of high false match rates (such as blur) can be expected to be absent. The images are encoded as ISO/IEC 10918-1 i.e. JPEG. Older images had a compression ration of about 16:1, while newer images, since 2010, are more lightly compressed at 4:1. When these images are provided as input into the algorithm, they are labeled with the type "iso". This report enrols 1 600 000 application images, one per person.
- ▷ **Border crossing photos:** Most images are have width 320 and height 240 pixels. They are JPEG compressed at 16:1 i.e. filesize just below 15KB. The images present challenges for face recognition in that subjects often exhibit non-zero yaw and pitch (associated with the rotational degrees of freedom of the camera mount), low contrast (due to varying and intense background lights), and poor spatial resolution (due to inexpensive cameras). There are often subjects standing in the background, usually at very low resolution (see Figure 4b). In such cases, algorithms should detect all faces and determine which is the largest and most centered. When these images are provided as input into the algorithm, they are labeled with the type "wild".
- ▷ **Kiosk photos:** These photos were collected from subjects whose attention was focused on interaction with an immigration kiosk. They images were not intended for use with automated face recognition. The camera is situated above a display which the user touches, and is triggered either without directing the subject to look at it, or without waiting for the subject to comply. The images are therefore characterized by pitch-down pose, sometimes exceeding 45 degrees, as in Figure 4c. Yaw-angle variation is mild, with most images close to frontal. The images

have width 320 pixels and height 240 pixels and therefore tall individuals are sometimes cropped. This is often just above the eyes and can occur at the nose or mouth. Conversely, short individuals are sometimes cropped such that only the top part of the face is visible. In a quite small number of cases, there other subjects standing just behind the primary subject such that algorithms should detect all faces and determine which is the largest and most centered. Background ceiling lighting is often visible and this sometimes leads to under-exposure of the face. When these images are provided as input into the algorithm, they are labeled with the type "wild".

## 2.2 Law enforcement images

The main mugshot dataset used is referred to as the FRVT 2018 set. This set was collected over the period 2002 to 2017 in routine United States law enforcement operations. This set yields three subsets

- ▷ **Mugshots:** Mugshots comprise about 86% of the database. They have reasonable compliance with the ANSI/NIST ITL1-2011 Type 10 standard's subject acquisition profiles levels 10-20 for frontal images [26]. The most common departure from the standard's requirements is the presence of mild pose variations around frontal - the images of Figure 5 are typical. The images vary in size, with many being 480x600 pixels with JPEG compression applied to produce filesizes of between 18 and 36KB with many images outside this range, implying that about 0.5 bits are being encoded per pixel. When these images are provided as input into the algorithm, they are labeled with the type "mugshot".

Example images appear in Fig. 5

[NIST Interagency Report 8238](#) includes a comparison of this set of mugshots with the smaller and easier sets of mugshots used in tests run in 2010 and 2014.

- ▷ **Profile images:** Profile-view images have been collected in law enforcement for more than 100 years, as human capability is improved with orthogonal information. The profile images used in this report were collected during the same session as the frontal mugshot photograph, in the same standardized photographic setup. These would not therefore be used with automated face recognition. A small subset, 200 000 images, were set aside for testing. When these images are provided as input into the algorithm, they are labeled with the type "wild".

Example images appear in Fig. 7

- ▷ **Webcam images:** The remaining 14% of the images were collected using an inexpensive webcam attached to a flexible operator-directed mount. These images are all of size 240x240 pixels, that are in considerable violation of most quality-related clauses of all face recognition standards. As evident in the figure, the most common defects are non-frontal pose (associated with the rotational degrees of freedom of the camera mount), low contrast (due to varying and intense background lights), and poor spatial resolution (due to inexpensive camera optics) - see examples in Fig 6. The images are overly JPEG compressed, to between 4 and 7KB, implying that only 0.5 to 1 bits are being encoded per color pixel. When these images are provided as input into the algorithm, they are labeled with the type "wild".

Example images appear in Fig. 6

These are drawn from NIST Special Database 32 which may be downloaded [here](#).

These images were partitioned in galleries and probesets for the various experiment listed in Table 1.

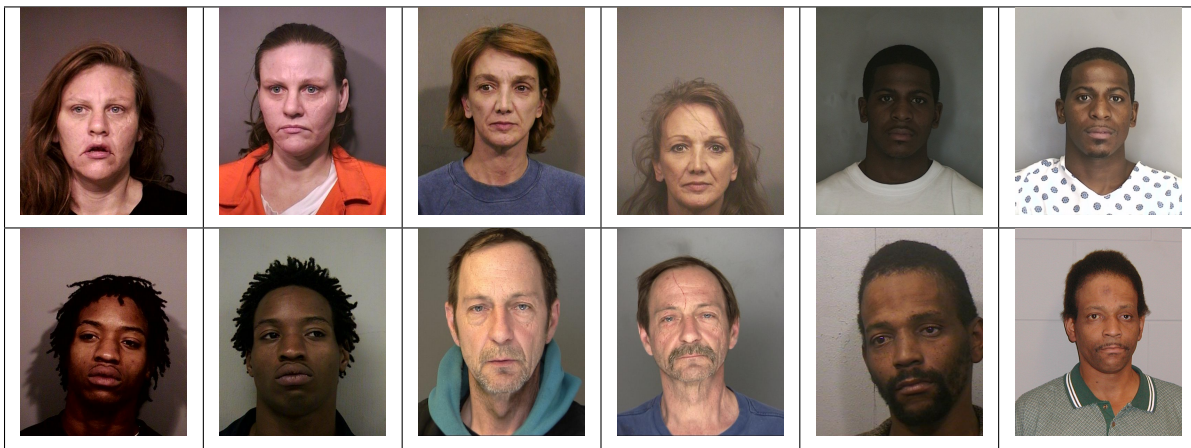


Figure 5: Six mated mugshot pairs representative of the FRVT-2014 (LEO) and FRVT-2018 datasets. The images are collected live, i.e. not scanned from paper. Image source: NIST Special Database 32 the Multiple Encounter Deceased Subjects dataset.



Figure 6: Twelve webcam images representative of probes against the FRVT-2018 mugshot gallery. The first eight images are four mated pairs. Such images present challenges to recognition including pose, non-uniform illumination, low contrast, compression, cropping, and low spatial sampling rate. Image source: NIST Special Database 32 the Multiple Encounter Deceased Subjects dataset.



Figure 7: **[Profile views]** The three images are a frontal enrollment, subsequent frontal probe, and same-session ninety degree profile view. While collection of both frontal and profile views has been typical in law enforcement for more than a century, the recognition of profile to frontal views has essentially been impossible. However, reasonably high accuracy results is now possible - see section E.

Image				
Encounter	1	...	$K_i - 1$	$K_i$
Capture Time	$T_1$	...	$T_{K_i-1}$	$T_{K_i}$
Role RECENT	Not used	Not used	Enrolled	Search
Role LIFETIME	Enrolled	Enrolled	Enrolled	Search

Figure 8: Depiction of the “recent” and “lifetime” enrollment types. Image source: NIST Special Database 32

## 2.3 Enrollment strategies

Many operational applications include collection and enrollment of biometric data from subjects on more than one occasion. This might be done on a regular basis, as might occur in credential (re-)issuance, or irregularly, as might happen in a criminal recidivist situation [4]. The number of images per person will depend on the application area. In civil identity credentialing (e.g. passports, driver’s licenses), the images will be acquired approximately uniformly over time (e.g. ten years for a passport). While the distribution of dates for such images of a person might be assumed uniform, a number of factors might undermine this assumption<sup>7</sup>. In criminal applications, the number of images would depend on the number of arrests. The distribution of dates for arrest records for a person (i.e. the recidivism distribution) has been modeled using the exponential distribution but is recognized to be more complicated<sup>8</sup>.

In any case, the 2010 NIST evaluation of face recognition showed that considerable accuracy benefits accrue with retention and use of *all* historical images [6].

To this end, the FRVT API document provides  $K \geq 1$  images of an individual to the enrollment software. The software is tasked with producing a single proprietary undocumented “black-box” template<sup>9</sup> from the  $K$  images. This affords the algorithm an ability to generate a *model* of the individual, rather than to simply extract features from each image on a sequential basis.

As depicted in Figure 8, the  $i$ -th individual in the FRVT 2018 dataset has  $K_i$  images. These are labelled as  $x_k$  for  $k = 1 \dots K_i$  in chronological order of capture date. To measure the utility of having multiple enrollment images, this report evaluates three kinds of enrollment:

- ▷ **Recent:** Only the second most recent image,  $x_{K_i-1}$  is enrolled. This strategy of enrollment mimics the operational policy of retaining the imagery from the most recent encounter. This might be done operationally to ameliorate the effects of face ageing. Obviously retaining only the most recent image should only be done if the identity of the person is trusted to be correct. For example, in an access control situation retention of the most recent successful *authentication* image would be hazardous if it could be a false positive.
- ▷ **Lifetime-consolidated:** All but the most recent image are enrolled,  $x_1 \dots x_{K_i-1}$ . This subject-centric strategy might be adopted if quality variations exist where an older image might be more suitable for matching, despite the ageing effect.

<sup>7</sup>For example, a person might skip applying for a passport for one cycle, letting it expire. In addition, a person might submit identical images (from the same photography session) to consecutive passport applications at five year intervals.

<sup>8</sup>A number of distributions have been considered to model recidivism, see for example [3].

<sup>9</sup>There are no formal face template standards. Template standards only exist for fingerprint minutiae - see ISO/IEC 19794-2:2011.

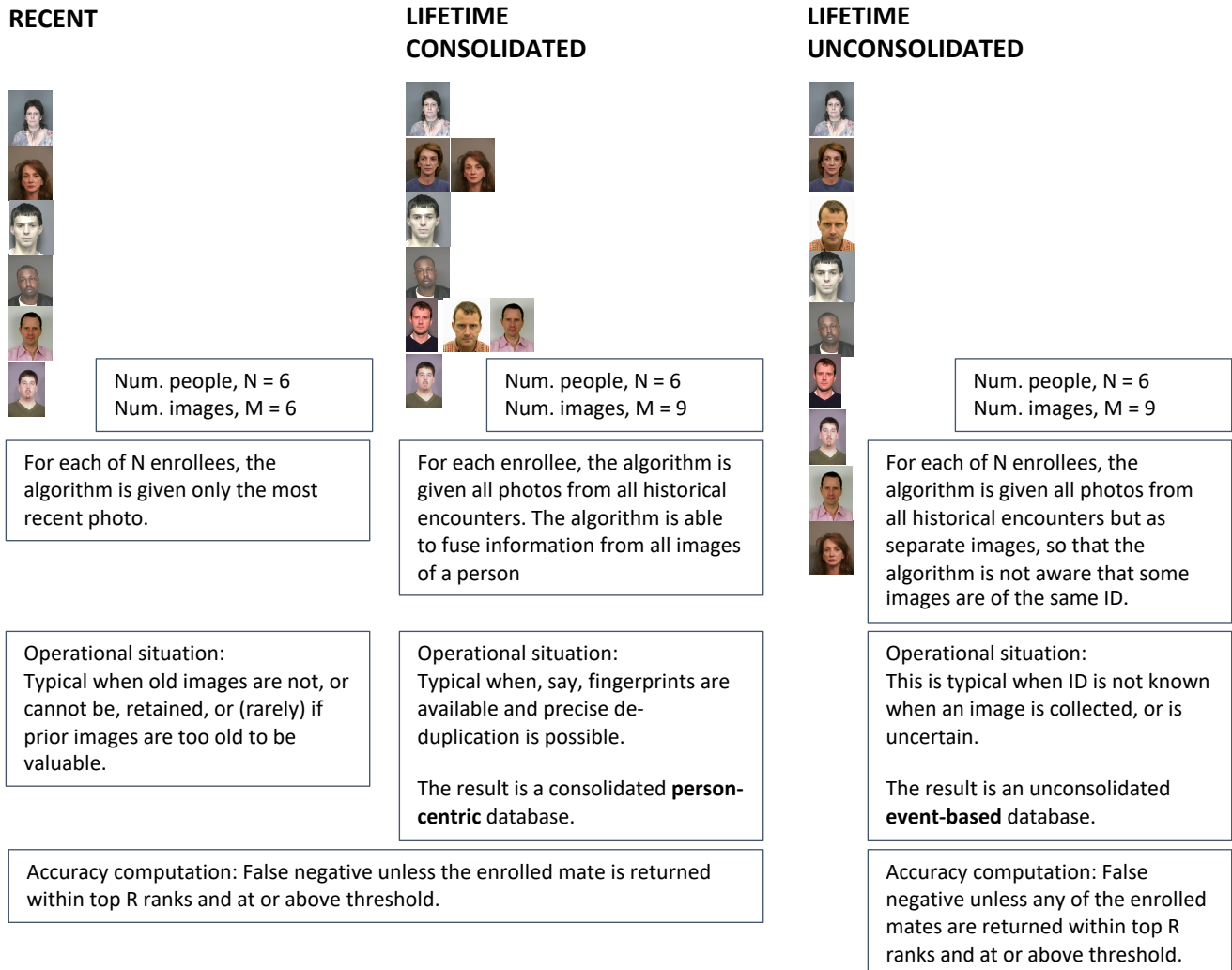


**Figure 9: Enrollment strategies.** The figure shows the three kinds of enrollment databases examined in this report. Image source: NIST Special Database 32

	ENROLLMENT				SEARCH			
	TYPE SEE SECTION 2.3	POPULATION FILTER	N-SUBJECTS	N-IMAGES	MATE N-SUBJECTS	NON-MATE N-IMAGES	N-SUBJECTS	N-IMAGES
<b>Mugshot trials from enrollment of single images</b>								
1	RECENT	NATURAL	640 000	640 000	154 549	154 549	331 254	331 254
2	RECENT	NATURAL	1 600 000	1 600 000				
3	RECENT	NATURAL	3 000 000	3 000 000				
4	RECENT	NATURAL	6 000 000	6 000 000				
5	RECENT	NATURAL	12 000 000	12 000 000				
<b>Cross-domain</b>								
13	MUGSHOTS AS ON ROW 2				82 106 WEBCAM	82 106 WEBCAM	331 254 WEBCAM	331 254 WEBCAM
<b>Cross-view</b>								
14	MUGSHOTS AS ON ROW 2				100 000 PROFILE	100 000 PROFILE	100 000 PROFILE	100 000 PROFILE
<b>Mugshot ageing</b>								
17	OLDEST	NATURAL	3 068 801	3 068 801	2 853 221	10 951 064	0	0
<b>Border crossing ageing</b>								
17	OLDEST	NATURAL	1 600 000	1 600 000	903 655	1 922 393	1 393 076	1 680 000
<b>Visa-border</b>								
19	PRIOR	NATURAL	1 600 000 VISA	1 600 000 VISA	80 000 BORDER	80 000 BORDER	80 000 BORDER	80 000 BORDER
20	VISA AS ON ROW 18				21 016 BORDER	21 016 BORDER	21 016 BORDER	21 016 BORDER

**Table 1: Enrollment and search sets.** Each row summarizes one identification trial. Unless stated otherwise, all entries refer to mugshot images. The term “natural” means that subjects were selected without heed to demographics, i.e. in the distribution native to this dataset. The probe images were collected in a different calendar year to the enrollment image. Missing values in rows 2-12 are the same as in row 1.

▷ **Lifetime-unconsolidated:** Again all but the most recent image are enrolled  $x_1 \dots x_{K_i-1}$  but now separately, with different identifiers, such that the algorithm is not aware that the images are from the same face. This kind of event- or encounter-centric enrollment is very common when operational constraints preclude reliable consolidation of the historical encounters into a single identity. This aspect also prevents the recognition algorithm from a) building a holistic model of identity (as is common in speaker recognition systems) and b) implementing fusion, for example template-level fusion of feature vectors, or post-search score-level fusion. The result is that searches will typically yield more than one image of a person in the top ranks. This has consequences for appropriate metrics, as detailed in section 3.2.1

NIST first evaluated this kind of enrollment in mid 2018, and the results tables include some comparison of accuracy available from all three enrollment styles.

In all cases, the most recent image,  $x_{K_i}$ , is reserved as the search image. For the 1.6 million subject enrollment partition of the FRVT 2018 data,  $1 \leq K_i \leq 33$  with  $K_i = 1$  in 80.1% of the individuals,  $K_i = 2$  in 13.4%,  $K_i = 3$  in 3.7%,  $K_i = 4$  in 1.4%,  $K_i = 5$  in 0.6%,  $K_i = 6$  in 0.3%, and  $K_i > 6$  is 0.2% for everyone else. This distribution is substantially dependent on United States recidivism rates.

We did not evaluate the case of retaining only the highest quality image, since automated quality assessment is out of scope for this report. We do not anticipate that such strategies will prove beneficial when the quality assessment apparatus is imperfect and unvalidated.

### 3 Performance metrics

This section gives specific definitions for accuracy and timing metrics. Tests of open-set biometric algorithms must quantify frequency of two error conditions:

- ▷ **False positives:** Type I errors occur when search data from a person who has never been seen before is incorrectly associated with one or more enrollees' data.
- ▷ **Misses:** Type II errors arise when a search of an enrolled person's biometric does not return the correct identity.

Many practitioners prefer to talk about "hit rates" instead of "miss rates" - the first is simply one minus the other as detailed below. Sections 3.1 and 3.2 define metrics for the Type I and Type II performance variables.

Additionally, because recognition algorithms sometimes fail to produce a template from an image, or fail to execute a one-to-many search, the occurrence of such events must be recorded. Further because algorithms might elect to not produce a template from, for example, a poor quality image, these failure rates must be combined with the recognition error rates to support algorithm comparison. This is addressed in section 3.5.

Finally, section 3.7 discusses measurement of computation duration, and section 3.8 addresses the uncertainty associated with various measurements. Template size measurement is included with the results.

#### 3.1 Quantifying false positives

It is typical for a search to be conducted into an enrolled population of  $N$  identities, and for the algorithm to be configured to return the closest  $L$  candidate identities. These candidates are ranked by their score, in descending order, with all scores required to be greater than or equal to zero. A human analyst might examine either all  $L$  candidates, or just the top  $R \leq L$  identities, or only those with score greater than threshold,  $T$ . The workload associated with such examination is discussed later, in 3.6.

False alarm performance is quantified in two related ways. These express how many searches produces false positives, and then, how many false positives are produced in a search.

**False positive identification rate:** The first quantity, FPIR, is the proportion of non-mate searches that produce an adverse outcome:

$$\text{FPIR}(N, T) = \frac{\text{Num. non-mate searches where one or more enrolled candidates are returned with score at or above threshold}}{\text{Num. non-mate searches attempted.}} \quad (1)$$

Under this definition, FPIR can be computed from the highest non-mate candidate produced in a search - it is not necessary to consider candidates at rank 2 and above. FPIR is the primary measure of Type I errors in this report.

**Selectivity:** However, note that in any given search, several non-mate may be returned above threshold. In order to quantify such events, a second quantity, selectivity (SEL), is defined as the *number* of non-mates returned on a candidate list, averaged over all searches.

$$\text{SEL}(N, T) = \frac{\text{Num. non-mate enrolled candidates returned with score at or above threshold}}{\text{Num. non-mate searches attempted.}} \quad (2)$$

where  $0 \leq \text{SEL}(N, T) \leq L$ . Both of these metrics are useful operationally. FPIR is useful for targeting how often an

adverse false positive outcome can occur, while SEL as a number is related to workload associated with adjudicating candidate lists. The relationship between the two quantities is complicated - it depends on whether an algorithm concentrates the false alarms in the results of a few searches or whether it disburses them across many. This was detailed in FRVT 2014, NISTIR 8009. It has not yet been detailed in FRVT 2018.

### 3.2 Quantifying hits and misses

If  $L$  candidates are returned in a search, a shorter candidate list can be prepared by taking the top  $R \leq L$  candidates for which the score is above some threshold,  $T \geq 0$ . This reduction of the candidate list is done because thresholds may be applied, and only short lists might be reviewed (according to policy or labor availability, for example). It is useful then to state accuracy in terms of  $R$  and  $T$ , so we define a “miss rate” with the general name **false negative identification rate** (FNIR), as follows:

$$\text{FNIR}(N, R, T) = \frac{\text{Num. mate searches with enrolled mate found outside top } R \text{ ranks or score below threshold}}{\text{Num. mate searches attempted.}} \quad (3)$$

This formulation is simple for evaluation in that it does not distinguish between causes of misses. Thus a mate that is not reported on a candidate list is treated the same as a miss arising from face finding failure, algorithm intolerance of poor quality, or software crashes. Thus if the algorithm fails to produce a candidate list, either because the search failed, or because a search template was not made, the result is regarded as a miss, adding to FNIR.

*Hit rates, and true positive identification rates:* While FNIR states the “miss rate” as how often the correct candidate is either not above threshold or not at good rank, many communities prefer to talk of “hit rates”. This is simply the **true positive identification rate**(TPIR) which is the complement of FNIR giving a positive statement of how often mated searches are successful:

$$\text{TPIR}(N, R, T) = 1 - \text{FNIR}(N, R, T) \quad (4)$$

This report does not report true positive “hit” rates, preferring false negative miss rates for two reasons. First, costs rise linearly with error rates. For example, if we double FNIR in an access control system, then we double user inconvenience and delay. If we express that as decrease of TPIR from, say 98.5% to 97%, then we mentally have to invert the scale to see a doubling in costs. More subtly, readers don’t perceive differences in numbers near 100% well, becoming inured to the “high nineties” effect where numbers close to 100 are perceived indifferently.

**Reliability** is a corresponding term, typically being identical to TPIR, and often cited in automated (fingerprint) identification system (AFIS) evaluations.

An important special case is the **cumulative match characteristic**(CMC) which summarizes accuracy of mated-searches only. It ignores similarity scores by relaxing the threshold requirement, and just reports the fraction of mated searches returning the mate at rank  $R$  or better.

$$\text{CMC}(N, R) = 1 - \text{FNIR}(N, R, 0) \quad (5)$$

We primarily cite the complement of this quantity,  $\text{FNIR}(N, R, 0)$ , the fraction of mates *not* in the top  $R$  ranks.

The **rank one hit rate** is the fraction of mated searches yielding the correct candidate at best rank, i.e.  $\text{CMC}(N, 1)$ . While this quantity is the most common summary indicator of an algorithm’s efficacy, it is not dependent on similarity scores, so it does not distinguish between strong (high scoring) and weak hits. It also ignores that an adjudicating reviewer is often willing to look at many candidates.

### 3.2.1 False negative rates for unconsolidated galleries

As detailed in section 2.3 a common type of gallery, here referred to as the lifetime unconsolidate type, is populated with all images of an individual without any association between them. That is, the gallery construction algorithm is not provided with any ID labels that would support processing of a person's images jointly. This contrasts with the lifetime consolidate type where an algorithm may explicitly fuse features from multiple images of a person, or select a best image. In such cases, where the number of enrolled images is a random variable, we define two false negative rates as follows.

The first demands that the algorithm place any of the  $K_i$  mates in the top  $R \geq 1$  ranks. The proportion of searches for which this does not occur forms a false negative identification rate:

$$\text{FNIR}_{\text{any}}(N, R, T) = 1 - \frac{\text{Num. mate searches where any enrolled mate is found in the top } R \text{ ranks and at-or-above threshold}}{\text{Num. mate searches attempted.}} \quad (6)$$

The second demands that the algorithm place all  $K_i$  mates in the top  $R \geq K_i$  ranks. The proportion of searches for which this does not occur forms a false negative identification rate:

$$\text{FNIR}_{\text{all}}(N, R, T) = 1 - \frac{\text{Num. mate searches where all enrolled mates are found in the top } R \text{ ranks and at-or-above threshold}}{\text{Num. mate searches attempted.}} \quad (7)$$

Placing all mates in the top ranks is a more difficult task than correctly retrieving any image, so it holds that:  $\text{FNIR}_{\text{all}} \geq \text{FNIR}_{\text{any}}$ . This is evident in the results presented for November 2018 algorithms in Tables starting at ??.

The information retrieval community might prefer to compute and plot *precision* and *recall*; this is a valid approach, but we advance the two metrics above because they relate to our normal definition of consolidated FNIR, and they cover the two extreme use-cases of wanting any hit vs. all hits.

## 3.3 DET interpretation

In biometrics, a false negative occurs when an algorithm fails to match two samples of one person – a Type II error. Correspondingly, a false positive occurs when samples from two persons are improperly associated – a Type I error.

Matches are declared by a biometric system when the native comparison score from the recognition algorithm meets some threshold. Comparison scores can be either similarity scores, in which case higher values indicate that the samples are more likely to come from the same person, or dissimilarity scores, in which case higher values indicate different people. Similarity scores are traditionally computed by fingerprint and face recognition algorithms, while dissimilarities are used in iris recognition. In some cases, the dissimilarity score is a distance possessing metric properties. In any case, scores can be either mate scores, coming from a comparison of one person's samples, or nonmate scores, coming from comparison of different persons' samples.

The words "genuine" or "authentic" are synonyms for mate, and the word "impostor" is used as a synonym for non-mate. The words "mate" and "nonmate" are traditionally used in identification applications (such as law enforcement search, or background checks) while genuine and impostor are used in verification applications (such as access control).

An error tradeoff characteristic represents the tradeoff between Type II and Type I classification errors. For identification this plots false negative vs. false positive identification rates i.e. FNIR vs. FPIR parametrically with T. Such plots

are often called detection error tradeoff (DET) characteristics or receiver operating characteristic (ROC). These serve the same function – to show error tradeoff – but differ, for example, in plotting the complement of an error rate (e.g.  $TPIR = 1 - FNIR$ ) and in transforming the axes, most commonly using logarithms, to show multiple decades of FPIR. More rarely, the function might be the inverse of the Gaussian cumulative distribution function.

The slides of Figures 10 through 15 discuss presentation and interpretation of DETs used in this document for reporting face identification accuracy. Further detail is provided in formal biometrics testing standards, see the various parts of ISO/IEC 19795 Biometrics Testing and Reporting. More terms, including and beyond those to do with accuracy, appear in ISO/IEC 2382-37 Information technology – Vocabulary – Part 37: Harmonized biometric vocabulary.

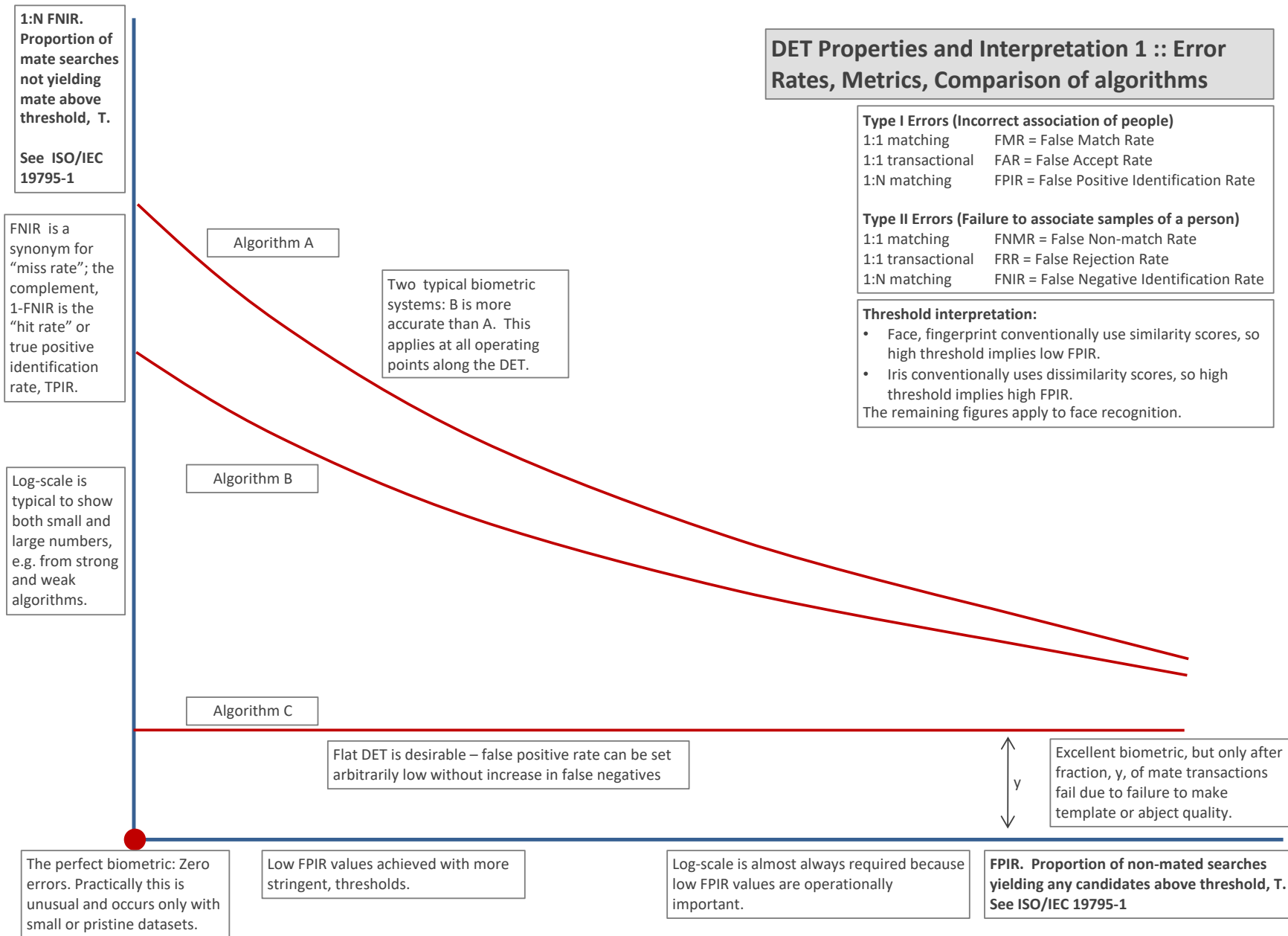


Figure 10: DET as the primary performance reporting mechanism.

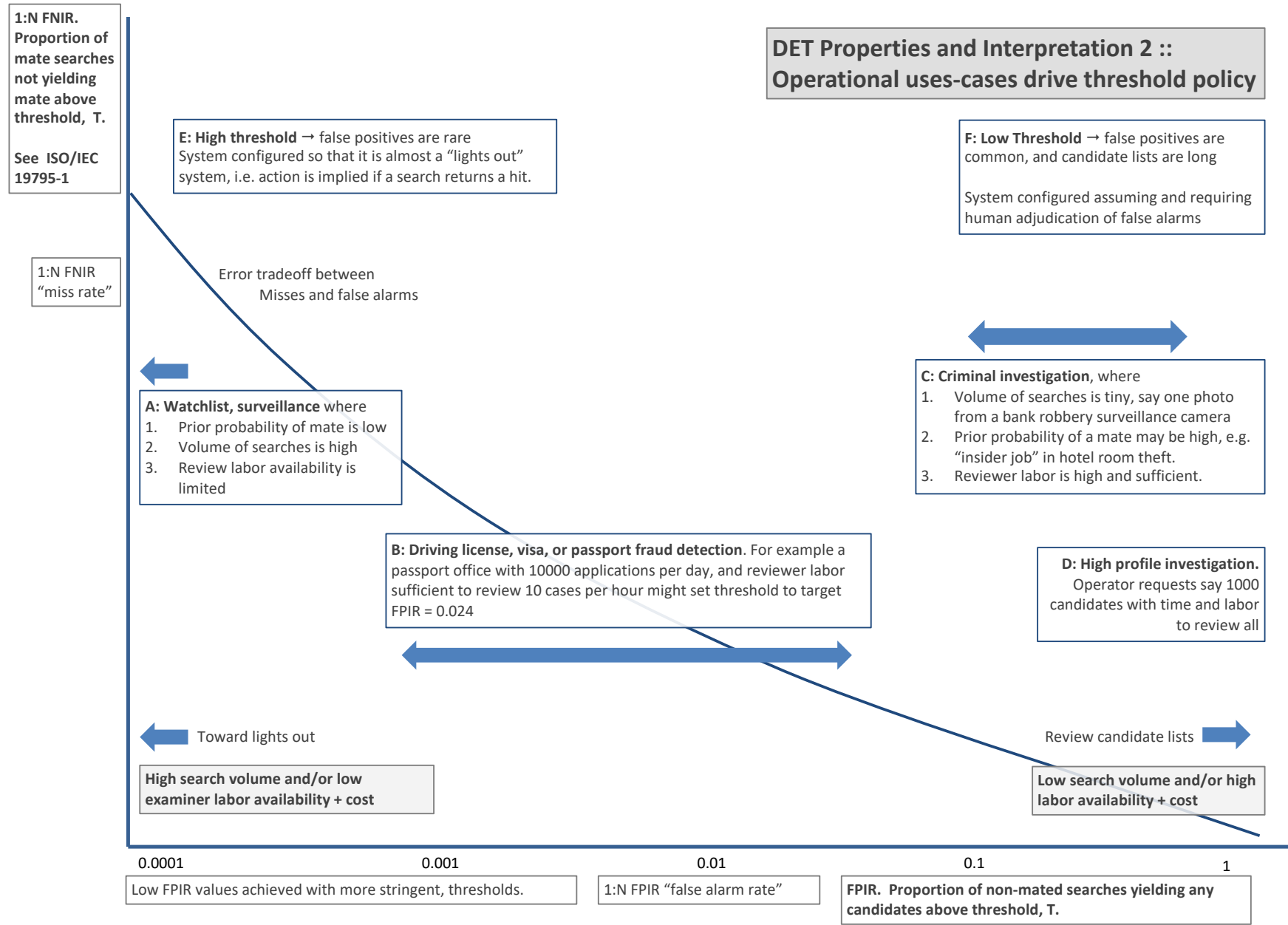


Figure 11: DET as the primary performance reporting mechanism.

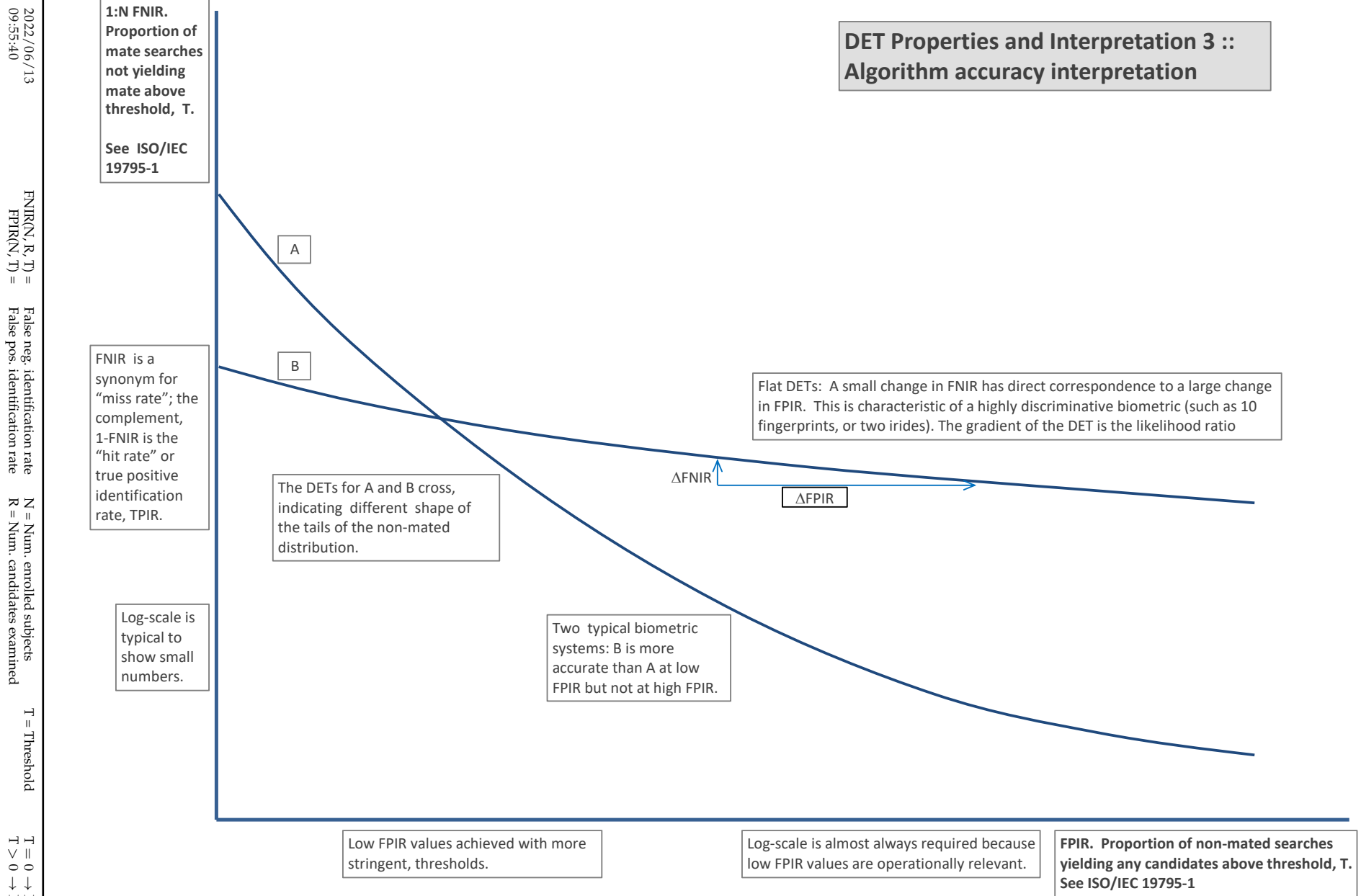


Figure 12: DET as the primary performance reporting mechanism.

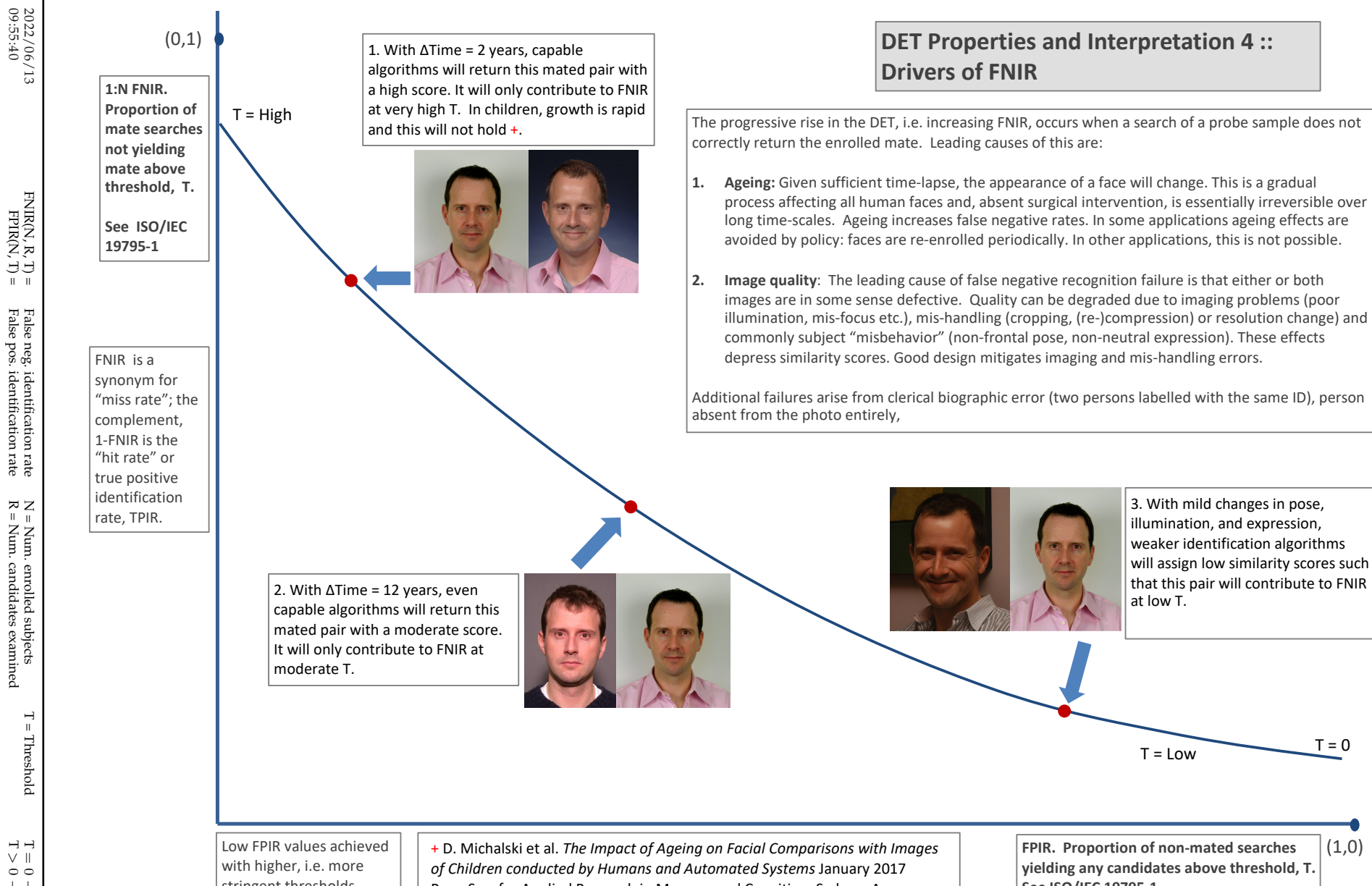
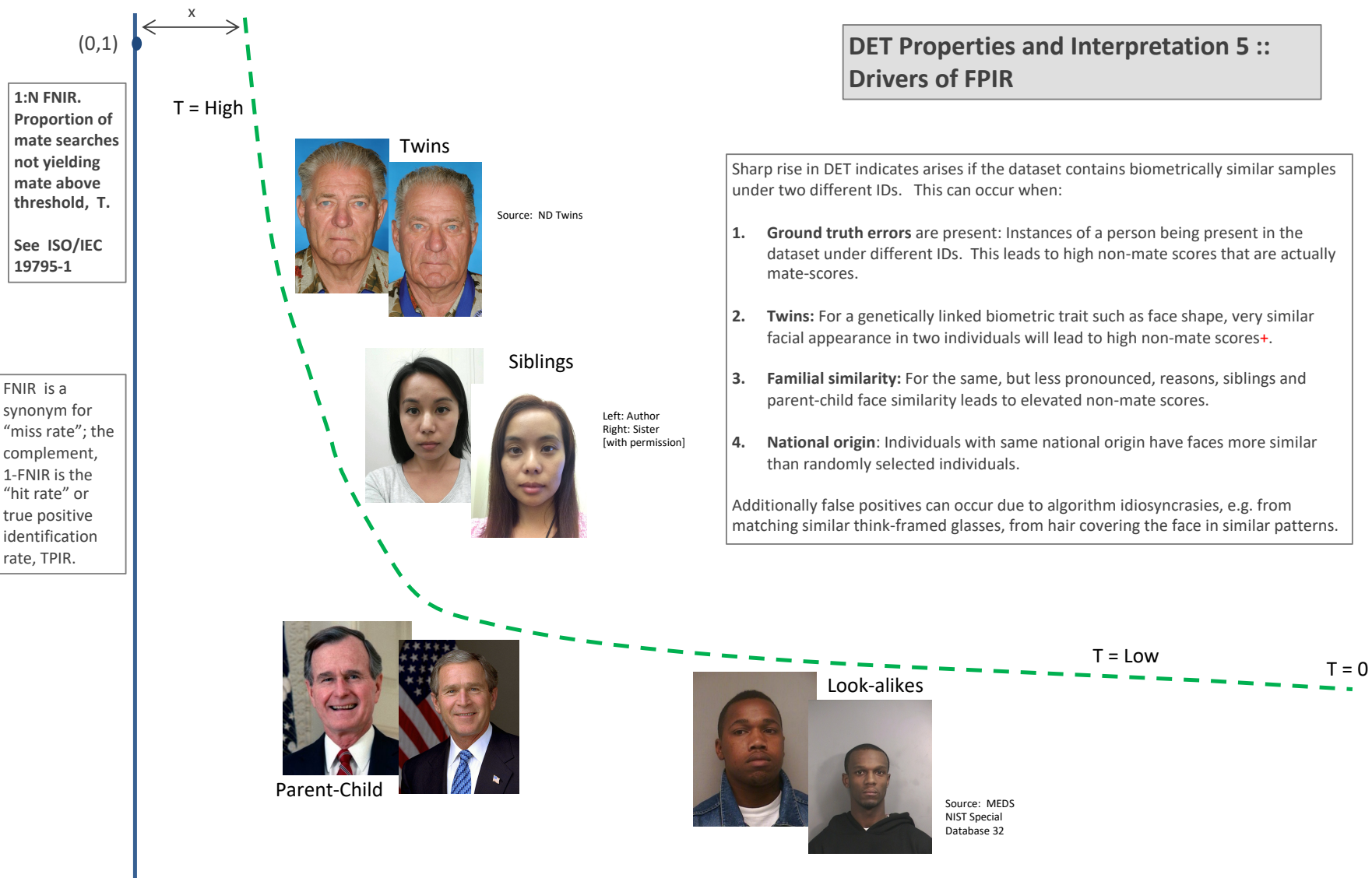


Figure 13: DET as the primary performance reporting mechanism.



Low FPIR values achieved with higher, i.e. more stringent thresholds.

+ NOTE: While most algorithms will not recognize twins correctly, there is at least one face recognition algorithm that can correctly distinguish twins [US Patent: [US7369685B2](#)].

**FPIR.** Proportion of non-mated searches yielding any candidates above threshold, T.  
See ISO/IEC 19795-1

Figure 14: DET as the primary performance reporting mechanism.

2022/06/13  
09:55:40

$\text{FNIR}(N, R, T) =$  False neg. identification rate  
 $\text{FPIR}(N, T) =$  False pos. identification rate

$N$  = Num. enrolled subjects  
 $R$  = Num. candidates examined

$T$  = Threshold

$T = 0 \rightarrow$  Investigation  
 $T > 0 \rightarrow$  Identification

**1:N FNIR.**  
Proportion of mate searches not yielding mate above threshold,  $T$ .  
See ISO/IEC 19795-1

Algorithm X,  
Condition 1

Algorithm X,  
Condition 2

If system X is used with images of different properties, say from different imaging systems, or from different populations, generally both FNIR and FPIR will change. The dotted line joins points of the same threshold. Horizontal (vertical) lines indicate change in FPIR (FNIR) only. Two cases concerning population size are shown below (A and B), for the blue curves.

FNIR is a synonym for "miss rate"; the complement, 1-FNIR is the "hit rate" or true positive identification rate, TPIR.

Log-scale is typical to show small numbers.

Algorithm Y,  
Condition 1

Algorithm Y,  
Condition 2

If DETs are computed for two categories (men and women) or (cameras A and B) or (indoor vs. outdoor), generally the Type I and Type II errors will differ and the line of constant threshold will be neither horizontal nor vertical.

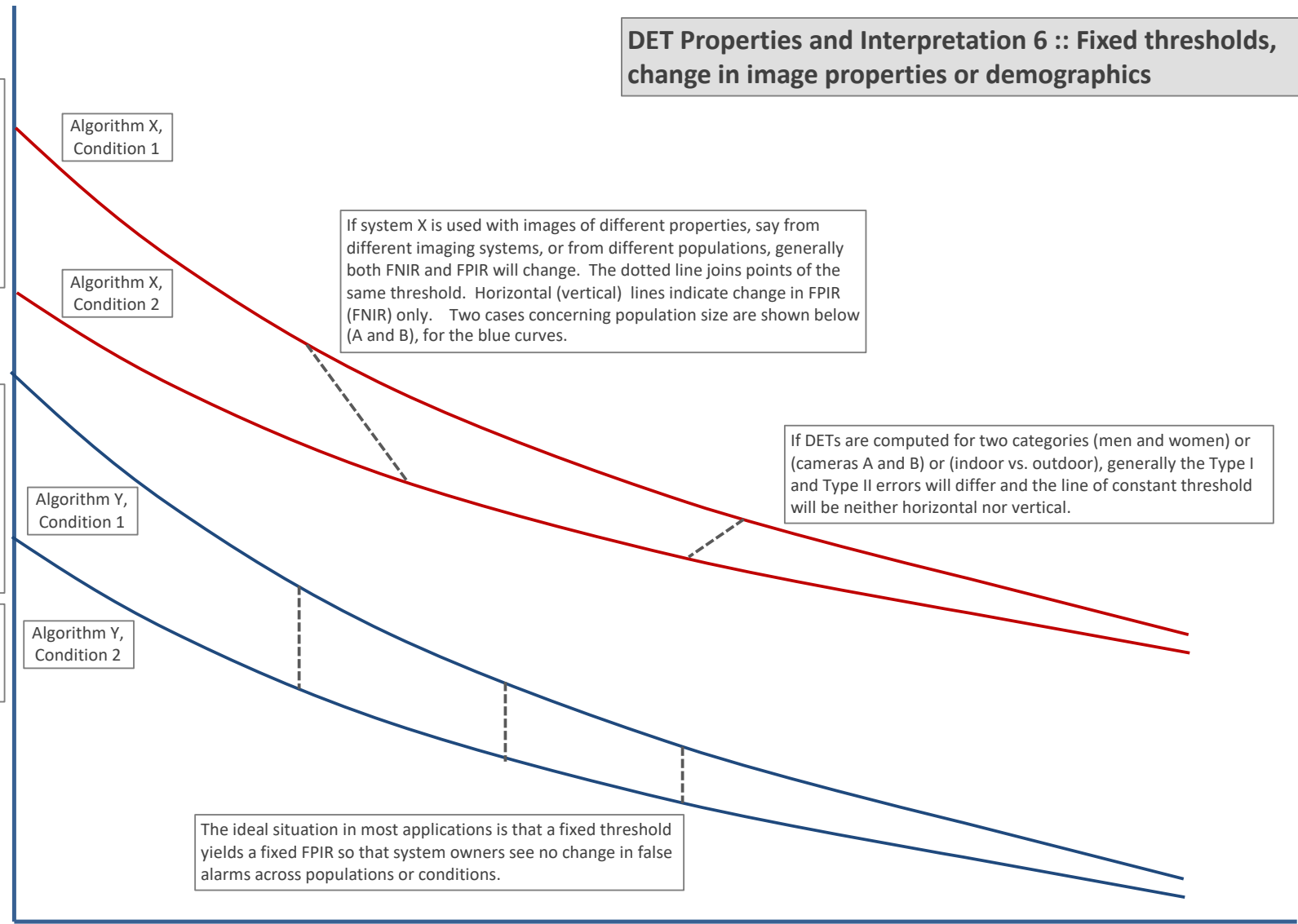
The ideal situation in most applications is that a fixed threshold yields a fixed FPIR so that system owners see no change in false alarms across populations or conditions.

Low FPIR values achieved with higher, i.e. more stringent, thresholds.

Log-scale is often required because low FPIR values are operationally relevant.

**FPIR.** Proportion of non-mated searches yielding any candidates above threshold,  $T$ . See ISO/IEC 19795-1

Figure 15: DET as the primary performance reporting mechanism.



2022/06/13  
09:55:40FNIR(N, R, T) = False neg. identification rate  
FPIR(N, T) = False pos. identification rateN = Num. enrolled subjects  
R = Num. candidates examined

T = Threshold

T = 0 → Investigation  
T > 0 → Identification

## DET Properties and Interpretation 7 :: Effect of enrolled population size.

**1:N FNIR.**  
Proportion of mate searches not yielding mate above threshold, T.  
See ISO/IEC 19795-1

FNIR is a synonym for "miss rate"; the complement, 1-FNIR is the "hit rate" or true positive identification rate, TPIR.

Log-scale is typical to show small numbers.

A: Typical case: In theory, and often in practice, a 1:N search is implemented by executing N 1:1 comparisons independently and then sorting by similarity score:

**Mate scores:** A mate comparison score is independent of the rest of enrollment data, and so independent of N. This implies the horizontal line above  $\text{FNIR}(T, N) = \text{FNMR}(T, 1)$ .

**Non-mate scores:** FPIR increases linearly with N from binomial theory:  $\text{FPIR}(N, T) = 1 - (1 - \text{FMR}(T))^N \rightarrow N \text{ FMR}(T)$  for small FPIR.

Pop. N1

Pop. N2 > N1

B: Special case: An enrollment database is not just a linear data structure, it could be an index, or tree, then search is not simply N 1:1 comparisons and a sort. In that case:

**Mate scores** become dependent on the enrollment data, either its size or actual content, then generally  $\text{FNIR}(T, N) \neq \text{FNIR}(T, 1)$ .

Non-mate scores are normally no longer just the highest 1:1 comparison score. Instead, for example, scores may be normalized as the implementation attempts to make FPIR independent of N will yield the vertical line linking points of equal threshold.

Low FPIR values achieved with higher, i.e. more stringent, thresholds.

Log-scale is often required because low FPIR values are operationally important.

**FPIR.** Proportion of non-mated searches yielding any candidates above threshold, T.  
See ISO/IEC 19795-1

Figure 16: DET as the primary performance reporting mechanism.

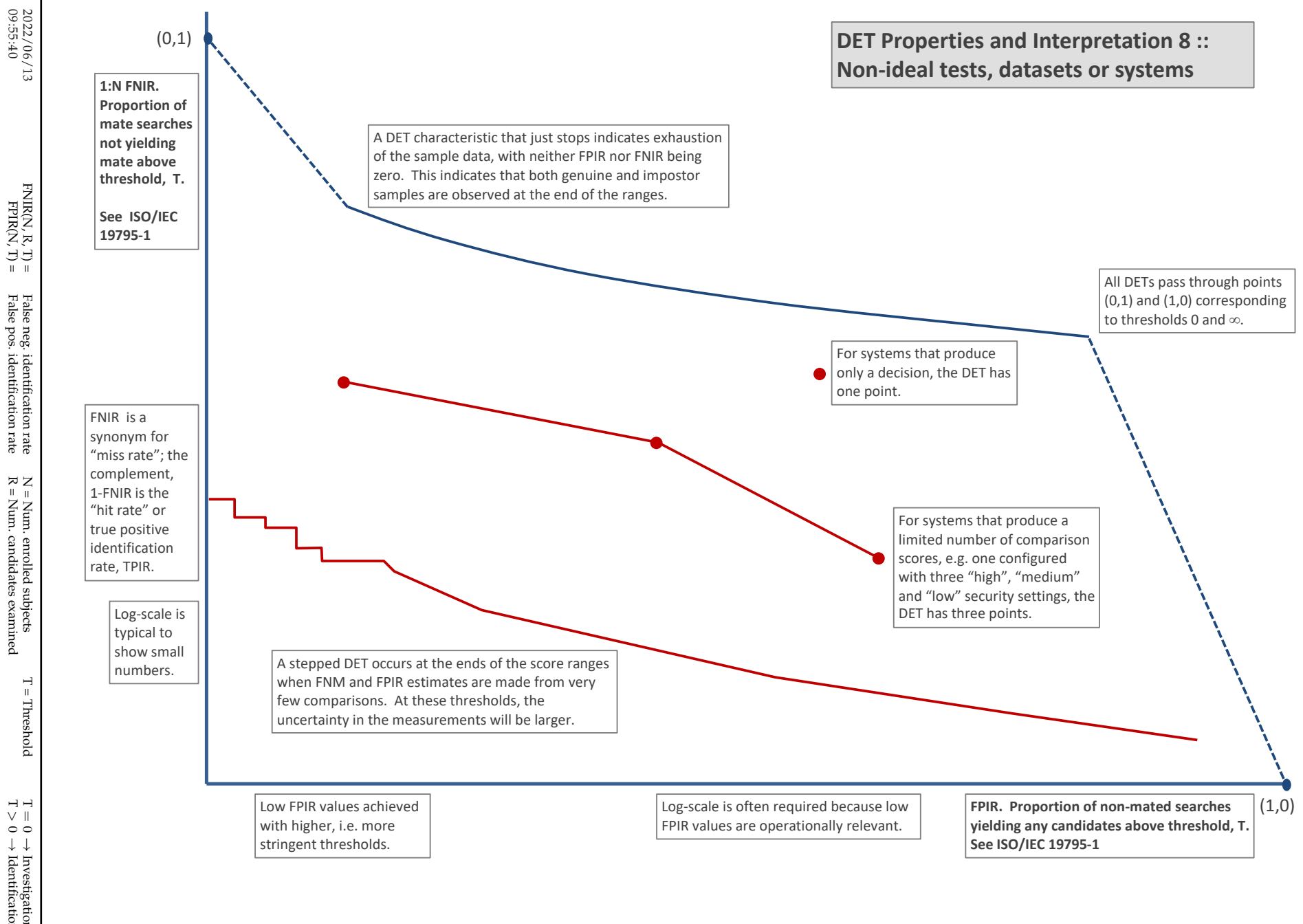


Figure 17: DET as the primary performance reporting mechanism.

### 3.4 Best practice testing requires execution of searches with and without mates

FRVT embeds 1:N searches of two kinds: Those for which there is an enrolled mate, and those for which there is not. The respective numbers for these types of searches appear in Table 1. However, it is common to conduct only mated searches<sup>10</sup>. The cumulative match characteristic is computed from candidate lists produced in mated searches. Even if the CMC is the only metric of interest, the actual trials executed in a test should nevertheless include searches for which no mate exists. As detailed in Table 1 the FRVT reserved disjoint populations of subjects for executing true non-mate searches.

### 3.5 Failure to extract features

During enrollment some algorithms fail to convert a face image to a template. The proportion of failures is the failure-to-enroll rate, denoted by FTE. Similarly, some search images are not converted to templates. The corresponding proportion is termed failure-to-extract, denoted by FTX.

We do not report FTX because we assume that the same underlying algorithm is used for template generation for enrollment and search.

Failure to extract rates are incorporated into FNIR and FPIR measurements as follows.

- ▷ **Enrollment templates:** Any failed enrollment is regarded as producing a zero length template. Algorithms are required by the API [10] to transparently process zero length templates. The effect of template generation failure on search accuracy depends on whether subsequent searches are mated, or non-mated: Mated searches will fail giving elevated FNIR; non-mated searches will not produce false positives so, to first order, FPIR will be reduced by a factor of  $1 - \text{FTE}$ .
- ▷ **Search templates and 1:N search:** In cases where the algorithm fails to produce a search template from input imagery, the result is taken to be a candidate list whose entries have no hypothesized identities and zero score. The effect of template generation failure on search accuracy depends on whether searches are mated, or non-mated: Mated searches will fail giving elevated FNIR; Non-mated searches will not produce false positives, so FPIR will be reduced. Thus given a measurement of false negative and positive rates made over only those where failures-to-extract did not occur, those rates - call them  $\text{FNIR}^\dagger$  and  $\text{FPIR}^\dagger$  - could be adjusted by an explicit measurement of FTX as follows

$$\text{FNIR} = \text{FTX} + (1 - \text{FTX})\text{FNIR}^\dagger \quad (8)$$

$$\text{FPIR} = (1 - \text{FTX})\text{FPIR}^\dagger \quad (9)$$

This approach is the correct treatment for positive-identification applications such as access control where cooperative users are enrolled and make attempts at recognition. This approach is not appropriate to negative identification applications, such as visa fraud detection, in which hostile individuals may attempt to evade detection by submitting poor quality samples. In those cases, template generation failures should be investigated as though a false alarm had occurred.

<sup>10</sup>For example, the [Megaface benchmark](#). This is bad practice for several reasons: First, if a developer knows, or can reasonably assume, that a mate always exists, then unrealistic gaming of the test is possible. A second reason is that it does not put FPIR on equal footing with FNIR and that matters because in most applications, not all searches have mates - not everyone has been previously enrolled in a driving license issuance or a criminal justice system - so addressing between-class separation becomes necessary.

### 3.6 Fixed length candidate lists, threshold independent workload

Suppose an automated face identification algorithm returns  $L$  candidates, and a human reviewer is retained to examine up to  $R$  candidates, where  $R \leq L$  might be set by policy, preference or labor availability. For now, assume also that the reviewer is not provided with, or ignores, similarity scores, and thresholds are not applied. Given the algorithm typically places mates at low (good) ranks, the number of candidates a reviewer can be expected to review can be derived as follows. Note that the reviewer will:

- ▷ Always inspect the first ranked image Frac. reviewed = 1
- ▷ Then inspect those candidates where mate not confirmed at rank 1 Frac. reviewed = 1-CMC(1)
- ▷ Then inspect those candidates where mate not confirmed at rank 1 or 2 Frac. reviewed = 1-CMC(2)

etc. Thus if the reviewer will stop after a maximum of  $R$  candidates, the expected number of candidate reviews is

$$M(R) = 1 + (1 - CMC(1)) + (1 - CMC(2)) + \dots + (1 - CMC(R - 1)) \quad (10)$$

$$= R - \sum_{r=1}^{R-1} CMC(r) \quad (11)$$

A recognition algorithm that front-loads the cumulative match characteristic will offer reduced workload for the reviewer. This workload is defined only over the searches for which a mate exists. In the cases where there truly is no mate, the reviewer would review all  $R$  candidates. Thus, if the proportion of searches for which a mate does exist is  $\beta$ , which in the law enforcement context would be the recidivism rate [3], the full expression for workload becomes:

$$M(R) = \beta \left( R - \sum_{r=1}^{R-1} CMC(r) \right) + (1 - \beta)R \quad (12)$$

$$= R - \beta \sum_{r=1}^{R-1} CMC(r) \quad (13)$$

### 3.7 Timing measurement

Algorithms were submitted to NIST as implementations of the application programming interface(API) specified by NIST in the Evaluation Plan [10]. The API includes functions for initialization, template generation, finalization, search, gallery insert, and gallery delete. Two template generation functions are required, one for the preparation of an enrollment template, and one for a search template.

In NIST's test harness, all functions were wrapped by calls to the C++ std::chrono::high\_resolution\_clock which on the dedicated timing machine counts 1ns clock ticks. Precision is somewhat worse than that however.

## 3.8 Uncertainty estimation

### 3.8.1 Random error

This study leverages operational datasets for measurement of recognition error rates. This affords several advantages. First, large numbers of searches are conducted (see Table 1) giving precision to the measurements. Moreover, for the two mugshot datasets, these do not involve reuse of individuals so binomial statistics can be expected to apply to recognition error counts. In that case, an observed count of a particular recognition outcome (i.e. a false negative or false positive) in  $M$  trials will sustain 95% confidence that the actual error rate is no larger than some value.

As an example, the minimum number of mugshot searches conducted in this report is  $M = 154\,549$ , and for an observed FNIR around 0.002, the measurement supports a conclusion that the actual FNIR is no higher than 0.00228 at 99% confidence level. On the false positive side, we tabulate FNIR at FPIR values as low as 0.001. Given estimates based on 331 254 non-mate trials, the actual FPIR values will be below 0.00115 at 99% confidence. In conclusion, large scale evaluation, without reuse of subjects, supports tight uncertainty bounds on the measured error rates.

### 3.8.2 Systematic error

The FRVT 2018 dataset includes anomalies discovered as a result of inspecting images involved in recognition failures from the most accurate algorithms. Two kinds of failure occur: False negatives (which, for the purpose here, include failures to make templates) and false positives.

**False negative errors:** We reviewed 600 false negative pairs for which either or both of the leading two algorithms did not put the correct mate in the top 50 candidates. Given 154 549 searches, this number represents 0.39% of the total, resulting in  $\text{FNIR} \sim 0.0039$ . Of the 600 pairs:

- ▷ **A: Poor quality:** About 20% of the pairs included images of very low quality, often greyscale, low resolution, blurred, low contrast, partially cropped, interlaced, or noisy scans of paper images. Additionally, in a few cases, the face is injured or occluded by bandages or heavy cosmetics.
- ▷ **B: Ground truth identity label bugs:** About 15% of the pairs are not actually mated. We only assigned this outcome when a pair is clearly not mated.
- ▷ **C: Profile views:** About 35% included an image of a profile (side) view of the face, or, more rarely, an image that was rotated 90 degrees in-plane (roll).
- ▷ **D: Tattoos:** About 30% included an image of a tattoo that contained a face image. These arise from mis-labelling in the parent dataset metadata.
- ▷ **E: Ageing:** There is considerable time-lapse between the two captures.

All these estimates are approximate. Of these, the tattoo and mislabelled images can never be matched. These constitute an accuracy floor in the sample implying that FNIR cannot be below 0.0018<sup>11</sup>. The profile-views, low-quality images, and images with considerable ageing can, in principle, be successfully matched - indeed some algorithms do so - so are not part of the accuracy floor.

<sup>11</sup>This value is the sum of two partial false negative rates:  $\text{FNIR}_B = 0.15 * 0.0039$  plus  $\text{FNIR}_D = 0.3 * 0.0039$

For the microsoft-4 algorithm the lowest miss rate from (recent entry in Table 24) is  $\text{FNIR}(640\,000, 50, 0) = 0.0018$ . This is close to the value estimated from the inspection of misses. It is below the 0.0039 figure because the algorithm does match some profile and poor quality images, that the yitu-2 algorithm does not.

For many tables (e.g. Table 24), the FNIR values obtained for the FRVT-2018 mugshots could be corrected by reducing them by 0.0018. The best values would then be indistinct from zero. The results in this report *were not* adjusted to account for this systematic error.

**False positive errors:** As shown in Figure 1 and discussed in Figure 14 many of the DET characteristics in this report exhibit a pronounced turn upward at low false positive rates. The shape can be caused by identity labelling errors in the ground truth of a dataset, specifically persons present in the database under two IDs such that some proportion of non-mate pairs are actually mated. To look for such possibilities, we merged the highest 1000 non-mate pairs produced by three different algorithms which resulted in 1839 unique pairs. This constitutes 0.56% of all non-mate searches. We assert that it is *very* difficult for human reviewers to assign the pairs into the following three categories: twins; doppelgangers; or ground-truth errors (instances of the same person under two IDs). Given this difficulty we made no attempt to correct any possible ground truth errors except by removing 57 pairs in the following categories:

- ▷ **A: Profile views:** Thirteen pairs included one or two profile-view images. As described in Figure 135, these can cause false positives.
- ▷ **B: Same-session photographs:** For twelve pairs, the images were identical or trivially altered (e.g. cropped) versions of the same photo. These were present under a different ID likely due to some clerical or procedural mistake.
- ▷ **C: Tattoos of faces:** There were fourteen instances of tattoo photographs that contained faces causing false matches.
- ▷ **D: T-shirt faces:** There were six instances of T-shirt photographs (of Bob Marley and Che Guevara) being detected instead of the face and causing false positives.
- ▷ **E: Background faces:** There were twelve instances of one subject appearing in the background of two otherwise correct portrait photos.

Note we did not remove any images where there was a chance that the pair was actually a different person.

In any case, the results in this report have not been adjusted for this systematic error.

## 4 Results

This section gives extensive results for algorithms submitted to FRVT 2018. Three page “report cards” for each algorithm are contained in a [separate supplement](#). Performance metrics were described in section 3. The main results are summarized in tabular form with more exhaustive data included as DET, CMC and related graphs in appendices as follows:

- ▷ The three tables 2-4 list algorithms alongside full developer names, acceptance date, size of the provided configuration data, template size and generation time, and search duration data.
  - The **template generation duration** is most important to applications that require fast response. For example, an eGate taking more than two seconds to produce a template might be unacceptable. Note that GPUs may be of utility in expediting this operation for some algorithms, though at additional expense. Two additional factors should be considered<sup>1213</sup>.
  - The **search duration** is the time taken for a search of a search template into a gallery of  $N$  enrollment templates. This performance variable, together with the volume of searches, is influential on the amount of hardware needed to sustain an operational deployment. This is measured here with the algorithm running on a single core of a contemporary CPU. Search is most simply implemented as  $N$  computations of a distance metric followed by a sort operation to find the closest enrollments. However, considerable optimization of this process is possible, up to and including fast-search algorithms that, by various means, avoid computation of all  $N$  distances.
  - The **template size** is the size of the extracted feature vector (or vectors) and any needed header information. Large template sizes may be influential on bus or network bandwidth, storage requirements, and on search duration. While the template itself is an opaque data blob, the feature dimensionality might be estimated by assuming a four-bytes-per-float encoding. There is a wide range of encodings. For the more accurate algorithm, sizes range from 256 bytes to about 2KB bytes, indicating essentially no consensus on face modeling and template design.
  - The **template size multiplier** column shows how, given  $k$  input images, the size of the template grows. Most implementations internally extract features from each image and concatenate them, and implement some score-level fusion logic during search. Other implementations, including many of the most accurate algorithms, produce templates whose size does not grow with  $k$ . This could be achieved via selection of the best quality image - but this is not optimal in handling ageing where the oldest image could be the best quality. Another mechanism would be feature-level fusion where information is fused from all  $k$  inputs. In any case, as a black-box test, the fusion scheme is proprietary and unknown.
  - The size of the **configuration data** is the total size of all files resident in a vendor-provided directory that contains arbitrary read-only files such as parameters, recognition models (e.g caffe). Generally a large value for this quantity may prohibit the use of the algorithm on a resource-constrained device.

<sup>12</sup>The FRVT 2018 API prohibited threading, so some gains from parallelism may be available on multiple-cores or multiple processors, if the feature extraction code could be distributed across them.

<sup>13</sup>Note also that factors of two or more may be realizable by exploiting modern vector processing instructions on CPUs. It is not clear in our measurements whether all developers exploited Intel’s AVX2 instructions, for example. Our machine was so equipped, but we insisted that the same compiled library should also run on older machines lacking that instruction. The more sophisticated implementations may have detected AVX2 presence and branched accordingly. The less sophisticated may be defaulted to the reduced instruction set. Readers should see the FRVT 2018 API document for the specific chip details.

▷ Tables 24-25 report core rank-based accuracy for mugshot images. The population size is limited to  $N = 1.6$  million identities because this is the largest gallery size on which all algorithms were executed. Notable observations from these tables are as follows:

- **Accuracy gains since 2018:** NIST Interagency Report 8238 documented massive gains over those reported in the FRVT 2014 report, NIST Interagency Report 8009. Further gains are documented in this report. Comparing the most accurate algorithm in November 2018, NEC-3, the value of  $\text{FNIR}(N, L, T)$  reduced from 0.0031 to 0.0024 for the Sensetime-004 algorithm with  $N = 12$  million recent images. The tables show broader gains: many developers have made advances since 2018 with between two and five-fold reduction in errors.
- **Wide range in accuracy:** The rank-1 miss rates vary from  $\text{FNIR}(N, 1, 0) = 0.0012$  for sensetime-004 up to about 0.5 for the very fast but inaccurate microfocus-x algorithms. Among the developers who are superior to NEC in 2013, the range is from 0.002 to 0.035 for camvi-3. This large accuracy range is consistent with the buyer-beware maxim, and indicates that face recognition software is far from being commoditized.

▷ Tables 29-30 report threshold-based error rates,  $\text{FNIR}(N, L, T)$ , for  $N = 1.6$  million for mugshot-mugshot accuracy on FRVT 2014, FRVT 2018, and also (in pink) mugshot-webcam accuracy using FRVT 2018 enrollments. Notable observations from these tables are as follows:

- **Order of magnitude accuracy gains since 2014:** As with rank-based results, the gains in accuracy are substantial, though somewhat reduced. At  $\text{FPIR} = 0.01$ , the best improvement over NEC in 2014 is a 27 fold reduction in FNIR using the NEC\_2 algorithm. At  $\text{FPIR} = 0.001$ , the largest gain is a six-fold reduction in FNIR via the NEC\_3 algorithm.
- **Broad gains across the industry:** About 19 companies realize accuracy better than the NEC benchmark from 2014. This is somewhat lower than the 28 developers who succeeded on the rank-1 metric. This may be due to the ubiquity of, and emphasis on, the rank-1 metric in many published algorithm development papers.
- **Webcam images:** Searches of webcam images give  $\text{FNIR}(N, T)$  values around 2 to 3 times higher than mugshot searches. Notably the leading developers with mugshots are approximately the same with poorer quality webcams. But some developers e.g. Camvi, Megvii, TongYi, and Neurotechnology do improve their relative rankings on webcams, perhaps indicating their algorithms were tailored to less constrained images.

▷ Tables 18, 21, 22 and show, respectively, high-threshold, rank 1, and rank 50 FNIR values for all algorithms performing searches into five different gallery sizes,  $N = 640\,000$ ,  $N = 1\,600\,000$ ,  $N = 3\,000\,000$ ,  $N = 6\,000\,000$  and  $12\,000\,000$ . The  $\text{FPIR} = 0.001$  table is included to inform high-volume duplicate detection applications. The Rank-1 table is included as a primary accuracy indicator. The Rank-50 table is included to inform agencies who routinely produce 50 candidates for human-review. The notable results are:

- **Slow growth in rank-based miss rates:**  $\text{FNIR}(N, R)$  generally grows as a power law,  $aN^b$ . From the straight lines of many graphs of Figure 20 this is clearly a reasonable model for most, but not all, algorithms. The coefficient  $a$  can be interpreted as FNIR in a gallery of size 1. The more important coefficient  $b$  indicates scalability, and often,  $b \ll 1$ , implies very benign growth in FNIR. The coefficients of the models appear in the Tables 21 and 22.
- **Slow growth in threshold-based miss rates:**  $\text{FNIR}(N, T)$  also generally grows as a power law,  $aN^b$  except at the high threshold values corresponding to low FPIR values. This is visible in the plots of Figure 36 which

show straight lines except for  $FPIR = 0.001$ , which increase more rapidly with  $N$  above 3 000 000. Each trace in those figures shows  $FNIR(N, T)$  at fixed  $FPIR$  with both  $N$  and  $T$  varying. Thus at large  $N$ , it is usually necessary to elevate  $T$  to maintain fixed  $FPIR$ . This causes increased  $FNIR$ . Why that would no-longer obey a power-law is not known. However, if we expect large galleries to contain individuals with familial relations to the non-mate search images - in the most extreme case, twins - then suppression of false positives becomes more difficult. This is discussed in the Figures starting at Fig. 10

▷ Figure ?? shows false positives from twins against their enrolled siblings, broken out by type of twin: fraternal or identical. The Figure is based on the enrollment of 104 single images on one of a pair of twins, and then the search of 2354 second images. Note that the dataset is heavily skewed towards identical twins which is not representative of the true population. There is also a skew towards same sex fraternal twin pairs compared to different sex fraternal twin pairs again not representative of the true population.

The notable results are:

- For all algorithms tested, the 1087 mated searches (Twin A vs. Twin A) produce scores almost always above typical operational thresholds, with (not shown) matches at rank 1. The images are of good quality, so this is the result expected from the rest of this report.
- For the 1066 identical twin searches (AB), almost all produce the twin at rank 1, with a few producing the mate at further down the candidate lists rank and low score.
- For the 169 fraternal searches (AB) from same sex pairs, most algorithms give a large number of very high scores, implying false positives at all thresholds. However, there are long tails containing lower scores that are correctly below threshold. In general, scores that are higher in this distribution are all rank 1 whereas the lower scores have much higher ranks.
- (Not shown) Of the 169, there are 24 fraternal searches (AB) involving different sex twins. Here most algorithms correctly report scores well below the lowest threshold, and usually not on the candidate list at all.

2022/06/13  
09:55:40  
FNIR(N, R, T) = False neg. identification rate  
FPIR(N, T) = False pos. identification rate  
N = Num. enrolled subjects  
R = Num. candidates examined  
T = Threshold  
T = 0 → Investigation  
T > 0 → Identification

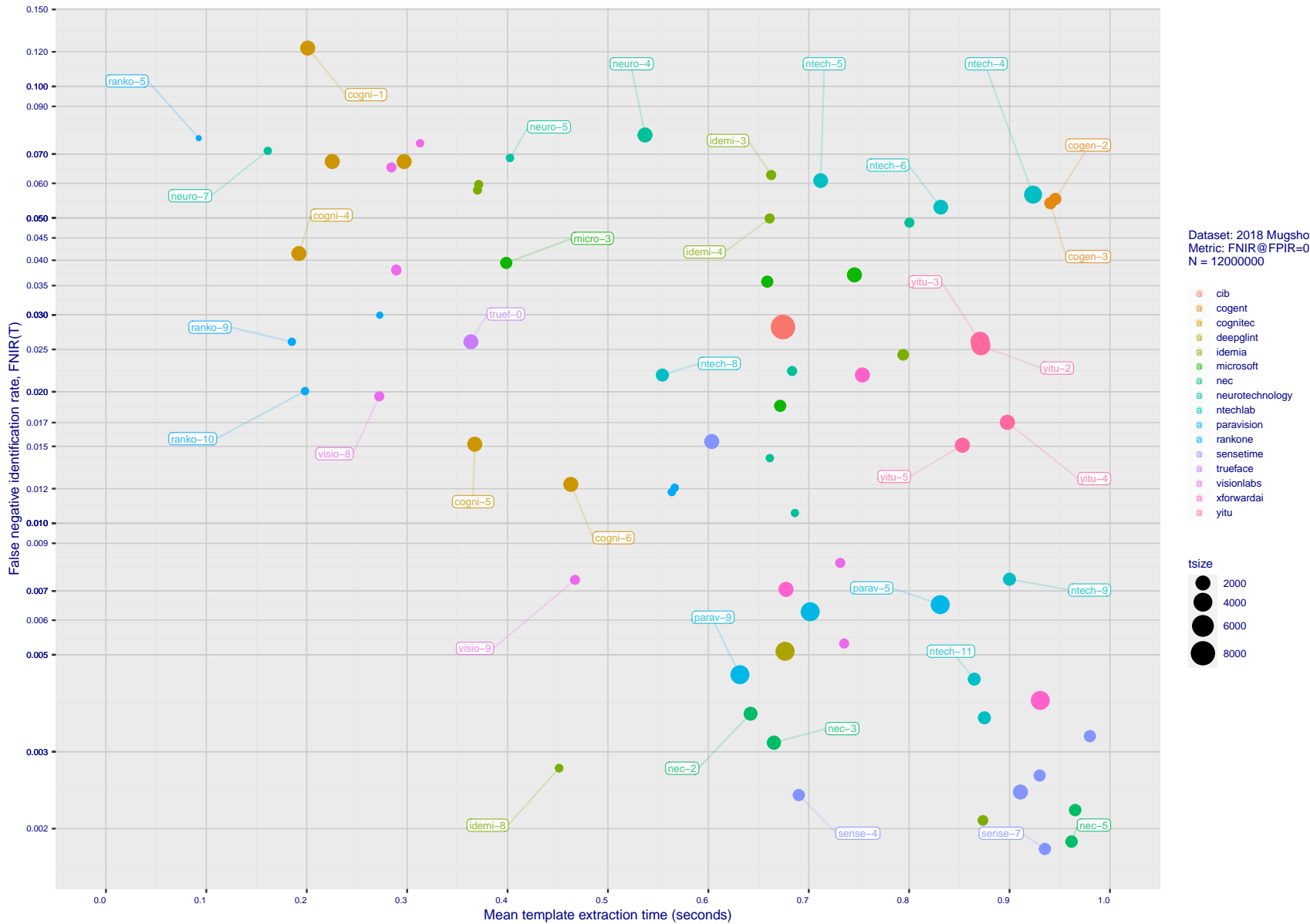


Figure 18: [Mugshot Dataset] Speed-accuracy tradeoff. For developers of the more accurate algorithms the plot shows the tradeoff of high-threshold recognition miss-rates, FNIR( $N, N, T$ ) for FPIR( $N, T$ ) = 0.003, and template generation time. Developers are coded by color. Template size is encoded by the size of the circle. Some labels are quite distant from the respective point, to avoid superposing text. Without any other influences, the assumption would be that taking time to localize the face, and extract features, would lead to better accuracy. The most notable result, for NEC, is that their slower algorithms are much more accurate than the version that extract features in fewer than 90 milliseconds.

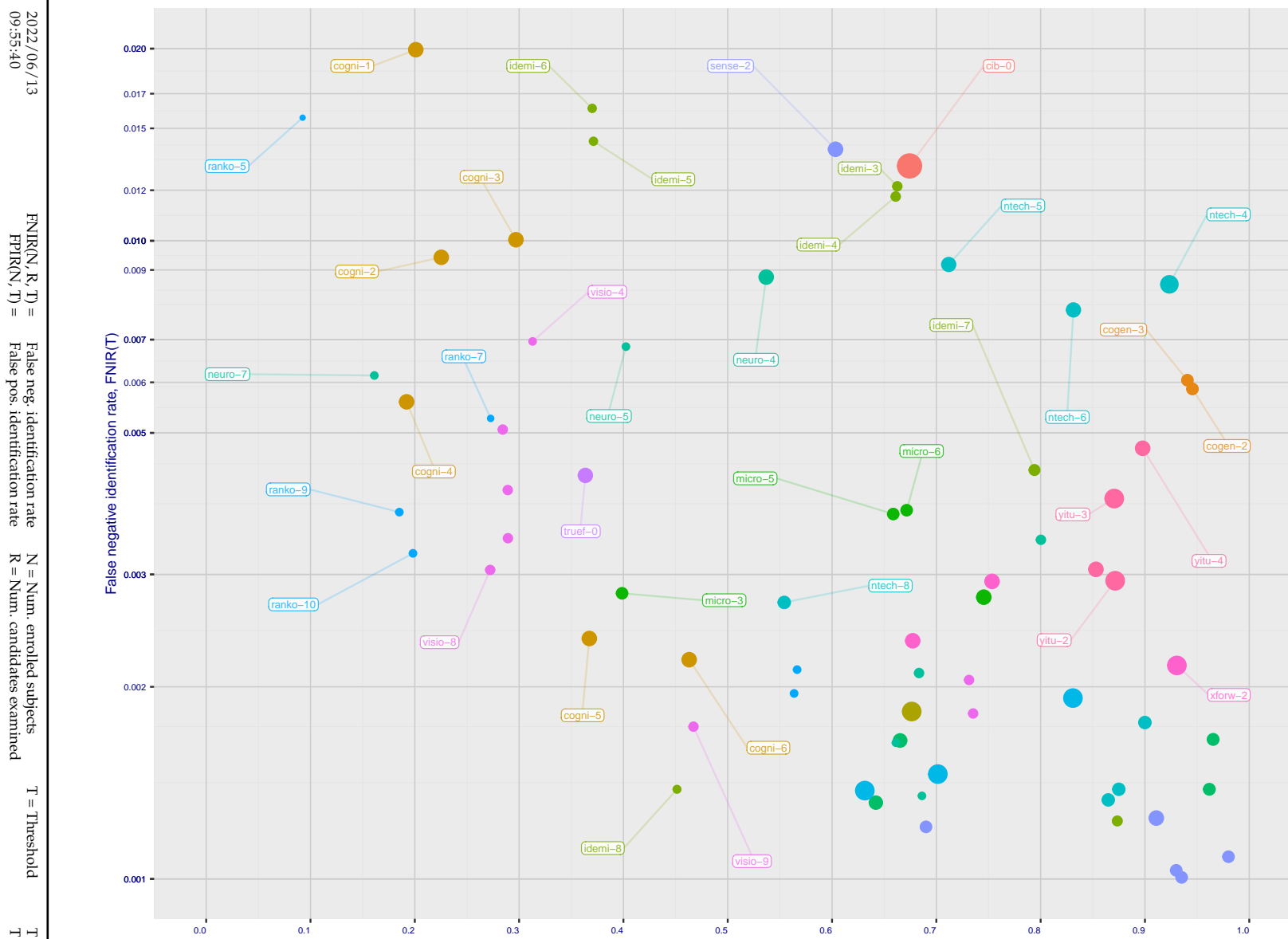


Figure 19: [Mugshot Dataset] Speed-accuracy tradeoff. For developers of the more accurate algorithms the plot shows the tradeoff of rank-one recognition miss-rates, FNIR( $N, 1, 0$ ), and template generation time. Developers are coded by color. Template size is encoded by the size of the circle. Some labels are quite distant from the respective point, to avoid superposing text. Without any other influences, the assumption would be that taking time to localize the face, and extract features, would lead to better accuracy. This occurs for NEC with their slower algorithm being much accurate than the version that extract features in fewer than 90 milliseconds.

	DEVELOPER	SHORT	SEQ.	VALIDATION	CONFIG <sup>1</sup>	LIB <sup>1</sup>	TEMPLATE GENERATION			FINALIZE <sup>2</sup>	SEARCH DURATION <sup>5</sup> MILLISEC						
							DATA (MB)	DATA (MB)	SIZE (B)		N=1.6M	N=1.6M	N=3M	N=6M	N=12M	( $\mu$ s)	
	FULL NAME	NAME	NUM.	DATE													
1	20Face	20face	000	2021-10-01	112	319	122	2048	-	20	236	67	9	(212)	6355	(214) 6341	
2	3Divi	3divi	5	2018-10-26	186	51	206	4096	k	113	638	178	28	(93)	538	(92) 537	
3	3Divi	3divi	6	2018-10-26	187	51	38	528	k	114	640	27	5	(13)	33	(13) 33	
4	Acer Incorporated	acer	000	2020-08-12	35	67	32	512	-	15	198	17	4	(59)	295	(59) 295	
5	Acer Incorporated	acer	001	2021-11-08	42	610	116	2048	-	11	184	64	9	(106)	619	(101) 575	
6	Akurat Satu Indonesia	ptakuratsatu	000	2020-10-23	0	572	41	538	-	212	905	226	28633	(7)	15	(6) 16	
7	Alchera Inc	alchera	2	2018-10-30	7	14	114	2048	k	6	114	20	63	(190)	2923	(193) 2929	
8	Alchera Inc	alchera	3	2018-10-30	251	14	92	2048	k	89	531	206	63	(191)	2955	(194) 2956	
9	Alchera Inc	alchera	004	2021-09-17	476	24	118	2048	-	187	853	187	35	(213)	6657	(220) 6851	
10	Alivia / Innovation Sys	isystems	3	2018-10-30	350	784	130	2048	1	177	825	146	16	(71)	385	(75) 389	
11	AllGoVision	allgogvision	000	2019-07-30	168	150	102	2048	k	53	404	95	12	(194)	3226	(197) 3193	
12	AllGoVision	allgogvision	001	2020-07-14	283	126	99	2048	-	164	777	101	13	(193)	3174	(196) 3183	
13	Anke Investments	anke	0	2018-10-30	779	27	190	2072	k	61	429	138	16	(109)	675	(115) 748	
14	Anke Investments	anke	1	2018-10-30	779	27	189	2072	k	62	430	131	15	(114)	707	(118) 769	
15	Anke Investments	anke	002	2019-06-27	341	401	176	2056	k	106	623	113	13	(109)	624	(109) 1306	
16	Aware	aware	5	2018-10-30	368	27	199	3100	k	169	792	187	34	(17)	95	(22) 98	
17	Aware	aware	6	2018-10-30	368	27	2	124	k	168	789	32	2	(33)	158	(35) 162	
18	Ayonix	ayonix	1	2018-10-29	74	2	63	1036	k	2	12	99	11	(55)	279	(56) 279	
19	Ayonix	ayonix	2	2018-10-30	74	2	64	1036	1	1	11	116	14	(54)	279	(55) 276	
20	Camvi Technologies	camvitech	4	2018-10-30	233	220	51	1024	1	131	686	181	31	(14)	33	(12) 32	
21	Camvi Technologies	camvitech	5	2018-10-30	257	220	49	1024	1	154	751	183	31	(12)	31	(10) 30	
22	Canon Inc	cib	000	2020-10-19	426	127	227	8196	-	125	674	212	113	(195)	3589	(199) 3604	
23	Canon Inc	canon	001	2021-10-27	1139	91	202	4096	-	202	885	161	21	(215)	6804	(218) 6789	
24	Canon Inc	canon	002	2022-04-26	1231	111	221	6200	-	208	897	203	58	(217)	7673	(221) 7559	
25	Clearview AI Inc	clearviewai	000	2021-11-12	358	316	205	4096	-	159	765	180	30	(120)	802	(106) 657	
26	Cloudwalk - Hengrui AI Technology	hr	000	2021-02-10	501	392	133	2048	-	213	905	124	15	(56)	282	(53) 276	
27	Cloudwalk - Moontime Smart Technology	cloudwalk	000	2022-01-31	716	573	119	2048	-	194	869	82	10	(82)	440	(71) 371	
28	Cognitec Systems GmbH	cognitec	2	2018-10-30	463	26	167	2052	k	19	225	170	27	(167)	1733	(169) 1763	
29	Cognitec Systems GmbH	cognitec	3	2018-10-30	465	26	160	2052	k	31	297	136	16	(166)	1719	(170) 1791	
30	Cognitec Systems GmbH	cognitec	004	2021-03-08	384	60	172	2052	-	14	192	108	13	(165)	1673	(167) 1727	
31	Cognitec Systems GmbH	cognitec	005	2021-07-30	460	61	163	2052	-	40	367	69	9	(157)	1556	(159) 1551	
32	Cognitec Systems GmbH	cognitec	006	2022-02-10	689	61	168	2052	-	72	463	79	10	(134)	1006	(133) 1002	
33	Cubox	cubox	000	2021-08-24	529	298	107	2048	-	216	917	79	10	(196)	3646	(201) 4076	
34	Cyberlink Corp	cyberlink	000	2019-06-12	217	93	170	2052	1	118	654	179	30	(111)	696	(111) 701	
35	Cyberlink Corp	cyberlink	001	2019-10-07	459	102	173	2052	1	59	423	176	28	(112)	698	(110) 700	
36	Cyberlink Corp	cyberlink	002	2020-07-31	333	109	219	4140	-	147	724	217	685	(154)	1353	(198) 3198	
37	Cyberlink Corp	cyberlink	003	2021-01-05	333	100	224	6212	-	135	691	191	35	(85)	488	(112) 723	
38	Cyberlink Corp	cyberlink	004	2021-07-16	371	100	223	6212	-	149	728	163	23	(87)	492	(90) 504	
39	Cyberlink Corp	cyberlink	005	2022-01-07	371	100	222	6212	-	151	733	182	30	(89)	501	(86) 498	
40	DAON	daon	000	2021-12-23	274	2	186	2069	-	96	583	49	8	(92)	524	(105) 625	
41	Dahua Technology Co Ltd	dahua	0	2018-10-29	276	167	110	2048	k	45	374	163	22	-	51	258	
42	Dahua Technology Co Ltd	dahua	1	2018-10-29	276	167	109	2048	k	41	369	173	28	-	50	257	
43	Dahua Technology Co Ltd	dahua	002	2019-12-02	607	137	123	2048	k	130	685	157	19	(45)	243	(52) 269	
44	Dahua Technology Co Ltd	dahua	003	2020-11-18	889	154	108	2048	-	146	723	148	18	(57)	283	(49) 249	
45	Dahua Technology Co Ltd	dahua	004	2021-11-18	812	116	132	2048	-	157	758	84	11	(70)	423	(74) 411	
46	Decatur Industries Inc	decatur	000	2022-02-09	411	383	174	2052	-	190	863	71	9	(168)	1761	(177) 2023	
47	Deepglint	deepglint	001	2019-11-15	448	265	212	4096	-	127	676	188	35	(110)	677	(157) 1495	
48	Dermalog	dermalog	5	2018-10-26	0	440	4	128	1	88	528	216	3155	(1)	0	(1)	0
49	Dermalog	dermalog	6	2018-10-26	0	453	12	256	1	84	507	4	2	(30)	442	(30) 444	
50	Dermalog	dermalog	007	2020-02-12	0	424	128	1	-	56	410	1	1	(23)	98	(20) 96	
51	Dermalog	dermalog	008	2021-01-25	0	531	29	512	-	42	370	19	4	(65)	335	(45) 246	
52	Dermalog	dermalog	009	2021-11-09	0	318	34	512	-	36	347	14	3	(49)	253	(46) 246	

Notes
1 Configuration size does not capture static data present in libraries. Libraries are included but the size also includes any ancillary libraries for image processing (e.g. openCV) or numerical computation (e.g. blas).
2 Finalization is the processing of converting N = 1600000 templates into a searchable data structure an operation which can be a simple copy, or the building of an index or tree, for example. The duration of the operation may be data dependent, and may not be linear in the number of input templates.
3 This multiplier expresses the increase in template size when $k$ images are passed to the template generation function.
4 All durations are measured on Intel®Xeon®@CPU E5-2630 v4 @ 2.20GHz processors. Estimates are made by wrapping the API function call in calls to std::chrono::high_resolution_clock which on the machine in (3) counts 1ns clock ticks. Precision is somewhat worse than that however.
5 Search durations are measured as in the prior note. The power-law model in the final column mostly fits the empirical results in Figure 136. However in certain cases the model is not correct and should not be used numerically.

Table 2: Summary of algorithms and properties included in this report. The blue superscripts give ranking for the quantity in that column. Missing search durations, denoted by “-”, are absent because those runs were not executed, usually because we did not run on the larger galleries. Caution: The power-law model is sometimes an incorrect model. It is included here only to show broad sublinear behavior, which is flagged in green. The models should not be used for prediction.

DEVELOPER FULL NAME	SHORT NAME	SEQ. NUM.	VALIDATION DATE	CONFIG <sup>1</sup> DATA (MB)	LIB <sup>1</sup> DATA (MB)	TEMPLATE GENERATION SIZE (B) MULT <sup>3</sup> TIME (MS) <sup>4</sup>	FINALIZE <sup>2</sup> TIME (S)	SEARCH DURATION <sup>5</sup> MILLISEC					
								N=1.6M	N=1.6M	N=1.6M	N=3M	N=6M	N=12M
53 Digidata	digidata	000	2022-06-03	248	33	139 2048 - 92 560	215 2444 (2) 0 (17) 95	-	-	-	-	-	-
54 DiluSense Technology	dilusense	000	2022-05-26	311	56	131 2048 - 23 247	169 26 (172) 1904 (172) 1898 (146) 3597 (143) 7256 (145) 14689	75 0.88N <sup>1.0</sup>					
55 FarBar Inc	f8	001	2019-10-03	266	19	134 2048 k 173 810	113 14 -	-	-	-	-	-	-
56 Fincore Ltd	fincore	000	2021-08-18	250	224	115 2048 - 76 475	99 9 (100) 562 (97) 560	-	-	-	-	-	-
57 Fujitsu Research and Development Center	fujitsulab	000	2021-10-12	497	337	56 1032 - 224 945	29 5 (164) 1668 (163) 1657 (140) 3140 (137) 6320 (136) 12723	740.78N <sup>1.0</sup>					
58 Fujitsu Research and Development Center	fujitsulab	001	2022-03-15	675	386	55 1032 - 201 882	60 9 (170) 1854 (171) 1817 (143) 3451 (141) 6986 (142) 14166	920.72N <sup>1.0</sup>					
59 Gorilla Technology	gorilla	2	2018-10-29	91	1252	71 1132 k 338	167 24 (31) 145 (31) 146 (26) 293 (25) 612 (27) 1509	141 0.02N <sup>1.1</sup>					
60 Gorilla Technology	gorilla	3	2018-10-26	94	1252	192 2156 k 91 559	221 12020 - (178) 2047	-	-	-	-	-	-
61 Gorilla Technology	gorilla	004	2020-01-06	182	1244	193 2192 k 48 388	193 41 (58) 286 (58) 285 (79) 1191 (80) 2416 (75) 5036	180 0.00N <sup>1.3</sup>					
62 Gorilla Technology	gorilla	005	2021-02-22	306	1420	225 6288 - 79 483	208 78 (119) 802 (119) 799 (96) 1514 (110) 4454 (104) 8820	165 0.05N <sup>1.2</sup>					
63 Gorilla Technology	gorilla	006	2021-09-30	377	691	228 8336 - 160 767	211 99 (160) 1626 (160) 1612 (120) 2422 (109) 4422 (109) 9363	73 0.59N <sup>1.0</sup>					
64 Gorilla Technology	gorilla	007	2022-02-16	392	322	226 6290 - 87 526	210 89 (117) 765 (114) 745 (90) 1408 (89) 2823 (83) 5764	580.42N <sup>1.0</sup>					
65 Griaule	griaule	000	2021-11-01	0	584	171 2052 - 58 417	43 8 (208) 5827 (212) 6150 (176) 11473 (174) 22952 (171) 46070	323.89N <sup>1.0</sup>					
66 Guangzhou Pixel Solutions Co Ltd	pixelall	002	2019-07-01	0	165	196 2560 k 13 190	128 15 (151) 1296 (153) 1334 (127) 2526 (122) 5136 (126) 11045	97 0.52N <sup>1.0</sup>					
67 Guangzhou Pixel Solutions Co Ltd	pixelall	003	2019-11-05	0	690	195 2560 k 140 703	164 22 (148) 1273 (149) 1307 (124) 2474 (123) 5198 (127) 11141	108 0.46N <sup>1.0</sup>					
68 Guangzhou Pixel Solutions Co Ltd	pixelall	004	2020-07-02	0	538	197 2560 k 64 449	147 17 (147) 1259 (148) 1300 (123) 2465 (128) 5492 (128) 11443	122 0.34N <sup>1.1</sup>					
69 Guangzhou Pixel Solutions Co Ltd	pixelall	005	2021-03-23	0	717	194 2560 - 183 840	88 11 (159) 1606 (158) 1528 (129) 2609 (119) 4926 (131) 11770	66 0.73N <sup>1.0</sup>					
70 Hangzhuo Allu Network Information Technology	hzailu	000	2022-03-18	855	97	53 1024 - 116 649	89 11 (187) 2609 (191) 2551 (162) 4813 (160) 9702 (159) 19338	51.150N <sup>1.0</sup>					
71 Hikvision Research Institute	hikvision	5	2018-10-29	593	9	76 1408 1 101 607	134 16 (127) 883 (128) 895 (106) 1908 (100) 3792 (110) 9387	152 0.10N <sup>1.1</sup>					
72 Hikvision Research Institute	hikvision	6	2018-10-29	593	9	77 1408 1 99 598	136 16 (125) 871 (127) 877	-	-	-	-	-	-
73 HyperVerge Inc	hyperverge	001	2021-08-11	1791	212	54 1024 - 186 845	25 5 (113) 705 (108) 681 (85) 1346 (86) 2681 (81) 5680	83 0.32N <sup>1.0</sup>					
74 HyperVerge Inc	hyperverge	002	2022-04-13	1140	1118	48 1024 - 219 934	63 9 (108) 661 (107) 659 (83) 1292 (73) 2188 (38) 2181	16 11.29N <sup>0.8</sup>					
75 Idemia	idemia	5	2018-10-29	417	48	24 352 1 44 371	26 5 (27) 137 (28) 138 (32) 437 (30) 724 (29) 1630	174 0.01N <sup>1.2</sup>					
76 Idemia	idemia	6	2018-10-29	417	48	23 352 1 43 370	23 4 (28) 137 (27) 138 (33) 442 (33) 827 (30) 1646	176 0.01N <sup>1.2</sup>					
77 Idemia	idemia	007	2020-01-17	738	113	47 860 1 170 794	114 14 (32) 151 (32) 152 (54) 683 (57) 1481 (55) 3022	185 0.00N <sup>1.4</sup>					
78 Idemia	idemia	008	2021-03-15	378	65	25 300 - 66 451	15 3 (26) 132 (26) 131 (24) 247 (22) 501 (21) 1013	61 0.07N <sup>1.0</sup>					
79 Idemia	idemia	009	2022-03-01	735	68	45 636 - 196 873	37 7 (41) 211 (40) 205 (31) 389 (32) 787 (28) 1615	78 0.10N <sup>1.0</sup>					
80 Imagus Technology Pty Ltd	imagus	005	2021-01-15	222	311	145 2048 - 167 786	112 14 (44) 236 (62) 313 (52) 651 (52) 1361 (43) 2461	150 0.03N <sup>1.1</sup>					
81 Imagus Technology Pty Ltd	imagus	006	2021-05-27	248	369	148 2048 - 211 904	72 9 (63) 317 (43) 234 (38) 499 (50) 1273 (46) 2727	171 0.01N <sup>1.2</sup>					
82 Imagus Technology Pty Ltd	imagus	007	2021-11-16	248	366	101 2048 - 102 609	55 9 (49) 234 (44) 238 (34) 442 (34) 881 (32) 1765	27 0.16N <sup>1.0</sup>					
83 Imagus Technology Pty Ltd	imagus	008	2022-05-26	204	335	135 2048 - 63 445	145 17 (98) 560 (100) 565 - - -						
84 Imperial College London	imperial	000	2019-08-28	461	15	120 2048 1 95 577	100 13 (65) 360 (74) 379 (99) 1626 (104) 4057 (124) 10291	188 0.00N <sup>1.5</sup>					
85 Incode Technologies Inc	incode	2	2018-10-29	71	31	103 2048 1 20 289	131 15 (77) 411 (76) 404 - - -						
86 Incode Technologies Inc	incode	3	2018-10-29	133	31	134 2048 1 138 697	123 15 (70) 408 (80) 412 (60) 847 (59) 1608 (69) 4486	145 0.05N <sup>1.1</sup>					
87 Incode Technologies Inc	incode	004	2019-06-24	254	50	136 2048 1 75 475	93 12 (69) 365 (73) 378 (79) 1482 (61) 1660 (53) 2954	120 0.12N <sup>1.1</sup>					
88 Incode Technologies Inc	incode	005	2021-07-29	259	21	95 2048 - 81 500	77 10 (62) 316 (84) 454 (65) 890 (67) 1843 (62) 3640	134 0.07N <sup>1.1</sup>					
89 Innovatrics	innovatrics	4	2018-10-30	0	400	68 1076 k 49 399	218 10902 (68) 8 (4) 8 (4) 11 (2) 9 (3) 13 9668.38N <sup>0.2</sup>						
90 Innovatrics	innovatrics	005	2019-09-30	0	455	39 538 1 179 827	220 11897 (5) 8 (5) 9 (3) 9 (2) 9 1405.65N <sup>0.1</sup>						
91 Innovatrics	innovatrics	007	2021-08-16	175	58	46 538 - 162 777	115 14 (22) 97 (23) 100 (18) 188 (19) 378 (18) 788	24 0.09N <sup>1.0</sup>					
92 Intellivision	intellivision	001	2022-03-08	62	130	183 2056 - 55 406	158 20 (72) 388 (72) 377 - - -						
93 IrexAI	irex	000	2021-02-09	724	46	198 3080 - 185 844	154 19 (108) 616 (102) 600 (74) 1120 (82) 2477 (84) 5863	126 0.13N <sup>1.1</sup>					
94 Kakao Enterprise	kakao	000	2021-06-23	404	124	164 2052 - 182 835	45 8 (42) 213 (41) 215 (39) 510 (36) 971 (36) 1955	130 0.05N <sup>1.1</sup>					
95 Kedacom International Pte	kedacom	001	2019-09-16	239	36	20 292 1 83 507	5 2 (116) 764 (116) 760 (107) 1940 (93) 2983 (93) 6623	102 0.31N <sup>1.0</sup>					
96 Kneron	kneron	000	2020-03-03	366	13	121 2048 k 86 523	105 13 (186) 2535 (189) 2506 (161) 4752 (159) 6966 (161) 2026	103 0.95N <sup>1.0</sup>					
97 Kneron	kneron	001	2021-06-10	270	69	111 2048 - 74 472	61 9 (188) 2690 (192) 2642 - - -						
98 Line Corporation	line	000	2021-06-02	138	397	141 2048 - 77 481	80 8 (203) 5433 (207) 5418 (174) 10144 - - -	30 3.65N <sup>1.0</sup>					
99 Line Corporation	line	001	2021-11-21	471	396	144 2048 - 214 907	51 8 (171) 1872 (175) 1934 (148) 3647 (149) 7675	110 0.64N <sup>1.0</sup>					
100 Lomonosov Moscow State University	intsymsu	000	2019-08-19	375	168	149 2048 1 104 614	106 13 (80) 430 (82) 431 (63) 860 (62) 1730 (78) 5353	160 0.03N <sup>1.1</sup>					
101 Lookman Electroplost Industries	lookman	3	2018-10-28	203	24	21 292 1 34 336	13 3 (115) 739 (113) 745 (89) 1394 (88) 2817 (99) 8286	138 0.13N <sup>1.1</sup>					
102 Lookman Electroplost Industries	lookman	4	2018-10-28	184	24	45 548 1 32 320	22 4 (131) 981 (132) 998 - - -						
103 Lookman Electroplost Industries	lookman	005	2019-09-16	239	36	42 548 1 83 506	18 4 (133) 1005 (134) 1008 (128) 2597 (127) 5446 (105) 8939	136 0.19N <sup>1.1</sup>					
104 Mantra Softech India	mantra	000	2021-10-28	460	61	166 2052 - 57 412	76 10 (129) 916 (129) 910 (101) 1714 (99) 3411 (95) 6841	36 0.57N <sup>1.0</sup>					

## Notes

- Configuration size does not capture static data present in libraries. Libraries are included but the size also includes any ancillary libraries for image processing (e.g. openCV) or numerical computation (e.g. blas).
- Finalization is the processing of converting  $N = 1600000$  templates into a searchable data structure an operation which can be a simple copy, or the building of an index or tree, for example. The duration of the operation may be data dependent, and may not be linear in the number of input templates.
- This multiplier expresses the increase in template size when  $k$  images are passed to the template generation function.
- All durations are measured on Intel®Xeon®@CPU E5-2630 v4 @ 2.20GHz processors. Estimates are made by wrapping the API function call in calls to std::chrono::high\_resolution\_clock which on the machine in (3) counts 1ns clock ticks. Precision is somewhat worse than that however.
- Search durations are measured as in the prior note. The power-law model in the final column mostly fits the empirical results in Figure 136. However in certain cases the model is not correct and should not be used numerically.

Table 3: Summary of algorithms and properties included in this report. The blue superscripts give ranking for the quantity in that column. Missing search durations, denoted by “-”, are absent because those runs were not executed, usually because we did not run on the larger galleries. Caution: The power-law model is sometimes an incorrect model. It is included here only to show broad sublinear behavior, which is flagged in green. The models should not be used for prediction.

DEVELOPER	SHORT	SEQ.	VALIDATION	CONFIG <sup>1</sup>	LIB <sup>1</sup>	TEMPLATE GENERATION	FINALIZE <sup>2</sup>	SEARCH DURATION <sup>5</sup> MILLISEC						POWER LAW	
								L=1	L=50	L=50	L=50	L=50	L=50		
								N=1.6M	N=1.6M	N=1.6M	N=3M	N=6M	N=12M	( $\mu$ s)	
105	Megvii/Face++	megvii	1	2018-10-28	1703	41	207 4096	1	108 631	180 32	105 552	98 561	82 1222	(78) 2321	(85) 5968 144 0.08N <sup>1.1</sup>
106	Megvii/Face++	megvii	2	2018-10-28	1735	42	213 4096	1	111 635	181 31	106 553	97 558	-	-	-
107	MicroFocus	microfocus	5	2018-10-29	94	26	256 k	k	24 262	8 2	188 186	(37) 186	(29) 354	(29) 708	(25) 1425 53 0.11N <sup>1.0</sup>
108	MicroFocus	microfocus	6	2018-10-29	94	26	256 k	k	25 262	10 2	(39) 183	(36) 186	-	-	-
109	Microsoft	microsoft	5	2018-10-29	381	155	50 1024	1	119 658	91 11	(158) 1606	(164) 1673	(139) 3076	(136) 6302	(139) 13160 72 0.79N <sup>1.0</sup>
110	Microsoft	microsoft	6	2018-10-29	478	155	52 1024	1	123 671	127 15	(161) 1642	(162) 1618	(150) 3710	(138) 6401	(137) 12892 91 0.68N <sup>1.0</sup>
111	N-Tech Lab	ntech	5	2018-10-30	1685	113	89 1940	k	144 711	202 55	(47) 243	48 246	(48) 538	(41) 1100	(49) 2867 156 0.02N <sup>1.1</sup>
112	N-Tech Lab	ntech	6	2018-10-30	1686	117	88 1940	k	181 831	209 63	(46) 243	(47) 246	(43) 546	(42) 1104	(50) 2873 158 0.02N <sup>1.1</sup>
113	N-Tech Lab	ntechlab	007	2019-06-25	2450	51	200 3348	k	171 795	207 73	(73) 393	(81) 427	(58) 780	(65) 1768	(61) 3499 100 0.16N <sup>1.0</sup>
114	N-Tech Lab	ntechlab	008	2020-01-06	1111	51	74 1300	k	90 554	197 36	(37) 179	(34) 184	(28) 341	(28) 683	(24) 1395 48 0.11N <sup>1.0</sup>
115	N-Tech Lab	ntechlab	009	2021-03-01	1208	42	75 1300	-	209 899	190 35	(36) 178	(35) 184	(27) 336	(27) 676	(31) 1704 121 0.05N <sup>1.1</sup>
116	N-Tech Lab	ntechlab	010	2021-06-24	351	213	73 1280	-	197 874	30 6	(81) 440	(83) 435	(59) 821	(60) 1645	(58) 3337 67 0.22N <sup>1.0</sup>
117	N-Tech Lab	ntechlab	011	2021-12-07	679	208	72 1280	-	191 864	32 6	(86) 488	(85) 483	(66) 912	(68) 1869	(73) 5003 140 0.07N <sup>1.1</sup>
118	NEC	nec	2	2018-10-30	705	35	84 1616	k	115 642	151 18	(74) 405	(78) 409	(72) 1072	(63) 1755	(68) 4255 147 0.06N <sup>1.1</sup>
119	NEC	nec	3	2018-10-30	774	110	85 1712	k	121 665	159 21	(4) 7	(3) 7	(5) 14	(9) 40	(10) 82 166 0.00N <sup>1.2</sup>
120	NEC	nec	004	2021-07-19	971	63	69 1104	-	228 965	33 7	(66) 349	(67) 351	(53) 662	(51) 1330	(45) 2685 56 0.20N <sup>1.0</sup>
121	NEC	nec	005	2021-12-13	922	88	70 1104	-	227 961	34 7	(84) 473	(95) 551	(70) 1017	(71) 2091	(66) 4242 64 0.28N <sup>1.0</sup>
122	Neurotechnology	neurotech	5	2018-10-30	266	53	13 256	k	51 402	9 2	(123) 835	(124) 839	(100) 1690	(98) 3219	(106) 8955 127 0.19N <sup>1.1</sup>
123	Neurotechnology	neurotech	6	2018-10-30	564	53	13 256	k	148 726	7 2	(124) 839	(125) 842	-	-	-
124	Neurotechnology	neurotech	007	2019-10-03	57	51	11 256	k	7 161	6 2	(139) 1118	(139) 1110	(113) 2143	(108) 4397	(107) 9045 71 0.55N <sup>1.0</sup>
125	Neurotechnology	neurotechnology	008	2021-03-22	355	49	3 514	-	172 800	21 4	(142) 1167	(142) 1149	(115) 2266	(113) 4573	(114) 9586 79 0.55N <sup>1.0</sup>
126	Neurotechnology	neurotechnology	009	2021-09-01	246	82	35 513	-	129 683	11 3	(136) 1035	(136) 1049	(109) 1977	(106) 4270	(102) 8756 114 0.32N <sup>1.1</sup>
127	Neurotechnology	neurotechnology	010	2022-01-07	247	83	14 256	-	120 661	2 2	(132) 988	(130) 984	(104) 1897	(103) 3977	(98) 8048 105 0.36N <sup>1.0</sup>
128	Neurotechnology	neurotechnology	012	2022-06-07	247	84	10 256	-	132 686	12 3	(137) 1036	(138) 1063	(110) 2046	(105) 4179	(101) 8624 101 0.41N <sup>1.1</sup>
129	Newland Computer Co Ltd	newland	2	2018-10-30	96	27	113 2048	-	189 855	129 15	(219) 8741	(224) 8854	(189) 17892	(186) 39356	- 142 1.32N <sup>1.1</sup>
130	Nobilis	noblis	1	2018-10-30	114	176	112 2048	1	17 206	125 15	(149) 1273	(146) 1272	-	-	-
131	Nobilis	noblis	2	2018-10-30	153	176	220 6144	1	85 517	193 43	(185) 2513	(190) 2522	(163) 5649	(164) 12432	(170) 44262 178 0.04N <sup>1.3</sup>
132	NotionTag Technologies Private Limited	notiontag	000	2022-01-14	265	945	191 2120	-	67 453	80 10	(218) 8619	(222) 8705	(188) 16652	(187) 38794	(182) 90607 146 1.15N <sup>1.1</sup>
133	Pangiam	pangiam	000	2022-02-22	453	23	156 2048	-	112 636	146 17	(51) 276	(63) 319	(48) 601	(47) 1210	(42) 2443 54 0.18N <sup>1.0</sup>
134	Paravision (EverAI)	everai	2	2018-10-30	224	304	129 2048	1	39 366	181 30	(53) 278	(57) 283	-	-	-
135	Paravision (EverAI)	everai	3	2018-10-30	438	304	128 2048	1	145 717	174 28	(52) 278	(56) 281	(45) 572	(43) 1146	(39) 2278 93 0.12N <sup>1.0</sup>
136	Paravision (EverAI)	everai-paravision	004	2019-06-19	527	128	210 4096	1	124 672	194 45	(97) 559	(96) 559	(130) 2611	(139) 6445	(143) 14519 186 0.00N <sup>1.5</sup>
137	Paravision (EverAI)	paravision	005	2019-12-11	543	154	211 4096	1	180 830	200 48	(99) 561	(99) 564	(71) 1056	(75) 2298	(72) 4966 118 0.16N <sup>1.1</sup>
138	Paravision (EverAI)	paravision	007	2021-02-01	529	235	204 4096	-	139 701	204 48	(101) 569	(94) 558	(73) 1086	(72) 2111	(67) 4254 21 1.11N <sup>0.9</sup>
139	Paravision	paravision	009	2021-12-14	672	300	214 4100	-	109 631	209 82	(197) 3690	(202) 4230	(171) 8037	(170) 16532	(166) 31422 95 1.62N <sup>1.0</sup>
140	Qnap Security	qnap	000	2021-07-28	182	15	100 2048	-	68 457	65 9	(144) 1231	(168) 1763	-	-	-
141	Qnap Security	qnap	001	2021-12-09	191	13	105 2048	-	103 613	46 8	(163) 1666	(156) 1429	(144) 3472	(146) 7375	(149) 15159 163 0.11N <sup>1.2</sup>
142	Qnap Security	qnap	002	2022-04-15	338	32	98 2048	-	176 822	143 17	(130) 958	(143) 1179	(117) 2312	(116) 4789	(121) 971 129 0.24N <sup>1.1</sup>
143	Quantasoft	quantasoft	1	2018-10-30	276	452	152 2048	k	47 385	31 6	(220) 15422	(225) 14858	(186) 14717	-	(153) 18323
144	Rank One Computing	rankone	4	2018-10-09	0	101	1 85	k	3 36	35 7	(24) 101	(24) 101	(19) 190	-	- 28 0.07N <sup>1.0</sup>
145	Rank One Computing	rankone	5	2018-10-24	0	101	5 133	k	9 92	36 7	(29) 140	(29) 144	(24) 266	(23) 525	(22) 1049 25 0.11N <sup>1.0</sup>
146	Rank One Computing	rankone	006	2019-06-03	0	133	7 165	k	22 245	44 8	-	-	-	-	-
147	Rank One Computing	rankone	007	2019-11-12	0	137	6 165	k	26 272	39 7	(25) 116	(25) 115	(21) 215	(21) 439	(19) 877 52 0.07N <sup>1.0</sup>
148	Rank One Computing	rankone	009	2020-06-26	0	105	16 260	k	12 185	87 11	(18) 95	(21) 96	(16) 181	(16) 362	(17) 727 38 0.06N <sup>1.0</sup>
149	Rank One Computing	rankone	010	2020-11-05	0	135	17 261	-	16 198	81 10	(19) 95	(16) 95	(14) 178	(14) 357	(15) 714 34 0.06N <sup>1.0</sup>
150	Rank One Computing	rankone	011	2021-08-27	0	175	18 261	-	94 566	52 8	(21) 96	(18) 95	(17) 183	(17) 370	(14) 714 46 0.06N <sup>1.0</sup>
151	Rank One Computing	rankone	012	2021-12-27	0	257	19 261	-	93 563	41 8	(20) 95	(19) 95	(15) 179	(15) 361	(16) 718 37 0.06N <sup>1.0</sup>
152	Realnetworks Inc	realnetworks	2	2018-10-30	105	104	215 4104	k	21 241	173 28	(173) 2008	(179) 2048	(153) 4194	(152) 8642	(148) 15035 65 1.08N <sup>1.0</sup>
153	Realnetworks Inc	realnetworks	003	2019-06-12	93	102	87 1848	k	10 173	99 13	(141) 1145	(140) 1132	(112) 2142	(124) 5241	(125) 10495 133 0.21N <sup>1.1</sup>
154	Realnetworks Inc	realnetworks	004	2019-10-17	94	102	86 1848	1	9 171	88 11	(140) 1143	(141) 1137	(114) 2149	(115) 4740	(117) 9693 113 0.36N <sup>1.0</sup>
155	Realnetworks Inc	realnetworks	005	2021-06-23	168	209	180 2056	-	33 332	58 9	(162) 1654	(161) 1616	(138) 3030	(134) 6068	(134) 12134 43 1.01N <sup>1.0</sup>
156	Realnetworks Inc	realnetworks	006	2021-12-02	250	56	179 2056	-	37 348	47 8	(94) 543	(91) 531	(69) 996	(70) 1998	(65) 3991 41 0.33N <sup>1.0</sup>

Notes
1 Configuration size does not capture static data present in libraries. Libraries are included but the size also includes any ancillary libraries for image processing (e.g. openCV) or numerical computation (e.g. blas).
2 Finalization is the processing of converting $N = 1600000$ templates into a searchable data structure an operation which can be a simple copy, or the building of an index or tree, for example. The duration of the operation may be data dependent, and may not be linear in the number of input templates.
3 This multiplier expresses the increase in template size when $k$ images are passed to the template generation function.
4 All durations are measured on Intel®Xeon®CPU E5-2630 v4 @ 2.20GHz processors. Estimates are made by wrapping the API function call in calls to std::chrono::high_resolution_clock which on the machine in (3) counts 1ns clock ticks. Precision is somewhat worse than that however.
5 Search durations are measured as in the prior note. The power-law model in the final column mostly fits the empirical results in Figure 136. However in certain cases the model is not correct and should not be used numerically.

	DEVELOPER	SHORT NAME	SEQ. NUM.	VALIDATION DATE	CONFIG <sup>1</sup>	LIB <sup>1</sup> DATA (MB)	TEMPLATE GENERATION TIME (MS) <sup>4</sup>	FINALIZE <sup>2</sup> TIME (S)	SEARCH DURATION <sup>5</sup> MILLISEC						
									L=1 N=1.6M	L=50 N=1.6M	L=50 N=3M	L=50 N=6M	L=50 N=12M	POWER LAW ( $\mu$ s)	
157	Realnetworks Inc	realnetworks	007	2022-04-11	455	99	182 <sup>2056</sup>	-	110 <sup>634</sup>	144 <sup>17</sup>	815 <sup>(122)</sup>	812 <sup>(97)</sup>	1559 <sup>(96)</sup>	3159 <sup>(92)</sup> 6361 <sup>109</sup> 0.27 $N^{1.0}$	
158	Remark Holdings	remarkai	0	2018-10-30	187	847	151 <sup>2048</sup>	k	97 <sup>593</sup>	118 <sup>14</sup>	206 <sup>(5685)</sup>	5723 <sup>(210)</sup>	-	-	
159	Remark Holdings	remarkai	000	2019-06-12	234	1092	97 <sup>2048</sup>	k	117 <sup>650</sup>	98 <sup>12</sup>	207 <sup>(5776)</sup>	5703 <sup>(177)</sup> 11604 <sup>(184)</sup> 32133 <sup>(183)</sup> 91436 <sup>179</sup> 0.05 $N^{1.3}$	-	-	
160	Remark Holdings	remarkai	1	2018-10-30	187	847	155 <sup>2048</sup>	k	60 <sup>427</sup>	122 <sup>14</sup>	205 <sup>(5680)</sup>	5761 <sup>(211)</sup> 12475 <sup>(180)</sup> 28726 <sup>(182)</sup> 59618 <sup>(180)</sup> 0.37 $N^{1.2}$	-	-	
161	Rendip	rendip	000	2021-05-21	0	416	125 <sup>2048</sup>	-	204 <sup>890</sup>	68 <sup>9</sup>	40 <sup>(40)</sup>	249 <sup>(69)</sup>	368 <sup>(56)</sup>	697 <sup>(56)</sup> 1452 <sup>(52)</sup> 2926 <sup>124</sup> 0.08 $N^{1.1}$	
162	Reveal Media Ltd	revealmedia	000	2022-02-02	287	196	158 <sup>2052</sup>	-	46 <sup>383</sup>	75 <sup>10</sup>	177 <sup>(177)</sup>	2322 <sup>(176)</sup>	2019 <sup>(152)</sup> 3838 <sup>(150)</sup> 7816 <sup>(152)</sup> 16559 <sup>(98)</sup> 0.78 $N^{1.0}$	-	-
163	SQLsoft	sqsoft	001	2021-12-20	271	377	181 <sup>2056</sup>	-	71 <sup>462</sup>	66 <sup>9</sup>	152 <sup>(152)</sup>	1310 <sup>(151)</sup> 1319 <sup>(122)</sup> 2456 <sup>(118)</sup> 4906 <sup>(120)</sup> 9755 <sup>29</sup> 0.90 $N^{1.0}$	-	-	
164	Samsung S1 Corp	s1	000	2021-06-03	257	196	203 <sup>4096</sup>	-	192 <sup>865</sup>	156 <sup>20</sup>	214 <sup>(6715)</sup>	6794 <sup>(184)</sup> 13032 <sup>(180)</sup> 26372 <sup>(178)</sup> 55723 <sup>90</sup> 2.82 $N^{1.0}$	-	-	
165	Samsung S1 Corp	s1	001	2021-11-01	240	198	108 <sup>2048</sup>	-	174 <sup>813</sup>	53 <sup>8</sup>	179 <sup>(179)</sup>	2415 <sup>(188)</sup> 2491 <sup>(160)</sup> 4718 <sup>(158)</sup> 9614 <sup>(162)</sup> 24472 <sup>128</sup> 0.53 $N^{1.1}$	-	-	
166	Samsung S1 Corp	s1	002	2022-05-04	244	93	91 <sup>2048</sup>	-	226 <sup>958</sup>	135 <sup>16</sup>	145 <sup>(145)</sup>	1234 <sup>(147)</sup> 1285 <sup>(119)</sup> 2111 <sup>(117)</sup> 4805 <sup>(118)</sup> 9705 <sup>49</sup> 0.77 $N^{1.0}$	-	-	
167	Scanovate Ltd	scanovate	000	2020-01-15	250	446	147 <sup>2048</sup>	-	141 <sup>705</sup>	120 <sup>14</sup>	156 <sup>(156)</sup>	1419 <sup>(155)</sup> 1412 <sup>(137)</sup> 3008 <sup>(161)</sup> 11616 <sup>(132)</sup> 12012 <sup>169</sup> 0.10 $N^{1.2}$	-	-	
168	Scanovate Ltd	scanovate	001	2020-09-10	250	446	104 <sup>2048</sup>	-	126 <sup>675</sup>	104 <sup>13</sup>	155 <sup>(153)</sup>	1321 <sup>(152)</sup> 1320 <sup>(125)</sup> 2502 <sup>(121)</sup> 5047 <sup>(122)</sup> 10163 <sup>69</sup> 0.65 $N^{1.0}$	-	-	
169	Sensetime Group	sensetime	0	2018-10-30	525	6	218 <sup>4104</sup>	k	137 <sup>693</sup>	194 <sup>41</sup>	88 <sup>(498)</sup>	501 <sup>(87)</sup> 501 <sup>(81)</sup> 1212 <sup>(74)</sup> 2281 <sup>(74)</sup> 5032 <sup>139</sup> 0.09 $N^{1.1}$	-	-	
170	Sensetime Group	sensetime	1	2018-10-30	525	6	217 <sup>4104</sup>	k	107 <sup>628</sup>	199 <sup>48</sup>	91 <sup>(516)</sup>	502 <sup>(88)</sup> 502 <sup>(76)</sup> 1146 <sup>(76)</sup> 2301 <sup>(70)</sup> 4765 <sup>137</sup> 0.09 $N^{1.1}$	-	-	
171	Sensetime Group	sensetime	002	2019-06-03	523	6	178 <sup>2056</sup>	k	100 <sup>603</sup>	148 <sup>18</sup>	67 <sup>(359)</sup>	370 <sup>(70)</sup> 370 <sup>(105)</sup> 1897 <sup>(111)</sup> 4508 <sup>(113)</sup> 9543 <sup>189</sup> 0.00 $N^{1.5}$	-	-	
172	Sensetime Group	sensetime	003	2019-12-02	769	76	177 <sup>2056</sup>	1	219 <sup>910</sup>	153 <sup>19</sup>	201 <sup>(4885)</sup>	4889 <sup>(206)</sup> 12325 <sup>(179)</sup> 2472 <sup>(176)</sup> 24712 <sup>(173)</sup> 9445 <sup>149</sup> 0.67 $N^{1.1}$	-	-	
173	Sensetime Group	sensetime	004	2020-08-10	456	29	61 <sup>1032</sup>	-	134 <sup>690</sup>	97 <sup>12</sup>	184 <sup>(2490)</sup>	2490 <sup>(185)</sup> 2477 <sup>(158)</sup> 4654 <sup>(157)</sup> 9402 <sup>(160)</sup> 19651 <sup>70</sup> 1.22 $N^{1.0}$	-	-	
174	Sensetime Group	sensetime	005	2020-12-17	631	39	60 <sup>1032</sup>	-	229 <sup>980</sup>	85 <sup>11</sup>	181 <sup>(2459)</sup>	2459 <sup>(200)</sup> 3939 <sup>(169)</sup> 7398 <sup>(167)</sup> 14768 <sup>(158)</sup> 19016 <sup>19</sup> 14.03 $N^{0.9}$	-	-	
175	Sensetime Group	sensetime	006	2021-07-26	526	54	59 <sup>1032</sup>	-	217 <sup>929</sup>	40 <sup>7</sup>	178 <sup>(2414)</sup>	2422 <sup>(184)</sup> 4527 <sup>(156)</sup> 9128 <sup>(154)</sup> 18640 <sup>59</sup> 1.35 $N^{1.0}$	-	-	
176	Sensetime Group	sensetime	007	2022-01-15	526	37	62 <sup>1032</sup>	-	229 <sup>935</sup>	54 <sup>8</sup>	180 <sup>(2432)</sup>	2406 <sup>(183)</sup> 2406 <sup>(155)</sup> 4513 <sup>(153)</sup> 8998 <sup>(156)</sup> 18796 <sup>63</sup> 1.28 $N^{1.0}$	-	-	
177	Shaman Software	shaman	6	2018-10-26	0	200	117 <sup>2048</sup>	k	142 <sup>706</sup>	119 <sup>14</sup>	104 <sup>(603)</sup>	603 <sup>(103)</sup> 612 <sup>-</sup> - <sup>-</sup> - <sup>-</sup> - <sup>-</sup> - <sup>-</sup>	-	-	
178	Shaman Software	shaman	7	2018-10-26	0	200	140 <sup>2048</sup>	k	143 <sup>707</sup>	121 <sup>14</sup>	103 <sup>(602)</sup>	602 <sup>(104)</sup> 614 <sup>(77)</sup> 1187 <sup>(81)</sup> 2448 <sup>(77)</sup> 5083 <sup>94</sup> 0.25 $N^{1.0}$	-	-	
179	Shanghai Yitu Technology	yitu	4	2018-10-30	2119	136	187 <sup>2070</sup>	1	20 <sup>897</sup>	197 <sup>45</sup>	180 <sup>(1288)</sup>	1288 <sup>(149)</sup> 1203 <sup>(121)</sup> 2440 <sup>(125)</sup> 5241 <sup>(116)</sup> 9671 <sup>89</sup> 0.52 $N^{1.0}$	-	-	
180	Shanghai Yitu Technology	yitu	5	2018-10-30	2043	136	188 <sup>2070</sup>	1	188 <sup>853</sup>	196 <sup>44</sup>	146 <sup>(1237)</sup>	1237 <sup>(144)</sup> 1199 <sup>(126)</sup> 2513 <sup>(120)</sup> 5013 <sup>(115)</sup> 9620 <sup>85</sup> 0.55 $N^{1.0}$	-	-	
181	Smilart	smilart	4	2018-10-30	65	89	28 <sup>512</sup>	k	8 <sup>167</sup>	20 <sup>4</sup>	221 <sup>(16137)</sup>	16137 <sup>(226)</sup> 15633 <sup>-</sup> - <sup>-</sup> - <sup>-</sup> - <sup>-</sup> - <sup>-</sup>	-	-	
182	Smilart	smilart	5	2018-10-30	562	89	150 <sup>2048</sup>	k	65 <sup>450</sup>	117 <sup>14</sup>	- <sup>-</sup>	- <sup>-</sup> - <sup>-</sup> - <sup>-</sup> - <sup>-</sup> - <sup>-</sup>	-	-	
183	Staqu Technologies	st aqu	000	2021-08-30	1018	690	20 <sup>4096</sup>	-	178 <sup>826</sup>	188 <sup>24</sup>	202 <sup>(4950)</sup>	4950 <sup>(205)</sup> 4933 <sup>-</sup> - <sup>-</sup> - <sup>-</sup> - <sup>-</sup> - <sup>-</sup>	-	-	
184	Synesis	synesis	3	2018-10-30	237	150	208 <sup>4096</sup>	k	5 <sup>99</sup>	177 <sup>29</sup>	118 <sup>(789)</sup>	789 <sup>(120)</sup> 801 <sup>(108)</sup> 1941 <sup>(102)</sup> 3888 <sup>(103)</sup> 8810 <sup>157</sup> 0.07 $N^{1.1}$	-	-	
185	Synesis	synesis	003	2019-07-04	143	17	97 <sup>2048</sup>	k	18 <sup>211</sup>	94 <sup>12</sup>	90 <sup>(507)</sup>	507 <sup>(89)</sup> 502 <sup>(116)</sup> 2297 <sup>(112)</sup> 4564 <sup>(111)</sup> 9452 <sup>184</sup> 0.00 $N^{1.4}$	-	-	
186	Synesis	synesis	005	2020-09-08	494	24	216 <sup>4104</sup>	-	156 <sup>756</sup>	166 <sup>24</sup>	126 <sup>(877)</sup>	877 <sup>(126)</sup> 865 <sup>(141)</sup> 3182 <sup>(114)</sup> 4658 <sup>(119)</sup> 9750 <sup>170</sup> 0.06 $N^{1.2}$	-	-	
187	Tech5 SA	tech5	001	2019-08-19	1394	116	79 <sup>1536</sup>	k	20 <sup>887</sup>	74 <sup>10</sup>	70 <sup>(383)</sup>	766 <sup>(117)</sup> 766 <sup>(132)</sup> 2767 <sup>(139)</sup> 6149 <sup>(88)</sup> 6178 <sup>148</sup> 0.12 $N^{1.1}$	-	-	
188	Tech5 SA	tech5	002	2021-04-07	727	112	36 <sup>513</sup>	-	222 <sup>940</sup>	16 <sup>4</sup>	200 <sup>(4682)</sup>	4682 <sup>(217)</sup> 6689 <sup>(181)</sup> 12541 <sup>(177)</sup> 25145 <sup>(175)</sup> 25145 <sup>40</sup> 4.18 $N^{1.0}$	-	-	
189	Tencent Deepsea Lab	deepsea	001	2019-07-29	250	323	127 <sup>2048</sup>	1	153 <sup>737</sup>	96 <sup>12</sup>	135 <sup>(1021)</sup>	1021 <sup>(135)</sup> 1020 <sup>(133)</sup> 2774 <sup>(131)</sup> 5767 <sup>(135)</sup> 12341 <sup>175</sup> 0.06 $N^{1.2}$	-	-	
190	Tevian	tevian	5	2018-10-30	773	15	126 <sup>2048</sup>	1	54 <sup>405</sup>	126 <sup>15</sup>	75 <sup>(405)</sup>	405 <sup>(77)</sup> 408 <sup>(61)</sup> 854 <sup>(64)</sup> 1757 <sup>(60)</sup> 3380 <sup>112</sup> 0.14 $N^{1.0}$	-	-	
191	Tevian	tevian	006	2021-04-16	769	19	57 <sup>1032</sup>	-	98 <sup>597</sup>	73 <sup>10</sup>	60 <sup>(295)</sup>	295 <sup>(60)</sup> 295 <sup>(46)</sup> 578 <sup>(45)</sup> 1187 <sup>(48)</sup> 2741 <sup>125</sup> 0.06 $N^{1.1}$	-	-	
192	Tevian	tevian	007	2021-10-12	703	19	58 <sup>1032</sup>	-	163 <sup>777</sup>	24 <sup>4</sup>	61 <sup>(298)</sup>	298 <sup>(61)</sup> 298 <sup>(47)</sup> 579 <sup>(44)</sup> 1179 <sup>(41)</sup> 2418 <sup>104</sup> 0.11 $N^{1.0}$	-	-	
193	Thales	cogent	2	2018-10-30	681	39	66 <sup>1043</sup>	k	223 <sup>945</sup>	171 <sup>27</sup>	2017 <sup>(184)</sup> 2144 <sup>(154)</sup> 4298 <sup>(151)</sup> 8472 <sup>(151)</sup> 8472 <sup>69</sup> 1.08 $N^{1.0}$	-	-		
194	Thales	cogent	3	2018-10-30	681	39	65 <sup>1043</sup>	k	221 <sup>940</sup>	70 <sup>9</sup>	143 <sup>(1230)</sup>	1230 <sup>(150)</sup> 1311 <sup>(131)</sup> 2687 <sup>(126)</sup> 5390 <sup>(123)</sup> 10184 <sup>80</sup> 0.62 $N^{1.0}$	-	-	
195	Thales	cogent	004	2021-02-10	1376	59	173 <sup>2053</sup>	-	223 <sup>947</sup>	111 <sup>14</sup>	189 <sup>(2903)</sup>	2903 <sup>(173)</sup> 1911 <sup>(191)</sup> 3566 <sup>(145)</sup> 7498 <sup>(150)</sup> 16370 <sup>111</sup> 0.64 $N^{1.0}$	-	-	
196	Thales	cogent	005	2021-09-13	1043	56	67 <sup>1062</sup>	-	161 <sup>769</sup>	28 <sup>5</sup>	128 <sup>(912)</sup>	912 <sup>(131)</sup> 996 <sup>(103)</sup> 1872 <sup>(101)</sup> 3845 <sup>(96)</sup> 7555 <sup>82</sup> 0.44 $N^{1.0}$	-	-	
197	Thales	cogent	006	2022-05-14	508	70	44 <sup>550</sup>	-	184 <sup>843</sup>	48 <sup>2</sup>	102 <sup>(587)</sup>	587 <sup>(123)</sup> 820 <sup>(88)</sup> 1202 <sup>(98)</sup> 1564 <sup>(97)</sup> 3173 <sup>(100)</sup> 8290 <sup>132</sup> 0.16 $N^{1.1}$	-	-	
198	TigerIT Americas LLC	tiger	2	2018-10-29	416	518	162 <sup>2052</sup>	k	70 <sup>461</sup>	130 <sup>15</sup>	169 <sup>(1816)</sup>	1816 <sup>(174)</sup> 1921 <sup>(151)</sup> 3833 <sup>(148)</sup> 7526 <sup>(146)</sup> 14820 <sup>87</sup> 0.83 $N^{1.0}$	-	-	
199	TigerIT Americas LLC	tiger	3	2018-10-30	416	518	166 <sup>2052</sup>	k	69 <sup>461</sup>	228 <sup>37431</sup>	401 <sup>(191)</sup>	189 <sup>(181)</sup> - <sup>-</sup> - <sup>-</sup> - <sup>-</sup> - <sup>-</sup>	-	-	
200	Toshiba	toshiba	0	2018-10-30	961	105	83 <sup>1548</sup>	k	199 <sup>876</sup>	92 <sup>12</sup>	211 <sup>(6153)</sup>	6153 <sup>(213)</sup> 2326 <sup>(178)</sup> 12221 <sup>(178)</sup> 25355 <sup>(174)</sup> 49448 <sup>164</sup> 0.36 $N^{1.2}$	-	-	
201	Toshiba	toshiba	1	2018-10-30	961	105	185 <sup>2050</sup>	k	198 <sup>875</sup>	229 <sup>44701</sup>	210 <sup>(607)</sup>	6355 <sup>(215)</sup> - <sup>-</sup> - <sup>-</sup> - <sup>-</sup> - <sup>-</sup>	-	-	
202	Tripleize	aize	001	2021-08-06	262	150	146 <sup>2048</sup>	-	50 <sup>402</sup>	62 <sup>9</sup>	192 <sup>(3087)</sup>	3087 <sup>(195)</sup> - <sup>-</sup> - <sup>-</sup> - <sup>-</sup> - <sup>-</sup>	-	-	
203	Trueface.ai	trueface	000	2021-01-27	247	119	96 <sup>2000</sup>	-	36 <sup>363</sup>	102 <sup>13</sup>	150 <sup>(271)</sup>	271 <sup>(66)</sup> 327 <sup>(50)</sup> 614 <sup>(48)</sup> 1239 <sup>(44)</sup> 2678 <sup>77</sup> 0.15 $N^{1.0}$	-	-	
204	Veridas Digital Authentication Solutions S.L.	veridas	001	2021-03-05	347	875	153<sup								

2022/06/13 09:55:40	FNIR(N, R, T) = FPFR(N, T) = False neg. identification rate False pos. identification rate	N = Num. enrolled subjects R = Num. candidates examined	T = Threshold T = 0 → Investigation T > 0 → Identification	SEARCH DURATION <sup>5</sup> MILLISEC																				
				DEVELOPER		SHORT	SEQ.	VALIDATION	CONFIG <sup>1</sup>	LIB <sup>1</sup>	TEMPLATE GENERATION			FINALIZE <sup>2</sup>	L=1	L=50	L=50	L=50	POWER LAW ( $\mu$ s)					
				FULL NAME	NAME	NUM.	DATE	DATA (MB)	DATA (MB)	SIZE (B)	MULT <sup>3</sup>	TIME (MS) <sup>4</sup>	TIME (S)	N=1.6M	N=1.6M	N=1.6M	N=3M	N=6M	N=12M					
209	Viettel Group	vts	001	2021-07-16	352	600	142	2048	-	205	891	16 <sup>21</sup>	(182)	2477	(187)	2487	(157)	4644	(155)	9313	(155)	18713	<sup>48</sup> 1.53 $N^{1.0}$	
210	Viettel Group	vts	002	2022-02-08	244	600	138	2048	-	210	903	178 <sup>29</sup>	(183)	2485	(186)	2485	(159)	4678	(156)	9370	(157)	18833	<sup>50</sup> 1.49 $N^{1.0}$	
211	Vigilant Solutions	vigilant	5	2018-10-30	335	122	82	1544	k	158	762	15 <sup>19</sup>	-	(166)	1720	-	-	-	-	-	-	-		
212	Vigilant Solutions	vigilant	6	2018-10-30	337	122	81	1544	k	178	816	160 <sup>21</sup>	-	(165)	1713	-	-	-	-	-	-	-		
213	Vigilant Solutions	vigilantsolutions	007	2021-01-08	340	51	80	1544	-	105	616	142 <sup>16</sup>	(155)	1354	(154)	1352	(135)	2911	(133)	5966	(129)	11466	<sup>131</sup> 0.27 $N^{1.1}$	
214	Vigilant Solutions	vigilantsolutions	008	2021-07-23	340	51	79	1544	-	52	403	107 <sup>13</sup>	(138)	1062	(137)	1061	(118)	2330	(129)	5520	(112)	9499	<sup>153</sup> 0.11 $N^{1.1}$	
215	Visidon	visidon	1	2018-10-30	166	42	165	2052	k	122	667	132 <sup>15</sup>	(198)	4370	(204)	4472	(172)	8454	(171)	17262	(167)	34288	<sup>62</sup> 2.40 $N^{1.0}$	
216	Visidon	vd	002	2021-05-18	248	42	161	2052	-	133	687	57 <sup>9</sup>	(175)	2089	(182)	2336	-	-	-	-	-	-	-	
217	Visidon	vd	003	2021-10-12	497	43	159	2052	-	136	692	48 <sup>8</sup>	(176)	2095	(180)	2082	-	-	-	-	-	-	-	
218	Visiob-Box	visionbox	000	2021-09-17	252	274	184	2059	-	78	481	141 <sup>16</sup>	(78)	422	(68)	359	(62)	855	(26)	631	(37)	2096	<sup>17</sup> 2.46 $N^{0.8}$	
219	VisionLabs	visionlabs	6	2018-10-30	360	17	30	512	1	28	289	225 <sup>36</sup>	(15)	20290	(14)	36	(12)	39	(11)	44	(9)	53	<sup>8</sup> 3211.93 $N^{0.2}$	
220	VisionLabs	visionlabs	7	2018-10-30	360	17	31	512	1	29	289	227 <sup>36</sup>	(16)	34666	(15)	63	(13)	72	(13)	80	(11)	115	<sup>10</sup> 2076.32 $N^{0.2}$	
221	VisionLabs	visionlabs	008	2019-06-18	348	17	26	512	1	27	272	223 <sup>23</sup>	12747	(10)	23	(8)	24	(7)	26	(6)	29	(5)	33	<sup>6</sup> 2539.61 $N^{0.2}$
222	VisionLabs	visionlabs	009	2020-08-04	689	20	27	512	-	73	467	224 <sup>23</sup>	13245	(11)	23	(9)	29	(9)	34	(12)	61	(12)	145	<sup>12</sup> 8.88 $N^{0.6}$
223	VisionLabs	visionlabs	010	2021-02-05	1042	20	27	512	-	150	731	219 <sup>21</sup>	11837	(8)	21	(11)	32	(10)	36	(8)	39	(9)	43	<sup>7</sup> 3183.79 $N^{0.2}$
224	VisionLabs	visionlabs	011	2021-10-20	1042	20	30	512	-	152	735	222 <sup>21</sup>	12255	(9)	21	(7)	23	(8)	26	(7)	34	(8)	51	<sup>11</sup> 301.26 $N^{0.3}$
225	Vocord	vocord	5	2018-10-30	1035	185	46	768	k	165	780	38 <sup>7</sup>	(34)	158	(39)	204	(30)	383	(31)	767	(26)	1466	<sup>47</sup> 0.12 $N^{1.0}$	
226	Vocord	vocord	6	2018-10-30	1035	185	229	10240	k	166	785	213 <sup>243</sup>	(35)	170	(42)	216	-	-	-	-	-	-	-	
227	Xforward AI Technology	xforwardai	000	2020-07-24	236	171	157	2048	-	155	753	109 <sup>13</sup>	(199)	4603	(222)	7647	(187)	15723	(175)	23900	(177)	53729	<sup>154</sup> 0.56 $N^{1.1}$	
228	Xforward AI Technology	xforwardai	001	2021-01-21	332	50	137	2048	-	128	677	139 <sup>16</sup>	(209)	5887	(203)	4384	(173)	8798	(172)	18553	(172)	48993	<sup>161</sup> 0.32 $N^{1.1}$	
229	Xforward AI Technology	xforwardai	002	2021-05-24	691	50	201	4096	-	218	930	150 <sup>18</sup>	(216)	6957	(216)	6400	(182)	12659	(183)	31077	(181)	65158	<sup>159</sup> 0.52 $N^{1.1}$	

## Notes

- Configuration size does not capture static data present in libraries. Libraries are included but the size also includes any ancillary libraries for image processing (e.g. openCV) or numerical computation (e.g. blas).
- Finalization is the processing of converting N = 1600000 templates into a searchable data structure an operation which can be a simple copy, or the building of an index or tree, for example. The duration of the operation may be data dependent, and may not be linear in the number of input templates.
- This multiplier expresses the increase in template size when  $k$  images are passed to the template generation function.
- All durations are measured on Intel®Xeon®CPU E5-2630 v4 @ 2.20GHz processors. Estimates are made by wrapping the API function call in calls to std::chrono::high\_resolution\_clock which on the machine in (3) counts 1ns clock ticks. Precision is somewhat worse than that however.
- Search durations are measured as in the prior note. The power-law model in the final column mostly fits the empirical results in Figure 136. However in certain cases the model is not correct and should not be used numerically.

Table 6: Summary of algorithms and properties included in this report. The blue superscripts give ranking for the quantity in that column. Missing search durations, denoted by “-”, are absent because those runs were not executed, usually because we did not run on the larger galleries. Caution: The power-law model is sometimes an incorrect model. It is included here only to show broad sublinear behavior, which is flagged in green. The models should not be used for prediction.

#	ALGORITHM	INVESTIGATION, FNIR(N, R = 1, T = 0)								IDENTIFICATION, FNIR(N, R = L, T ≥ 0) FOR FPIR = 0.001							
		(0, 2]	(2, 4]	(4, 6]	(6, 8]	(8, 10]	(10, 12]	(12, 14]	(14, 18]	(0, 2]	(2, 4]	(4, 6]	(6, 8]	(8, 10]	(10, 12]	(12, 14]	(14, 18]
1	3DIVI-005	<sup>97</sup> 0.0207	<sup>97</sup> 0.0304	<sup>97</sup> 0.0415	<sup>97</sup> 0.0533	<sup>97</sup> 0.0646	<sup>114</sup> 0.0735	<sup>114</sup> 0.0884	<sup>115</sup> 0.1148	<sup>107</sup> 0.1580	<sup>98</sup> 0.2316	<sup>98</sup> 0.3033	<sup>98</sup> 0.3740	<sup>98</sup> 0.4285	<sup>113</sup> 0.4742	<sup>113</sup> 0.5329	<sup>113</sup> 0.5975
2	ANKE-000	<sup>95</sup> 0.0162	<sup>95</sup> 0.0245	<sup>95</sup> 0.0333	<sup>95</sup> 0.0428	<sup>95</sup> 0.0515	<sup>95</sup> 0.0615	<sup>112</sup> 0.0780	<sup>111</sup> 0.1028	<sup>96</sup> 0.1132	<sup>96</sup> 0.1761	<sup>96</sup> 0.2402	<sup>96</sup> 0.3057	<sup>95</sup> 0.3640	<sup>112</sup> 0.4200	<sup>112</sup> 0.4928	<sup>112</sup> 0.5680
3	ANKE-002	<sup>4</sup> 0.0055	<sup>50</sup> 0.0074	<sup>50</sup> 0.0090	<sup>49</sup> 0.0103	<sup>48</sup> 0.0116	<sup>66</sup> 0.0135	<sup>65</sup> 0.0162	<sup>65</sup> 0.0202	<sup>54</sup> 0.0329	<sup>54</sup> 0.0560	<sup>56</sup> 0.0843	<sup>57</sup> 0.1169	<sup>57</sup> 0.1481	<sup>73</sup> 0.1820	<sup>74</sup> 0.2280	<sup>73</sup> 0.2831
4	AWARE-005	<sup>106</sup> 0.0328	<sup>106</sup> 0.0519	<sup>106</sup> 0.0712	<sup>109</sup> 0.0910	<sup>104</sup> 0.1078	<sup>121</sup> 0.1235	<sup>121</sup> 0.1457	<sup>121</sup> 0.1831	<sup>108</sup> 0.3605	<sup>107</sup> 0.4949	<sup>107</sup> 0.5948	<sup>107</sup> 0.6783	<sup>108</sup> 0.7393	<sup>125</sup> 0.7905	<sup>125</sup> 0.8408	<sup>126</sup> 0.8831
5	AWARE-006	<sup>110</sup> 0.0702	<sup>111</sup> 0.1110	<sup>111</sup> 0.1502	<sup>118</sup> 0.2253	<sup>126</sup> 0.2614	<sup>127</sup> 0.3045	<sup>127</sup> 0.3659									
6	AYONIX-002	<sup>113</sup> 0.3360	<sup>114</sup> 0.4389	<sup>114</sup> 0.5144	<sup>114</sup> 0.5814	<sup>114</sup> 0.6340	<sup>131</sup> 0.6818	<sup>131</sup> 0.7297	<sup>132</sup> 0.7774	<sup>116</sup> 0.8288	<sup>111</sup> 0.9013	<sup>111</sup> 0.9375	<sup>111</sup> 0.9603	<sup>111</sup> 0.9744	<sup>129</sup> 0.9837	<sup>129</sup> 0.9893	<sup>129</sup> 0.9927
7	CAMVI-004	<sup>109</sup> 0.0623	<sup>109</sup> 0.0944	<sup>109</sup> 0.1243	<sup>108</sup> 0.1548	<sup>108</sup> 0.1812	<sup>125</sup> 0.2056	<sup>125</sup> 0.2344	<sup>123</sup> 0.2672	<sup>91</sup> 0.0810	<sup>91</sup> 0.1267	<sup>88</sup> 0.1721	<sup>88</sup> 0.2203	<sup>88</sup> 0.2619	<sup>103</sup> 0.3040	<sup>103</sup> 0.3543	<sup>98</sup> 0.4124
8	CAMVI-005	<sup>111</sup> 0.0849	<sup>111</sup> 0.1255	<sup>111</sup> 0.1631	<sup>111</sup> 0.1989	<sup>117</sup> 0.2298	<sup>127</sup> 0.2585	<sup>126</sup> 0.2915	<sup>126</sup> 0.3246								
9	CANON-001						<sup>25</sup> 0.0052	<sup>24</sup> 0.0057	<sup>19</sup> 0.0042						<sup>29</sup> 0.0491	<sup>29</sup> 0.0606	<sup>30</sup> 0.0826
10	CIB-000	<sup>114</sup> 0.0022	<sup>114</sup> 0.0030	<sup>115</sup> 0.0037	<sup>115</sup> 0.0044	<sup>117</sup> 0.0049	<sup>29</sup> 0.0057	<sup>29</sup> 0.0069	<sup>29</sup> 0.0062	<sup>25</sup> 0.0139	<sup>26</sup> 0.0240	<sup>27</sup> 0.0373	<sup>28</sup> 0.0525	<sup>28</sup> 0.0689	<sup>39</sup> 0.0859	<sup>40</sup> 0.1109	<sup>40</sup> 0.1454
11	CLEARVIEWAI-000	<sup>1</sup> 0.0017	<sup>4</sup> 0.0023	<sup>4</sup> 0.0028	<sup>9</sup> 0.0034	<sup>111</sup> 0.0039	<sup>19</sup> 0.0046	<sup>23</sup> 0.0056	<sup>24</sup> 0.0047	<sup>16</sup> 0.0066	<sup>18</sup> 0.0121	<sup>18</sup> 0.0194	<sup>19</sup> 0.0287	<sup>19</sup> 0.0385	<sup>36</sup> 0.0493	<sup>32</sup> 0.0662	<sup>32</sup> 0.0873
12	CLOUDWALK-HR-000	<sup>8</sup> 0.0019	<sup>7</sup> 0.0024	<sup>8</sup> 0.0029	<sup>6</sup> 0.0032	<sup>5</sup> 0.0036	<sup>5</sup> 0.0041	<sup>3</sup> 0.0020	<sup>1</sup> 0.0029	<sup>1</sup> 0.0041	<sup>1</sup> 0.0054	<sup>1</sup> 0.0064	<sup>2</sup> 0.0073	<sup>4</sup> 0.0085	<sup>4</sup> 0.0102	<sup>4</sup> 0.0112	
13	CLOUDWALK-MT-000							<sup>1</sup> 0.0038	<sup>1</sup> 0.0013						<sup>1</sup> 0.0065	<sup>1</sup> 0.0072	<sup>1</sup> 0.0075
14	COGENT-000	<sup>91</sup> 0.0128	<sup>91</sup> 0.0184	<sup>92</sup> 0.0250	<sup>93</sup> 0.0327	<sup>93</sup> 0.0407	<sup>108</sup> 0.0488	<sup>107</sup> 0.0611	<sup>106</sup> 0.0794	<sup>77</sup> 0.0559	<sup>78</sup> 0.0923	<sup>76</sup> 0.1342	<sup>76</sup> 0.1812	<sup>78</sup> 0.2243	<sup>92</sup> 0.2675	<sup>93</sup> 0.3240	<sup>94</sup> 0.3992
15	COGENT-001	<sup>95</sup> 0.0128	<sup>96</sup> 0.0184	<sup>95</sup> 0.0250	<sup>92</sup> 0.0327	<sup>92</sup> 0.0407	<sup>105</sup> 0.0488	<sup>108</sup> 0.0611	<sup>107</sup> 0.0794	<sup>78</sup> 0.0559	<sup>79</sup> 0.0923	<sup>77</sup> 0.1342	<sup>77</sup> 0.1812	<sup>78</sup> 0.2243	<sup>91</sup> 0.2675	<sup>91</sup> 0.3240	<sup>95</sup> 0.3992
16	COGENT-002	<sup>69</sup> 0.0081	<sup>66</sup> 0.0105	<sup>63</sup> 0.0123	<sup>64</sup> 0.0137	<sup>62</sup> 0.0157	<sup>79</sup> 0.0175	<sup>77</sup> 0.0215	<sup>77</sup> 0.0280	<sup>69</sup> 0.0499	<sup>68</sup> 0.0827	<sup>67</sup> 0.1207	<sup>67</sup> 0.1639	<sup>67</sup> 0.2037	<sup>83</sup> 0.2432	<sup>84</sup> 0.2972	<sup>85</sup> 0.3638
17	COGENT-003	<sup>71</sup> 0.0082	<sup>67</sup> 0.0108	<sup>65</sup> 0.0128	<sup>67</sup> 0.0145	<sup>66</sup> 0.0168	<sup>85</sup> 0.0191	<sup>86</sup> 0.0239	<sup>83</sup> 0.0312	<sup>80</sup> 0.0582	<sup>80</sup> 0.0971	<sup>80</sup> 0.1417	<sup>80</sup> 0.1918	<sup>80</sup> 0.2380	<sup>98</sup> 0.2836	<sup>101</sup> 0.3440	<sup>101</sup> 0.4207
18	COGENT-004	<sup>59</sup> 0.0066	<sup>59</sup> 0.0080	<sup>45</sup> 0.0085	<sup>39</sup> 0.0080	<sup>31</sup> 0.0083	<sup>47</sup> 0.0092	<sup>48</sup> 0.0106	<sup>51</sup> 0.0130	<sup>63</sup> 0.0410	<sup>65</sup> 0.0720	<sup>65</sup> 0.1099	<sup>65</sup> 0.1539	<sup>64</sup> 0.1974	<sup>84</sup> 0.2443	<sup>87</sup> 0.3043	<sup>87</sup> 0.3757
19	COGENT-006							<sup>17</sup> 0.0045	<sup>15</sup> 0.0049	<sup>17</sup> 0.0038					<sup>24</sup> 0.0370	<sup>20</sup> 0.0448	<sup>20</sup> 0.0602
20	COGNITEC-000	<sup>105</sup> 0.0265	<sup>105</sup> 0.0423	<sup>105</sup> 0.0588	<sup>105</sup> 0.0757	<sup>105</sup> 0.0894	<sup>119</sup> 0.1014	<sup>119</sup> 0.1169	<sup>118</sup> 0.1381	<sup>108</sup> 0.1522	<sup>99</sup> 0.2330	<sup>97</sup> 0.3051	<sup>97</sup> 0.3751	<sup>97</sup> 0.4300	<sup>111</sup> 0.4779	<sup>111</sup> 0.5307	<sup>111</sup> 0.5913
21	COGNITEC-001	<sup>93</sup> 0.0149	<sup>93</sup> 0.0228	<sup>94</sup> 0.0312	<sup>94</sup> 0.0399	<sup>94</sup> 0.0479	<sup>111</sup> 0.0546	<sup>110</sup> 0.0656	<sup>108</sup> 0.0806	<sup>93</sup> 0.0963	<sup>93</sup> 0.1562	<sup>93</sup> 0.2157	<sup>93</sup> 0.2771	<sup>110</sup> 0.3771	<sup>109</sup> 0.4343	<sup>108</sup> 0.4959	
22	COGNITEC-002	<sup>7</sup> 0.0101	<sup>80</sup> 0.0138	<sup>81</sup> 0.0170	<sup>81</sup> 0.0201	<sup>81</sup> 0.0237	<sup>97</sup> 0.0264	<sup>95</sup> 0.0309	<sup>94</sup> 0.0389	<sup>72</sup> 0.0517	<sup>71</sup> 0.0879	<sup>72</sup> 0.1269	<sup>71</sup> 0.1707	<sup>71</sup> 0.2098	<sup>88</sup> 0.2463	<sup>83</sup> 0.2919	<sup>83</sup> 0.3535
23	COGNITEC-003	<sup>78</sup> 0.0104	<sup>81</sup> 0.0140	<sup>82</sup> 0.0174	<sup>82</sup> 0.0205	<sup>82</sup> 0.0238	<sup>98</sup> 0.0266	<sup>96</sup> 0.0311	<sup>96</sup> 0.0401	<sup>71</sup> 0.0504	<sup>70</sup> 0.0855	<sup>69</sup> 0.1235	<sup>69</sup> 0.1662	<sup>68</sup> 0.2045	<sup>82</sup> 0.2403	<sup>82</sup> 0.2854	<sup>81</sup> 0.3451
24	COGNITEC-004	<sup>6</sup> 0.0073	<sup>62</sup> 0.0099	<sup>62</sup> 0.0118	<sup>59</sup> 0.0130	<sup>78</sup> 0.0147	<sup>74</sup> 0.0189	<sup>72</sup> 0.0239	<sup>83</sup> 0.0325	<sup>83</sup> 0.0548	<sup>82</sup> 0.0798	<sup>81</sup> 0.1074	<sup>80</sup> 0.1325	<sup>67</sup> 0.1591	<sup>64</sup> 0.1952	<sup>63</sup> 0.2414	
25	COGNITEC-006						<sup>41</sup> 0.0081	<sup>39</sup> 0.0086	<sup>40</sup> 0.0090					<sup>36</sup> 0.0777	<sup>36</sup> 0.0926	<sup>36</sup> 0.1274	
26	CUBOX-000	<sup>7</sup> 0.0019	<sup>5</sup> 0.0024	<sup>5</sup> 0.0028	<sup>4</sup> 0.0031	<sup>4</sup> 0.0032	<sup>9</sup> 0.0037	<sup>9</sup> 0.0044	<sup>7</sup> 0.0027	<sup>6</sup> 0.0039	<sup>6</sup> 0.0059	<sup>7</sup> 0.0083	<sup>8</sup> 0.0111	<sup>8</sup> 0.0141	<sup>13</sup> 0.0185	<sup>13</sup> 0.0252	<sup>13</sup> 0.0339
27	CYBERLINK-002	<sup>50</sup> 0.0055	<sup>45</sup> 0.0068	<sup>41</sup> 0.0075	<sup>35</sup> 0.0078	<sup>32</sup> 0.0084	<sup>48</sup> 0.0094	<sup>49</sup> 0.0107	<sup>47</sup> 0.0114	<sup>32</sup> 0.0180	<sup>33</sup> 0.0302	<sup>35</sup> 0.0460	<sup>32</sup> 0.0643	<sup>33</sup> 0.0837	<sup>48</sup> 0.1058	<sup>47</sup> 0.1370	<sup>47</sup> 0.1787
28	CYBERLINK-003	<sup>35</sup> 0.0041	<sup>34</sup> 0.0052	<sup>27</sup> 0.0057	<sup>25</sup> 0.0058	<sup>25</sup> 0.0061	<sup>38</sup> 0.0068	<sup>35</sup> 0.0078	<sup>37</sup> 0.0078	<sup>19</sup> 0.0109	<sup>19</sup> 0.0175	<sup>20</sup> 0.0259	<sup>21</sup> 0.0356	<sup>21</sup> 0.0468	<sup>33</sup> 0.0594	<sup>34</sup> 0.0787	<sup>34</sup> 0.1072
29	DAHUA-002	<sup>30</sup> 0.0035	<sup>29</sup> 0.0047	<sup>28</sup> 0.0058	<sup>27</sup> 0.0067	<sup>28</sup> 0.0074	<sup>42</sup> 0.0082	<sup>45</sup> 0.0100	<sup>40</sup> 0.0108	<sup>30</sup> 0.0169	<sup>32</sup> 0.0294	<sup>31</sup> 0.0449	<sup>30</sup> 0.0635	<sup>30</sup> 0.0817	<sup>45</sup> 0.1013	<sup>44</sup> 0.1291	<sup>43</sup> 0.1638
30	DAHUA-003	<sup>19</sup> 0.0026	<sup>19</sup> 0.0036	<sup>19</sup> 0.0043	<sup>20</sup> 0.0050	<sup>20</sup> 0.0055	<sup>31</sup> 0.0062	<sup>37</sup> 0.0080	<sup>32</sup> 0.0073	<sup>29</sup> 0.0160	<sup>30</sup> 0.0280	<sup>29</sup> 0.0432	<sup>29</sup> 0.0794	<sup>43</sup> 0.0987	<sup>43</sup> 0.1270	<sup>41</sup> 0.1587	
31	DEEPLINT-001	<sup>1</sup> 0.0024	<sup>16</sup> 0.0032	<sup>14</sup> 0.0037	<sup>13</sup> 0.0040	<sup>13</sup> 0.0043	<sup>23</sup> 0.0049	<sup>25</sup> 0.0060	<sup>22</sup> 0.0052	<sup>12</sup> 0.0058	<sup>10</sup> 0.0087	<sup>11</sup> 0.0119	<sup>11</sup> 0.0155	<sup>11</sup> 0.0199	<sup>16</sup> 0.0249	<sup>16</sup> 0.0388	<sup>16</sup> 0.0463
32	DEEPESEA-001	<sup>70</sup> 0.0081	<sup>70</sup> 0.0116	<sup>73</sup> 0.0149	<sup>76</sup> 0.0182	<sup>76</sup> 0.0216	<sup>96</sup> 0.0260	<sup>98</sup> 0.0332	<sup>66</sup> 0.0458	<sup>66</sup> 0.0734	<sup>64</sup> 0.1086	<sup>63</sup> 0.1460	<sup>63</sup> 0.1812	<sup>80</sup> 0.2186	<sup>80</sup> 0.2663	<sup>79</sup> 0.3213	
33	DERMALOG-006	<sup>8</sup> 0.0113	<sup>82</sup> 0.0142	<sup>78</sup> 0.0163	<sup>77</sup> 0.0183	<sup>74</sup> 0.0200	<sup>90</sup> 0.0218	<sup>88</sup> 0.0251	<sup>79</sup> 0.0329	<sup>75</sup> 0.0545	<sup>73</sup> 0.0889	<sup>73</sup> 0.1271	<sup>73</sup> 0.1697	<sup>73</sup> 0.2090	<sup>88</sup> 0.2498	<sup>86</sup> 0.3028	<sup>86</sup> 0.3670
34	DERMALOG-007	<sup>88</sup> 0.0125	<sup>88</sup> 0.0170	<sup>88</sup> 0.0214	<sup>88</sup> 0.0264	<sup>87</sup> 0.0309	<sup>103</sup> 0.0356	<sup>104</sup> 0.0432	<sup>104</sup> 0.0579	<sup>92</sup> 0.0910	<sup>92</sup> 0.1453	<sup>92</sup> 0.2009	<sup>92</sup> 0.3134	<sup>109</sup> 0.3649	<sup>108</sup> 0.4289	<sup>109</sup> 0.5007	
35	DERMALOG-008	<sup>5</sup> 0.0057	<sup>52</sup> 0.0077	<sup>54</sup> 0.0095	<sup>54</sup> 0.0110	<sup>53</sup> 0.0128	<sup>72</sup> 0.0148	<sup>72</sup> 0.0180	<sup>72</sup> 0.0223	<sup>70</sup> 0.0501	<sup>69</sup> 0.0850	<sup>70</sup> 0.1247	<sup>71</sup> 0.1692	<sup>72</sup> 0.2105	<sup>88</sup> 0.2541	<sup>88</sup> 0.3102	<sup>88</sup> 0.3762
36	FUJITSULAB-001						<sup>46</sup> 0.0089	<sup>44</sup> 0.0098	<sup>46</sup> 0.0111					<sup>57</sup> 0.1403	<sup>56</sup> 0.1723	<sup>54</sup> 0.2165	
37	GORILLA-002	<sup>100</sup> 0.0213	<sup>100</sup> 0.0359	<sup>101</sup> 0.0528	<sup>102</sup> 0.0716	<sup>103</sup> 0.0895	<sup>120</sup> 0.1088	<sup>120</sup> 0.									

MISS RATES		INVESTIGATION, FNIR( $N, R = 1, T = 0$ )								IDENTIFICATION, FNIR( $N, R = L, T \geq 0$ ) FOR FPIR = 0.001							
#	ALGORITHM	(0, 2]	(2, 4]	(4, 6]	(6, 8]	(8, 10]	(10, 12]	(12, 14]	(14, 18]	(0, 2]	(2, 4]	(4, 6]	(6, 8]	(8, 10]	(10, 12]	(12, 14]	(14, 18]
45	IDEMIA-008	<sup>3</sup> 0.0018	<sup>6</sup> 0.0024	<sup>6</sup> 0.0029	<sup>5</sup> 0.0032	<sup>7</sup> 0.0035	<sup>9</sup> 0.0039	<sup>12</sup> 0.0046	<sup>12</sup> 0.0033	<sup>3</sup> 0.0034	<sup>3</sup> 0.0051	<sup>7</sup> 0.0069	<sup>5</sup> 0.0087	<sup>7</sup> 0.0102	<sup>8</sup> 0.0123	<sup>7</sup> 0.0146	<sup>7</sup> 0.0186
46	IDEMIA-009						<sup>11</sup> 0.0040	<sup>10</sup> 0.0042	<sup>10</sup> 0.0024						<sup>5</sup> 0.0094	<sup>5</sup> 0.0103	<sup>5</sup> 0.0123
47	IMAGUS-005	<sup>33</sup> 0.0039	<sup>33</sup> 0.0052	<sup>31</sup> 0.0061	<sup>29</sup> 0.0067	<sup>30</sup> 0.0077	<sup>45</sup> 0.0088	<sup>46</sup> 0.0103	<sup>45</sup> 0.0109	<sup>39</sup> 0.0212	<sup>39</sup> 0.0357	<sup>40</sup> 0.0539	<sup>40</sup> 0.0755	<sup>38</sup> 0.0967	<sup>53</sup> 0.1183	<sup>52</sup> 0.1485	<sup>50</sup> 0.1893
48	IMPERIAL-000	<sup>38</sup> 0.0040	<sup>38</sup> 0.0054	<sup>36</sup> 0.0067	<sup>38</sup> 0.0079	<sup>40</sup> 0.0093	<sup>38</sup> 0.0112	<sup>37</sup> 0.0139	<sup>39</sup> 0.0178	<sup>49</sup> 0.0286	<sup>31</sup> 0.0503	<sup>31</sup> 0.0779	<sup>51</sup> 0.1116	<sup>51</sup> 0.1455	<sup>74</sup> 0.1844	<sup>77</sup> 0.2341	<sup>76</sup> 0.2951
49	INCODE-003	<sup>94</sup> 0.0155	<sup>96</sup> 0.0247	<sup>96</sup> 0.0348	<sup>96</sup> 0.0463	<sup>96</sup> 0.0571	<sup>113</sup> 0.0674	<sup>113</sup> 0.0856	<sup>114</sup> 0.1114	<sup>102</sup> 0.1627	<sup>102</sup> 0.2507	<sup>102</sup> 0.3322	<sup>100</sup> 0.4122	<sup>100</sup> 0.4772	<sup>118</sup> 0.5368	<sup>118</sup> 0.6059	<sup>118</sup> 0.6766
50	INCODE-004	<sup>56</sup> 0.0061	<sup>59</sup> 0.0087	<sup>59</sup> 0.0110	<sup>61</sup> 0.0136	<sup>64</sup> 0.0161	<sup>81</sup> 0.0185	<sup>84</sup> 0.0238	<sup>88</sup> 0.0309	<sup>73</sup> 0.0532	<sup>74</sup> 0.0908	<sup>73</sup> 0.1334	<sup>77</sup> 0.1808	<sup>77</sup> 0.2245	<sup>93</sup> 0.2675	<sup>92</sup> 0.3249	<sup>91</sup> 0.3932
51	INNOVATRICS-004	<sup>114</sup> 0.3594	<sup>113</sup> 0.3629	<sup>113</sup> 0.3688	<sup>112</sup> 0.3754	<sup>112</sup> 0.3813	<sup>129</sup> 0.3870	<sup>129</sup> 0.3960	<sup>129</sup> 0.4135	<sup>102</sup> 0.4234	<sup>106</sup> 0.4642	<sup>106</sup> 0.5073	<sup>106</sup> 0.5522	<sup>105</sup> 0.5902	<sup>122</sup> 0.6274	<sup>120</sup> 0.6736	<sup>120</sup> 0.7253
52	INNOVATRICS-005	<sup>41</sup> 0.0046	<sup>41</sup> 0.0063	<sup>42</sup> 0.0078	<sup>45</sup> 0.0092	<sup>45</sup> 0.0106	<sup>60</sup> 0.0124	<sup>60</sup> 0.0149	<sup>69</sup> 0.0178	<sup>85</sup> 0.0343	<sup>56</sup> 0.0590	<sup>88</sup> 0.0888	<sup>56</sup> 0.1222	<sup>51</sup> 0.1544	<sup>77</sup> 0.1881	<sup>76</sup> 0.2321	<sup>74</sup> 0.2874
53	IREX-000	<sup>24</sup> 0.0031	<sup>24</sup> 0.0042	<sup>25</sup> 0.0051	<sup>26</sup> 0.0060	<sup>26</sup> 0.0068	<sup>40</sup> 0.0080	<sup>42</sup> 0.0095	<sup>45</sup> 0.0107	<sup>52</sup> 0.0313	<sup>52</sup> 0.0539	<sup>53</sup> 0.0815	<sup>56</sup> 0.1137	<sup>53</sup> 0.1442	<sup>71</sup> 0.1755	<sup>72</sup> 0.2181	<sup>70</sup> 0.2718
54	ISYSTEMS-002	<sup>78</sup> 0.0101	<sup>79</sup> 0.0135	<sup>80</sup> 0.0169	<sup>79</sup> 0.0197	<sup>80</sup> 0.0228	<sup>94</sup> 0.0256	<sup>94</sup> 0.0304	<sup>96</sup> 0.0398	<sup>90</sup> 0.0779	<sup>90</sup> 0.1258	<sup>91</sup> 0.1759	<sup>96</sup> 0.2299	<sup>91</sup> 0.2758	<sup>106</sup> 0.3204	<sup>108</sup> 0.3763	<sup>108</sup> 0.4401
55	ISYSTEMS-003	<sup>75</sup> 0.0089	<sup>69</sup> 0.0115	<sup>69</sup> 0.0139	<sup>69</sup> 0.0158	<sup>70</sup> 0.0177	<sup>87</sup> 0.0198	<sup>83</sup> 0.0234	<sup>80</sup> 0.0303	<sup>84</sup> 0.0647	<sup>84</sup> 0.1056	<sup>84</sup> 0.1502	<sup>84</sup> 0.1986	<sup>83</sup> 0.2402	<sup>96</sup> 0.2819	<sup>95</sup> 0.3351	<sup>93</sup> 0.3976
56	KEDACOM-001	<sup>81</sup> 0.0116	<sup>75</sup> 0.0130	<sup>67</sup> 0.0135	<sup>60</sup> 0.0133	<sup>57</sup> 0.0135	<sup>67</sup> 0.0141	<sup>81</sup> 0.0151	<sup>58</sup> 0.0176	<sup>41</sup> 0.0241	<sup>41</sup> 0.0360	<sup>39</sup> 0.0513	<sup>38</sup> 0.0689	<sup>41</sup> 0.0866	<sup>49</sup> 0.1060	<sup>45</sup> 0.1327	<sup>45</sup> 0.1694
57	LOOKMAN-003	<sup>86</sup> 0.0123	<sup>83</sup> 0.0144	<sup>77</sup> 0.0158	<sup>70</sup> 0.0168	<sup>71</sup> 0.0178	<sup>83</sup> 0.0188	<sup>76</sup> 0.0212	<sup>76</sup> 0.0260	<sup>64</sup> 0.0438	<sup>62</sup> 0.0687	<sup>61</sup> 0.0978	<sup>61</sup> 0.1296	<sup>60</sup> 0.1581	<sup>76</sup> 0.1879	<sup>75</sup> 0.2294	<sup>72</sup> 0.2756
58	LOOKMAN-005	<sup>88</sup> 0.0118	<sup>77</sup> 0.0134	<sup>70</sup> 0.0142	<sup>66</sup> 0.0144	<sup>61</sup> 0.0150	<sup>77</sup> 0.0160	<sup>69</sup> 0.0176	<sup>60</sup> 0.0213	<sup>51</sup> 0.0310	<sup>49</sup> 0.0480	<sup>46</sup> 0.0698	<sup>48</sup> 0.0954	<sup>48</sup> 0.1216	<sup>62</sup> 0.1491	<sup>62</sup> 0.1890	<sup>62</sup> 0.2381
59	MICROFOCUS-005	<sup>115</sup> 0.4269	<sup>115</sup> 0.5527	<sup>115</sup> 0.6355	<sup>116</sup> 0.7024	<sup>116</sup> 0.7503	<sup>133</sup> 0.7876	<sup>133</sup> 0.8234	<sup>134</sup> 0.8601	<sup>111</sup> 0.8338	<sup>112</sup> 0.9113	<sup>112</sup> 0.9468	<sup>112</sup> 0.9667	<sup>112</sup> 0.9771	<sup>128</sup> 0.9836	<sup>128</sup> 0.9924	
60	MICROSOFT-003	<sup>28</sup> 0.0034	<sup>32</sup> 0.0050	<sup>33</sup> 0.0064	<sup>36</sup> 0.0078	<sup>38</sup> 0.0092	<sup>54</sup> 0.0107	<sup>56</sup> 0.0135	<sup>57</sup> 0.0166	<sup>56</sup> 0.0288	<sup>50</sup> 0.0503	<sup>50</sup> 0.0763	<sup>58</sup> 0.1067	<sup>51</sup> 0.1359	<sup>56</sup> 0.1680	<sup>68</sup> 0.2116	<sup>66</sup> 0.2644
61	MICROSOFT-004	<sup>29</sup> 0.0032	<sup>22</sup> 0.0047	<sup>29</sup> 0.0060	<sup>32</sup> 0.0075	<sup>35</sup> 0.0087	<sup>51</sup> 0.0103	<sup>55</sup> 0.0131	<sup>55</sup> 0.0159	<sup>47</sup> 0.0268	<sup>48</sup> 0.0470	<sup>49</sup> 0.0716	<sup>48</sup> 0.1007	<sup>48</sup> 0.1291	<sup>68</sup> 0.1610	<sup>66</sup> 0.2052	<sup>65</sup> 0.2590
62	MICROSOFT-005	<sup>22</sup> 0.0031	<sup>29</sup> 0.0047	<sup>35</sup> 0.0066	<sup>43</sup> 0.0084	<sup>43</sup> 0.0103	<sup>64</sup> 0.0131	<sup>66</sup> 0.0164	<sup>62</sup> 0.0185	<sup>43</sup> 0.0243	<sup>44</sup> 0.0432	<sup>44</sup> 0.0658	<sup>44</sup> 0.0913	<sup>45</sup> 0.1172	<sup>59</sup> 0.1476	<sup>61</sup> 0.1874	<sup>59</sup> 0.2272
63	MICROSOFT-006	<sup>29</sup> 0.0032	<sup>31</sup> 0.0049	<sup>34</sup> 0.0065	<sup>42</sup> 0.0081	<sup>42</sup> 0.0096	<sup>59</sup> 0.0117	<sup>58</sup> 0.0144	<sup>56</sup> 0.0160	<sup>24</sup> 0.0134	<sup>24</sup> 0.0233	<sup>25</sup> 0.0346	<sup>29</sup> 0.0462	<sup>29</sup> 0.0578	<sup>39</sup> 0.0713	<sup>35</sup> 0.0903	<sup>35</sup> 0.1156
64	NEC-000	<sup>97</sup> 0.0195	<sup>99</sup> 0.0415	<sup>99</sup> 0.0445	<sup>98</sup> 0.0581	<sup>98</sup> 0.0699	<sup>116</sup> 0.0817	<sup>116</sup> 0.0998	<sup>116</sup> 0.1237	<sup>89</sup> 0.0759	<sup>89</sup> 0.1245	<sup>89</sup> 0.1729	<sup>89</sup> 0.2240	<sup>89</sup> 0.2671	<sup>105</sup> 0.3117	<sup>103</sup> 0.3639	<sup>103</sup> 0.4348
65	NEC-001	<sup>104</sup> 0.0246	<sup>102</sup> 0.0382	<sup>103</sup> 0.0524	<sup>108</sup> 0.0672	<sup>107</sup> 0.0793	<sup>118</sup> 0.0904	<sup>117</sup> 0.1076	<sup>117</sup> 0.1317	<sup>94</sup> 0.1019	<sup>94</sup> 0.1623	<sup>94</sup> 0.2214	<sup>94</sup> 0.2834	<sup>91</sup> 0.3341	<sup>111</sup> 0.3844	<sup>111</sup> 0.4440	<sup>118</sup> 0.5183
66	NEC-002	<sup>27</sup> 0.0033	<sup>22</sup> 0.0041	<sup>18</sup> 0.0043	<sup>16</sup> 0.0044	<sup>15</sup> 0.0045	<sup>22</sup> 0.0049	<sup>22</sup> 0.0056	<sup>18</sup> 0.0041	<sup>15</sup> 0.0066	<sup>11</sup> 0.0090	<sup>10</sup> 0.0111	<sup>10</sup> 0.0131	<sup>9</sup> 0.0149	<sup>11</sup> 0.0171	<sup>12</sup> 0.0207	<sup>12</sup> 0.0267
67	NEC-003	<sup>31</sup> 0.0036	<sup>26</sup> 0.0046	<sup>24</sup> 0.0051	<sup>24</sup> 0.0055	<sup>24</sup> 0.0059	<sup>35</sup> 0.0067	<sup>35</sup> 0.0077	<sup>36</sup> 0.0073	<sup>9</sup> 0.0056	<sup>9</sup> 0.0076	<sup>9</sup> 0.0091	<sup>7</sup> 0.0105	<sup>6</sup> 0.0119	<sup>10</sup> 0.0137	<sup>9</sup> 0.0162	<sup>9</sup> 0.0209
68	NEC-004	<sup>32</sup> 0.0039	<sup>29</sup> 0.0045	<sup>22</sup> 0.0047	<sup>18</sup> 0.0046	<sup>14</sup> 0.0044	<sup>21</sup> 0.0046	<sup>20</sup> 0.0052	<sup>15</sup> 0.0036	<sup>7</sup> 0.0046	<sup>5</sup> 0.0057	<sup>2</sup> 0.0063	<sup>2</sup> 0.0066	<sup>1</sup> 0.0069	<sup>2</sup> 0.0076	<sup>2</sup> 0.0090	<sup>2</sup> 0.0105
69	NEC-005						<sup>8</sup> 0.0037	<sup>4</sup> 0.0044	<sup>4</sup> 0.0020					<sup>3</sup> 0.0080	<sup>3</sup> 0.0091	<sup>3</sup> 0.0107	
70	NEUROTECHNOLOGY-003	<sup>101</sup> 0.0234	<sup>101</sup> 0.0379	<sup>102</sup> 0.0549	<sup>101</sup> 0.0682	<sup>108</sup> 0.0720	<sup>115</sup> 0.0747	<sup>115</sup> 0.0886	<sup>113</sup> 0.1066	<sup>108</sup> 0.6802	<sup>108</sup> 0.8187	<sup>110</sup> 0.8920	<sup>110</sup> 0.9355	<sup>110</sup> 0.9594	<sup>127</sup> 0.9738	<sup>127</sup> 0.9828	<sup>127</sup> 0.9885
71	NEUROTECHNOLOGY-004	<sup>79</sup> 0.0104	<sup>78</sup> 0.0134	<sup>76</sup> 0.0156	<sup>73</sup> 0.0173	<sup>72</sup> 0.0195	<sup>89</sup> 0.0212	<sup>87</sup> 0.0245	<sup>84</sup> 0.0320	<sup>83</sup> 0.0462	<sup>82</sup> 0.1015	<sup>81</sup> 0.1426	<sup>79</sup> 0.1881	<sup>73</sup> 0.2299	<sup>92</sup> 0.3269	<sup>92</sup> 0.3943	
72	NEUROTECHNOLOGY-005	<sup>79</sup> 0.0089	<sup>71</sup> 0.0116	<sup>68</sup> 0.0136	<sup>68</sup> 0.0152	<sup>69</sup> 0.0173	<sup>86</sup> 0.0196	<sup>82</sup> 0.0233	<sup>81</sup> 0.0306	<sup>76</sup> 0.0556	<sup>76</sup> 0.0913	<sup>74</sup> 0.1315	<sup>71</sup> 0.1766	<sup>70</sup> 0.2192	<sup>89</sup> 0.2617	<sup>89</sup> 0.3174	<sup>89</sup> 0.3843
73	NEUROTECHNOLOGY-007	<sup>66</sup> 0.0078	<sup>63</sup> 0.0103	<sup>64</sup> 0.0124	<sup>65</sup> 0.0140	<sup>63</sup> 0.0161	<sup>80</sup> 0.0185	<sup>79</sup> 0.0225	<sup>78</sup> 0.0290	<sup>82</sup> 0.0641	<sup>85</sup> 0.1069	<sup>85</sup> 0.1546	<sup>85</sup> 0.2075	<sup>86</sup> 0.2572	<sup>104</sup> 0.3081	<sup>105</sup> 0.3713	<sup>105</sup> 0.4421
74	NEUROTECHNOLOGY-010								<sup>26</sup> 0.0053	<sup>26</sup> 0.0061	<sup>27</sup> 0.0053			<sup>40</sup> 0.0863	<sup>38</sup> 0.1050	<sup>38</sup> 0.1333	
75	NOBLIS-002	<sup>112</sup> 0.1520	<sup>112</sup> 0.2419	<sup>112</sup> 0.3296	<sup>113</sup> 0.4114	<sup>113</sup> 0.4856	<sup>130</sup> 0.5528	<sup>130</sup> 0.6061	<sup>130</sup> 0.6532	<sup>113</sup> 0.9984	<sup>113</sup> 0.9996	<sup>113</sup> 0.9998	<sup>113</sup> 0.9999	<sup>113</sup> 0.9999	<sup>130</sup> 1.0000	<sup>134</sup> 1.0000	<sup>132</sup> 1.0000
76	NTECHLAB-003	<sup>67</sup> 0.0078	<sup>76</sup> 0.0131	<sup>82</sup> 0.0202	<sup>90</sup> 0.0295	<sup>91</sup> 0.0405	<sup>110</sup> 0.0543	<sup>111</sup> 0.0761	<sup>112</sup> 0.1035	<sup>68</sup> 0.0491	<sup>72</sup> 0.0881	<sup>70</sup> 0.1384	<sup>81</sup> 0.1985	<sup>81</sup> 0.2594	<sup>107</sup> 0.3270	<sup>107</sup> 0.4065	<sup>107</sup> 0.4891
77	NTECHLAB-004	<sup>62</sup> 0.0068	<sup>68</sup> 0.0110	<sup>79</sup> 0.0167	<sup>86</sup> 0.0239	<sup>89</sup> 0.0330	<sup>102</sup> 0.0447	<sup>109</sup> 0.0641	<sup>110</sup> 0.0891	<sup>60</sup> 0.0379	<sup>63</sup> 0.0688	<sup>66</sup> 0.1108	<sup>66</sup> 0.1629	<sup>73</sup> 0.2192	<sup>99</sup> 0.2846	<sup>104</sup> 0.3657	<sup>106</sup> 0.4524
78	NTECHLAB-006	<sup>51</sup> 0.0056	<sup>62</sup> 0.0095	<sup>72</sup> 0.0148	<sup>83</sup> 0.0218	<sup>85</sup> 0.0301	<sup>105</sup> 0.0413	<sup>109</sup> 0.0591	<sup>109</sup> 0.0814	<sup>56</sup> 0.0349	<sup>63</sup> 0.0636	<sup>63</sup> 0.1023	<sup>63</sup> 0.1506	<sup>67</sup> 0.2024	<sup>89</sup> 0.2617	<sup>96</sup> 0.3374	<sup>104</sup> 0.4185
79	NTECHLAB-007	<sup>37</sup> 0.0044	<sup>43</sup> 0.0066	<sup>49</sup> 0.0089	<sup>57</sup> 0.0118	<sup>60</sup> 0.0150	<sup>84</sup> 0.018										

MISS RATES		INVESTIGATION, FNIR(N, R = 1, T = 0)								IDENTIFICATION, FNIR(N, R = L, T ≥ 0) FOR FPIR = 0.001							
#	ALGORITHM	(0, 2]	(2, 4]	(4, 6]	(6, 8]	(8, 10]	(10, 12]	(12, 14]	(14, 18]	(0, 2]	(2, 4]	(4, 6]	(6, 8]	(8, 10]	(10, 12]	(12, 14]	(14, 18]
89	PARAVISION-009																
90	PIXELALL-002	<sup>72</sup> 0.0085	<sup>78</sup> 0.0119	<sup>71</sup> 0.0147	<sup>72</sup> 0.0172	<sup>73</sup> 0.0198	<sup>91</sup> 0.0225	<sup>90</sup> 0.0270	<sup>91</sup> 0.0349	<sup>97</sup> 0.1193	<sup>97</sup> 0.1900	<sup>97</sup> 0.2601	<sup>97</sup> 0.3332	<sup>97</sup> 0.3955	<sup>114</sup> 0.4565	<sup>114</sup> 0.5268	<sup>111</sup> 0.6030
91	PIXELALL-003	<sup>46</sup> 0.0050	<sup>42</sup> 0.0063	<sup>39</sup> 0.0072	<sup>34</sup> 0.0077	<sup>33</sup> 0.0085	<sup>49</sup> 0.0095	<sup>50</sup> 0.0113	<sup>48</sup> 0.0119	<sup>44</sup> 0.0248	<sup>43</sup> 0.0418	<sup>43</sup> 0.0622	<sup>43</sup> 0.0861	<sup>43</sup> 0.1104	<sup>55</sup> 0.1364	<sup>55</sup> 0.1723	<sup>55</sup> 0.2167
92	PIXELALL-004	<sup>45</sup> 0.0049	<sup>48</sup> 0.0063	<sup>48</sup> 0.0072	<sup>37</sup> 0.0079	<sup>36</sup> 0.0089	<sup>53</sup> 0.0103	<sup>53</sup> 0.0127	<sup>53</sup> 0.0146	<sup>38</sup> 0.0211	<sup>40</sup> 0.0360	<sup>42</sup> 0.0553	<sup>42</sup> 0.0792	<sup>39</sup> 0.1045	<sup>51</sup> 0.1317	<sup>54</sup> 0.1700	<sup>58</sup> 0.2246
93	PTAKURATSATU-000	<sup>54</sup> 0.0061	<sup>55</sup> 0.0082	<sup>55</sup> 0.0097	<sup>53</sup> 0.0109	<sup>49</sup> 0.0120	<sup>63</sup> 0.0131	<sup>59</sup> 0.0146	<sup>61</sup> 0.0180	<sup>59</sup> 0.0375	<sup>57</sup> 0.0596	<sup>55</sup> 0.1116	<sup>53</sup> 0.1357	<sup>59</sup> 0.1553	<sup>61</sup> 0.1820	<sup>61</sup> 0.2326	
94	RANKONE-002	<sup>99</sup> 0.0212	<sup>98</sup> 0.0313	<sup>98</sup> 0.0431	<sup>98</sup> 0.0562	<sup>99</sup> 0.0712	<sup>117</sup> 0.0881	<sup>118</sup> 0.1130	<sup>119</sup> 0.1543	<sup>95</sup> 0.1111	<sup>95</sup> 0.1707	<sup>95</sup> 0.2305	<sup>95</sup> 0.2968	<sup>98</sup> 0.3646	<sup>113</sup> 0.4345	<sup>113</sup> 0.5172	<sup>116</sup> 0.6110
95	RANKONE-004	<sup>108</sup> 0.0424	<sup>107</sup> 0.0643	<sup>107</sup> 0.0875	<sup>107</sup> 0.1127	<sup>107</sup> 0.1364	<sup>122</sup> 0.1579	<sup>122</sup> 0.1914	<sup>122</sup> 0.2378	<sup>104</sup> 0.1855	<sup>103</sup> 0.2681	<sup>103</sup> 0.3431	<sup>101</sup> 0.4155	<sup>117</sup> 0.4785	<sup>117</sup> 0.5350	<sup>117</sup> 0.5980	<sup>117</sup> 0.6722
96	RANKONE-005	<sup>92</sup> 0.0136	<sup>93</sup> 0.0192	<sup>91</sup> 0.0246	<sup>91</sup> 0.0303	<sup>90</sup> 0.0362	<sup>108</sup> 0.0422	<sup>105</sup> 0.0521	<sup>105</sup> 0.0694	<sup>81</sup> 0.0582	<sup>75</sup> 0.0910	<sup>71</sup> 0.1260	<sup>88</sup> 0.1645	<sup>81</sup> 0.2005	<sup>81</sup> 0.2816	<sup>82</sup> 0.3522	
97	RANKONE-007	<sup>67</sup> 0.0078	<sup>64</sup> 0.0099	<sup>61</sup> 0.0113	<sup>58</sup> 0.0123	<sup>58</sup> 0.0139	<sup>76</sup> 0.0156	<sup>75</sup> 0.0191	<sup>74</sup> 0.0242	<sup>42</sup> 0.0242	<sup>42</sup> 0.0376	<sup>41</sup> 0.0542	<sup>38</sup> 0.0737	<sup>37</sup> 0.0935	<sup>51</sup> 0.1130	<sup>49</sup> 0.1416	<sup>49</sup> 0.1811
98	RANKONE-009	<sup>48</sup> 0.0054	<sup>49</sup> 0.0072	<sup>46</sup> 0.0085	<sup>47</sup> 0.0098	<sup>47</sup> 0.0113	<sup>62</sup> 0.0130	<sup>67</sup> 0.0169	<sup>71</sup> 0.0220	<sup>37</sup> 0.0208	<sup>38</sup> 0.0345	<sup>37</sup> 0.0504	<sup>36</sup> 0.0706	<sup>36</sup> 0.0930	<sup>50</sup> 0.1174	<sup>50</sup> 0.1504	<sup>52</sup> 0.2002
99	RANKONE-010	<sup>42</sup> 0.0047	<sup>38</sup> 0.0061	<sup>38</sup> 0.0070	<sup>33</sup> 0.0076	<sup>34</sup> 0.0087	<sup>50</sup> 0.0098	<sup>51</sup> 0.0113	<sup>49</sup> 0.0120	<sup>31</sup> 0.0177	<sup>29</sup> 0.0269	<sup>26</sup> 0.0368	<sup>26</sup> 0.0479	<sup>26</sup> 0.0590	<sup>34</sup> 0.0688	<sup>34</sup> 0.0803	<sup>33</sup> 0.0991
100	RANKONE-011	<sup>23</sup> 0.0031	<sup>23</sup> 0.0041	<sup>23</sup> 0.0047	<sup>23</sup> 0.0053	<sup>22</sup> 0.0058	<sup>36</sup> 0.0067	<sup>32</sup> 0.0077	<sup>34</sup> 0.0073	<sup>23</sup> 0.0127	<sup>20</sup> 0.0194	<sup>21</sup> 0.0265	<sup>20</sup> 0.0345	<sup>20</sup> 0.0422	<sup>31</sup> 0.0499	<sup>30</sup> 0.0611	<sup>22</sup> 0.0756
101	RANKONE-012																
102	REALNETWORKS-002	<sup>102</sup> 0.0381	<sup>108</sup> 0.0687	<sup>108</sup> 0.1062	<sup>108</sup> 0.1495	<sup>109</sup> 0.1963	<sup>126</sup> 0.2513	<sup>128</sup> 0.3206	<sup>128</sup> 0.3927	<sup>105</sup> 0.2153	<sup>108</sup> 0.3323	<sup>108</sup> 0.4444	<sup>108</sup> 0.5485	<sup>108</sup> 0.6355	<sup>123</sup> 0.7132	<sup>124</sup> 0.7855	<sup>124</sup> 0.8437
103	REALNETWORKS-003	<sup>103</sup> 0.0245	<sup>105</sup> 0.0437	<sup>105</sup> 0.0686	<sup>108</sup> 0.0975	<sup>108</sup> 0.1312	<sup>124</sup> 0.1719	<sup>124</sup> 0.2294	<sup>125</sup> 0.2907	<sup>98</sup> 0.1468	<sup>108</sup> 0.2370	<sup>101</sup> 0.3313	<sup>105</sup> 0.4269	<sup>103</sup> 0.5142	<sup>121</sup> 0.5979	<sup>122</sup> 0.6815	<sup>122</sup> 0.7567
104	REALNETWORKS-004	<sup>102</sup> 0.0244	<sup>104</sup> 0.0428	<sup>104</sup> 0.0663	<sup>105</sup> 0.0939	<sup>105</sup> 0.1251	<sup>123</sup> 0.1634	<sup>123</sup> 0.2785	<sup>99</sup> 0.1484	<sup>101</sup> 0.2377	<sup>100</sup> 0.3303	<sup>102</sup> 0.4249	<sup>102</sup> 0.5106	<sup>120</sup> 0.5924	<sup>121</sup> 0.6758	<sup>121</sup> 0.7534	
105	REALNETWORKS-006																
106	S1-002																
107	SCANOVATE-001	<sup>68</sup> 0.0079	<sup>72</sup> 0.0117	<sup>75</sup> 0.0151	<sup>78</sup> 0.0185	<sup>78</sup> 0.0221	<sup>95</sup> 0.0259	<sup>97</sup> 0.0321	<sup>97</sup> 0.0427	<sup>88</sup> 0.0727	<sup>88</sup> 0.1169	<sup>87</sup> 0.1650	<sup>87</sup> 0.2115	<sup>84</sup> 0.2528	<sup>101</sup> 0.2925	<sup>98</sup> 0.3437	<sup>97</sup> 0.4084
108	SENSETIME-002	<sup>96</sup> 0.0186	<sup>97</sup> 0.0191	<sup>84</sup> 0.0183	<sup>75</sup> 0.0179	<sup>68</sup> 0.0173	<sup>65</sup> 0.0133	<sup>41</sup> 0.0089	<sup>28</sup> 0.0059	<sup>40</sup> 0.0220	<sup>25</sup> 0.0236	<sup>19</sup> 0.0237	<sup>18</sup> 0.0240	<sup>17</sup> 0.0245	<sup>14</sup> 0.0219	<sup>11</sup> 0.0195	<sup>10</sup> 0.0222
109	SENSETIME-003	<sup>117</sup> 0.0021	<sup>12</sup> 0.0028	<sup>11</sup> 0.0031	<sup>7</sup> 0.0033	<sup>6</sup> 0.0035	<sup>10</sup> 0.0040	<sup>13</sup> 0.0047	<sup>13</sup> 0.0033	<sup>8</sup> 0.0046	<sup>8</sup> 0.0064	<sup>6</sup> 0.0076	<sup>4</sup> 0.0086	<sup>4</sup> 0.0101	<sup>7</sup> 0.0122	<sup>8</sup> 0.0155	<sup>8</sup> 0.0196
110	SENSETIME-004	<sup>3</sup> 0.0016	<sup>3</sup> 0.0022	<sup>3</sup> 0.0025	<sup>3</sup> 0.0028	<sup>30</sup> 0.0030	<sup>4</sup> 0.0035	<sup>8</sup> 0.0043	<sup>7</sup> 0.0025	<sup>40</sup> 0.0036	<sup>4</sup> 0.0052	<sup>3</sup> 0.0066	<sup>3</sup> 0.0081	<sup>3</sup> 0.0099	<sup>9</sup> 0.0169	<sup>11</sup> 0.0230	
111	SENSETIME-005	<sup>2</sup> 0.0015	<sup>2</sup> 0.0020	<sup>2</sup> 0.0024	<sup>2</sup> 0.0026	<sup>2</sup> 0.0029	<sup>3</sup> 0.0035	<sup>7</sup> 0.0043	<sup>10</sup> 0.0028	<sup>5</sup> 0.0036	<sup>7</sup> 0.0059	<sup>8</sup> 0.0089	<sup>9</sup> 0.0128	<sup>10</sup> 0.0177	<sup>15</sup> 0.0240	<sup>17</sup> 0.0345	<sup>17</sup> 0.0493
112	SENSETIME-006	<sup>1</sup> 0.0015	<sup>1</sup> 0.0019	<sup>1</sup> 0.0022	<sup>1</sup> 0.0027	<sup>1</sup> 0.0033	<sup>3</sup> 0.0040	<sup>5</sup> 0.0021	<sup>2</sup> 0.0031	<sup>2</sup> 0.0049	<sup>4</sup> 0.0068	<sup>6</sup> 0.0097	<sup>7</sup> 0.0132	<sup>12</sup> 0.0184	<sup>14</sup> 0.0262	<sup>14</sup> 0.0359	
113	SENSETIME-007																
114	SIAT-002	<sup>117</sup> 0.8309	<sup>117</sup> 0.8310	<sup>117</sup> 0.8311	<sup>117</sup> 0.8306	<sup>117</sup> 0.8296	<sup>134</sup> 0.8302	<sup>134</sup> 0.8300	<sup>135</sup> 0.8301	<sup>117</sup> 0.8340	<sup>116</sup> 0.8368	<sup>109</sup> 0.8404	<sup>126</sup> 0.8480	<sup>126</sup> 0.8532	<sup>126</sup> 0.8595	<sup>12</sup> 0.8691	
115	SYNESIS-003	<sup>89</sup> 0.0125	<sup>85</sup> 0.0151	<sup>83</sup> 0.0174	<sup>80</sup> 0.0199	<sup>79</sup> 0.0223	<sup>92</sup> 0.0240	<sup>92</sup> 0.0279	<sup>87</sup> 0.0331	<sup>85</sup> 0.0568	<sup>83</sup> 0.1052	<sup>83</sup> 0.1483	<sup>82</sup> 0.1968	<sup>82</sup> 0.2399	<sup>97</sup> 0.2834	<sup>96</sup> 0.3405	
116	SYNESIS-005	<sup>9</sup> 0.0044	<sup>3</sup> 0.0058	<sup>3</sup> 0.0070	<sup>46</sup> 0.0080	<sup>37</sup> 0.0091	<sup>52</sup> 0.0103	<sup>52</sup> 0.0125	<sup>24</sup> 0.0152	<sup>46</sup> 0.0262	<sup>45</sup> 0.0444	<sup>45</sup> 0.0666	<sup>45</sup> 0.0923	<sup>4</sup> 0.1156	<sup>39</sup> 0.1399	<sup>57</sup> 0.1736	<sup>56</sup> 0.2185
117	TECH5-001	<sup>57</sup> 0.0061	<sup>61</sup> 0.0093	<sup>66</sup> 0.0128	<sup>71</sup> 0.0171	<sup>77</sup> 0.0221	<sup>99</sup> 0.0289	<sup>102</sup> 0.0412	<sup>102</sup> 0.0560	<sup>86</sup> 0.0660	<sup>87</sup> 0.1156	<sup>90</sup> 0.1733	<sup>91</sup> 0.2385	<sup>91</sup> 0.2998	<sup>108</sup> 0.3629	<sup>110</sup> 0.4424	<sup>111</sup> 0.5284
118	TOSHIBA-001	<sup>73</sup> 0.0088	<sup>74</sup> 0.0119	<sup>71</sup> 0.0150	<sup>74</sup> 0.0178	<sup>75</sup> 0.0209	<sup>93</sup> 0.0241	<sup>93</sup> 0.0292	<sup>92</sup> 0.0365								
119	TRUEFACE-000	<sup>36</sup> 0.0043	<sup>36</sup> 0.0057	<sup>36</sup> 0.0061	<sup>29</sup> 0.0067	<sup>27</sup> 0.0073	<sup>43</sup> 0.0084	<sup>43</sup> 0.0097	<sup>41</sup> 0.0099	<sup>35</sup> 0.0200	<sup>37</sup> 0.0338	<sup>38</sup> 0.0504	<sup>35</sup> 0.0705	<sup>35</sup> 0.0904	<sup>30</sup> 0.1112	<sup>48</sup> 0.1401	<sup>48</sup> 0.1792
120	VERIDAS-001	<sup>30</sup> 0.0063	<sup>30</sup> 0.0083	<sup>30</sup> 0.0099	<sup>56</sup> 0.0113	<sup>56</sup> 0.0132	<sup>71</sup> 0.0148	<sup>72</sup> 0.0184	<sup>61</sup> 0.0219	<sup>61</sup> 0.0403	<sup>61</sup> 0.0684	<sup>62</sup> 0.1012	<sup>62</sup> 0.1386	<sup>62</sup> 0.1741	<sup>79</sup> 0.2113	<sup>79</sup> 0.2611	<sup>80</sup> 0.3233
121	VISIONLABS-004	<sup>45</sup> 0.0048	<sup>46</sup> 0.0069	<sup>59</sup> 0.0091	<sup>59</sup> 0.0111	<sup>59</sup> 0.0130	<sup>74</sup> 0.0152	<sup>73</sup> 0.0187	<sup>75</sup> 0.0242	<sup>74</sup> 0.0540	<sup>77</sup> 0.0916	<sup>78</sup> 0.1358	<sup>78</sup> 0.1855	<sup>79</sup> 0.2303	<sup>95</sup> 0.2745	<sup>94</sup> 0.3312	<sup>90</sup> 0.3913
122	VISIONLABS-005	<sup>39</sup> 0.0044	<sup>39</sup> 0.0063	<sup>43</sup> 0.0081	<sup>46</sup> 0.0095	<sup>46</sup> 0.0109	<sup>61</sup> 0.0125	<sup>62</sup> 0.0151	<sup>63</sup> 0.0187	<sup>67</sup> 0.0479	<sup>67</sup> 0.0812	<sup>68</sup> 0.1212	<sup>69</sup> 0.1644	<sup>69</sup> 0.2078	<sup>81</sup> 0.2473	<sup>84</sup> 0.2999	<sup>85</sup> 0.3577
123	VISIONLABS-006	<sup>29</sup> 0.0035	<sup>30</sup> 0.0048	<sup>30</sup> 0.0061	<sup>30</sup> 0.0069	<sup>29</sup> 0.0077	<sup>44</sup> 0.0087	<sup>47</sup> 0.0105	<sup>50</sup> 0.0120	<sup>48</sup> 0.0273	<sup>47</sup> 0.0465	<sup>47</sup> 0.0702	<sup>47</sup> 0.0970	<sup>47</sup> 0.1228	<sup>61</sup> 0.1486	<sup>60</sup> 0.1847	<sup>60</sup> 0.2295
124	VISIONLABS-008	<sup>21</sup> 0.0028	<sup>20</sup> 0.0037	<sup>21</sup> 0.0047	<sup>22</sup> 0.0053	<sup>23</sup> 0.0058	<sup>34</sup> 0.0067	<sup>38</sup> 0.0081	<sup>39</sup> 0.0085	<sup>27</sup> 0.0143	<sup>27</sup> 0.0241	<sup>28</sup> 0.0373	<sup>27</sup> 0.0519	<sup>27</sup> 0.0677	<sup>38</sup> 0.0850	<sup>39</sup> 0.1104	<sup>39</sup> 0.1444
125	VISIONLABS-009	<sup>10</sup> 0.0020	<sup>10</sup> 0.0026	<sup>10</sup> 0.0030	<sup>10</sup> 0.0034	<sup>16</sup> 0.0044	<sup>19</sup> 0.0052	<sup>21</sup> 0.0046	<sup>14</sup> 0.0065	<sup>15</sup> 0.0105	<sup>15</sup> 0.0156	<sup>15</sup> 0.0217	<sup>15</sup> 0.0289	<sup>20</sup> 0.0368	<sup>23</sup> 0.0499	<sup>23</sup> 0.0681	
126	VISIONLABS-010	<sup>9</sup> 0.0020	<sup>9</sup> 0.0025	<sup>9</sup> 0.0030	<sup>11</sup> 0.0034	<sup>9</sup> 0.0036	<sup>16</sup> 0.0043	<sup>16</sup> 0.0151	<sup>23</sup> 0.0047	<sup>17</sup> 0.0069	<sup>1</sup>						

MISS RATES		INVESTIGATION, FNIR(N, R = 1, T = 0)								IDENTIFICATION, FNIR(N, R = L, T ≥ 0) FOR FPIR = 0.001							
#	ALGORITHM	(0, 2]	(2, 4]	(4, 6]	(6, 8]	(8, 10]	(10, 12]	(12, 14]	(14, 18]	(0, 2]	(2, 4]	(4, 6]	(6, 8]	(8, 10]	(10, 12]	(12, 14]	(14, 18]
133	YITU-004	<sup>35</sup> 0.0061	<sup>31</sup> 0.0075	<sup>44</sup> 0.0081	<sup>41</sup> 0.0081	<sup>39</sup> 0.0092	<sup>35</sup> 0.0107	<sup>64</sup> 0.0154	<sup>66</sup> 0.0207	<sup>22</sup> 0.0125	<sup>22</sup> 0.0204	<sup>23</sup> 0.0314	<sup>25</sup> 0.0469	<sup>26</sup> 0.0671	<sup>42</sup> 0.0955	<sup>51</sup> 0.1421	<sup>53</sup> 0.2006
134	YITU-005	<sup>61</sup> 0.0067	<sup>34</sup> 0.0080	<sup>47</sup> 0.0087	<sup>45</sup> 0.0085	<sup>41</sup> 0.0094	<sup>56</sup> 0.0108	<sup>63</sup> 0.0151	<sup>65</sup> 0.0204	<sup>21</sup> 0.0124	<sup>21</sup> 0.0198	<sup>22</sup> 0.0308	<sup>22</sup> 0.0462	<sup>25</sup> 0.0667	<sup>41</sup> 0.0953	<sup>50</sup> 0.1418	<sup>51</sup> 0.1930

Table 10: **Accuracy for the FRVT 2018 mugshot sets under ageing.** The second row shows the time lapse between gallery and subsequent probe images, in years. The first two columns identify the algorithm. The next 8 values give rank-based FNIR with  $R = 1$ ,  $T = 0$  and FPIR = 1. All these are relevant to investigational uses where candidates from all searches would need human review. The second 8 values give threshold-based FNIR with  $T \geq 0$ , FPIR = 0.001 and no rank criterion. The shaded cells indicate the three most accurate algorithms for that elapsed time. The gallery size is 3068801. The total number of searches is 10951064.

#	ALGORITHM	INVESTIGATION MODE						IDENTIFICATION MODE						FAILURE TO EXTRACT FEATURES						FEATURES									
		RANK ONE MISS RATE, FNIR(N, 0, 1)						HIGH T → FPIR = 0.001, FNIR(N, T, L)						N=1.6M						N=1.6M									
		GALLERY		MUGSHOT	MUGSHOT	MUGSHOT	VISA	BORDER	BOR <sub>L</sub> 10YR	KIOSK	MUGSHOT	MUGSHOT	MUGSHOT	VISA	BORDER	BOR <sub>L</sub> 10YR	KIOSK	MUGSHOT	MUGSHOT	MUGSHOT	VISA	BORDER	KIOSK						
1	20FACE-000	25 <sup>0.055</sup>	24 <sup>0.085</sup>	15 <sup>0.736</sup>	17 <sup>0.056</sup>	10 <sup>0.239</sup>	17 <sup>0.243</sup>	25 <sup>0.348</sup>	24 <sup>0.450</sup>	22 <sup>1.000</sup>	18 <sup>0.424</sup>	10 <sup>0.772</sup>	17 <sup>0.938</sup>	0.000	0.000	0.000	0.000	0.000	0.000	0.000	0.000	0.000	0.000	0.000	0.000				
2	3DIVI-003	26 <sup>0.083</sup>	26 <sup>0.206</sup>	19 <sup>0.141</sup>	19 <sup>0.474</sup>	20 <sup>0.400</sup>	26 <sup>0.626</sup>	19 <sup>0.605</sup>	15 <sup>0.821</sup>	0.005	15 <sup>0.821</sup>	0.002	0.002	0.005	0.000	0.000	0.000	0.000	0.000	0.000	0.000	0.000	0.000	0.000	0.000				
3	3DIVI-004	22 <sup>0.018</sup>	23 <sup>0.062</sup>	17 <sup>0.035</sup>	17 <sup>0.279</sup>	23 <sup>0.169</sup>	23 <sup>0.343</sup>	17 <sup>0.277</sup>	13 <sup>0.607</sup>	0.005	13 <sup>0.607</sup>	0.002	0.002	0.005	0.000	0.000	0.000	0.000	0.000	0.000	0.000	0.000	0.000	0.000	0.000				
4	3DIVI-005	22 <sup>0.018</sup>	23 <sup>0.062</sup>	20 <sup>0.930</sup>	21 <sup>0.821</sup>	17 <sup>0.279</sup>	22 <sup>0.166</sup>	23 <sup>0.339</sup>	14 <sup>0.996</sup>	20 <sup>0.864</sup>	13 <sup>0.597</sup>	0.002	0.005	0.442	0.000	0.000	0.000	0.000	0.000	0.000	0.000	0.000	0.000	0.000	0.000	0.000			
5	3DIVI-006	23 <sup>0.024</sup>	23 <sup>0.074</sup>	17 <sup>0.047</sup>	17 <sup>0.342</sup>	18 <sup>0.312</sup>	23 <sup>0.168</sup>	23 <sup>0.342</sup>	17 <sup>0.283</sup>	14 <sup>0.615</sup>	0.002	0.005	0.000	0.000	0.000	0.000	0.000	0.000	0.000	0.000	0.000	0.000	0.000	0.000	0.000				
6	ACER-000	20 <sup>0.011</sup>	19 <sup>0.036</sup>	18 <sup>0.827</sup>	19 <sup>0.025</sup>	16 <sup>0.209</sup>	22 <sup>0.146</sup>	21 <sup>0.246</sup>	10 <sup>0.981</sup>	16 <sup>0.201</sup>	12 <sup>0.490</sup>	0.000	0.000	0.042	0.000	0.000	0.000	0.000	0.000	0.000	0.000	0.000	0.000	0.000	0.000	0.000			
7	ACER-001	15 <sup>0.005</sup>	14 <sup>0.020</sup>	9 <sup>0.422</sup>	12 <sup>0.008</sup>	9 <sup>0.050</sup>	8 <sup>0.098</sup>	16 <sup>0.056</sup>	14 <sup>0.109</sup>	17 <sup>0.999</sup>	13 <sup>0.068</sup>	9 <sup>0.406</sup>	12 <sup>0.479</sup>	0.001	0.001	0.041	0.000	0.000	0.000	0.000	0.000	0.000	0.000	0.000	0.000	0.000			
8	AIZE-001	16 <sup>0.006</sup>	15 <sup>0.022</sup>	14 <sup>0.683</sup>	14 <sup>0.016</sup>	9 <sup>0.050</sup>	14 <sup>0.165</sup>	18 <sup>0.077</sup>	17 <sup>0.143</sup>	12 <sup>0.994</sup>	14 <sup>0.101</sup>	8 <sup>0.364</sup>	10 <sup>0.387</sup>	0.001	0.001	0.047	0.000	0.000	0.000	0.000	0.000	0.000	0.000	0.000	0.000	0.000			
9	ALCHERA-000	21 <sup>0.016</sup>	21 <sup>0.047</sup>	18 <sup>0.870</sup>	17 <sup>0.046</sup>	18 <sup>0.292</sup>	21 <sup>0.138</sup>	19 <sup>0.216</sup>	16 <sup>0.999</sup>	16 <sup>0.176</sup>	15 <sup>0.803</sup>	0.006	0.006	0.328	0.000	0.000	0.000	0.000	0.000	0.000	0.000	0.000	0.000	0.000	0.000	0.000			
10	ALCHERA-001	29 <sup>0.987</sup>	28 <sup>1.000</sup>	21 <sup>1.000</sup>	29 <sup>1.000</sup>	28 <sup>0.999</sup>	28 <sup>1.000</sup>	28 <sup>0.999</sup>	28 <sup>1.000</sup>	26 <sup>1.000</sup>	26 <sup>1.000</sup>	0.006	0.006	0.324	0.000	0.000	0.000	0.000	0.000	0.000	0.000	0.000	0.000	0.000	0.000	0.000			
11	ALCHERA-002	26 <sup>0.095</sup>	25 <sup>0.166</sup>	21 <sup>0.954</sup>	20 <sup>0.668</sup>	19 <sup>0.446</sup>	26 <sup>0.486</sup>	25 <sup>0.591</sup>	18 <sup>0.100</sup>	19 <sup>0.827</sup>	15 <sup>0.811</sup>	0.001	0.001	0.106	0.000	0.000	0.000	0.000	0.000	0.000	0.000	0.000	0.000	0.000	0.000	0.000			
12	ALCHERA-003	19 <sup>0.010</sup>	19 <sup>0.035</sup>	15 <sup>0.741</sup>	14 <sup>0.016</sup>	10 <sup>0.088</sup>	13 <sup>0.144</sup>	25 <sup>0.394</sup>	25 <sup>0.529</sup>	12 <sup>0.991</sup>	18 <sup>0.424</sup>	9 <sup>0.708</sup>	13 <sup>0.546</sup>	0.001	0.001	0.046	0.000	0.000	0.000	0.000	0.000	0.000	0.000	0.000	0.000	0.000			
13	ALCHERA-004	20 <sup>0.011</sup>	19 <sup>0.038</sup>	9 <sup>0.345</sup>	14 <sup>0.017</sup>	10 <sup>0.088</sup>	18 <sup>0.144</sup>	21 <sup>0.239</sup>	17 <sup>0.999</sup>	16 <sup>0.172</sup>	11 <sup>0.464</sup>	0.001	0.001	0.106	0.000	0.000	0.000	0.000	0.000	0.000	0.000	0.000	0.000	0.000	0.000	0.000			
14	ALLGOVISION-000	20 <sup>0.011</sup>	18 <sup>0.033</sup>	16 <sup>0.894</sup>	15 <sup>0.021</sup>	18 <sup>0.282</sup>	19 <sup>0.088</sup>	18 <sup>0.166</sup>	11 <sup>0.990</sup>	14 <sup>0.117</sup>	13 <sup>0.526</sup>	0.002	0.002	0.122	0.000	0.000	0.000	0.000	0.000	0.000	0.000	0.000	0.000	0.000	0.000	0.000			
15	ALLGOVISION-001	18 <sup>0.009</sup>	20 <sup>0.038</sup>	13 <sup>0.661</sup>	15 <sup>0.021</sup>	17 <sup>0.241</sup>	19 <sup>0.102</sup>	20 <sup>0.221</sup>	10 <sup>0.986</sup>	15 <sup>0.150</sup>	12 <sup>0.491</sup>	0.001	0.001	0.042	0.000	0.000	0.000	0.000	0.000	0.000	0.000	0.000	0.000	0.000	0.000	0.000			
16	ANKE-000	21 <sup>0.013</sup>	19 <sup>0.038</sup>	20 <sup>0.931</sup>	25 <sup>1.000</sup>	24 <sup>1.000</sup>	20 <sup>0.117</sup>	20 <sup>0.220</sup>	12 <sup>0.994</sup>	23 <sup>1.000</sup>	22 <sup>1.000</sup>	0.000	0.000	0.080	0.000	0.000	0.000	0.000	0.000	0.000	0.000	0.000	0.000	0.000	0.000	0.000			
17	ANKE-001	21 <sup>0.013</sup>	19 <sup>0.038</sup>	20 <sup>0.946</sup>	27 <sup>1.000</sup>	24 <sup>1.000</sup>	20 <sup>0.119</sup>	20 <sup>0.220</sup>	13 <sup>0.994</sup>	23 <sup>1.000</sup>	22 <sup>1.000</sup>	0.000	0.000	0.080	0.000	0.000	0.000	0.000	0.000	0.000	0.000	0.000	0.000	0.000	0.000	0.000			
18	ANKE-002	11 <sup>0.003</sup>	11 <sup>0.016</sup>	11 <sup>0.522</sup>	8 <sup>0.005</sup>	10 <sup>0.119</sup>	12 <sup>0.032</sup>	11 <sup>0.079</sup>	7 <sup>0.948</sup>	9 <sup>0.034</sup>	7 <sup>0.245</sup>	0.001	0.001	0.049	0.000	0.000	0.000	0.000	0.000	0.000	0.000	0.000	0.000	0.000	0.000	0.000	0.000		
19	AWARE-003	24 <sup>0.031</sup>	24 <sup>0.090</sup>	22 <sup>0.966</sup>	19 <sup>0.316</sup>	18 <sup>0.290</sup>	21 <sup>0.128</sup>	22 <sup>0.298</sup>	10 <sup>0.984</sup>	18 <sup>0.428</sup>	13 <sup>0.530</sup>	0.004	0.003	0.874	0.000	0.000	0.000	0.000	0.000	0.000	0.000	0.000	0.000	0.000	0.000	0.000	0.000		
20	AWARE-004	25 <sup>0.068</sup>	25 <sup>0.176</sup>	23 <sup>0.976</sup>	19 <sup>0.122</sup>	19 <sup>0.414</sup>	24 <sup>0.269</sup>	25 <sup>0.509</sup>	19 <sup>1.000</sup>	17 <sup>0.397</sup>	15 <sup>0.816</sup>	0.003	0.003	0.776	0.000	0.000	0.000	0.000	0.000	0.000	0.000	0.000	0.000	0.000	0.000	0.000	0.000		
21	AWARE-005	24 <sup>0.031</sup>	23 <sup>0.067</sup>	23 <sup>0.978</sup>	17 <sup>0.048</sup>	18 <sup>0.308</sup>	25 <sup>0.364</sup>	21 <sup>0.253</sup>	19 <sup>0.960</sup>	17 <sup>0.255</sup>	17 <sup>0.916</sup>	0.001	0.001	0.189	0.000	0.000	0.000	0.000	0.000	0.000	0.000	0.000	0.000	0.000	0.000	0.000	0.000		
22	AWARE-006	26 <sup>0.070</sup>	25 <sup>0.128</sup>	23 <sup>0.983</sup>	18 <sup>0.111</sup>	19 <sup>0.421</sup>	24 <sup>0.276</sup>	25 <sup>0.398</sup>	18 <sup>0.999</sup>	17 <sup>0.368</sup>	14 <sup>0.749</sup>	0.001	0.001	0.189	0.000	0.000	0.000	0.000	0.000	0.000	0.000	0.000	0.000	0.000	0.000	0.000	0.000		
23	AYONIX-000	28 <sup>0.450</sup>	28 <sup>0.685</sup>	24 <sup>0.996</sup>	20 <sup>0.607</sup>	20 <sup>0.867</sup>	27 <sup>0.811</sup>	26 <sup>0.939</sup>	15 <sup>0.998</sup>	20 <sup>0.954</sup>	18 <sup>0.982</sup>	0.010	0.010	0.939	0.000	0.000	0.000	0.000	0.000	0.000	0.000	0.000	0.000	0.000	0.000	0.000	0.000	0.000	
24	AYONIX-001	28 <sup>0.341</sup>	27 <sup>0.527</sup>	24 <sup>0.993</sup>	21 <sup>0.994</sup>	20 <sup>0.778</sup>	27 <sup>0.824</sup>	27 <sup>0.920</sup>	18 <sup>0.999</sup>	20 <sup>0.999</sup>	18 <sup>0.969</sup>	0.010	0.010	0.939	0.000	0.000	0.000	0.000	0.000	0.000	0.000	0.000	0.000	0.000	0.000	0.000	0.000	0.000	
25	AYONIX-002	27 <sup>0.341</sup>	27 <sup>0.527</sup>	24 <sup>0.993</sup>	20 <sup>0.464</sup>	20 <sup>0.778</sup>	27 <sup>0.824</sup>	27 <sup>0.920</sup>	18 <sup>0.999</sup>	20 <sup>0.915</sup>	18 <sup>0.969</sup>	0.010	0.010	0.939	0.000	0.000	0.000	0.000	0.000	0.000	0.000	0.000	0.000	0.000	0.000	0.000	0.000	0.000	
26	CAMVI-003	25 <sup>0.052</sup>	24 <sup>0.090</sup>	19 <sup>0.911</sup>	18 <sup>0.093</sup>	19 <sup>0.360</sup>	17 <sup>0.071</sup>	16 <sup>0.132</sup>	8 <sup>0.970</sup>	14 <sup>0.114</sup>	10 <sup>0.402</sup>	0.006	0.006	0.675	0.000	0.000	0.000	0.000	0.000	0.000	0.000	0.000	0.000	0.000	0.000	0.000	0.000	0.000	0.000
27	CAMVI-004	25 <sup>0.047</sup>	25 <sup>0.077</sup>	15 <sup>0.744</sup>	18 <sup>0.072</sup>	18 <sup>0.296</sup>	17 <sup>0.072</sup>	16 <sup>0.136</sup>	17 <sup>0.999</sup>	14 <sup>0.100</sup>	15 <sup>0.787</sup>	0.000	0.000	0.000	0.000	0.000	0.000	0.000	0.000	0.000	0.000	0.000	0.000	0.000	0.000	0.000	0.000	0.000	
28	CAMVI-005	25 <sup>0.065</sup>	25 <sup>0.103</sup>	15 <sup>0.746</sup>	18 <sup>0.098</sup>	18 <sup>0.341</sup>	19 <sup>0.099</sup>	15 <sup>0.179</sup>	15 <sup>0.156</sup>	15 <sup>0.999</sup>	14 <sup>0.999</sup>	0.000	0.000	0.000	0.000	0.000	0.000	0.000	0.000	0.000	0.000	0.000	0.000	0.000	0.000	0.000	0.000	0.000	0.000
29	CANON-001	14 <sup>0.001</sup>	27 <sup>0.068</sup>	16 <sup>0.001</sup>	14 <sup>0.007</sup>	14 <sup>0.062</sup>	3 <sup>0.005</sup>	2 <sup>0.023</sup>	17 <sup>0.365</sup>	21 <sup>0.008</sup>	24 <sup>0.068</sup>	3 <sup>0.139</sup>	0.001																

#	ALGORITHM	INVESTIGATION MODE						IDENTIFICATION MODE						FAILURE TO EXTRACT FEATURES					
		RANK ONE MISS RATE, FNIR(N, 0, 1)						HIGH T → FPIR = 0.001, FNIR(N, T, L)											
		N=1.6M						N=1.6M											
	GALLERY	MUGSHOT	MUGSHOT	MUGSHOT	VISA	BORDER	VISA	MUGSHOT	MUGSHOT	MUGSHOT	VISA	BORDER	VISA	MUGSHOT	MUGSHOT	MUGSHOT	VISA	BORDER	KIOSK
PROBE		MUGSHOT	WEBCAM	PROFILE	BORDER	BOR <sub>E</sub> 10YR	KIOSK	MUGSHOT	WEBCAM	PROFILE	BORDER	BOR <sub>E</sub> 10YR	KIOSK	MUGSHOT	WEBCAM	PROFILE	BORDER	BOR <sub>E</sub> 10YR	KIOSK
47	COGNITEC-005	<sup>30</sup> 0.002	<sup>47</sup> 0.010	<sup>150</sup> 0.021	<sup>131</sup> 0.021	<sup>87</sup> 0.037	<sup>104</sup> 0.115	<sup>46</sup> 0.010	<sup>33</sup> 0.041	<sup>271</sup> 1.000	<sup>101</sup> 0.041	<sup>51</sup> 0.157	<sup>52</sup> 0.179	0.002	0.001	0.614	0.017	0.017	0.017
48	COGNITEC-006	<sup>48</sup> 0.002	<sup>37</sup> 0.010	<sup>147</sup> 0.703	<sup>115</sup> 0.007	<sup>70</sup> 0.024	<sup>97</sup> 0.111	<sup>41</sup> 0.008	<sup>49</sup> 0.040	<sup>286</sup> 1.000	<sup>79</sup> 0.030	<sup>50</sup> 0.171	<sup>144</sup> 0.681	0.002	0.001	0.568	0.003	0.003	0.003
49	CUBOX-000	<sup>35</sup> 0.001	<sup>44</sup> 0.010	<sup>4</sup> 0.058	<sup>19</sup> 0.002	<sup>5</sup> 0.004	<sup>1</sup> 0.049	<sup>16</sup> 0.003	<sup>17</sup> 0.019	<sup>4</sup> 0.168	<sup>7</sup> 0.004	<sup>8</sup> 0.028	<sup>2</sup> 0.073	0.001	0.000	0.042	0.000	0.000	0.000
50	CYBERLINK-000	<sup>13</sup> 0.004	<sup>144</sup> 0.020	<sup>151</sup> 0.717	<sup>118</sup> 0.007	<sup>122</sup> 0.134	<sup>163</sup> 0.056	<sup>149</sup> 0.116	<sup>141</sup> 0.995	<sup>126</sup> 0.063	<sup>96</sup> 0.339	0.001	0.001	0.063	0.000	0.000	0.000	0.000	0.000
51	CYBERLINK-001	<sup>129</sup> 0.004	<sup>132</sup> 0.018	<sup>152</sup> 0.731	<sup>111</sup> 0.007	<sup>125</sup> 0.133	<sup>156</sup> 0.054	<sup>146</sup> 0.109	<sup>136</sup> 0.995	<sup>123</sup> 0.062	<sup>141</sup> 0.652	0.000	0.000	0.040	0.000	0.000	0.000	0.000	0.000
52	CYBERLINK-002	<sup>10</sup> 0.003	<sup>72</sup> 0.012	<sup>131</sup> 0.577	<sup>71</sup> 0.004	<sup>96</sup> 0.107	<sup>69</sup> 0.015	<sup>77</sup> 0.053	<sup>112</sup> 0.988	<sup>67</sup> 0.024	<sup>88</sup> 0.288	0.001	0.000	0.042	0.000	0.000	0.000	0.000	0.000
53	CYBERLINK-003	<sup>49</sup> 0.002	<sup>29</sup> 0.009	<sup>108</sup> 0.474	<sup>52</sup> 0.003	<sup>38</sup> 0.012	<sup>48</sup> 0.082	<sup>42</sup> 0.008	<sup>43</sup> 0.035	<sup>85</sup> 0.972	<sup>40</sup> 0.012	<sup>34</sup> 0.100	<sup>101</sup> 0.368	0.000	0.000	0.039	0.000	0.000	0.000
54	CYBERLINK-004	<sup>56</sup> 0.002	<sup>68</sup> 0.011	<sup>100</sup> 0.423	<sup>56</sup> 0.003	<sup>36</sup> 0.011	<sup>81</sup> 0.104	<sup>39</sup> 0.007	<sup>40</sup> 0.036	<sup>224</sup> 1.000	<sup>42</sup> 0.013	<sup>36</sup> 0.109	<sup>18</sup> 0.954	0.000	0.000	0.011	0.000	0.000	0.000
55	CYBERLINK-005	<sup>66</sup> 0.002	<sup>54</sup> 0.011	<sup>57</sup> 0.209	<sup>34</sup> 0.002	<sup>31</sup> 0.010	<sup>69</sup> 0.098	<sup>50</sup> 0.010	<sup>56</sup> 0.041	<sup>193</sup> 1.000	<sup>43</sup> 0.014	<sup>30</sup> 0.089	<sup>177</sup> 0.926	0.000	0.000	0.034	0.000	0.000	0.000
56	DAHUA-000	<sup>192</sup> 0.009	<sup>177</sup> 0.026					<sup>190</sup> 0.086	<sup>165</sup> 0.135					0.004	0.003	0.000	0.000	0.000	0.000
57	DAHUA-001	<sup>17</sup> 0.007	<sup>169</sup> 0.024	<sup>148</sup> 0.703				<sup>180</sup> 0.073	<sup>159</sup> 0.122	<sup>97</sup> 0.980				0.002	0.002	0.346	0.000	0.000	0.000
58	DAHUA-002	<sup>69</sup> 0.002	<sup>71</sup> 0.012	<sup>80</sup> 0.304	<sup>48</sup> 0.003	<sup>50</sup> 0.084	<sup>70</sup> 0.015	<sup>59</sup> 0.046	<sup>37</sup> 0.638	<sup>48</sup> 0.017	<sup>42</sup> 0.159	0.001	0.000	0.099	0.000	0.000	0.000	0.000	0.000
59	DAHUA-003	<sup>27</sup> 0.001	<sup>12</sup> 0.007	<sup>55</sup> 0.206	<sup>27</sup> 0.002	<sup>29</sup> 0.009	<sup>29</sup> 0.073	<sup>64</sup> 0.014	<sup>55</sup> 0.041	<sup>32</sup> 0.579	<sup>41</sup> 0.013	<sup>28</sup> 0.081	<sup>29</sup> 0.134	0.000	0.000	0.000	0.000	0.000	0.000
60	DAHUA-004	<sup>12</sup> 0.001	<sup>16</sup> 0.008	<sup>42</sup> 0.144	<sup>20</sup> 0.002	<sup>17</sup> 0.007	<sup>20</sup> 0.069	<sup>38</sup> 0.007	<sup>29</sup> 0.026	<sup>26</sup> 0.485	<sup>28</sup> 0.008	<sup>15</sup> 0.051	<sup>22</sup> 0.113	0.000	0.000	0.000	0.000	0.000	0.000
61	DAON-000	<sup>13</sup> 0.004	<sup>126</sup> 0.017	<sup>120</sup> 0.530	<sup>89</sup> 0.005	<sup>62</sup> 0.020	<sup>11</sup> 0.125	<sup>98</sup> 0.023	<sup>81</sup> 0.061	<sup>194</sup> 1.000	<sup>68</sup> 0.225	<sup>69</sup> 0.173	<sup>16</sup> 0.846	0.002	0.002	0.108	0.001	0.001	0.001
62	DECATUR-000	<sup>86</sup> 0.002	<sup>70</sup> 0.011	<sup>63</sup> 0.229	<sup>81</sup> 0.004	<sup>59</sup> 0.019	<sup>93</sup> 0.109	<sup>101</sup> 0.023	<sup>91</sup> 0.066	<sup>42</sup> 0.675	<sup>72</sup> 0.027	<sup>59</sup> 0.173	<sup>69</sup> 0.239	0.001	0.000	0.044	0.001	0.001	0.001
63	DEEPLINT-001	<sup>39</sup> 0.001	<sup>10</sup> 0.007	<sup>53</sup> 0.200	<sup>41</sup> 0.002	<sup>29</sup> 0.073	<sup>26</sup> 0.003	<sup>11</sup> 0.014	<sup>185</sup> 1.000	<sup>16</sup> 0.006	<sup>41</sup> 0.159	0.000	0.000	0.038	0.000	0.000	0.000	0.000	0.000
64	DEEPSEA-001	<sup>143</sup> 0.004	<sup>116</sup> 0.016	<sup>128</sup> 0.814	<sup>122</sup> 0.010	<sup>132</sup> 0.140	<sup>143</sup> 0.046	<sup>137</sup> 0.101	<sup>105</sup> 0.985	<sup>134</sup> 0.077	<sup>95</sup> 0.326	0.000	0.001	0.047	0.000	0.000	0.000	0.000	0.000
65	DERMALOG-003	<sup>26</sup> 0.126	<sup>262</sup> 0.217		<sup>19</sup> 0.296		<sup>20</sup> 0.560	<sup>26</sup> 0.482	<sup>26</sup> 0.655	<sup>198</sup> 0.677	<sup>16</sup> 0.870	0.002	0.002	0.103	0.000	0.000	0.000	0.000	0.000
66	DERMALOG-004	<sup>288</sup> 0.125	<sup>261</sup> 0.215	<sup>201</sup> 0.930	<sup>191</sup> 0.135	<sup>196</sup> 0.467	<sup>264</sup> 0.480	<sup>263</sup> 0.657	<sup>142</sup> 0.995	<sup>193</sup> 0.603	<sup>165</sup> 0.856	0.001	0.001	0.107	0.000	0.000	0.000	0.000	0.000
67	DERMALOG-005	<sup>21</sup> 0.015	<sup>196</sup> 0.037	<sup>146</sup> 0.701	<sup>196</sup> 0.242	<sup>193</sup> 0.384	<sup>193</sup> 0.088	<sup>17</sup> 0.154	<sup>116</sup> 0.990	<sup>174</sup> 0.300	<sup>139</sup> 0.614	0.001	0.002	0.102	0.000	0.000	0.000	0.000	0.000
68	DERMALOG-006	<sup>18</sup> 0.008	<sup>173</sup> 0.024	<sup>137</sup> 0.619	<sup>128</sup> 0.010	<sup>141</sup> 0.155	<sup>150</sup> 0.052	<sup>140</sup> 0.105	<sup>99</sup> 0.981	<sup>121</sup> 0.059	<sup>93</sup> 0.318	0.003	0.006	0.181	0.000	0.000	0.000	0.000	0.000
69	DERMALOG-007	<sup>19</sup> 0.009	<sup>178</sup> 0.027	<sup>141</sup> 0.675	<sup>143</sup> 0.014	<sup>147</sup> 0.170	<sup>191</sup> 0.086	<sup>177</sup> 0.152	<sup>115</sup> 0.990	<sup>141</sup> 0.099	<sup>135</sup> 0.557	0.001	0.002	0.102	0.000	0.000	0.000	0.000	0.000
70	DERMALOG-008	<sup>11</sup> 0.003	<sup>108</sup> 0.015	<sup>115</sup> 0.516	<sup>108</sup> 0.007	<sup>84</sup> 0.029	<sup>13</sup> 0.139	<sup>141</sup> 0.045	<sup>126</sup> 0.094	<sup>216</sup> 1.000	<sup>118</sup> 0.057	<sup>88</sup> 0.382	<sup>17</sup> 0.940	0.000	0.000	0.002	<sup>1</sup> 0.000	<sup>0</sup> 0.000	<sup>0</sup> 0.000
71	DERMALOG-009	<sup>115</sup> 0.003	<sup>104</sup> 0.014	<sup>49</sup> 0.167	<sup>116</sup> 0.007	<sup>109</sup> 0.999	<sup>84</sup> 0.106	<sup>91</sup> 0.021	<sup>92</sup> 0.066	<sup>204</sup> 1.000	<sup>81</sup> 0.031	<sup>106</sup> 0.999	<sup>162</sup> 0.840	0.001	0.001	0.018	<sup>0</sup> 0.003	<sup>0</sup> 0.000	<sup>0</sup> 0.000
72	DIGIDATA-000	<sup>28</sup> 0.590	<sup>276</sup> 0.548	<sup>191</sup> 0.895	<sup>20</sup> 0.642	<sup>107</sup> 0.707	<sup>208</sup> 0.813	<sup>27</sup> 0.610	<sup>25</sup> 0.577	<sup>130</sup> 0.994	<sup>196</sup> 0.646	<sup>105</sup> 0.789	<sup>167</sup> 0.824	1.000	1.000	1.000	1.000	1.000	1.000
73	DILUSENSE-000	<sup>91</sup> 0.002	<sup>76</sup> 0.012	<sup>78</sup> 0.297	<sup>121</sup> 0.008	<sup>81</sup> 0.028	<sup>73</sup> 0.099	<sup>120</sup> 0.030	<sup>109</sup> 0.078	<sup>38</sup> 0.655	<sup>98</sup> 0.039	<sup>96</sup> 0.664	<sup>60</sup> 0.203	1.000	1.000	1.000	1.000	1.000	1.000
74	EYDEA-003	<sup>26</sup> 0.080	<sup>255</sup> 0.148	<sup>220</sup> 0.960	<sup>188</sup> 0.101	<sup>19</sup> 0.379	<sup>25</sup> 0.388	<sup>25</sup> 0.543	<sup>133</sup> 0.994	<sup>191</sup> 0.570	<sup>137</sup> 0.792	0.001	0.003	0.161	0.000	0.000	0.000	0.000	0.000
75	F8-001	<sup>210</sup> 0.012		<sup>140</sup> 0.669	<sup>251</sup> 1.000		<sup>247</sup> 1.000	<sup>226</sup> 0.166	<sup>162</sup> 0.998					0.004	1.000	0.158	0.000	0.000	0.000
76	FINCORE-000	<sup>20</sup> 0.011	<sup>19</sup> 0.034	<sup>164</sup> 0.767	<sup>166</sup> 0.032	<sup>102</sup> 0.117	<sup>159</sup> 0.191	<sup>216</sup> 0.134	<sup>206</sup> 0.217	<sup>198</sup> 1.000	<sup>163</sup> 0.187	<sup>95</sup> 0.598	<sup>117</sup> 0.458	0.000	0.001	0.043	0.000	0.000	0.000
77	FUJITSULAB-000	<sup>92</sup> 0.002	<sup>97</sup> 0.014	<sup>103</sup> 0.440	<sup>73</sup> 0.004	<sup>65</sup> 0.023	<sup>70</sup> 0.098	<sup>92</sup> 0.021	<sup>78</sup> 0.056	<sup>65</sup> 0.024	<sup>61</sup> 0.177	<sup>70</sup> 0.240	0.000	0.001	0.016	0.000	0.000	0.000	
78	FUJITSULAB-001	<sup>7</sup> 0.002	<sup>89</sup> 0.013	<sup>105</sup> 0.455	<sup>78</sup> 0.004	<sup>70</sup> 0.026	<sup>88</sup> 0.106	<sup>82</sup> 0.018	<sup>80</sup> 0.058	<sup>122</sup> 0.992	<sup>66</sup> 0.024	<sup>66</sup> 0.739	<sup>71</sup> 0.247	1.000	1.000	1.000	1.000	1.000	1.000
79	GLORY-000	<sup>273</sup> 0.178	<sup>268</sup> 0.320	<sup>245</sup> 0.994	<sup>195</sup> 0.228		<sup>202</sup> 0.678	<sup>254</sup> 0.367	<sup>255</sup> 0.547	<sup>135</sup> 0.995	<sup>186</sup> 0.453	<sup>161</sup> 0.839	0.011	0.013	0.985	0.000	0.000	0.000	
80	GLORY-001	<sup>27</sup> 0.127	<sup>265</sup> 0.267	<sup>240</sup> 0.992	<sup>194</sup> 0.178		<sup>20</sup> 0.594	<sup>246</sup> 0.305	<sup>25</sup> 0.537	<sup>125</sup> 0.993	<sup>181</sup> 0.408	<sup>189</sup> 0.819	0.011	0.013	0.988	0.000	0.000	0.000	
81	GORILLA-001	<sup>258</sup> 0.060	<sup>247</sup> 0.095	<sup>205</sup> 0.936	<sup>183</sup> 0.069		<sup>187</sup> 0.329	<sup>260</sup> 0.406	<sup>247</sup> 0.453	<sup>223</sup> 1.000	<sup>187</sup> 0.468	<sup>264</sup> 1.000	0.001	0.001	0.069	0.000	0.000	0.000	
82	GORILLA-002	<sup>22</sup> 0.020	<sup>212</sup> 0.044	<sup>160</sup> 0.753	<sup>160</sup> 0.027		<sup>161</sup> 0.214	<sup>233</sup> 0.188	<sup>22</sup> 0.268	<sup>209</sup> 1.000	<sup>170</sup> 0.250	<sup>196</sup> 1.000	0.001	0.001	0.069	0.0			

Table 13: **Miss rates by dataset**: At left, rank 1 miss rates relevant to investigations; at right, with threshold set to target FPIR = 0.01 for higher volume, low prior, uses. Yellow indicates most accurate algorithm. Throughout blue superscripts indicate the rank of the algorithm for that column.

2022/08/13  
09:55:40

$FNIR(N, K, T) =$  False neg. identification rate  
 $FPIR(N, T) =$  False pos. identification rate

N = Null. enrolled subjects  
R = Num. candidates examined

1 = 1mesjou

$I = 0 \rightarrow$  Investigation  
 $T > 0 \rightarrow$  Identification

#	ALGORITHM	INVESTIGATION MODE						IDENTIFICATION MODE						FAILURE TO EXTRACT FEATURES															
		RANK ONE MISS RATE, FNIR(N, 0, 1)						HIGH T → FPIR = 0.001, FNIR(N, T, L)						N=1.6M															
		N=1.6M			N=1.6M			N=1.6M			N=1.6M			N=1.6M			N=1.6M												
		GALLERY	MUGSHOT	MUGSHOT	WEBCAM	PROFILE	BORDER	BOR <sub>L</sub> 10YR	KIOSK	MUGSHOT	WEBCAM	PROFILE	BORDER	BOR <sub>L</sub> 10YR	KIOSK	MUGSHOT	WEBCAM	PROFILE	BORDER	BOR <sub>L</sub> 10YR	KIOSK								
139	MICROFOCUS-004	286	0.576	284	0.758	209	0.701	211	0.904	287	0.999	278	0.975	205	0.974	188	0.989	0.001	0.005										
140	MICROFOCUS-005	282	0.424	279	0.601	204	0.494	204	0.777	279	0.835	274	0.928	203	0.935	187	0.985	0.001	0.005										
141	MICROFOCUS-006	283	0.427	278	0.583	203	0.490	207	0.782	284	0.978	273	0.923	202	0.923	184	0.971	0.001	0.005										
142	MICROSOFT-003	50	0.002	78	0.012	70	0.004	94	0.109	115	0.028	124	0.091	91	0.036	68	0.233	0.000	0.001										
143	MICROSOFT-004	42	0.001	77	0.012	63	0.004	95	0.109	107	0.026	118	0.087	89	0.033	64	0.222	0.000	0.001										
144	MICROSOFT-005	73	0.002	58	0.011	43	0.144	57	0.099	104	0.026	98	0.070	33	0.587	70	0.027	53	0.180	0.000	0.001	0.049							
145	MICROSOFT-006	79	0.002	69	0.011	47	0.150	67	0.004	74	0.100	55	0.012	45	0.037	18	0.386	85	0.032	49	0.178	0.000	0.001	0.049					
146	NEC-002	221	0.017	210	0.041	219	0.959	158	0.025	172	0.243	186	0.079	170	0.140	94	0.979	121	0.474	0.001	0.002	0.890							
147	NEC-001	230	0.021	223	0.056	227	0.967	160	0.033	176	0.277	203	0.106	197	0.197	108	0.986	130	0.133	120	0.468	0.005	0.003	0.934					
148	NEC-002	10	0.001	28	0.009	94	0.363	62	0.003	105	0.117	14	0.003	20	0.020	178	0.999	24	0.008	143	0.676	0.000	0.001	0.041					
149	NEC-003	31	0.001	43	0.010	97	0.352	66	0.004	41	0.013	111	0.120	12	0.002	16	0.017	56	0.824	27	0.008	12	0.036	142	0.668				
150	NEC-004	37	0.001	26	0.009	12	0.538	55	0.003	22	0.007	33	0.075	5	0.002	7	0.013	36	0.622	8	0.004	3	0.019	14	0.100				
151	NEC-005	21	0.001	17	0.008	29	0.081	22	0.002	7	0.005	30	0.073	3	0.002	3	0.012	41	0.673	3	0.003	11	0.099	0.000	0.001	0.040			
152	NEUROTECHNOLOGY-003	231	0.022	211	0.042	227	0.961			272	0.636	221	0.266	289	1.000					0.000	0.001	0.131							
153	NEUROTECHNOLOGY-004	198	0.006	143	0.020	227	0.970			173	0.063	150	0.117	129	0.994					0.000	0.001	0.131							
154	NEUROTECHNOLOGY-005	142	0.004	172	0.024	189	0.893			160	0.054	162	0.130	154	0.998					0.000	0.000	0.030							
155	NEUROTECHNOLOGY-006	225	0.018	214	0.045	135	0.606			242	0.249	241	0.418							0.000	0.000								
156	NEUROTECHNOLOGY-007	134	0.004	151	0.021	170	0.796	126	0.009	153	0.180	172	0.062	191	0.173	201	1.000	176	0.339	280	1.000	0.001	0.001	0.041					
157	NEUROTECHNOLOGY-008	89	0.002	102	0.014	106	0.457	74	0.004	67	0.023	77	0.101	154	0.053	112	0.080	219	1.000	93	0.035	79	0.293	59	0.203	0.001			
158	NEUROTECHNOLOGY-009	38	0.001	55	0.011	57	0.179	32	0.002	44	0.013	42	0.079	73	0.015	69	0.052	56	0.020	51	0.153	44	0.165	0.001	0.046	0.000			
159	NEUROTECHNOLOGY-010	24	0.001	33	0.009	19	0.070	12	0.001	21	0.007	19	0.068	49	0.010	47	0.037	14	0.277	36	0.010	27	0.075	25	0.126	0.000	0.041	0.000	
160	NEUROTECHNOLOGY-012	8	0.001	19	0.008	4	0.001	9	0.005	9	0.057	27	0.007	42	0.032	39	0.008	21	0.061	173	0.916	1.000	1.000	1.000	1.000				
161	NEWLAND-002	261	0.079	252	0.117	204	0.936			262	0.438	248	0.466	170	0.999					0.007	0.012	0.200							
162	NOBLIS-001	278	0.249	273	0.522	247	0.993			289	1.000	283	1.000	225	1.000					0.000	0.000	0.000							
163	NOBLIS-002	274	0.179	270	0.392	238	0.982			285	0.997	282	1.000	228	1.000					0.000	0.000	0.000							
164	NOTIONTAG-000	105	0.002	79	0.012	51	0.204	76	0.004	51	0.016	63	0.095	76	0.017	83	0.059	38	0.611	69	0.021	49	0.150	48	0.176	0.000	0.000	0.000	
165	NTECHLAB-003	164	0.006	162	0.023	117	0.504			158	0.054	151	0.118	38	0.837					0.000	0.000	0.040							
166	NTECHLAB-004	151	0.005	138	0.019	117	0.506	120	0.008	119	0.129	133	0.041	141	0.105	57	0.833	116	0.053	78	0.263	0.000	0.000	0.040					
167	NTECHLAB-005	149	0.005	134	0.018	97	0.367	123	0.008	107	0.118	134	0.042	139	0.102	50	0.771	132	0.073	86	0.294	0.000	0.000	0.040					
168	NTECHLAB-006	139	0.004	125	0.017	97	0.347	117	0.007	103	0.113	128	0.037	127	0.094	49	0.754	119	0.057	77	0.260	0.000	0.000	0.040					
169	NTECHLAB-007	110	0.003	80	0.012	87	0.326	81	0.004	88	0.107	103	0.026	93	0.067	48	0.750	80	0.032	65	0.223	0.000	0.000	0.042					
170	NTECHLAB-008	38	0.002	35	0.010	48	0.157	61	0.003	51	0.084	66	0.014	38	0.045	29	0.529	90	0.033	54	0.183	0.000	0.000	0.044					
171	NTECHLAB-009	26	0.001	20	0.008	46	0.138	31	0.002	46	0.013	32	0.074	30	0.005	22	0.022	40	0.15	36	0.109	32	0.142	0.000	0.000	0.041	0.001		
172	NTECHLAB-010	15	0.001	23	0.008	29	0.085	25	0.002	25	0.008	10	0.057	15	0.003	14	0.015	15	0.252	17	0.007	20	0.059	10	0.098	0.001	0.043	0.000	
173	NTECHLAB-011	9	0.001	8	0.007	29	0.072	14	0.001	24	0.007	4	0.051	17	0.003	13	0.015	10	0.228	39	0.009	26	0.074	7	0.091	0.000	0.040	0.000	
174	PANGIAM-000	20	0.001	18	0.008	27	0.074	26	0.002	23	0.007	17	0.065	36	0.006	37	0.030	16	0.318	38	0.009	41	0.136	17	0.105	1.000	1.000	1.000	
175	PARAVISION-000	226	0.019	201	0.038	121	0.534	201	0.423			199	0.529	197	0.889	189	0.170	172	0.999	187	0.470	176	0.926	0.000	0.000				
176	PARAVISION-001	132	0.004	148	0.020	87	0.329	200	0.414			198	0.484	147	0.049	161	0.128	164	0.999	188	0.444	148	0.739	0.000	0.000				
177	PARAVISION-002	137	0.004	135	0.022	89	0.335	145	0.015			149	0.175	148	0.050	154	0.119	102	0.983	135	0.080	125	0.497	0.000	0.000	0.032			
178	PARAVISION-003	122	0.003	140	0.019	67	0.252	146	0.015			146	0.167	126	0.035	131	0.096	131	0.994	120	0.058	87	0.296	0.000	0.000	0.032			
179	PARAVISION-004	51	0.002	48	0.010	33	0.104	98	0.006			99	0.112	53	0.010	48	0.038	215	1.000	52	0.018	171	0.908	0.000	0.000	0.032			
180	PARAVISION-005	46	0.002	38	0.010	27	0.079	112	0.007			85	0.106	23	0.004	25	0.024	96	0.980	37	0.011	27	0.132	0.000	0.000	0.038			
181	PARAVISION-007	18	0.001	21	0.008	13	0.066	91	0.005	32	0.010	75	0.101	22	0.004	26	0.025	211	1.000	31	0.009	37	0.113	243	1.000	0.000	0.000	0.000	
182	PARAVISION-009	7	0.001	13	0.007	1	0.067	11	0.001	4	0.004	5	0.054	15	0.003	18	0.019	46	0.735	7	0.003	8	0.033	3	0.073	0.000	0.001	0.025	0.000</

#	ALGORITHM	INVESTIGATION MODE										IDENTIFICATION MODE										FAILURE TO EXTRACT FEATURES															
		RANK ONE MISS RATE, FNIR(N, 0, 1)					N=1.6M					HIGH T → FPIR = 0.001, FNIR(N, T, L)					N=1.6M																				
		GALLERY	MUGSHOT	MUGSHOT	MUGSHOT	VISA	BORDER	BOR <sub>L</sub> 10YR	KIOSK	MUGSHOT	MUGSHOT	MUGSHOT	VISA	BORDER	KIOSK	MUGSHOT	MUGSHOT	MUGSHOT	WEBCAM	PROFILE	BORDER	BOR <sub>L</sub> 10YR	KIOSK	MUGSHOT	MUGSHOT	MUGSHOT	VISA	BORDER	BOR <sub>L</sub> 10YR	KIOSK							
185	PIXELALL-004	<sup>84</sup> 0.002	<sup>107</sup> 0.015	<sup>118</sup> 0.523	<sup>95</sup> 0.005	<sup>139</sup> 0.152	<sup>84</sup> 0.018	<sup>111</sup> 0.079	<sup>205</sup> 1.000	<sup>111</sup> 0.051	<sup>191</sup> 0.994	<sup>0.000</sup>	<sup>0.000</sup>	<sup>0.000</sup>	<sup>0.000</sup>	<sup>0.000</sup>	<sup>0.000</sup>	<sup>0.000</sup>	<sup>0.000</sup>	<sup>0.000</sup>	<sup>0.000</sup>	<sup>0.000</sup>	<sup>0.000</sup>	<sup>0.000</sup>	<sup>0.000</sup>	<sup>0.000</sup>	<sup>0.000</sup>	<sup>0.000</sup>	<sup>0.000</sup>	<sup>0.000</sup>							
186	PIXELALL-005	<sup>74</sup> 0.002	<sup>57</sup> 0.011	<sup>71</sup> 0.264	<sup>13</sup> 0.012	<sup>78</sup> 0.028	<sup>135</sup> 0.146	<sup>82</sup> 0.012	<sup>217</sup> 1.000	<sup>71</sup> 0.051	<sup>217</sup> 0.203	<sup>196</sup> 1.000	<sup>0.000</sup>	<sup>0.000</sup>	<sup>0.000</sup>	<sup>0.000</sup>	<sup>0.000</sup>	<sup>0.000</sup>	<sup>0.000</sup>	<sup>0.000</sup>	<sup>0.000</sup>	<sup>0.000</sup>	<sup>0.000</sup>	<sup>0.000</sup>	<sup>0.000</sup>	<sup>0.000</sup>	<sup>0.000</sup>	<sup>0.000</sup>	<sup>0.000</sup>	<sup>0.000</sup>	<sup>0.000</sup>						
187	PTAKURATSATU-000	<sup>120</sup> 0.003	<sup>124</sup> 0.017	<sup>134</sup> 0.605	<sup>94</sup> 0.005	<sup>76</sup> 0.027	<sup>82</sup> 0.105	<sup>127</sup> 0.037	<sup>159</sup> 0.124	<sup>69</sup> 0.924	<sup>108</sup> 0.046	<sup>69</sup> 0.206	<sup>67</sup> 0.232	<sup>0.000</sup>	<sup>0.001</sup>	<sup>0.039</sup>	<sup>0.000</sup>	<sup>0.000</sup>	<sup>0.000</sup>	<sup>0.000</sup>	<sup>0.000</sup>	<sup>0.000</sup>	<sup>0.000</sup>	<sup>0.000</sup>	<sup>0.000</sup>	<sup>0.000</sup>	<sup>0.000</sup>	<sup>0.000</sup>	<sup>0.000</sup>	<sup>0.000</sup>	<sup>0.000</sup>	<sup>0.000</sup>					
188	QNAP-000	<sup>179</sup> 0.008	<sup>183</sup> 0.027	<sup>116</sup> 0.522	<sup>14</sup> 0.013	<sup>95</sup> 0.054	<sup>142</sup> 0.158	<sup>213</sup> 0.129	<sup>209</sup> 0.238	<sup>227</sup> 1.000	<sup>16</sup> 0.191	<sup>95</sup> 0.539	<sup>193</sup> 0.998	<sup>0.001</sup>	<sup>0.000</sup>	<sup>0.054</sup>	<sup>0.000</sup>	<sup>0.000</sup>	<sup>0.000</sup>	<sup>0.000</sup>	<sup>0.000</sup>	<sup>0.000</sup>	<sup>0.000</sup>	<sup>0.000</sup>	<sup>0.000</sup>	<sup>0.000</sup>	<sup>0.000</sup>	<sup>0.000</sup>	<sup>0.000</sup>	<sup>0.000</sup>	<sup>0.000</sup>	<sup>0.000</sup>					
189	QNAP-001	<sup>140</sup> 0.004	<sup>156</sup> 0.022	<sup>110</sup> 0.498	<sup>105</sup> 0.006	<sup>91</sup> 0.041	<sup>101</sup> 0.112	<sup>157</sup> 0.054	<sup>167</sup> 0.928	<sup>70</sup> 0.081	<sup>86</sup> 0.368	<sup>97</sup> 0.331	<sup>0.000</sup>	<sup>0.000</sup>	<sup>0.000</sup>	<sup>0.000</sup>	<sup>0.000</sup>	<sup>0.000</sup>	<sup>0.000</sup>	<sup>0.000</sup>	<sup>0.000</sup>	<sup>0.000</sup>	<sup>0.000</sup>	<sup>0.000</sup>	<sup>0.000</sup>	<sup>0.000</sup>	<sup>0.000</sup>	<sup>0.000</sup>	<sup>0.000</sup>	<sup>0.000</sup>	<sup>0.000</sup>						
190	QNAP-002	<sup>152</sup> 0.005	<sup>150</sup> 0.021	<sup>51</sup> 0.172	<sup>88</sup> 0.004	<sup>86</sup> 0.031	<sup>115</sup> 0.125	<sup>168</sup> 0.026	<sup>143</sup> 0.106	<sup>51</sup> 0.772	<sup>111</sup> 0.052	<sup>78</sup> 0.281	<sup>83</sup> 0.272	<sup>1.000</sup>	<sup>1.000</sup>	<sup>1.000</sup>	<sup>1.000</sup>	<sup>1.000</sup>	<sup>1.000</sup>	<sup>1.000</sup>	<sup>1.000</sup>	<sup>1.000</sup>	<sup>1.000</sup>	<sup>1.000</sup>	<sup>1.000</sup>	<sup>1.000</sup>	<sup>1.000</sup>	<sup>1.000</sup>	<sup>1.000</sup>	<sup>1.000</sup>	<sup>1.000</sup>	<sup>1.000</sup>					
191	QUANTASOFT-001	<sup>275</sup> 0.218	<sup>283</sup> 0.727						<sup>273</sup> 0.639																												
192	RANKONE-002	<sup>228</sup> 0.019	<sup>225</sup> 0.071						<sup>260</sup> 0.118	<sup>217</sup> 0.261																											
193	RANKONE-003	<sup>227</sup> 0.019	<sup>223</sup> 0.068						<sup>207</sup> 0.118	<sup>216</sup> 0.255																											
194	RANKONE-004	<sup>249</sup> 0.041	<sup>254</sup> 0.141						<sup>234</sup> 0.193	<sup>243</sup> 0.426																											
195	RANKONE-005	<sup>193</sup> 0.009	<sup>209</sup> 0.041	<sup>238</sup> 0.986					<sup>169</sup> 0.059	<sup>192</sup> 0.173	<sup>156</sup> 0.998																										
196	RANKONE-006	<sup>154</sup> 0.005	<sup>150</sup> 0.021	<sup>172</sup> 0.797					<sup>129</sup> 0.037	<sup>90</sup> 0.977																											
197	RANKONE-007	<sup>126</sup> 0.003	<sup>136</sup> 0.019	<sup>167</sup> 0.796					<sup>97</sup> 0.022	<sup>128</sup> 0.095	<sup>78</sup> 0.967																										
198	RANKONE-009	<sup>100</sup> 0.002	<sup>82</sup> 0.013	<sup>125</sup> 0.549	<sup>97</sup> 0.006				<sup>127</sup> 0.134	<sup>79</sup> 0.018	<sup>105</sup> 0.076	<sup>81</sup> 0.969	<sup>122</sup> 0.062	<sup>96</sup> 0.328																							
199	RANKONE-010	<sup>94</sup> 0.002	<sup>39</sup> 0.010	<sup>96</sup> 0.374	<sup>90</sup> 0.005	<sup>74</sup> 0.027	<sup>117</sup> 0.126	<sup>63</sup> 0.014	<sup>81</sup> 0.058	<sup>54</sup> 0.802	<sup>111</sup> 0.052	<sup>70</sup> 0.208	<sup>75</sup> 0.259																								
200	RANKONE-011	<sup>43</sup> 0.002	<sup>67</sup> 0.011	<sup>61</sup> 0.223	<sup>65</sup> 0.004	<sup>38</sup> 0.019	<sup>49</sup> 0.082	<sup>45</sup> 0.009	<sup>60</sup> 0.048	<sup>96</sup> 0.037	<sup>62</sup> 0.182	<sup>185</sup> 0.977																									
201	RANKONE-012	<sup>30</sup> 0.001	<sup>51</sup> 0.010	<sup>39</sup> 0.127	<sup>56</sup> 0.003	<sup>48</sup> 0.014	<sup>21</sup> 0.069	<sup>40</sup> 0.008	<sup>73</sup> 0.053																												
202	REALNETWORKS-000	<sup>248</sup> 0.040	<sup>242</sup> 0.078						<sup>240</sup> 0.234	<sup>232</sup> 0.319																											
203	REALNETWORKS-001	<sup>247</sup> 0.040	<sup>341</sup> 0.078						<sup>239</sup> 0.234	<sup>233</sup> 0.319																											
204	REALNETWORKS-002	<sup>244</sup> 0.039	<sup>240</sup> 0.078						<sup>238</sup> 0.231	<sup>231</sup> 0.315																											
205	REALNETWORKS-003	<sup>234</sup> 0.024	<sup>229</sup> 0.062	<sup>168</sup> 0.771	<sup>165</sup> 0.031				<sup>160</sup> 0.209	<sup>224</sup> 0.159	<sup>220</sup> 0.266	<sup>160</sup> 0.998	<sup>159</sup> 0.164				<sup>126</sup> 0.500																				
206	REALNETWORKS-004	<sup>232</sup> 0.024	<sup>227</sup> 0.059	<sup>171</sup> 0.797	<sup>168</sup> 0.031				<sup>165</sup> 0.213	<sup>222</sup> 0.158	<sup>218</sup> 0.263	<sup>173</sup> 0.999	<sup>169</sup> 0.170				<sup>138</sup> 0.613																				
207	REALNETWORKS-005	<sup>96</sup> 0.002	<sup>82</sup> 0.013	<sup>102</sup> 0.433	<sup>82</sup> 0.004	<sup>66</sup> 0.023	<sup>79</sup> 0.102	<sup>114</sup> 0.028	<sup>103</sup> 0.074	<sup>83</sup> 0.971	<sup>95</sup> 0.037	<sup>71</sup> 0.223	<sup>62</sup> 0.215				<sup>0.006</sup>																				
208	REALNETWORKS-006	<sup>34</sup> 0.001	<sup>41</sup> 0.010	<sup>76</sup> 0.287	<sup>46</sup> 0.002	<sup>35</sup> 0.010	<sup>40</sup> 0.078	<sup>40</sup> 0.015	<sup>71</sup> 0.053	<sup>98</sup> 0.980	<sup>40</sup> 0.016	<sup>28</sup> 0.120	<sup>38</sup> 0.154				<sup>0.000</sup>																				
209	REALNETWORKS-007	<sup>28</sup> 0.001	<sup>32</sup> 0.009	<sup>72</sup> 0.267	<sup>21</sup> 0.002	<sup>27</sup> 0.009	<sup>27</sup> 0.072	<sup>47</sup> 0.010	<sup>56</sup> 0.043	<sup>93</sup> 0.979	<sup>39</sup> 0.012	<sup>92</sup> 0.463	<sup>31</sup> 0.140				<sup>1.000</sup>																				
210	REMARKAI-000	<sup>128</sup> 0.003	<sup>135</sup> 0.018	<sup>136</sup> 0.660	<sup>119</sup> 0.008				<sup>136</sup> 0.148	<sup>161</sup> 0.055	<sup>150</sup> 0.120	<sup>171</sup> 0.999	<sup>134</sup> 0.069	<sup>146</sup> 0.717				<sup>0.000</sup>																			
211	REMARKAI-000	<sup>186</sup> 0.009	<sup>186</sup> 0.030						<sup>211</sup> 0.128	<sup>198</sup> 0.203																											
212	REMARKAI-002	<sup>184</sup> 0.008	<sup>185</sup> 0.029	<sup>173</sup> 0.802					<sup>210</sup> 0.124	<sup>196</sup> 0.196	<sup>119</sup> 0.991																										
213	RENDIP-000	<sup>47</sup> 0.002	<sup>109</sup> 0.015	<sup>101</sup> 0.424	<sup>103</sup> 0.006	<sup>77</sup> 0.028	<sup>52</sup> 0.084	<sup>56</sup> 0.012	<sup>82</sup> 0.059	<sup>66</sup> 0.894	<sup>61</sup> 0.022	<sup>64</sup> 0.185	<sup>45</sup> 0.167				<sup>0.000</sup>																				
214	REVEALMEDIA-000	<sup>71</sup> 0.002	<sup>36</sup> 0.010	<sup>73</sup> 0.275	<sup>32</sup> 0.002	<sup>40</sup> 0.012	<sup>31</sup> 0.074	<sup>58</sup> 0.012	<sup>54</sup> 0.042	<sup>43</sup> 0.680	<sup>59</sup> 0.021	<sup>33</sup> 0.093	<sup>33</sup> 0.143				<sup>0.000</sup>																				
215	S1-000	<sup>102</sup> 0.002	<sup>123</sup> 0.017	<sup>70</sup> 0.258	<sup>96</sup> 0.005	<sup>72</sup> 0.025	<sup>57</sup> 0.090	<sup>116</sup> 0.028	<sup>115</sup> 0.085	<sup>229</sup> 1.000	<sup>111</sup> 0.047	<sup>224</sup> 1.000	<sup>277</sup> 1.000				<sup>0.000</sup>																				
216	S1-001	<sup>121</sup> 0.003	<sup>98</sup> 0.014	<sup>60</sup> 0.215	<sup>51</sup> 0.003	<sup>56</sup> 0.018	<sup>35</sup> 0.077	<sup>74</sup> 0.016	<sup>68</sup> 0.052	<sup>108</sup> 0.																											

#	ALGORITHM	INVESTIGATION MODE										IDENTIFICATION MODE										FAILURE TO EXTRACT FEATURES																
		RANK ONE MISS RATE, FNIR(N, 0, 1)										HIGH T → FPIR = 0.001, FNIR(N, T, L)																										
		N=1.6M										N=1.6M																										
		GALLERY	MUGSHOT	MUGSHOT	MUGSHOT	VISA	BORDER	BOR <sub>L</sub> 10YR	KIOSK	MUGSHOT	MUGSHOT	MUGSHOT	WEBCAM	PROFILE	BORDER	BOR <sub>L</sub> 10YR	KIOSK	MUGSHOT	MUGSHOT	WEBCAM	PROFILE	BORDER	BOR <sub>L</sub> 10YR	KIOSK	MUGSHOT	MUGSHOT	WEBCAM	PROFILE	BORDER	BOR <sub>L</sub> 10YR	KIOSK							
231	SHAMAN-007	245	0.040	224	0.057	269	0.333	83	0.004	72	0.099	77	0.018	237	0.365	89	0.031	0.020	0.010																			
232	SIAT-001	65	0.002	271	0.446	199	0.348	78	0.102	94	0.022	249	0.478	178	0.372	175	0.923	0.000	0.000																			
233	SIAT-002	67	0.002	271	0.446	199	0.348	78	0.102	282	0.968	279	0.976																									
234	SMILART-004	290	0.965	286	0.974					282	0.968	279	0.976																									
235	SMILART-005																																					
236	SQISOFT-001	141	0.004	139	0.019	75	0.282	92	0.005	75	0.027	67	0.097	215	0.132	214	0.252	52	0.797	160	0.040	83	0.317	111	0.420	0.000	0.000	0.039	0.000									
237	STAUQ-000	175	0.007	146	0.020	136	0.613	152	0.020	96	0.055	143	0.159	170	0.062	245	0.443	199	1.000	190	0.535	104	0.961	270	1.000	0.000	0.000	0.000	0.000									
238	SYNESIS-003	219	0.016	166	0.023	181	0.827	157	0.013	129	0.136	174	0.065	138	0.123	76	0.960	133	0.075	91	0.314	0.000	0.001	0.063														
239	SYNESIS-003	272	0.170	263	0.235					268	0.582	261	0.646																									
240	SYNESIS-005	185	0.009	83	0.013	157	0.744	59	0.003	60	0.092	102	0.025	99	0.072	103	0.984	87	0.032	61	0.214	0.001	0.000	0.135														
241	TECH5-001	136	0.004	122	0.017	137	0.584	109	0.007	89	0.107	164	0.057	275	0.935	229	1.000	167	0.244	192	0.994	0.000	0.000	0.006														
242	TECH5-002	111	0.003	56	0.011	82	0.312	58	0.003	83	0.029	56	0.089	111	0.027	97	0.070	51	0.805	99	0.039	68	0.205	114	0.440	0.001	0.000	0.041	0.000									
243	TEVIAN-003	216	0.015	220	0.052					231	0.177	227	0.298																									
244	TEVIAN-004	203	0.011	200	0.038					205	0.117	193	0.176																									
245	TEVIAN-005	176	0.007	184	0.028	107	0.467			192	0.087	173	0.144	77	0.962																							
246	TEVIAN-006	103	0.002	63	0.011	37	0.123	49	0.003	47	0.013	25	0.071	48	0.010	40	0.032	19	0.425	46	0.016	31	0.093	180	0.951	0.001	0.000	0.062	0.000									
247	TEVIAN-007	63	0.002	31	0.009	34	0.093	28	0.002	30	0.009	18	0.067	22	0.005	21	0.022	15	0.301	34	0.009	23	0.065	23	0.122	0.000	0.000	0.062	0.000									
248	TIGER-000	256	0.062	248	0.095					257	0.390	250	0.500																									
249	TIGER-002	159	0.006	163	0.023	113	0.514			188	0.086	183	0.158	168	0.999																							
250	TIGER-003	160	0.006	164	0.023					189	0.086	182	0.158																									
251	TONGYITRANS-000	171	0.007	160	0.022					181	0.074	147	0.112																									
252	TONGYITRANS-001	172	0.007	161	0.022					175	0.066	138	0.101																									
253	TOSHIBA-000	145	0.004	151	0.022	163	0.766			171	0.062	152	0.118	140	0.995																							
254	TOSHIBA-001	150	0.005	157	0.022					166	0.058	125	0.092																									
255	TRUEFACE-000	125	0.003	92	0.014	61	0.230	114	0.007	69	0.024	61	0.092	83	0.018	86	0.062	61	0.882	78	0.030	66	0.194	56	0.188	0.001	0.001	0.047	0.003									
256	VD-000	285	0.474	277	0.551					280	0.917	277	0.946																									
257	VD-001	238	0.028	221	0.053					235	0.201	224	0.281																									
258	VD-002	194	0.010	182	0.027	188	0.893	140	0.013	93	0.050	150	0.176	185	0.079	175	0.148	143	0.996	140	0.095	85	0.367	102	0.372	0.004	0.003	0.156	0.002									
259	VD-003	177	0.008	154	0.022	166	0.773	122	0.008	85	0.030	130	0.137	142	0.046	136	0.100	169	0.999	112	0.051	73	0.244	93	0.315	0.003	0.003	0.144	0.002									
260	VERIDAS-001	114	0.003	100	0.014	122	0.550	104	0.006	79	0.028	121	0.131	131	0.037	113	0.082	111	0.987	104	0.044	75	0.266	80	0.264	0.000	0.002	0.093	0.001									
261	VERIDAS-002	113	0.003	99	0.014	122	0.550	106	0.006	80	0.028	120	0.131	120	0.037	114	0.082	110	0.987	103	0.044	76	0.266	79	0.264	0.000	0.002	0.093	0.001									
262	VERIDAS-003	66	0.002	62	0.011	72	0.297	73	0.004	52	0.016	91	0.108	75	0.017	76	0.055	149	0.997	50	0.020	48	0.150	51	0.178	0.000	0.002	0.093	0.001									
263	VIGILANTSOLUTIONS-003	259	0.069	256	0.151	210	0.958			261	0.408	264	0.660	163	0.999																							
264	VIGILANTSOLUTIONS-004	267	0.125	264	0.244	223	0.965			267	0.549	269	0.817	146	0.996																							
265	VIGILANTSOLUTIONS-005	190	0.009	199	0.920					256	0.388			218	1.000																							
266	VIGILANTSOLUTIONS-006	196	0.010	196	0.921					251	0.353			214	1.000																							
267	VIGILANTSOLUTIONS-007	127	0.003	127	0.017	197	0.925	158	0.013	98	0.068	148	0.175	118	0.028	119	0.088	145	0.996	137	0.081	87	0.371	105	0.391	0.000	0.001	0.127	0.001									
268	VIGILANTSOLUTIONS-008	119	0.003	128	0.017	194	0.913	142	0.014	99	0.072	151	0.178	98	0.021	106	0.077	167	0.999	144	0.104	89	0.398	127	0.511	0.000	0.001	0.127	0.001									
269	VISIONBOX-000	75	0.002	64	0.011	157	0.752	86	0.005	54	0.017	41	0.078	80	0.018	79	0.057	118	0.990	61	0.023	47	0.146	43	0.162	0.000	0.001	0.043	0.001									
270	VISIONLABS-004	112	0.003	142	0.020	93	0.343																															

#	ALGORITHM	INVESTIGATION MODE						IDENTIFICATION MODE						FAILURE TO EXTRACT FEATURES						
		RANK ONE MISS RATE, FNIR(N, 0, 1)						HIGH T → FPIR = 0.001, FNIR(N, T, L)												
		N=1.6M						N=1.6M												
	GALLERY	MUGSHOT	MUGSHOT	MUGSHOT	VISA	BORDER	KIOSK	MUGSHOT	MUGSHOT	MUGSHOT	VISA	BORDER	KIOSK	MUGSHOT	MUGSHOT	MUGSHOT	VISA	BORDER	KIOSK	
277	VISIONLABS-011	22.001	27.009	11.064	7.001	6.004	15.063	19.003	19.020	9.004	10.034	6.090	0.000	0.000	0.032	0.000	0.000	0.000		
278	VNP1-001	88.002	105.014	41.045	45.002	68.023	26.071	65.014	95.068	48.0718	92.035	105.090	100.362	1.000	1.000	1.000	1.000	1.000	1.000	
279	VOCORD-003	165.006	171.024	174.0804	182.061	153.0188	209.0122	180.0155	157.0998	158.0157	108.0404	0.001	0.011	0.425						
280	VOCORD-004	180.008	149.021	168.0792	136.012	118.0127	252.0355	196.0173	209.1.000	166.0193	189.0991	0.000	0.000	0.000						
281	VOCORD-005	174.007	167.023	176.0812	178.055	158.0206	222.0158	163.0130	149.0997	153.0138	103.0381	0.001	0.009	0.554						
282	VOCORD-006	293.1.000	297.1.000	286.1.000	289.1.000	227.1.000	290.1.000	293.1.000	237.1.000	230.1.000	244.1.000	0.001	0.009	0.554						
283	VTS-000	288.0594	280.0608	192.0909	205.0607	108.0724	208.0739	269.0598	259.0619	175.0999	195.0613	100.760	150.0761	0.000	0.001	0.047	0.000			
284	VTS-001	45.002	47.010	59.0167	99.006	57.018	36.077	62.013	66.051	128.0994	62.022	44.0141	57.0192	0.000	0.000	0.040	0.000			
285	VTS-002	77.002	81.013	65.0233	144.014	90.038	115.0125	105.026	104.075	186.1.000	106.045	72.0231	110.0417	0.000	0.000	0.029	0.000			
286	XFORWARDAI-000	95.002	96.014	28.089	69.004	49.015	62.094	71.015	74.053	21.0440	58.0201	53.0159	46.0169	0.000	0.000	0.000	0.000			
287	XFORWARDAI-001	85.002	81.013	16.067	54.003	28.009	47.0882	29.005	36.028	29.0448	26.0008	22.0062	24.0123	0.000	0.000	0.000	0.000			
288	XFORWARDAI-002	78.002	75.012	5.059	44.002	16.007	36.077	18.003	15.016	27.0525	12.005	13.041	13.099	0.000	0.000	0.000	0.000	0.000	0.000	
289	YISHENG-001	237.027	222.060	181.058	181.0287	249.0346	260.0808	197.0666		174.0919	0.002	0.005								
290	YITU-002	70.002	46.010					78.018	61.049			0.000	0.000							
291	YITU-003	118.003	117.016					86.019	70.052			0.003	0.001							
292	YITU-004	27.001	21.008	186.0866				45.010	32.027	71.0936			0.000	0.000	0.000	0.000	0.000			
293	YITU-005	97.002	105.014					52.010	41.032				0.003	0.001						

Table 17: **Miss rates by dataset:** At left, rank 1 miss rates relevant to investigations; at right, with threshold set to target FPIR = 0.01 for higher volume, low prior, uses. Yellow indicates most accurate algorithm. Throughout blue superscripts indicate the rank of the algorithm for that column.

2022/06/13 09:55:40

FNIR(N, R, T) = False neg. identification rate

N = Num. enrolled subjects

T = Threshold

T = 0 → Investigation  
T > 0 → Identification

FPTR(N, T) = False pos. identification rate

R = Num. candidates examined

#	ALGORITHM	ENROL, MOST RECENT				
		DATASET: FRVT 2018 MUGSHOTS				
		N=0.64M	N=1.6M	N=3.0M	N=6.0M	N=12.0M
1	3DIVI-005	<sup>22</sup> 0.1358	<sup>22</sup> 0.1664	<sup>20</sup> 0.1915	<sup>19</sup> 0.2370	<sup>18</sup> 0.3054
2	ACER-000	<sup>21</sup> 0.1185	<sup>22</sup> 0.1455	<sup>19</sup> 0.1714	<sup>18</sup> 0.2074	<sup>17</sup> 0.2537
3	ALCHERA-003	<sup>21</sup> 0.1176	<sup>22</sup> 0.1553	<sup>19</sup> 0.1853	<sup>19</sup> 0.2409	<sup>19</sup> 0.3553
4	ALLGOVISION-000	<sup>19</sup> 0.0688	<sup>19</sup> 0.0881	<sup>17</sup> 0.1084	<sup>16</sup> 0.1389	<sup>16</sup> 0.2129
5	ALLGOVISION-001	<sup>19</sup> 0.0785	<sup>19</sup> 0.1017	<sup>18</sup> 0.1218	<sup>17</sup> 0.1584	<sup>16</sup> 0.2273
6	ANKE-000	<sup>20</sup> 0.0942	<sup>20</sup> 0.1169	<sup>18</sup> 0.1404	<sup>18</sup> 0.1776	<sup>17</sup> 0.2559
7	ANKE-002	<sup>12</sup> 0.0229	<sup>12</sup> 0.0318	<sup>12</sup> 0.0406	<sup>11</sup> 0.0605	<sup>10</sup> 0.1466
8	AWARE-003	<sup>21</sup> 0.1098	<sup>21</sup> 0.1283	<sup>19</sup> 0.1447	<sup>19</sup> 0.1768	<sup>18</sup> 0.2364
9	AWARE-005	<sup>25</sup> 0.3389	<sup>25</sup> 0.3643	<sup>20</sup> 0.3993	<sup>20</sup> 0.4526	<sup>17</sup> 0.2531
10	AYONIX-002	<sup>27</sup> 0.7862	<sup>27</sup> 0.8242	<sup>21</sup> 0.8508	<sup>20</sup> 0.8704	<sup>19</sup> 0.8939
11	CAMVI-004	<sup>14</sup> 0.0367	<sup>17</sup> 0.0716	<sup>17</sup> 0.0983	<sup>19</sup> 0.2508	<sup>18</sup> 0.2701
12	CANON-001	<sup>33</sup> 0.0039	<sup>33</sup> 0.0054	<sup>33</sup> 0.0074	<sup>30</sup> 0.0158	<sup>38</sup> 0.0924
13	CANON-002	<sup>28</sup> 0.0036	<sup>27</sup> 0.0047	<sup>28</sup> 0.0061	<sup>24</sup> 0.0124	<sup>24</sup> 0.0808
14	CIB-000	<sup>56</sup> 0.0086	<sup>59</sup> 0.0125	<sup>59</sup> 0.0160	<sup>63</sup> 0.0303	<sup>80</sup> 0.1251
15	CLEARVIEWAI-000	<sup>38</sup> 0.0040	<sup>35</sup> 0.0058	<sup>36</sup> 0.0078	<sup>31</sup> 0.0159	<sup>41</sup> 0.0971
16	CLOUDWALK-HR-000	<sup>10</sup> 0.0019	<sup>10</sup> 0.0020	<sup>8</sup> 0.0023	<sup>13</sup> 0.0072	<sup>17</sup> 0.0701
17	CLOUDWALK-MT-000	<sup>11</sup> 0.0019	<sup>9</sup> 0.0020	<sup>7</sup> 0.0022	<sup>5</sup> 0.0049	<sup>7</sup> 0.0466
18	COGENT-000	<sup>16</sup> 0.0430	<sup>15</sup> 0.0527	<sup>15</sup> 0.0695	<sup>15</sup> 0.1133	<sup>14</sup> 0.1960
19	COGENT-001	<sup>16</sup> 0.0430	<sup>15</sup> 0.0527	<sup>15</sup> 0.0695	<sup>15</sup> 0.1133	<sup>14</sup> 0.1960
20	COGENT-002	<sup>15</sup> 0.0322	<sup>13</sup> 0.0444	<sup>13</sup> 0.0610	<sup>15</sup> 0.1116	<sup>15</sup> 0.2180
21	COGENT-003	<sup>13</sup> 0.0328	<sup>14</sup> 0.0463	<sup>13</sup> 0.0683	<sup>16</sup> 0.1294	<sup>17</sup> 0.2445
22	COGENT-004	<sup>12</sup> 0.0210	<sup>12</sup> 0.0331	<sup>13</sup> 0.0527	<sup>15</sup> 0.1138	<sup>15</sup> 0.2119
23	COGENT-005	<sup>45</sup> 0.0064	<sup>44</sup> 0.0091	<sup>44</sup> 0.0123	<sup>64</sup> 0.0303	<sup>26</sup> 0.1233
24	COGENT-006	<sup>24</sup> 0.0032	<sup>24</sup> 0.0044	<sup>24</sup> 0.0057	<sup>22</sup> 0.0120	<sup>24</sup> 0.0830
25	COGNITEC-000	<sup>22</sup> 0.1377	<sup>22</sup> 0.1606	<sup>19</sup> 0.1870	<sup>18</sup> 0.2176	<sup>18</sup> 0.2831
26	COGNITEC-001	<sup>20</sup> 0.0807	<sup>20</sup> 0.1017	<sup>18</sup> 0.1214	<sup>17</sup> 0.1513	<sup>16</sup> 0.2238
27	COGNITEC-002	<sup>16</sup> 0.0406	<sup>15</sup> 0.0531	<sup>14</sup> 0.0666	<sup>14</sup> 0.0935	<sup>14</sup> 0.1874
28	COGNITEC-003	<sup>15</sup> 0.0400	<sup>15</sup> 0.0526	<sup>14</sup> 0.0650	<sup>15</sup> 0.0895	<sup>13</sup> 0.1772
29	COGNITEC-004	<sup>12</sup> 0.0222	<sup>12</sup> 0.0313	<sup>12</sup> 0.0388	<sup>11</sup> 0.0540	<sup>58</sup> 0.1103
30	COGNITEC-005	<sup>44</sup> 0.0063	<sup>46</sup> 0.0096	<sup>52</sup> 0.0144	<sup>57</sup> 0.0287	<sup>40</sup> 0.0967
31	COGNITEC-006	<sup>40</sup> 0.0053	<sup>41</sup> 0.0077	<sup>41</sup> 0.0117	<sup>45</sup> 0.0254	<sup>31</sup> 0.0919
32	CYBERLINK-000	<sup>16</sup> 0.0414	<sup>16</sup> 0.0565	<sup>15</sup> 0.0707	<sup>14</sup> 0.1031	<sup>15</sup> 0.2050
33	CYBERLINK-001	<sup>15</sup> 0.0392	<sup>15</sup> 0.0536	<sup>15</sup> 0.0695	<sup>14</sup> 0.0973	<sup>13</sup> 0.1794
34	CYBERLINK-002	<sup>66</sup> 0.0105	<sup>69</sup> 0.0148	<sup>71</sup> 0.0202	<sup>85</sup> 0.0399	<sup>81</sup> 0.1255
35	CYBERLINK-003	<sup>4</sup> 0.0056	<sup>42</sup> 0.0077	<sup>39</sup> 0.0100	<sup>41</sup> 0.0235	<sup>7</sup> 0.1237
36	CYBERLINK-004	<sup>39</sup> 0.0051	<sup>39</sup> 0.0071	<sup>41</sup> 0.0102	<sup>35</sup> 0.0199	<sup>84</sup> 0.1269
37	CYBERLINK-005	<sup>47</sup> 0.0067	<sup>50</sup> 0.0099	<sup>50</sup> 0.0138	<sup>82</sup> 0.0394	<sup>118</sup> 0.1566
38	DAIHUA-001	<sup>18</sup> 0.0569	<sup>18</sup> 0.0727	<sup>16</sup> 0.0878	<sup>15</sup> 0.1148	<sup>15</sup> 0.1867
39	DAIHUA-002	<sup>71</sup> 0.0108	<sup>70</sup> 0.0151	<sup>69</sup> 0.0191	<sup>59</sup> 0.0291	<sup>69</sup> 0.1153
40	DAIHUA-003	<sup>63</sup> 0.0100	<sup>64</sup> 0.0139	<sup>67</sup> 0.0180	<sup>60</sup> 0.0296	<sup>63</sup> 0.1130
41	DAIHUA-004	<sup>38</sup> 0.0048	<sup>38</sup> 0.0069	<sup>37</sup> 0.0090	<sup>33</sup> 0.0164	<sup>27</sup> 0.0853
42	DAON-000	<sup>98</sup> 0.0161	<sup>98</sup> 0.0226	<sup>10</sup> 0.0293	<sup>11</sup> 0.0562	<sup>12</sup> 0.1702
43	DECATUR-000	<sup>100</sup> 0.0173	<sup>101</sup> 0.0229	<sup>101</sup> 0.0305	<sup>95</sup> 0.0464	<sup>101</sup> 0.1433
44	DEEPLINT-001	<sup>29</sup> 0.0027	<sup>20</sup> 0.0033	<sup>19</sup> 0.0043	<sup>23</sup> 0.0121	<sup>31</sup> 0.0922
45	DEEPSEA-001	<sup>145</sup> 0.0347	<sup>143</sup> 0.0462	<sup>138</sup> 0.0586	<sup>133</sup> 0.0802	<sup>129</sup> 0.1708
46	DERMALOG-005	<sup>19</sup> 0.0700	<sup>19</sup> 0.0880	<sup>17</sup> 0.1144	<sup>17</sup> 0.1578	<sup>17</sup> 0.2451
47	DERMALOG-006	<sup>154</sup> 0.0395	<sup>150</sup> 0.0517	<sup>143</sup> 0.0659	<sup>144</sup> 0.0973	<sup>132</sup> 0.1745
48	DERMALOG-007	<sup>19</sup> 0.0691	<sup>19</sup> 0.0863	<sup>17</sup> 0.1107	<sup>17</sup> 0.1504	<sup>16</sup> 0.2299
49	DERMALOG-008	<sup>141</sup> 0.0338	<sup>141</sup> 0.0455	<sup>141</sup> 0.0626	<sup>149</sup> 0.1060	<sup>164</sup> 0.2276
50	DERMALOG-009	<sup>91</sup> 0.0148	<sup>91</sup> 0.0206	<sup>92</sup> 0.0268	<sup>89</sup> 0.0416	<sup>91</sup> 0.1374
51	DILUSENSE-000	<sup>119</sup> 0.0208	<sup>120</sup> 0.0305	<sup>118</sup> 0.0377	<sup>114</sup> 0.0543	<sup>97</sup> 0.1429
52	FUJITSULAB-000	<sup>92</sup> 0.0148	<sup>92</sup> 0.0206	<sup>98</sup> 0.0277	<sup>112</sup> 0.0541	<sup>13</sup> 0.1739
53	FUJITSULAB-001	<sup>76</sup> 0.0126	<sup>82</sup> 0.0182	<sup>87</sup> 0.0251	<sup>121</sup> 0.0646	<sup>152</sup> 0.2079
54	GORILLA-002	<sup>233</sup> 0.1539	<sup>233</sup> 0.1880	<sup>203</sup> 0.2184	<sup>195</sup> 0.2596	<sup>190</sup> 0.3398
55	GORILLA-004	<sup>196</sup> 0.0699	<sup>196</sup> 0.0892	<sup>178</sup> 0.1048	<sup>167</sup> 0.1370	<sup>148</sup> 0.1969
56	GORILLA-005	<sup>172</sup> 0.0453	<sup>167</sup> 0.0583	<sup>157</sup> 0.0704	<sup>146</sup> 0.0974	<sup>105</sup> 0.1474
57	GORILLA-006	<sup>113</sup> 0.0196	<sup>113</sup> 0.0275	<sup>108</sup> 0.0331	<sup>103</sup> 0.0516	<sup>6</sup> 0.1113
58	GORILLA-007	<sup>110</sup> 0.0190	<sup>112</sup> 0.0271	<sup>112</sup> 0.0348	<sup>106</sup> 0.0520	<sup>62</sup> 0.1129
59	GRIAULE-000	<sup>88</sup> 0.0145	<sup>89</sup> 0.0201	<sup>88</sup> 0.0253	<sup>87</sup> 0.0407	<sup>10</sup> 0.1440
60	HIK-003	<sup>202</sup> 0.0828	<sup>201</sup> 0.1028	<sup>182</sup> 0.1202	<sup>174</sup> 0.1525	<sup>173</sup> 0.2480
61	HIK-004	<sup>20</sup> 0.0796	<sup>197</sup> 0.0988	<sup>180</sup> 0.1147	<sup>170</sup> 0.1474	<sup>17</sup> 0.2483
62	HIK-005	<sup>133</sup> 0.0312	<sup>136</sup> 0.0436	<sup>137</sup> 0.0560	<sup>137</sup> 0.0911	<sup>157</sup> 0.2129
63	HYPERVERGE-001	<sup>2</sup> 0.0033	<sup>25</sup> 0.0045	<sup>23</sup> 0.0059	<sup>19</sup> 0.0117	<sup>2</sup> 0.0872
64	HYPERVERGE-002	<sup>21</sup> 0.0028	<sup>21</sup> 0.0037	<sup>21</sup> 0.0046	<sup>10</sup> 0.0064	<sup>1</sup> 0.0064
65	HZAILU-000	<sup>87</sup> 0.0143	<sup>88</sup> 0.0197	<sup>89</sup> 0.0255	<sup>88</sup> 0.0411	<sup>22</sup> 0.1174
66	IDEARIA-003	<sup>143</sup> 0.0346	<sup>146</sup> 0.0471	<sup>16</sup> 0.0892	<sup>197</sup> 0.2789	<sup>194</sup> 0.4311
67	IDEARIA-004	<sup>132</sup> 0.0300	<sup>132</sup> 0.0373	<sup>126</sup> 0.0447	<sup>119</sup> 0.0617	<sup>126</sup> 0.1635
68	IDEARIA-005	<sup>148</sup> 0.0360	<sup>138</sup> 0.0440	<sup>138</sup> 0.0537	<sup>132</sup> 0.0764	<sup>14</sup> 0.1915
69	IDEARIA-006	<sup>146</sup> 0.0351	<sup>135</sup> 0.0433	<sup>133</sup> 0.0525	<sup>129</sup> 0.0734	<sup>159</sup> 0.2201
70	IDEARIA-007	<sup>81</sup> 0.0136	<sup>81</sup> 0.0181	<sup>76</sup> 0.0228	<sup>75</sup> 0.0357	<sup>96</sup> 0.1402
71	IDEARIA-008	<sup>8</sup> 0.0016	<sup>8</sup> 0.0019	<sup>10</sup> 0.0024	<sup>6</sup> 0.0053	<sup>10</sup> 0.0470
72	IDEARIA-009	<sup>2</sup> 0.0013	<sup>2</sup> 0.0016	<sup>2</sup> 0.0018	<sup>7</sup> 0.0061	<sup>14</sup> 0.0550

**Table 18: Identification-mode: Effect of N on FNIR at high threshold.** Values are threshold-based miss rates i.e. FNIR at FPIR = 0.001 for five enrollment population sizes, N. The right six columns apply for enrollment of one image. Missing entries usually apply because another algorithm from the same developer was run instead. Some developers are missing because less accurate algorithms were not run on galleries with  $N \geq 3\ 000\ 000$ . Throughout blue superscripts indicate the rank of the algorithm for that column.

#	ALGORITHM	MISSES BELOW THRESHOLD, T		ENROL MOST RECENT				
		FNIR(N, T > 0, R > L)		DATASET: FRVT 2018 MUGSHOTS				
		N=0.64M	N=1.6M	N=3.0M	N=6.0M	N=12.0M		
73	IMAGUS-005	<sup>84</sup> 0.0137	<sup>85</sup> 0.0185	<sup>82</sup> 0.0237	<sup>77</sup> 0.0368	<sup>54</sup> 0.1067		
74	IMAGUS-006	<sup>85</sup> 0.0137	<sup>87</sup> 0.0190	<sup>80</sup> 0.0244	<sup>83</sup> 0.0396	<sup>70</sup> 0.1159		
75	IMAGUS-007	<sup>96</sup> 0.0160	<sup>100</sup> 0.0228	<sup>96</sup> 0.0284	<sup>92</sup> 0.0444	<sup>73</sup> 0.1179		
76	IMPERIAL-000	<sup>106</sup> 0.0187	<sup>106</sup> 0.0259	<sup>116</sup> 0.0358	<sup>128</sup> 0.0733	<sup>135</sup> 0.1794		
77	INCODE-003	<sup>22</sup> 0.1324	<sup>228</sup> 0.1672	<sup>20</sup> 0.1961	<sup>189</sup> 0.2345	<sup>182</sup> 0.3123		
78	INCODE-004	<sup>158</sup> 0.0403	<sup>159</sup> 0.0538	<sup>146</sup> 0.0662	<sup>139</sup> 0.0917	<sup>123</sup> 0.1619		
79	INCODE-005	<sup>54</sup> 0.0083	<sup>54</sup> 0.0113	<sup>56</sup> 0.0145	<sup>42</sup> 0.0247	<sup>32</sup> 0.0912		
80	INNOVATRICS-007	<sup>60</sup> 0.0093	<sup>60</sup> 0.0125	<sup>56</sup> 0.0159	<sup>47</sup> 0.0259	<sup>35</sup> 0.1092		
81	INTSYSMSU-000	<sup>28</sup> 0.9982	<sup>286</sup> 0.9984	<sup>21</sup> 0.9985	<sup>218</sup> 0.9987	<sup>20</sup> 0.9988		
82	IREX-000	<sup>111</sup> 0.0190	<sup>117</sup> 0.0280	<sup>121</sup> 0.0391	<sup>124</sup> 0.0677	<sup>108</sup> 0.1479		
83	ISYSTEMS-002	<sup>184</sup> 0.0584	<sup>184</sup> 0.0783	<sup>171</sup> 0.0973	<sup>168</sup> 0.1373	<sup>161</sup> 0.2295		
84	ISYSTEMS-003	<sup>170</sup> 0.0438	<sup>168</sup> 0.0590	<sup>164</sup> 0.0807	<sup>160</sup> 0.1259	<sup>167</sup> 0.2357		
85	KAKAO-000	<sup>72</sup> 0.0109	<sup>72</sup> 0.0151	<sup>71</sup> 0.0196	<sup>70</sup> 0.0324	<sup>44</sup> 0.1010		
86	KEDACOM-001	<sup>102</sup> 0.0181	<sup>99</sup> 0.0227	<sup>96</sup> 0.0265	<sup>91</sup> 0.0422	<sup>92</sup> 0.1340		
87	LOOKMAN-003	<sup>141</sup> 0.0346	<sup>137</sup> 0.0437	<sup>135</sup> 0.0514	<sup>127</sup> 0.0724	<sup>124</sup> 0.1620		
88	LOOKMAN-005	<sup>124</sup> 0.0240	<sup>119</sup> 0.0301	<sup>115</sup> 0.0356	<sup>102</sup> 0.0512	<sup>91</sup> 0.1334		
89	MANTRA-000	<sup>46</sup> 0.0065	<sup>51</sup> 0.0101	<sup>54</sup> 0.0151	<sup>65</sup> 0.0308	<sup>48</sup> 0.1035		
90	MEGVII-001	<sup>180</sup> 0.0562	<sup>179</sup> 0.0722	<sup>166</sup> 0.0872	<sup>164</sup> 0.1309	<sup>181</sup> 0.2713		
91	MICROFOCUS-005	<sup>28</sup> 0.9732	<sup>29</sup> 0.8354	<sup>21</sup> 0.8555	<sup>28</sup> 0.8755	<sup>20</sup> 0.8954		
92	MICROSOFT-003	<sup>114</sup> 0.0198	<sup>115</sup> 0.0278	<sup>114</sup> 0.0356	<sup>109</sup> 0.0538	<sup>114</sup> 0.1539		
93	MICROSOFT-004	<sup>105</sup> 0.0185	<sup>107</sup> 0.0259	<sup>107</sup> 0.0333	<sup>104</sup> 0.0517	<sup>112</sup> 0.1510		
94	MICROSOFT-005	<sup>103</sup> 0.0181	<sup>104</sup> 0.0256	<sup>103</sup> 0.0320	<sup>101</sup> 0.0512	<sup>110</sup> 0.1491		
95	MICROSOFT-006	<sup>59</sup> 0.0091	<sup>55</sup> 0.0120	<sup>60</sup> 0.0162	<sup>62</sup> 0.0301	<sup>109</sup> 0.1482		
96	NEC-000	<sup>18</sup> 0.0637	<sup>186</sup> 0.0789	<sup>171</sup> 0.0933	<sup>159</sup> 0.1163	<sup>14</sup> 0.1941		
97	NEC-001	<sup>203</sup> 0.0863	<sup>203</sup> 0.1055	<sup>185</sup> 0.1249	<sup>173</sup> 0.1519	<sup>162</sup> 0.2223		
98	NEC-002	<sup>14</sup> 0.0020	<sup>14</sup> 0.0026	<sup>14</sup> 0.0033	<sup>26</sup> 0.0135	<sup>18</sup> 0.0653		
99	NEC-003	<sup>15</sup> 0.0021	<sup>12</sup> 0.0024	<sup>11</sup> 0.0028	<sup>8</sup> 0.0059	<sup>12</sup> 0.0540		
100	NEC-004	<sup>9</sup> 0.0017	<sup>5</sup> 0.0018	<sup>4</sup> 0.0020	<sup>2</sup> 0.0037	<sup>4</sup> 0.0329		
101	NEC-005	<sup>4</sup> 0.0015	<sup>3</sup> 0.0017	<sup>3</sup> 0.0019	<sup>11</sup> 0.0065	<sup>2</sup> 0.0307		
102	NEUROTECHNOLOGY-003	<sup>221</sup> 0.5698	<sup>222</sup> 0.6362	<sup>212</sup> 0.7035	<sup>204</sup> 0.7602	<sup>198</sup> 0.8224		
103	NEUROTECHNOLOGY-004	<sup>17</sup> 0.0466	<sup>173</sup> 0.0629	<sup>159</sup> 0.0779	<sup>156</sup> 0.1135	<sup>15</sup> 0.2102		
104	NEUROTECHNOLOGY-005	<sup>155</sup> 0.0396	<sup>160</sup> 0.0538	<sup>149</sup> 0.0675	<sup>143</sup> 0.0950	<sup>147</sup> 0.1966		
105	NEUROTECHNOLOGY-007	<sup>16</sup> 0.0436	<sup>172</sup> 0.0623	<sup>161</sup> 0.0802	<sup>165</sup> 0.1320	<sup>167</sup> 0.2393		
106	NEUROTECHNOLOGY-008	<sup>142</sup> 0.0339	<sup>154</sup> 0.0530	<sup>168</sup> 0.0893	<sup>180</sup> 0.1769	<sup>188</sup> 0.3288		
107	NEUROTECHNOLOGY-009	<sup>70</sup> 0.0108	<sup>73</sup> 0.0152	<sup>77</sup> 0.0196	<sup>68</sup> 0.0324	<sup>59</sup> 0.1102		
108	NEUROTECHNOLOGY-010	<sup>50</sup> 0.0069	<sup>49</sup> 0.0099	<sup>51</sup> 0.0138	<sup>94</sup> 0.0449	<sup>130</sup> 0.1727		
109	NEUROTECHNOLOGY-012	<sup>37</sup> 0.0047	<sup>37</sup> 0.0068	<sup>38</sup> 0.0097	<sup>51</sup> 0.0265	<sup>94</sup> 0.1343		
110	NOTIONTAG-000	<sup>7</sup> 0.0128	<sup>76</sup> 0.0175	<sup>77</sup> 0.0228	<sup>76</sup> 0.0357	<sup>8</sup> 0.1270		
111	NTECHLAB-003	<sup>164</sup> 0.0421	<sup>158</sup> 0.0537	<sup>148</sup> 0.0674	<sup>136</sup> 0.0907	<sup>120</sup> 0.1582		
112	NTECHLAB-004	<sup>134</sup> 0.0312	<sup>133</sup> 0.0405	<sup>135</sup> 0.0519	<sup>126</sup> 0.0722	<sup>111</sup> 0.1503		
113	NTECHLAB-005	<sup>138</sup> 0.0334	<sup>134</sup> 0.0424	<sup>136</sup> 0.0537	<sup>131</sup> 0.0760	<sup>117</sup> 0.1543		
114	NTECHLAB-006	<sup>13</sup> 0.0288	<sup>128</sup> 0.0367	<sup>129</sup> 0.0471	<sup>123</sup> 0.0670	<sup>113</sup> 0.1523		
115	NTECHLAB-007	<sup>107</sup> 0.0188	<sup>103</sup> 0.0256	<sup>102</sup> 0.0317	<sup>100</sup> 0.0495	<sup>90</sup> 0.1306		
116	NTECHLAB-008	<sup>69</sup> 0.0107	<sup>66</sup> 0.0145	<sup>67</sup> 0.0187	<sup>56</sup> 0.0286	<sup>48</sup> 0.0995		
117	NTECHLAB-009	<sup>30</sup> 0.0037	<sup>30</sup> 0.0049	<sup>29</sup> 0.0062	<sup>25</sup> 0.0125	<sup>20</sup> 0.0735		
118	NTECHLAB-010	<sup>12</sup> 0.0020	<sup>13</sup> 0.0025	<sup>12</sup> 0.0030	<sup>15</sup> 0.0077	<sup>19</sup> 0.0710		
119	NTECHLAB-011	<sup>16</sup> 0.0022	<sup>17</sup> 0.0030	<sup>16</sup> 0.0038	<sup>14</sup> 0.0075	<sup>14</sup> 0.0625		
120	PANGIAM-000	<sup>36</sup> 0.0042	<sup>36</sup> 0.0060	<sup>36</sup> 0.0080	<sup>32</sup> 0.0160	<sup>30</sup> 0.0876		
121	PARAVISION-003	<sup>126</sup> 0.0260	<sup>126</sup> 0.0351	<sup>127</sup> 0.0447	<sup>122</sup> 0.0657	<sup>12</sup> 0.1630		
122	PARAVISION-004	<sup>51</sup> 0.0074	<sup>53</sup> 0.0101	<sup>49</sup> 0.0136	<sup>52</sup> 0.0267	<sup>82</sup> 0.1256		
123	PARAVISION-005	<sup>22</sup> 0.0032	<sup>23</sup> 0.0041	<sup>23</sup> 0.0057	<sup>34</sup> 0.0174	<sup>49</sup> 0.1037		
124	PARAVISION-007	<sup>22</sup> 0.0030	<sup>22</sup> 0.0040	<sup>22</sup> 0.0055	<sup>36</sup> 0.0211	<sup>56</sup> 0.1097		
125	PARAVISION-009	<sup>12</sup> 0.0020	<sup>15</sup> 0.0026	<sup>17</sup> 0.0038	<sup>18</sup> 0.0098	<sup>28</sup> 0.0857		
126	PIXELALL-002	<sup>198</sup> 0.0716	<sup>202</sup> 0.1052	<sup>192</sup> 0.1475	<sup>193</sup> 0.2489	<sup>193</sup> 0.3904		
127	PIXELALL-003	<sup>99</sup> 0.0158	<sup>95</sup> 0.0218	<sup>97</sup> 0.0288	<sup>96</sup> 0.0474	<sup>69</sup> 0.1138		
128	PIXELALL-004	<sup>79</sup> 0.0129	<sup>84</sup> 0.0183	<sup>86</sup> 0.0245	<sup>78</sup> 0.0378	<sup>96</sup> 0.1375		
129	PIXELALL-005	<sup>57</sup> 0.0087	<sup>57</sup> 0.0121	<sup>62</sup> 0.0171	<sup>44</sup> 0.0250	<sup>51</sup> 0.1052		
130	PTAKURATSATU-000	<sup>12</sup> 0.0275	<sup>127</sup> 0.0366	<sup>128</sup> 0.0458	<sup>107</sup> 0.0523	<sup>11</sup> 0.0523		
131	QNAP-001	<sup>159</sup> 0.0404	<sup>157</sup> 0.0536	<sup>148</sup> 0.0661	<sup>138</sup> 0.0916	<sup>121</sup> 0.1595		
132	QNAP-002	<sup>115</sup> 0.0200	<sup>108</sup> 0.0265	<sup>108</sup> 0.0327	<sup>98</sup> 0.0490	<sup>93</sup> 0.1341		
133	QUANTASOFT-001	<sup>273</sup> 0.6387	<sup>273</sup> 0.6387	<sup>211</sup> 0.6387		<sup>196</sup> 0.6387		
134	RANKONE-002	<sup>211</sup> 0.0973	<sup>206</sup> 0.1175	<sup>187</sup> 0.1359	<sup>177</sup> 0.1718	<sup>179</sup> 0.2613		
135	RANKONE-003	<sup>212</sup> 0.0973	<sup>207</sup> 0.1175	<sup>186</sup> 0.1359	<sup>178</sup> 0.1718	<sup>178</sup> 0.2613		
136	RANKONE-005	<sup>17</sup> 0.0473	<sup>169</sup> 0.0592	<sup>157</sup> 0.0700	<sup>141</sup> 0.0944	<sup>148</sup> 0.1998		
137	RANKONE-007	<sup>99</sup> 0.0168	<sup>97</sup> 0.0222	<sup>91</sup> 0.0266	<sup>80</sup> 0.0381	<sup>64</sup> 0.1132		
138	RANKONE-009	<sup>80</sup> 0.0132	<sup>79</sup> 0.0177	<sup>78</sup> 0.0230	<sup>72</sup> 0.0344	<sup>36</sup> 0.0921		
139	RANKONE-010	<sup>67</sup> 0.0106	<sup>63</sup> 0.0136	<sup>65</sup> 0.0174	<sup>50</sup> 0.0265	<sup>22</sup> 0.0785		
140	RANKONE-011	<sup>43</sup> 0.0063	<sup>43</sup> 0.0087	<sup>41</sup> 0.0115	<sup>33</sup> 0.0269	<sup>66</sup> 0.1135		
141	RANKONE-012	<sup>42</sup> 0.0058	<sup>40</sup> 0.0077	<sup>40</sup> 0.0100	<sup>37</sup> 0.0220	<sup>60</sup> 0.1111		
142	REALNETWORKS-002	<sup>239</sup> 0.1943	<sup>238</sup> 0.2314	<sup>206</sup> 0.2656	<sup>199</sup> 0.3134	<sup>187</sup> 0.3208		
143	REALNETWORKS-003	<sup>22</sup> 0.1300	<sup>224</sup> 0.1594	<sup>198</sup> 0.1858	<sup>187</sup> 0.2246	<sup>181</sup> 0.3076		
144	REALNETWORKS-004	<sup>224</sup> 0.1279	<sup>223</sup> 0.1581	<sup>197</sup> 0.1857	<sup>188</sup> 0.2329	<sup>186</sup> 0.3179		

**Table 19: Identification-mode: Effect of N on FNIR at high threshold.** Values are threshold-based miss rates i.e. FNIR at FPIR = 0.001 for five enrollment population sizes, N. The right six columns apply for enrollment of one image. Missing entries usually apply because another algorithm from the same developer was run instead. Some developers are missing because less accurate algorithms were not run on galleries with  $N \geq 3\ 000\ 000$ . Throughout blue superscripts indicate the rank of the algorithm for that column.

#	ALGORITHM	MISSES BELOW THRESHOLD, T FNIR(N, T > 0, R > L)		ENROL MOST RECENT DATASET: FRVT 2018 MUGSHOTS					
		N=0.64M	N=1.6M	N=3.0M	N=6.0M	N=12.0M			
145	REALNETWORKS-005	<sup>116</sup> 0.0202	<sup>114</sup> 0.0277	<sup>117</sup> 0.0355	<sup>116</sup> 0.0560	<sup>100</sup> 0.1431			
146	REALNETWORKS-006	<sup>62</sup> 0.0097	<sup>67</sup> 0.0145	<sup>66</sup> 0.0182	<sup>66</sup> 0.0308	<sup>42</sup> 0.0991			
147	REALNETWORKS-007	<sup>49</sup> 0.0068	<sup>47</sup> 0.0097	<sup>48</sup> 0.0125	<sup>39</sup> 0.0233	<sup>33</sup> 0.0917			
148	REMARKAI-000	<sup>161</sup> 0.0406	<sup>161</sup> 0.0552	<sup>159</sup> 0.0676	<sup>147</sup> 0.1028	<sup>159</sup> 0.2003			
149	RENDIP-000	<sup>35</sup> 0.0085	<sup>56</sup> 0.0121	<sup>56</sup> 0.0156	<sup>35</sup> 0.0277	<sup>74</sup> 0.1182			
150	REVEALMEDIA-000	<sup>38</sup> 0.0090	<sup>38</sup> 0.0122	<sup>37</sup> 0.0158	<sup>34</sup> 0.0277	<sup>45</sup> 0.1019			
151	S1-000	<sup>118</sup> 0.0204	<sup>116</sup> 0.0279	<sup>119</sup> 0.0382	<sup>120</sup> 0.0630	<sup>128</sup> 0.1707			
152	S1-001	<sup>75</sup> 0.0115	<sup>74</sup> 0.0156	<sup>73</sup> 0.0199	<sup>81</sup> 0.0392	<sup>83</sup> 0.1256			
153	S1-002	<sup>34</sup> 0.0040	<sup>34</sup> 0.0056	<sup>34</sup> 0.0077	<sup>49</sup> 0.0264	<sup>87</sup> 0.1285			
154	SCANOVATE-000	<sup>126</sup> 0.0498	<sup>176</sup> 0.0667	<sup>162</sup> 0.0804	<sup>151</sup> 0.1097	<sup>39</sup> 0.1109			
155	SCANOVATE-001	<sup>187</sup> 0.0630	<sup>187</sup> 0.0815	<sup>177</sup> 0.0993	<sup>161</sup> 0.1292	<sup>146</sup> 0.1960			
156	SENSETIME-000	<sup>94</sup> 0.0158	<sup>93</sup> 0.0208	<sup>91</sup> 0.0270	<sup>84</sup> 0.0398	<sup>75</sup> 0.1232			
157	SENSETIME-001	<sup>97</sup> 0.0161	<sup>96</sup> 0.0219	<sup>97</sup> 0.0277	<sup>90</sup> 0.0420	<sup>88</sup> 0.1304			
158	SENSETIME-002	<sup>89</sup> 0.0146	<sup>68</sup> 0.0148	<sup>59</sup> 0.0153	<sup>40</sup> 0.0234	<sup>16</sup> 0.0657			
159	SENSETIME-003	<sup>6</sup> 0.0016	<sup>7</sup> 0.0018	<sup>6</sup> 0.0021	<sup>7</sup> 0.0054	<sup>7</sup> 0.0451			
160	SENSETIME-004	<sup>3</sup> 0.0015	<sup>4</sup> 0.0018	<sup>3</sup> 0.0021	<sup>3</sup> 0.0040	<sup>3</sup> 0.0354			
161	SENSETIME-005	<sup>7</sup> 0.0016	<sup>11</sup> 0.0022	<sup>13</sup> 0.0031	<sup>17</sup> 0.0089	<sup>8</sup> 0.0454			
162	SENSETIME-006	<sup>1</sup> 0.0014	<sup>6</sup> 0.0018	<sup>7</sup> 0.0023	<sup>4</sup> 0.0047	<sup>10</sup> 0.0372			
163	SENSETIME-007	<sup>1</sup> 0.0012	<sup>1</sup> 0.0014	<sup>1</sup> 0.0016	<sup>1</sup> 0.0036	<sup>1</sup> 0.0316			
164	SHAMAN-007	<sup>223</sup> 0.1212	<sup>219</sup> 0.1413	<sup>193</sup> 0.1587	<sup>182</sup> 0.1879	<sup>172</sup> 0.2460			
165	SIAT-001	<sup>82</sup> 0.0136	<sup>77</sup> 0.0176	<sup>89</sup> 0.0230	<sup>71</sup> 0.0344	<sup>47</sup> 0.1035			
166	SIAT-002	<sup>93</sup> 0.0154	<sup>94</sup> 0.0216	<sup>95</sup> 0.0273	<sup>86</sup> 0.0404	<sup>36</sup> 0.1283			
167	SQISOFT-001	<sup>204</sup> 0.0921	<sup>215</sup> 0.1322	<sup>199</sup> 0.1781	<sup>190</sup> 0.2348	<sup>201</sup> 0.9271			
168	SYNESIS-003	<sup>127</sup> 0.0499	<sup>174</sup> 0.0652	<sup>163</sup> 0.0804	<sup>150</sup> 0.1095	<sup>142</sup> 0.1916			
169	SYNESIS-003	<sup>269</sup> 0.5341	<sup>268</sup> 0.5821	<sup>219</sup> 0.6113	<sup>203</sup> 0.6479	<sup>197</sup> 0.6822			
170	SYNESIS-005	<sup>101</sup> 0.0181	<sup>102</sup> 0.0248	<sup>103</sup> 0.0319	<sup>105</sup> 0.0518	<sup>119</sup> 0.1580			
171	TECH5-001	<sup>163</sup> 0.0420	<sup>164</sup> 0.0574	<sup>167</sup> 0.0911	<sup>185</sup> 0.2106	<sup>192</sup> 0.3725			
172	TECH5-002	<sup>112</sup> 0.0194	<sup>111</sup> 0.0269	<sup>111</sup> 0.0346	<sup>108</sup> 0.0537	<sup>122</sup> 0.1607			
173	TEVIAN-005	<sup>195</sup> 0.0692	<sup>192</sup> 0.0873	<sup>179</sup> 0.1066	<sup>163</sup> 0.1301	<sup>139</sup> 0.1840			
174	TEVIAN-006	<sup>35</sup> 0.0078	<sup>48</sup> 0.0098	<sup>47</sup> 0.0130	<sup>48</sup> 0.0261	<sup>89</sup> 0.1305			
175	TEVIAN-007	<sup>32</sup> 0.0038	<sup>32</sup> 0.0052	<sup>36</sup> 0.0065	<sup>29</sup> 0.0154	<sup>39</sup> 0.0957			
176	TIGER-002	<sup>190</sup> 0.0647	<sup>188</sup> 0.0861	<sup>174</sup> 0.1036	<sup>166</sup> 0.1332	<sup>160</sup> 0.2231			
177	TOSHIBA-000	<sup>173</sup> 0.0460	<sup>171</sup> 0.0620	<sup>168</sup> 0.0780	<sup>153</sup> 0.1117	<sup>153</sup> 0.2082			
178	TRUEFACE-000	<sup>81</sup> 0.0134	<sup>83</sup> 0.0182	<sup>83</sup> 0.0238	<sup>79</sup> 0.0380	<sup>97</sup> 0.1385			
179	VD-001	<sup>238</sup> 0.1642	<sup>235</sup> 0.2015	<sup>206</sup> 0.2351	<sup>196</sup> 0.2736	<sup>186</sup> 0.3293			
180	VERIDAS-001	<sup>129</sup> 0.0278	<sup>131</sup> 0.0373	<sup>130</sup> 0.0491	<sup>130</sup> 0.0753	<sup>115</sup> 0.1541			
181	VERIDAS-002	<sup>128</sup> 0.0278	<sup>130</sup> 0.0373	<sup>117</sup> 0.0373	<sup>99</sup> 0.0491	<sup>21</sup> 0.0753			
182	VERIDAS-003	<sup>74</sup> 0.0117	<sup>75</sup> 0.0166	<sup>79</sup> 0.0219	<sup>93</sup> 0.0446	<sup>116</sup> 0.1543			
183	VIGILANTSOLUTIONS-008	<sup>90</sup> 0.0146	<sup>90</sup> 0.0205	<sup>93</sup> 0.0269	<sup>97</sup> 0.0489	<sup>21</sup> 0.1164			
184	VISIONBOX-000	<sup>75</sup> 0.0122	<sup>80</sup> 0.0177	<sup>89</sup> 0.0239		<sup>202</sup> 0.9538			
185	VISIONLABS-004	<sup>166</sup> 0.0427	<sup>165</sup> 0.0578	<sup>156</sup> 0.0703	<sup>142</sup> 0.0949	<sup>138</sup> 0.1853			
186	VISIONLABS-005	<sup>151</sup> 0.0369	<sup>149</sup> 0.0502	<sup>148</sup> 0.0626	<sup>134</sup> 0.0847	<sup>136</sup> 0.1815			
187	VISIONLABS-006	<sup>108</sup> 0.0188	<sup>110</sup> 0.0267	<sup>109</sup> 0.0336	<sup>113</sup> 0.0542	<sup>106</sup> 0.1478			
188	VISIONLABS-007	<sup>109</sup> 0.0188	<sup>109</sup> 0.0266	<sup>108</sup> 0.0335	<sup>111</sup> 0.0540	<sup>107</sup> 0.1479			
189	VISIONLABS-008	<sup>61</sup> 0.0096	<sup>61</sup> 0.0131	<sup>61</sup> 0.0166	<sup>58</sup> 0.0291	<sup>29</sup> 0.1247			
190	VISIONLABS-009	<sup>29</sup> 0.0034	<sup>26</sup> 0.0046	<sup>29</sup> 0.0060	<sup>27</sup> 0.0140	<sup>31</sup> 0.0881			
191	VISIONLABS-010	<sup>31</sup> 0.0038	<sup>31</sup> 0.0051	<sup>32</sup> 0.0070	<sup>28</sup> 0.0149	<sup>35</sup> 0.0920			
192	VISIONLABS-011	<sup>18</sup> 0.0025	<sup>19</sup> 0.0033	<sup>20</sup> 0.0044	<sup>21</sup> 0.0120	<sup>25</sup> 0.0825			
193	VNPIT-001	<sup>65</sup> 0.0104	<sup>65</sup> 0.0143	<sup>69</sup> 0.0190	<sup>61</sup> 0.0296	<sup>46</sup> 0.1028			
194	VOCORD-005	<sup>220</sup> 0.1179	<sup>222</sup> 0.1577	<sup>208</sup> 0.2183	<sup>198</sup> 0.3122	<sup>195</sup> 0.4490			
195	VTS-001	<sup>64</sup> 0.0102	<sup>62</sup> 0.0133	<sup>69</sup> 0.0175	<sup>67</sup> 0.0322	<sup>78</sup> 0.1243			
196	VTS-002	<sup>104</sup> 0.0185	<sup>105</sup> 0.0259	<sup>110</sup> 0.0344	<sup>115</sup> 0.0549	<sup>103</sup> 0.1447			
197	XFORWARDAI-000	<sup>69</sup> 0.0107	<sup>71</sup> 0.0151	<sup>70</sup> 0.0195	<sup>69</sup> 0.0324	<sup>32</sup> 0.1057			
198	XFORWARDAI-001	<sup>29</sup> 0.0037	<sup>29</sup> 0.0049	<sup>27</sup> 0.0060	<sup>20</sup> 0.0120	<sup>23</sup> 0.0800			
199	XFORWARDAI-002	<sup>19</sup> 0.0026	<sup>18</sup> 0.0030	<sup>16</sup> 0.0035	<sup>16</sup> 0.0078	<sup>18</sup> 0.0706			
200	YITU-002	<sup>78</sup> 0.0129	<sup>78</sup> 0.0177	<sup>78</sup> 0.0228	<sup>73</sup> 0.0345	<sup>65</sup> 0.1133			
201	YITU-003	<sup>86</sup> 0.0138	<sup>86</sup> 0.0185	<sup>81</sup> 0.0236	<sup>74</sup> 0.0353	<sup>68</sup> 0.1148			
202	YITU-004	<sup>48</sup> 0.0067	<sup>45</sup> 0.0096	<sup>46</sup> 0.0129	<sup>38</sup> 0.0232	<sup>50</sup> 0.1046			
203	YITU-005	<sup>32</sup> 0.0074	<sup>52</sup> 0.0101	<sup>46</sup> 0.0135	<sup>46</sup> 0.0255	<sup>32</sup> 0.1057			

**Table 20: Identification-mode: Effect of N on FNIR at high threshold.** Values are threshold-based miss rates i.e. FNIR at FPIR = 0.001 for five enrollment population sizes, N. The right six columns apply for enrollment of one image. Missing entries usually apply because another algorithm from the same developer was run instead. Some developers are missing because less accurate algorithms were not run on galleries with  $N \geq 3\,000\,000$ . Throughout blue superscripts indicate the rank of the algorithm for that column.

MISSES AT GIVEN RANK		ENROL MOST RECENT													
#	ALGORITHM	RANK 1					$aN^b$	RANK 50					$aN^b$		
		N=0.64M	N=1.6M	N=3.0M	N=6.0M	N=12.0M		N=0.64M	N=1.6M	N=3.0M	N=6.0M	N=12.0M			
1	3DIVI-005	<sup>225</sup> 0.0137	<sup>223</sup> 0.0176	<sup>193</sup> 0.0210	<sup>187</sup> 0.0253	<sup>182</sup> 0.0302	<sup>146</sup> 0.0004 N <sup>0.271</sup> <sup>164</sup>	<sup>206</sup> 0.0040	<sup>206</sup> 0.0049	<sup>183</sup> 0.0057	<sup>179</sup> 0.0068	<sup>174</sup> 0.0081	<sup>48</sup> 0.0002 N <sup>0.240</sup> <sup>169</sup>		
2	ACER-000	<sup>194</sup> 0.0081	<sup>200</sup> 0.0106	<sup>181</sup> 0.0128	<sup>179</sup> 0.0157	<sup>174</sup> 0.0195	<sup>61</sup> 0.0001 N <sup>0.299</sup> <sup>188</sup>	<sup>153</sup> 0.0020	<sup>170</sup> 0.0026	<sup>160</sup> 0.0031	<sup>160</sup> 0.0037	<sup>156</sup> 0.0045	<sup>19</sup> 0.0000 N <sup>0.284</sup> <sup>182</sup>		
3	ALCHERA-003	<sup>190</sup> 0.0079	<sup>19</sup> 0.0104	<sup>178</sup> 0.0123	<sup>178</sup> 0.0147	<sup>173</sup> 0.0180	<sup>92</sup> 0.0002 N <sup>0.278</sup> <sup>175</sup>	<sup>187</sup> 0.0027	<sup>186</sup> 0.0032	<sup>166</sup> 0.0035	<sup>166</sup> 0.0042	<sup>159</sup> 0.0048	<sup>56</sup> 0.0002 N <sup>0.199</sup> <sup>159</sup>		
4	ALLGOVISION-000	<sup>208</sup> 0.0101	<sup>205</sup> 0.0114	<sup>180</sup> 0.0127	<sup>177</sup> 0.0145	<sup>172</sup> 0.0166	<sup>179</sup> 0.0010 N <sup>0.171</sup> <sup>100</sup>	<sup>226</sup> 0.0063	<sup>222</sup> 0.0067	<sup>188</sup> 0.0071	<sup>182</sup> 0.0075	<sup>173</sup> 0.0081	<sup>185</sup> 0.0020 N <sup>0.086</sup> <sup>117</sup>		
5	ALLGOVISION-001	<sup>182</sup> 0.0069	<sup>18</sup> 0.0094	<sup>174</sup> 0.0107	<sup>172</sup> 0.0128	<sup>167</sup> 0.0157	<sup>78</sup> 0.0002 N <sup>0.277</sup> <sup>173</sup>	<sup>174</sup> 0.0023	<sup>175</sup> 0.0027	<sup>161</sup> 0.0031	<sup>158</sup> 0.0036	<sup>154</sup> 0.0043	<sup>41</sup> 0.0001 N <sup>0.211</sup> <sup>164</sup>		
6	ANKE-000	<sup>211</sup> 0.0102	<sup>213</sup> 0.0132	<sup>188</sup> 0.0155	<sup>184</sup> 0.0188	<sup>178</sup> 0.0225	<sup>128</sup> 0.0003 N <sup>0.270</sup> <sup>163</sup>	<sup>196</sup> 0.0032	<sup>198</sup> 0.0040	<sup>172</sup> 0.0046	<sup>172</sup> 0.0056	<sup>165</sup> 0.0066	<sup>40</sup> 0.0001 N <sup>0.247</sup> <sup>171</sup>		
7	ANKE-002	<sup>115</sup> 0.0024	<sup>118</sup> 0.0026	<sup>112</sup> 0.0032	<sup>107</sup> 0.0037	<sup>107</sup> 0.0043	<sup>71</sup> 0.0002 N <sup>0.203</sup> <sup>117</sup>	<sup>125</sup> 0.0016	<sup>125</sup> 0.0017	<sup>118</sup> 0.0017	<sup>108</sup> 0.0018	<sup>103</sup> 0.0019	<sup>108</sup> 0.0006 N <sup>0.076</sup> <sup>105</sup>		
8	AWARE-003	<sup>242</sup> 0.0238	<sup>240</sup> 0.0306	<sup>201</sup> 0.0361	<sup>198</sup> 0.0431	<sup>193</sup> 0.0506	<sup>178</sup> 0.0008 N <sup>0.258</sup> <sup>158</sup>	<sup>220</sup> 0.0055	<sup>228</sup> 0.0075	<sup>198</sup> 0.0092	<sup>193</sup> 0.0113	<sup>192</sup> 0.0143	<sup>30</sup> 0.0001 N <sup>0.323</sup> <sup>192</sup>		
9	AWARE-005	<sup>243</sup> 0.0245	<sup>241</sup> 0.0311	<sup>203</sup> 0.0366	<sup>199</sup> 0.0434	<sup>186</sup> 0.0312	<sup>196</sup> 0.0056 N <sup>0.118</sup> <sup>56</sup>	<sup>224</sup> 0.0062	<sup>234</sup> 0.0082	<sup>200</sup> 0.0101	<sup>196</sup> 0.0128	<sup>176</sup> 0.0089	<sup>130</sup> 0.0007 N <sup>0.169</sup> <sup>154</sup>		
10	AYONIX-002	<sup>239</sup> 0.2935	<sup>27</sup> 0.3414	<sup>218</sup> 0.3736	<sup>207</sup> 0.4101	<sup>201</sup> 0.4465	<sup>201</sup> 0.0440 N <sup>0.143</sup> <sup>73</sup>	<sup>278</sup> 0.0950	<sup>280</sup> 0.1274	<sup>215</sup> 0.1524	<sup>208</sup> 0.1828	<sup>201</sup> 0.2150	<sup>108</sup> 0.0023 N <sup>0.279</sup> <sup>180</sup>		
11	CAMVI-004	<sup>218</sup> 0.0124	<sup>251</sup> 0.0468	<sup>209</sup> 0.0719	<sup>206</sup> 0.2363	<sup>203</sup> 0.2367	<sup>3</sup> 0.0000 N <sup>0.055</sup> <sup>202</sup>	<sup>202</sup> 0.0117	<sup>268</sup> 0.0464	<sup>211</sup> 0.0715	<sup>207</sup> 0.2361	<sup>201</sup> 0.2364	<sup>3</sup> 0.0000 N <sup>0.191</sup> <sup>202</sup>		
12	CANON-001	<sup>15</sup> 0.0011	<sup>14</sup> 0.0011	<sup>19</sup> 0.0012	<sup>16</sup> 0.0013	<sup>14</sup> 0.0014	<sup>108</sup> 0.0002 N <sup>0.113</sup> <sup>49</sup>	<sup>18</sup> 0.0009	<sup>18</sup> 0.0009	<sup>19</sup> 0.0009	<sup>18</sup> 0.0010	<sup>105</sup> 0.0006 N <sup>0.024</sup> <sup>80</sup>			
13	CANON-002	<sup>18</sup> 0.0011	<sup>19</sup> 0.0012	<sup>22</sup> 0.0013	<sup>22</sup> 0.0014	<sup>21</sup> 0.0016	<sup>71</sup> 0.0002 N <sup>0.142</sup> <sup>72</sup>	<sup>19</sup> 0.0009	<sup>16</sup> 0.0009	<sup>14</sup> 0.0009	<sup>14</sup> 0.0009	<sup>131</sup> 0.0007 N <sup>0.105</sup> <sup>26</sup>			
14	CIB-000	<sup>49</sup> 0.0014	<sup>44</sup> 0.0015	<sup>48</sup> 0.0017	<sup>48</sup> 0.0019	<sup>163</sup> 0.0131	<sup>4</sup> 0.0000 N <sup>0.635</sup> <sup>201</sup>	<sup>59</sup> 0.0012	<sup>53</sup> 0.0012	<sup>51</sup> 0.0012	<sup>49</sup> 0.0012	<sup>48</sup> 0.0012	<sup>188</sup> 0.0122	<sup>4</sup> 0.0000 N <sup>0.647</sup> <sup>201</sup>	
15	CLEARVIEWAI-000	<sup>12</sup> 0.0010	<sup>13</sup> 0.0011	<sup>14</sup> 0.0012	<sup>17</sup> 0.0013	<sup>18</sup> 0.0015	<sup>83</sup> 0.0002 N <sup>0.129</sup> <sup>65</sup>	<sup>21</sup> 0.0009	<sup>17</sup> 0.0009	<sup>17</sup> 0.0009	<sup>15</sup> 0.0009	<sup>120</sup> 0.0007 N <sup>0.109</sup> <sup>40</sup>			
16	CLOUDWALK-HR-000	<sup>53</sup> 0.0015	<sup>41</sup> 0.0015	<sup>38</sup> 0.0015	<sup>33</sup> 0.0016	<sup>29</sup> 0.0017	<sup>171</sup> 0.0007 N <sup>0.054</sup> <sup>11</sup>	<sup>111</sup> 0.0014	<sup>92</sup> 0.0014	<sup>87</sup> 0.0014	<sup>80</sup> 0.0014	<sup>62</sup> 0.0014	<sup>168</sup> 0.0012 N <sup>0.102</sup> <sup>18</sup>		
17	CLOUDWALK-MT-000	<sup>80</sup> 0.0018	<sup>61</sup> 0.0018	<sup>53</sup> 0.0018	<sup>43</sup> 0.0019	<sup>36</sup> 0.0020	<sup>180</sup> 0.0011 N <sup>0.036</sup> <sup>6</sup>	<sup>138</sup> 0.0018	<sup>133</sup> 0.0018	<sup>121</sup> 0.0018	<sup>105</sup> 0.0018	<sup>92</sup> 0.0018	<sup>182</sup> 0.0017 N <sup>0.002</sup> <sup>4</sup>		
18	COGENT-000	<sup>210</sup> 0.0101	<sup>198</sup> 0.0105	<sup>176</sup> 0.0109	<sup>167</sup> 0.0115	<sup>160</sup> 0.0125	<sup>194</sup> 0.0038 N <sup>0.071</sup> <sup>18</sup>	<sup>162</sup> 0.0021	<sup>163</sup> 0.0024	<sup>156</sup> 0.0028	<sup>159</sup> 0.0036	<sup>159</sup> 0.0095	<sup>3</sup> 0.0000 N <sup>0.466</sup> <sup>197</sup>		
19	COGENT-001	<sup>209</sup> 0.0101	<sup>179</sup> 0.0105	<sup>175</sup> 0.0109	<sup>168</sup> 0.0115	<sup>161</sup> 0.0125	<sup>194</sup> 0.0038 N <sup>0.071</sup> <sup>17</sup>	<sup>163</sup> 0.0021	<sup>164</sup> 0.0024	<sup>155</sup> 0.0028	<sup>158</sup> 0.0036	<sup>159</sup> 0.0095	<sup>9</sup> 0.0000 N <sup>0.466</sup> <sup>198</sup>		
20	COGENT-002	<sup>128</sup> 0.0029	<sup>13</sup> 0.0036	<sup>129</sup> 0.0041	<sup>127</sup> 0.0049	<sup>123</sup> 0.0059	<sup>43</sup> 0.0001 N <sup>0.244</sup> <sup>150</sup>	<sup>107</sup> 0.0014	<sup>116</sup> 0.0015	<sup>112</sup> 0.0017	<sup>111</sup> 0.0019	<sup>110</sup> 0.0021	<sup>51</sup> 0.0002 N <sup>0.144</sup> <sup>148</sup>		
21	COGENT-003	<sup>134</sup> 0.0031	<sup>133</sup> 0.0038	<sup>134</sup> 0.0043	<sup>130</sup> 0.0051	<sup>127</sup> 0.0060	<sup>57</sup> 0.0001 N <sup>0.230</sup> <sup>139</sup>	<sup>118</sup> 0.0015	<sup>127</sup> 0.0017	<sup>131</sup> 0.0018	<sup>126</sup> 0.0020	<sup>120</sup> 0.0022	<sup>58</sup> 0.0002 N <sup>0.143</sup> <sup>147</sup>		
22	COGENT-004	<sup>81</sup> 0.0018	<sup>80</sup> 0.0026	<sup>78</sup> 0.0022	<sup>77</sup> 0.0025	<sup>69</sup> 0.0025	<sup>96</sup> 0.0002 N <sup>0.159</sup> <sup>89</sup>	<sup>99</sup> 0.0013	<sup>94</sup> 0.0014	<sup>88</sup> 0.0014	<sup>85</sup> 0.0015	<sup>79</sup> 0.0015	<sup>113</sup> 0.0007 N <sup>0.050</sup> <sup>84</sup>		
23	COGENT-005	<sup>60</sup> 0.0016	<sup>55</sup> 0.0017	<sup>54</sup> 0.0018	<sup>51</sup> 0.0020	<sup>45</sup> 0.0021	<sup>145</sup> 0.0004 N <sup>0.108</sup> <sup>149</sup>	<sup>101</sup> 0.0013	<sup>86</sup> 0.0013	<sup>80</sup> 0.0014	<sup>69</sup> 0.0014	<sup>61</sup> 0.0014	<sup>165</sup> 0.0011 N <sup>0.117</sup> <sup>31</sup>		
24	COGENT-006	<sup>27</sup> 0.0012	<sup>28</sup> 0.0012	<sup>23</sup> 0.0013	<sup>20</sup> 0.0014	<sup>19</sup> 0.0015	<sup>146</sup> 0.0004 N <sup>0.088</sup> <sup>31</sup>	<sup>43</sup> 0.0011	<sup>42</sup> 0.0011	<sup>39</sup> 0.0011	<sup>31</sup> 0.0011	<sup>28</sup> 0.0011	<sup>143</sup> 0.0008 N <sup>0.119</sup> <sup>38</sup>		
25	COGNITEC-000	<sup>236</sup> 0.0195	<sup>235</sup> 0.0252	<sup>20</sup> 0.0297	<sup>196</sup> 0.0352	<sup>190</sup> 0.0417	<sup>168</sup> 0.0006 N <sup>0.259</sup> <sup>159</sup>	<sup>216</sup> 0.0050	<sup>220</sup> 0.0065	<sup>195</sup> 0.0077	<sup>192</sup> 0.0097	<sup>187</sup> 0.0122	<sup>37</sup> 0.0001 N <sup>0.305</sup> <sup>186</sup>		
26	COGNITEC-001	<sup>204</sup> 0.0090	<sup>204</sup> 0.0117	<sup>186</sup> 0.0139	<sup>182</sup> 0.0166	<sup>176</sup> 0.0199	<sup>118</sup> 0.0002 N <sup>0.271</sup> <sup>166</sup>	<sup>192</sup> 0.0030	<sup>191</sup> 0.0034	<sup>175</sup> 0.0040	<sup>171</sup> 0.0046	<sup>161</sup> 0.0054	<sup>51</sup> 0.0002 N <sup>0.207</sup> <sup>163</sup>		
27	COGNITEC-002	<sup>164</sup> 0.0048	<sup>162</sup> 0.0057	<sup>154</sup> 0.0067	<sup>147</sup> 0.0079	<sup>147</sup> 0.0094	<sup>100</sup> 0.0002 N <sup>0.232</sup> <sup>141</sup>	<sup>176</sup> 0.0024	<sup>172</sup> 0.0026	<sup>158</sup> 0.0030	<sup>150</sup> 0.0030	<sup>140</sup> 0.0034	<sup>88</sup> 0.0005 N <sup>0.117</sup> <sup>134</sup>		
28	COGNITEC-003	<sup>167</sup> 0.0053	<sup>166</sup> 0.0062	<sup>157</sup> 0.0072	<sup>154</sup> 0.0085	<sup>150</sup> 0.0100	<sup>125</sup> 0.0003 N <sup>0.222</sup> <sup>130</sup>	<sup>189</sup> 0.0028	<sup>183</sup> 0.0030	<sup>163</sup> 0.0032	<sup>153</sup> 0.0035	<sup>146</sup> 0.0037	<sup>138</sup> 0.0008 N <sup>0.097</sup> <sup>125</sup>		
29	COGNITEC-004	<sup>123</sup> 0.0027	<sup>12</sup> 0.0032	<sup>124</sup> 0.0037	<sup>120</sup> 0.0045	<sup>119</sup> 0.0056	<sup>33</sup> 0.0001 N <sup>0.253</sup> <sup>156</sup>	<sup>97</sup> 0.0013	<sup>98</sup> 0.0014	<sup>92</sup> 0.0014	<sup>88</sup> 0.0014	<sup>80</sup> 0.0014	<sup>62</sup> 0.0002 N <sup>0.123</sup> <sup>139</sup>		
30	COGNITEC-005	<sup>50</sup> 0.0014	<sup>52</sup> 0.0016	<sup>56</sup> 0.0018	<sup>54</sup> 0.0021	<sup>58</sup> 0.0024	<sup>62</sup> 0.0001 N <sup>0.169</sup> <sup>97</sup>	<sup>47</sup> 0.0011	<sup>47</sup> 0.0011	<sup>46</sup> 0.0012	<sup>45</sup> 0.0012	<sup>41</sup> 0.0012	<sup>111</sup> 0.0007 N <sup>0.109</sup> <sup>129</sup>		
31	COGNITEC-006	<sup>46</sup> 0.0014	<sup>48</sup> 0.0016	<sup>44</sup> 0.0017	<sup>47</sup> 0.0019	<sup>47</sup> 0.0022	<sup>81</sup> 0.0002 N <sup>0.154</sup> <sup>81</sup>	<sup>50</sup> 0.0011	<sup>46</sup> 0.0011	<sup>46</sup> 0.0011	<sup>41</sup> 0.0012	<sup>40</sup> 0.0012	<sup>112</sup> 0.0007 N <sup>0.136</sup> <sup>63</sup>		
32	CYBERLINK-000	<sup>140</sup> 0.0034	<sup>135</sup> 0.0040	<sup>133</sup> 0.0045	<sup>129</sup> 0.0063	<sup>129</sup> 0.0063	<sup>94</sup> 0.0002 N <sup>0.209</sup> <sup>123</sup>	<sup>160</sup> 0.0021	<sup>155</sup> 0.0022	<sup>147</sup> 0.0023	<sup>145</sup> 0.0025	<sup>134</sup> 0.0027	<sup>102</sup> 0.0006 N <sup>0.092</sup> <sup>122</sup>		
33	CYBERLINK-001	<sup>131</sup> 0.0030	<sup>130</sup> 0.0035	<sup>134</sup> 0.0042	<sup>129</sup> 0.0050	<sup>126</sup> 0.0060	<sup>44</sup> 0.0001 N <sup>0.243</sup> <sup>149</sup>	<sup>129</sup> 0.0016	<sup>120</sup> 0.0017	<sup>118</sup> 0.0020	<sup>111</sup> 0.0020	<sup>110</sup> 0.0020	<sup>77</sup> 0.0009 N <sup>0.109</sup> <sup>129</sup>		
34	CYBERLINK-002	<sup>116</sup> 0.0024	<sup>102</sup> 0.0026	<sup>108</sup> 0.0028	<sup>101</sup> 0.0031	<sup>91</sup> 0.0035	<sup>138</sup> 0.0005 N <sup>0.110</sup> <sup>46</sup>	<sup>130</sup> 0.0020	<sup>130</sup> 0.0035	<sup>124</sup> 0.0021	<sup>122</sup> 0.0021	<sup>122</sup> 0.0022	<sup>172</sup> 0.0012 N <sup>0.053</sup> <sup>62</sup>		
35	CYBERLINK-003	<sup>51</sup> 0.0015	<sup>46</sup> 0.0016	<sup>46</sup> 0.0017	<sup>40</sup> 0.0018	<sup>39</sup> 0.0020	<sup>130</sup> 0.0003 N <sup>0.110</sup> <sup>46</sup>	<sup>52</sup> 0.0011	<sup>51</sup> 0.0012	<sup>49</sup> 0.0012	<sup>45</sup> 0.0013	<sup>43</sup> 0.0013	<sup>98</sup> 0.0006 N <sup>0.107</sup> <sup>80</sup>		
36	CYBERLINK-004	<sup>64</sup> 0.0016	<sup>59</sup> 0.0017	<sup>58</sup> 0.0018	<sup>44</sup> 0.0019	<sup>40</sup> 0.0021	<sup>166</sup> 0.0006 N <sup>0.190</sup> <sup>111</sup>	<sup>108</sup> 0.0014	<sup>100</sup> 0.0						

MISSES AT GIVEN RANK			ENROL MOST RECENT											
#	ALGORITHM	FNIR(N, T= 0, R)	RANK 1					$aN^b$	RANK 50					$aN^b$
			N=0.64M	N=1.6M	N=3.0M	N=6.0M	N=12.0M		N=0.64M	N=1.6M	N=3.0M	N=6.0M	N=12.0M	
73	IMAGUS-005	79.0018	76.0019	77.0022	78.0025	69.0028	97.00002 N <sup>0.158</sup> 88	81.00013	87.00013	82.00014	79.00014	78.00016	92.00005 N <sup>0.066</sup> 104	
74	IMAGUS-006	82.0018	81.00020	76.00022	74.00025	71.00029	102.00002 N <sup>0.156</sup> 82	106.00014	103.00014	99.00015	87.00015	83.00016	123.00007 N <sup>0.049</sup> 83	
75	IMAGUS-007	77.00017	83.00020	82.00022	81.00026	79.00030	56.00001 N <sup>0.189</sup> 109	66.00012	66.00013	62.00013	60.00013	65.00015	91.00005 N <sup>0.064</sup> 102	
76	IMPERIAL-000	108.00022	104.00024	103.00027	108.00030	93.00035	124.00003 N <sup>0.157</sup> 84	132.00016	128.00017	120.00017	107.00018	95.00018	156.00009 N <sup>0.041</sup> 71	
77	INCODE-003	207.00098	212.00019	185.00015	180.00191	172.00233	88.00002 N <sup>0.286</sup> 185	177.00024	184.00031	175.00036	170.00046	163.00056	23.00001 N <sup>0.285</sup> 183	
78	INCODE-004	129.00029	130.00035	130.00041	129.00049	129.00060	45.00001 N <sup>0.244</sup> 151	144.00018	138.00019	137.00020	132.00021	119.00022	104.00006 N <sup>0.077</sup> 112	
79	INCODE-005	56.00015	53.00017	51.00018	52.00020	52.00023	109.00002 N <sup>0.140</sup> 70	73.00012	65.00013	64.00013	62.00013	59.00014	122.00007 N <sup>0.041</sup> 68	
80	INNOVATRICS-007	62.00016	56.00017	58.00019	59.00021	56.00024	106.00002 N <sup>0.143</sup> 75	71.00012	63.00012	60.00013	57.00013	51.00013	128.00007 N <sup>0.037</sup> 65	
81	INTSYSMSU-000	271.01395	271.01457	211.01498	203.01544	197.01591	203.00768 N <sup>0.045</sup> 8	280.01098	278.01163	214.01206	205.01252	199.01296	203.00519 N <sup>0.056</sup> 91	
82	IREX-000	135.00043	144.00044	135.00044	129.00046	114.00048	190.00028 N <sup>0.032</sup> 5	211.00043	202.00043	177.00043	165.00043	151.00043	193.00042 N <sup>0.032</sup> 5	
83	ISYSTEMS-002	168.00053	168.00064	158.00072	152.00083	148.00096	141.00003 N <sup>0.204</sup> 119	198.00033	192.00034	188.00036	161.00038	149.00041	173.00013 N <sup>0.033</sup> 107	
84	ISYSTEMS-003	159.00046	156.00052	147.00057	147.00066	136.00076	150.00004 N <sup>0.174</sup> 102	194.00031	188.00033	164.00034	154.00035	147.00037	174.00013 N <sup>0.063</sup> 101	
85	KAKAO-000	32.00013	40.00015	42.00016	46.00019	49.00022	37.00001 N <sup>0.192</sup> 113	23.00009	25.00010	24.00010	25.00010	25.00011	84.00005 N <sup>0.050</sup> 85	
86	KEDACOM-001	187.00076	178.00077	163.00079	151.00083	141.00087	195.00040 N <sup>0.047</sup> 9	231.00071	224.00072	192.00072	180.00073	167.00073	198.00063 N <sup>0.049</sup> 15	
87	KNERON-000	163.00048	163.00059	155.00067	149.00079	146.00093	111.00002 N <sup>0.226</sup> 135	213.00048	215.00059	187.00067	185.00079	178.00093	61.00002 N <sup>0.226</sup> 167	
88	LOOKMAN-003	196.00083	187.00088	170.00091	165.00096	159.00104	191.00030 N <sup>0.076</sup> 20	239.00072	227.00074	194.00075	185.00076	171.00077	196.00054 N <sup>0.022</sup> 43	
89	LOOKMAN-005	189.00078	181.00080	167.00083	155.00086	144.00092	192.00038 N <sup>0.053</sup> 10	233.00072	225.00072	193.00073	181.00073	168.00074	197.00060 N <sup>0.013</sup> 23	
90	MANTRA-000	57.00015	59.00017	61.00019	69.00022	58.00025	65.00002 N <sup>0.171</sup> 99	64.00012	57.00012	55.00012	53.00013	47.00013	110.00007 N <sup>0.042</sup> 72	
91	MEGVII-001	213.00105	208.00118	182.00128	176.00142	170.00161	185.0015 N <sup>0.143</sup> 74	237.00077	233.00080	196.00082	190.00089	177.00089	192.00040 N <sup>0.048</sup> 82	
92	MICROFOCUS-005	282.03700	282.04242	210.04610	205.05000	202.05391	202.00674 N <sup>0.128</sup> 64	281.01300	283.01724	216.02046	208.02425	202.02810	191.00040 N <sup>0.263</sup> 177	
93	MICROSOFT-003	29.00013	50.00016	57.00018	63.00022	68.00028	14.00000 N <sup>0.271</sup> 167	1.00006	1.00006	1.00007	1.00008	1.00009	28.00001 N <sup>0.158</sup> 153	
94	MICROSOFT-004	28.00012	42.00015	51.00018	59.00021	69.00028	15.00000 N <sup>0.281</sup> 176	1.00006	1.00006	1.00007	1.00007	1.00009	38.00001 N <sup>0.139</sup> 145	
95	MICROSOFT-005	55.0015	73.0019	85.0023	97.0030	98.0037	9.00000 N <sup>0.320</sup> 193	3.00006	3.00006	2.00007	2.00008	2.00009	39.00001 N <sup>0.136</sup> 144	
96	MICROSOFT-006	59.0016	79.0020	94.0025	96.0030	100.0038	15.00000 N <sup>0.305</sup> 189	4.00006	4.00007	10.00009	21.00010	22.00000 N <sup>0.184</sup> 156		
97	NEC-000	221.00131	221.00170	192.00203	186.00244	181.00294	139.00003 N <sup>0.276</sup> 172	191.00029	197.00038	180.00048	175.00059	169.00074	16.00000 N <sup>0.319</sup> 190	
98	NEC-001	233.00180	230.00209	195.00233	196.00266	188.00304	180.0016 N <sup>0.179</sup> 104	246.00109	241.00113	201.00116	194.00121	189.00129	195.00051 N <sup>0.056</sup> 89	
99	NEC-002	5.00009	10.00010	10.00011	10.00012	7.00013	96.00002 N <sup>0.113</sup> 31	3.00008	3.00008	5.00008	4.00008	4.00008	83.00005 N <sup>0.038</sup> 66	
100	NEC-003	34.00013	31.00014	30.00015	28.00016	23.00016	135.00005 N <sup>0.079</sup> 22	63.00012	54.00012	52.00012	47.00012	41.00012	152.00009 N <sup>0.019</sup> 39	
101	NEC-004	42.00014	37.00014	32.00015	29.00016	24.00017	167.00000 N <sup>0.059</sup> 13	89.00013	73.00013	70.00013	67.00013	63.00013	163.00010 N <sup>0.016</sup> 29	
102	NEC-005	25.00011	21.00012	18.00012	14.00013	12.00014	157.00005 N <sup>0.066</sup> 15	45.00011	41.00011	36.00011	32.00011	31.00011	151.00009 N <sup>0.013</sup> 22	
103	NEUROTECHNOLOGY-003	232.0179	231.0225	193.0263	193.0306	188.0361	174.00007 N <sup>0.239</sup> 147	210.00042	214.00057	191.00072	191.00090	186.00012	21.00000 N <sup>0.334</sup> 193	
104	NEUROTECHNOLOGY-004	160.00046	158.00056	153.00064	147.00074	142.00088	119.00002 N <sup>0.220</sup> 129	166.00022	165.00025	157.00028	151.00031	142.00034	65.00003 N <sup>0.154</sup> 150	
105	NEUROTECHNOLOGY-005	144.00035	142.00043	140.00049	136.00057	134.00066	84.00002 N <sup>0.223</sup> 132	161.00021	159.00023	150.00024	144.00025	136.00028	103.00006 N <sup>0.092</sup> 123	
106	NEUROTECHNOLOGY-007	137.00032	134.00039	136.00044	131.00052	128.00062	74.00002 N <sup>0.222</sup> 131	156.00020	152.00022	146.00023	138.00024	129.00027 N <sup>0.076</sup> 111		
107	NEUROTECHNOLOGY-008	85.0019	89.00022	87.00025	93.00029	89.00034	45.00001 N <sup>0.205</sup> 121	94.00013	81.00013	79.00013	74.00014	68.00015	127.00007 N <sup>0.043</sup> 73	
108	NEUROTECHNOLOGY-009	35.00013	38.00014	39.00016	41.00018	41.00021	60.00001 N <sup>0.223</sup> 91	46.00011	45.00011	42.00011	38.00012	35.00012	134.00007 N <sup>0.029</sup> 56	
109	NEUROTECHNOLOGY-010	23.00011	24.00012	24.00013	24.00015	22.00016	99.00002 N <sup>0.125</sup> 62	38.00010	35.00010	26.00010	24.00010	23.00011	145.00008 N <sup>0.014</sup> 24	
110	NEUROTECHNOLOGY-012	11.00010	20.00010	21.00012	19.00014	17.00013	117.00002 N <sup>0.102</sup> 41	34.00010	23.00009	19.00009	17.00009	17.00010	144.00008 N <sup>0.009</sup> 14	
111	NOTIONTAG-000	113.00023	105.00024	99.00026	91.00029	82.00032	156.00005 N <sup>0.117</sup> 54	150.0019	145.00199	139.00200	128.00020	114.00021	175.00013 N <sup>0.027</sup> 52	
112	NTECHLAB-003	161.00046	164.00062	167.00076	169.00094	159.00114	28.00001 N <sup>0.310</sup> 190	91.00013	119.00116	129.00118	134.00026	124.00022	24.00001 N <sup>0.237</sup> 168	
113	NTECHLAB-004	147.00037	151.00048	148.00058	144.00071	140.00085	28.00001 N <sup>0.291</sup> 181	54.00011	85.00013	102.00015	101.00017	112.00021	34.00001 N <sup>0.198</sup> 158	
114	NTECHLAB-005	141.00035	149.00047	149.00058	148.00073	140.00092	16.00000 N <sup>0.334</sup> 196	16.00008	39.00011	54.00012	52.00015	101.00019	11.00000 N <sup>0.283</sup> 181	
115	NTECHLAB-006	130.00030	139.00041	141.00050	138.00062	137.00078	15.00000 N <sup>0.326</sup> 195	6.00008	19.00009	38.00011	35.00013	34.00016	13.00000 N <sup>0.253</sup> 172	
116	NTECHLAB-007	104.00022	110.00027	111.00031	111.00037	106.00044	36.00001 N <sup>0.245</sup> 152	57.00011	58.00012	63.00013	76.00014	69.00015	6.00003 N <sup>0.109</sup> 130	
117	NTECHLAB-008	48.00014	58.00017	61.00020	62.00024	63.00027	23.00001 N <sup>0.224</sup> 134	39.00010	36.00010	34.00011	37.00011	36.00012	7.00004 N <sup>0.065</sup> 103	
118	NTECHLAB-009	26.00012	26.00013	27.00014	29.00015	29.00018	32.00002 N <sup>0.140</sup> 69	23.00099	24.00009	23.00010	23.00010	22.00010	35.00005 N <sup>0.041</sup> 69	
119	NTECHLAB-010	16.00011	15.00011	13.00012	13.00013	13.00014	133.00003 N <sup>0.091</sup> 34	36.00010	32.00010	25.00010	22.00010	20.00010	157.00009 N <sup>0.005</sup> 10	
120	NTECHLAB-011	10.00010	9.00010	8.00011	8.00012	8.00013	115.00002 N <sup>0.103</sup> 42	15.00009	13.00009	14.00009	12.00009	10.00009	118.00007 N <sup>0.017</sup> 32	
121	PANGAM-000	2												

MISSES AT GIVEN RANK		ENROL MOST RECENT											
FNIR(N, T = 0, R)		RANK 1						RANK 50					
#	ALGORITHM	N=0.64M	N=1.6M	N=3.0M	N=6.0M	N=12.0M	aN <sup>b</sup>	N=0.64M	N=1.6M	N=3.0M	N=6.0M	N=12.0M	aN <sup>b</sup>
145	REALNETWORKS-004	<sup>231</sup> 0.0175	<sup>232</sup> 0.0236	<sup>199</sup> 0.0284	<sup>194</sup> 0.0347	<sup>189</sup> 0.0416	<sup>140</sup> 0.0003 N <sup>0.295</sup> 183	<sup>205</sup> 0.0040	<sup>207</sup> 0.0050	<sup>184</sup> 0.0061	<sup>184</sup> 0.0078	<sup>181</sup> 0.0099	<sup>26</sup> 0.0001 N <sup>0.315</sup> 188
146	REALNETWORKS-005	<sup>94</sup> 0.0020	<sup>96</sup> 0.0023	<sup>16</sup> 0.0026	<sup>96</sup> 0.0030	<sup>99</sup> 0.0037	<sup>48</sup> 0.0001 N <sup>0.207</sup> 122	<sup>56</sup> 0.0012	<sup>60</sup> 0.0012	<sup>67</sup> 0.0013	<sup>72</sup> 0.0014	<sup>66</sup> 0.0015	<sup>76</sup> 0.0004 N <sup>0.081</sup> 114
147	REALNETWORKS-006	<sup>33</sup> 0.0013	<sup>34</sup> 0.0014	<sup>40</sup> 0.0016	<sup>39</sup> 0.0018	<sup>39</sup> 0.0021	<sup>58</sup> 0.0001 N <sup>0.163</sup> 93	<sup>33</sup> 0.0010	<sup>30</sup> 0.0010	<sup>34</sup> 0.0011	<sup>34</sup> 0.0011	<sup>32</sup> 0.0012	<sup>79</sup> 0.0004 N <sup>0.060</sup> 97
148	REALNETWORKS-007	<sup>30</sup> 0.0013	<sup>28</sup> 0.0013	<sup>27</sup> 0.0014	<sup>29</sup> 0.0016	<sup>30</sup> 0.0018	<sup>112</sup> 0.0002 N <sup>0.124</sup> 61	<sup>29</sup> 0.0010	<sup>26</sup> 0.0010	<sup>28</sup> 0.0011	<sup>29</sup> 0.0011	<sup>81</sup> 0.0004 N <sup>0.057</sup> 92	
149	REMARKAI-000	<sup>125</sup> 0.0027	<sup>128</sup> 0.0034	<sup>128</sup> 0.0040	<sup>128</sup> 0.0048	<sup>122</sup> 0.0058	<sup>32</sup> 0.0001 N <sup>0.260</sup> 161	<sup>116</sup> 0.0014	<sup>115</sup> 0.0015	<sup>111</sup> 0.0016	<sup>106</sup> 0.0018	<sup>104</sup> 0.0020	<sup>69</sup> 0.0003 N <sup>0.108</sup> 127
150	RENDIP-000	<sup>47</sup> 0.0014	<sup>47</sup> 0.0015	<sup>48</sup> 0.0017	<sup>48</sup> 0.0019	<sup>48</sup> 0.0022	<sup>76</sup> 0.0002 N <sup>0.158</sup> 86	<sup>57</sup> 0.0012	<sup>56</sup> 0.0012	<sup>53</sup> 0.0012	<sup>48</sup> 0.0012	<sup>42</sup> 0.0013	<sup>147</sup> 0.0008 N <sup>0.025</sup> 48
151	REVEALMEDIA-000	<sup>69</sup> 0.0017	<sup>71</sup> 0.0019	<sup>63</sup> 0.0020	<sup>69</sup> 0.0023	<sup>57</sup> 0.0025	<sup>126</sup> 0.0003 N <sup>0.134</sup> 66	<sup>69</sup> 0.0012	<sup>62</sup> 0.0012	<sup>57</sup> 0.0012	<sup>52</sup> 0.0013	<sup>46</sup> 0.0013	<sup>137</sup> 0.0007 N <sup>0.335</sup> 61
152	S1-000	<sup>99</sup> 0.0021	<sup>102</sup> 0.0024	<sup>106</sup> 0.0028	<sup>104</sup> 0.0032	<sup>99</sup> 0.0037	<sup>55</sup> 0.0001 N <sup>0.203</sup> 118	<sup>117</sup> 0.0014	<sup>110</sup> 0.0015	<sup>105</sup> 0.0015	<sup>98</sup> 0.0016	<sup>90</sup> 0.0017	<sup>114</sup> 0.0007 N <sup>0.055</sup> 88
153	S1-001	<sup>135</sup> 0.0031	<sup>121</sup> 0.0031	<sup>119</sup> 0.0034	<sup>108</sup> 0.0036	<sup>104</sup> 0.0040	<sup>176</sup> 0.0000 N <sup>0.092</sup> 35	<sup>171</sup> 0.0023	<sup>161</sup> 0.0023	<sup>148</sup> 0.0024	<sup>140</sup> 0.0024	<sup>128</sup> 0.0025	<sup>181</sup> 0.0017 N <sup>0.023</sup> 47
154	S1-002	<sup>41</sup> 0.0014	<sup>36</sup> 0.0014	<sup>33</sup> 0.0015	<sup>32</sup> 0.0016	<sup>29</sup> 0.0018	<sup>152</sup> 0.0004 N <sup>0.085</sup> 27	<sup>93</sup> 0.0013	<sup>84</sup> 0.0013	<sup>74</sup> 0.0013	<sup>59</sup> 0.0013	<sup>52</sup> 0.0013	<sup>167</sup> 0.0011 N <sup>0.011</sup> 17
155	SCANOVATE-000	<sup>150</sup> 0.0038	<sup>183</sup> 0.0050	<sup>151</sup> 0.0059	<sup>146</sup> 0.0073	<sup>137</sup> 0.0073	<sup>79</sup> 0.0002 N <sup>0.235</sup> 143	<sup>109</sup> 0.0014	<sup>117</sup> 0.0015	<sup>117</sup> 0.0017	<sup>129</sup> 0.0020	<sup>110</sup> 0.0020	<sup>85</sup> 0.0002 N <sup>0.142</sup> 46
156	SCANOVATE-001	<sup>153</sup> 0.0041	<sup>157</sup> 0.0053	<sup>152</sup> 0.0064	<sup>150</sup> 0.0079	<sup>149</sup> 0.0098	<sup>27</sup> 0.0001 N <sup>0.299</sup> 186	<sup>103</sup> 0.0013	<sup>114</sup> 0.0015	<sup>116</sup> 0.0017	<sup>130</sup> 0.0021	<sup>122</sup> 0.0024	<sup>36</sup> 0.0001 N <sup>0.127</sup> 162
157	SENSETIME-000	<sup>105</sup> 0.0022	<sup>98</sup> 0.0023	<sup>98</sup> 0.0026	<sup>96</sup> 0.0028	<sup>88</sup> 0.0032	<sup>142</sup> 0.0003 N <sup>0.135</sup> 67	<sup>131</sup> 0.0016	<sup>132</sup> 0.0017	<sup>125</sup> 0.0018	<sup>112</sup> 0.0018	<sup>106</sup> 0.0020	<sup>133</sup> 0.0007 N <sup>0.060</sup> 96
158	SENSETIME-001	<sup>103</sup> 0.0022	<sup>99</sup> 0.0023	<sup>95</sup> 0.0025	<sup>94</sup> 0.0029	<sup>96</sup> 0.0037	<sup>90</sup> 0.0002 N <sup>0.177</sup> 103	<sup>130</sup> 0.0016	<sup>120</sup> 0.0016	<sup>115</sup> 0.0017	<sup>109</sup> 0.0018	<sup>125</sup> 0.0024	<sup>66</sup> 0.0003 N <sup>0.125</sup> 140
159	SENSETIME-002	<sup>224</sup> 0.0136	<sup>215</sup> 0.0137	<sup>178</sup> 0.0138	<sup>164</sup> 0.0139	<sup>199</sup> 0.0124 N <sup>0.07</sup> 2	<sup>259</sup> 0.0136	<sup>247</sup> 0.0136	<sup>203</sup> 0.0136	<sup>197</sup> 0.0136	<sup>191</sup> 0.0136	<sup>209</sup> 0.0135 N <sup>0.011</sup> 3	
160	SENSETIME-003	<sup>8</sup> 0.0010	<sup>6</sup> 0.0010	<sup>6</sup> 0.0010	<sup>6</sup> 0.0011	<sup>6</sup> 0.0012	<sup>132</sup> 0.0003 N <sup>0.085</sup> 29	<sup>24</sup> 0.0009	<sup>22</sup> 0.0009	<sup>21</sup> 0.0009	<sup>20</sup> 0.0010	<sup>16</sup> 0.0010	<sup>140</sup> 0.0008 N <sup>0.113</sup> 20
161	SENSETIME-004	<sup>6</sup> 0.0010	<sup>5</sup> 0.0010	<sup>4</sup> 0.0010	<sup>4</sup> 0.0011	<sup>4</sup> 0.0012	<sup>134</sup> 0.0003 N <sup>0.081</sup> 24	<sup>11</sup> 0.0008	<sup>10</sup> 0.0009	<sup>9</sup> 0.0009	<sup>8</sup> 0.0009	<sup>8</sup> 0.0009	<sup>109</sup> 0.0007 N <sup>0.18</sup> 37
162	SENSETIME-005	<sup>2</sup> 0.0008	<sup>3</sup> 0.0009	<sup>0</sup> 0.0009	<sup>3</sup> 0.0010	<sup>1</sup> 0.0011	<sup>123</sup> 0.0003 N <sup>0.085</sup> 28	<sup>7</sup> 0.0008	<sup>6</sup> 0.0008	<sup>6</sup> 0.0008	<sup>5</sup> 0.0008	<sup>4</sup> 0.0008	<sup>142</sup> 0.0008 N <sup>0.002</sup> 6
163	SENSETIME-006	<sup>3</sup> 0.0008	<sup>2</sup> 0.0009	<sup>1</sup> 0.0009	<sup>1</sup> 0.0010	<sup>0</sup> 0.0009	<sup>136</sup> 0.0003 N <sup>0.069</sup> 16	<sup>8</sup> 0.0008	<sup>7</sup> 0.0008	<sup>6</sup> 0.0008	<sup>5</sup> 0.0008	<sup>4</sup> 0.0008	<sup>121</sup> 0.0007 N <sup>0.011</sup> 16
164	SENSETIME-007	<sup>1</sup> 0.0008	<sup>1</sup> 0.0008	<sup>0</sup> 0.0009	<sup>1</sup> 0.0009	<sup>0</sup> 0.0009	<sup>144</sup> 0.0004 N <sup>0.061</sup> 14	<sup>9</sup> 0.0008	<sup>8</sup> 0.0008	<sup>8</sup> 0.0008	<sup>7</sup> 0.0008	<sup>6</sup> 0.0008	<sup>132</sup> 0.0007 N <sup>0.008</sup> 13
165	SHAMAN-007	<sup>252</sup> 0.0371	<sup>245</sup> 0.0396	<sup>206</sup> 0.0416	<sup>208</sup> 0.0443	<sup>194</sup> 0.0473	<sup>198</sup> 0.0122 N <sup>0.085</sup> 25	<sup>267</sup> 0.0308	<sup>261</sup> 0.0314	<sup>209</sup> 0.0319	<sup>201</sup> 0.0326	<sup>195</sup> 0.0337	<sup>201</sup> 0.0207 N <sup>0.29</sup> 57
166	SIAT-001	<sup>67</sup> 0.0017	<sup>65</sup> 0.0018	<sup>6</sup> 0.0020	<sup>69</sup> 0.0023	<sup>62</sup> 0.0027	<sup>69</sup> 0.0002 N <sup>0.173</sup> 101	<sup>41</sup> 0.0010	<sup>44</sup> 0.0011	<sup>47</sup> 0.0012	<sup>51</sup> 0.0013	<sup>50</sup> 0.0013	<sup>70</sup> 0.0003 N <sup>0.085</sup> 16
167	SIAT-002	<sup>65</sup> 0.0016	<sup>67</sup> 0.0018	<sup>70</sup> 0.0020	<sup>69</sup> 0.0023	<sup>61</sup> 0.0027	<sup>73</sup> 0.0002 N <sup>0.171</sup> 98	<sup>50</sup> 0.0011	<sup>61</sup> 0.0012	<sup>61</sup> 0.0013	<sup>57</sup> 0.0014	<sup>50</sup> 0.0015 N <sup>0.062</sup> 99	
168	SQISOFT-001	<sup>127</sup> 0.0028	<sup>141</sup> 0.0042	<sup>150</sup> 0.0059	<sup>150</sup> 0.0084	<sup>205</sup> 0.0207	<sup>200</sup> 0.0000 N <sup>0.164</sup> 203	<sup>36</sup> 0.0010	<sup>37</sup> 0.0010	<sup>40</sup> 0.0011	<sup>44</sup> 0.0012	<sup>203</sup> 0.0198	<sup>2</sup> 0.0000 N <sup>0.188</sup> 203
169	SYNSES-003	<sup>230</sup> 0.0161	<sup>219</sup> 0.0162	<sup>190</sup> 0.0163	<sup>181</sup> 0.0165	<sup>180</sup> 0.0254	<sup>189</sup> 0.0027 N <sup>0.123</sup> 63	<sup>257</sup> 0.0160	<sup>252</sup> 0.0160	<sup>205</sup> 0.0160	<sup>199</sup> 0.0160	<sup>194</sup> 0.0245	<sup>158</sup> 0.0009 N <sup>0.192</sup> 157
170	SYNSES-003	<sup>272</sup> 0.1456	<sup>272</sup> 0.1700	<sup>217</sup> 0.1876	<sup>208</sup> 0.2088	<sup>194</sup> 0.2317	<sup>200</sup> 0.0177 N <sup>0.158</sup> 87	<sup>278</sup> 0.0828	<sup>274</sup> 0.0869	<sup>212</sup> 0.0920	<sup>204</sup> 0.0998	<sup>197</sup> 0.1104	<sup>202</sup> 0.0218 N <sup>0.098</sup> 126
171	SYNSES-005	<sup>199</sup> 0.0085	<sup>188</sup> 0.0085	<sup>186</sup> 0.0086	<sup>145</sup> 0.0088	<sup>197</sup> 0.0072 N <sup>0.032</sup> 3	<sup>241</sup> 0.0085	<sup>238</sup> 0.0085	<sup>197</sup> 0.0085	<sup>192</sup> 0.0085	<sup>187</sup> 0.0085	<sup>199</sup> 0.0085 N <sup>0.000</sup> 200	
172	TECH5-001	<sup>136</sup> 0.0032	<sup>136</sup> 0.0040	<sup>139</sup> 0.0047	<sup>136</sup> 0.0057	<sup>133</sup> 0.0071	<sup>31</sup> 0.0001 N <sup>0.271</sup> 165	<sup>128</sup> 0.0016	<sup>126</sup> 0.0017	<sup>120</sup> 0.0018	<sup>122</sup> 0.0020	<sup>68</sup> 0.0003 N <sup>0.119</sup> 135	
173	TECH5-002	<sup>96</sup> 0.0020	<sup>111</sup> 0.0027	<sup>114</sup> 0.0031	<sup>110</sup> 0.0037	<sup>112</sup> 0.0047	<sup>17</sup> 0.0000 N <sup>0.285</sup> 179	<sup>29</sup> 0.0009	<sup>28</sup> 0.0010	<sup>37</sup> 0.0011	<sup>39</sup> 0.0012	<sup>48</sup> 0.0013	<sup>49</sup> 0.0002 N <sup>0.122</sup> 142
174	TEVIAN-005	<sup>174</sup> 0.0056	<sup>176</sup> 0.0073	<sup>167</sup> 0.0084	<sup>166</sup> 0.0105	<sup>162</sup> 0.0130	<sup>58</sup> 0.0001 N <sup>0.283</sup> 178	<sup>158</sup> 0.0200	<sup>153</sup> 0.0203	<sup>147</sup> 0.0208	<sup>141</sup> 0.0304	<sup>90</sup> 0.0054 N <sup>0.178</sup> 155	
175	TEVIAN-006	<sup>112</sup> 0.0023	<sup>103</sup> 0.0024	<sup>101</sup> 0.0026	<sup>88</sup> 0.0028	<sup>79</sup> 0.0031	<sup>165</sup> 0.0005 N <sup>0.106</sup> 43	<sup>128</sup> 0.0016	<sup>123</sup> 0.0017	<sup>113</sup> 0.0017	<sup>104</sup> 0.0017	<sup>93</sup> 0.0018	<sup>154</sup> 0.0009 N <sup>0.041</sup> 201
176	TEVIAN-007	<sup>75</sup> 0.0017	<sup>63</sup> 0.0018	<sup>55</sup> 0.0018	<sup>53</sup> 0.0020	<sup>42</sup> 0.0021	<sup>169</sup> 0.0006 N <sup>0.073</sup> 19	<sup>78</sup> 0.0013	<sup>70</sup> 0.0013	<sup>69</sup> 0.0013	<sup>63</sup> 0.0013	<sup>53</sup> 0.0013	<sup>149</sup> 0.0009 N <sup>0.026</sup> 49
177	TIGER-002	<sup>156</sup> 0.0044	<sup>159</sup> 0.0056	<sup>156</sup> 0.0068	<sup>157</sup> 0.0086	<sup>155</sup> 0.0105	<sup>29</sup> 0.0001 N <sup>0.299</sup> 187	<sup>86</sup> 0.0013	<sup>111</sup> 0.0015	<sup>122</sup> 0.0018	<sup>131</sup> 0.0021	<sup>132</sup> 0.0027	<sup>18</sup> 0.0000 N <sup>0.255</sup> 173
178	TOSHIBA-000	<sup>143</sup> 0.0035	<sup>145</sup> 0.0045	<sup>146</sup> 0.0052	<sup>137</sup> 0.0061	<sup>167</sup> 0.0154	<sup>6</sup> 0.0000 N <sup>0.144</sup> 199	<sup>127</sup> 0.0016	<sup>136</sup> 0.0018	<sup>135</sup> 0.0019	<sup>133</sup> 0.0021	<sup>185</sup> 0.0105	<sup>5</sup> 0.0000 N <sup>0.153</sup> 200
179	TRUEFACE-000	<sup>133</sup> 0.0031	<sup>125</sup> 0.0033	<sup>121</sup> 0.0035	<sup>119</sup> 0.0039	<sup>106</sup> 0.0043	<sup>170</sup> 0.0006 N <sup>0.115</sup> 53	<sup>181</sup> 0.0025	<sup>168</sup> 0.0026	<sup>154</sup> 0.0026	<sup>146</sup> 0.0027	<sup>137</sup> 0.0028	<sup>179</sup> 0.0015 N <sup>0.038</sup> 67
180	VD-001	<sup>241</sup> 0.0230	<sup>238</sup> 0.0276	<sup>202</sup> 0.0315	<sup>197</sup> 0.0363	<sup>191</sup> 0.0418	<sup>184</sup> 0.0015 N <sup>0.204</sup> 120	<sup>251</sup> 0.0120	<sup>246</sup> 0.0130	<sup>204</sup> 0.0140	<sup>198</sup> 0.0154	<sup>193</sup> 0.0170	<sup>188</sup> 0.0024 N <sup>0.120</sup> 136
181	VERIDAS-001	<sup>111</sup> 0.0023	<sup>114</sup> 0.0028	<sup>115</sup> 0.0032	<sup>115</sup> 0.0037	<sup>110</sup> 0.0045	<sup>49</sup> 0.0001 N <sup>0.231</sup> 140	<sup>114</sup> 0.0014	<sup>107</sup> 0.0015	<sup>101</sup> 0.0015	<sup>99</sup> 0.0016	<sup>82</sup> 0.0005 N <sup>0.083</sup> 115	
182	VERIDAS-002	<sup>110</sup> 0.0023	<sup>113</sup> 0.0028	<sup>109</sup> 0.0032	<sup>102</sup> 0.0032	<sup>97</sup> 0.0037	<sup>127</sup> 0.0003 N <sup>0.188</sup> 85	<sup>110</sup> 0.0014	<sup>108</sup> 0.0015	<sup>94</sup> 0.0015	<sup>91</sup> 0.0015	<sup>85</sup> 0.0016	<sup>135</sup> 0.0007 N <sup>0.047</sup> 81
183	VERIDAS-003	<sup>68</sup> 0.0017	<sup>66</sup> 0.0018	<sup>62</sup> 0.0020									

#	ALGORITHM	MISSES OUTSIDE RANK R		RESOURCE USAGE		ENROL MOST RECENT, N = 1.6M						
		FNIR(N, T=0, R)		TEMPLATE		R=1	R=5	R=10	R=20	R=50	WORK-10	
		BYTES	MSEC									
1	20FACE-000	188	2048	57	247	254	0.0552	248	0.0269	247	0.0198	
2	3DIVI-003	88	512	158	625	263	0.0833	258	0.0444	258	0.0349	
3	3DIVI-004	275	4096	159	628	22	0.0175	215	0.0091	211	0.0075	
4	3DIVI-005	266	4096	166	653	223	0.0176	216	0.0091	211	0.0074	
5	3DIVI-006	71	528	167	653	233	0.0240	240	0.0171	243	0.0160	
6	ACER-000	50	512	47	201	203	0.0106	184	0.0051	180	0.0041	
7	ACER-001	135	2048	38	184	159	0.0051	157	0.0032	156	0.0028	
8	AIZE-001	169	2048	97	403	161	0.0056	161	0.0037	166	0.0033	
9	ALCHERA-000	167	2048	66	263	218	0.0161	227	0.0124	232	0.0117	
10	ALCHERA-001	188	2048	29	66	29	0.9869	291	0.9782	291	0.9735	
11	ALCHERA-002	200	2048	31	115	265	0.0949	263	0.0555	261	0.0443	
12	ALCHERA-003	168	2048	142	548	19	0.0104	187	0.0054	187	0.0045	
13	ALCHERA-004	148	2048	250	854	202	0.0110	183	0.0049	176	0.0038	
14	ALLGOVISION-000	19	2048	107	425	205	0.0114	210	0.0084	216	0.0078	
15	ALLGOVISION-001	153	2048	229	792	188	0.0090	181	0.0048	179	0.0040	
16	ANKE-000	241	2072	431	218	0.0132	201	0.0073	206	0.0060	197	0.0050
17	ANKE-001	242	2072	110	433	214	0.0132	202	0.0073	205	0.0061	
18	ANKE-002	230	2056	162	641	180	0.0028	116	0.0020	114	0.0018	
19	AWARE-003	245	2076	203	716	240	0.0306	237	0.0162	234	0.0127	
20	AWARE-004	19	92	205	712	258	0.0679	255	0.0348	252	0.0274	
21	AWARE-005	25	3100	237	827	24	0.0311	238	0.0167	235	0.0134	
22	AWARE-006	20	124	233	818	260	0.0697	257	0.0369	253	0.0288	
23	AYONIX-000	108	1036	18	10	28	0.4505	285	0.3540	287	0.3176	
24	AYONIX-001	101	1036	20	12	280	0.3414	279	0.2338	280	0.1977	
25	AYONIX-002	99	1036	19	11	278	0.3414	280	0.2338	280	0.1977	
26	CAMVI-003	90	1024	196	707	253	0.0520	262	0.0517	267	0.0517	
27	CAMVI-004	87	1024	205	718	259	0.0468	260	0.0465	264	0.0464	
28	CAMVI-005	83	1024	220	769	257	0.0652	264	0.0648	268	0.0648	
29	CANON-001	26	4096	266	893	18	0.0011	21	0.0010	19	0.0010	
30	CANON-002	16	0	16	6	19	0.0012	17	0.0010	15	0.0009	
31	CIB-000	291	8196	175	674	44	0.0015	51	0.0013	48	0.0012	
32	CLEARVIEWAI-000	268	4096	217	765	13	0.0011	20	0.0010	21	0.0009	
33	CLOUDWALK-HR-000	164	2048	273	908	41	0.0015	70	0.0014	77	0.0014	
34	CLOUDWALK-MT-000	188	2048	288	870	61	0.0018	97	0.0018	108	0.0018	
35	COGENT-000	67	525	145	551	191	0.0105	220	0.0096	226	0.0095	
36	COGENT-001	68	525	144	552	190	0.0105	221	0.0096	229	0.0095	
37	COGENT-002	103	1043	291	987	131	0.0036	126	0.0022	124	0.0020	
38	COGENT-003	104	1043	288	960	13	0.0038	137	0.0024	135	0.0019	
39	COGENT-004	229	2053	285	952	80	0.0200	83	0.0116	84	0.0015	
40	COGENT-005	108	1062	223	774	38	0.0017	68	0.0014	69	0.0014	
41	COGENT-006	4	0	1	25	0.0012	32	0.0011	32	0.0011	37	0.0011
42	COGNITEC-000	209	2052	36	176	23	0.0252	233	0.0136	231	0.0107	
43	COGNITEC-001	229	2052	48	202	206	0.0117	194	0.0062	193	0.0051	
44	COGNITEC-002	208	2052	53	227	162	0.0057	160	0.0037	161	0.0032	
45	COGNITEC-003	22	2052	71	297	16	0.0062	169	0.0040	171	0.0036	
46	COGNITEC-004	211	2052	44	192	124	0.0032	119	0.0020	109	0.0018	
47	COGNITEC-005	229	2052	85	367	35	0.0016	45	0.0013	45	0.0012	
48	COGNITEC-006	228	2052	119	463	48	0.0016	44	0.0013	41	0.0012	
49	CUBOX-000	14	2048	277	918	39	0.0014	60	0.0014	70	0.0014	
50	CYBERLINK-000	212	2052	191	699	135	0.0040	147	0.0028	151	0.0026	
51	CYBERLINK-001	205	2052	111	433	12	0.0035	132	0.0023	131	0.0021	
52	CYBERLINK-002	28	4140	212	738	109	0.0026	128	0.0023	137	0.0022	
53	CYBERLINK-003	28	6212	189	696	49	0.0016	49	0.0013	56	0.0012	
54	CYBERLINK-004	28	6212	213	738	39	0.0017	74	0.0015	89	0.0014	
55	CYBERLINK-005	287	6212	214	739	64	0.0018	84	0.0016	90	0.0015	
56	DAHUA-000	191	2048	91	378	192	0.0093	197	0.0066	201	0.0061	
57	DAHUA-001	191	2048	87	371	170	0.0067	170	0.0040	167	0.0036	
58	DAHUA-002	148	2048	190	699	69	0.0018	72	0.0015	86	0.0014	
59	DAHUA-003	179	2048	208	725	25	0.0012	11	0.0010	12	0.0009	
60	DAHUA-004	204	2048	216	759	14	0.0011	14	0.0010	14	0.0009	
61	DAON-000	238	2069	149	584	138	0.0041	162	0.0038	171	0.0037	
62	DECATAR-000	225	2052	260	874	88	0.0021	85	0.0016	85	0.0014	
63	DEEPLINT-001	270	4096	180	687	39	0.0014	57	0.0014	59	0.0013	
64	DEEPSA-001	206	2048	226	780	14	0.0043	127	0.0022	112	0.0018	
65	DERMALOG-003	21	128	501	211	269	0.1259	268	0.0744	268	0.0603	
66	DERMALOG-004	24	128	49	208	26	0.1251	267	0.0739	265	0.0598	
67	DERMALOG-005	23	128	136	532	21	0.0149	230	0.0129	231	0.0125	
68	DERMALOG-006	39	256	134	514	183	0.0081	200	0.0069	203	0.0066	
69	DERMALOG-007	22	128	104	413	19	0.0092	198	0.0066	199	0.0060	
70	DERMALOG-008	54	512	86	370	117	0.0029	115	0.0020	111	0.0018	
71	DERMALOG-009	51	512	82	347	110	0.0028	135	0.0024	144	0.0023	
72	DIGIDATA-000	1	1	1	2	287	0.5897	288	0.5892	288	0.5891	

Table 24: Rank-based accuracy for the FRVT 2018 mugshot sets. In columns 3 and 4 are template size and template generation duration. Thereafter values are rank-based FNIR with  $T = 0$  and FPIR = 1. This is appropriate to investigational uses but not those with higher volumes where candidates from all searches would need review. The next column is a workload statistic, a small value shows an algorithm front-loads mates into the first 10 candidates. Throughout, blue superscripts indicate the rank of the algorithm for that column, and the best value is highlighted in yellow.

MISSES OUTSIDE RANK R		RESOURCE USAGE		ENROL MOST RECENT, N = 1.6M					
FNIR(N, T=0, R)		TEMPLATE		R=1	R=5	R=10	R=20	R=50	WORK=10
#	ALGORITHM	BYTES	MSEC						
73	DILUSENSE-000	<sup>8</sup> 0	<sup>9</sup> 2	<sup>21</sup> 0.0022	<sup>81</sup> 0.0015	<sup>75</sup> 0.0014	<sup>75</sup> 0.0013	<sup>64</sup> 0.0013	<sup>82</sup> 1.015
74	EYEDEA-003	<sup>102</sup> 1036	<sup>93</sup> 385	<sup>262</sup> 0.0800	<sup>259</sup> 0.0451	<sup>259</sup> 0.0362	<sup>255</sup> 0.0289	<sup>255</sup> 0.0211	<sup>260</sup> 1.448
75	F8-001	<sup>170</sup> 2048	<sup>249</sup> 851	<sup>210</sup> 0.0120	<sup>222</sup> 0.0105	<sup>222</sup> 0.0102	<sup>232</sup> 0.0100	<sup>237</sup> 0.0099	<sup>222</sup> 1.096
76	FINCORE-000	<sup>156</sup> 2048	<sup>124</sup> 477	<sup>201</sup> 0.0108	<sup>186</sup> 0.0052	<sup>182</sup> 0.0042	<sup>180</sup> 0.0034	<sup>175</sup> 0.0026	<sup>187</sup> 1.054
77	FUJITSULAB-000	<sup>96</sup> 1032	<sup>284</sup> 950	<sup>92</sup> 0.0022	<sup>90</sup> 0.0016	<sup>91</sup> 0.0015	<sup>91</sup> 0.0015	<sup>90</sup> 0.0014	<sup>90</sup> 1.015
78	FUJITSULAB-001	<sup>8</sup> 0	<sup>4</sup> 1	<sup>72</sup> 0.0019	<sup>78</sup> 0.0015	<sup>80</sup> 0.0015	<sup>86</sup> 0.0014	<sup>92</sup> 0.0014	<sup>75</sup> 1.014
79	GLORY-000	<sup>49</sup> 418	<sup>32</sup> 160	<sup>273</sup> 0.1781	<sup>275</sup> 0.1391	<sup>271</sup> 0.1266	<sup>275</sup> 0.1154	<sup>275</sup> 0.1007	<sup>274</sup> 2.298
80	GLORY-001	<sup>128</sup> 1726	<sup>99</sup> 405	<sup>270</sup> 0.1268	<sup>270</sup> 0.0967	<sup>270</sup> 0.0869	<sup>271</sup> 0.0778	<sup>272</sup> 0.0673	<sup>271</sup> 1.903
81	GORILLA-001	<sup>248</sup> 2156	<sup>34</sup> 169	<sup>235</sup> 0.0603	<sup>250</sup> 0.0304	<sup>249</sup> 0.0230	<sup>249</sup> 0.0174	<sup>242</sup> 0.0117	<sup>250</sup> 1.309
82	GORILLA-002	<sup>109</sup> 1132	<sup>30</sup> 341	<sup>220</sup> 0.0197	<sup>217</sup> 0.0092	<sup>207</sup> 0.0070	<sup>202</sup> 0.0054	<sup>200</sup> 0.0041	<sup>221</sup> 1.096
83	GORILLA-003	<sup>247</sup> 2156	<sup>147</sup> 563	<sup>242</sup> 0.0361	<sup>235</sup> 0.0146	<sup>230</sup> 0.0106	<sup>224</sup> 0.0078	<sup>212</sup> 0.0054	<sup>237</sup> 1.158
84	GORILLA-004	<sup>249</sup> 2192	<sup>95</sup> 395	<sup>16</sup> 0.0063	<sup>156</sup> 0.0032	<sup>155</sup> 0.0026	<sup>149</sup> 0.0023	<sup>135</sup> 0.0018	<sup>157</sup> 1.033
85	GORILLA-005	<sup>290</sup> 6288	<sup>127</sup> 483	<sup>123</sup> 0.0032	<sup>104</sup> 0.0019	<sup>102</sup> 0.0017	<sup>96</sup> 0.0015	<sup>74</sup> 0.0013	<sup>114</sup> 1.018
86	GORILLA-006	<sup>292</sup> 8336	<sup>218</sup> 768	<sup>60</sup> 0.0017	<sup>43</sup> 0.0013	<sup>45</sup> 0.0012	<sup>45</sup> 0.0011	<sup>46</sup> 0.0011	<sup>41</sup> 1.012
87	GORILLA-007	<sup>12</sup> 0	<sup>17</sup> 6	<sup>57</sup> 0.0017	<sup>39</sup> 0.0012	<sup>39</sup> 0.0012	<sup>35</sup> 0.0011	<sup>38</sup> 0.0011	<sup>41</sup> 1.012
88	GRIAULE-000	<sup>223</sup> 2052	<sup>106</sup> 419	<sup>107</sup> 0.0025	<sup>112</sup> 0.0020	<sup>117</sup> 0.0019	<sup>122</sup> 0.0018	<sup>122</sup> 0.0017	<sup>111</sup> 1.018
89	HIK-003	<sup>117</sup> 1408	<sup>160</sup> 633	<sup>207</sup> 0.0117	<sup>192</sup> 0.0060	<sup>191</sup> 0.0048	<sup>191</sup> 0.0039	<sup>182</sup> 0.0030	<sup>199</sup> 1.061
90	HIK-004	<sup>110</sup> 1152	<sup>132</sup> 510	<sup>204</sup> 0.0113	<sup>190</sup> 0.0059	<sup>196</sup> 0.0047	<sup>184</sup> 0.0037	<sup>175</sup> 0.0030	<sup>192</sup> 1.060
91	HIK-005	<sup>116</sup> 1408	<sup>157</sup> 619	<sup>14</sup> 0.0046	<sup>140</sup> 0.0025	<sup>128</sup> 0.0020	<sup>114</sup> 0.0017	<sup>105</sup> 0.0015	<sup>141</sup> 1.025
92	HIK-006	<sup>115</sup> 1408	<sup>153</sup> 610	<sup>148</sup> 0.0046	<sup>139</sup> 0.0025	<sup>128</sup> 0.0020	<sup>113</sup> 0.0017	<sup>108</sup> 0.0015	<sup>140</sup> 1.025
93	HYPERVERGE-001	<sup>88</sup> 1024	<sup>248</sup> 846	<sup>32</sup> 0.0014	<sup>46</sup> 0.0013	<sup>51</sup> 0.0013	<sup>62</sup> 0.0013	<sup>76</sup> 0.0013	<sup>41</sup> 1.012
94	HYPERVERGE-002	<sup>13</sup> 0	<sup>6</sup> 1	<sup>29</sup> 0.0014	<sup>47</sup> 0.0013	<sup>53</sup> 0.0013	<sup>61</sup> 0.0013	<sup>68</sup> 0.0013	<sup>43</sup> 1.012
95	HZALIU-000	<sup>7</sup> 0	<sup>5</sup> 1	<sup>90</sup> 0.0022	<sup>88</sup> 0.0016	<sup>91</sup> 0.0015	<sup>94</sup> 0.0015	<sup>104</sup> 0.0014	<sup>88</sup> 1.015
96	IDEMIA-003	<sup>70</sup> 528	<sup>182</sup> 689	<sup>173</sup> 0.0069	<sup>177</sup> 0.0045	<sup>177</sup> 0.0039	<sup>179</sup> 0.0034	<sup>176</sup> 0.0027	<sup>174</sup> 1.043
97	IDEMIA-004	<sup>67</sup> 528	<sup>173</sup> 669	<sup>169</sup> 0.0066	<sup>166</sup> 0.0038	<sup>167</sup> 0.0032	<sup>161</sup> 0.0027	<sup>150</sup> 0.0021	<sup>167</sup> 1.038
98	IDEMIA-005	<sup>48</sup> 352	<sup>89</sup> 374	<sup>182</sup> 0.0081	<sup>174</sup> 0.0044	<sup>171</sup> 0.0036	<sup>173</sup> 0.0032	<sup>181</sup> 0.0030	<sup>177</sup> 1.044
99	IDEMIA-006	<sup>47</sup> 352	<sup>88</sup> 373	<sup>193</sup> 0.0096	<sup>185</sup> 0.0052	<sup>187</sup> 0.0042	<sup>189</sup> 0.0039	<sup>195</sup> 0.0037	<sup>184</sup> 1.052
100	IDEMIA-007	<sup>80</sup> 860	<sup>231</sup> 807	<sup>108</sup> 0.0026	<sup>86</sup> 0.0016	<sup>79</sup> 0.0014	<sup>60</sup> 0.0013	<sup>55</sup> 0.0012	<sup>91</sup> 1.015
101	IDEMIA-008	<sup>49</sup> 300	<sup>114</sup> 451	<sup>11</sup> 0.0011	<sup>10</sup> 0.0009	<sup>15</sup> 0.0009	<sup>16</sup> 0.0009	<sup>15</sup> 0.0009	<sup>1</sup> 1.009
102	IDEMIA-009	<sup>11</sup> 0	<sup>3</sup> 0	<sup>4</sup> 0.0010	<sup>4</sup> 0.0009	<sup>7</sup> 0.0009	<sup>9</sup> 0.0009	<sup>9</sup> 0.0009	<sup>4</sup> 1.008
103	IMAGUS-002	<sup>59</sup> 512	<sup>24</sup> 76	<sup>226</sup> 0.2203	<sup>274</sup> 0.1342	<sup>273</sup> 0.1090	<sup>272</sup> 0.0871	<sup>270</sup> 0.0632	<sup>275</sup> 2.308
104	IMAGUS-003	<sup>6</sup> 512	<sup>22</sup> 57	<sup>281</sup> 0.3559	<sup>281</sup> 0.2491	<sup>281</sup> 0.2132	<sup>281</sup> 0.1791	<sup>281</sup> 0.1397	<sup>28</sup> 3.363
105	IMAGUS-005	<sup>138</sup> 2048	<sup>228</sup> 788	<sup>76</sup> 0.0019	<sup>87</sup> 0.0016	<sup>85</sup> 0.0015	<sup>83</sup> 0.0014	<sup>82</sup> 0.0013	<sup>83</sup> 1.015
106	IMAGUS-006	<sup>155</sup> 2048	<sup>27</sup> 905	<sup>81</sup> 0.0020	<sup>92</sup> 0.0016	<sup>91</sup> 0.0015	<sup>95</sup> 0.0015	<sup>103</sup> 0.0014	<sup>88</sup> 1.015
107	IMAGUS-007	<sup>163</sup> 2048	<sup>150</sup> 590	<sup>83</sup> 0.0020	<sup>75</sup> 0.0015	<sup>72</sup> 0.0014	<sup>65</sup> 0.0013	<sup>66</sup> 0.0013	<sup>73</sup> 1.014
108	IMAGUS-008	<sup>7</sup> 0	<sup>11</sup> 2	<sup>264</sup> 0.0860	<sup>265</sup> 0.0701	<sup>26</sup> 0.0646	<sup>267</sup> 0.0590	<sup>26</sup> 0.0518	<sup>26</sup> 1.648
109	IMPERIAL-000	<sup>158</sup> 2048	<sup>169</sup> 654	<sup>104</sup> 0.0024	<sup>106</sup> 0.0019	<sup>113</sup> 0.0018	<sup>120</sup> 0.0018	<sup>128</sup> 0.0017	<sup>106</sup> 1.018
110	INCODE-000	<sup>85</sup> 1024	<sup>41</sup> 190	<sup>252</sup> 0.0489	<sup>247</sup> 0.0261	<sup>246</sup> 0.0204	<sup>246</sup> 0.0160	<sup>245</sup> 0.0117	<sup>247</sup> 1.262
111	INCODE-001	<sup>137</sup> 2048	<sup>183</sup> 690	<sup>220</sup> 0.0166	<sup>211</sup> 0.0084	<sup>208</sup> 0.0067	<sup>204</sup> 0.0055	<sup>205</sup> 0.0043	<sup>217</sup> 1.086
112	INCODE-002	<sup>192</sup> 2048	<sup>68</sup> 291	<sup>224</sup> 0.0178	<sup>214</sup> 0.0090	<sup>208</sup> 0.0070	<sup>205</sup> 0.0056	<sup>204</sup> 0.0043	<sup>218</sup> 1.092
113	INCODE-003	<sup>163</sup> 2048	<sup>704</sup> 704	<sup>212</sup> 0.0129	<sup>196</sup> 0.0064	<sup>194</sup> 0.0051	<sup>192</sup> 0.0040	<sup>184</sup> 0.0031	<sup>200</sup> 1.066
114	INCODE-004	<sup>157</sup> 2048	<sup>131</sup> 508	<sup>130</sup> 0.0035	<sup>133</sup> 0.0024	<sup>135</sup> 0.0021	<sup>138</sup> 0.0020	<sup>138</sup> 0.0019	<sup>132</sup> 1.023
115	INCODE-005	<sup>183</sup> 2048	<sup>130</sup> 500	<sup>53</sup> 0.0017	<sup>59</sup> 0.0014	<sup>6</sup> 0.0014	<sup>63</sup> 0.0013	<sup>59</sup> 0.0013	<sup>1</sup> 1.013
116	INNOVATRICS-002	<sup>73</sup> 530	<sup>59</sup> 255	<sup>250</sup> 0.0451	<sup>252</sup> 0.0342	<sup>255</sup> 0.0322	<sup>257</sup> 0.0308	<sup>259</sup> 0.0297	<sup>254</sup> 1.321
117	INNOVATRICS-003	<sup>7</sup> 530	<sup>58</sup> 255	<sup>236</sup> 0.0263	<sup>228</sup> 0.0126	<sup>225</sup> 0.0095	<sup>219</sup> 0.0074	<sup>205</sup> 0.0053	<sup>23</sup> 1.129
118	INNOVATRICS-004	<sup>106</sup> 1076	<sup>101</sup> 406	<sup>211</sup> 0.0123	<sup>195</sup> 0.0063	<sup>192</sup> 0.0050	<sup>193</sup> 0.0040	<sup>182</sup> 0.0032	<sup>199</sup> 1.064
119	INNOVATRICS-005	<sup>74</sup> 538	<sup>245</sup> 842	<sup>185</sup> 0.0024	<sup>100</sup> 0.0018	<sup>103</sup> 0.0017	<sup>106</sup> 0.0016	<sup>102</sup> 0.0014	<sup>100</sup> 1.017
120	INNOVATRICS-007	<sup>76</sup> 538	<sup>227</sup> 785	<sup>56</sup> 0.0017	<sup>65</sup> 0.0014	<sup>61</sup> 0.0013	<sup>58</sup> 0.0013	<sup>63</sup> 0.0012	<sup>62</sup> 1.013
121	INTELLIVISION-001	<sup>17</sup> 0	<sup>15</sup> 2	<sup>243</sup> 0.0365	<sup>245</sup> 0.0199	<sup>241</sup> 0.0160	<sup>240</sup> 0.0126	<sup>234</sup> 0.0095	<sup>243</sup> 1.199
122	INTSYSMSU-000	<sup>198</sup> 2048	<sup>176</sup> 675	<sup>271</sup> 0.1457	<sup>273</sup> 0.1320	<sup>270</sup> 0.1272	<sup>26</sup> 0.1225	<sup>278</sup> 0.1163	<sup>272</sup> 2.203
123	IREX-000	<sup>256</sup> 3080	<sup>237</sup> 2379	<sup>144</sup> 0.0044	<sup>171</sup> 0.0043	<sup>180</sup> 0.0043	<sup>198</sup> 0.0043	<sup>202</sup> 0.0043	<sup>169</sup> 1.039
124	ISYSTEMS-002	<sup>166</sup> 2048	<sup>76</sup> 316	<sup>168</sup> 0.0064	<sup>172</sup> 0.0043	<sup>177</sup> 0.0039	<sup>182</sup> 0.0037	<sup>192</sup> 0.0034	<sup>177</sup> 1.041
125	ISYSTEMS-003	<sup>182</sup> 2048	<sup>251</sup> 856	<sup>156</sup> 0.0052	<sup>167</sup> 0.0039	<sup>172</sup> 0.0036	<sup>181</sup> 0.0034	<sup>188</sup> 0.0033	<sup>163</sup> 1.037
126	KAKAO-000	<sup>216</sup> 2052	<sup>243</sup> 840	<sup>40</sup> 0.0015	<sup>30</sup> 0.0011	<sup>28</sup> 0.0011	<sup>24</sup> 0.0010	<sup>25</sup> 0.0010	<sup>31</sup> 1.010
127	KEDACOM-001	<sup>44</sup> 292	<sup>138</sup> 537	<sup>178</sup> 0.0077	<sup>203</sup> 0.0074	<sup>209</sup> 0.0073	<sup>216</sup> 0.0072	<sup>224</sup> 0.0072	<sup>201</sup> 1.067
128	KNERON-000	<sup>173</sup> 2048	<sup>133</sup> 530	<sup>163</sup> 0.0059	<sup>191</sup> 0.0059	<sup>198</sup> 0.0059	<sup>208</sup> 0.0059	<sup>215</sup> 0.0059	<sup>188</sup> 1.053
129	KNERON-001	<sup>187</sup> 2048	<sup>123</sup> 468	<sup>239</sup> 0.0295	<sup>249</sup> 0.0295	<sup>254</sup> 0.0295	<sup>256</sup> 0.0295	<sup>258</sup> 0.0295	<sup>248</sup> 1.266
130	LINE-000	<sup>152</sup> 2048	<sup>128</sup> 482	<sup>93</sup> 0.0022	<sup>80</sup> 0.0015	<sup>71</sup> 0.0014	<sup>55</sup> 0.0013	<sup>52</sup> 0.0012	<sup>81</sup> 1.015
131	LINE-001	<sup>177</sup> 2048	<sup>276</sup> 910	<sup>16</sup> 0.0011	<sup>19</sup> 0.0010	<sup>22</sup> 0.0010	<sup>19</sup> 0.0009	<sup>20</sup> 0.0009	<sup>18</sup> 1.009
132	LOOKMAN-003	<sup>47</sup> 292	<sup>81</sup> 342	<sup>18</sup> 0.0088	<sup>207</sup> 0.0078	<sup>217</sup> 0.0076	<sup>221</sup> 0.0075	<sup>227</sup> 0.0074	<sup>207</sup> 1.071
133	LOOKMAN-004	<sup>78</sup> 548	<sup>77</sup> 325	<sup>189</sup> 0.0091	<sup>208</sup> 0.0079	<sup>214</sup> 0.0076	<sup>220</sup> 0.0075	<sup>226</sup> 0.0073	<sup>205</sup> 1.072
134	LOOKMAN-005	<sup>77</sup> 548	<sup>133</sup> 514	<sup>18</sup> 0.0080	<sup>205</sup> 0.0075	<sup>218</sup> 0.0074	<sup>218</sup> 0.0073	<sup>225</sup> 0.0072	<sup>205</sup> 1.068
135	MANTRA-000	<sup>217</sup> 2052	<sup>102</sup> 412	<sup>59</sup> 0.0017	<sup>53</sup> 0.0013	<sup>55</sup> 0.0013	<sup>54</sup> 0.0012	<sup>52</sup> 0.0012	<sup>57</sup> 1.013
136	MEGVII-001	<sup>264</sup> 4096	<sup>165</sup> 652	<sup>208</sup> 0.0118	<sup>218</sup> 0.0093	<sup>218</sup> 0.0087	<sup>228</sup> 0.0084	<sup>233</sup> 0.0080	<sup>218</sup> 1.086
137	MEGVII-002	<sup>271</sup> 4096	<sup>170</sup> 656	<sup					

MISSES OUTSIDE RANK R FNIR(N, T=0, R)		RESOURCE USAGE TEMPLATE		ENROL MOST RECENT, N = 1.6M FRVT 2018 MUGSHOTS					
#	ALGORITHM	BYTES	MSEC	R=1	R=5	R=10	R=20	R=50	WORK-10
145	MICROSOFT-006	84 1024	187 695	79 0.0020	31 0.0011	29 0.0010	4 0.0008	4 0.0007	36 1.011
146	NEC-000	254 2592	25 82	221 0.0170	213 0.0086	204 0.0066	201 0.0052	197 0.0038	215 1.087
147	NEC-001	250 2592	26 88	230 0.0209	234 0.0141	238 0.0128	238 0.0119	241 0.0113	233 1.135
148	NEC-002	126 1616	168 653	10 0.0010	5 0.0009	5 0.0008	6 0.0008	5 0.0008	5 1.008
149	NEC-003	127 1712	184 690	31 0.0014	42 0.0012	45 0.0012	52 0.0012	54 0.0012	38 1.011
150	NEC-004	107 1104	296 967	37 0.0014	55 0.0013	65 0.0013	66 0.0013	73 0.0013	53 1.012
151	NEC-005	108 1104	289 964	21 0.0012	29 0.0011	34 0.0011	36 0.0011	41 0.0011	29 1.010
152	NEUROTECHNOLOGY-003	201 2048	141 547	231 0.0225	229 0.0126	225 0.0100	225 0.0078	214 0.0057	230 1.125
153	NEUROTECHNOLOGY-004	139 2048	140 543	158 0.0056	159 0.0036	164 0.0032	166 0.0029	165 0.0025	160 1.035
154	NEUROTECHNOLOGY-005	36 256	105 412	142 0.0043	149 0.0029	159 0.0027	153 0.0024	159 0.0023	150 1.028
155	NEUROTECHNOLOGY-006	31 256	215 746	225 0.0180	209 0.0079	197 0.0059	197 0.0046	189 0.0033	211 1.083
156	NEUROTECHNOLOGY-007	35 256	39 169	134 0.0039	144 0.0027	149 0.0025	150 0.0023	150 0.0022	14 1.026
157	NEUROTECHNOLOGY-008	66 514	238 804	89 0.0022	76 0.0015	79 0.0014	81 0.0014	81 0.0013	79 1.015
158	NEUROTECHNOLOGY-009	65 513	179 686	38 0.0014	38 0.0012	40 0.0012	41 0.0011	45 0.0011	37 1.011
159	NEUROTECHNOLOGY-010	35 256	172 663	24 0.0012	23 0.0011	24 0.0010	26 0.0010	30 0.0010	24 1.010
160	NEUROTECHNOLOGY-012	10 0	4 0	8 0.0010	16 0.0010	16 0.0010	20 0.0009	23 0.0009	11 1.009
161	NEWLAND-002	143 2048	256 868	261 0.0786	261 0.0480	260 0.0397	260 0.0332	257 0.0263	262 1.468
162	NOBLIS-001	193 2048	51 211	278 0.2492	278 0.1772	278 0.1542	278 0.1339	276 0.1112	278 2.679
163	NOBLIS-002	256 6144	137 535	247 0.1794	271 0.1108	277 0.0903	270 0.0722	269 0.0535	272 2.077
164	NOTIONTAG-000	246 2120	118 461	105 0.0024	123 0.0021	130 0.0021	141 0.0020	145 0.0019	119 1.019
165	NTECHLAB-003	260 3484	239 831	164 0.0062	152 0.0029	143 0.0023	136 0.0019	117 0.0016	155 1.030
166	NTECHLAB-004	259 3484	278 929	151 0.0048	130 0.0023	119 0.0019	109 0.0016	85 0.0013	138 1.024
167	NTECHLAB-005	131 1940	204 717	149 0.0047	125 0.0022	166 0.0017	68 0.0013	39 0.0011	131 1.023
168	NTECHLAB-006	132 1940	244 841	139 0.0041	108 0.0019	88 0.0015	48 0.0012	19 0.0009	120 1.019
169	NTECHLAB-007	258 3348	242 834	110 0.0027	93 0.0017	79 0.0014	74 0.0013	56 0.0012	95 1.016
170	NTECHLAB-008	114 1300	145 562	38 0.0017	37 0.0012	38 0.0012	38 0.0011	36 0.0010	40 1.012
171	NTECHLAB-009	113 1300	269 900	26 0.0013	25 0.0011	25 0.0010	23 0.0010	24 0.0009	27 1.010
172	NTECHLAB-010	111 1280	267 875	15 0.0011	22 0.0010	25 0.0010	25 0.0010	35 0.0010	20 1.009
173	NTECHLAB-011	112 1280	254 865	9 0.0010	7 0.0009	11 0.0009	13 0.0009	13 0.0009	7 1.008
174	PANGIAM-000	5 0	8 2	20 0.0012	27 0.0011	29 0.0011	29 0.0010	34 0.0010	26 1.010
175	PARAVISION-000	180 2048	113 438	226 0.0188	239 0.0171	245 0.0167	248 0.0165	253 0.0164	236 1.156
176	PARAVISION-001	174 2048	151 590	132 0.0038	136 0.0024	130 0.0022	142 0.0020	139 0.0019	136 1.023
177	PARAVISION-002	134 2048	90 377	137 0.0040	141 0.0025	142 0.0022	144 0.0021	141 0.0019	139 1.025
178	PARAVISION-003	16 2048	210 735	122 0.0031	124 0.0022	122 0.0020	132 0.0019	131 0.0017	12 1.021
179	PARAVISION-004	269 4096	207 720	51 0.0016	62 0.0014	64 0.0013	72 0.0013	80 0.0013	61 1.013
180	PARAVISION-005	272 4096	252 858	46 0.0015	58 0.0014	60 0.0013	73 0.0013	83 0.0013	56 1.013
181	PARAVISION-007	265 4096	194 706	18 0.0012	26 0.0011	28 0.0010	28 0.0010	29 0.0010	23 1.010
182	PARAVISION-009	276 4100	161 638	7 0.0010	12 0.0010	17 0.0010	22 0.0009	21 0.0009	10 1.009
183	PIXELALL-002	250 2560	45 198	146 0.0045	151 0.0029	159 0.0025	147 0.0022	144 0.0019	151 1.028
184	PIXELALL-003	253 2560	206 719	87 0.0021	89 0.0016	92 0.0015	90 0.0014	99 0.0014	89 1.015
185	PIXELALL-004	252 2560	115 453	84 0.0020	79 0.0015	88 0.0015	88 0.0014	89 0.0013	71 1.014
186	PIXELALL-005	251 2560	247 845	74 0.0019	95 0.0017	97 0.0016	108 0.0016	118 0.0016	87 1.015
187	PTAKURATSU-000	75 538	274 910	120 0.0030	122 0.0021	124 0.0019	118 0.0018	121 0.0016	12 1.020
188	QNAP-000	144 2048	116 457	129 0.0078	178 0.0044	174 0.0037	175 0.0033	177 0.0028	175 1.043
189	QNAP-001	172 2048	151 615	140 0.0041	150 0.0029	159 0.0027	156 0.0025	166 0.0023	14 1.028
190	QNAP-002	14 0	14 2	152 0.0049	173 0.0044	186 0.0043	196 0.0043	201 0.0042	171 1.040
191	QUANTASOFT-001	154 2048	96 396	275 0.2177	277 0.1643	277 0.1468	277 0.1312	277 0.1116	277 2.539
192	RANKONE-002	26 133	29 113	228 0.0194	223 0.0112	223 0.0093	223 0.0077	217 0.0060	223 1.111
193	RANKONE-003	27 133	30 114	227 0.0194	224 0.0112	224 0.0093	223 0.0077	218 0.0060	224 1.111
194	RANKONE-004	18 85	21 36	249 0.0415	246 0.0226	246 0.0177	242 0.0141	239 0.0102	246 1.225
195	RANKONE-005	25 133	27 94	193 0.0094	188 0.0054	188 0.0046	190 0.0039	188 0.0032	188 1.054
196	RANKONE-006	28 165	60 261	154 0.0050	155 0.0030	158 0.0027	152 0.0024	148 0.0021	154 1.030
197	RANKONE-007	29 165	67 278	126 0.0034	131 0.0023	133 0.0021	128 0.0018	124 0.0017	128 1.022
198	RANKONE-009	40 260	43 191	100 0.0024	91 0.0016	96 0.0015	97 0.0015	96 0.0014	92 1.015
199	RANKONE-010	42 261	46 200	94 0.0022	98 0.0018	99 0.0016	104 0.0015	108 0.0015	97 1.016
200	RANKONE-011	43 261	148 567	43 0.0015	41 0.0012	43 0.0012	46 0.0012	50 0.0012	39 1.011
201	RANKONE-012	41 261	146 563	30 0.0014	35 0.0012	39 0.0011	40 0.0011	48 0.0011	33 1.011
202	REALNETWORKS-000	277 4100	53 244	248 0.0402	241 0.0195	239 0.0149	238 0.0111	230 0.0077	245 1.201
203	REALNETWORKS-001	280 4104	54 243	247 0.0402	244 0.0195	246 0.0149	236 0.0111	231 0.0077	244 1.201
204	REALNETWORKS-002	281 4104	56 245	244 0.0393	242 0.0189	242 0.0142	234 0.0108	229 0.0076	242 1.195
205	REALNETWORKS-003	130 1848	37 178	234 0.0242	226 0.0117	224 0.0090	215 0.0070	217 0.0054	228 1.120
206	REALNETWORKS-004	129 1848	39 185	232 0.0236	225 0.0112	219 0.0087	213 0.0068	209 0.0050	225 1.116
207	REALNETWORKS-005	23 2056	75 337	96 0.0023	82 0.0016	76 0.0014	76 0.0013	66 0.0012	81 1.015
208	REALNETWORKS-006	230 2056	83 350	34 0.0014	36 0.0012	35 0.0011	32 0.0011	36 0.0010	34 1.011
209	REALNETWORKS-007	15 0	15 2	28 0.0013	33 0.0012	31 0.0011	30 0.0011	26 0.0010	32 1.011
210	REMARKAI-000	136 2048	183 691	128 0.0034	121 0.0021	116 0.0019	111 0.0017	118 0.0015	123 1.020
211	REMARKAI-000	151 2048	154 615	186 0.0086	176 0.0044	169 0.0036	169 0.0031	166 0.0025	178 1.045
212	REMARKAI-002	156 2048	112 434	184 0.0081	168 0.0040	167 0.0031	157 0.0026	147 0.0021	12 1.041
213	RENDIP-000	154 2048	26 894	47 0.0015	48 0.0013	47 0.0012	49 0.0012	56 0.0012	50 1.012
214	REVEALMEDIA-000	221 2052	92 385	71 0.0019	52 0.0013	58 0.0013	57 0.0013	62 0.0012	60 1.013
215	S1-000	273 4096	255 865	102 0.0024	96 0.0018	100 0.0017	105 0.0016	112 0.0015	99 1.017
216	S1-001	142 2048	237 814	121 0.0031	138 0.0025	146 0.0024	151 0.0024	161 0.0023	134 1.023

Table 26: **Rank-based accuracy for the FRVT 2018 mugshot sets.** In columns 3 and 4 are template size and template generation duration. Thereafter values are rank-based FNIR with  $T = 0$  and FPIR = 1. This is appropriate to investigational uses but not those with higher volumes where candidates from all searches would need review. The next column is a workload statistic, a small value shows an algorithm front-loads mates into the first 10 candidates. Throughout, blue superscripts indicate the rank of the algorithm for that column, and the best value is highlighted in yellow.

MISSES OUTSIDE RANK R FNIR(N, T=0, R)		RESOURCE USAGE TEMPLATE		ENROL MOST RECENT, N = 1.6M FRVT 2018 MUGSHOTS						
#	ALGORITHM	BYTES	MSEC	R=1	R=5	R=10	R=20	R=50	WORK-10	
217	S1-002	<sup>10</sup> 0	<sup>7</sup> 2	<sup>3</sup> 0.0014	<sup>54</sup> 0.0013	<sup>60</sup> 0.0013	<sup>70</sup> 0.0013	<sup>84</sup> 0.0013	<sup>51</sup> 0.012	
218	SCANOVATE-000	<sup>171</sup> 2048	<sup>199</sup> 712	<sup>153</sup> 0.0050	<sup>143</sup> 0.0026	<sup>139</sup> 0.0022	<sup>126</sup> 0.0018	<sup>117</sup> 0.0015	<sup>148</sup> 1.026	
219	SCANOVATE-001	<sup>194</sup> 2048	<sup>177</sup> 675	<sup>157</sup> 0.0053	<sup>145</sup> 0.0027	<sup>141</sup> 0.0022	<sup>122</sup> 0.0018	<sup>114</sup> 0.0015	<sup>146</sup> 1.028	
220	SENSETIME-000	<sup>278</sup> 4104	<sup>202</sup> 715	<sup>97</sup> 0.0023	<sup>117</sup> 0.0020	<sup>121</sup> 0.0019	<sup>124</sup> 0.0018	<sup>132</sup> 0.0017	<sup>112</sup> 1.018	
221	SENSETIME-001	<sup>282</sup> 4104	<sup>171</sup> 656	<sup>99</sup> 0.0023	<sup>114</sup> 0.0020	<sup>118</sup> 0.0019	<sup>115</sup> 0.0017	<sup>120</sup> 0.0016	<sup>109</sup> 1.018	
222	SENSETIME-002	<sup>231</sup> 2056	<sup>164</sup> 650	<sup>217</sup> 0.0137	<sup>232</sup> 0.0136	<sup>237</sup> 0.0136	<sup>241</sup> 0.0136	<sup>247</sup> 0.0136	<sup>229</sup> 1.122	
223	SENSETIME-003	<sup>232</sup> 2056	<sup>282</sup> 940	<sup>6</sup> 0.0010	<sup>15</sup> 0.0010	<sup>18</sup> 0.0010	<sup>21</sup> 0.0009	<sup>22</sup> 0.0009	<sup>9</sup> 1.009	
224	SENSETIME-004	<sup>97</sup> 1032	<sup>198</sup> 710	<sup>7</sup> 0.0010	<sup>6</sup> 0.0009	<sup>9</sup> 0.0009	<sup>10</sup> 0.0009	<sup>10</sup> 0.0009	<sup>6</sup> 1.008	
225	SENSETIME-005	<sup>95</sup> 1032	<sup>292</sup> 1007	<sup>3</sup> 0.0009	<sup>2</sup> 0.0008	<sup>2</sup> 0.0008	<sup>3</sup> 0.0008	<sup>6</sup> 0.0008	<sup>2</sup> 1.008	
226	SENSETIME-006	<sup>94</sup> 1032	<sup>286</sup> 956	<sup>1</sup> 0.0009	<sup>3</sup> 0.0008	<sup>4</sup> 0.0008	<sup>3</sup> 0.0008	<sup>7</sup> 0.0008	<sup>3</sup> 1.008	
227	SENSETIME-007	<sup>92</sup> 1032	<sup>287</sup> 958	<sup>1</sup> 0.0008	<sup>1</sup> 0.0008	<sup>3</sup> 0.0008	<sup>7</sup> 0.0008	<sup>8</sup> 0.0008	<sup>1</sup> 1.007	
228	SHAMAN-003	<sup>160</sup> 2048	<sup>192</sup> 704	<sup>26</sup> 0.1243	<sup>269</sup> 0.0823	<sup>269</sup> 0.0708	<sup>26</sup> 0.0616	<sup>268</sup> 0.0518	<sup>266</sup> 1.789	
229	SHAMAN-004	<sup>176</sup> 2048	<sup>163</sup> 642	<sup>27</sup> 0.2221	<sup>276</sup> 0.1473	<sup>274</sup> 0.1241	<sup>274</sup> 0.1049	<sup>273</sup> 0.0825	<sup>276</sup> 2.411	
230	SHAMAN-006	<sup>199</sup> 2048	<sup>195</sup> 706	<sup>246</sup> 0.0398	<sup>254</sup> 0.0344	<sup>257</sup> 0.0332	<sup>259</sup> 0.0323	<sup>262</sup> 0.0315	<sup>253</sup> 1.316	
231	SHAMAN-007	<sup>172</sup> 2048	<sup>197</sup> 709	<sup>24</sup> 0.0396	<sup>253</sup> 0.0342	<sup>256</sup> 0.0331	<sup>259</sup> 0.0322	<sup>261</sup> 0.0314	<sup>251</sup> 1.315	
232	SIAT-001	<sup>218</sup> 2052	<sup>246</sup> 842	<sup>67</sup> 0.0018	<sup>63</sup> 0.0014	<sup>52</sup> 0.0013	<sup>47</sup> 0.0012	<sup>44</sup> 0.0011	<sup>63</sup> 1.013	
233	SIAT-002	<sup>210</sup> 2052	<sup>272</sup> 906	<sup>6</sup> 0.0018	<sup>61</sup> 0.0014	<sup>66</sup> 0.0013	<sup>61</sup> 0.0013	<sup>66</sup> 0.0012	<sup>66</sup> 1.013	
234	SMILART-004	<sup>56</sup> 512	<sup>33</sup> 167	<sup>290</sup> 0.9648	<sup>290</sup> 0.9641	<sup>290</sup> 0.9640	<sup>290</sup> 0.9639	<sup>291</sup> 0.9638	<sup>293</sup> 9.678	
235	SMILART-005	<sup>159</sup> 2048	<sup>121</sup> 464						<sup>10</sup> 0.0000	
236	SQISOFT-001	<sup>234</sup> 2056	<sup>117</sup> 460	<sup>141</sup> 0.0042	<sup>69</sup> 0.0014	<sup>49</sup> 0.0013	<sup>42</sup> 0.0012	<sup>37</sup> 0.0010	<sup>96</sup> 1.016	
237	STAQU-000	<sup>274</sup> 4096	<sup>236</sup> 827	<sup>17</sup> 0.0071	<sup>193</sup> 0.0060	<sup>195</sup> 0.0057	<sup>20</sup> 0.0055	<sup>208</sup> 0.0053	<sup>190</sup> 1.056	
238	SYNESIS-003	<sup>181</sup> 2048	<sup>52</sup> 215	<sup>219</sup> 0.0162	<sup>236</sup> 0.0160	<sup>242</sup> 0.0160	<sup>247</sup> 0.0160	<sup>252</sup> 0.0160	<sup>235</sup> 1.144	
239	SYNESIS-003	<sup>262</sup> 4096	<sup>28</sup> 103	<sup>27</sup> 0.1700	<sup>272</sup> 0.1172	<sup>272</sup> 0.1047	<sup>274</sup> 0.0953	<sup>274</sup> 0.0869	<sup>272</sup> 2.120	
240	SYNESIS-005	<sup>279</sup> 4104	<sup>221</sup> 772	<sup>187</sup> 0.0085	<sup>212</sup> 0.0085	<sup>217</sup> 0.0085	<sup>229</sup> 0.0085	<sup>235</sup> 0.0085	<sup>209</sup> 1.076	
241	TECH5-001	<sup>118</sup> 1536	<sup>268</sup> 898	<sup>13</sup> 0.0040	<sup>134</sup> 0.0024	<sup>134</sup> 0.0021	<sup>122</sup> 0.0018	<sup>126</sup> 0.0017	<sup>137</sup> 1.024	
242	TECH5-002	<sup>64</sup> 513	<sup>283</sup> 941	<sup>11</sup> 0.0027	<sup>67</sup> 0.0014	<sup>46</sup> 0.0012	<sup>39</sup> 0.0011	<sup>28</sup> 0.0010	<sup>76</sup> 1.014	
243	TEVIAN-003	<sup>141</sup> 2048	<sup>74</sup> 300	<sup>218</sup> 0.0147	<sup>204</sup> 0.0074	<sup>196</sup> 0.0059	<sup>198</sup> 0.0047	<sup>196</sup> 0.0037	<sup>208</sup> 1.075	
244	TEVIAN-004	<sup>180</sup> 2048	<sup>72</sup> 299	<sup>20</sup> 0.0113	<sup>189</sup> 0.0057	<sup>189</sup> 0.0047	<sup>188</sup> 0.0037	<sup>180</sup> 0.0030	<sup>191</sup> 1.058	
245	TEVIAN-005	<sup>195</sup> 2048	<sup>105</sup> 416	<sup>178</sup> 0.0073	<sup>165</sup> 0.0038	<sup>159</sup> 0.0031	<sup>160</sup> 0.0027	<sup>158</sup> 0.0023	<sup>167</sup> 1.038	
246	TEVIAN-006	<sup>98</sup> 1032	<sup>152</sup> 599	<sup>107</sup> 0.0024	<sup>101</sup> 0.0018	<sup>107</sup> 0.0018	<sup>111</sup> 0.0017	<sup>123</sup> 0.0017	<sup>101</sup> 1.017	
247	TEVIAN-007	<sup>93</sup> 1032	<sup>225</sup> 779	<sup>63</sup> 0.0018	<sup>56</sup> 0.0014	<sup>62</sup> 0.0013	<sup>71</sup> 0.0013	<sup>70</sup> 0.0013	<sup>58</sup> 1.013	
248	TIGER-000	<sup>213</sup> 2052	<sup>108</sup> 428	<sup>25</sup> 0.0616	<sup>251</sup> 0.0310	<sup>250</sup> 0.0236	<sup>259</sup> 0.0178	<sup>244</sup> 0.0120	<sup>252</sup> 1.315	
249	TIGER-002	<sup>215</sup> 2052	<sup>120</sup> 464	<sup>159</sup> 0.0056	<sup>153</sup> 0.0029	<sup>147</sup> 0.0024	<sup>131</sup> 0.0019	<sup>111</sup> 0.0015	<sup>152</sup> 1.030	
250	TIGER-003	<sup>223</sup> 2052	<sup>122</sup> 464	<sup>16</sup> 0.0056	<sup>154</sup> 0.0029	<sup>146</sup> 0.0024	<sup>139</sup> 0.0019	<sup>110</sup> 0.0015	<sup>153</sup> 1.030	
251	TONGYITRANS-000	<sup>240</sup> 2070	<sup>42</sup> 190	<sup>17</sup> 0.0069	<sup>163</sup> 0.0038	<sup>163</sup> 0.0032	<sup>165</sup> 0.0029	<sup>171</sup> 0.0026	<sup>168</sup> 1.038	
252	TONGYITRANS-001	<sup>242</sup> 2070	<sup>40</sup> 189	<sup>172</sup> 0.0069	<sup>164</sup> 0.0038	<sup>163</sup> 0.0032	<sup>167</sup> 0.0029	<sup>169</sup> 0.0026	<sup>166</sup> 1.038	
253	TOSHIBA-000	<sup>125</sup> 1548	<sup>29</sup> 930	<sup>14</sup> 0.0045	<sup>142</sup> 0.0026	<sup>140</sup> 0.0022	<sup>139</sup> 0.0020	<sup>136</sup> 0.0018	<sup>143</sup> 1.026	
254	TOSHIBA-001	<sup>237</sup> 2060	<sup>280</sup> 931	<sup>150</sup> 0.0048	<sup>146</sup> 0.0027	<sup>143</sup> 0.0023	<sup>142</sup> 0.0020	<sup>137</sup> 0.0018	<sup>147</sup> 1.027	
255	TRUEFACE-000	<sup>133</sup> 2000	<sup>84</sup> 365	<sup>12</sup> 0.0033	<sup>148</sup> 0.0028	<sup>157</sup> 0.0028	<sup>159</sup> 0.0026	<sup>168</sup> 0.0026	<sup>144</sup> 1.026	
256	VD-000	<sup>91</sup> 1028	<sup>78</sup> 337	<sup>28</sup> 0.4737	<sup>284</sup> 0.3204	<sup>284</sup> 0.2695	<sup>28</sup> 0.2215	<sup>282</sup> 0.1678	<sup>284</sup> 4.058	
257	VD-001	<sup>219</sup> 2052	<sup>188</sup> 695	<sup>23</sup> 0.0276	<sup>241</sup> 0.0181	<sup>244</sup> 0.0162	<sup>243</sup> 0.0146	<sup>246</sup> 0.0130	<sup>241</sup> 1.174	
258	VD-002	<sup>214</sup> 2052	<sup>181</sup> 689	<sup>194</sup> 0.0095	<sup>206</sup> 0.0077	<sup>210</sup> 0.0073	<sup>214</sup> 0.0070	<sup>223</sup> 0.0068	<sup>203</sup> 1.071	
259	VD-003	<sup>222</sup> 2052	<sup>186</sup> 693	<sup>17</sup> 0.0076	<sup>199</sup> 0.0069	<sup>206</sup> 0.0067	<sup>217</sup> 0.0066	<sup>221</sup> 0.0066	<sup>197</sup> 1.063	
260	VERIDAS-001	<sup>202</sup> 2048	<sup>263</sup> 885	<sup>118</sup> 0.0028	<sup>110</sup> 0.0019	<sup>104</sup> 0.0017	<sup>103</sup> 0.0015	<sup>107</sup> 0.0015	<sup>110</sup> 1.018	
261	VERIDAS-002	<sup>162</sup> 2048	<sup>264</sup> 888	<sup>11</sup> 0.0028	<sup>109</sup> 0.0019	<sup>101</sup> 0.0017	<sup>105</sup> 0.0015	<sup>108</sup> 0.0018	<sup>108</sup> 1.018	
262	VERIDAS-003	<sup>203</sup> 2048	<sup>262</sup> 877	<sup>69</sup> 0.0018	<sup>73</sup> 0.0015	<sup>74</sup> 0.0014	<sup>77</sup> 0.0013	<sup>77</sup> 0.0013	<sup>70</sup> 1.014	
263	VIGILANTSOLUTIONS-003	<sup>123</sup> 1544	<sup>240</sup> 832	<sup>29</sup> 0.0694	<sup>256</sup> 0.0349	<sup>251</sup> 0.0262	<sup>25</sup> 0.0201	<sup>248</sup> 0.0140	<sup>256</sup> 1.355	
264	VIGILANTSOLUTIONS-004	<sup>124</sup> 1544	<sup>238</sup> 830	<sup>26</sup> 0.1249	<sup>266</sup> 0.0706	<sup>264</sup> 0.0557	<sup>262</sup> 0.0434	<sup>260</sup> 0.0305	<sup>266</sup> 1.699	
265	VIGILANTSOLUTIONS-005	<sup>122</sup> 1544	<sup>224</sup> 778	<sup>19</sup> 0.0092	<sup>178</sup> 0.0045	<sup>168</sup> 0.0306	<sup>167</sup> 0.0299	<sup>153</sup> 0.0222	<sup>179</sup> 1.046	
266	VIGILANTSOLUTIONS-006	<sup>120</sup> 1544	<sup>241</sup> 834	<sup>19</sup> 0.0099	<sup>180</sup> 0.0048	<sup>178</sup> 0.0038	<sup>168</sup> 0.0030	<sup>157</sup> 0.0022	<sup>182</sup> 1.049	
267	VIGILANTSOLUTIONS-007	<sup>119</sup> 1544	<sup>156</sup> 618	<sup>12</sup> 0.0034	<sup>113</sup> 0.0020	<sup>105</sup> 0.0017	<sup>108</sup> 0.0015	<sup>82</sup> 0.0013	<sup>118</sup> 1.019	
268	VIGILANTSOLUTIONS-008	<sup>121</sup> 1544	<sup>100</sup> 405	<sup>11</sup> 0.0029	<sup>103</sup> 0.0018	<sup>96</sup> 0.0016	<sup>93</sup> 0.0015	<sup>71</sup> 0.0013	<sup>107</sup> 1.018	
269	VISIONBOX-000	<sup>236</sup> 2059	<sup>126</sup> 482	<sup>75</sup> 0.0019	<sup>77</sup> 0.0015	<sup>81</sup> 0.0014	<sup>78</sup> 0.0013	<sup>69</sup> 0.0013	<sup>74</sup> 1.014	
270	VISIONLABS-004	<sup>32</sup> 256	<sup>75</sup> 315	<sup>11</sup> 0.0027	<sup>99</sup> 0.0018	<sup>98</sup> 0.0016	<sup>99</sup> 0.0015	<sup>95</sup> 0.0014	<sup>103</sup> 1.017	
271	VISIONLABS-005	<sup>53</sup> 512	<sup>73</sup> 300	<sup>101</sup> 0.0024	<sup>94</sup> 0.0017	<sup>89</sup> 0.0015	<sup>82</sup> 0.0014	<sup>78</sup> 0.0013	<sup>94</sup> 1.016	
272	VISIONLABS-006	<sup>58</sup> 512	<sup>69</sup> 292	<sup>6</sup> 0.0018	<sup>71</sup> 0.0015	<sup>68</sup> 0.0014	<sup>69</sup> 0.0013	<sup>72</sup> 0.0013	<sup>69</sup> 1.014	
273	VISIONLABS-007	<sup>60</sup> 512	<sup>70</sup> 293	<sup>67</sup> 0.0018	<sup>66</sup> 0.0014	<sup>57</sup> 0.0013	<sup>56</sup> 0.0013	<sup>59</sup> 0.0012	<sup>65</sup> 1.013	
274	VISIONLABS-008	<sup>62</sup> 512	<sup>66</sup> 277	<sup>82</sup> 0.0020	<sup>102</sup> 0.0018	<sup>110</sup> 0.0018	<sup>117</sup> 0.0018	<sup>129</sup> 0.0017	<sup>98</sup> 1.017	
275	VISIONLABS-009	<sup>52</sup> 512	<sup>129</sup> 494	<sup>17</sup> 0.0011	<sup>24</sup> 0.0011	<sup>26</sup> 0.0010	<sup>27</sup> 0.0010	<sup>27</sup> 0.0010	<sup>22</sup> 1.010	
276	VISIONLABS-010	<sup>57</sup> 512	<sup>209</sup> 732	<sup>33</sup> 0.0014	<sup>50</sup> 0.0013	<sup>56</sup> 0.0013	<sup>59</sup> 0.0013	<sup>47</sup> 0.0013	<sup>47</sup> 1.012	
277	VISIONLABS-011	<sup>61</sup> 512	<sup>211</sup> 736	<sup>2</sup> 0.0012	<sup>28</sup> 0.0011	<sup>33</sup> 0.0011	<sup>31</sup> 0.0011	<sup>40</sup> 0.0011	<sup>28</sup> 1.010	
278	VNPPT-001	<sup>0</sup> 0	<sup>10</sup> 2	<sup>88</sup> 0.0022	<sup>102</sup> 0.0019	<sup>113</sup> 0.0018	<sup>123</sup> 0.0018	<sup>134</sup> 0.0018	<sup>104</sup> 1.017	
279	VOCORD-003	<sup>82</sup> 896	<sup>201</sup> 714	<sup>16</sup> 0.0062	<sup>188</sup> 0.0035	<sup>158</sup> 0.0030	<sup>150</sup> 0.0026	<sup>160</sup> 0.0023	<sup>159</sup> 1.035	
280	VOCORD-004	<sup>81</sup> 896	<sup>139</sup> 538	<sup>180</sup> 0.0079	<sup>182</sup> 0.0049	<sup>184</sup> 0.0043	<sup>188</sup> 0.0038	<sup>190</sup> 0.0034	<sup>180</sup> 1.048	
281	VOCORD-005	<sup>79</sup> 768	<sup>234</sup> 822	<sup>17</sup> 0.0070	<sup>179</sup> 0.0046	<sup>181</sup> 0.0041	<sup>187</sup> 0.0038	<sup>193</sup> 0.		

#	ALGORITHM	MISSES OUTSIDE RANK R		RESOURCE USAGE		ENROL MOST RECENT, N = 1.6M					
		FNIR(N, T=0, R)		TEMPLATE		FRVT 2018 MUGSHOTS					
		BYTES	MSEC	R=1	R=5	R=10	R=20	R=50	WORK-10		
289	YISHENG-001	<sup>261</sup> 3704	<sup>94</sup> 387	<sup>237</sup> 0.0265	<sup>231</sup> 0.0130	<sup>228</sup> 0.0102	<sup>226</sup> 0.0080	<sup>216</sup> 0.0059	<sup>232</sup> 1.134		
290	YITU-002	<sup>287</sup> 4138	<sup>257</sup> 870	<sup>70</sup> 0.0018	<sup>40</sup> 0.0012	<sup>36</sup> 0.0011	<sup>34</sup> 0.0011	<sup>33</sup> 0.0010	<sup>46</sup> 1.012		
291	YITU-003	<sup>284</sup> 4138	<sup>259</sup> 871	<sup>118</sup> 0.0029	<sup>129</sup> 0.0023	<sup>138</sup> 0.0022	<sup>146</sup> 0.0021	<sup>151</sup> 0.0021	<sup>126</sup> 1.021		
292	YITU-004	<sup>241</sup> 2070	<sup>275</sup> 910	<sup>27</sup> 0.0013	<sup>8</sup> 0.0009	<sup>10</sup> 0.0009	<sup>11</sup> 0.0009	<sup>11</sup> 0.0009	<sup>16</sup> 1.009		
293	YITU-005	<sup>239</sup> 2070	<sup>253</sup> 861	<sup>97</sup> 0.0023	<sup>120</sup> 0.0021	<sup>127</sup> 0.0020	<sup>140</sup> 0.0020	<sup>146</sup> 0.0020	<sup>115</sup> 1.019		

**Table 28: Rank-based accuracy for the FRVT 2018 mugshot sets.** In columns 3 and 4 are template size and template generation duration. Thereafter values are rank-based FNIR with  $T = 0$  and FPIR = 1. This is appropriate to investigational uses but not those with higher volumes where candidates from all searches would need review. The next column is a workload statistic, a small value shows an algorithm front-loads mates into the first 10 candidates. Throughout, blue superscripts indicate the rank of the algorithm for that column, and the best value is highlighted in yellow.

MISSES BELOW THRESHOLD, T		ENROL RECENT MUGSHOT, N = 1.6M												ENROL APPLICATION PORTRAIT, N = 1.6M																		
#	ALGORITHM	ENROL: MUGSHOT			ENROL: MUGSHOT			ENROL: MUGSHOT			ENROL: VISA			ENROL: BORDER			ENROL: BORDER 10+YR			ENROL: KIOSK												
		FPIR=0.0003	FPIR=0.001	FPIR=0.01	FPIR=0.0003	FPIR=0.001	FPIR=0.01	FPIR=0.0003	FPIR=0.001	FPIR=0.01	FPIR=0.0001	FPIR=0.001	FPIR=0.01	FPIR=0.001	FPIR=0.001	FPIR=0.01	FPIR=0.001	FPIR=0.001	FPIR=0.01	FPIR=0.001	FPIR=0.001	FPIR=0.01	FPIR=0.001	FPIR=0.01								
1	20FACE-000	241	0.462	250	0.348	257	0.230	253	0.763	246	0.450	246	0.301	200	1.000	222	1.000	225	1.000	182	0.424	182	0.255	101	0.772	105	0.599	176	0.938	189	0.836	
2	3DIVI-003	243	0.482	259	0.400	263	0.282	248	0.685	260	0.626	262	0.497					194	0.605	199	0.445					159	0.821	179	0.717			
3	3DIVI-004	214	0.256	230	0.169	234	0.093	218	0.400	236	0.343	240	0.237					172	0.277	176	0.172					137	0.607	159	0.485			
4	3DIVI-005	213	0.255	227	0.166	231	0.093	217	0.395	231	0.339	239	0.234	143	0.998	147	0.996	159	0.990	200	0.864	207	0.846					136	0.597	159	0.484	
5	3DIVI-006	212	0.253	229	0.168	236	0.096	221	0.403	235	0.342	241	0.238					173	0.283	177	0.174					140	0.615	169	0.490			
6	ACER-000	198	0.208	220	0.146	222	0.074	202	0.300	213	0.246	215	0.157	92	0.987	106	0.981	124	0.955	167	0.201	177	0.114					123	0.490	144	0.363	
7	ACER-001	144	0.109	162	0.056	166	0.026	138	0.136	145	0.109	148	0.069	172	1.000	179	0.999	204	0.998	130	0.068	129	0.036	90	0.406	93	0.250	122	0.479	99	0.206	
8	AIZE-001	155	0.127	182	0.077	181	0.034	168	0.187	172	0.143	171	0.087	116	0.995	125	0.994	148	0.983	143	0.101	144	0.052	84	0.364	96	0.216	104	0.387	128	0.289	
9	ALCHERA-000	205	0.231	217	0.138	218	0.070	191	0.259	199	0.216	209	0.146	153	0.999	163	0.999	187	0.996	162	0.176	170	0.111					155	0.803	159	0.456	
10	ALCHERA-001	288	1.000	288	0.999	299	0.999	28	1.000	281	1.000	292	1.000					289	1.000	277	1.000					260	1.000	227	1.000			
11	ALCHERA-002	266	0.807	266	0.486	266	0.302	247	0.685	257	0.591	257	0.442	189	1.000	189	1.000	209	0.999	199	0.827	199	0.770					156	0.811	179	0.705	
12	ALCHERA-003	237	0.450	221	0.155	219	0.070	203	0.304	210	0.239	214	0.152	184	1.000	174	0.999	192	0.997	161	0.172	167	0.097					118	0.464	143	0.362	
13	ALCHERA-004	248	0.520	258	0.394	256	0.211	244	0.642	252	0.529	251	0.327	117	0.995	120	0.991	86	0.813	183	0.424	188	0.232	97	0.708	100	0.515	133	0.546	159	0.398	
14	ALLGOVISION-000	164	0.138	194	0.088	200	0.045	159	0.202	188	0.166	195	0.106	102	0.993	117	0.990	148	0.982	146	0.117	151	0.066					130	0.526	151	0.396	
15	ALLGOVISION-001	173	0.155	199	0.102	206	0.053	176	0.275	203	0.221	208	0.141	102	0.993	107	0.986	107	0.933	156	0.150	159	0.081					124	0.491	159	0.389	
16	ANKE-000	184	0.184	204	0.117	215	0.063	190	0.256	201	0.220	212	0.151	113	0.995	126	0.994	157	0.990	245	1.000	218	1.000					200	1.000	256	1.000	
17	ANKE-001	182	0.183	208	0.119	216	0.063	189	0.256	202	0.220	213	0.151	119	0.995	132	0.994	167	0.992	231	1.000	259	1.000					232	1.000	299	1.000	
18	ANKE-002	108	0.062	123	0.032	125	0.014	104	0.103	110	0.079	112	0.050	71	0.975	72	0.948	81	0.795	91	0.034	94	0.018					71	0.245	92	0.190	
19	AWARE-003	181	0.174	212	0.128	221	0.082	21	0.351	222	0.298	233	0.204	89	0.987	104	0.984	147	0.977	184	0.428	188	0.378					131	0.530	157	0.443	
20	AWARE-004	229	0.355	243	0.269	252	0.175	240	0.619	251	0.509	255	0.375	187	1.000	191	1.000	212	0.999	179	0.397	184	0.279					157	0.816	170	0.631	
21	AWARE-005	254	0.608	253	0.364	228	0.085	26	0.342	21	0.253	217	0.163	183	1.000	196	1.000	21	0.999	171	0.255	174	0.122					172	0.916	177	0.714	
22	AWARE-006	242	0.475	244	0.276	253	0.175	230	0.466	239	0.398	244	0.283	168	1.000	184	0.999	205	0.999	177	0.368	181	0.254					149	0.749	167	0.623	
23	AYONIX-000	269	0.846	276	0.811	28	0.724	26	0.956	276	0.939	278	0.892	144	0.998	153	0.998	18	0.995	204	0.954	20	0.891					186	0.982	196	0.959	
24	AYONIX-001	270	0.875	278	0.824	280	0.701	261	0.946	271	0.920	274	0.845	180	1.000	182	0.999	188	0.996	208	0.999	208	0.998					183	0.969	192	0.926	
25	AYONIX-002	271	0.876	277	0.824	281	0.702	262	0.946	272	0.920	273	0.845	181	1.000	181	0.999	189	0.996	201	0.915	200	0.821					182	0.969	193	0.926	
26	CAMVI-003	133	0.094	177	0.071	211	0.058	148	0.152	164	0.132	196	0.108	77	0.979	82	0.970	111	0.940	145	0.114	167	0.100					107	0.402	147	0.377	
27	CAMVI-004	142	0.107	178	0.072	209	0.054	156	0.240	166	0.136	185	0.100	169	1.000	177	0.999	195	0.998	142	0.100	158	0.081					153	0.787	161	0.507	
28	CAMVI-005	165	0.139	198	0.099	227	0.076	19	0.451	179	0.179	203	0.132	176	1.000	187	1.000	207	0.998	157	0.156	177	0.112					194	0.999	205	0.983	
29	CANON-001	27	0.012	33	0.005	33	0.021	23	0.031	23	0.015	26	0.033	17	0.365	25	0.217	21	0.008	23	0.004	24	0.068	27	0.034	30	0.139	21	0.092			
30	CANON-002	19	0.010	27	0.005	29	0.002	28	0.034	31	0.027	38	0.020	66	0.956	73	0.952	117	0.947	127	0.064	148	0.056	105	0.542	168	0.881	191	0.878			
31	CIB-000	78	0.044	59	0.012	54	0.005	75	0.077	57	0.045	53	0.025	208	1.000	207	1.000	221	1.000	51	0.017	43	0.008	43	0.141	43	0.068	169	0.894	162	0.521	
32	CLEARVIEWAI-000	29	0.013	35	0.006	31	0.002	30	0.036	27	0.025	27	0.016	156	0.999	87	0.974	13	0.149	22	0.008	17	0.004	19	0.057	16	0.027	82	0.268	12	0.080	
33	CLOUDWALK-HR-000	8	0.004	10	0.002	14	0.002	8	0.015	10	0.013	13	0.012	2	0.188	2	0.133	4	0.095	11	0.005	11	0.003	7	0.033	10	0.018	12	0.099	7	0.075	
34	CLOUDWALK-MT-000	4	0.003	9	0.002	17	0.002	5	0.015	9	0.013	15	0.012	10	0.169	10	0.109	1	0.077	1	0.002	3	0.002	1	0.018	1	0.009	1	0.072	3	0.063	
35	COGENT-000	169	0.143	152	0.053	171	0.029	159	0.175	169	0.140	187	0.100	123	0.996	137	0.995	163	0.991													
36	COGENT-001	168	0.143	153	0.053	172	0.029	160	0.175	168	0.140	188	0.100	124	0.996	138	0.995	167	0.991													
37	COGENT-002	179	0.159	139	0.044	135	0.017	123	0.124	135	0.098	139	0.063	148	0.																	

MISSES BELOW THRESHOLD, T		ENROL RECENT MUGSHOT, N = 1.6M												ENROL APPLICATION PORTRAIT, N = 1.6M																		
		ENROL: MUGSHOT				ENROL: MUGSHOT				ENROL: MUGSHOT				ENROL: VISA				ENROL: BORDER		ENROL: BORDER 10+YR		ENROL: KIOSK										
#	ALGORITHM	FPIR=0.0003	FPIR=0.001	FPIR=0.01	FPIR=0.0003	FPIR=0.001	FPIR=0.01	FPIR=0.0003	FPIR=0.001	FPIR=0.01	FPIR=0.0003	FPIR=0.001	FPIR=0.01	FPIR=0.001	FPIR=0.01	FPIR=0.001	FPIR=0.01	FPIR=0.001	FPIR=0.01	FPIR=0.001	FPIR=0.01	FPIR=0.001	FPIR=0.01	FPIR=0.001	FPIR=0.01							
47	COGNITEC-005	10 <sup>2</sup>	0.055	40 <sup>1</sup>	0.010	43 <sup>1</sup>	0.004	50 <sup>1</sup>	0.058	53 <sup>1</sup>	0.041	41 <sup>1</sup>	0.022	253 <sup>1</sup>	1.000	271 <sup>1</sup>	1.000	96 <sup>1</sup>	0.878	10 <sup>1</sup>	0.041	11 <sup>1</sup>	0.028	5 <sup>1</sup>	0.157	61 <sup>1</sup>	0.092	5 <sup>1</sup>	0.179	63 <sup>1</sup>	0.145	
48	COGNITEC-006	56 <sup>1</sup>	0.029	41 <sup>1</sup>	0.008	40 <sup>1</sup>	0.003	56 <sup>1</sup>	0.065	49 <sup>1</sup>	0.040	42 <sup>1</sup>	0.022	227 <sup>1</sup>	1.000	286 <sup>1</sup>	1.000	206 <sup>1</sup>	0.999	79 <sup>1</sup>	0.030	74 <sup>1</sup>	0.013	58 <sup>1</sup>	0.171	54 <sup>1</sup>	0.081	14 <sup>1</sup>	0.681	102 <sup>1</sup>	0.214	
49	CUBOX-000	1 <sup>1</sup>	0.005	16 <sup>1</sup>	0.003	19 <sup>1</sup>	0.002	17 <sup>1</sup>	0.022	17 <sup>1</sup>	0.019	19 <sup>1</sup>	0.014	6 <sup>1</sup>	0.276	41 <sup>1</sup>	0.168	7 <sup>1</sup>	0.104	7 <sup>1</sup>	0.004	8 <sup>1</sup>	0.003	6 <sup>1</sup>	0.028	6 <sup>1</sup>	0.014	3 <sup>1</sup>	0.073	2 <sup>1</sup>	0.062	
50	CYBERLINK-000	163 <sup>1</sup>	0.137	163 <sup>1</sup>	0.056	153 <sup>1</sup>	0.023	154 <sup>1</sup>	0.162	149 <sup>1</sup>	0.116	151 <sup>1</sup>	0.070	136 <sup>1</sup>	0.997	141 <sup>1</sup>	0.995	142 <sup>1</sup>	0.981	126 <sup>1</sup>	0.063	124 <sup>1</sup>	0.032					98 <sup>1</sup>	0.339	112 <sup>1</sup>	0.232	
51	CYBERLINK-001	13 <sup>1</sup>	0.096	156 <sup>1</sup>	0.054	151 <sup>1</sup>	0.022	141 <sup>1</sup>	0.138	146 <sup>1</sup>	0.109	144 <sup>1</sup>	0.067	134 <sup>1</sup>	0.997	136 <sup>1</sup>	0.995	150 <sup>1</sup>	0.984	12 <sup>1</sup>	0.062	120 <sup>1</sup>	0.031					14 <sup>1</sup>	0.652	114 <sup>1</sup>	0.239	
52	CYBERLINK-002	70 <sup>1</sup>	0.038	69 <sup>1</sup>	0.015	69 <sup>1</sup>	0.006	65 <sup>1</sup>	0.068	72 <sup>1</sup>	0.053	71 <sup>1</sup>	0.032	109 <sup>1</sup>	0.994	112 <sup>1</sup>	0.988	126 <sup>1</sup>	0.957	67 <sup>1</sup>	0.024	68 <sup>1</sup>	0.013					85 <sup>1</sup>	0.288	72 <sup>1</sup>	0.157	
53	CYBERLINK-003	8 <sup>1</sup>	0.045	4 <sup>1</sup>	0.008	42 <sup>1</sup>	0.004	38 <sup>1</sup>	0.045	43 <sup>1</sup>	0.035	40 <sup>1</sup>	0.021	110 <sup>1</sup>	0.995	28 <sup>1</sup>	0.972	90 <sup>1</sup>	0.845	40 <sup>1</sup>	0.012	41 <sup>1</sup>	0.007	34 <sup>1</sup>	0.100	36 <sup>1</sup>	0.051	10 <sup>1</sup>	0.368	42 <sup>1</sup>	0.126	
54	CYBERLINK-004	192 <sup>1</sup>	0.188	39 <sup>1</sup>	0.007	39 <sup>1</sup>	0.003	54 <sup>1</sup>	0.063	44 <sup>1</sup>	0.036	44 <sup>1</sup>	0.022	220 <sup>1</sup>	1.000	224 <sup>1</sup>	1.000	214 <sup>1</sup>	0.999	42 <sup>1</sup>	0.013	40 <sup>1</sup>	0.007	35 <sup>1</sup>	0.109	34 <sup>1</sup>	0.050	181 <sup>1</sup>	0.954	131 <sup>1</sup>	0.291	
55	CYBERLINK-005	19 <sup>1</sup>	0.208	50 <sup>1</sup>	0.010	48 <sup>1</sup>	0.004	45 <sup>1</sup>	0.054	50 <sup>1</sup>	0.041	55 <sup>1</sup>	0.026	194 <sup>1</sup>	1.000	193 <sup>1</sup>	1.000	97 <sup>1</sup>	0.888	43 <sup>1</sup>	0.014	42 <sup>1</sup>	0.007	30 <sup>1</sup>	0.089	31 <sup>1</sup>	0.043	17 <sup>1</sup>	0.926	122 <sup>1</sup>	0.266	
56	DAHUA-000	15 <sup>1</sup>	0.128	19 <sup>1</sup>	0.086	19 <sup>1</sup>	0.045	163 <sup>1</sup>	0.179	165 <sup>1</sup>	0.135	169 <sup>1</sup>	0.083																			
57	DAHUA-001	14 <sup>1</sup>	0.106	18 <sup>1</sup>	0.073	184 <sup>1</sup>	0.037	147 <sup>1</sup>	0.151	157 <sup>1</sup>	0.122	160 <sup>1</sup>	0.075	91 <sup>1</sup>	0.987	97 <sup>1</sup>	0.980	108 <sup>1</sup>	0.933													
58	DAHUA-002	36 <sup>1</sup>	0.026	70 <sup>1</sup>	0.015	67 <sup>1</sup>	0.006	51 <sup>1</sup>	0.060	59 <sup>1</sup>	0.046	60 <sup>1</sup>	0.029	31 <sup>1</sup>	0.681	37 <sup>1</sup>	0.638	51 <sup>1</sup>	0.522	48 <sup>1</sup>	0.017	47 <sup>1</sup>	0.008					42 <sup>1</sup>	0.159	46 <sup>1</sup>	0.125	
59	DAHUA-003	42 <sup>1</sup>	0.025	64 <sup>1</sup>	0.014	58 <sup>1</sup>	0.005	44 <sup>1</sup>	0.054	52 <sup>1</sup>	0.041	51 <sup>1</sup>	0.024	27 <sup>1</sup>	0.647	32 <sup>1</sup>	0.579	42 <sup>1</sup>	0.447	41 <sup>1</sup>	0.013	39 <sup>1</sup>	0.006	28 <sup>1</sup>	0.081	32 <sup>1</sup>	0.043	29 <sup>1</sup>	0.134	31 <sup>1</sup>	0.098	
60	DAHUA-004	31 <sup>1</sup>	0.014	38 <sup>1</sup>	0.007	38 <sup>1</sup>	0.003	27 <sup>1</sup>	0.033	29 <sup>1</sup>	0.026	28 <sup>1</sup>	0.016	18 <sup>1</sup>	0.552	26 <sup>1</sup>	0.485	34 <sup>1</sup>	0.345	28 <sup>1</sup>	0.008	26 <sup>1</sup>	0.004	15 <sup>1</sup>	0.051	17 <sup>1</sup>	0.027	22 <sup>1</sup>	0.113	24 <sup>1</sup>	0.094	
61	DAO-N-000	161 <sup>1</sup>	0.135	98 <sup>1</sup>	0.023	96 <sup>1</sup>	0.009	79 <sup>1</sup>	0.079	83 <sup>1</sup>	0.061	88 <sup>1</sup>	0.039	190 <sup>1</sup>	1.000	194 <sup>1</sup>	1.000	201 <sup>1</sup>	0.998	68 <sup>1</sup>	0.025	69 <sup>1</sup>	0.013	60 <sup>1</sup>	0.173	60 <sup>1</sup>	0.091	164 <sup>1</sup>	0.846	80 <sup>1</sup>	0.172	
62	DECATUR-000	7 <sup>1</sup>	0.043	101 <sup>1</sup>	0.023	101 <sup>1</sup>	0.010	84 <sup>1</sup>	0.085	91 <sup>1</sup>	0.066	90 <sup>1</sup>	0.040	34 <sup>1</sup>	0.757	42 <sup>1</sup>	0.675	47 <sup>1</sup>	0.509	72 <sup>1</sup>	0.027	78 <sup>1</sup>	0.014	59 <sup>1</sup>	0.173	67 <sup>1</sup>	0.098	60 <sup>1</sup>	0.239	70 <sup>1</sup>	0.156	
63	DEEPLINKL-001	21 <sup>1</sup>	0.101	20 <sup>1</sup>	0.003	20 <sup>1</sup>	0.002	11 <sup>1</sup>	0.018	11 <sup>1</sup>	0.014	8 <sup>1</sup>	0.010	209 <sup>1</sup>	1.000	185 <sup>1</sup>	1.000	46 <sup>1</sup>	0.503	16 <sup>1</sup>	0.006	25 <sup>1</sup>	0.004					41 <sup>1</sup>	0.159	25 <sup>1</sup>	0.097	
64	DEEPSA-001	120 <sup>1</sup>	0.073	143 <sup>1</sup>	0.046	149 <sup>1</sup>	0.022	130 <sup>1</sup>	0.129	137 <sup>1</sup>	0.101	131 <sup>1</sup>	0.059	95 <sup>1</sup>	0.988	105 <sup>1</sup>	0.985	137 <sup>1</sup>	0.973	134 <sup>1</sup>	0.077	133 <sup>1</sup>	0.041					95 <sup>1</sup>	0.326	117 <sup>1</sup>	0.251	
65	DERMALOG-003	250 <sup>1</sup>	0.550	262 <sup>1</sup>	0.482	269 <sup>1</sup>	0.360	251 <sup>1</sup>	0.715	262 <sup>1</sup>	0.655	266 <sup>1</sup>	0.526							198 <sup>1</sup>	0.677	196 <sup>1</sup>	0.554					16 <sup>1</sup>	0.870	185 <sup>1</sup>	0.791	
66	DERMALOG-004	252 <sup>1</sup>	0.554	264 <sup>1</sup>	0.480	268 <sup>1</sup>	0.358	250 <sup>1</sup>	0.711	263 <sup>1</sup>	0.657	264 <sup>1</sup>	0.526	128 <sup>1</sup>	0.997	142 <sup>1</sup>	0.995	167 <sup>1</sup>	0.991	193 <sup>1</sup>	0.603	195 <sup>1</sup>	0.458					16 <sup>1</sup>	0.856	181 <sup>1</sup>	0.751	
67	DERMALOG-005	193 <sup>1</sup>	0.189	193 <sup>1</sup>	0.088	192 <sup>1</sup>	0.043	175 <sup>1</sup>	0.201	179 <sup>1</sup>	0.154	182 <sup>1</sup>	0.096	125 <sup>1</sup>	0.996	116 <sup>1</sup>	0.990	120 <sup>1</sup>	0.950	174 <sup>1</sup>	0.300	183 <sup>1</sup>	0.267					16 <sup>1</sup>	0.614	155 <sup>1</sup>	0.459	
68	DERMALOG-006	13 <sup>1</sup>	0.098	150 <sup>1</sup>	0.052	165 <sup>1</sup>	0.026	140 <sup>1</sup>	0.137	140 <sup>1</sup>	0.105	143 <sup>1</sup>	0.067	96 <sup>1</sup>	0.989	99 <sup>1</sup>	0.981	105 <sup>1</sup>	0.933	121 <sup>1</sup>	0.059	122 <sup>1</sup>	0.020					9 <sup>1</sup>	0.318	110 <sup>1</sup>	0.230	
69	DERMALOG-007	19 <sup>1</sup>	0.188	191 <sup>1</sup>	0.086	190 <sup>1</sup>	0.040	174 <sup>1</sup>	0.200	177 <sup>1</sup>	0.152	179 <sup>1</sup>	0.093	126 <sup>1</sup>	0.996	115 <sup>1</sup>	0.990	119 <sup>1</sup>	0.950	141 <sup>1</sup>	0.099	143 <sup>1</sup>	0.052					135 <sup>1</sup>	0.557	135 <sup>1</sup>	0.299	
70	DERMALOG-008	21 <sup>1</sup>	0.268	14 <sup>1</sup>	0.045	132 <sup>1</sup>	0.017	184 <sup>1</sup>	0.231	126 <sup>1</sup>	0.094	122 <sup>1</sup>	0.054	210 <sup>1</sup>	1.000	216 <sup>1</sup>	1.000	222 <sup>1</sup>	1.000	118 <sup>1</sup>	0.057	111 <sup>1</sup>	0.025	88 <sup>1</sup>	0.382	86 <sup>1</sup>	0.158	17 <sup>1</sup>	0.940	173 <sup>1</sup>	0.678	
71	DERMALOG-009	74 <sup>1</sup>	0.041	91 <sup>1</sup>	0.021	93 <sup>1</sup>	0.009	86 <sup>1</sup>	0.086	92 <sup>1</sup>	0.066	93 <sup>1</sup>	0.040	195 <sup>1</sup>	1.000	204 <sup>1</sup>	1.000	219 <sup>1</sup>	1.000	81 <sup>1</sup>	0.031	85 <sup>1</sup>	0.016	106 <sup>1</sup>	0.999	108 <sup>1</sup>	0.098	162 <sup>1</sup>	0.840	106 <sup>1</sup>	0.222	
72	DIGIDATA-000	25 <sup>1</sup>	0.620	27 <sup>1</sup>	0.610	278 <sup>1</sup>	0.598	238 <sup>1</sup>	0.588	256 <sup>1</sup>	0.577	267 <sup>1</sup>	0.560	158 <sup>1</sup>	0.999	130 <sup>1</sup>	0.994	115 <sup>1</sup>	0.942	196 <sup>1</sup>	0.646	198 <sup>1</sup>	0.643	102 <sup>1</sup>	0.789	106 <sup>1</sup>	0.722	160 <sup>1</sup>	0.824	187 <sup>1</sup>	0.816	
73	DILUSENSE-000	96 <sup>1</sup>	0.053	120 <sup>1</sup>	0.030	118 <sup>1</sup>	0.012	109 <sup>1</sup>	0.100	109 <sup>1</sup>	0.078	109 <sup>1</sup>	0.047	45 <sup>1</sup>	0.852	38 <sup>1</sup>	0.655	44 <sup>1</sup>	0.488	98 <sup>1</sup>	0.039	106 <sup>1</sup>	0.022	96 <sup>1</sup>	0.664	93 <sup>1</sup>	0.242	60 <sup>1</sup>	0.203	69 <sup>1</sup>	0.154	
74	EYEDEA-003	24 <sup>1</sup>	0.509	25 <sup>1</sup>	0.388	261 <sup>1</sup>	0.265	242 <sup>1</sup>	0.625	254 <sup>1</sup>	0.543	256 <sup>1</sup>	0.404	127 <sup>1</sup>	0.997	133 <sup>1</sup>	0.994	156 <sup>1</sup>	0.990	191 <sup>1</sup>	0.570	196 <sup>1</sup>	0.392					15 <sup>1</sup>	0.792	172 <sup>1</sup>	0.658	
75	F8-001	29 <sup>1</sup>	0.458	226 <sup>1</sup>	0.166	181 <sup>1</sup>	0.036							155 <sup>1</sup>	0.999	162 <sup>1</sup>	0.998	186 <sup>1</sup>	0.995													
76	FINCORE-000	18 <sup>1</sup>	0.187	216 <sup>1</sup>	0.134	222 <sup>1</sup>	0.071	195 <sup>1</sup>	0.267	200 <sup>1</sup>	0.217	206 <sup>1</sup>	0.140	185 <sup>1</sup>	1.000	198 <sup>1</sup>	1.000	179 <sup>1</sup>	1.000	163 <sup>1</sup>	0.187	169 <sup>1</sup>	0.108	95 <sup>1</sup>	0.598	99 <sup>1</sup>	0.418	117 <sup>1</sup>	0.458	140 <sup>1</sup>	0.349	
77	FUJITSULAB-000	20 <sup>1</sup>	0.246	92 <sup>1</sup>	0.021	89 <sup>1</sup>	0.008	68 <sup>1</sup>	0.070	78 <sup>1</sup>	0.056	81 <sup>1</sup>	0.035							65 <sup>1</sup>	0.024	73 <sup>1</sup>	0.013	61 <sup>1</sup>	0.177	65 <sup>1</sup>	0.093	70 <sup>1</sup>	0.240	71 <sup>1</sup>	0.156	
78	FUJITSULAB-001</td																															

Table 30: **Threshold-based accuracy.** Values are FNIR( $N, T, L$ ) with  $N = 1.6$  million with thresholds set to produce FPIR = 0.0003, 0.001, and 0.01 in non-mate searches. Throughout blue superscripts indicate the rank of the algorithm for that column. Caution: The Power-low models are mostly intended to draw attention to the kind of behavior, not as a model to be used for prediction.

2022/06/13  
09:55:40

FNIK(N, k,  
FPIR(N,

False neg. identification rate  
False pos. identification rate

N = Num. enrolled subjects  
 R = Num. candidates examined

$\equiv$  threshold

$T \geq 0 \rightarrow$  Identification

MISSSES BELOW THRESHOLD, T		ENROL RECENT MUGSHOT, N = 1.6M												ENROL APPLICATION PORTRAIT, N = 1.6M													
#	ALGORITHM	ENROL: MUGSHOT			ENROL: MUGSHOT			PROBE: WEBCAM			ENROL: MUGSHOT			PROBE: PROFILE			ENROL: VISA		ENROL: BORDER		ENROL: BORDER 1+YR		ENROL: KIOSK				
		FPIR=0.0003	FPIR=0.001	FPIR=0.01	FPIR=0.0003	FPIR=0.001	FPIR=0.01	FPIR=0.0003	FPIR=0.001	FPIR=0.01	FPIR=0.0003	FPIR=0.001	FPIR=0.01	FPIR=0.0003	FPIR=0.001	FPIR=0.01	FPIR=0.001	FPIR=0.01	FPIR=0.001	FPIR=0.01	FPIR=0.001	FPIR=0.01	FPIR=0.001	FPIR=0.01			
93	HYPERVERGE-001	18.009	25.004	28.002	34.039	39.031	39.020	5.0275	9.220	12.146	19.007	22.004	17.053	20.027	15.101	13.083	15.101	13.083	15.101	13.083	15.101	13.083	15.101	13.083			
94	HYPERVERGE-002	17.008	21.004	22.002	29.034	30.027	33.018	8.0278	8.0210	8.0131	13.006	16.003	14.048	16.023	9.093	7.077	9.093	7.077	9.093	7.077	9.093	7.077	9.093	7.077	9.093	7.077	
95	HZAILU-000	65.035	88.020	92.009	64.064	65.051	65.031	83.0983	29.0967	87.0813	57.020	53.010	81.0316	50.077	36.153	48.120	151.766	168.630	151.766	168.630	151.766	168.630	151.766	168.630	151.766	168.630	
96	IDEMIA-003	251.552	146.047	144.021	288.1000	187.0165	164.079	278.1000	147.0000	274.0976	86.0973	128.0968	148.0123	144.061	152.766	168.630	167.879	179.743	167.879	179.743	167.879	179.743	167.879	179.743	167.879	179.743	
97	IDEMIA-004	100.055	132.037	143.021	144.0144	151.0118	163.079	74.0976	86.0973	128.0968	148.0123	144.061	149.0130	153.070	152.733	168.531	167.733	168.531	167.733	168.531	167.733	168.531	167.733	168.531	167.733	168.531	
98	IDEMIA-005	115.066	138.044	164.026	165.0181	176.0150	193.0102	78.0979	92.0978	135.0973	149.0130	153.070	152.036	168.0109	152.036	152.036	168.0109	152.036	152.036	168.0109	152.036	152.036	168.0109	152.036	152.036	168.0109	
99	IDEMIA-006	113.065	135.043	162.025	194.0266	209.0226	216.0161	88.0984	101.0982	146.0980	135.0144	161.0090	152.036	152.036	168.0109	152.036	152.036	168.0109	152.036	152.036	168.0109	152.036	152.036	168.0109	152.036	152.036	
100	IDEMIA-007	66.035	81.018	84.008	73.073	73.055	74.0033	283.1000	234.1000	268.1000	113.0052	108.0022	63.0182	71.109	239.1000	208.982	152.036	152.036	152.036	152.036	152.036	152.036	152.036	152.036	152.036	152.036	152.036
101	IDEMIA-008	6.004	8.002	9.001	10.016	10.013	9.009	7.0276	7.0204	8.0136	10.0005	9.0003	11.036	12.019	18.0106	20.0092	152.036	152.036	152.036	152.036	152.036	152.036	152.036	152.036	152.036	152.036	152.036
102	IDEMIA-009	5.004	2.002	3.001	4.012	4.011	2.008	3.0202	3.0141	5.099	3.003	4.002	5.027	5.013	4.074	4.064	152.036	152.036	152.036	152.036	152.036	152.036	152.036	152.036	152.036	152.036	152.036
103	IMAGUS-002	274.908	274.749	276.564	264.944	268.816	270.645	207.1000	221.1000	229.1000	152.036	152.036	152.036	152.036	152.036	152.036	152.036	152.036	152.036	152.036	152.036	152.036	152.036	152.036	152.036		
104	IMAGUS-003	273.898	275.807	279.669	268.954	270.909	272.809	196.1000	207.1000	223.1000	152.036	152.036	152.036	152.036	152.036	152.036	152.036	152.036	152.036	152.036	152.036	152.036	152.036	152.036	152.036		
105	IMAGUS-005	63.034	83.018	85.008	87.088	91.066	91.040	55.0926	59.0838	66.0647	75.029	86.0116	55.0161	66.094	66.094	66.094	66.094	66.094	66.094	66.094	66.094	66.094	66.094	66.094	66.094	66.094	
106	IMAGUS-006	71.039	87.019	86.008	91.093	90.069	99.042	81.0980	67.0897	60.0621	74.028	80.015	54.0161	62.092	76.0260	88.0181	152.036	152.036	152.036	152.036	152.036	152.036	152.036	152.036	152.036	152.036	152.036
107	IMAGUS-007	76.044	100.023	108.010	97.100	102.073	103.045	69.0973	65.0893	65.0651	82.031	80.016	57.0169	66.098	81.265	88.0181	152.036	152.036	152.036	152.036	152.036	152.036	152.036	152.036	152.036	152.036	152.036
108	IMAGUS-008	283.995	283.974	278.523	268.058	268.774	245.285	177.1000	144.0996	229.0700	189.0520	150.0071	102.0000	102.0540	128.0518	115.0245	152.036	152.036	152.036	152.036	152.036	152.036	152.036	152.036	152.036	152.036	152.036
109	IMPERIAL-000	172.054	106.026	97.009	89.089	94.068	96.041	211.0000	166.0999	178.0995	102.0042	103.020	72.0245	77.0168	77.0168	77.0168	77.0168	77.0168	77.0168	77.0168	77.0168	77.0168	77.0168	77.0168	77.0168	77.0168	
110	INCODE-000	235.423	247.310	254.199	238.486	248.420	248.304	178.1000	158.0998	179.0994	152.036	152.036	152.036	152.036	152.036	152.036	152.036	152.036	152.036	152.036	152.036	152.036	152.036	152.036	152.036		
111	INCODE-001	224.319	236.212	241.112	212.348	228.296	229.198	216.1000	208.1000	220.1000	152.036	152.036	152.036	152.036	152.036	152.036	152.036	152.036	152.036	152.036	152.036	152.036	152.036	152.036	152.036		
112	INCODE-002	221.285	232.184	239.100	206.333	222.269	225.176	139.0998	124.0993	144.0976	152.036	152.036	152.036	152.036	152.036	152.036	152.036	152.036	152.036	152.036	152.036	152.036	152.036	152.036	152.036		
113	INCODE-003	222.286	228.167	222.084	216.372	219.264	219.164	186.1000	180.0999	190.0996	152.036	152.036	152.036	152.036	152.036	152.036	152.036	152.036	152.036	152.036	152.036	152.036	152.036	152.036	152.036		
114	INCODE-004	138.099	159.054	158.023	156.017	156.120	152.070	135.0997	134.0995	108.0929	125.063	121.031	90.016	90.0153	90.0153	90.0153	90.0153	90.0153	90.0153	90.0153	90.0153	90.0153	90.0153	90.0153	90.0153	90.0153	
115	INCODE-005	38.021	54.011	52.005	47.055	55.043	56.026	24.0614	28.0528	38.0372	50.017	50.009	46.145	47.073	47.073	47.073	47.073	47.073	47.073	47.073	47.073	47.073	47.073	47.073	47.073	47.073	
116	INNOVATRICS-002	233.379	241.234	249.139	230.403	230.310	235.209	217.1000	212.1000	219.0999	152.036	152.036	152.036	152.036	152.036	152.036	152.036	152.036	152.036	152.036	152.036	152.036	152.036	152.036	152.036		
117	INNOVATRICS-003	223.297	237.221	248.132	214.351	226.297	232.203	188.1000	190.1000	200.0998	152.036	152.036	152.036	152.036	152.036	152.036	152.036	152.036	152.036	152.036	152.036	152.036	152.036	152.036	152.036		
118	INNOVATRICS-004	187.184	214.132	224.074	192.262	204.222	210.149	87.0984	95.0980	134.0973	152.036	152.036	152.036	152.036	152.036	152.036	152.036	152.036	152.036	152.036	152.036	152.036	152.036	152.036	152.036		
119	INNOVATRICS-005	104.057	125.034	124.014	113.0114	121.089	118.052	49.0890	60.0846	77.0723	109.047	109.022	74.0251	87.0182	152.036	152.036	152.036	152.036	152.036	152.036	152.036	152.036	152.036	152.036	152.036	152.036	152.036
120	INNOVATRICS-007	43.024	60.013	59.005	57.065	65.051	67.032	41.0806	47.0743	56.0567	49.017	51.009	32.093	38.053	37.0154	44.0120	152.036	152.036	152.036	152.036	152.036	152.036	152.036	152.036	152.036	152.036	152.036
121	INTELLIVISION-001	246.508	245.029	251.158	229.0459	240.404	247.302	191.1000	197.1000	219.0999	152.036	152.036	152.036	152.036	152.036	152.036	152.036	152.036	152.036	152.036	152.036	152.036	152.036	152.036	152.036		
122	INTSYSMSU-000	284.099	286.998	289.0990	279.1000	281.0000	282.0998	182.1000	192.1000	196.0998	207.0999	207.0989	152.036	152.036	152.036	152.036	152.036	152.036	152.036	152.036	152.036	152.036	152.036	152.036	152.036	152.036	
123	IREX-000	117.068	117.028	83.008	98.099	84.060	69.032	94.0988	74.0957	71.0680	105.044	60.0111	80.0302	40.062	47.0170	45.0130	50.0364	288.0988	152.036	152.036	152.036	152.036	152.036	152.036	152.036	152.036	
124	ISYSTEMS-002	174.155	184.078	177.032	152.161	160.126	166.080	146.0998	151.0998	170.0993	152.036	152.036	152.036	152.036	152.036	152.036	152.036	152.036	152.036	152.036	152.036	152.036	152.036	152.036	152.036		
125	ISYSTEMS-003	197.204	168.059	158.024	137.0135	144.0107	146.0668	193.1000	195.1000	199.0997	152.036	152.036	152.036	152.036	152.036	152.036	152.036	152.036	152.036	152.036	152.036	152.036	152.036	152.036	152.036		
126	KAKAO-000	54.028	72.015	71.006	71.071	77.056	79.034	17.0539	23.0468	33.0327	54.019	52.010	42.141	48.075	40.0158	43.0120	41.0183	40.0158	43.0120								

**Table 31: Threshold-based accuracy.** Values are  $FNIR(N, T, L)$  with  $N = 1.6$  million with thresholds set to produce  $FPIR = 0.0003, 0.001$ , and  $0.01$  in non-mate searches. Throughout blue superscripts indicate the rank of the algorithm for that column. Caution: The Power-low models are mostly intended to draw attention to the kind of behavior, not as a model to be used for prediction.

2022/06/13  
09:55:40

$FNIR(N, R, I) =$  False neg. identification rate  
 $FPIR(N, T) =$  False pos. identification rate

N = Num. enrolled subjects  
R = Num. candidates examined

1 = Threshold

$T \geq 0 \rightarrow$  Investigation  
 $T > 0 \rightarrow$  Identification

MISSES BELOW THRESHOLD, T		ENROL RECENT MUGSHOT, N = 1.6M												ENROL APPLICATION PORTRAIT, N = 1.6M							
		ENROL: MUGSHOT			ENROL: MUGSHOT			ENROL: PROFILE			ENROL: VISA		ENROL: BORDER		ENROL: KIOSK						
#	ALGORITHM	FPIR=0.0003	FPIR=0.001	FPIR=0.01	FPIR=0.0003	FPIR=0.001	FPIR=0.01	FPIR=0.0003	FPIR=0.001	FPIR=0.01	FPIR=0.001	FPIR=0.01	FPIR=0.001	FPIR=0.01	FPIR=0.001	FPIR=0.01	FPIR=0.001	FPIR=0.01	FPIR=0.001	FPIR=0.01	
139	MICROFOCUS-004	<sup>286</sup> 0.999	<sup>287</sup> 0.999	<sup>29</sup> 0.999	<sup>27</sup> 0.984	<sup>27</sup> 0.975	<sup>29</sup> 0.940				<sup>205</sup> 0.974	<sup>205</sup> 0.935					<sup>188</sup> 0.989	<sup>198</sup> 0.976			
140	MICROFOCUS-005	<sup>272</sup> 0.883	<sup>29</sup> 0.835	<sup>283</sup> 0.736	<sup>264</sup> 0.951	<sup>274</sup> 0.928	<sup>27</sup> 0.865				<sup>203</sup> 0.935	<sup>203</sup> 0.848					<sup>187</sup> 0.985	<sup>197</sup> 0.965			
141	MICROFOCUS-006	<sup>281</sup> 0.983	<sup>284</sup> 0.978	<sup>286</sup> 0.963	<sup>265</sup> 0.950	<sup>277</sup> 0.923	<sup>275</sup> 0.858				<sup>202</sup> 0.923	<sup>201</sup> 0.843					<sup>184</sup> 0.971	<sup>194</sup> 0.939			
142	MICROSOFT-003	<sup>90</sup> 0.049	<sup>115</sup> 0.028	<sup>113</sup> 0.012	<sup>114</sup> 0.117	<sup>124</sup> 0.091	<sup>127</sup> 0.056				<sup>94</sup> 0.036	<sup>100</sup> 0.019					<sup>68</sup> 0.233	<sup>82</sup> 0.176			
143	MICROSOFT-004	<sup>85</sup> 0.046	<sup>107</sup> 0.026	<sup>107</sup> 0.011	<sup>110</sup> 0.111	<sup>115</sup> 0.087	<sup>121</sup> 0.053				<sup>89</sup> 0.033	<sup>95</sup> 0.018					<sup>61</sup> 0.222	<sup>79</sup> 0.170			
144	MICROSOFT-005	<sup>87</sup> 0.047	<sup>104</sup> 0.026	<sup>104</sup> 0.010	<sup>90</sup> 0.090	<sup>98</sup> 0.070	<sup>97</sup> 0.041	<sup>164</sup> 0.999	<sup>33</sup> 0.587	<sup>38</sup> 0.354	<sup>70</sup> 0.027	<sup>72</sup> 0.013					<sup>53</sup> 0.180	<sup>54</sup> 0.134			
145	MICROSOFT-006	<sup>47</sup> 0.025	<sup>55</sup> 0.012	<sup>66</sup> 0.006	<sup>41</sup> 0.048	<sup>45</sup> 0.037	<sup>52</sup> 0.024	<sup>14</sup> 0.452	<sup>18</sup> 0.386	<sup>27</sup> 0.281	<sup>85</sup> 0.032	<sup>81</sup> 0.015					<sup>49</sup> 0.178	<sup>56</sup> 0.138			
146	NEC-000	<sup>147</sup> 0.113	<sup>186</sup> 0.079	<sup>201</sup> 0.047	<sup>157</sup> 0.171	<sup>170</sup> 0.140	<sup>177</sup> 0.093	<sup>84</sup> 0.983	<sup>94</sup> 0.979	<sup>131</sup> 0.969							<sup>121</sup> 0.474	<sup>148</sup> 0.377			
147	NEC-001	<sup>171</sup> 0.148	<sup>203</sup> 0.106	<sup>214</sup> 0.060	<sup>189</sup> 0.238	<sup>197</sup> 0.197	<sup>204</sup> 0.133	<sup>98</sup> 0.991	<sup>109</sup> 0.986	<sup>133</sup> 0.972	<sup>150</sup> 0.133	<sup>160</sup> 0.082					<sup>124</sup> 0.468	<sup>149</sup> 0.378			
148	NEC-002	<sup>34</sup> 0.018	<sup>14</sup> 0.003	<sup>12</sup> 0.002	<sup>22</sup> 0.029	<sup>20</sup> 0.020	<sup>17</sup> 0.013	<sup>171</sup> 1.000	<sup>178</sup> 0.999	<sup>180</sup> 0.995	<sup>24</sup> 0.008	<sup>35</sup> 0.005					<sup>143</sup> 0.676	<sup>132</sup> 0.292			
149	NEC-003	<sup>10</sup> 0.005	<sup>12</sup> 0.002	<sup>16</sup> 0.002	<sup>16</sup> 0.021	<sup>16</sup> 0.017	<sup>16</sup> 0.013	<sup>51</sup> 0.902	<sup>56</sup> 0.824	<sup>62</sup> 0.628	<sup>27</sup> 0.008	<sup>36</sup> 0.006	<sup>12</sup> 0.036	<sup>13</sup> 0.023			<sup>14</sup> 0.668	<sup>120</sup> 0.261			
150	NEC-004	<sup>1</sup> 0.003	<sup>3</sup> 0.002	<sup>11</sup> 0.002	<sup>7</sup> 0.015	<sup>7</sup> 0.013	<sup>10</sup> 0.010	<sup>28</sup> 0.654	<sup>36</sup> 0.622	<sup>50</sup> 0.575	<sup>8</sup> 0.004	<sup>15</sup> 0.004	<sup>1</sup> 0.019	<sup>4</sup> 0.012			<sup>14</sup> 0.100	<sup>16</sup> 0.088			
151	NEC-005	<sup>15</sup> 0.007	<sup>3</sup> 0.002	<sup>8</sup> 0.001	<sup>3</sup> 0.014	<sup>3</sup> 0.012	<sup>6</sup> 0.009	<sup>50</sup> 0.901	<sup>41</sup> 0.673	<sup>20</sup> 0.177	<sup>5</sup> 0.003	<sup>6</sup> 0.002	<sup>7</sup> 0.019	<sup>2</sup> 0.011			<sup>11</sup> 0.099	<sup>15</sup> 0.087			
152	NEUROTECHNOLOGY-003	<sup>285</sup> 0.999	<sup>272</sup> 0.636	<sup>239</sup> 0.099	<sup>254</sup> 0.773	<sup>221</sup> 0.266	<sup>218</sup> 0.164	<sup>228</sup> 1.000	<sup>289</sup> 1.000	<sup>261</sup> 1.000											
153	NEUROTECHNOLOGY-004	<sup>149</sup> 0.120	<sup>173</sup> 0.063	<sup>169</sup> 0.028	<sup>144</sup> 0.146	<sup>150</sup> 0.117	<sup>154</sup> 0.073	<sup>127</sup> 0.996	<sup>129</sup> 0.994	<sup>158</sup> 0.990											
154	NEUROTECHNOLOGY-005	<sup>148</sup> 0.117	<sup>160</sup> 0.054	<sup>150</sup> 0.022	<sup>188</sup> 0.252	<sup>167</sup> 0.130	<sup>157</sup> 0.074	<sup>152</sup> 0.999	<sup>154</sup> 0.998	<sup>155</sup> 0.989											
155	NEUROTECHNOLOGY-006	<sup>282</sup> 0.987	<sup>242</sup> 0.249	<sup>243</sup> 0.121	<sup>285</sup> 1.000	<sup>241</sup> 0.418	<sup>234</sup> 0.206														
156	NEUROTECHNOLOGY-007	<sup>211</sup> 0.252	<sup>172</sup> 0.062	<sup>147</sup> 0.021	<sup>276</sup> 0.996	<sup>197</sup> 0.173	<sup>145</sup> 0.068	<sup>201</sup> 1.000	<sup>201</sup> 1.000	<sup>193</sup> 0.997	<sup>176</sup> 0.339	<sup>128</sup> 0.036					<sup>280</sup> 1.000	<sup>205</sup> 0.989			
157	NEUROTECHNOLOGY-008	<sup>265</sup> 0.797	<sup>154</sup> 0.053	<sup>117</sup> 0.012	<sup>108</sup> 0.110	<sup>112</sup> 0.080	<sup>108</sup> 0.047	<sup>205</sup> 1.000	<sup>219</sup> 1.000	<sup>230</sup> 1.000	<sup>95</sup> 0.035	<sup>91</sup> 0.017	<sup>79</sup> 0.293	<sup>82</sup> 0.149	<sup>50</sup> 0.203	<sup>67</sup> 0.152					
158	NEUROTECHNOLOGY-009	<sup>51</sup> 0.027	<sup>73</sup> 0.015	<sup>63</sup> 0.006	<sup>60</sup> 0.066	<sup>67</sup> 0.052	<sup>68</sup> 0.032	<sup>29</sup> 0.661	<sup>34</sup> 0.588	<sup>41</sup> 0.436	<sup>56</sup> 0.020	<sup>55</sup> 0.010	<sup>41</sup> 0.165	<sup>51</sup> 0.153	<sup>57</sup> 0.082	<sup>44</sup> 0.165	<sup>50</sup> 0.129				
159	NEUROTECHNOLOGY-010	<sup>226</sup> 0.346	<sup>49</sup> 0.010	<sup>41</sup> 0.003	<sup>40</sup> 0.047	<sup>47</sup> 0.037	<sup>49</sup> 0.023	<sup>12</sup> 0.377	<sup>14</sup> 0.277	<sup>18</sup> 0.170	<sup>36</sup> 0.010	<sup>30</sup> 0.005	<sup>27</sup> 0.075	<sup>30</sup> 0.039	<sup>28</sup> 0.126	<sup>26</sup> 0.097					
160	NEUROTECHNOLOGY-012	<sup>132</sup> 0.092	<sup>37</sup> 0.007	<sup>30</sup> 0.002	<sup>39</sup> 0.045	<sup>42</sup> 0.032	<sup>36</sup> 0.019				<sup>30</sup> 0.008	<sup>18</sup> 0.004	<sup>21</sup> 0.061	<sup>22</sup> 0.028	<sup>173</sup> 0.916	<sup>17</sup> 0.088					
161	NEWLAND-002	<sup>249</sup> 0.523	<sup>262</sup> 0.438	<sup>23</sup> 0.294	<sup>53</sup> 0.535	<sup>246</sup> 0.466	<sup>232</sup> 0.335	<sup>161</sup> 0.999	<sup>170</sup> 0.999	<sup>199</sup> 0.998											
162	NOBLIS-001	<sup>289</sup> 1.000	<sup>289</sup> 1.000	<sup>287</sup> 0.991	<sup>284</sup> 1.000	<sup>283</sup> 1.000	<sup>293</sup> 1.000	<sup>199</sup> 1.000	<sup>225</sup> 1.000	<sup>234</sup> 1.000											
163	NOBLIS-002	<sup>287</sup> 1.000	<sup>285</sup> 0.997	<sup>277</sup> 0.488	<sup>282</sup> 1.000	<sup>291</sup> 1.000	<sup>197</sup> 1.000	<sup>226</sup> 1.000	<sup>234</sup> 1.000												
164	NOTIONTAG-000	<sup>61</sup> 0.032	<sup>76</sup> 0.017	<sup>81</sup> 0.007	<sup>74</sup> 0.076	<sup>83</sup> 0.059	<sup>84</sup> 0.036	<sup>30</sup> 0.671	<sup>35</sup> 0.611	<sup>43</sup> 0.467	<sup>60</sup> 0.021	<sup>62</sup> 0.011	<sup>49</sup> 0.150	<sup>58</sup> 0.084	<sup>48</sup> 0.176	<sup>58</sup> 0.140					
165	NTECHLAB-003	<sup>124</sup> 0.080	<sup>158</sup> 0.054	<sup>176</sup> 0.028	<sup>148</sup> 0.148	<sup>151</sup> 0.118	<sup>159</sup> 0.075	<sup>47</sup> 0.873	<sup>58</sup> 0.837	<sup>80</sup> 0.752											
166	NTECHLAB-004	<sup>111</sup> 0.063	<sup>133</sup> 0.041	<sup>148</sup> 0.021	<sup>132</sup> 0.131	<sup>144</sup> 0.105	<sup>142</sup> 0.065	<sup>46</sup> 0.868	<sup>57</sup> 0.833	<sup>78</sup> 0.746	<sup>116</sup> 0.053	<sup>119</sup> 0.030					<sup>28</sup> 0.263	<sup>104</sup> 0.214			
167	NTECHLAB-005	<sup>110</sup> 0.062	<sup>134</sup> 0.042	<sup>146</sup> 0.021	<sup>131</sup> 0.130	<sup>137</sup> 0.102	<sup>141</sup> 0.063	<sup>42</sup> 0.816	<sup>50</sup> 0.771	<sup>69</sup> 0.661	<sup>132</sup> 0.073	<sup>132</sup> 0.039					<sup>89</sup> 0.294	<sup>109</sup> 0.227			
168	NTECHLAB-006	<sup>103</sup> 0.056	<sup>128</sup> 0.037	<sup>138</sup> 0.018	<sup>121</sup> 0.121	<sup>127</sup> 0.094	<sup>129</sup> 0.059	<sup>40</sup> 0.802	<sup>49</sup> 0.754	<sup>64</sup> 0.635	<sup>119</sup> 0.057	<sup>122</sup> 0.032					<sup>77</sup> 0.260	<sup>100</sup> 0.207			
169	NTECHLAB-007	<sup>72</sup> 0.040	<sup>103</sup> 0.026	<sup>114</sup> 0.012	<sup>83</sup> 0.085	<sup>93</sup> 0.067	<sup>95</sup> 0.041	<sup>39</sup> 0.796	<sup>48</sup> 0.750	<sup>62</sup> 0.642	<sup>86</sup> 0.032	<sup>92</sup> 0.017					<sup>61</sup> 0.223	<sup>81</sup> 0.176			
170	NTECHLAB-008	<sup>45</sup> 0.024	<sup>66</sup> 0.014	<sup>74</sup> 0.007	<sup>49</sup> 0.057	<sup>50</sup> 0.045	<sup>61</sup> 0.029	<sup>21</sup> 0.601	<sup>29</sup> 0.529	<sup>40</sup> 0.391	<sup>90</sup> 0.033	<sup>96</sup> 0.018					<sup>51</sup> 0.183	<sup>59</sup> 0.140			
171	NTECHLAB-009	<sup>20</sup> 0.010	<sup>30</sup> 0.005	<sup>35</sup> 0.003	<sup>21</sup> 0.028	<sup>22</sup> 0.022	<sup>21</sup> 0.014	<sup>16</sup> 0.522	<sup>20</sup> 0.430	<sup>29</sup> 0.311	<sup>44</sup> 0.015	<sup>45</sup> 0.008	<sup>36</sup> 0.109	<sup>39</sup> 0.061			<sup>32</sup> 0.142	<sup>32</sup> 0.114			
172	NTECHLAB-010	<sup>12</sup> 0.005	<sup>13</sup> 0.003	<sup>10</sup> 0.002	<sup>13</sup> 0.018	<sup>14</sup> 0.015	<sup>12</sup> 0.011	<sup>11</sup> 0.334	<sup>13</sup> 0.252	<sup>17</sup> 0.169	<sup>17</sup> 0.007	<sup>21</sup> 0.004	<sup>20</sup> 0.059	<sup>24</sup> 0.031			<sup>10</sup> 0.098	<sup>8</sup> 0.077			
173	NTECHLAB-011	<sup>13</sup> 0.006	<sup>17</sup> 0.003	<sup>12</sup> 0.002	<sup>10</sup> 0.018	<sup>13</sup> 0.015	<sup>11</sup> 0.010	<sup>9</sup> 0.291	<sup>10</sup> 0.228	<sup>13</sup> 0.150	<sup>32</sup> 0.009	<sup>28</sup> 0.004	<sup>26</sup> 0.074	<sup>29</sup> 0.038			<sup>7</sup> 0.091	<sup>6</sup> 0.075			
174	PANGIAM-000	<sup>30</sup> 0.014	<sup>36</sup> 0.006	<sup>34</sup> 0.003	<sup>36</sup> 0.039	<sup>37</sup> 0.030	<sup>34</sup> 0.018	<sup>70</sup> 0.974	<sup>16</sup> 0.318	<sup>19</sup> 0.175	<sup>35</sup> 0.009	<sup>29</sup> 0.005	<sup>41</sup> 0.136	<sup>26</sup> 0.033			<sup>17</sup> 0.105	<sup>14</sup> 0.083			
175	PARAVISION-000	<sup>220</sup> 0.278	<sup>195</sup> 0.089	<sup>199</sup> 0.045	<sup>226</sup> 0.447	<sup>189</sup> 0.170	<sup>189</sup> 0.100	<sup>206</sup> 1.000	<sup>172</sup> 0.999	<sup>191</sup> 0.997	<sup>188</sup> 0.470	<sup>193</sup> 0.443					<sup>126</sup> 0.926	<sup>184</sup> 0.779			
176	PARAVISION-001	<sup>166</sup> 0.140	<sup>147</sup> 0.049																		

MISSSES BELOW THRESHOLD, T		ENROL RECENT MUGSHOT, N = 1.6M												ENROL APPLICATION PORTRAIT, N = 1.6M																							
		ENROL: MUGSHOT			ENROL: MUGSHOT			ENROL: MUGSHOT			ENROL: VISA			ENROL: BORDER			ENROL: BORDER 10+YR			ENROL: KIOSK																	
#	ALGORITHM	FPIR=0.0003	FPIR=0.001	FPIR=0.01	FPIR=0.0003	FPIR=0.001	FPIR=0.01	FPIR=0.0003	FPIR=0.001	FPIR=0.01	FPIR=0.0001	FPIR=0.001	FPIR=0.01	FPIR=0.0001	FPIR=0.001	FPIR=0.01	FPIR=0.0001	FPIR=0.001	FPIR=0.01	FPIR=0.0001	FPIR=0.001	FPIR=0.01	FPIR=0.0001	FPIR=0.001	FPIR=0.01												
185	PIXELAIL-004	150	0.120	84	0.018	78	0.007	250	0.783	111	0.076	86	0.037	205	1.000	208	0.999	111	0.051	82	0.015	191	0.994	195	0.942												
186	PIXELAIL-005	123	0.079	57	0.012	53	0.005	229	0.456	62	0.050	58	0.027	217	1.000	218	0.999	71	0.027	88	0.017	67	0.203	44	0.071												
187	PTAKURATSATU-000	105	0.057	127	0.037	131	0.017	159	0.165	159	0.124	153	0.071	63	0.947	69	0.924	93	0.868	108	0.046	105	0.022	69	0.206	73	0.120										
188	QNAP-000	280	0.972	213	0.129	209	0.052	279	0.998	209	0.238	199	0.117	222	1.000	227	1.000	164	0.191	159	0.068	93	0.539	97	0.263	193	0.998										
189	QNAP-001	128	0.083	157	0.054	159	0.024	161	0.176	167	0.137	170	0.085	59	0.943	70	0.928	94	0.870	136	0.081	136	0.041	86	0.368	92	0.227	92	0.331								
190	QNAP-002	81	0.045	108	0.026	120	0.013	139	0.136	147	0.106	147	0.068	43	0.820	51	0.772	61	0.622	115	0.052	112	0.025	78	0.281	87	0.171	83	0.272								
191	QUANTASOFT-001	263	0.713	273	0.639	274	0.493																					105	0.214								
192	RANKONE-002	186	0.184	206	0.118	221	0.071	208	0.308	217	0.261	228	0.190																								
193	RANKONE-003	188	0.184	207	0.118	230	0.071	201	0.300	216	0.255	226	0.187																								
194	RANKONE-004	210	0.250	234	0.193	244	0.124	251	0.482	241	0.426	280	0.324																								
195	RANKONE-005	135	0.096	169	0.059	178	0.033	181	0.212	192	0.173	200	0.119	162	0.999	156	0.998	177	0.994																		
196	RANKONE-006	107	0.061	129	0.037	138	0.020							90	0.987	90	0.977	110	0.937																		
197	RANKONE-007	62	0.034	97	0.022	110	0.011	118	0.118	128	0.095	134	0.061	73	0.975	78	0.967	108	0.924																		
198	RANKONE-009	58	0.031	79	0.018	87	0.008	95	0.098	105	0.076	102	0.045	82	0.983	81	0.969	92	0.859	122	0.062	118	0.029					96	0.328	99	0.206						
199	RANKONE-010	40	0.023	63	0.014	79	0.007	76	0.077	81	0.058	85	0.036	52	0.905	54	0.802	69	0.652	114	0.052	115	0.027	70	0.208	74	0.119	75	0.259	95	0.194						
200	RANKONE-011	145	0.109	43	0.009	49	0.004	80	0.079	60	0.048	62	0.029					96	0.037	93	0.017	62	0.182	63	0.092	185	0.977	156	0.465								
201	RANKONE-012	20	0.020	40	0.008	45	0.004	72	0.072	73	0.053	63	0.030					77	0.029	77	0.014	45	0.144	43	0.072	119	0.465	49	0.128								
202	REALNETWORKS-000	232	0.374	248	0.234	248	0.138	222	0.433	238	0.319	237	0.209																								
203	REALNETWORKS-001	231	0.374	239	0.234	241	0.138	224	0.433	233	0.319	236	0.209																								
204	REALNETWORKS-002	230	0.370	238	0.231	246	0.137	229	0.416	231	0.315	238	0.209																126	0.500	145	0.364					
205	REALNETWORKS-003	218	0.273	224	0.159	230	0.090	209	0.342	220	0.266	224	0.172	159	0.999	160	0.998	152	0.987	159	0.164	168	0.103						138	0.613	146	0.370					
206	REALNETWORKS-004	208	0.242	223	0.158	229	0.090	217	0.353	216	0.263	221	0.169	175	1.000	173	0.999	167	0.992	160	0.170	168	0.103														
207	REALNETWORKS-005	95	0.052	114	0.028	116	0.012	93	0.094	103	0.074	107	0.047	86	0.984	83	0.971	98	0.896	95	0.037	89	0.017	71	0.223	77	0.123	62	0.215	75	0.165						
208	REALNETWORKS-006	48	0.025	67	0.015	62	0.006	66	0.068	71	0.053	72	0.032	103	0.993	98	0.980	89	0.838	45	0.016	46	0.008	38	0.120	41	0.063	38	0.154	34	0.116						
209	REALNETWORKS-007	36	0.019	47	0.010	47	0.004	48	0.057	50	0.043	57	0.027	99	0.992	93	0.979	91	0.855	39	0.012	34	0.005	32	0.463	42	0.063	31	0.140	28	0.100						
210	REMARKAI-000	154	0.125	161	0.055	154	0.023	156	0.173	150	0.120	150	0.070	167	0.999	171	0.999	181	0.995	131	0.069	122	0.033						146	0.717	130	0.315					
211	REMARKAI-000	195	0.197	211	0.128	215	0.059	193	0.263	198	0.203	202	0.123																								
212	REMARKAI-002	191	0.188	210	0.124	212	0.059	187	0.248	196	0.196	201	0.122	106	0.993	119	0.991	145	0.980																		
213	RENDIP-000	41	0.023	56	0.012	57	0.005	170	0.189	87	0.059	78	0.034	62	0.945	66	0.894	77	0.744	61	0.022	70	0.013	64	0.185	59	0.089	45	0.167	51	0.130						
214	REVEALMEDIA-000	42	0.024	58	0.012	61	0.006	46	0.054	54	0.042	54	0.025	33	0.755	43	0.680	53	0.539	59	0.021	33	0.093	37	0.051	33	0.143	37	0.118								
215	S1-000	162	0.137	116	0.028	108	0.011	129	0.129	117	0.085	110	0.048	221	1.000	229	1.000	56	0.596	110	0.047	97	0.018	224	1.000	76	0.123	277	1.000	171	0.632						
216	S1-001	99	0.054	74	0.016	76	0.007	59	0.066	68	0.052	77	0.033	100	0.992	106	0.985	123	0.952	53	0.019	54	0.010	40	0.136	49	0.075	34	0.148	38	0.119						
217	S1-002	106	0.060	34	0.006	32	0.002	89	0.085	36	0.031	32	0.018	54	0.924	6	0.196	5	0.095	20	0.007	12	0.003	103	0.792	89	0.151	163	0.841	61	0.144						
218	SCANOVATE-000	140	0.103	176	0.067	174	0.030	209	0.296	212	0.240	211	0.150	57	0.931	64	0.893	83	0.803	168	0.215	173	0.118						106	0.400	134	0.299					
219	SCANOVATE-001	156	0.128	187	0.081	186	0.037	197	0.281	208	0.227	207	0.140	38	0.935	68	0.911	89	0.834	165	0.192	16	0.103						109	0.404	130	0.290					
220	SENSETIME-000	67	0.036	93	0.021	99	0.009	77	0.078	87	0.063	92	0.040	271	1.000	255	1.000	153	0.988																		
221	SENSETIME-001	68	0.036	96	0.022	99	0.010	81	0.080	89	0.064	98	0.041																		129	0.523	74	0.160			
222	SENSETIME-002	69	0.037	68	0.015	129	0.014	129	0.124	37	0.028	47	0.023	130	0.997	127	0.994	144	0.979	84	0.032	90	0.017														
223	SENSETIME-003	7	0.004	7	0.002	6	0.001	4	0.014	4	0.012	4	0.009	23	0.607	24	0.477	30	0.311	25	0.008	33	0.005										28	0.133	33	0.115	
224	SENSETIME-004	3	0.003	4	0.002	5	0.001	4	0.015	4	0.013	9	0.010	10	0.301	11	0.229	14	0.149	14	0.006	16	0.004									21	0.113	27	0.100		
225	SENSETIME-005	24	0.011	11	0.002	4	0.001	14	0.018	12	0.014	7	0.010	4	0.259	5	0.173	8	0.103	18	0.007	20	0.004	16	0.051	15	0.023	16	0.104	22	0.093		22	0.293			
226	SENSETIME-006	7	0.005	6	0.002	7	0.001	9	0.016	3	0.012	3	0.009	1	0.007	173	1.000	176	0.999	52	0.538	2	0.003	1	0.001	4	0.024	3	0.011	5	0.085	3	0.074				
227	SENSETIME-007	2	0.003	1	0.001	1	0.001	1	0.012	1	0.009	1	0.007	1	0.007	173	1.000																				
228	SHAMAN-003	245	0.506	263	0.451	267	0.347	245	0.650	25																											

Table 33: **Threshold-based accuracy**. Values are FNIR( $N, T, L$ ) with  $N = 1.6$  million with thresholds set to produce FPIR = 0.0003, 0.001, and 0.01 in non-mate searches. Throughout blue superscripts indicate the rank of the algorithm for that column. Caution: The Power-low models are mostly intended to draw attention to the kind of behavior, not as a model to be used for prediction.

2022/06/13  
09:55:40

FNIK(N, k,  
FPIR(N,

False neg. identification rate

$N =$  Num. enrolled subjects  
 $R =$  Num. candidates examined

= 1 hreshold

$T \geq 0 \rightarrow$  Identification

MISSES BELOW THRESHOLD, T			ENROL RECENT MUGSHOT, N = 1.6M												ENROL APPLICATION PORTRAIT, N = 1.6M											
#	ALGORITHM	FPIR=0.0003	ENROL: MUGSHOT			ENROL: MUGSHOT			ENROL: MUGSHOT			ENROL: PROFILE			ENROL: VISA		ENROL: BORDER		ENROL: VISA							
			PROBE: MUGSHOT	FPIR=0.001	FPIR=0.01	PROBE: WEBCAM	FPIR=0.001	FPIR=0.01	PROBE: PROFILE	FPIR=0.0003	PROBE: BORDER	FPIR=0.01	FPIR=0.001	PROBE: BORDER	FPIR=0.01	FPIR=0.001	FPIR=0.01	FPIR=0.001	FPIR=0.01	FPIR=0.001	FPIR=0.01					
231	SHAMAN-007	<sup>183</sup> 0.183	<sup>219</sup> 0.141	<sup>231</sup> 0.092	<sup>199</sup> 0.280	<sup>217</sup> 0.240	<sup>222</sup> 0.169								<sup>89</sup> 0.031	<sup>76</sup> 0.014										
232	SIAT-001	<sup>159</sup> 0.132	<sup>77</sup> 0.018	<sup>73</sup> 0.007	<sup>243</sup> 0.641	<sup>237</sup> 0.365	<sup>235</sup> 0.348								<sup>178</sup> 0.372	<sup>187</sup> 0.356					<sup>175</sup> 0.923	<sup>78</sup> 0.169				
233	SIAT-002	<sup>234</sup> 0.417	<sup>94</sup> 0.022	<sup>80</sup> 0.007	<sup>259</sup> 0.942	<sup>249</sup> 0.478	<sup>239</sup> 0.460																			
234	SMILART-004	<sup>279</sup> 0.970	<sup>282</sup> 0.968	<sup>287</sup> 0.965	<sup>270</sup> 0.977	<sup>279</sup> 0.976	<sup>281</sup> 0.973																			
235	SMILART-005																									
236	SQISOFT-001	<sup>204</sup> 0.226	<sup>215</sup> 0.132	<sup>198</sup> 0.044	<sup>207</sup> 0.340	<sup>214</sup> 0.252	<sup>192</sup> 0.111	<sup>65</sup> 0.956	<sup>52</sup> 0.797	<sup>59</sup> 0.608	<sup>100</sup> 0.040	<sup>99</sup> 0.019	<sup>83</sup> 0.317	<sup>83</sup> 0.150	<sup>111</sup> 0.420	<sup>91</sup> 0.189										
237	STAQU-000	<sup>225</sup> 0.334	<sup>170</sup> 0.062	<sup>148</sup> 0.022	<sup>257</sup> 0.848	<sup>247</sup> 0.443	<sup>135</sup> 0.061	<sup>192</sup> 1.000	<sup>199</sup> 1.000	<sup>210</sup> 0.999	<sup>190</sup> 0.535	<sup>133</sup> 0.039	<sup>104</sup> 0.961	<sup>88</sup> 0.183	<sup>270</sup> 1.000	<sup>206</sup> 0.999							<sup>91</sup> 0.314	<sup>113</sup> 0.235		
238	SYNESIS-003	<sup>146</sup> 0.111	<sup>174</sup> 0.065	<sup>178</sup> 0.032	<sup>159</sup> 0.155	<sup>158</sup> 0.123	<sup>162</sup> 0.078	<sup>68</sup> 0.973	<sup>76</sup> 0.960	<sup>108</sup> 0.911	<sup>133</sup> 0.075	<sup>131</sup> 0.039														
239	SYNESIS-003	<sup>257</sup> 0.648	<sup>268</sup> 0.582	<sup>277</sup> 0.443	<sup>247</sup> 0.708	<sup>26</sup> 0.646	<sup>263</sup> 0.524															<sup>61</sup> 0.214	<sup>73</sup> 0.158			
240	SYNESIS-005	<sup>91</sup> 0.050	<sup>102</sup> 0.025	<sup>112</sup> 0.011	<sup>88</sup> 0.088	<sup>99</sup> 0.072	<sup>101</sup> 0.043	<sup>114</sup> 0.995	<sup>103</sup> 0.984	<sup>82</sup> 0.795	<sup>87</sup> 0.032	<sup>84</sup> 0.016									<sup>19</sup> 0.994	<sup>188</sup> 0.817				
241	TECH5-001	<sup>267</sup> 0.807	<sup>164</sup> 0.057	<sup>134</sup> 0.018	<sup>277</sup> 0.994	<sup>126</sup> 0.055	<sup>251</sup> 1.000	<sup>228</sup> 1.000	<sup>224</sup> 1.000	<sup>169</sup> 0.244	<sup>117</sup> 0.028										<sup>114</sup> 0.440	<sup>88</sup> 0.182				
242	TECH5-002	<sup>98</sup> 0.053	<sup>111</sup> 0.027	<sup>118</sup> 0.012	<sup>92</sup> 0.094	<sup>97</sup> 0.070	<sup>94</sup> 0.040	<sup>48</sup> 0.874	<sup>55</sup> 0.805	<sup>62</sup> 0.627	<sup>99</sup> 0.039	<sup>98</sup> 0.019	<sup>68</sup> 0.205	<sup>72</sup> 0.111												
243	TEVIAN-003	<sup>207</sup> 0.239	<sup>231</sup> 0.177	<sup>259</sup> 0.096	<sup>211</sup> 0.346	<sup>227</sup> 0.298	<sup>230</sup> 0.198																			
244	TEVIAN-004	<sup>180</sup> 0.170	<sup>205</sup> 0.117	<sup>217</sup> 0.063	<sup>188</sup> 0.216	<sup>197</sup> 0.176	<sup>198</sup> 0.115																			
245	TEVIAN-005	<sup>158</sup> 0.129	<sup>192</sup> 0.087	<sup>198</sup> 0.045	<sup>164</sup> 0.180	<sup>173</sup> 0.144	<sup>174</sup> 0.089	<sup>93</sup> 0.988	<sup>77</sup> 0.962	<sup>83</sup> 0.796											<sup>189</sup> 0.951	<sup>36</sup> 0.117				
246	TEVIAN-006	<sup>44</sup> 0.024	<sup>48</sup> 0.010	<sup>56</sup> 0.005	<sup>37</sup> 0.041	<sup>40</sup> 0.032	<sup>41</sup> 0.021	<sup>19</sup> 0.562	<sup>19</sup> 0.425	<sup>28</sup> 0.291	<sup>46</sup> 0.016	<sup>49</sup> 0.009	<sup>31</sup> 0.093	<sup>35</sup> 0.050								<sup>23</sup> 0.033	<sup>30</sup> 0.102			
247	TEVIAN-007	<sup>25</sup> 0.011	<sup>32</sup> 0.005	<sup>36</sup> 0.003	<sup>20</sup> 0.028	<sup>21</sup> 0.022	<sup>22</sup> 0.015	<sup>15</sup> 0.504	<sup>15</sup> 0.301	<sup>23</sup> 0.183	<sup>34</sup> 0.009	<sup>31</sup> 0.005	<sup>23</sup> 0.065	<sup>25</sup> 0.033	<sup>23</sup> 0.122	<sup>30</sup> 0.102										
248	TIGER-000	<sup>240</sup> 0.462	<sup>257</sup> 0.390	<sup>269</sup> 0.261	<sup>235</sup> 0.565	<sup>259</sup> 0.500	<sup>254</sup> 0.366																			
249	TIGER-002	<sup>176</sup> 0.158	<sup>188</sup> 0.086	<sup>189</sup> 0.039	<sup>178</sup> 0.202	<sup>183</sup> 0.158	<sup>181</sup> 0.095	<sup>166</sup> 0.999	<sup>168</sup> 0.999	<sup>141</sup> 0.975																
250	TIGER-003	<sup>177</sup> 0.158	<sup>189</sup> 0.086	<sup>188</sup> 0.039	<sup>177</sup> 0.202	<sup>182</sup> 0.158	<sup>180</sup> 0.095																			
251	TONGYITRANS-000	<sup>143</sup> 0.107	<sup>181</sup> 0.074	<sup>187</sup> 0.038	<sup>142</sup> 0.141	<sup>147</sup> 0.112	<sup>149</sup> 0.069																			
252	TONGYITRANS-001	<sup>153</sup> 0.124	<sup>175</sup> 0.066	<sup>176</sup> 0.032	<sup>128</sup> 0.128	<sup>130</sup> 0.101	<sup>138</sup> 0.062																			
253	TOSHIBA-000	<sup>152</sup> 0.123	<sup>171</sup> 0.062	<sup>168</sup> 0.027	<sup>146</sup> 0.150	<sup>159</sup> 0.118	<sup>155</sup> 0.074	<sup>132</sup> 0.997	<sup>140</sup> 0.995	<sup>154</sup> 0.988																
254	TOSHIBA-001	<sup>202</sup> 0.225	<sup>166</sup> 0.058	<sup>159</sup> 0.019	<sup>135</sup> 0.133	<sup>125</sup> 0.092	<sup>125</sup> 0.054																			
255	TRUEFACE-000	<sup>84</sup> 0.046	<sup>83</sup> 0.018	<sup>88</sup> 0.008	<sup>78</sup> 0.079	<sup>80</sup> 0.062	<sup>89</sup> 0.039	<sup>118</sup> 0.995	<sup>61</sup> 0.882	<sup>48</sup> 0.499	<sup>78</sup> 0.030	<sup>82</sup> 0.016	<sup>66</sup> 0.194	<sup>73</sup> 0.111	<sup>56</sup> 0.188	<sup>62</sup> 0.145										
256	VD-000	<sup>276</sup> 0.950	<sup>280</sup> 0.917	<sup>284</sup> 0.827	<sup>268</sup> 0.968	<sup>277</sup> 0.946	<sup>277</sup> 0.871																			
257	VD-001	<sup>219</sup> 0.278	<sup>235</sup> 0.201	<sup>242</sup> 0.116	<sup>209</sup> 0.331	<sup>223</sup> 0.281	<sup>227</sup> 0.188																			
258	VD-002	<sup>170</sup> 0.144	<sup>185</sup> 0.079	<sup>182</sup> 0.036	<sup>169</sup> 0.188	<sup>178</sup> 0.148	<sup>175</sup> 0.092	<sup>141</sup> 0.998	<sup>143</sup> 0.996	<sup>151</sup> 0.987	<sup>140</sup> 0.095	<sup>142</sup> 0.048	<sup>85</sup> 0.367	<sup>91</sup> 0.220	<sup>102</sup> 0.372	<sup>126</sup> 0.280										
259	VD-003	<sup>206</sup> 0.234	<sup>142</sup> 0.046	<sup>139</sup> 0.020	<sup>135</sup> 0.133	<sup>130</sup> 0.100	<sup>137</sup> 0.061	<sup>163</sup> 0.999	<sup>169</sup> 0.999	<sup>175</sup> 0.994	<sup>112</sup> 0.051	<sup>114</sup> 0.027	<sup>75</sup> 0.244	<sup>78</sup> 0.133	<sup>95</sup> 0.315	<sup>95</sup> 0.203										
260	VERIDAS-001	<sup>125</sup> 0.080	<sup>131</sup> 0.037	<sup>129</sup> 0.016	<sup>106</sup> 0.106	<sup>113</sup> 0.082	<sup>114</sup> 0.051	<sup>104</sup> 0.993	<sup>111</sup> 0.987	<sup>111</sup> 0.938	<sup>104</sup> 0.044	<sup>110</sup> 0.023	<sup>75</sup> 0.266	<sup>80</sup> 0.146	<sup>80</sup> 0.264	<sup>96</sup> 0.204										
261	VERIDAS-002	<sup>126</sup> 0.080	<sup>130</sup> 0.037	<sup>128</sup> 0.016	<sup>107</sup> 0.106	<sup>111</sup> 0.082	<sup>115</sup> 0.051	<sup>105</sup> 0.993	<sup>110</sup> 0.987	<sup>112</sup> 0.938	<sup>103</sup> 0.044	<sup>109</sup> 0.023	<sup>76</sup> 0.266	<sup>81</sup> 0.146	<sup>79</sup> 0.264	<sup>97</sup> 0.204										
262	VERIDAS-003	<sup>118</sup> 0.072	<sup>75</sup> 0.017	<sup>68</sup> 0.006	<sup>69</sup> 0.071	<sup>76</sup> 0.055	<sup>75</sup> 0.033	<sup>147</sup> 0.998	<sup>148</sup> 0.997	<sup>108</sup> 0.927	<sup>35</sup> 0.020	<sup>57</sup> 0.011	<sup>48</sup> 0.150	<sup>51</sup> 0.078	<sup>31</sup> 0.178	<sup>60</sup> 0.142										
263	VIGILANTSOLUTIONS-003	<sup>244</sup> 0.482	<sup>261</sup> 0.408	<sup>268</sup> 0.282	<sup>257</sup> 0.730	<sup>265</sup> 0.660	<sup>265</sup> 0.526	<sup>160</sup> 0.999	<sup>165</sup> 0.999	<sup>182</sup> 0.995																
264	VIGILANTSOLUTIONS-004	<sup>256</sup> 0.624	<sup>267</sup> 0.549	<sup>270</sup> 0.422	<sup>258</sup> 0.858	<sup>269</sup> 0.817	<sup>271</sup> 0.709	<sup>145</sup> 0.998	<sup>146</sup> 0.996	<sup>167</sup> 0.991	<sup>202</sup> 1.000	<sup>218</sup> 1.000	<sup>221</sup> 1.000													
265	VIGILANTSOLUTIONS-005	<sup>275</sup> 0.936	<sup>256</sup> 0.388	<sup>191</sup> 0.043																						
266	VIGILANTSOLUTIONS-006	<sup>278</sup> 0.959	<sup>251</sup> 0.353	<sup>194</sup> 0.043																						
267	VIGILANTSOLUTIONS-007	<sup>122</sup> 0.076	<sup>118</sup> 0.028	<sup>111</sup> 0.011	<sup>112</sup> 0.113	<sup>119</sup> 0.088	<sup>120</sup> 0.053	<sup>138</sup> 0.997	<sup>145</sup> 0.996	<sup>166</sup> 0.991	<sup>137</sup> 0.081	<sup>140</sup> 0.047	<sup>87</sup> 0.371	<sup>94</sup> 0.242	<sup>105</sup> 0.391	<sup>133</sup> 0.295										
268	VIGILANTSOLUTIONS-008	<sup>94</sup> 0.051	<sup>90</sup> 0.021	<sup>98</sup> 0.010	<sup>105</sup> 0.105	<sup>107</sup> 0.077	<sup>105</sup> 0.046	<sup>170</sup> 1.000	<sup>167</sup> 0.999	<sup>162</sup> 0.991	<sup>144</sup> 0.104	<sup>145</sup> 0.054	<sup>89</sup> 0.398	<sup>96</sup> 0.259	<sup>12</sup> 0.511	<sup>139</sup> 0.316										
269	VISIONLABS-000	<sup>119</sup> 0.073	<sup>80</sup> 0.018	<sup>77</sup> 0.007	<sup>70</sup> 0.071	<sup>79</sup> 0.057	<sup>82</sup> 0.035	<sup>111</sup> 0.995	<sup>118</sup>																	

MISSES BELOW THRESHOLD, T		ENROL RECENT MUGSHOT, N = 1.6M												ENROL APPLICATION PORTRAIT, N = 1.6M												
#	ALGORITHM	ENROL: MUGSHOT			ENROL: MUGSHOT			ENROL: WEBCAM			PROBE: PROFILE			ENROL: VISA			ENROL: BORDER			ENROL: BORDER 10+YR			ENROL: VISA			
		FPIR=0.0003	FPIR=0.001	FPIR=0.01	FPIR=0.0003	FPIR=0.001	FPIR=0.01	FPIR=0.0003	FPIR=0.001	FPIR=0.01	FPIR=0.068	FPIR=0.036	FPIR=0.022	FPIR=0.01	FPIR=0.001	FPIR=0.01	FPIR=0.001	FPIR=0.01	FPIR=0.034	FPIR=0.017	FPIR=0.090	FPIR=0.079	FPIR=0.001	FPIR=0.01	FPIR=0.001	
277	VISIONLABS-011	<sup>26</sup> 0.011	<sup>19</sup> 0.003	<sup>15</sup> 0.002	<sup>20</sup> 0.006	<sup>15</sup> 0.158	<sup>25</sup> 0.068	<sup>18</sup> 0.024	<sup>19</sup> 0.020	<sup>20</sup> 0.014	<sup>35</sup> 0.068	<sup>83</sup> 0.036	<sup>35</sup> 0.922	<sup>45</sup> 0.718	<sup>35</sup> 0.373	<sup>9</sup> 0.004	<sup>7</sup> 0.002	<sup>10</sup> 0.034	<sup>9</sup> 0.017	<sup>10</sup> 0.990	<sup>10</sup> 0.537	<sup>100</sup> 0.362	<sup>53</sup> 0.134	<sup>108</sup> 0.404	<sup>12</sup> 0.289	
278	VNPNT-001	<sup>52</sup> 0.027	<sup>65</sup> 0.014	<sup>20</sup> 0.006	<sup>15</sup> 0.158	<sup>25</sup> 0.068	<sup>18</sup> 0.024	<sup>15</sup> 0.093	<sup>16</sup> 0.099	<sup>15</sup> 0.099	<sup>15</sup> 0.999	<sup>15</sup> 0.999	<sup>15</sup> 0.999	<sup>15</sup> 0.999	<sup>15</sup> 0.999	<sup>15</sup> 0.999	<sup>15</sup> 0.999	<sup>15</sup> 0.999	<sup>15</sup> 0.999	<sup>15</sup> 0.999	<sup>15</sup> 0.999	<sup>15</sup> 0.999	<sup>15</sup> 0.999	<sup>15</sup> 0.999	<sup>15</sup> 0.999	<sup>15</sup> 0.999
279	VOCORD-003	<sup>22</sup> 0.354	<sup>20</sup> 0.122	<sup>20</sup> 0.048	<sup>17</sup> 0.195	<sup>18</sup> 0.155	<sup>17</sup> 0.093	<sup>16</sup> 0.099	<sup>16</sup> 0.099	<sup>16</sup> 0.099	<sup>16</sup> 0.099	<sup>16</sup> 0.099	<sup>16</sup> 0.099	<sup>16</sup> 0.099	<sup>16</sup> 0.099	<sup>16</sup> 0.099	<sup>16</sup> 0.099	<sup>16</sup> 0.099	<sup>16</sup> 0.099							
280	VOCORD-004	<sup>268</sup> 0.826	<sup>252</sup> 0.355	<sup>203</sup> 0.051	<sup>219</sup> 0.401	<sup>190</sup> 0.173	<sup>176</sup> 0.093	<sup>200</sup> 1.000	<sup>207</sup> 0.999	<sup>166</sup> 0.193	<sup>150</sup> 0.065	<sup>166</sup> 0.193	<sup>150</sup> 0.065	<sup>166</sup> 0.193	<sup>150</sup> 0.065	<sup>166</sup> 0.193	<sup>150</sup> 0.065	<sup>166</sup> 0.193	<sup>150</sup> 0.065	<sup>166</sup> 0.193	<sup>150</sup> 0.065	<sup>166</sup> 0.193	<sup>150</sup> 0.065	<sup>166</sup> 0.193	<sup>150</sup> 0.065	<sup>166</sup> 0.193
281	VOCORD-005	<sup>261</sup> 0.689	<sup>222</sup> 0.158	<sup>19</sup> 0.044	<sup>15</sup> 0.161	<sup>16</sup> 0.130	<sup>165</sup> 0.080	<sup>157</sup> 0.999	<sup>149</sup> 0.997	<sup>138</sup> 0.968	<sup>153</sup> 0.138	<sup>168</sup> 0.090	<sup>153</sup> 0.138	<sup>168</sup> 0.090	<sup>153</sup> 0.138	<sup>168</sup> 0.090	<sup>153</sup> 0.138	<sup>168</sup> 0.090	<sup>153</sup> 0.138	<sup>168</sup> 0.090	<sup>153</sup> 0.138	<sup>168</sup> 0.090	<sup>153</sup> 0.138	<sup>168</sup> 0.090	<sup>153</sup> 0.138	<sup>168</sup> 0.090
282	VOCORD-006	<sup>292</sup> 1.000	<sup>290</sup> 1.000	<sup>293</sup> 1.000	<sup>290</sup> 1.000	<sup>293</sup> 1.000	<sup>286</sup> 1.000	<sup>292</sup> 1.000	<sup>287</sup> 1.000	<sup>266</sup> 1.000	<sup>230</sup> 1.000	<sup>245</sup> 1.000	<sup>230</sup> 1.000	<sup>245</sup> 1.000	<sup>230</sup> 1.000	<sup>245</sup> 1.000	<sup>230</sup> 1.000	<sup>245</sup> 1.000	<sup>230</sup> 1.000	<sup>245</sup> 1.000	<sup>230</sup> 1.000	<sup>245</sup> 1.000	<sup>230</sup> 1.000	<sup>245</sup> 1.000	<sup>230</sup> 1.000	<sup>245</sup> 1.000
283	VTS-000	<sup>253</sup> 0.605	<sup>269</sup> 0.598	<sup>27</sup> 0.595	<sup>24</sup> 0.624	<sup>259</sup> 0.619	<sup>268</sup> 0.613	<sup>165</sup> 0.999	<sup>175</sup> 0.999	<sup>20</sup> 0.998	<sup>195</sup> 0.613	<sup>19</sup> 0.609	<sup>100</sup> 0.760	<sup>107</sup> 0.739	<sup>150</sup> 0.761	<sup>18</sup> 0.749										
284	VTS-001	<sup>64</sup> 0.035	<sup>62</sup> 0.013	<sup>63</sup> 0.006	<sup>63</sup> 0.067	<sup>66</sup> 0.051	<sup>64</sup> 0.031	<sup>140</sup> 0.998	<sup>128</sup> 0.994	<sup>48</sup> 0.510	<sup>62</sup> 0.022	<sup>67</sup> 0.012	<sup>44</sup> 0.141	<sup>52</sup> 0.079	<sup>57</sup> 0.192	<sup>48</sup> 0.126	<sup>62</sup> 0.022	<sup>67</sup> 0.012	<sup>44</sup> 0.141	<sup>52</sup> 0.079	<sup>57</sup> 0.192	<sup>48</sup> 0.126	<sup>62</sup> 0.022	<sup>67</sup> 0.012	<sup>44</sup> 0.141	<sup>52</sup> 0.079
285	VTS-002	<sup>97</sup> 0.053	<sup>105</sup> 0.026	<sup>106</sup> 0.010	<sup>97</sup> 0.098	<sup>104</sup> 0.075	<sup>106</sup> 0.046	<sup>179</sup> 1.000	<sup>186</sup> 1.000	<sup>12</sup> 0.953	<sup>106</sup> 0.045	<sup>11</sup> 0.026	<sup>72</sup> 0.231	<sup>79</sup> 0.133	<sup>110</sup> 0.417	<sup>89</sup> 0.187	<sup>106</sup> 0.045	<sup>11</sup> 0.026	<sup>72</sup> 0.231	<sup>79</sup> 0.133	<sup>110</sup> 0.417	<sup>89</sup> 0.187	<sup>106</sup> 0.045	<sup>11</sup> 0.026	<sup>72</sup> 0.231	<sup>79</sup> 0.133
286	XFORWARDAI-000	<sup>55</sup> 0.029	<sup>71</sup> 0.015	<sup>72</sup> 0.006	<sup>67</sup> 0.070	<sup>74</sup> 0.053	<sup>80</sup> 0.034	<sup>32</sup> 0.698	<sup>21</sup> 0.440	<sup>26</sup> 0.250	<sup>58</sup> 0.021	<sup>56</sup> 0.011	<sup>53</sup> 0.159	<sup>56</sup> 0.082	<sup>46</sup> 0.169	<sup>52</sup> 0.134	<sup>58</sup> 0.021	<sup>56</sup> 0.011	<sup>53</sup> 0.159	<sup>56</sup> 0.082	<sup>46</sup> 0.169	<sup>52</sup> 0.134	<sup>58</sup> 0.021	<sup>56</sup> 0.011	<sup>53</sup> 0.159	<sup>56</sup> 0.082
287	XFORWARDAI-001	<sup>22</sup> 0.010	<sup>29</sup> 0.005	<sup>3</sup> 0.003	<sup>32</sup> 0.036	<sup>30</sup> 0.028	<sup>37</sup> 0.020	<sup>44</sup> 0.838	<sup>22</sup> 0.448	<sup>10</sup> 0.143	<sup>26</sup> 0.008	<sup>34</sup> 0.005	<sup>22</sup> 0.062	<sup>24</sup> 0.030	<sup>28</sup> 0.102	<sup>22</sup> 0.062	<sup>24</sup> 0.030	<sup>28</sup> 0.102	<sup>22</sup> 0.062	<sup>24</sup> 0.030	<sup>28</sup> 0.102	<sup>22</sup> 0.062	<sup>24</sup> 0.030	<sup>28</sup> 0.102	<sup>22</sup> 0.062	<sup>24</sup> 0.030
288	XFORWARDAI-002	<sup>14</sup> 0.007	<sup>18</sup> 0.003	<sup>25</sup> 0.002	<sup>15</sup> 0.018	<sup>15</sup> 0.016	<sup>18</sup> 0.014	<sup>72</sup> 0.975	<sup>27</sup> 0.525	<sup>2</sup> 0.095	<sup>12</sup> 0.005	<sup>13</sup> 0.003	<sup>13</sup> 0.041	<sup>11</sup> 0.018	<sup>13</sup> 0.099	<sup>18</sup> 0.089	<sup>12</sup> 0.005	<sup>13</sup> 0.003	<sup>13</sup> 0.041	<sup>11</sup> 0.018	<sup>13</sup> 0.099	<sup>18</sup> 0.089	<sup>12</sup> 0.005	<sup>13</sup> 0.003	<sup>13</sup> 0.041	<sup>11</sup> 0.018
289	YISHENG-001	<sup>28</sup> 0.452	<sup>24</sup> 0.346	<sup>25</sup> 0.206	<sup>27</sup> 0.983	<sup>26</sup> 0.808	<sup>24</sup> 0.269	<sup>197</sup> 0.666	<sup>19</sup> 0.396	<sup>19</sup> 0.396	<sup>197</sup> 0.666	<sup>19</sup> 0.396	<sup>19</sup> 0.396	<sup>197</sup> 0.666	<sup>19</sup> 0.396	<sup>19</sup> 0.396	<sup>197</sup> 0.666	<sup>19</sup> 0.396	<sup>19</sup> 0.396	<sup>197</sup> 0.666	<sup>19</sup> 0.396	<sup>19</sup> 0.396	<sup>197</sup> 0.666	<sup>19</sup> 0.396	<sup>19</sup> 0.396	
290	YITU-002	<sup>59</sup> 0.031	<sup>78</sup> 0.018	<sup>82</sup> 0.008	<sup>55</sup> 0.063	<sup>61</sup> 0.049	<sup>59</sup> 0.028	<sup>59</sup> 0.028	<sup>59</sup> 0.028	<sup>59</sup> 0.028	<sup>59</sup> 0.028	<sup>59</sup> 0.028	<sup>59</sup> 0.028	<sup>59</sup> 0.028	<sup>59</sup> 0.028	<sup>59</sup> 0.028	<sup>59</sup> 0.028	<sup>59</sup> 0.028								
291	YITU-003	<sup>60</sup> 0.032	<sup>86</sup> 0.019	<sup>90</sup> 0.009	<sup>61</sup> 0.067	<sup>70</sup> 0.052	<sup>76</sup> 0.033	<sup>59</sup> 0.033	<sup>59</sup> 0.033	<sup>59</sup> 0.033	<sup>59</sup> 0.033	<sup>59</sup> 0.033	<sup>59</sup> 0.033	<sup>59</sup> 0.033	<sup>59</sup> 0.033	<sup>59</sup> 0.033	<sup>59</sup> 0.033	<sup>59</sup> 0.033	<sup>59</sup> 0.033							
292	YITU-004	<sup>35</sup> 0.019	<sup>45</sup> 0.010	<sup>50</sup> 0.004	<sup>31</sup> 0.035	<sup>32</sup> 0.027	<sup>31</sup> 0.017	<sup>64</sup> 0.948	<sup>71</sup> 0.936	<sup>101</sup> 0.913	<sup>59</sup> 0.033	<sup>59</sup> 0.033	<sup>59</sup> 0.033	<sup>59</sup> 0.033	<sup>59</sup> 0.033	<sup>59</sup> 0.033	<sup>59</sup> 0.033	<sup>59</sup> 0.033	<sup>59</sup> 0.033	<sup>59</sup> 0.033	<sup>59</sup> 0.033	<sup>59</sup> 0.033	<sup>59</sup> 0.033	<sup>59</sup> 0.033		
293	YITU-005	<sup>39</sup> 0.022	<sup>52</sup> 0.010	<sup>55</sup> 0.005	<sup>35</sup> 0.039	<sup>41</sup> 0.032	<sup>46</sup> 0.023	<sup>59</sup> 0.033	<sup>59</sup> 0.033	<sup>59</sup> 0.033	<sup>59</sup> 0.033	<sup>59</sup> 0.033	<sup>59</sup> 0.033	<sup>59</sup> 0.033	<sup>59</sup> 0.033	<sup>59</sup> 0.033	<sup>59</sup> 0.033	<sup>59</sup> 0.033								

09:55:40

2022/06/13

FNIR(N, R, T) = False neg. identification rate

N = Num. enrolled subjects

T = Threshold

T = 0 → Investigation

R = Num. candidates examined

T &gt; 0 → Identification

# Appendices

## Appendix A Accuracy on large-population FRVT 2018 mugshots

2022/06/13 09:55:40	$\text{FNIR}(N, R, T) =$ $\text{FPTR}(N, T) =$	False neg. identification rate False pos. identification rate	$N =$ Num. enrolled subjects $R =$ Num. candidates examined	$T =$ Threshold $T > 0 \rightarrow$ Identification	$T = 0 \rightarrow$ Investigation
------------------------	---------------------------------------------------	------------------------------------------------------------------	----------------------------------------------------------------	-------------------------------------------------------	-----------------------------------

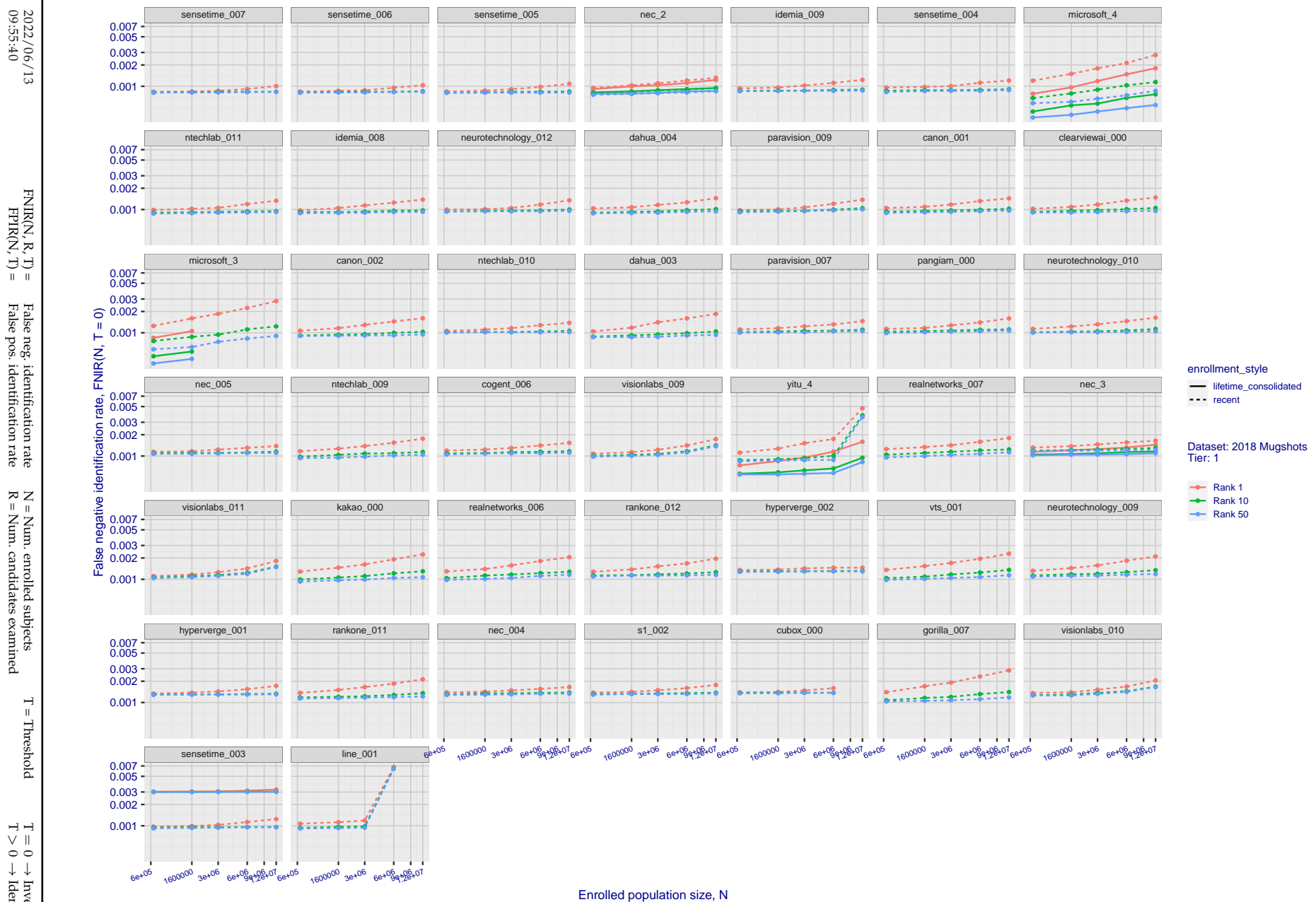


Figure 20: [FRVT-2018 Mugshot Dataset] Rank-based identification miss rates vs. number of enrolled subjects. The figure shows false negative identification rates,  $\text{FNIR}(N, R)$ , across various gallery sizes and ranks 1, 10 and 50. The threshold is set to zero, so this metric rewards even weak scoring rank 1 mates. This also means  $\text{FPIR} = 1$ , so any search without an enrolled mate will return non-mated candidates. For clarity, results are sorted and reported into tiers spanning multiple pages, the tiering criteria being rank 1 hit rate on a gallery size of 640 000.

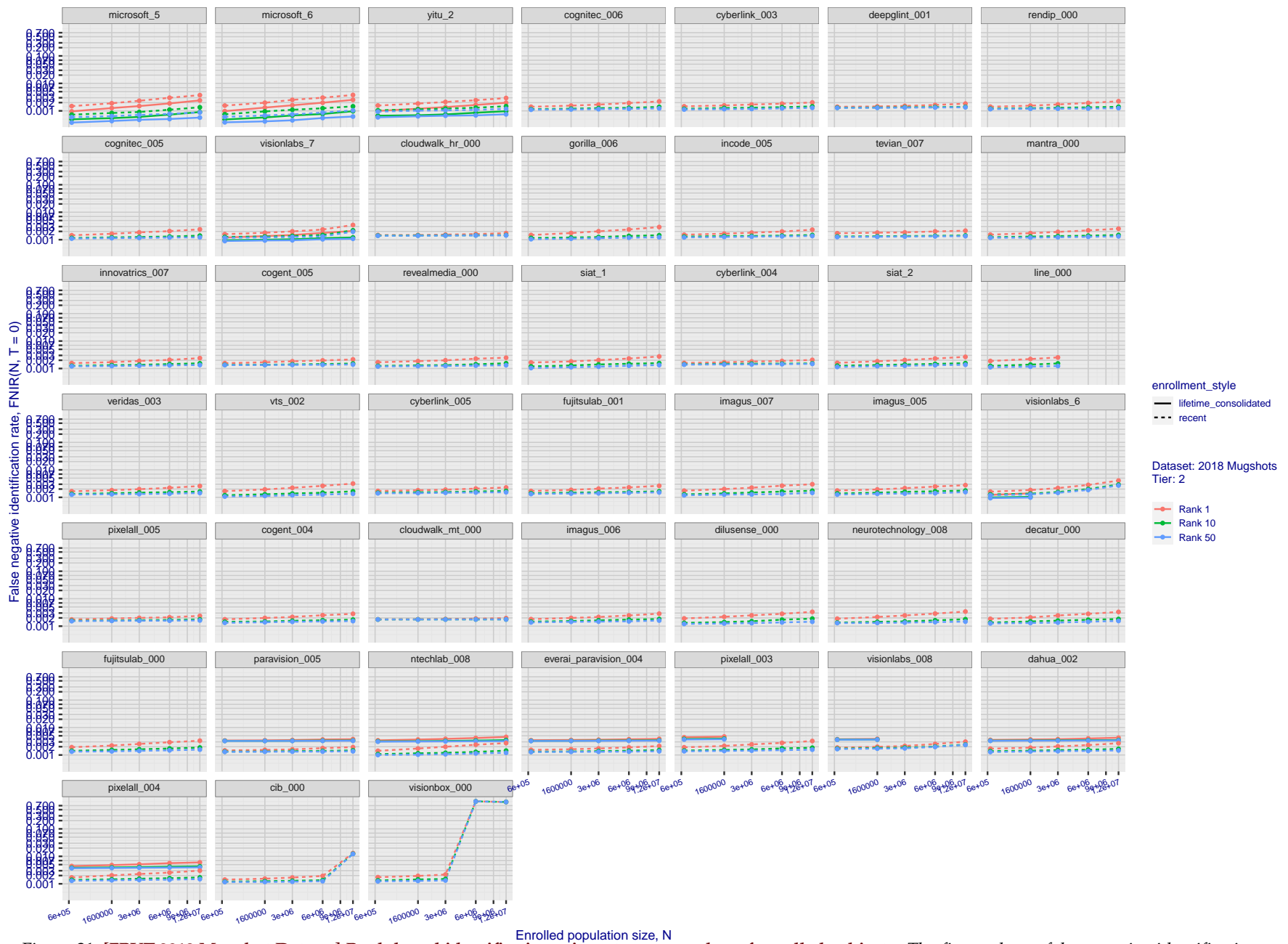
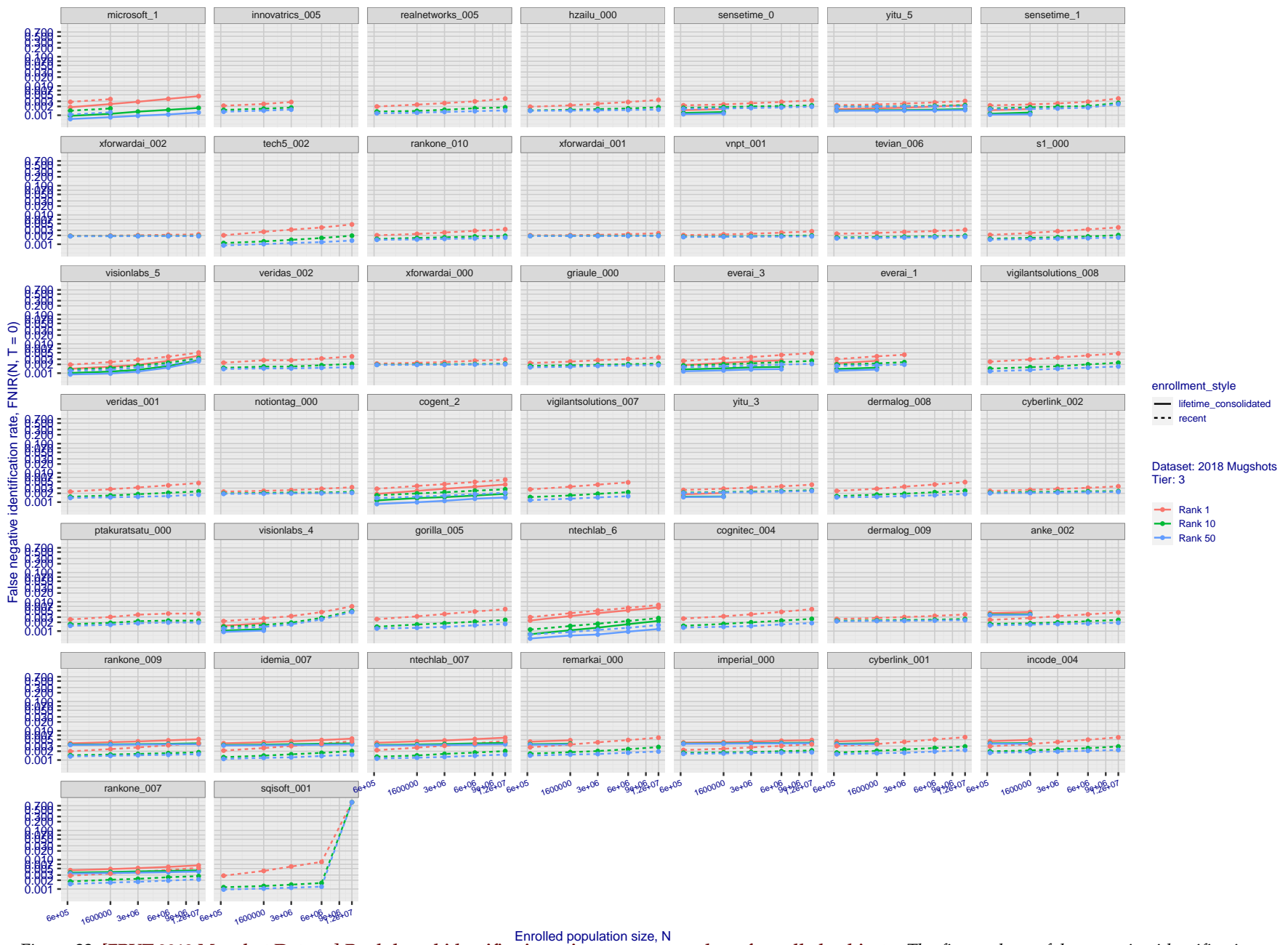


Figure 21: [FRVT-2018 Mugshot Dataset] Rank-based identification miss rates vs. number of enrolled subjects. The figure shows false negative identification rates,  $\text{FNIR}(N, R)$ , across various gallery sizes and ranks 1, 10 and 50. The threshold is set to zero, so this metric rewards even weak scoring rank 1 mates. This also means  $\text{FPIR} = 1$ , so any search without an enrolled mate will return non-mated candidates. For clarity, results are sorted and reported into tiers spanning multiple pages, the tiering criteria being rank 1 hit rate on a gallery size of 640 000.



**Figure 22: [FRVT-2018 Mugshot Dataset] Rank-based identification miss rates vs. number of enrolled subjects.** The figure shows false negative identification rates,  $\text{FNIR}(N, R)$ , across various gallery sizes and ranks 1, 10 and 50. The threshold is set to zero, so this metric rewards even weak scoring rank 1 mates. This also means  $\text{FPIR} = 1$ , so any search without an enrolled mate will return non-mated candidates. For clarity, results are sorted and reported into tiers spanning multiple pages, the tiering criteria being rank 1 hit rate on a gallery size of 640 000.

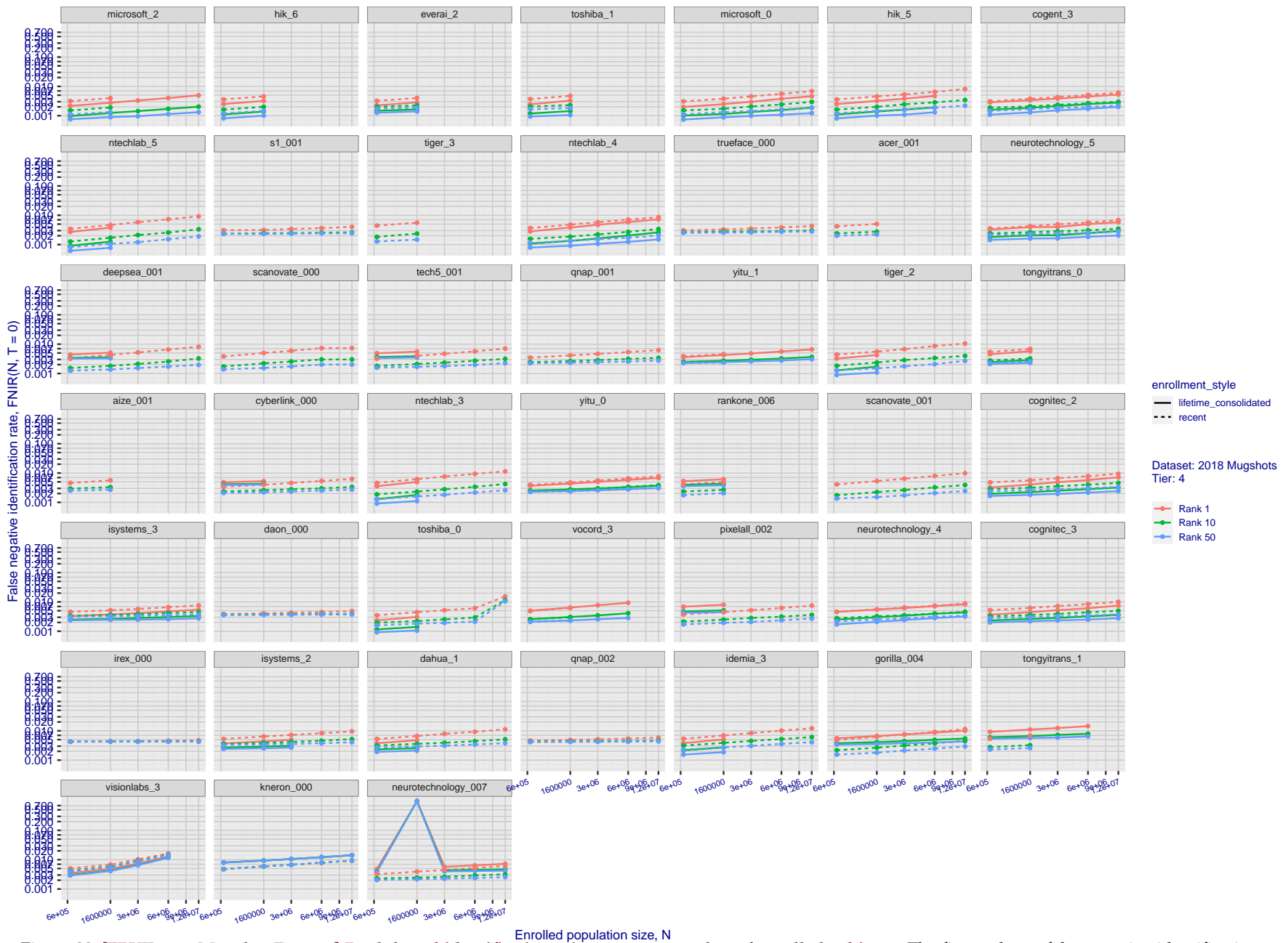


Figure 23: [FRVT-2018 Mugshot Dataset] Rank-based identification miss rates vs. number of enrolled subjects. The figure shows false negative identification rates,  $\text{FNIR}(N, R)$ , across various gallery sizes and ranks 1, 10 and 50. The threshold is set to zero, so this metric rewards even weak scoring rank 1 mates. This also means  $\text{FPIR} = 1$ , so any search without an enrolled mate will return non-mated candidates. For clarity, results are sorted and reported into tiers spanning multiple pages, the tiering criteria being rank 1 hit rate on a gallery size of 640 000.

2022/06/13 09:55:40

FNIR( $N, R, T$ ) = False neg. identification rate  
FPIR( $N, T$ ) = False pos. identification rate $N$  = Num. enrolled subjects  
 $R$  = Num. candidates examined $T$  = Threshold  
 $T = 0 \rightarrow$  Investigation $T > 0 \rightarrow$  Identification

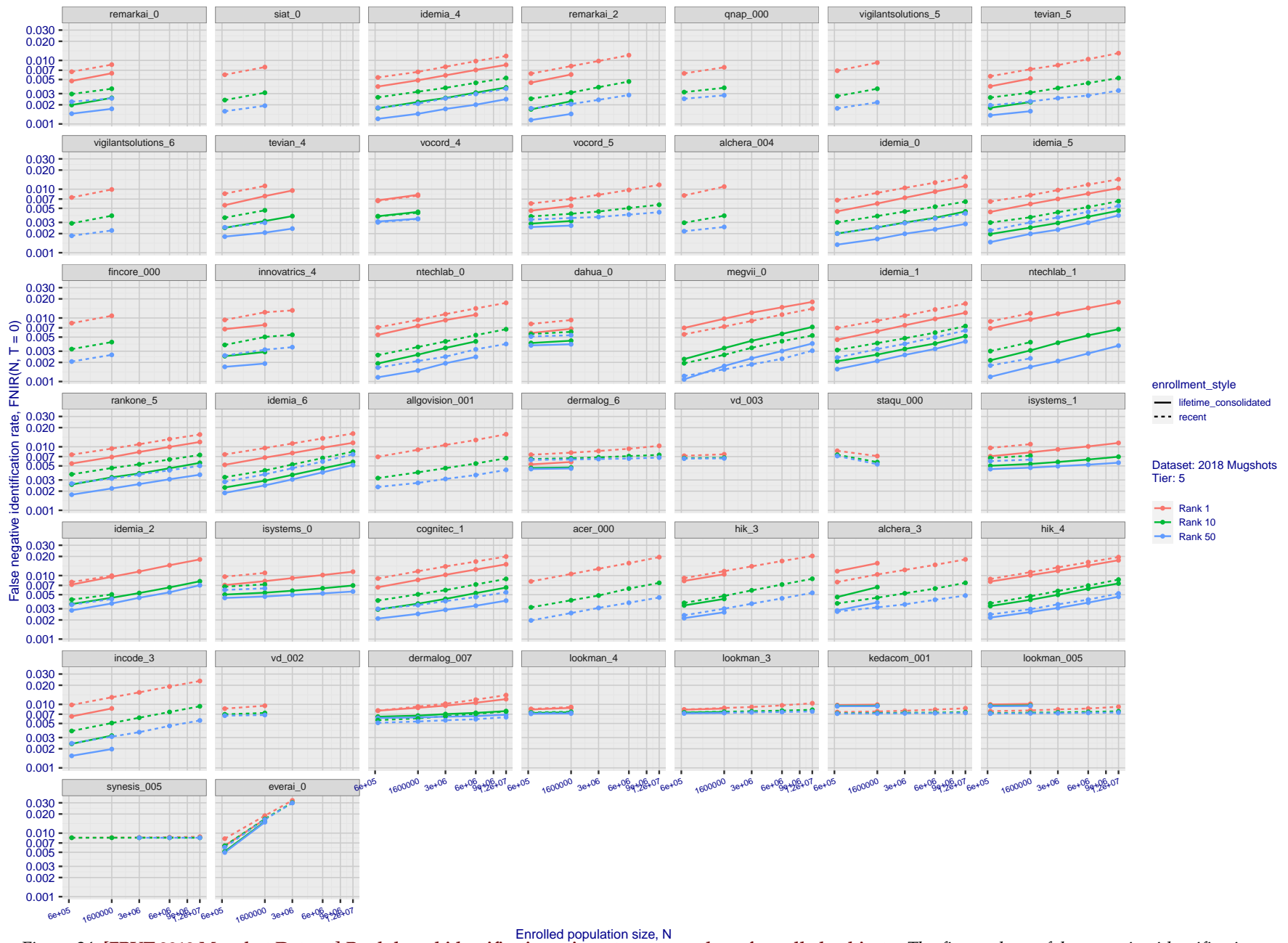
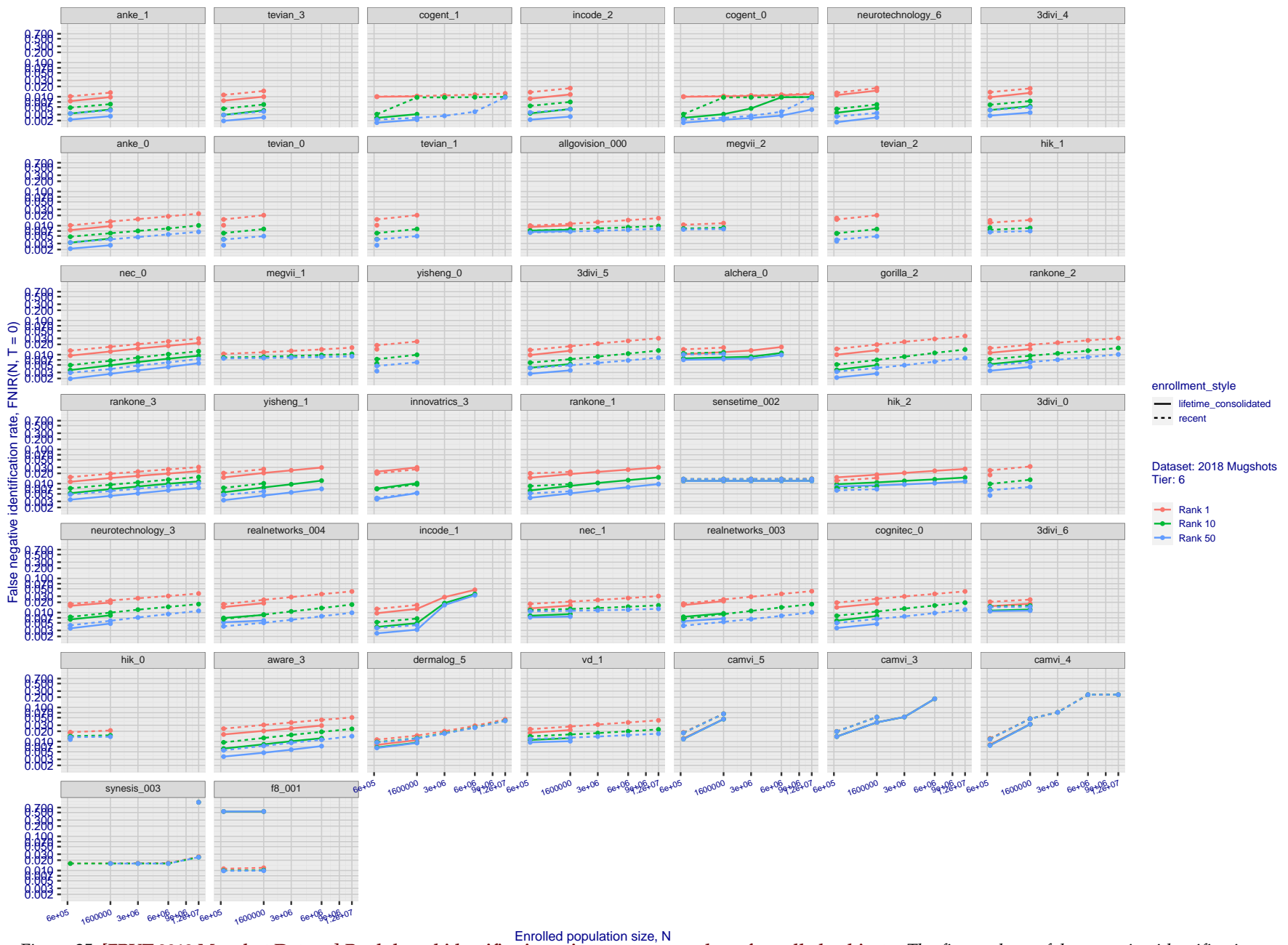


Figure 24: [FRVT-2018 Mugshot Dataset] Rank-based identification miss rates vs. number of enrolled subjects. The figure shows false negative identification rates,  $\text{FNIR}(N, R)$ , across various gallery sizes and ranks 1, 10 and 50. The threshold is set to zero, so this metric rewards even weak scoring rank 1 mates. This also means  $\text{FPIR} = 1$ , so any search without an enrolled mate will return non-mated candidates. For clarity, results are sorted and reported into tiers spanning multiple pages, the tiering criteria being rank 1 hit rate on a gallery size of 640 000.

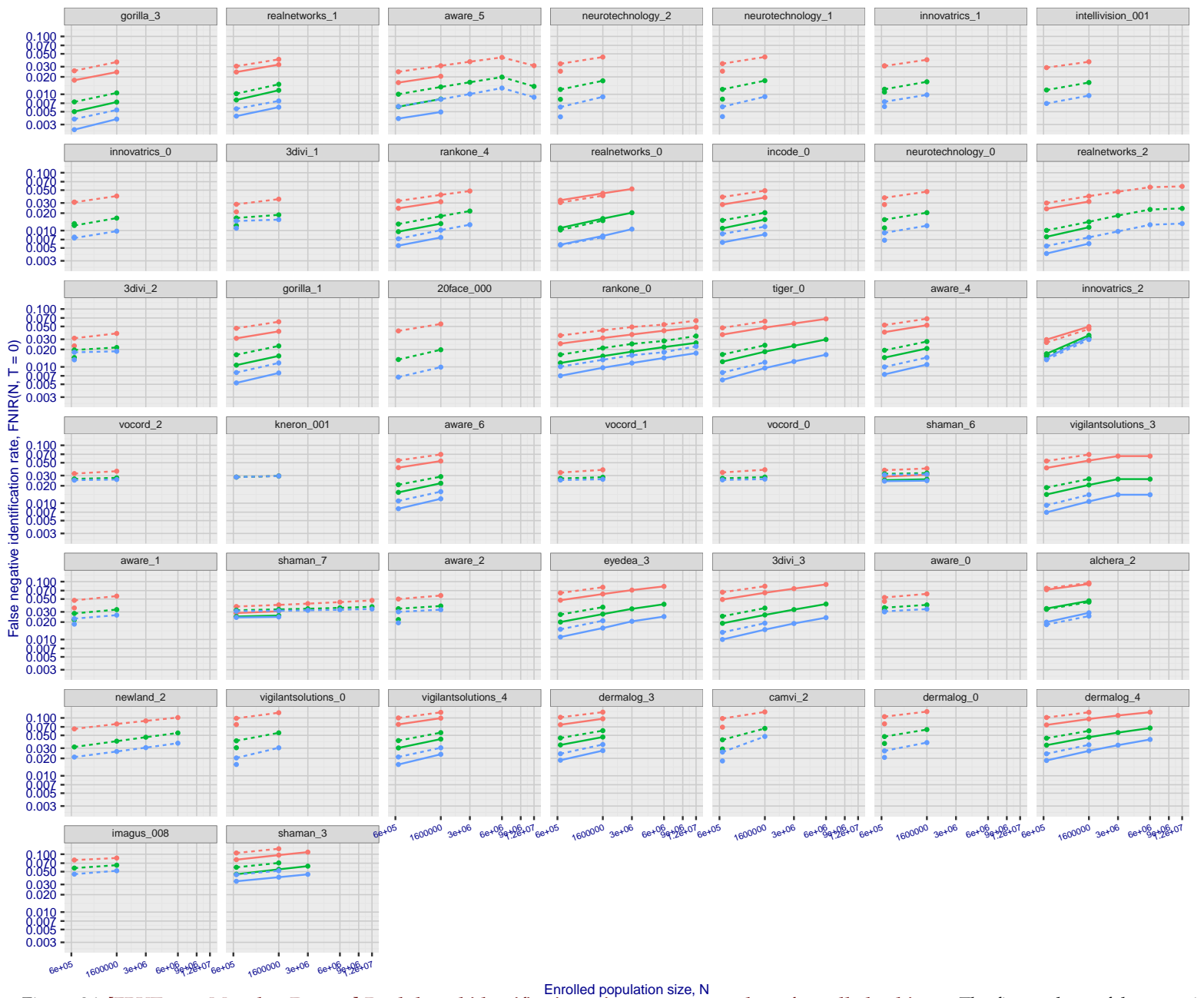
2022 / 06 / 13  
09:55:40FNIR( $N, R, T = 0$ ) = False neg. identification rate  
FPIR( $N, T = 0$ ) = False pos. identification rate $N = \text{Num. enrolled subjects}$   
 $R = \text{Num. candidates examined}$  $T = \text{Threshold}$  $T = 0 \rightarrow \text{Investigation}$   
 $T > 0 \rightarrow \text{Identification}$



2022/06/13

09:55:40

FNIR( $N, R, T = 0$ )  
FPIR( $N, T = 0$ )  
False pos. identification rate $N = \text{Num. enrolled subjects}$  $T = \text{Threshold}$   
 $T = 0 \rightarrow \text{Investigation}$   
 $T > 0 \rightarrow \text{Identification}$



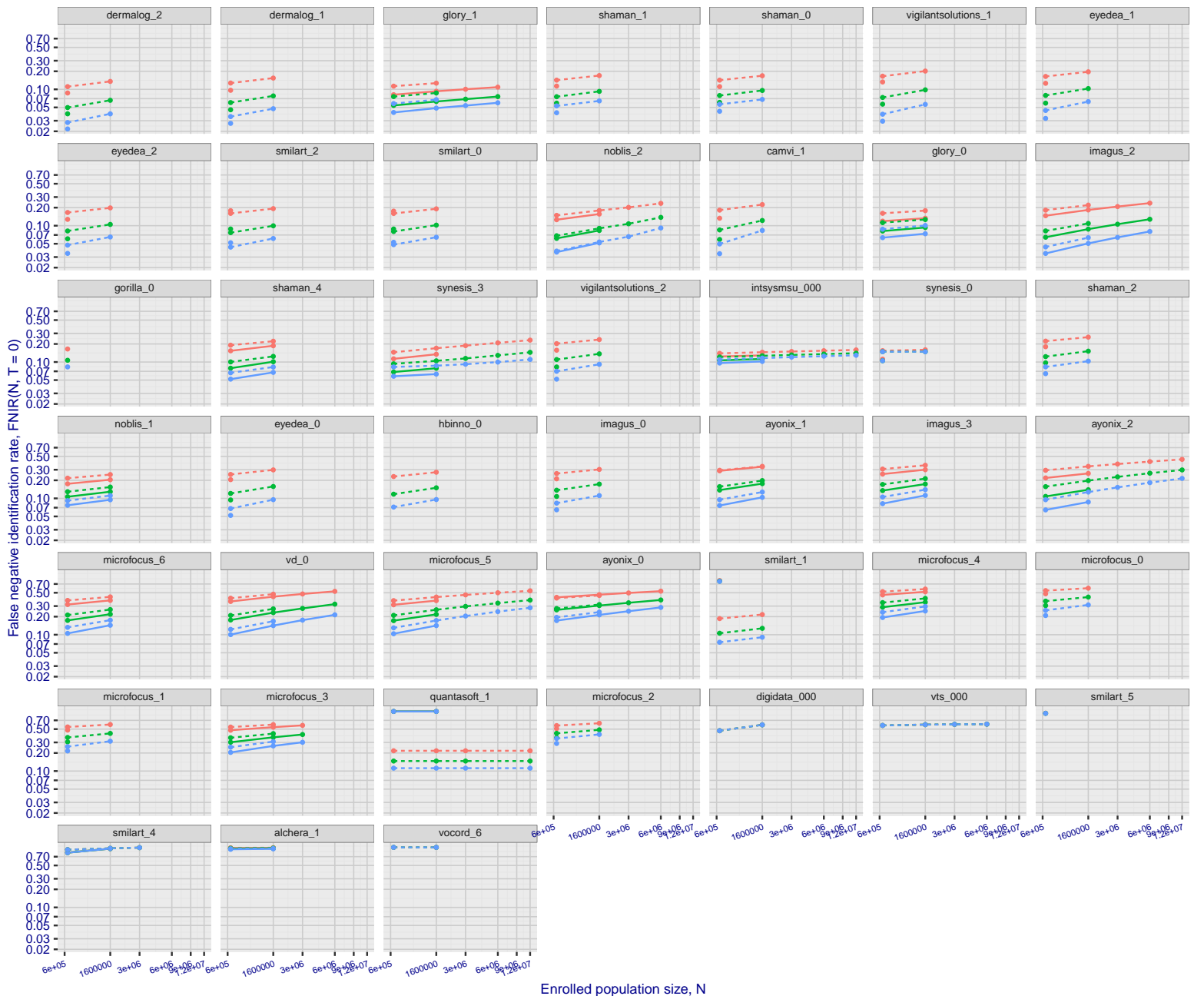


**Figure 27: [FRVT-2018 Mugshot Dataset] Rank-based identification miss rates vs. number of enrolled subjects.** The figure shows false negative identification rates,  $\text{FNIR}(N, R)$ , across various gallery sizes and ranks 1, 10 and 50. The threshold is set to zero, so this metric rewards even weak scoring rank 1 mates. This also means  $\text{FPIR} = 1$ , so any search without an enrolled mate will return non-mated candidates. For clarity, results are sorted and reported into tiers spanning multiple pages, the tiering criteria being rank 1 hit rate on a gallery size of 640 000.

2022/06/13  
09:55:40FNIR(N, R, T) =  
FPIR(N, T) =  
False neg. identification rate  
False pos. identification rateN = Num. enrolled subjects  
R = Num. candidates examined

T = Threshold

T = 0 → Investigation  
T > 0 → Identification

2022/06/13 09:55:40	$\text{FNIR}(N, R, T) =$ $\text{FPTR}(N, T) =$	False neg. identification rate False pos. identification rate	$N =$ Num. enrolled subjects $R =$ Num. candidates examined	$T =$ Threshold $T > 0 \rightarrow$ Identification	$T = 0 \rightarrow$ Investigation
------------------------	---------------------------------------------------	------------------------------------------------------------------	----------------------------------------------------------------	-------------------------------------------------------	-----------------------------------

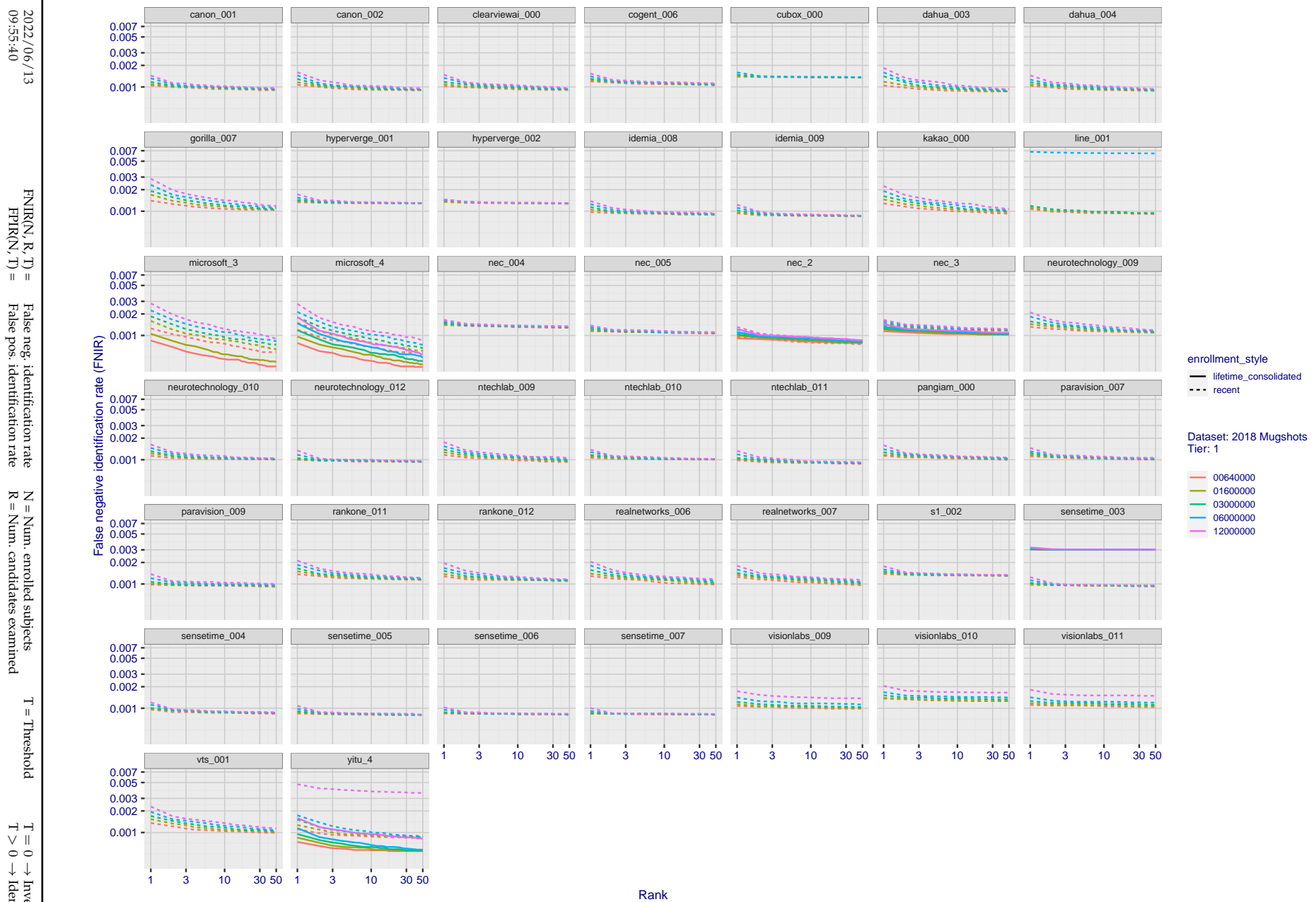


**Figure 28: [FRVT-2018 Mugshot Dataset] Rank-based identification miss rates vs. rank.** The figure shows false negative identification rates (FNIR) for ranks up to 50. This metric is appropriate to investigational applications where human reviewers will adjudicate sorted candidate lists. Note that with threshold set to zero, FPIR = 1, i.e. any search without an enrolled mate will return non-mated candidates. Results are sorted and reported into tiers for clarity, with the tiering criteria being rank 1 hit rate on a gallery size of N = 640 000 subjects.

2022 / 06 / 13  
09:55:40  
  
 $\text{FNIR}(N, R, T) = \text{False neg. identification rate}$   
 $\text{FPIR}(N, T) = \text{False pos. identification rate}$   
 $N = \text{Num. enrolled subjects}$   
 $R = \text{Num. candidates examined}$   
 $T = \text{Threshold}$   
 $T = 0 \rightarrow \text{Investigation}$   
 $T > 0 \rightarrow \text{Identification}$

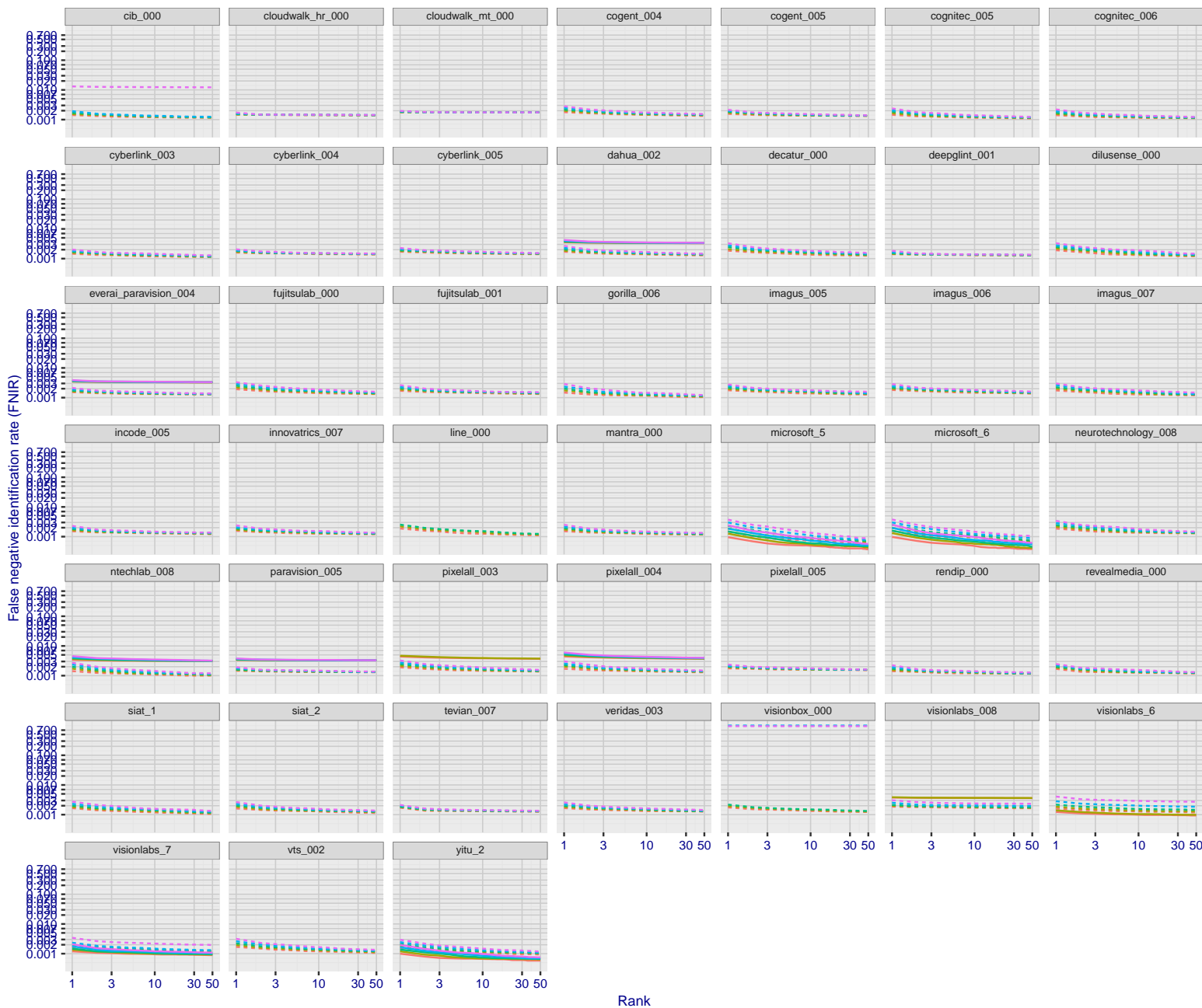


Figure 29: [FRVT-2018 Mugshot Dataset] Rank-based identification miss rates vs. rank. The figure shows false negative identification rates (FNIR) for ranks up to 50. This metric is appropriate to investigational applications where human reviewers will adjudicate sorted candidate lists. Note that with threshold set to zero, FPIR = 1, i.e. any search without an enrolled mate will return non-mated candidates. Results are sorted and reported into tiers for clarity, with the tiering criteria being rank 1 hit rate on a gallery size of  $N = 640\,000$  subjects.

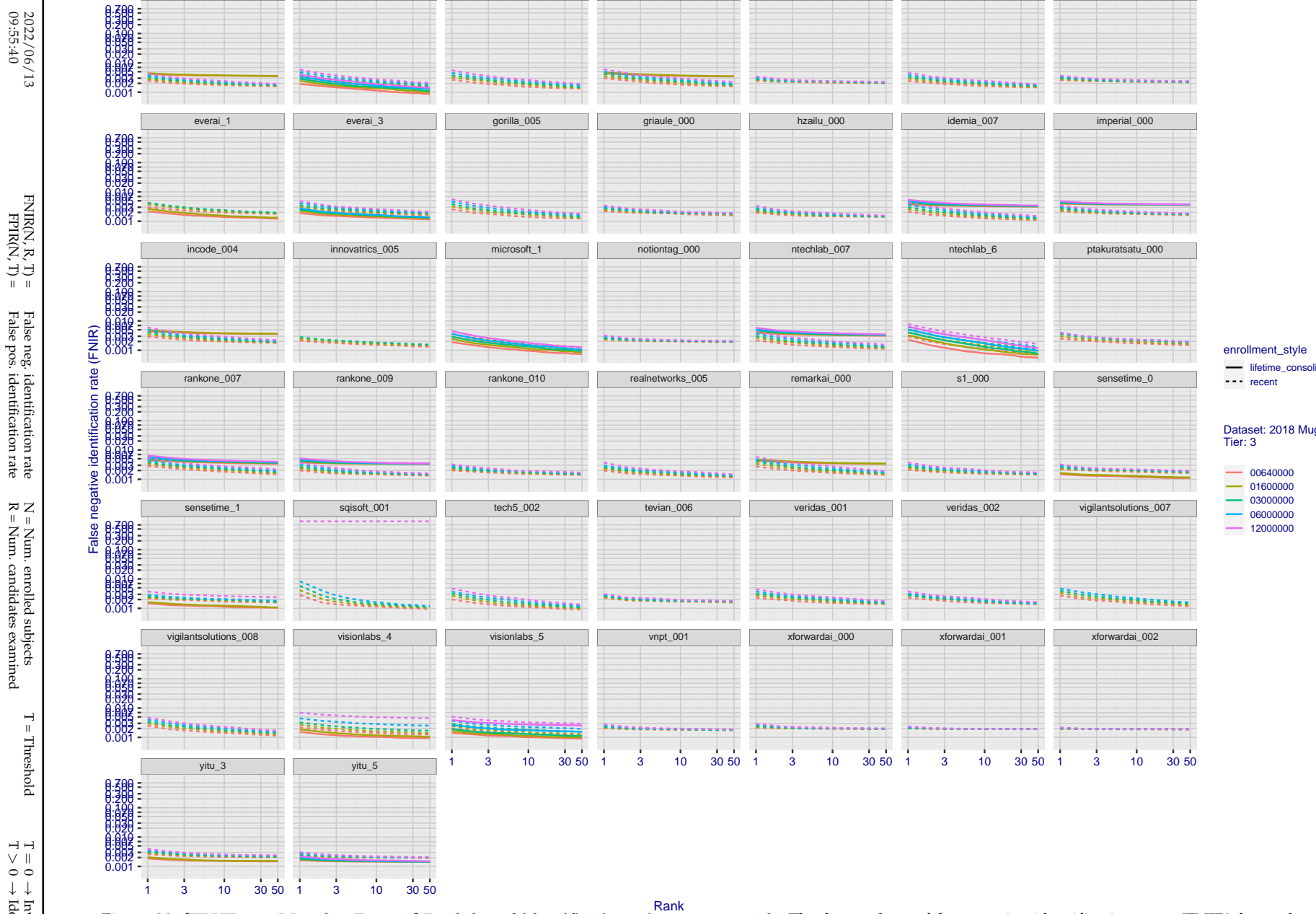
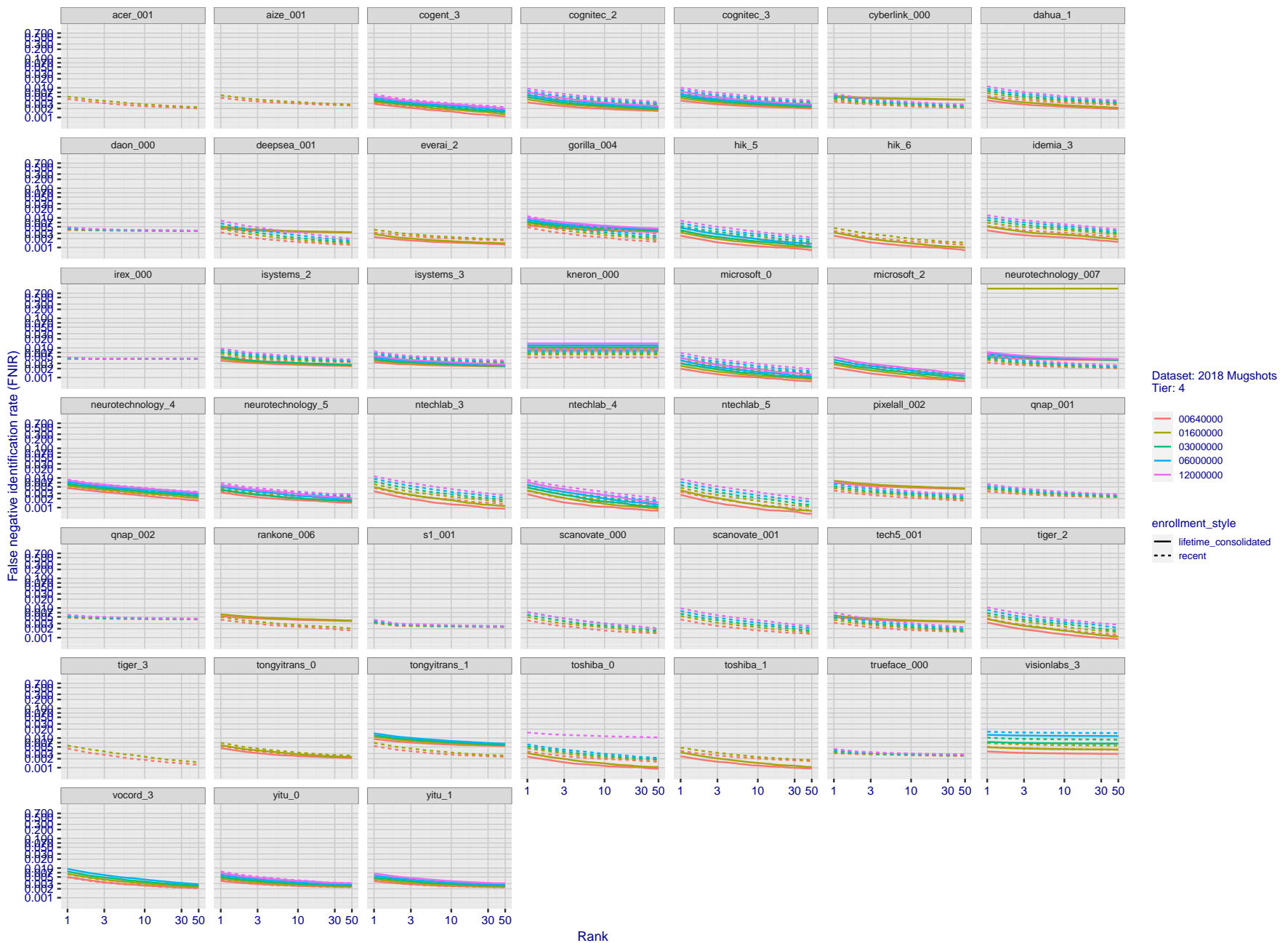


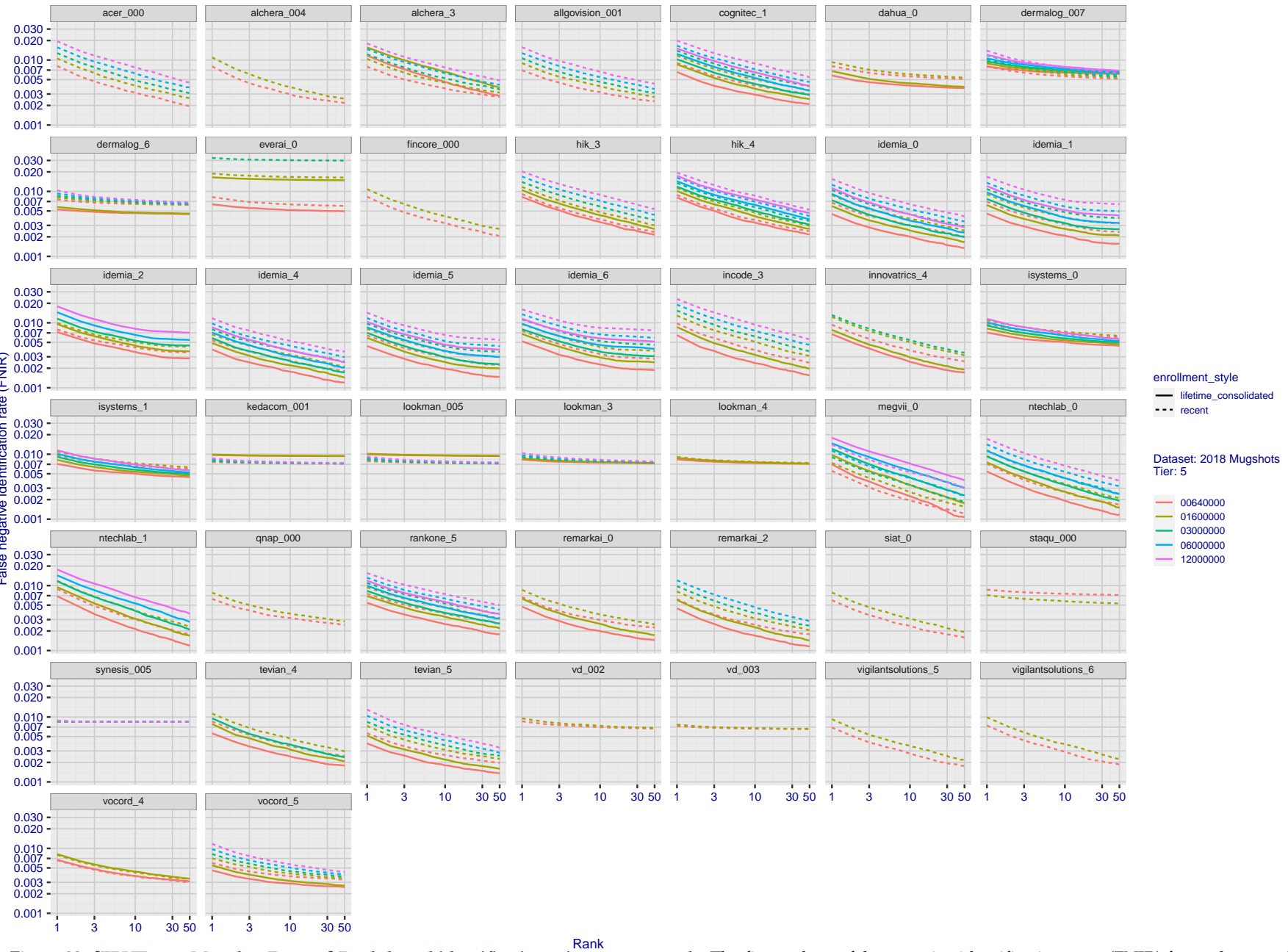
Figure 30: [FRVT-2018 Mugshot Dataset] Rank-based identification miss rates vs. rank. The figure shows false negative identification rates (FNIR) for ranks up to 50. This metric is appropriate to investigational applications where human reviewers will adjudicate sorted candidate lists. Note that with threshold set to zero, FPIR = 1, i.e. any search without an enrolled mate will return non-mated candidates. Results are sorted and reported into tiers for clarity, with the tiering criteria being rank 1 hit rate on a gallery size of N = 640 000 subjects.



**Figure 31: [FRVT-2018 Mugshot Dataset] Rank-based identification miss rates vs. rank.** The figure shows false negative identification rates (FNIR) for ranks up to 50. This metric is appropriate to investigational applications where human reviewers will adjudicate sorted candidate lists. Note that with threshold set to zero, FPIR = 1, i.e. any search without an enrolled mate will return non-mated candidates. Results are sorted and reported into tiers for clarity, with the tiering criteria being rank 1 hit rate on a gallery size of N = 640 000 subjects.

2022/06/13  
09:55:40FNIR(N, R, T) = False neg. identification rate  
FPIR(N, T) = False pos. identification rateN = Num. enrolled subjects  
R = Num. candidates examined

T = Threshold

T = 0 → Investigation  
 $T > 0 \rightarrow$  Identification

**Figure 32: [FRVT-2018 Mugshot Dataset] Rank-based identification miss rates vs. rank.** The figure shows false negative identification rates (FNIR) for ranks up to 50. This metric is appropriate to investigational applications where human reviewers will adjudicate sorted candidate lists. Note that with threshold set to zero, FPIR = 1, i.e. any search without an enrolled mate will return non-mated candidates. Results are sorted and reported into tiers for clarity, with the tiering criteria being rank 1 hit rate on a gallery size of N = 640 000 subjects.

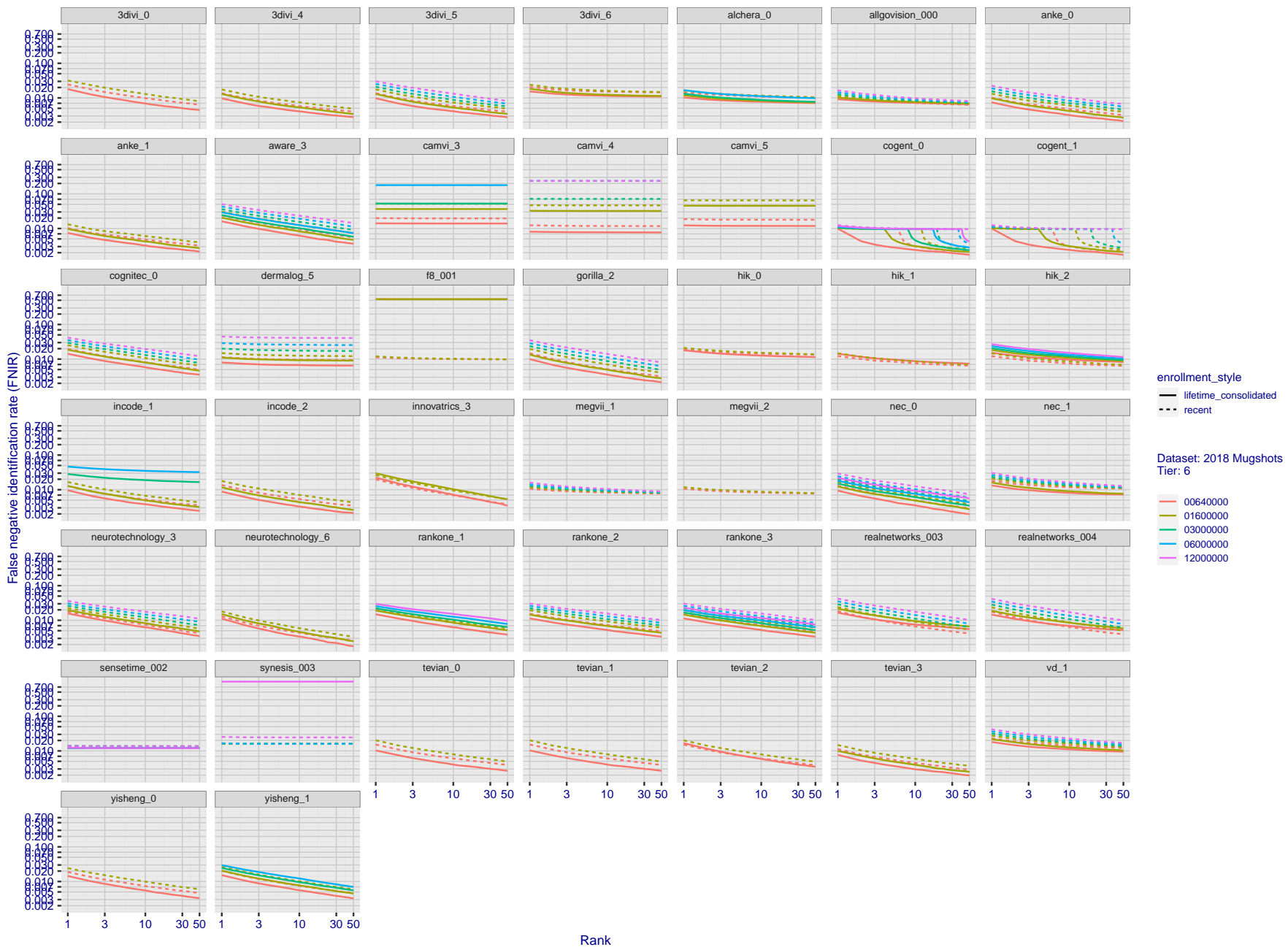


Figure 33: [FRVT-2018 Mugshot Dataset] Rank-based identification miss rates vs. rank. The figure shows false negative identification rates (FNIR) for ranks up to 50. This metric is appropriate to investigational applications where human reviewers will adjudicate sorted candidate lists. Note that with threshold set to zero, FPIR = 1, i.e. any search without an enrolled mate will return non-mated candidates. Results are sorted and reported into tiers for clarity, with the tiering criteria being rank 1 hit rate on a gallery size of  $N = 640\,000$  subjects.

2022 / 06 / 13

09:55:40

FNIR( $N, R, T$ ) = False neg. identification rateFPIR( $N, T$ ) = False pos. identification rate $N =$  Num. enrolled subjects

T = Threshold

T = 0 → Investigation

T &gt; 0 → Identification

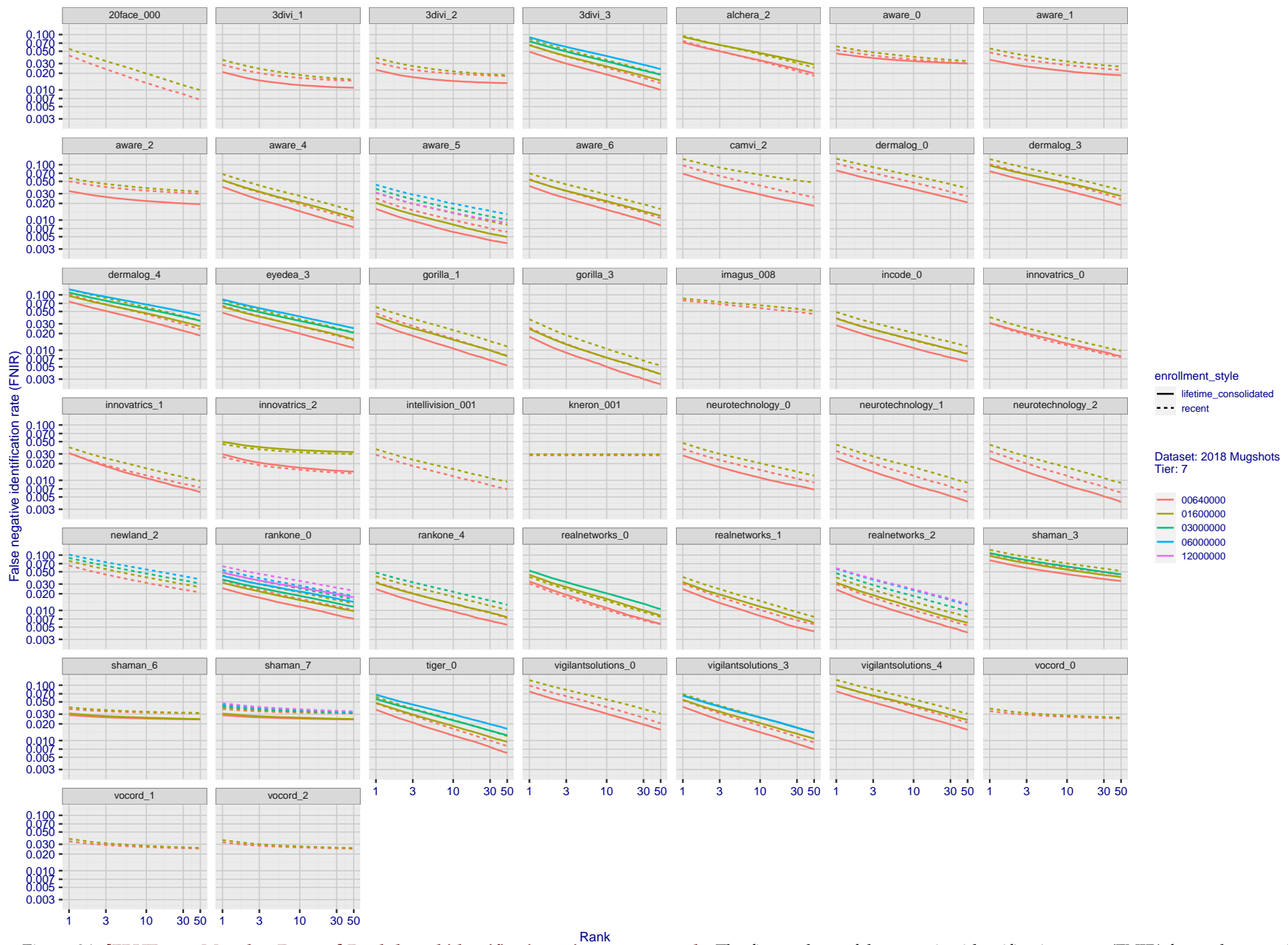


Figure 34: [FRVT-2018 Mugshot Dataset] Rank-based identification miss rates vs. rank. The figure shows false negative identification rates (FNIR) for ranks up to 50. This metric is appropriate to investigational applications where human reviewers will adjudicate sorted candidate lists. Note that with threshold set to zero, FPIR = 1, i.e. any search without an enrolled mate will return non-mated candidates. Results are sorted and reported into tiers for clarity, with the tiering criteria being rank 1 hit rate on a gallery size of  $N = 640\,000$  subjects.

2022/06/13  
09:55:40FNIR( $N, R, T$ ) = False neg. identification rate  
FPIR( $N, T$ ) = False pos. identification rate $N$  = Num. enrolled subjects  
 $R$  = Num. candidates examined $T$  = Threshold $T = 0 \rightarrow$  Investigation  
 $T > 0 \rightarrow$  Identification

2022/06/13  
09:55:40  
  
 $\text{FNIR}(N, R, T) = \text{False neg. identification rate}$   
 $\text{FPIR}(N, T) = \text{False pos. identification rate}$   
 $N = \text{Num. enrolled subjects}$   
 $R = \text{Num. candidates examined}$   
 $T = \text{Threshold}$   
 $T = 0 \rightarrow \text{Investigation}$   
 $T > 0 \rightarrow \text{Identification}$

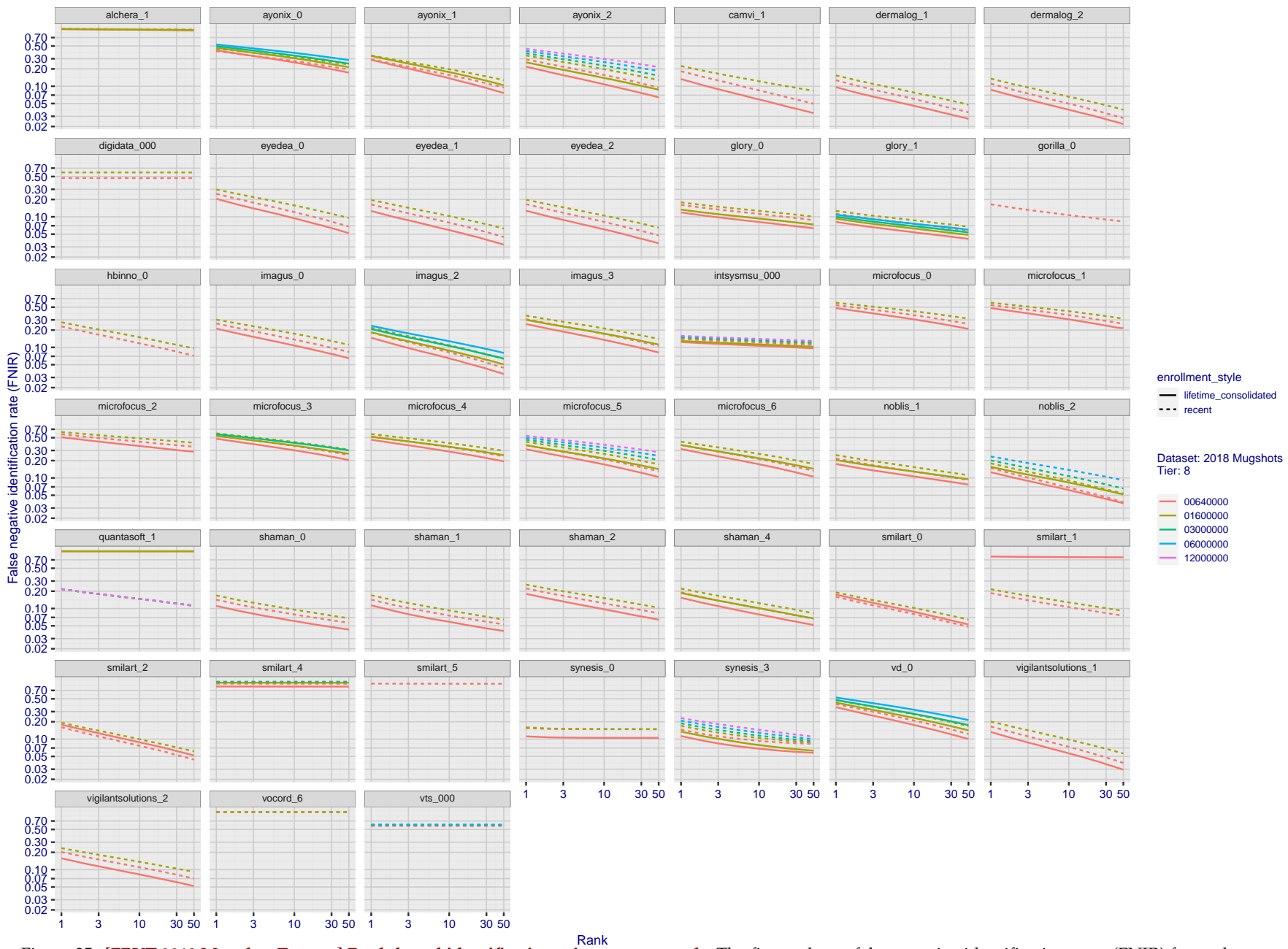
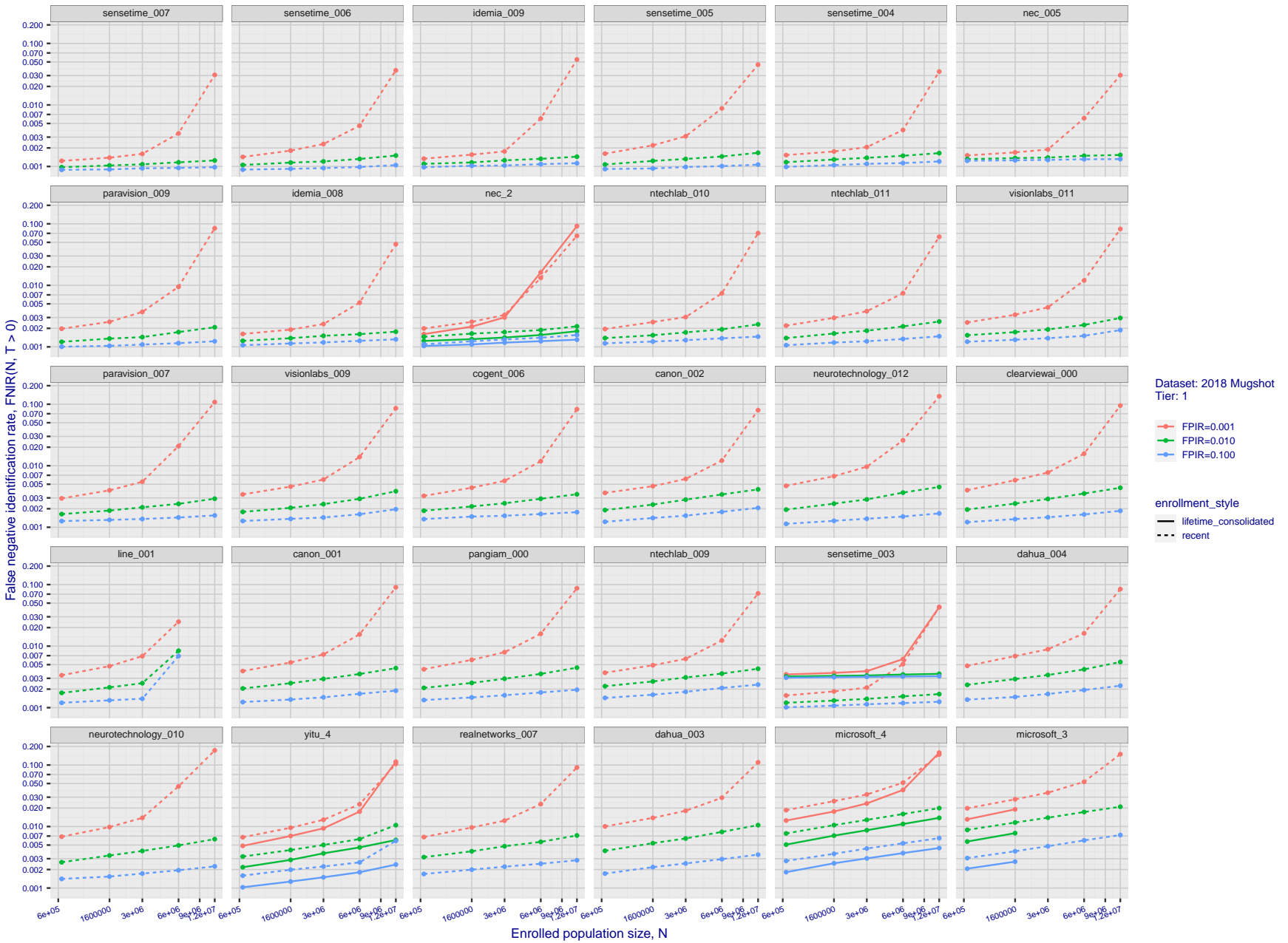


Figure 35: [FRVT-2018 Mugshot Dataset] Rank-based identification miss rates vs. rank. The figure shows false negative identification rates (FNIR) for ranks up to 50. This metric is appropriate to investigational applications where human reviewers will adjudicate sorted candidate lists. Note that with threshold set to zero, FPIR = 1, i.e. any search without an enrolled mate will return non-mated candidates. Results are sorted and reported into tiers for clarity, with the tiering criteria being rank 1 hit rate on a gallery size of  $N = 640\,000$  subjects.

2022/06/13 09:55:40	$\text{FNIR}(N, R, T) =$ $\text{FPTR}(N, T) =$	False neg. identification rate False pos. identification rate	$N =$ Num. enrolled subjects $R =$ Num. candidates examined	$T =$ Threshold $T > 0 \rightarrow$ Identification	$T = 0 \rightarrow$ Investigation
------------------------	---------------------------------------------------	------------------------------------------------------------------	----------------------------------------------------------------	-------------------------------------------------------	-----------------------------------



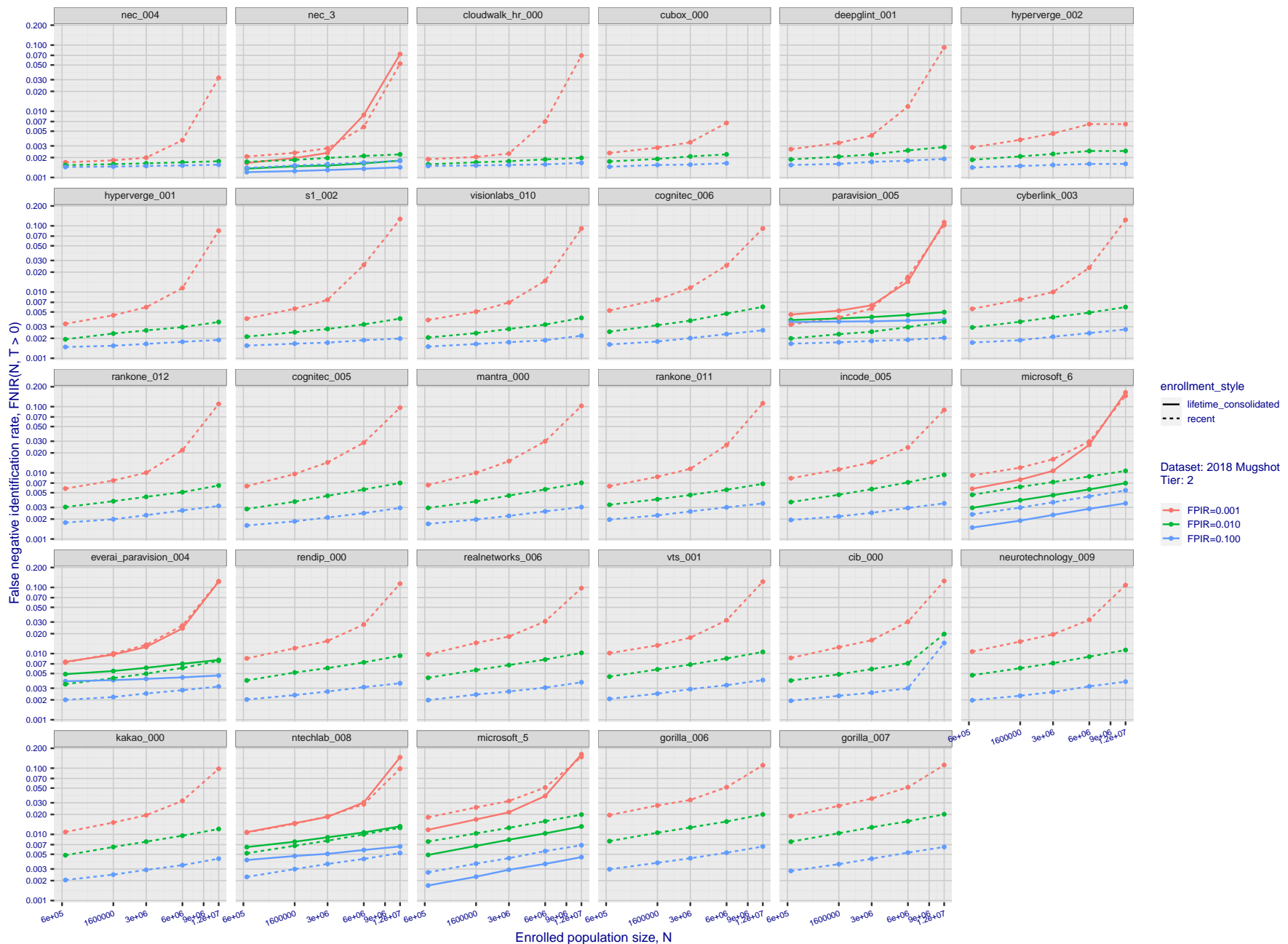


Figure 37: [FRVT-2018 Mugshot Dataset] Threshold-based identification miss rates vs. number of enrolled subjects. The figure shows FNIR( $N, T$ ) across various gallery sizes when the threshold is set to achieve the given FPIRs. The rank criterion is irrelevant at high thresholds as mates are always at rank 1. The results are computed from the trials listed in rows 1-10 of Table 1. Less accurate algorithms were not run on large  $N$ , so results are missing. For clarity, results are sorted and reported into tiers spanning multiple pages. The tiering criteria is complicated: First paging by  $\text{FNIR}(N_b, 1, 0)$ , then sorting by median  $\text{FNIR}(N_b, T)$ ,  $N_b = 640\,000$ .

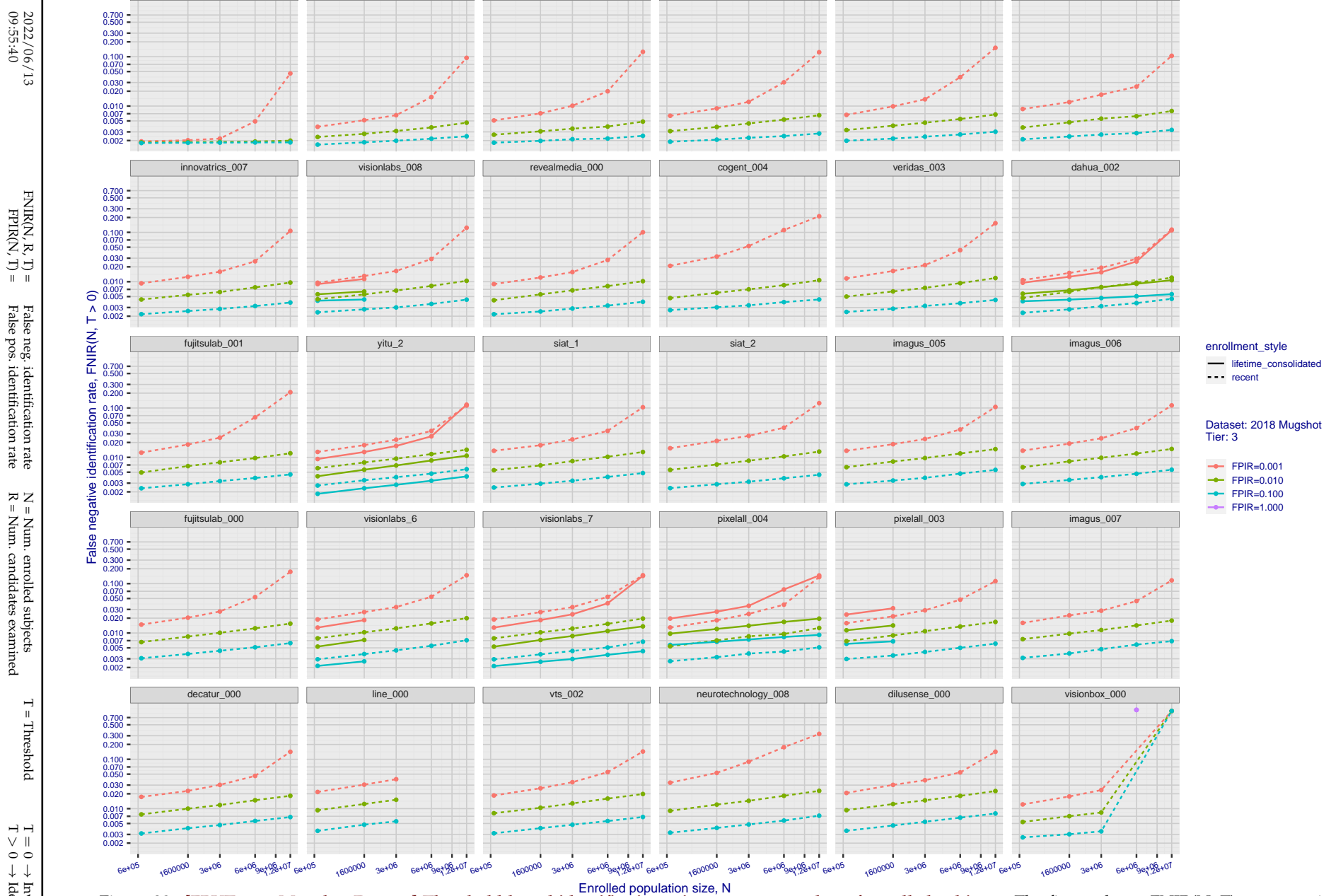


Figure 38: [FRVT-2018 Mugshot Dataset] Threshold-based identification miss rates vs. number of enrolled subjects. The figure shows  $\text{FNIR}(N, T)$  across various gallery sizes when the threshold is set to achieve the given FPIRs. The rank criterion is irrelevant at high thresholds as mates are always at rank 1. The results are computed from the trials listed in rows 1-10 of Table 1. Less accurate algorithms were not run on large  $N$ , so results are missing. For clarity, results are sorted and reported into tiers spanning multiple pages. The tiering criteria is complicated: First paging by  $\text{FNIR}(N_b, 1, 0)$ , then sorting by median  $\text{FNIR}(N_b, T)$ ,  $N_b = 640\,000$ .

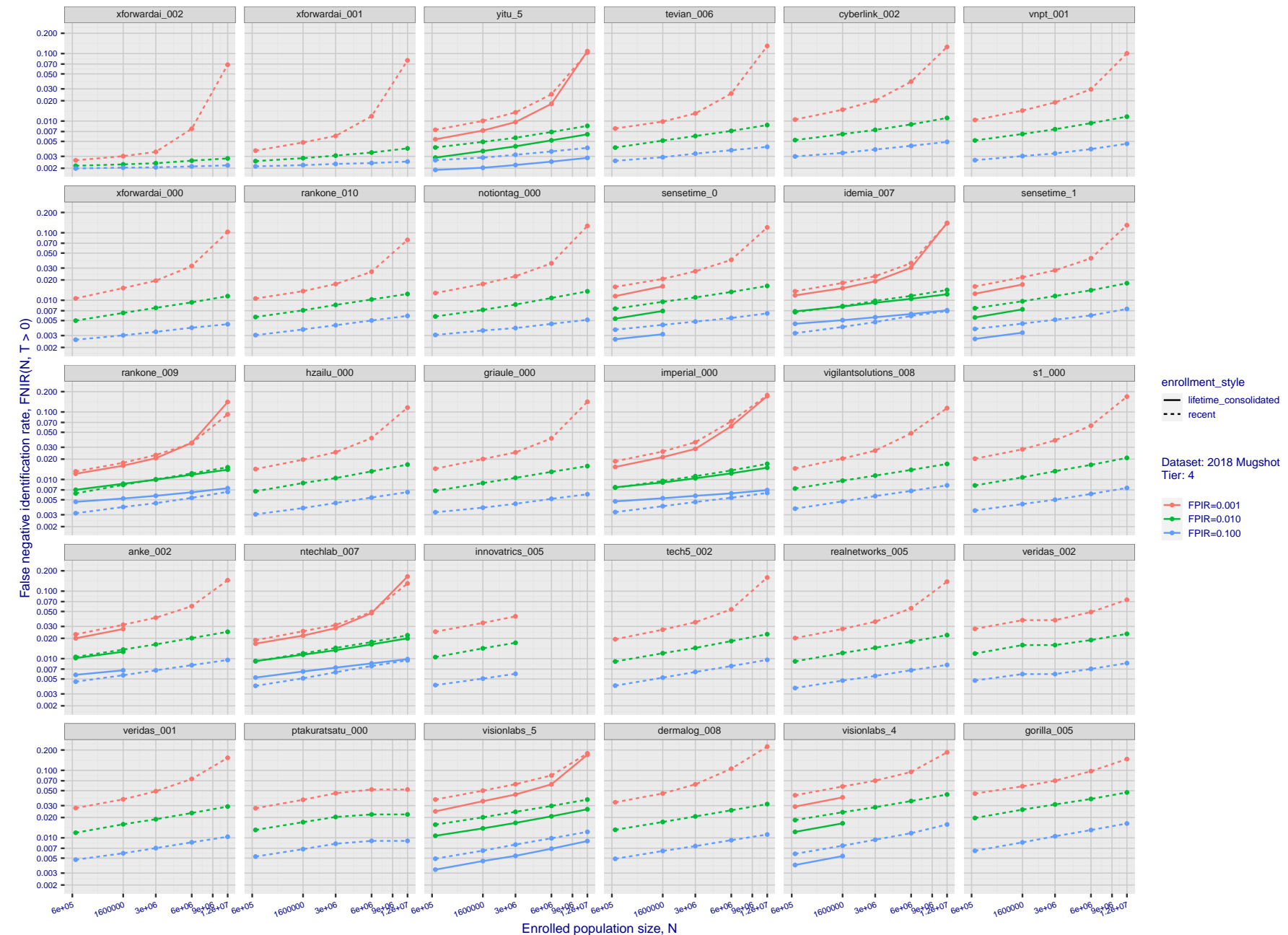


Figure 39: [FRVT-2018 Mugshot Dataset] Threshold-based identification miss rates vs. number of enrolled subjects. The figure shows  $\text{FNIR}(N, T)$  across various gallery sizes when the threshold is set to achieve the given FPIRs. The rank criterion is irrelevant at high thresholds as mates are always at rank 1. The results are computed from the trials listed in rows 1-10 of Table 1. Less accurate algorithms were not run on large  $N$ , so results are missing. For clarity, results are sorted and reported into tiers spanning multiple pages. The tiering criteria is complicated: First paging by  $\text{FNIR}(N_b, 1, 0)$ , then sorting by median  $\text{FNIR}(N_b, T)$ ,  $N_b = 640\,000$ .

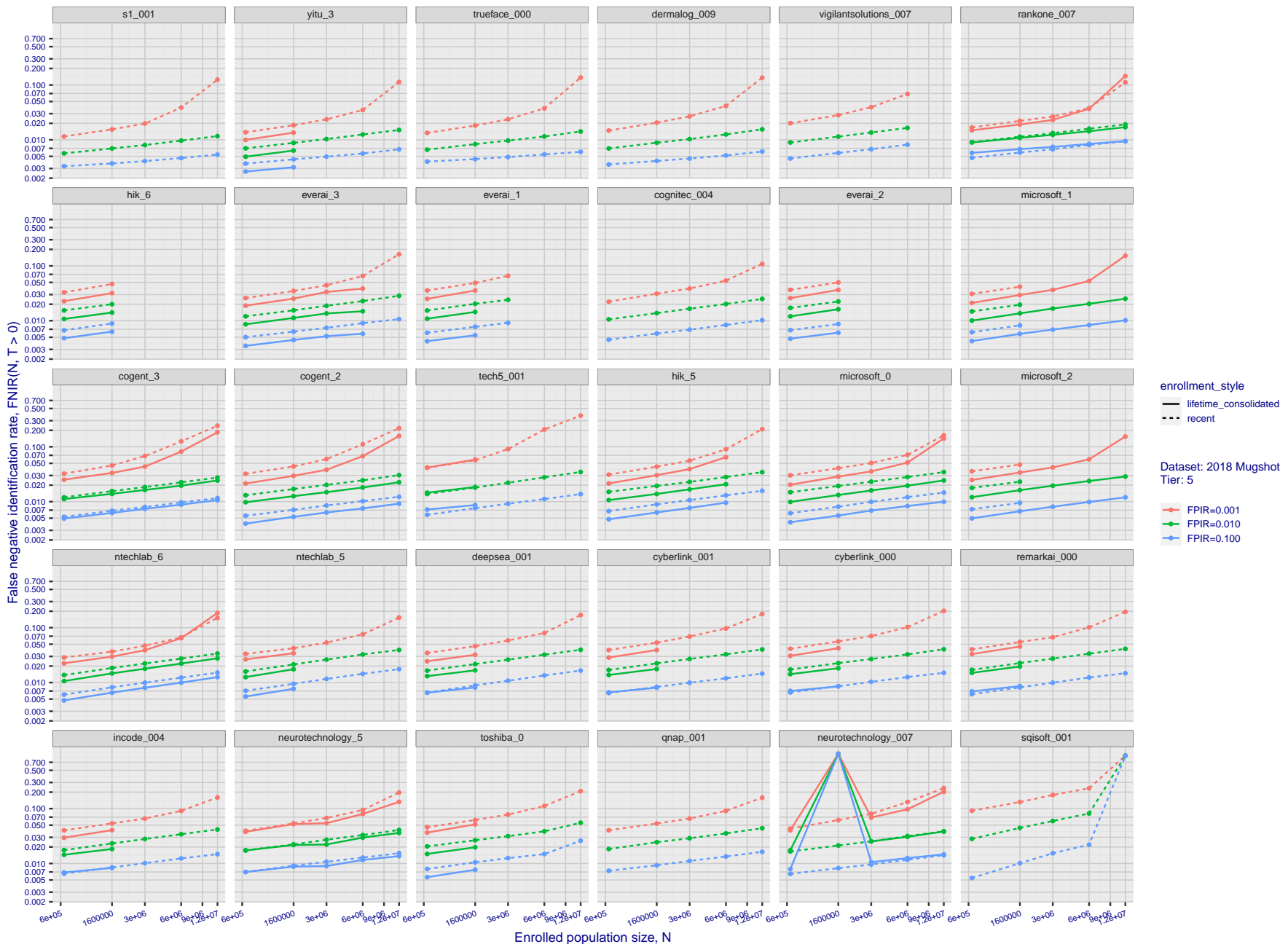
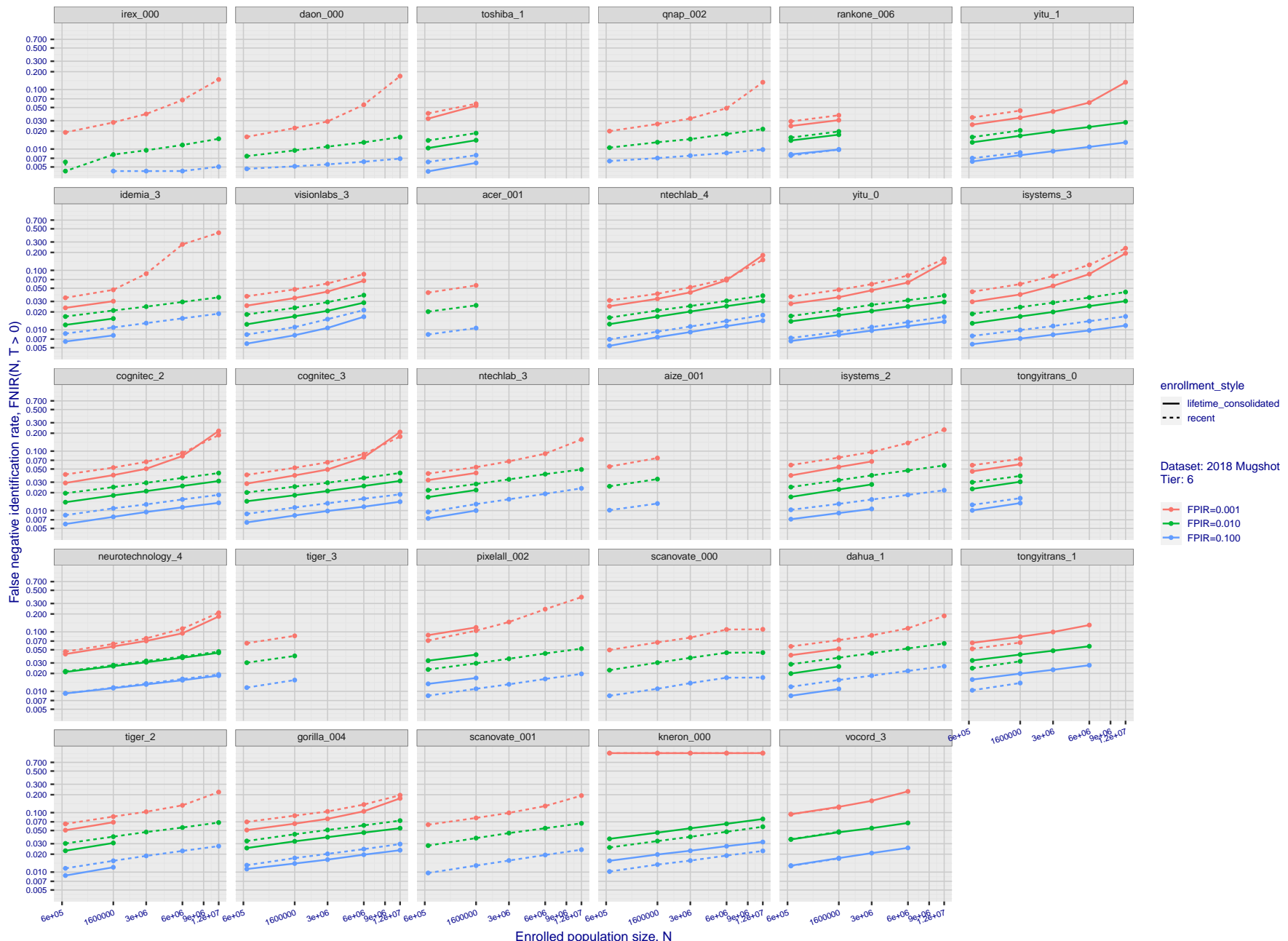
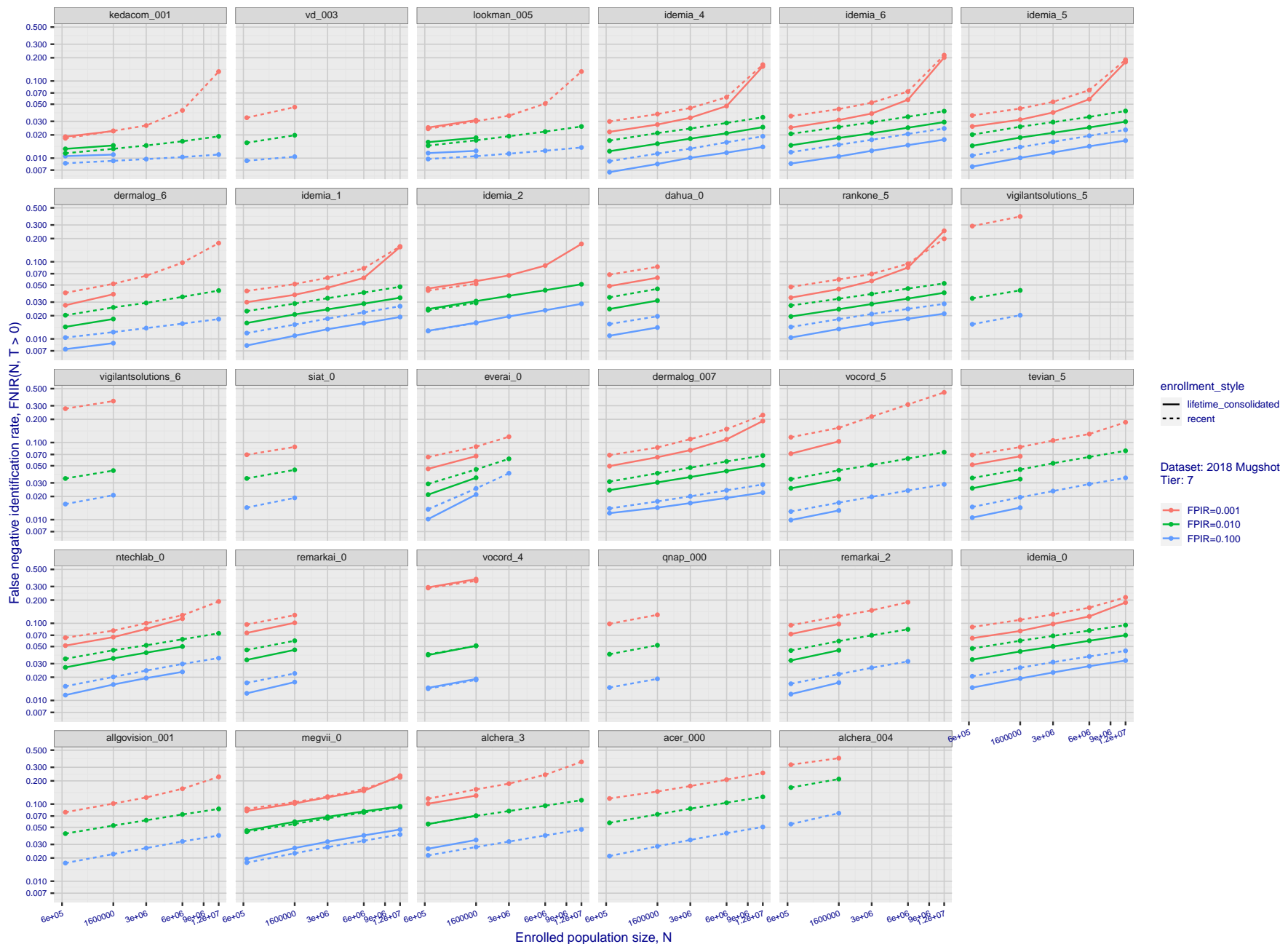


Figure 40: [FRVT-2018 Mugshot Dataset] Threshold-based identification miss rates vs. number of enrolled subjects. The figure shows FNIR( $N, T$ ) across various gallery sizes when the threshold is set to achieve the given FPIRs. The rank criterion is irrelevant at high thresholds as mates are always at rank 1. The results are computed from the trials listed in rows 1-10 of Table 1. Less accurate algorithms were not run on large  $N$ , so results are missing. For clarity, results are sorted and reported into tiers spanning multiple pages. The tiering criteria is complicated: First paging by FNIR( $N_b, 1, 0$ ), then sorting by median FNIR( $N_b, T$ ),  $N_b = 640\,000$ .



**Figure 41: [FRVT-2018 Mugshot Dataset] Threshold-based identification miss rates vs. number of enrolled subjects.** The figure shows FNIR( $N, T$ ) across various gallery sizes when the threshold is set to achieve the given FPIRs. The rank criterion is irrelevant at high thresholds as mates are always at rank 1. The results are computed from the trials listed in rows 1-10 of Table 1. Less accurate algorithms were not run on large  $N$ , so results are missing. For clarity, results are sorted and reported into tiers spanning multiple pages. The tiering criteria is complicated: First paging by  $\text{FNIR}(N_b, 1, 0)$ , then sorting by median  $\text{FNIR}(N_b, T)$ ,  $N_b = 640\,000$ .



**Figure 42: [FRVT-2018 Mugshot Dataset] Threshold-based identification miss rates vs. number of enrolled subjects.** The figure shows FNIR( $N, T$ ) across various gallery sizes when the threshold is set to achieve the given FPIRs. The rank criterion is irrelevant at high thresholds as mates are always at rank 1. The results are computed from the trials listed in rows 1-10 of Table 1. Less accurate algorithms were not run on large  $N$ , so results are missing. For clarity, results are sorted and reported into tiers spanning multiple pages. The tiering criteria is complicated: First paging by  $\text{FNIR}(N_b, 1, 0)$ , then sorting by median  $\text{FNIR}(N_b, T)$ ,  $N_b = 640\,000$ .

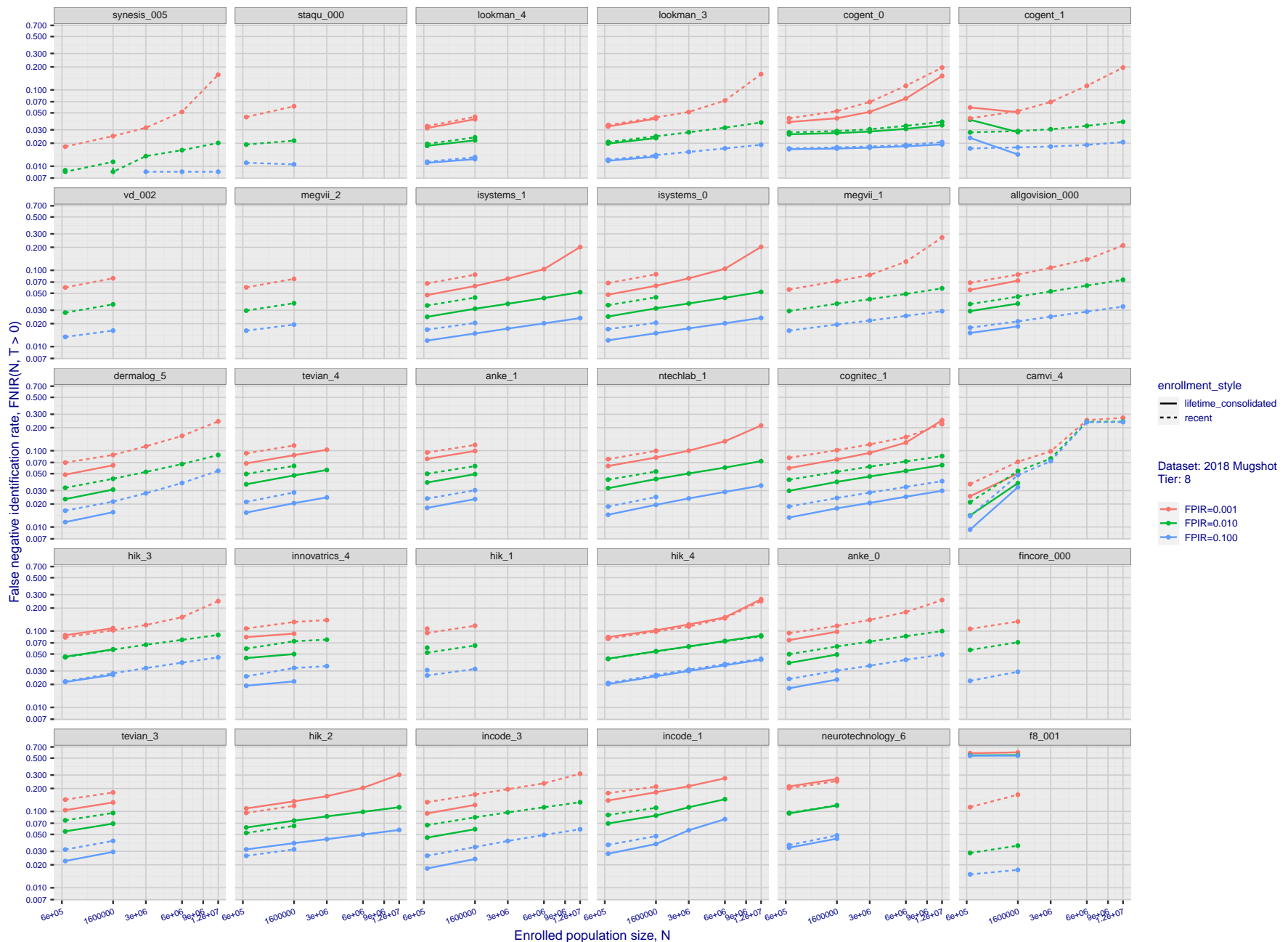
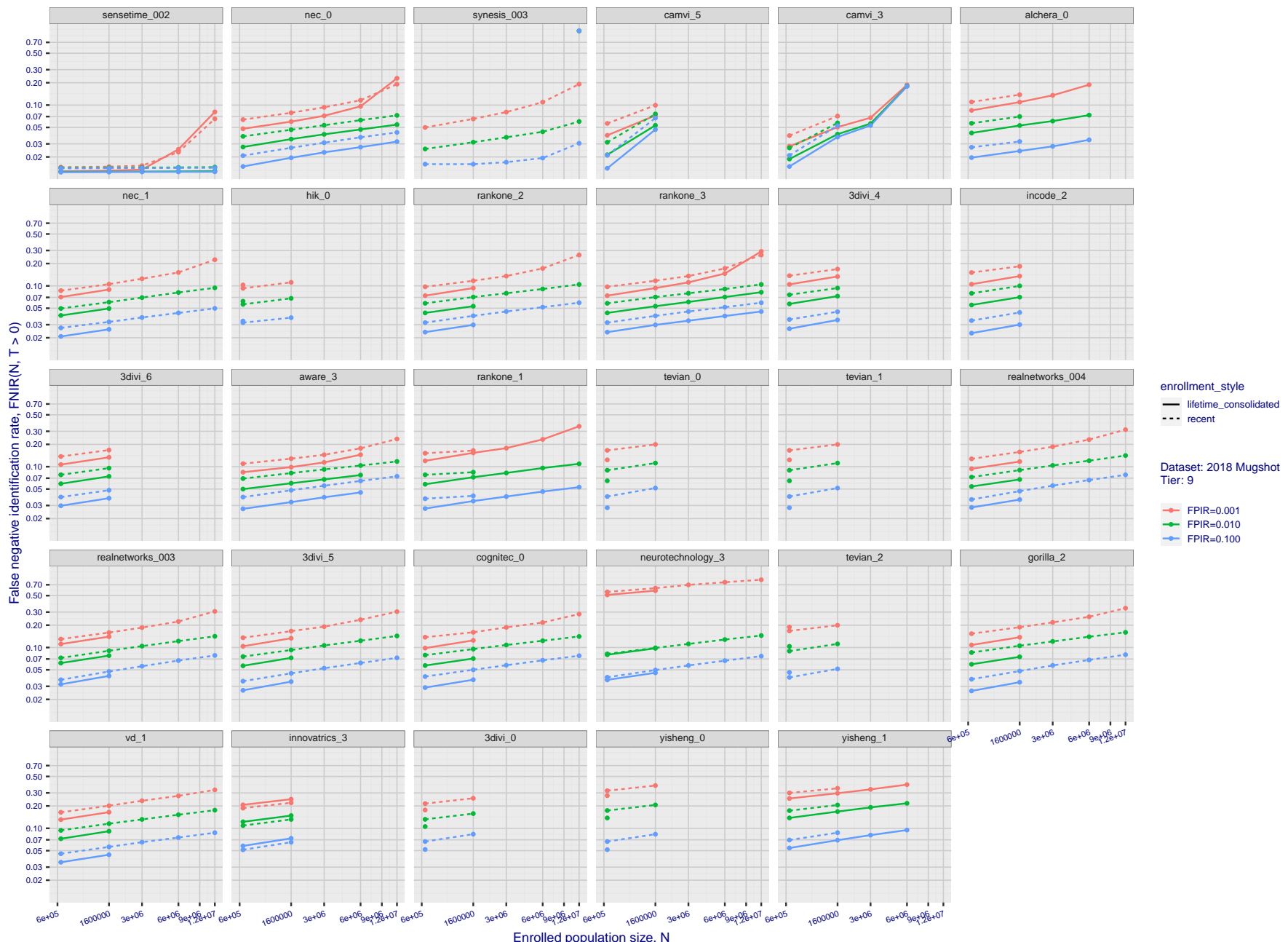


Figure 43: [FRVT-2018 Mugshot Dataset] Threshold-based identification miss rates vs. number of enrolled subjects. The figure shows FNIR( $N, T$ ) across various gallery sizes when the threshold is set to achieve the given FPIRs. The rank criterion is irrelevant at high thresholds as mates are always at rank 1. The results are computed from the trials listed in rows 1-10 of Table 1. Less accurate algorithms were not run on large  $N$ , so results are missing. For clarity, results are sorted and reported into tiers spanning multiple pages. The tiering criteria is complicated: First paging by FNIR( $N_b, 1, 0$ ), then sorting by median FNIR( $N_b, T$ ),  $N_b = 640\,000$ .



**Figure 44: [FRVT-2018 Mugshot Dataset] Threshold-based identification miss rates vs. number of enrolled subjects.** The figure shows FNIR( $N, T$ ) across various gallery sizes when the threshold is set to achieve the given FPIRs. The rank criterion is irrelevant at high thresholds as mates are always at rank 1. The results are computed from the trials listed in rows 1-10 of Table 1. Less accurate algorithms were not run on large  $N$ , so results are missing. For clarity, results are sorted and reported into tiers spanning multiple pages. The tiering criteria is complicated: First paging by  $\text{FNIR}(N_b, 1, 0)$ , then sorting by median  $\text{FNIR}(N_b, T)$ ,  $N_b = 640\,000$ .

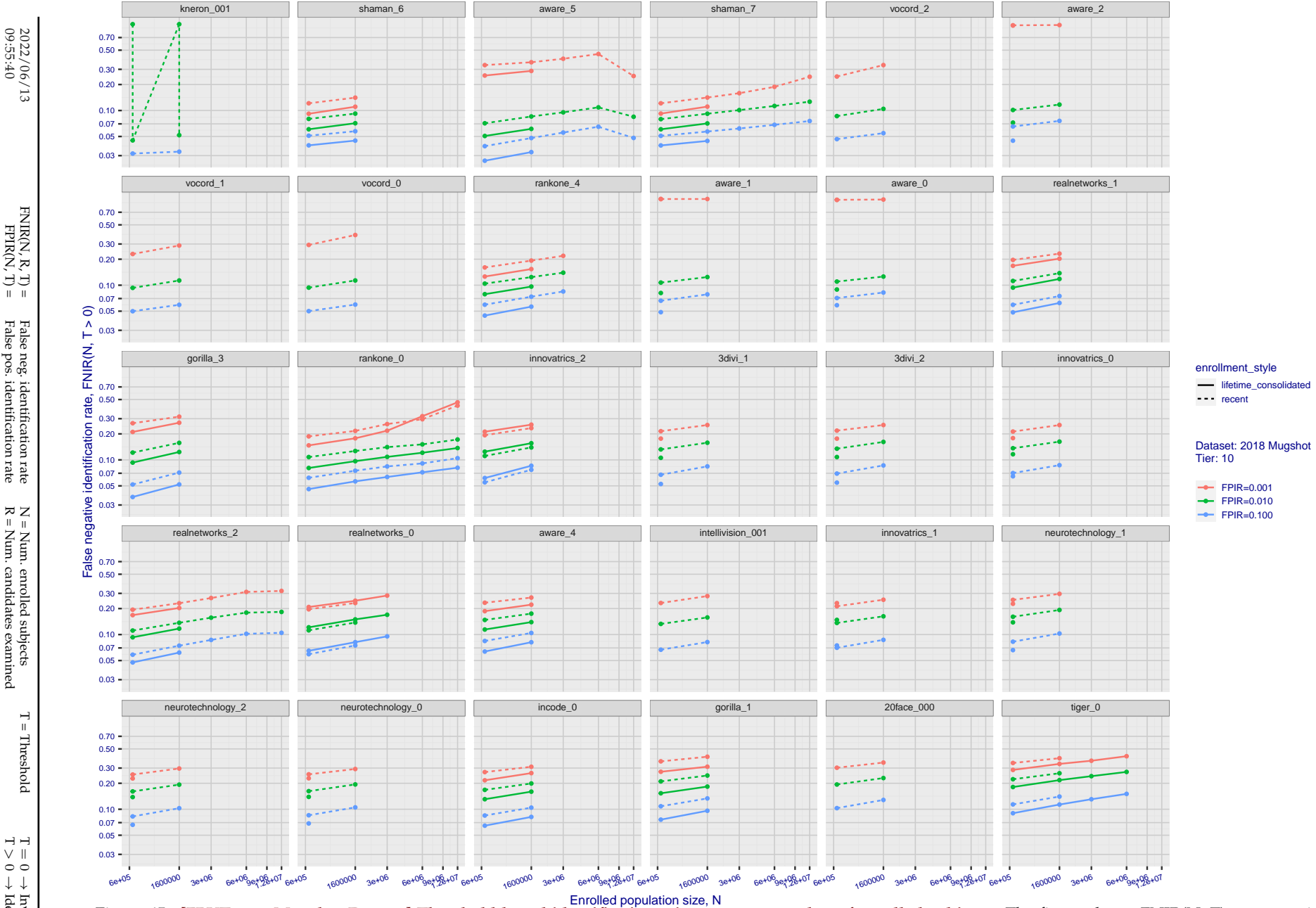
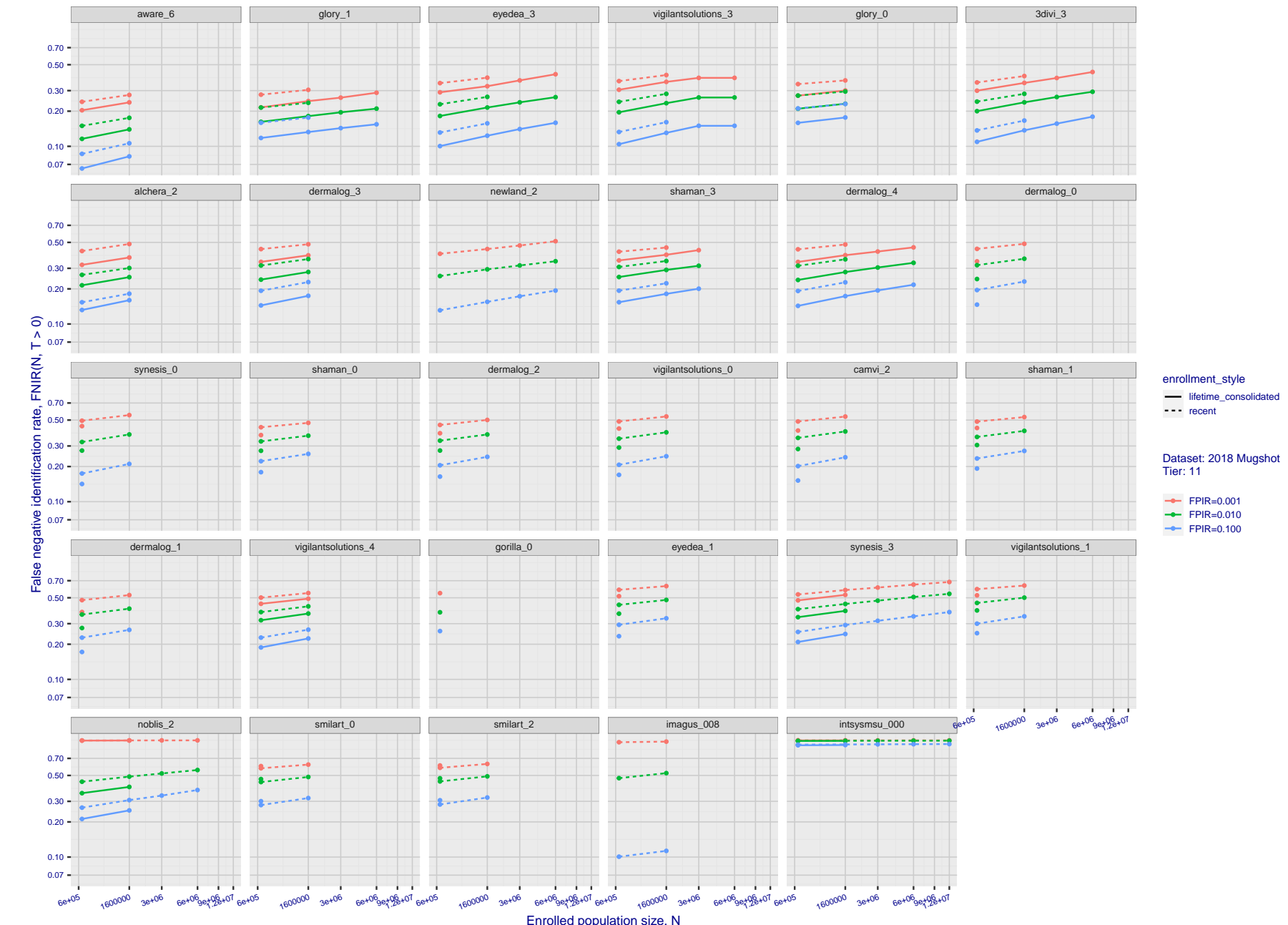


Figure 45: [FRVT-2018 Mugshot Dataset] Threshold-based identification miss rates vs. number of enrolled subjects. The figure shows  $\text{FNIR}(N, T)$  across various gallery sizes when the threshold is set to achieve the given FPIRs. The rank criterion is irrelevant at high thresholds as mates are always at rank 1. The results are computed from the trials listed in rows 1-10 of Table 1. Less accurate algorithms were not run on large  $N$ , so results are missing. For clarity, results are sorted and reported into tiers spanning multiple pages. The tiering criteria is complicated: First paging by  $\text{FNIR}(N_b, 1, 0)$ , then sorting by median  $\text{FNIR}(N_b, T)$ ,  $N_b = 640\,000$ .



**Figure 46: [FRVT-2018 Mugshot Dataset] Threshold-based identification miss rates vs. number of enrolled subjects.** The figure shows  $FNIR(N, T)$  across various gallery sizes when the threshold is set to achieve the given FPIRs. The rank criterion is irrelevant at high thresholds as mates are always at rank 1. The results are computed from the trials listed in rows 1-10 of Table 1. Less accurate algorithms were not run on large  $N$ , so results are missing. For clarity, results are sorted and reported into tiers spanning multiple pages. The tiering criteria is complicated: First paging by  $FNIR(N_b, 1, 0)$ , then sorting by median  $FNIR(N_b, T)$ ,  $N_b = 640\,000$ .

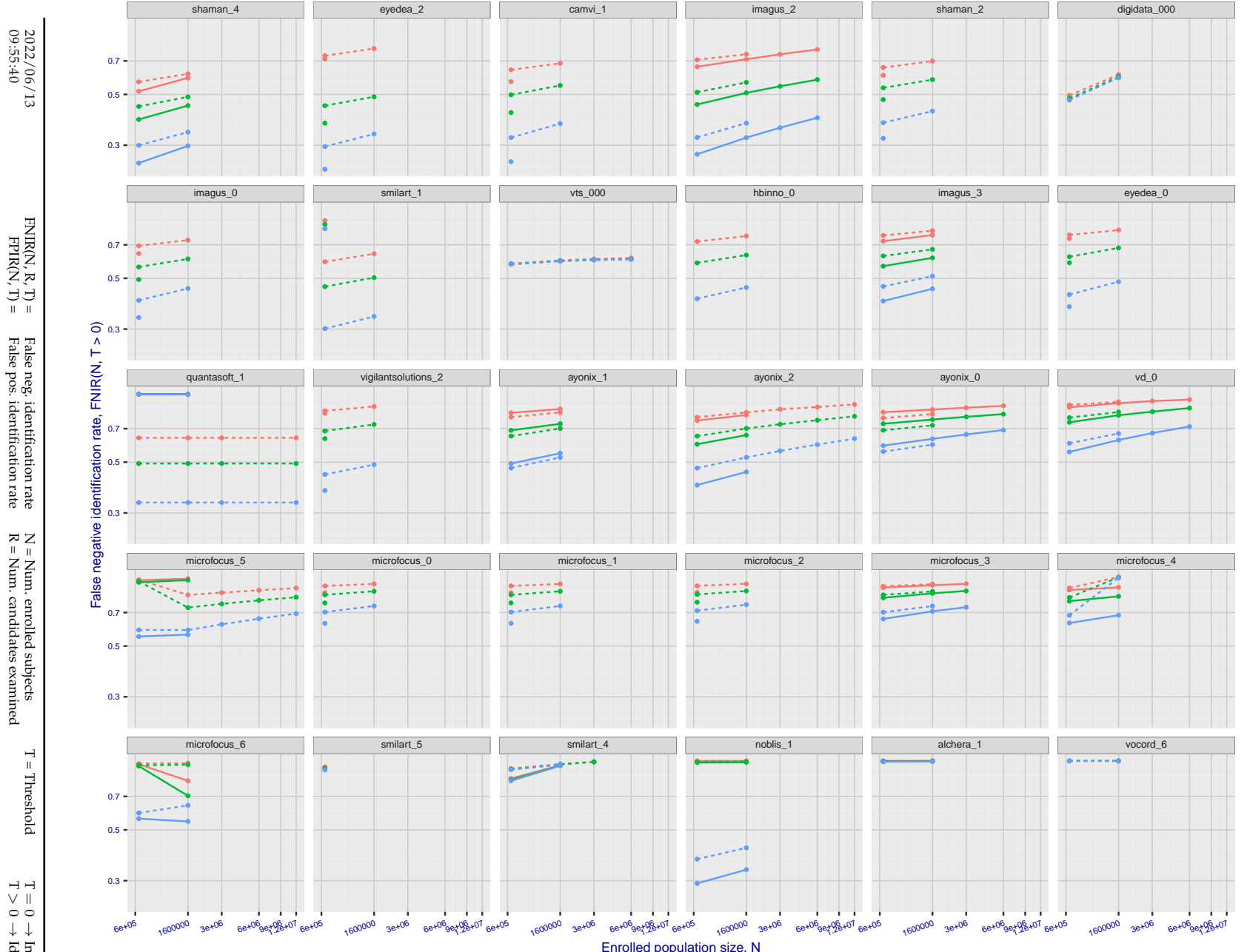
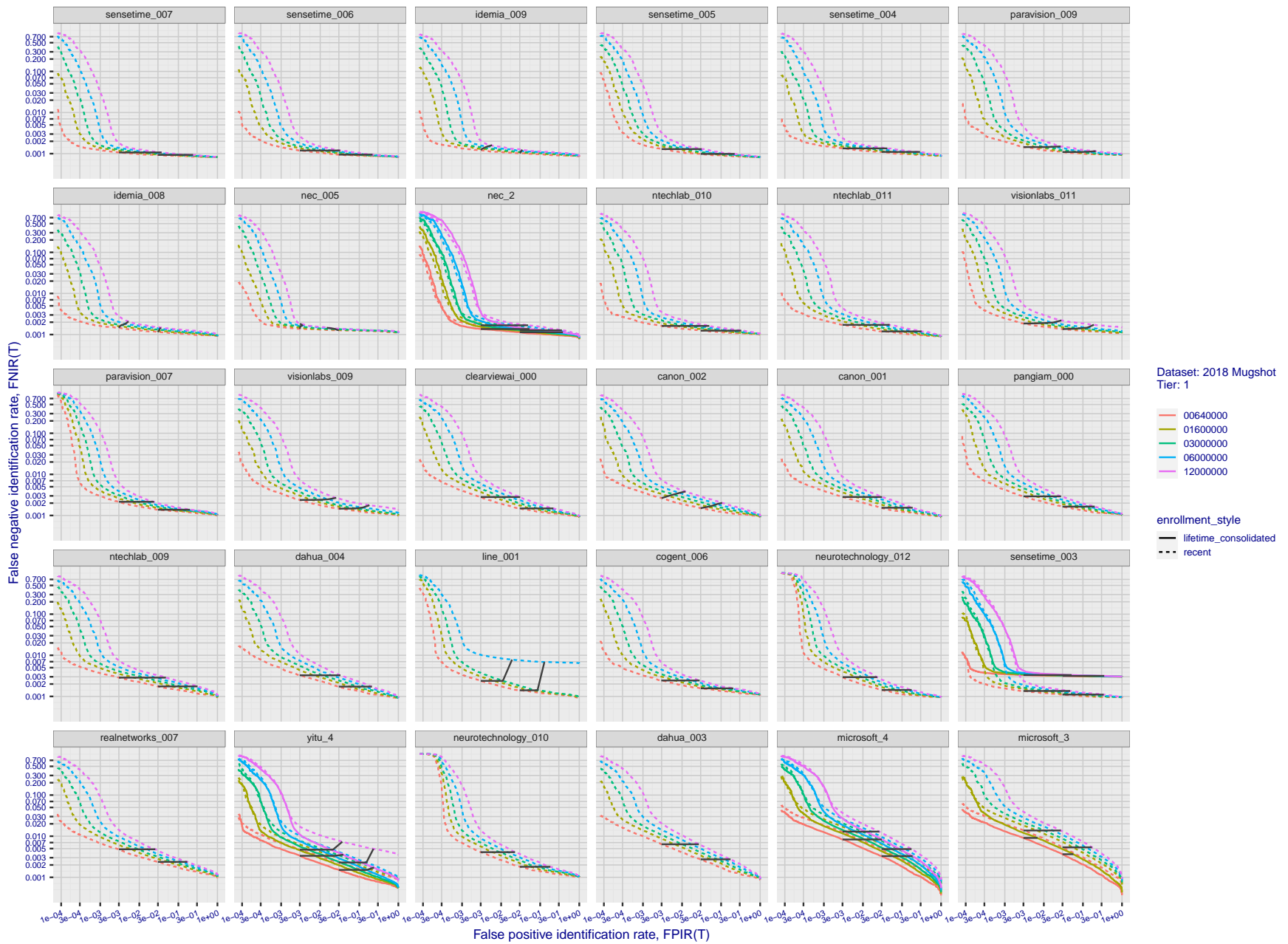


Figure 47: [FRVT-2018 Mugshot Dataset] Threshold-based identification miss rates vs. number of enrolled subjects. The figure shows FNIR( $N, T$ ) across various gallery sizes when the threshold is set to achieve the given FPIRs. The rank criterion is irrelevant at high thresholds as mates are always at rank 1. The results are computed from the trials listed in rows 1-10 of Table 1. Less accurate algorithms were not run on large  $N$ , so results are missing. For clarity, results are sorted and reported into tiers spanning multiple pages. The tiering criteria is complicated: First paging by FNIR( $N_b, 1, 0$ ), then sorting by median FNIR( $N_b, T$ ),  $N_b = 640\,000$ .

2022/06/13 09:55:40	$FNIR(N, R, T) =$ $FPIR(N, T) =$	False neg. identification rate False pos. identification rate	$N =$ Num. enrolled subjects $R =$ Num. candidates examined	$T =$ Threshold $T > 0 \rightarrow$ Identification	$T = 0 \rightarrow$ Investigation
------------------------	-------------------------------------	------------------------------------------------------------------	----------------------------------------------------------------	-------------------------------------------------------	-----------------------------------

2022/06/13  
09:55:40FNIR(N, R, T) = False neg. identification rate  
FPIR(N, T) = False pos. identification rateN = Num. enrolled subjects  
R = Num. candidates examined

T = Threshold

T = 0 → Investigation  
 $T > 0 \rightarrow$  Identification

**Figure 48: [FRVT-2018 Mugshot Dataset] Identification miss rates vs. false positive rates.** The figure shows miss rates  $\text{FNIR}(N, L, T)$  as a function of  $\text{FPIR}(N, T)$ , with  $N$  ranging from 640 000 to 12 000 000 as noted in rows 1-10 of Table 1. These error tradeoff characteristics are useful for applications where a threshold must be elevated to limit false positives, such as when human reviewer labor is not matched to the volume of searches. Dark lines join points of equal threshold: If horizontal,  $\text{FPIR}(T)$  rises with  $N$ , and mate scores are independent of  $N$ . Other algorithms adjust scores in an attempt to make  $\text{FPIR}$  independent of  $N$ .

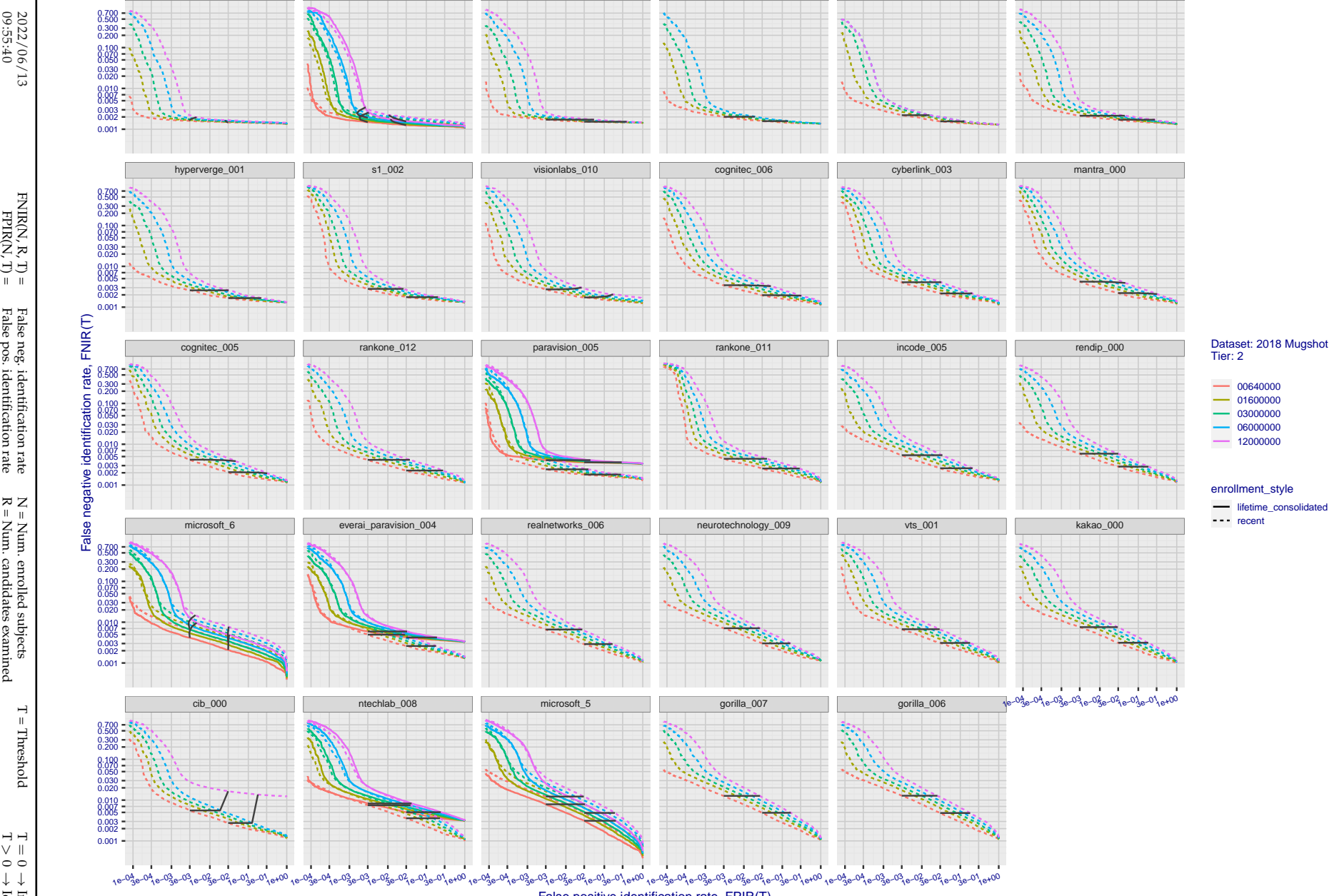


Figure 49: [FRVT-2018 Mugshot Dataset] Identification miss rates vs. false positive rates. The figure shows miss rates  $\text{FNIR}(N, L, T)$  as a function of  $\text{FPIR}(N, T)$ , with  $N$  ranging from 64 000 to 12 000 000 as noted in rows 1-10 of Table 1. These error tradeoff characteristics are useful for applications where a threshold must be elevated to limit false positives, such as when human reviewer labor is not matched to the volume of searches. Dark lines join points of equal  $N$ . If horizontal,  $\text{FPIR}(T)$  rises with  $N$ , and mate scores are independent of  $N$ . Other algorithms adjust scores in an attempt to make  $\text{FPIR}$  independent of  $N$ .

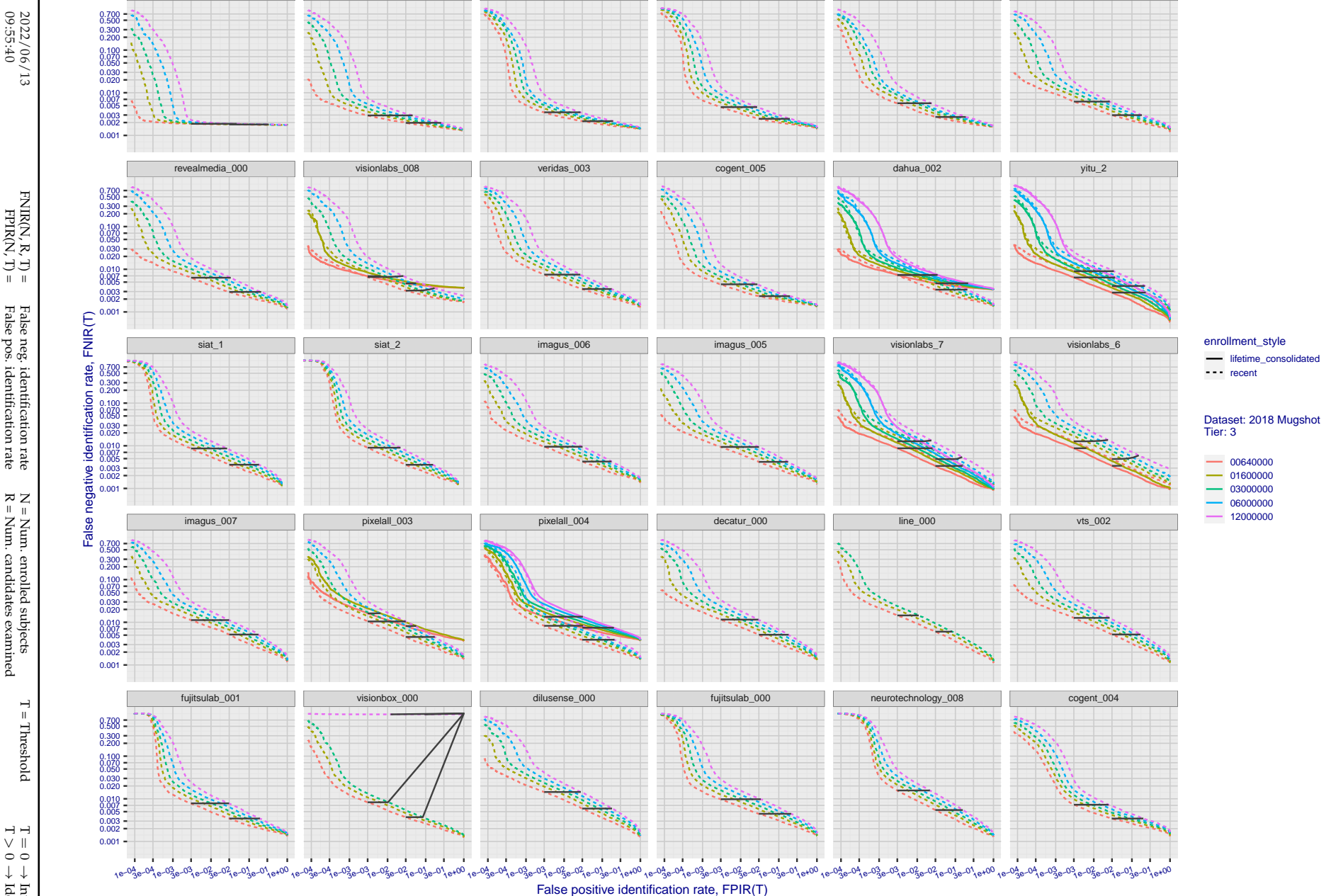
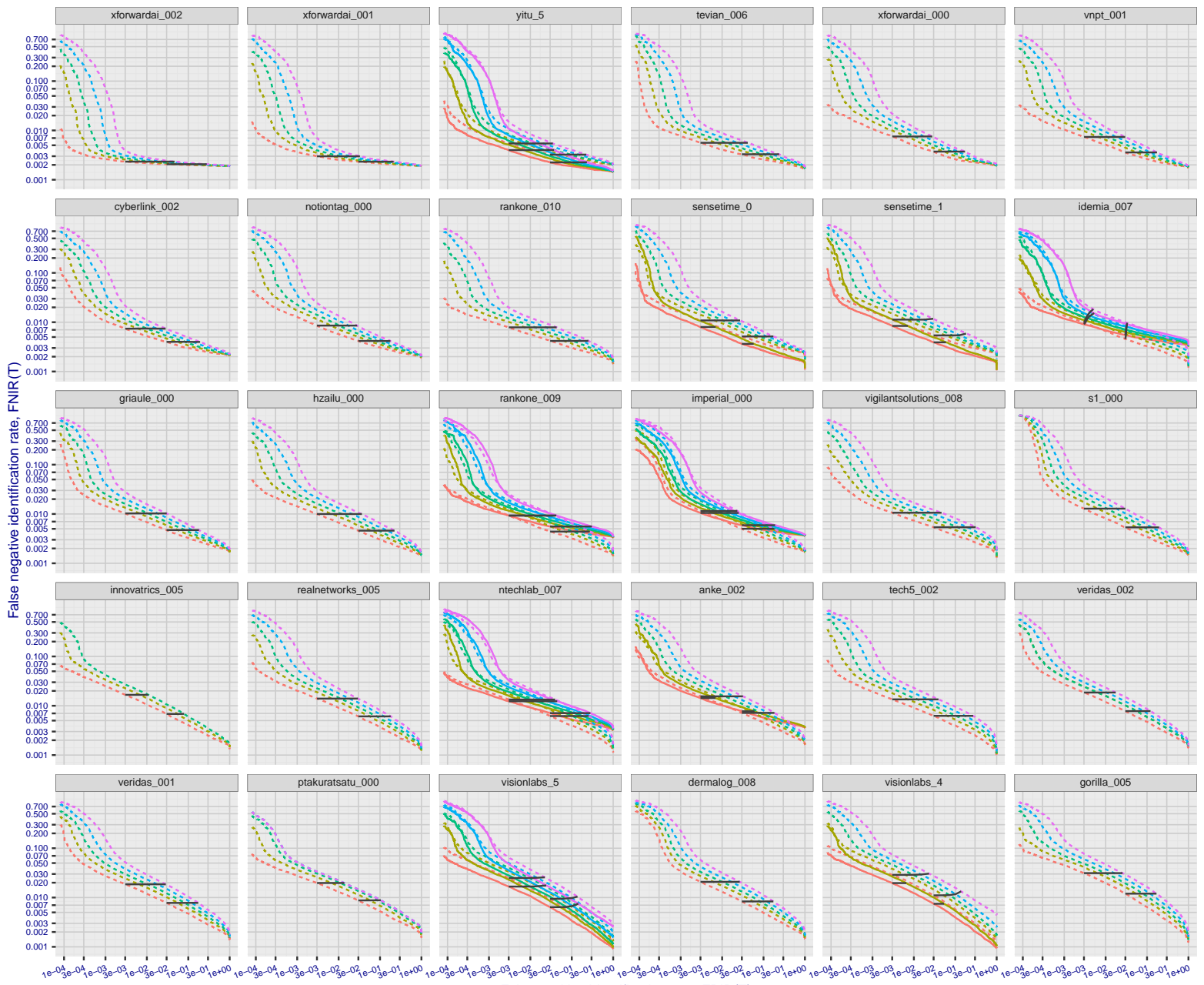


Figure 50: [FRVT-2018 Mugshot Dataset] Identification miss rates vs. false positive rates. The figure shows miss rates  $\text{FNIR}(N, L, T)$  as a function of  $\text{FPIR}(N, T)$ , with  $N$  ranging from 640 000 to 12 000 000 as noted in rows 1-10 of Table 1. These error tradeoff characteristics are useful for applications where a threshold must be elevated to limit false positives, such as when human reviewer labor is not matched to the volume of searches. Dark lines join points of equal threshold: If horizontal,  $\text{FPIR}(T)$  rises with  $N$ , and mate scores are independent of  $N$ . Other algorithms adjust scores in an attempt to make  $\text{FPIR}$  independent of  $N$ .



**Figure 51: [FRVT-2018 Mugshot Dataset] Identification miss rates vs. false positive rates.** The figure shows miss rates  $\text{FNIR}(N, L, T)$  as a function of  $\text{FPIR}(N, T)$ , with  $N$  ranging from 640 000 to 12 000 000 as noted in rows 1-10 of Table 1. These error tradeoff characteristics are useful for applications where a threshold must be elevated to limit false positives, such as when human reviewer labor is not matched to the volume of searches. Dark lines join points of equal threshold: If horizontal,  $\text{FPIR}(T)$  rises with  $N$ , and mate scores are independent of  $N$ . Other algorithms adjust scores in an attempt to make  $\text{FPIR}$  independent of  $N$ .

2022/06/13

09:55:40

 $\text{FNIR}(N, R, T) = \text{False neg. identification rate}$  $\text{FPIR}(N, T) = \text{False pos. identification rate}$  $N = \text{Num. enrolled subjects}$  $T = \text{Threshold}$  $T = 0 \rightarrow \text{Investigation}$  $T > 0 \rightarrow \text{Identification}$

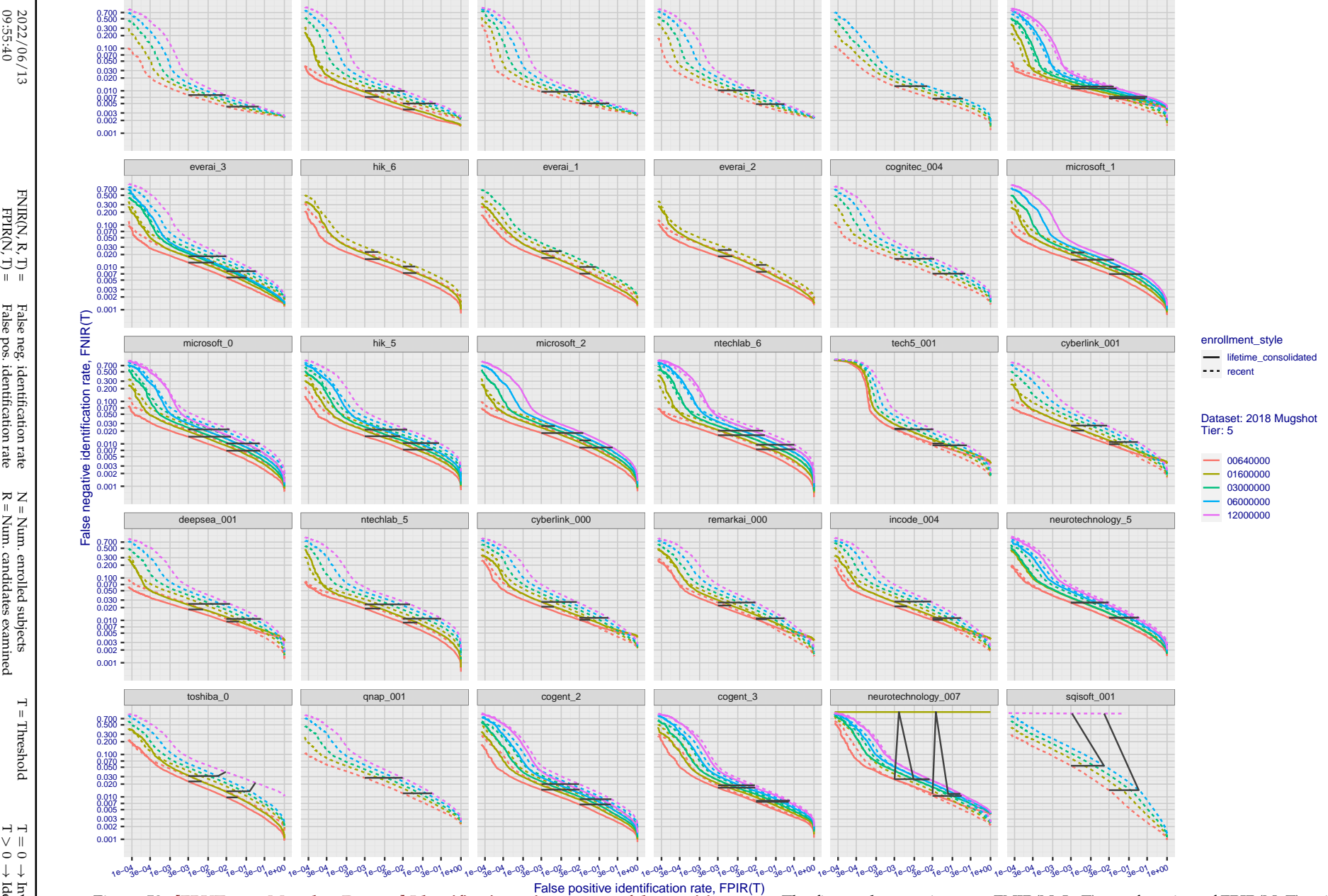


**Figure 52: [FRVT-2018 Mugshot Dataset] Identification miss rates vs. false positive rates.** The figure shows miss rates  $FNIR(N, L, T)$  as a function of  $FPIR(N, T)$ , with  $N$  ranging from 640 000 to 12 000 000 as noted in rows 1-10 of Table 1. These error tradeoff characteristics are useful for applications where a threshold must be elevated to limit false positives, such as when human reviewer labor is not matched to the volume of searches. Dark lines join points of equal threshold: If horizontal,  $FPIR(T)$  rises with  $N$ , and mate scores are independent of  $N$ . Other algorithms adjust scores in an attempt to make  $FPIR$  independent of  $N$ .

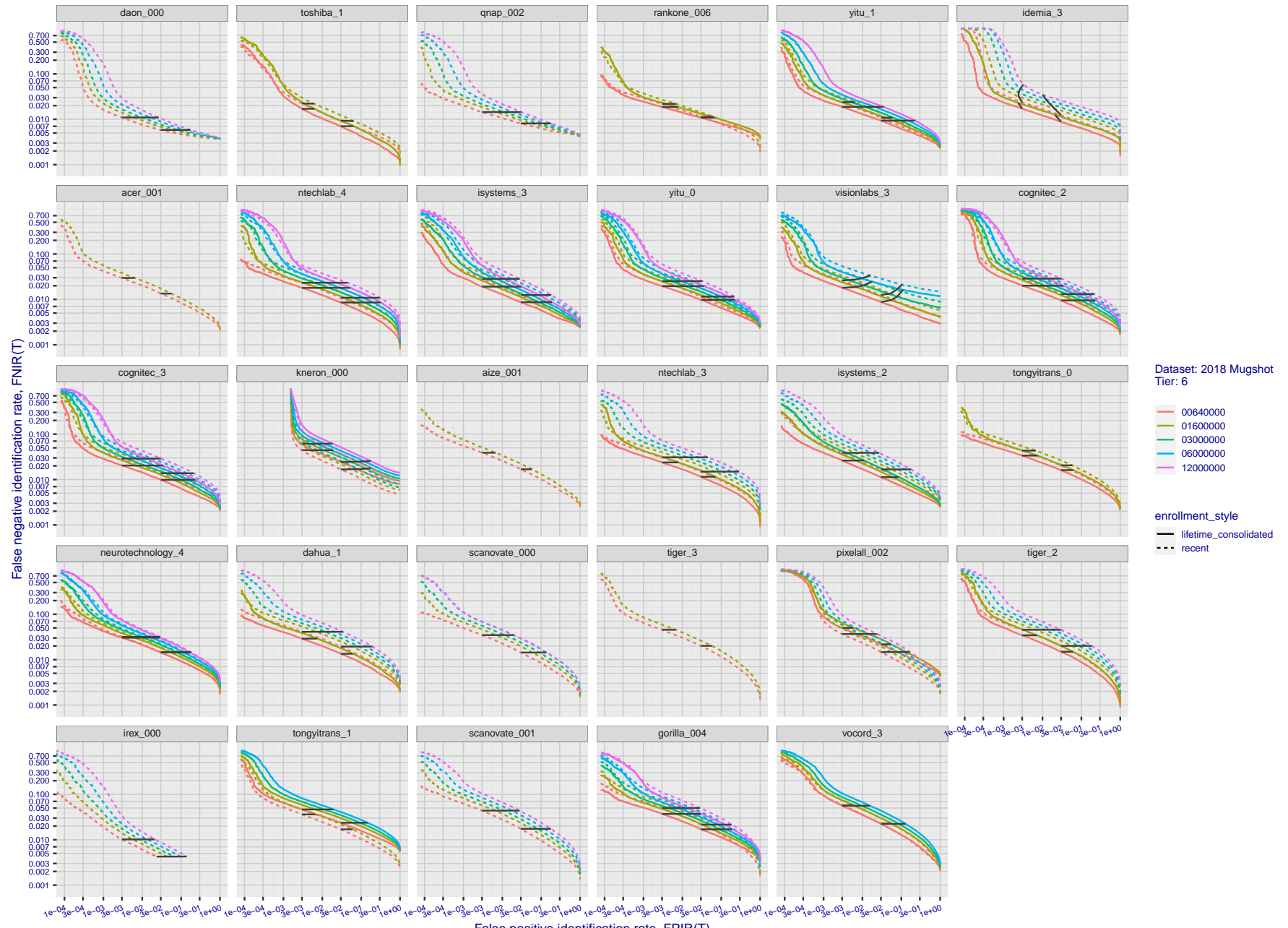
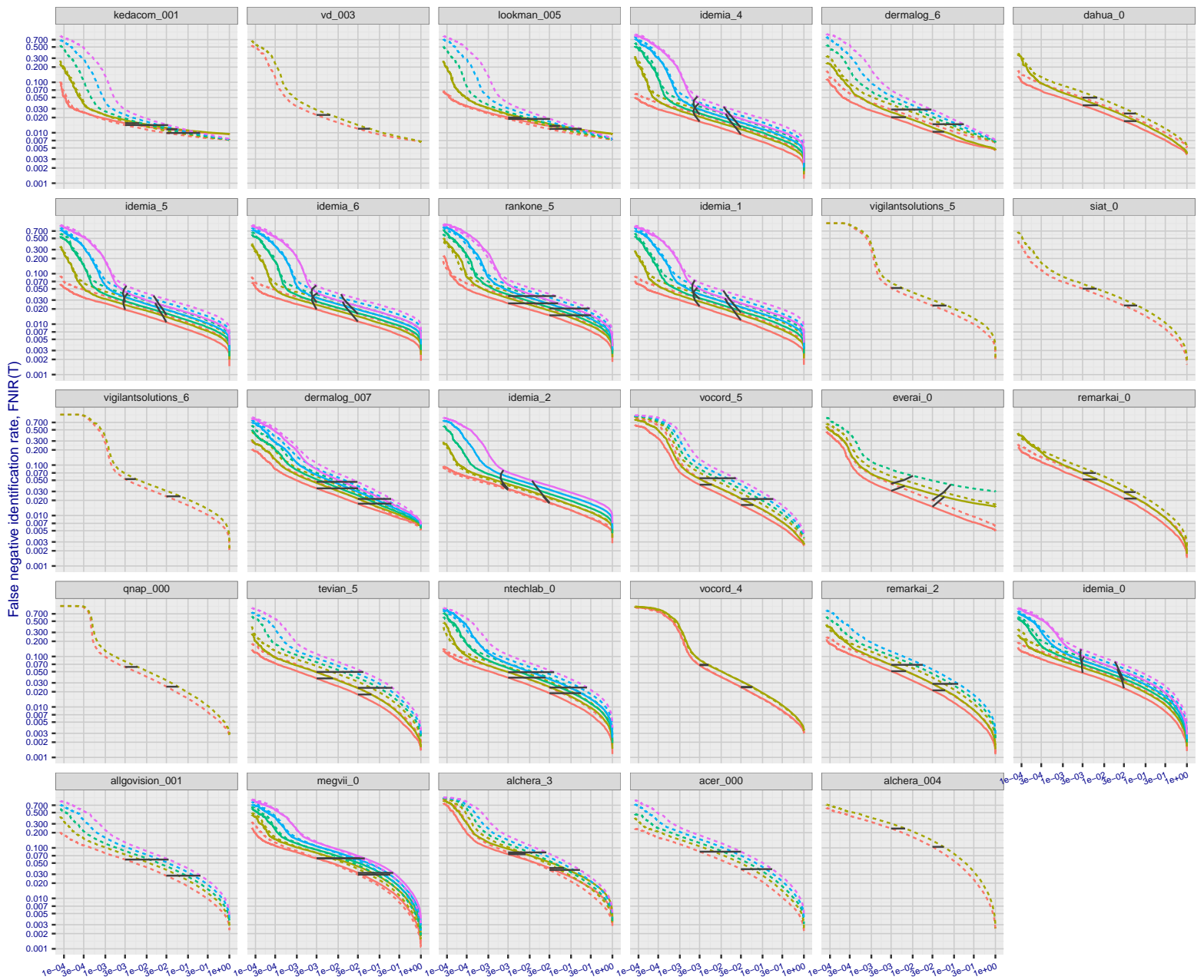


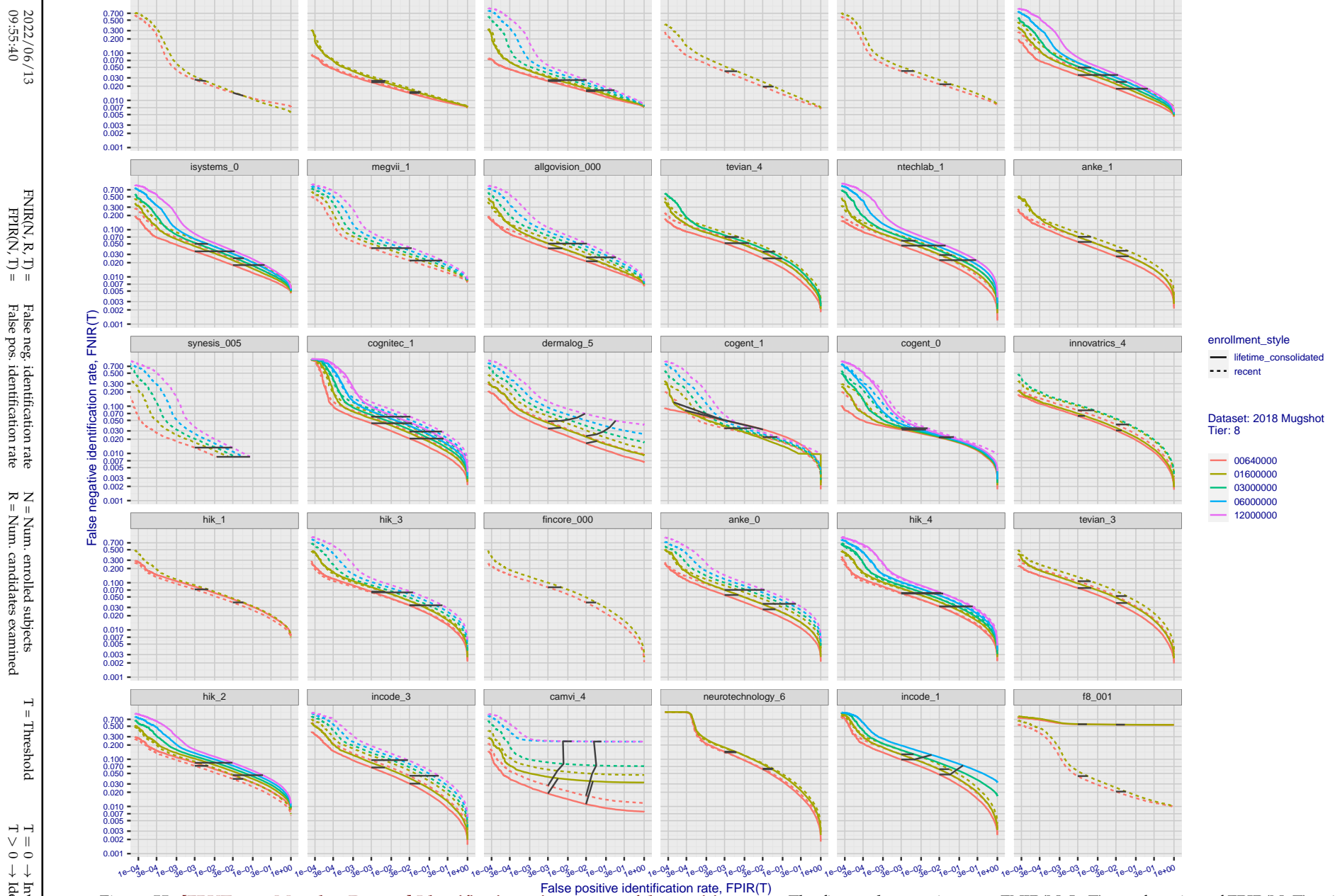
Figure 53: [FRVT-2018 Mugshot Dataset] Identification miss rates vs. false positive rates. The figure shows miss rates  $\text{FNIR}(N, L, T)$  as a function of  $\text{FPIR}(N, T)$ , with  $N$  ranging from 64 000 to 12 000 000 as noted in rows 1-10 of Table 1. These error tradeoff characteristics are useful for applications where a threshold must be elevated to limit false positives, such as when human reviewer labor is not matched to the volume of searches. Dark lines join points of equal threshold: If horizontal,  $\text{FPIR}(T)$  rises with  $N$ , and mate scores are independent of  $N$ . Other algorithms adjust scores in an attempt to make  $\text{FPIR}$  independent of  $N$ .

2022 / 06 / 13  
09:55:40FNIR(N, R, T) = False neg. identification rate  
FPIR(N, T) = False pos. identification rate  
N = Num. enrolled subjects  
R = Num. candidates examined

T = Threshold

T = 0 → Investigation  
 $T > 0 \rightarrow$  Identification

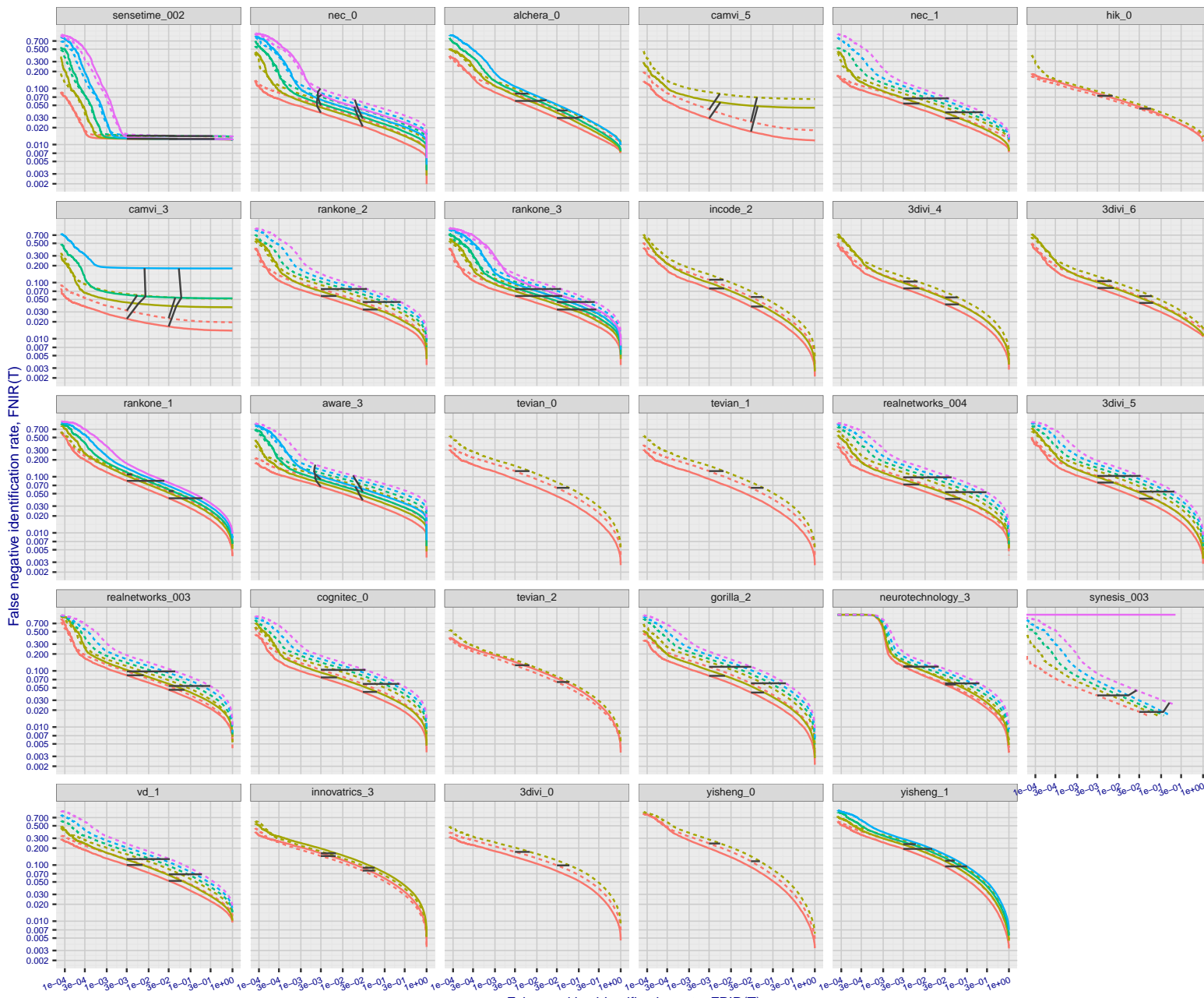
**Figure 54: [FRVT-2018 Mugshot Dataset] Identification miss rates vs. false positive rates.** The figure shows miss rates  $\text{FNIR}(N, L, T)$  as a function of  $\text{FPIR}(N, T)$ , with  $N$  ranging from 640 000 to 12 000 000 as noted in rows 1-10 of Table 1. These error tradeoff characteristics are useful for applications where a threshold must be elevated to limit false positives, such as when human reviewer labor is not matched to the volume of searches. Dark lines join points of equal  $N$ . Other algorithms adjust scores in an attempt to make  $\text{FPIR}$  independent of  $N$ .



**Figure 55: [FRVT-2018 Mugshot Dataset] Identification miss rates vs. false positive rates.** The figure shows miss rates  $\text{FNIR}(N, L, T)$  as a function of  $\text{FPIR}(N, T)$ , with  $N$  ranging from 640 000 to 12 000 000 as noted in rows 1-10 of Table 1. These error tradeoff characteristics are useful for applications where a threshold must be elevated to limit false positives, such as when human reviewer labor is not matched to the volume of searches. Dark lines join points of equal threshold: If horizontal,  $\text{FPIR}(T)$  rises with  $N$ , and mate scores are independent of  $N$ . Other algorithms adjust scores in an attempt to make  $\text{FPIR}$  independent of  $N$ .

2022/06/13  
09:55:40FNIR(N, R, T) = False neg. identification rate  
FPIR(N, T) = False pos. identification rateN = Num. enrolled subjects  
R = Num. candidates examined

T = Threshold

T = 0 → Investigation  
 $T > 0 \rightarrow$  Identification

**Figure 56: [FRVT-2018 Mugshot Dataset] Identification miss rates vs. false positive rates.** The figure shows miss rates  $\text{FNIR}(N, L, T)$  as a function of  $\text{FPIR}(N, T)$ , with  $N$  ranging from 640 000 to 12 000 000 as noted in rows 1-10 of Table 1. These error tradeoff characteristics are useful for applications where a threshold must be elevated to limit false positives, such as when human reviewer labor is not matched to the volume of searches. Dark lines join points of equal threshold: If horizontal,  $\text{FPIR}(T)$  rises with  $N$ , and mate scores are independent of  $N$ . Other algorithms adjust scores in an attempt to make  $\text{FPIR}$  independent of  $N$ .

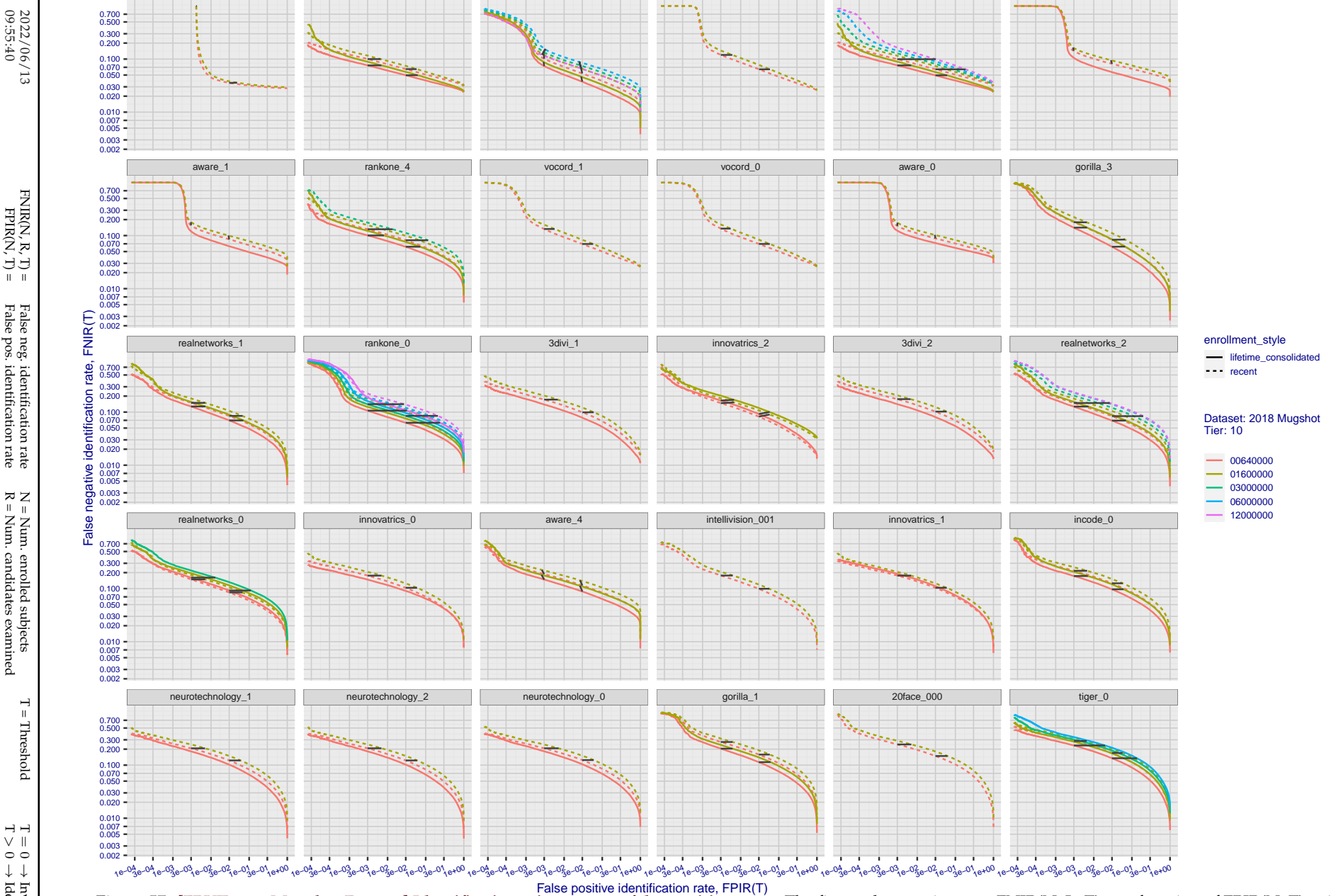


Figure 57: [FRVT-2018 Mugshot Dataset] Identification miss rates vs. false positive rates. The figure shows miss rates  $\text{FNIR}(N, L, T)$  as a function of  $\text{FPIR}(N, T)$ , with  $N$  ranging from 640 000 to 12 000 000 as noted in rows 1-10 of Table 1. These error tradeoff characteristics are useful for applications where a threshold must be elevated to limit false positives, such as when human reviewer labor is not matched to the volume of searches. Dark lines join points of equal threshold: If horizontal,  $\text{FPIR}(T)$  rises with  $N$ , and mate scores are independent of  $N$ . Other algorithms adjust scores in an attempt to make  $\text{FPIR}$  independent of  $N$ .

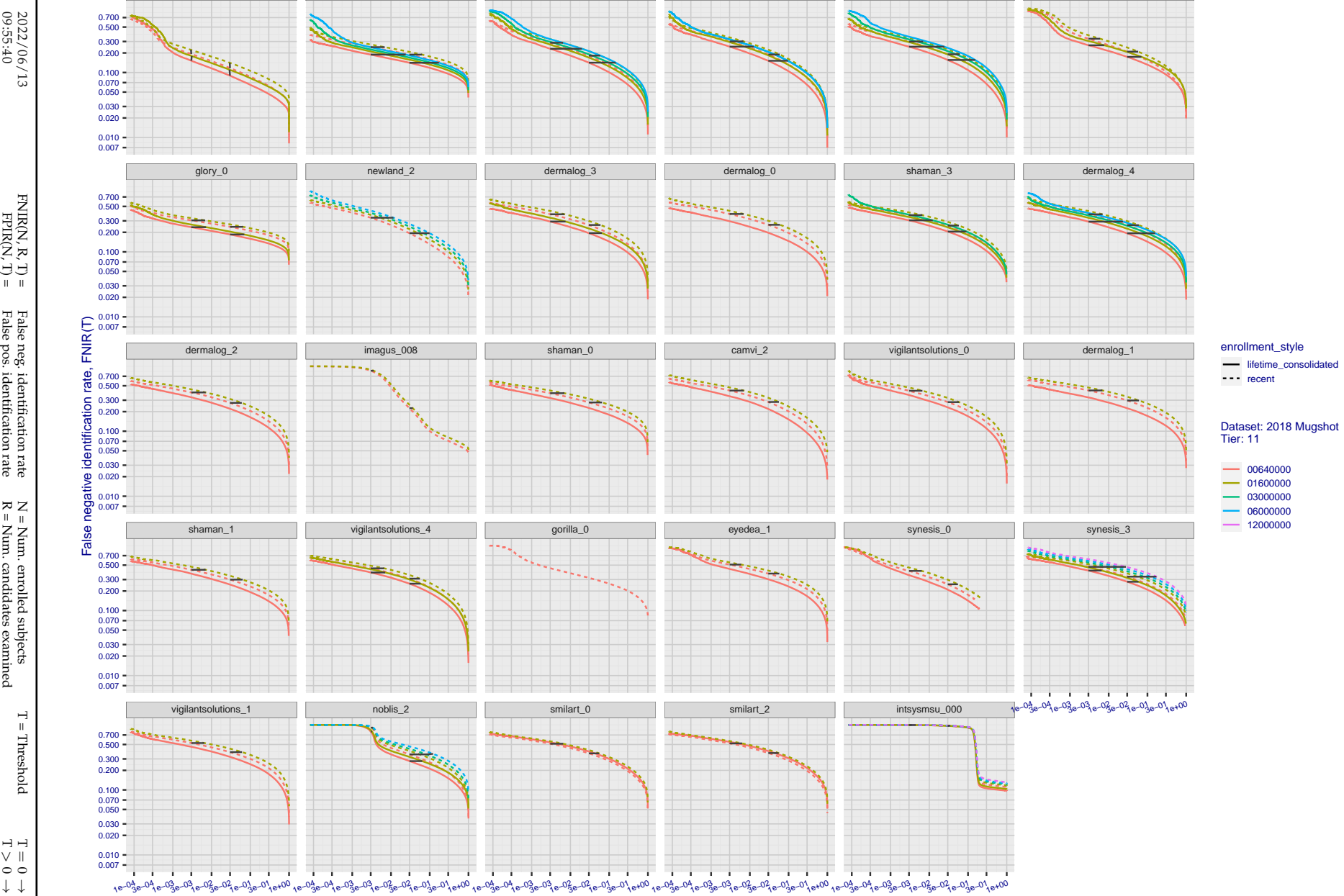


Figure 58: [FRVT-2018 Mugshot Dataset] Identification miss rates vs. false positive rates. The figure shows miss rates  $\text{FNIR}(N, L, T)$  as a function of  $\text{FPIR}(N, T)$ , with  $N$  ranging from 640 000 to 12 000 000 as noted in rows 1-10 of Table 1. These error tradeoff characteristics are useful for applications where a threshold must be elevated to limit false positives, such as when human reviewer labor is not matched to the volume of searches. Dark lines join points of equal threshold: If horizontal,  $\text{FPIR}(T)$  rises with  $N$ , and mate scores are independent of  $N$ . Other algorithms adjust scores in an attempt to make  $\text{FPIR}$  independent of  $N$ .

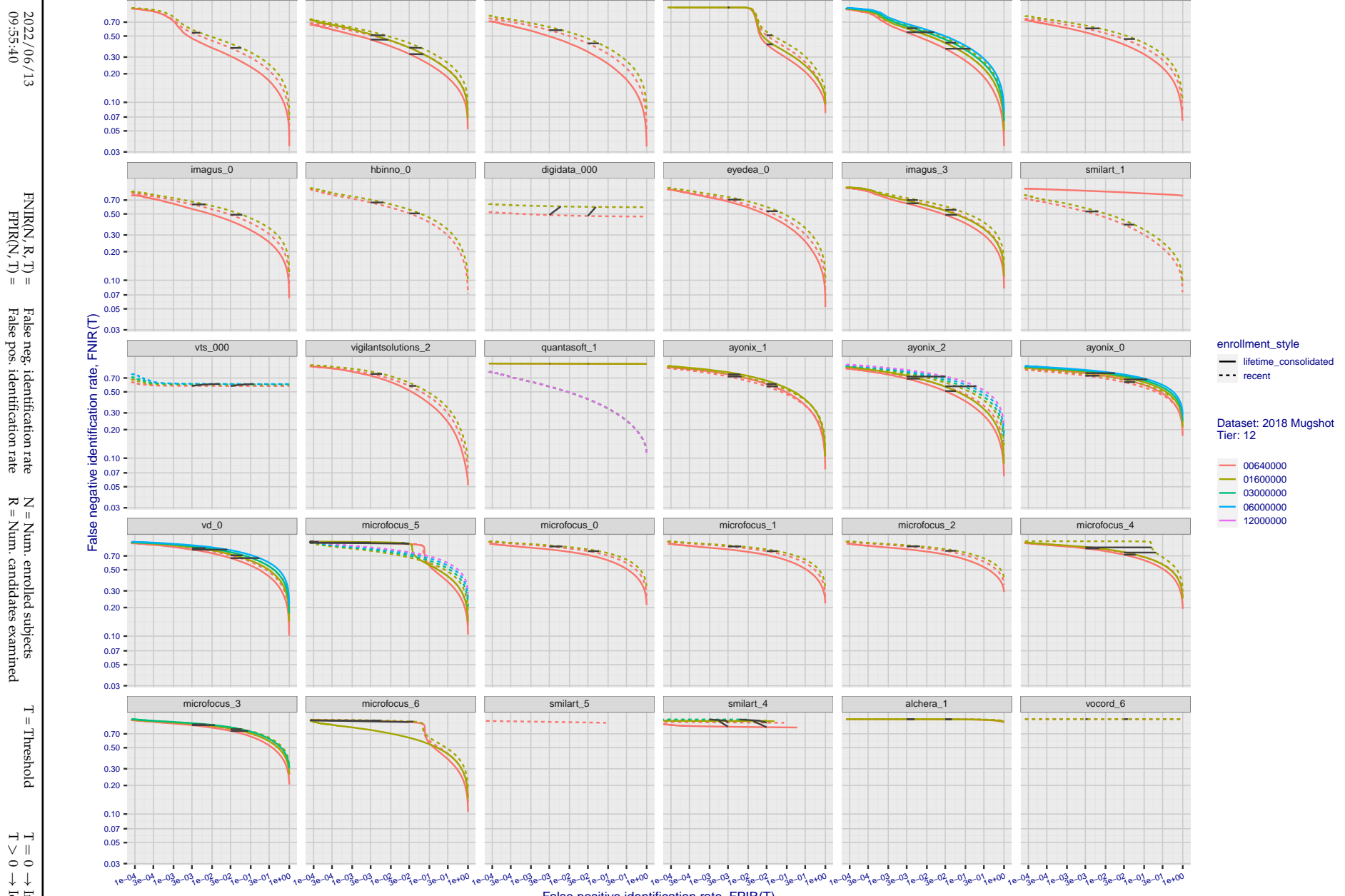


Figure 59: [FRVT-2018 Mugshot Dataset] Identification miss rates vs. false positive rates. The figure shows miss rates  $\text{FNIR}(N, L, T)$  as a function of  $\text{FPIR}(N, T)$ , with  $N$  ranging from 640 000 to 12 000 000 as noted in rows 1-10 of Table 1. These error tradeoff characteristics are useful for applications where a threshold must be elevated to limit false positives, such as when human reviewer labor is not matched to the volume of searches. Dark lines join points of equal threshold: If horizontal,  $\text{FPIR}(T)$  rises with  $N$ , and mate scores are independent of  $N$ . Other algorithms adjust scores in an attempt to make  $\text{FPIR}$  independent of  $N$ .

## Appendix B Effect of time-lapse: Accuracy after face ageing

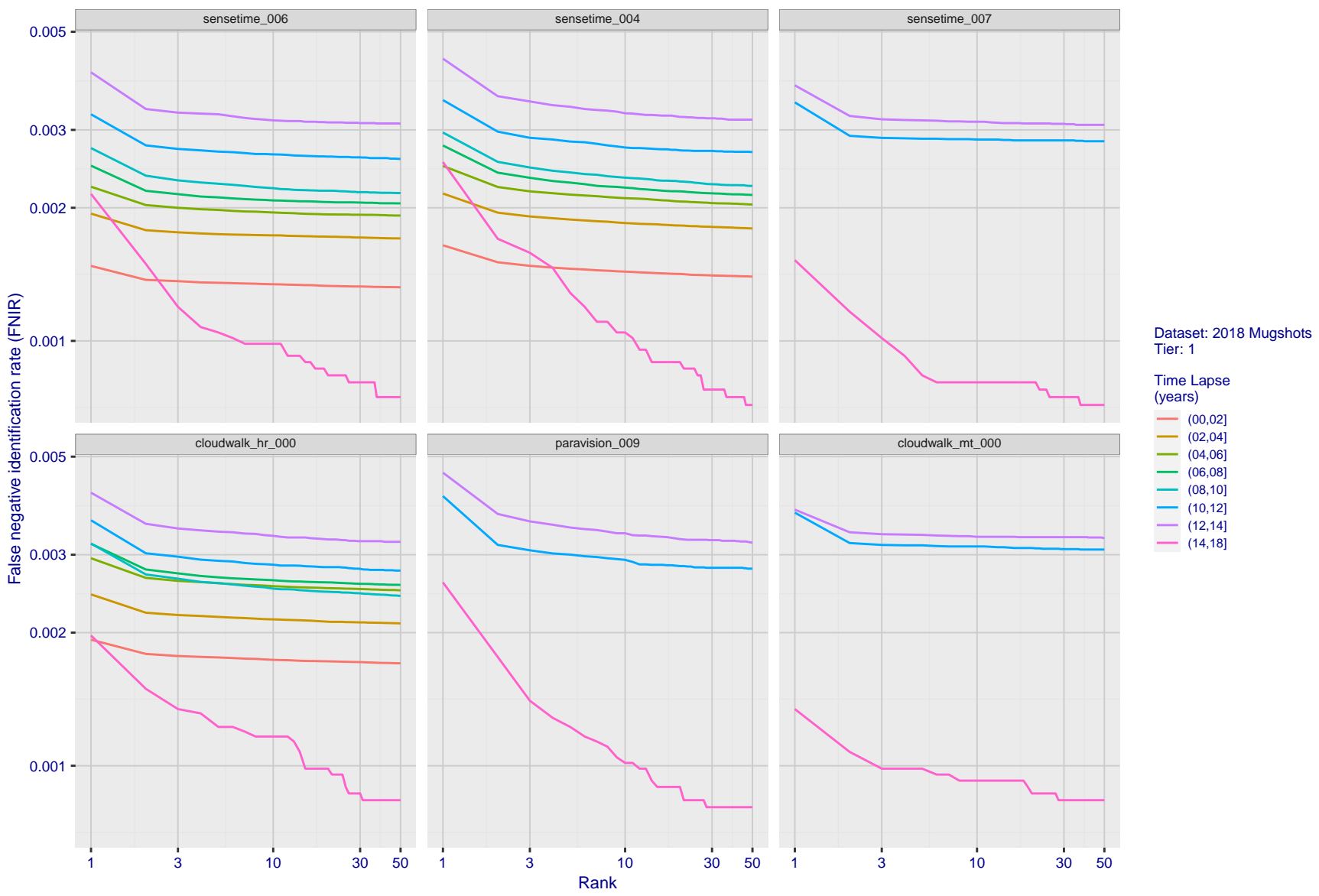
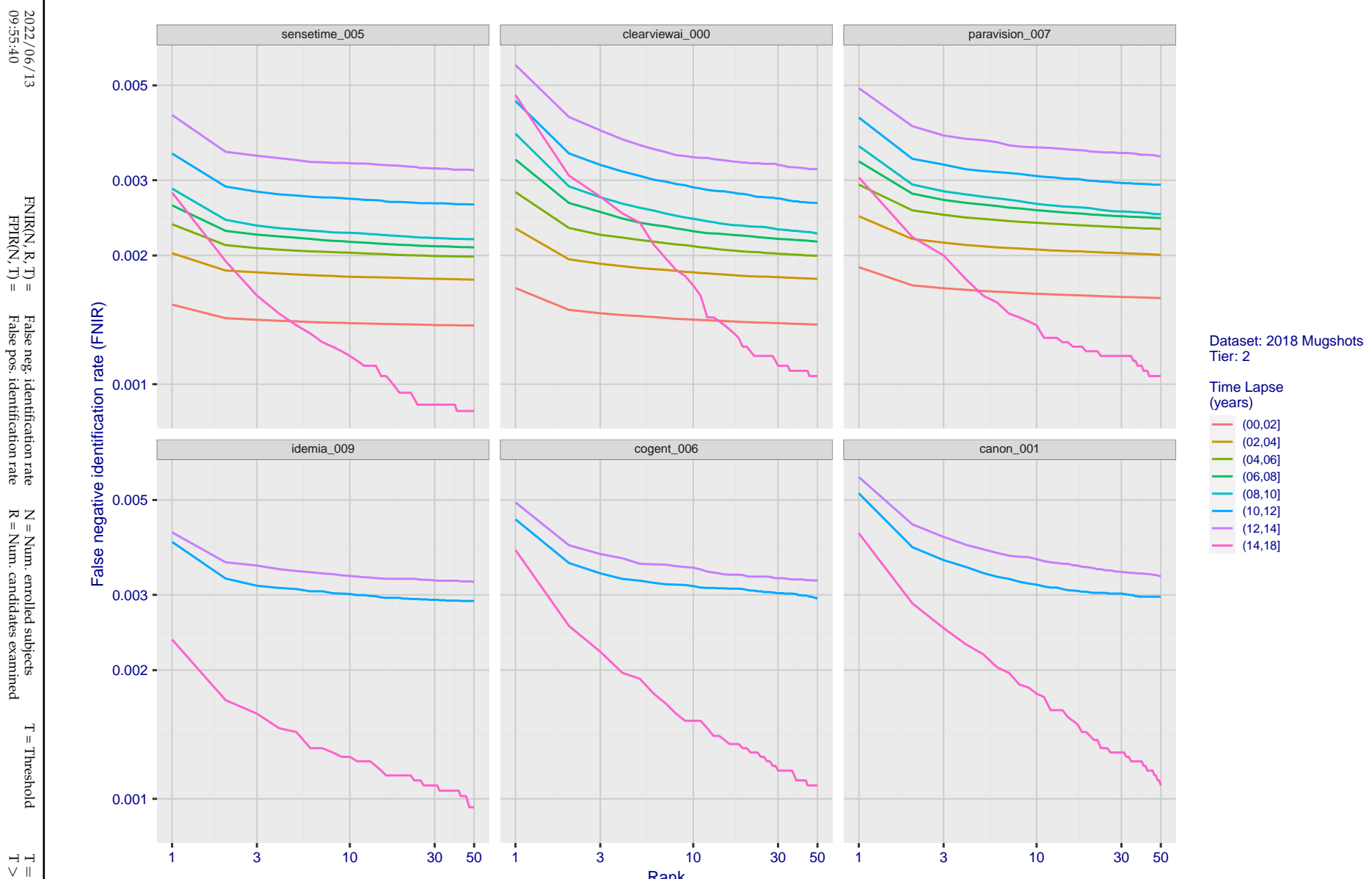


Figure 60: [FRVT-2018 Mugshot Ageing Dataset] Identification miss rates vs. rank by time-elapsed. The oldest image of each individual is enrolled. Thereafter, all more recent images are searched. Miss rates are computed over all searches noted in row 17 of Table 1 and binned by number of years between search and initial enrollment.



**Figure 61: [FRVT-2018 Mugshot Ageing Dataset] Identification miss rates vs. rank by time-elapsed.** The oldest image of each individual is enrolled. Thereafter, all more recent images are searched. Miss rates are computed over all searches noted in row 17 of Table 1 and binned by number of years between search and initial enrollment.

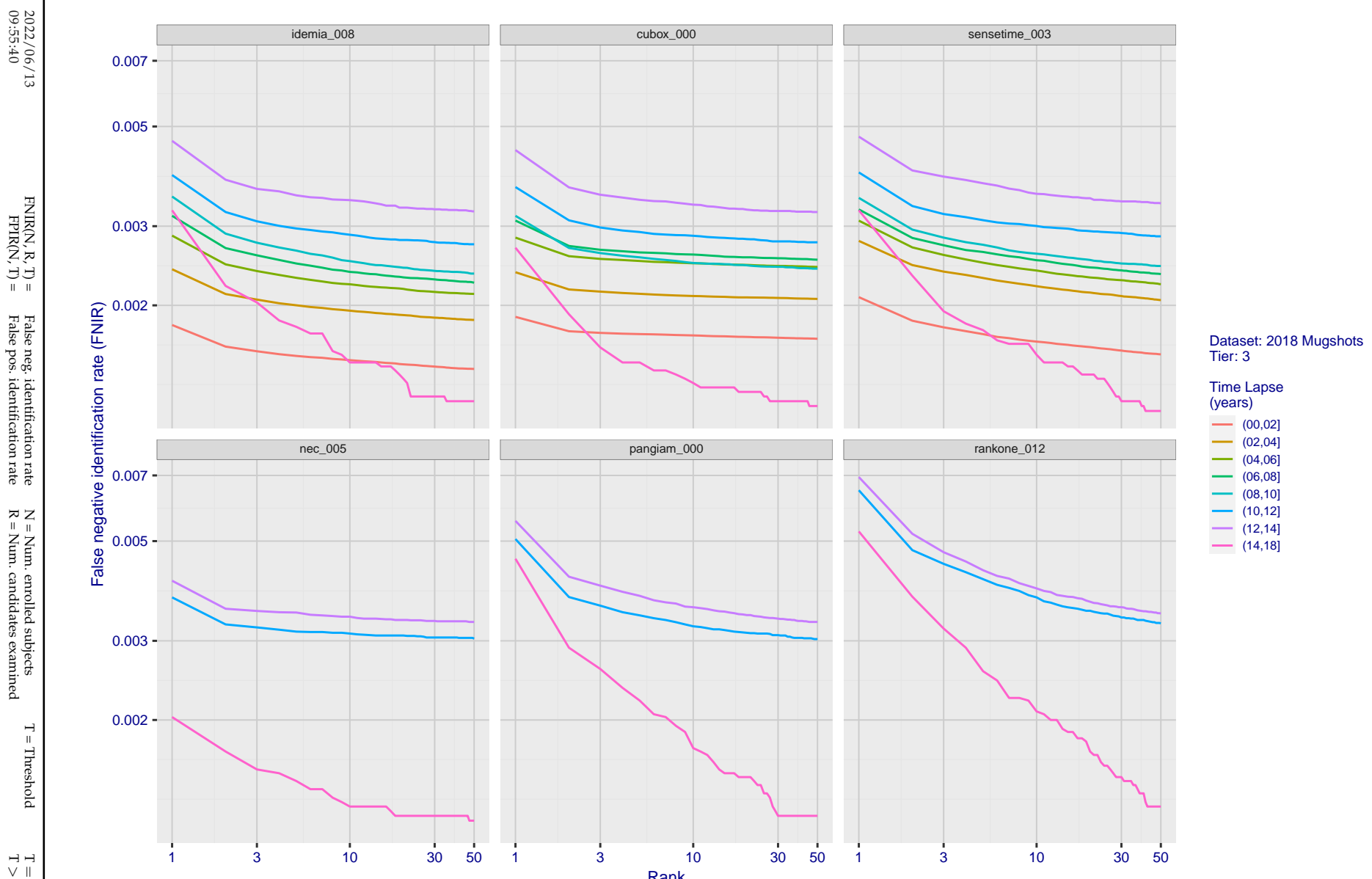


Figure 62: [FRVT-2018 Mugshot Ageing Dataset] Identification miss rates vs. rank by time-elapsed. The oldest image of each individual is enrolled. Thereafter, all more recent images are searched. Miss rates are computed over all searches noted in row 17 of Table 1 and binned by number of years between search and initial enrollment.

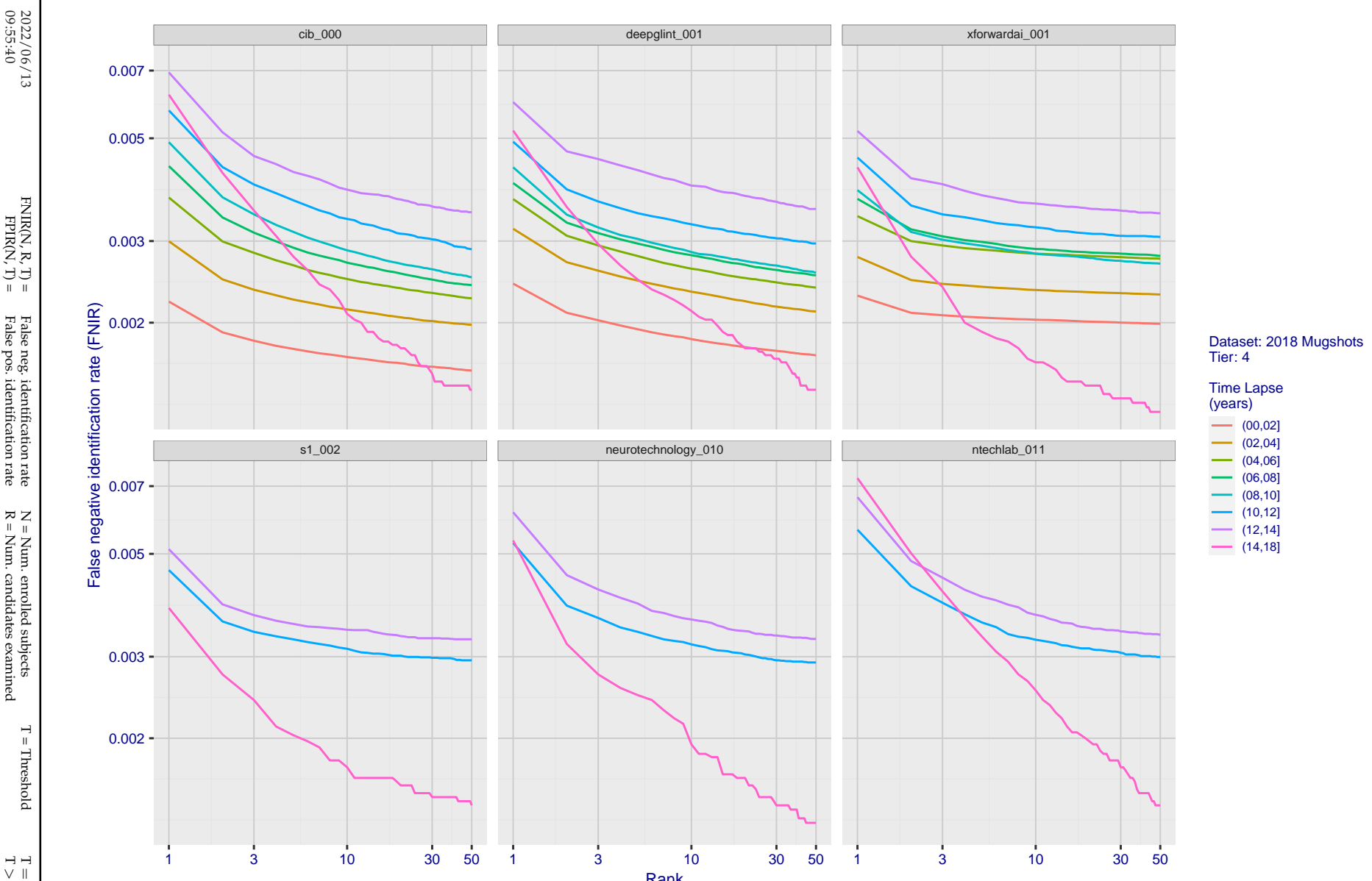


Figure 63: [FRVT-2018 Mugshot Ageing Dataset] Identification miss rates vs. rank by time-elapsed. The oldest image of each individual is enrolled. Thereafter, all more recent images are searched. Miss rates are computed over all searches noted in row 17 of Table 1 and binned by number of years between search and initial enrollment.

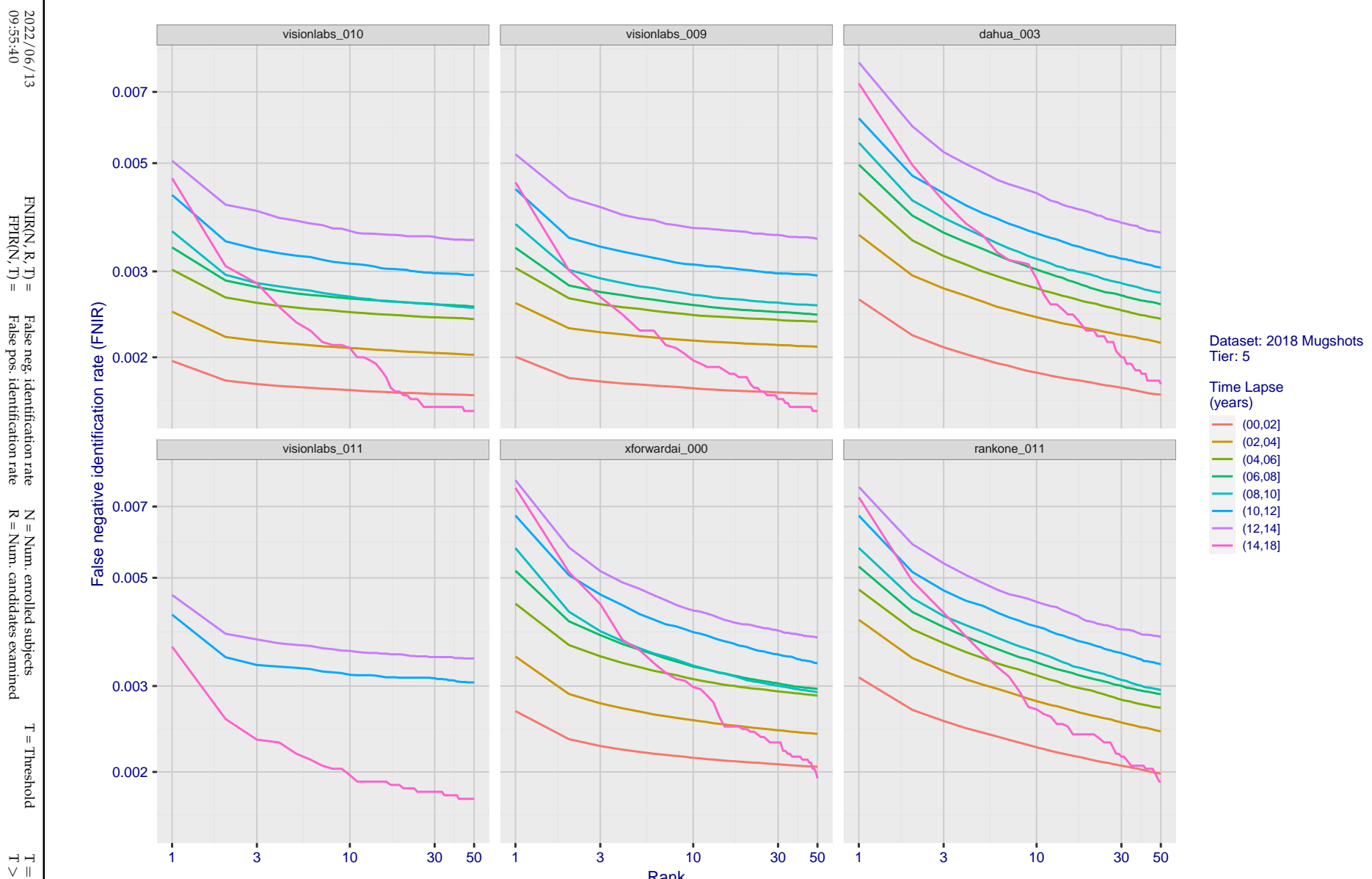
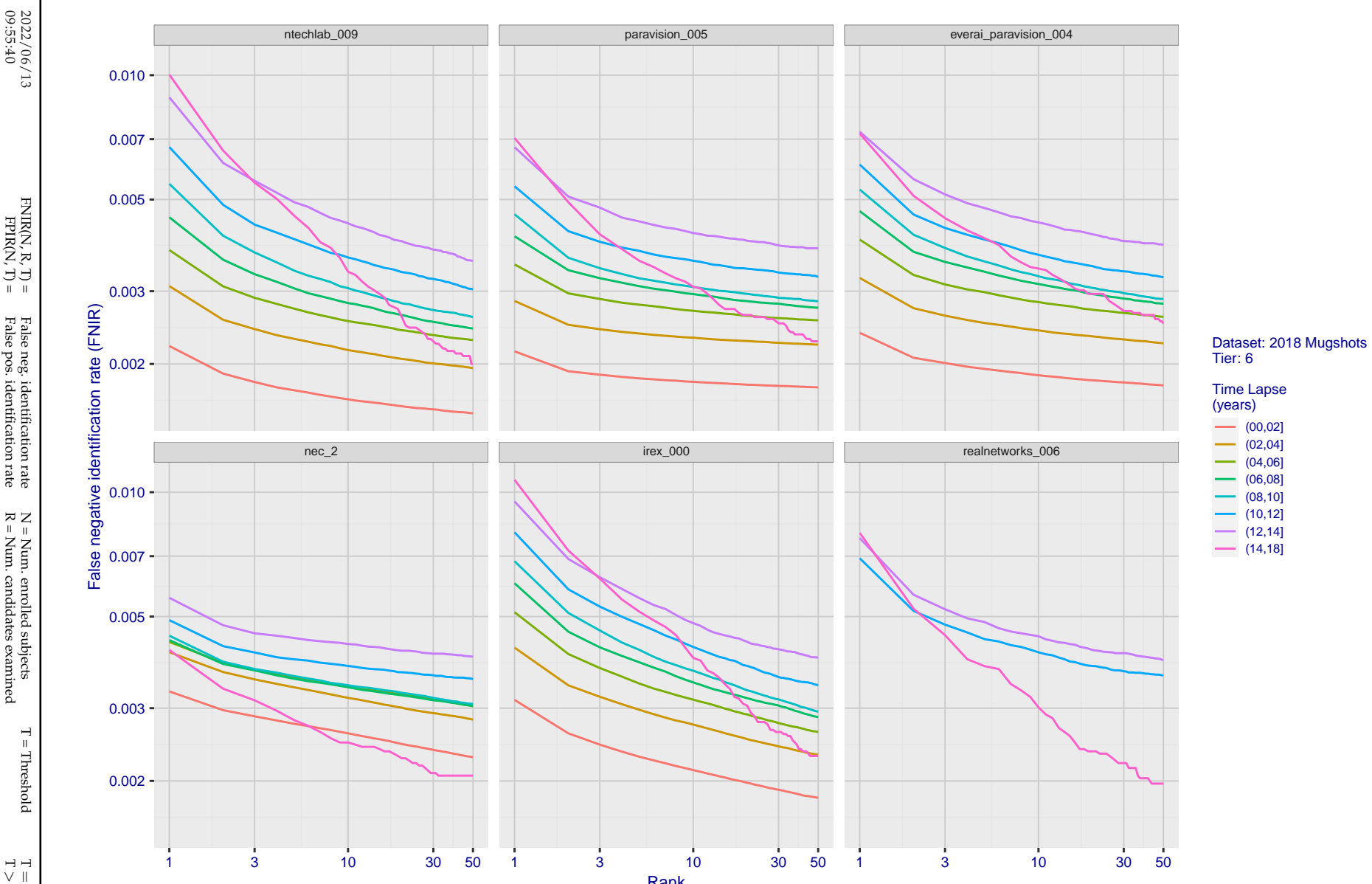
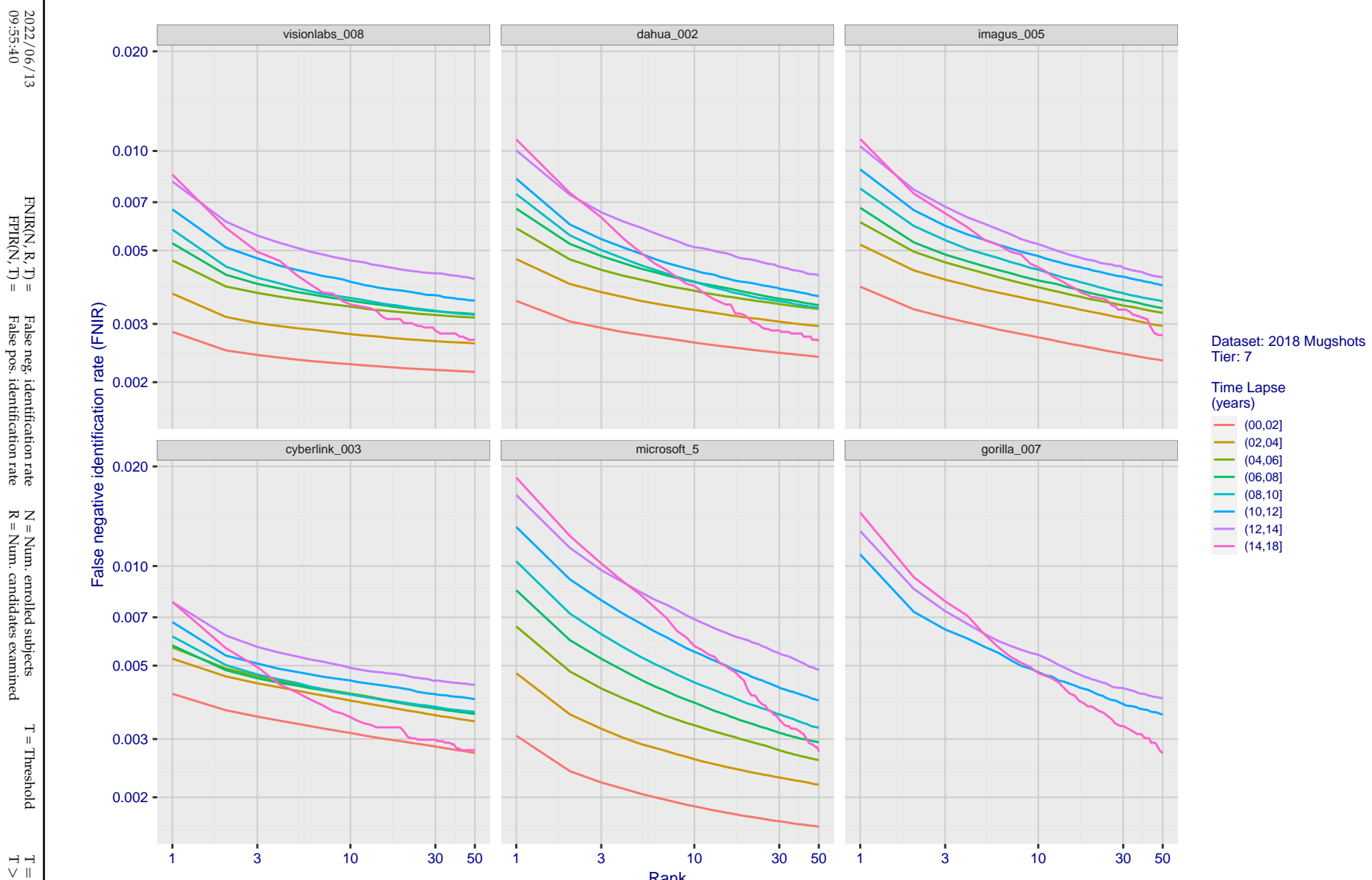


Figure 64: [FRVT-2018 Mugshot Ageing Dataset] Identification miss rates vs. rank by time-elapsed. The oldest image of each individual is enrolled. Thereafter, all more recent images are searched. Miss rates are computed over all searches noted in row 17 of Table 1 and binned by number of years between search and initial enrollment.



**Figure 65: [FRVT-2018 Mugshot Ageing Dataset] Identification miss rates vs. rank by time-elapsed.** The oldest image of each individual is enrolled. Thereafter, all more recent images are searched. Miss rates are computed over all searches noted in row 17 of Table 1 and binned by number of years between search and initial enrollment.



**Figure 66: [FRVT-2018 Mugshot Ageing Dataset] Identification miss rates vs. rank by time-elapsed.** The oldest image of each individual is enrolled. Thereafter, all more recent images are searched. Miss rates are computed over all searches noted in row 17 of Table 1 and binned by number of years between search and initial enrollment.

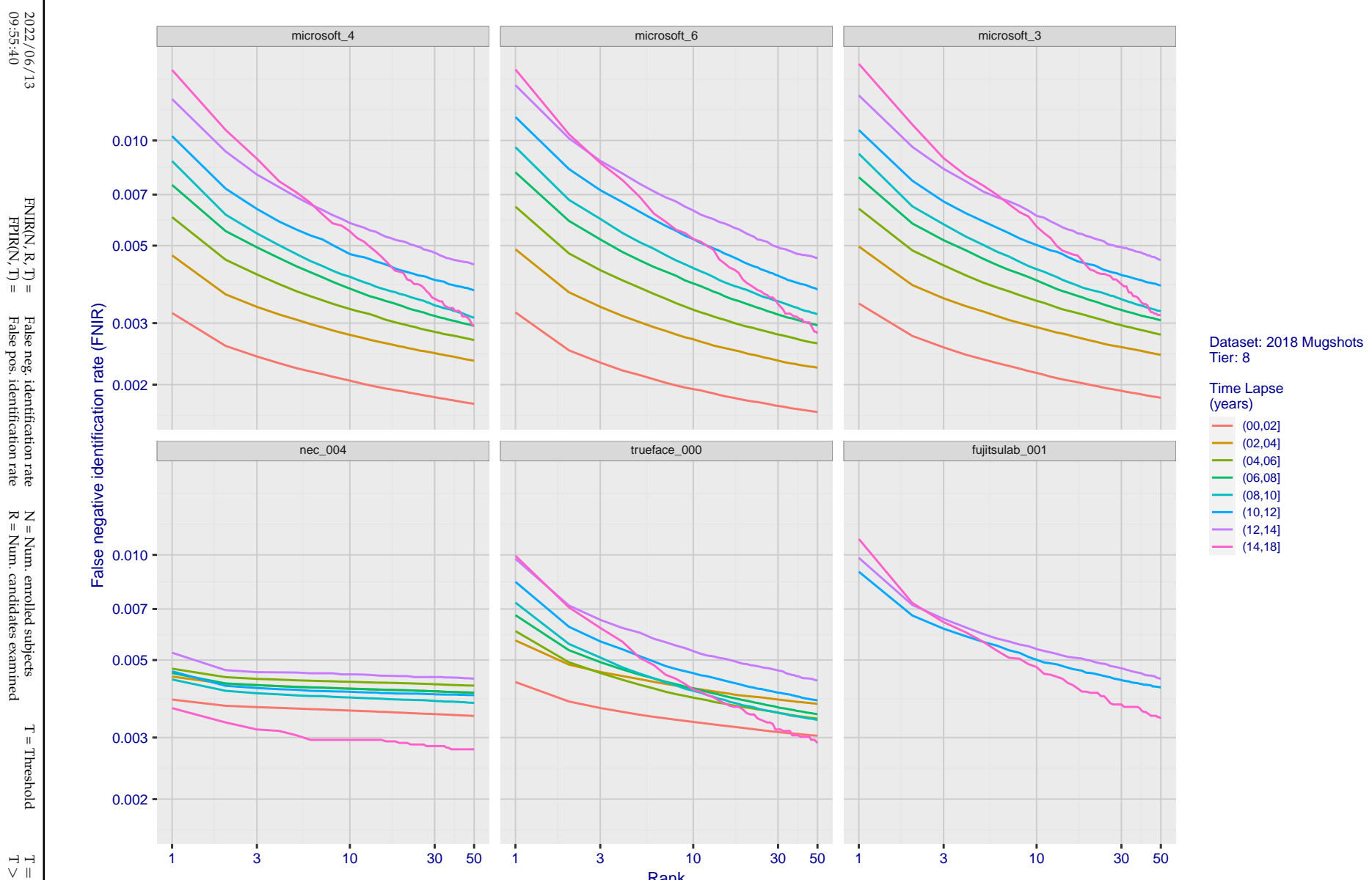


Figure 67: [FRVT-2018 Mugshot Ageing Dataset] Identification miss rates vs. rank by time-elapsed. The oldest image of each individual is enrolled. Thereafter, all more recent images are searched. Miss rates are computed over all searches noted in row 17 of Table 1 and binned by number of years between search and initial enrollment.

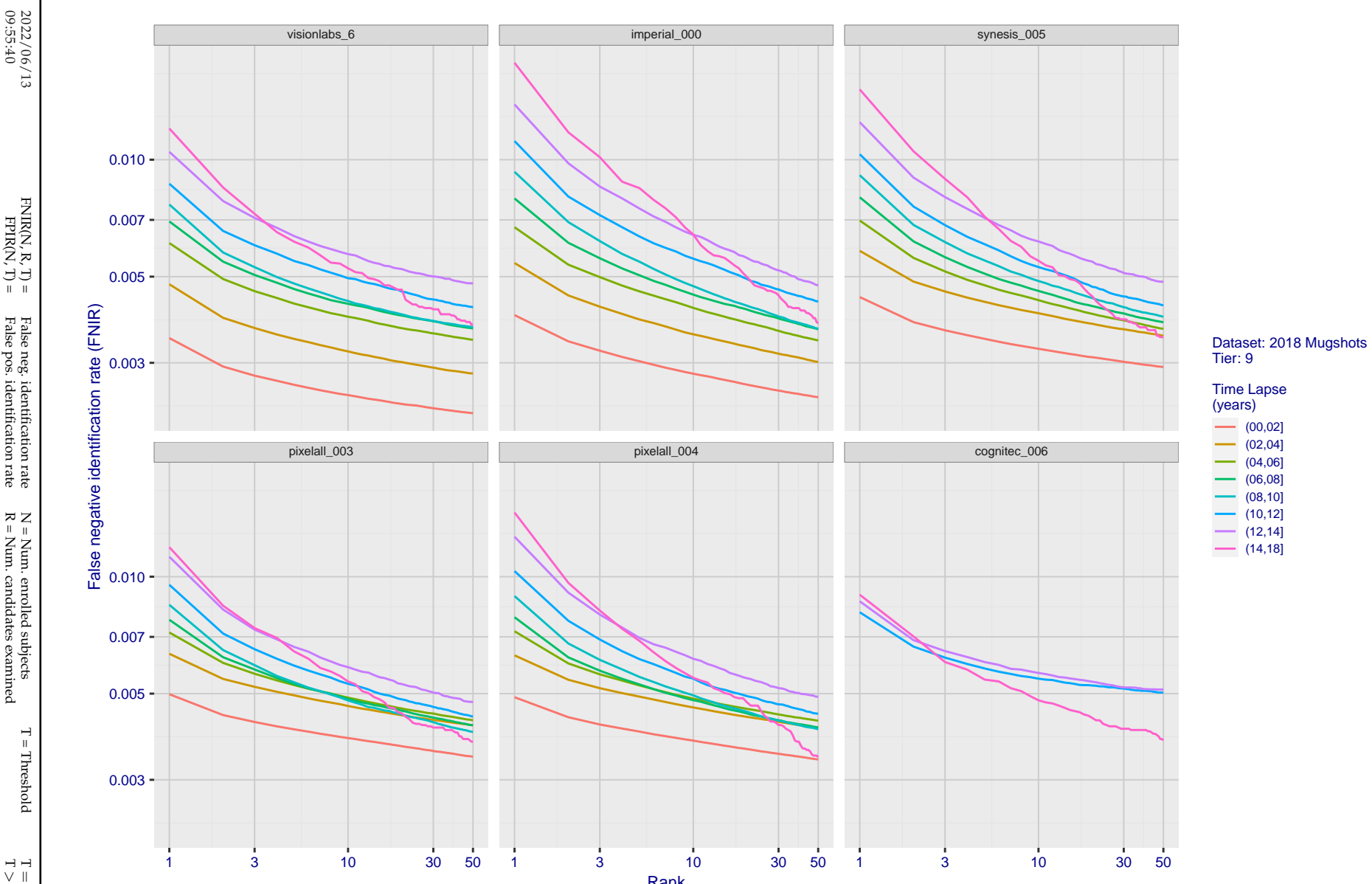
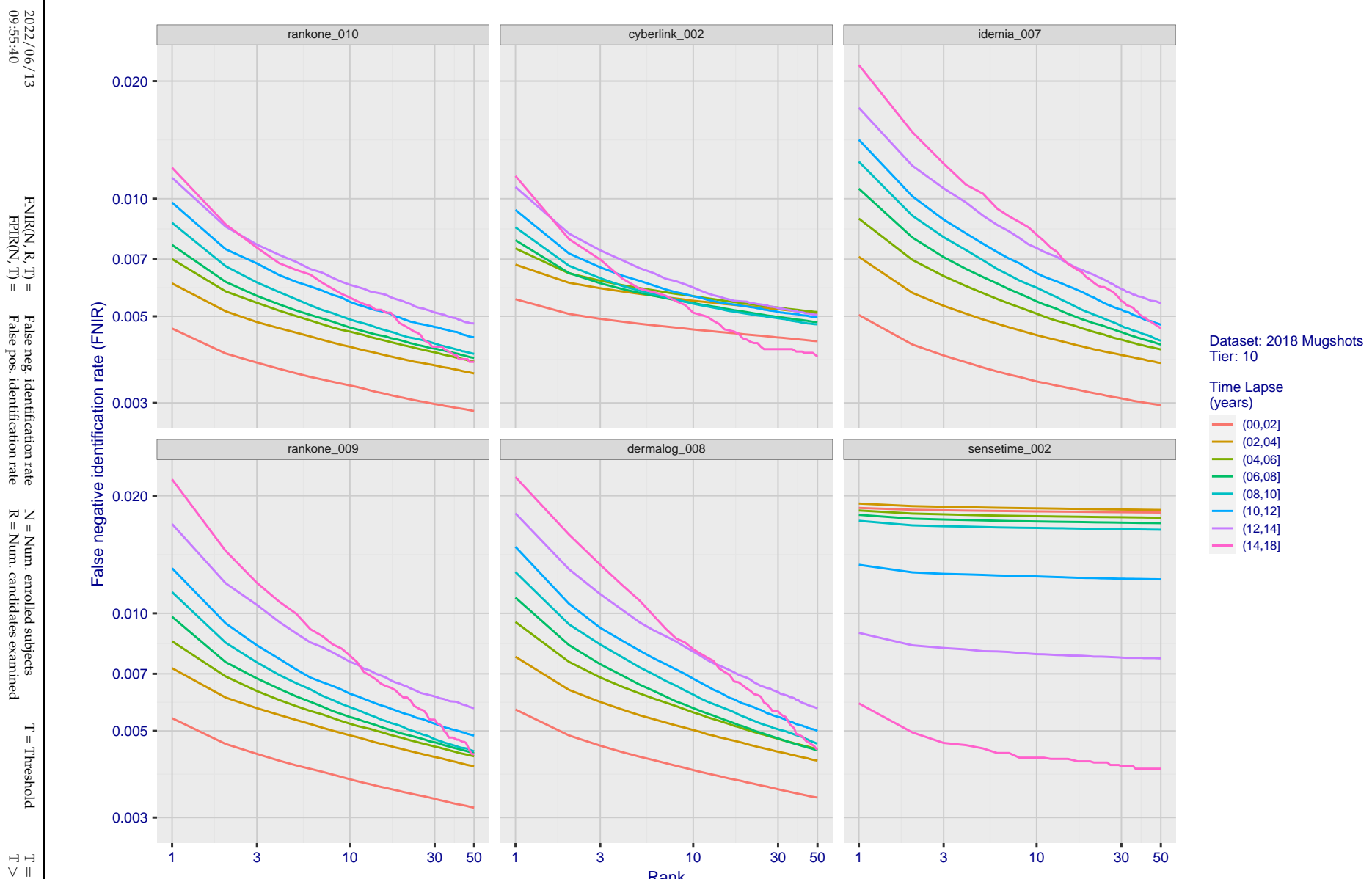


Figure 68: [FRVT-2018 Mugshot Ageing Dataset] Identification miss rates vs. rank by time-elapsed. The oldest image of each individual is enrolled. Thereafter, all more recent images are searched. Miss rates are computed over all searches noted in row 17 of Table 1 and binned by number of years between search and initial enrollment.



**Figure 69: [FRVT-2018 Mugshot Ageing Dataset] Identification miss rates vs. rank by time elapsed.** The oldest image of each individual is enrolled. Thereafter, all more recent images are searched. Miss rates are computed over all searches noted in row 17 of Table 1 and binned by number of years between search and initial enrollment.

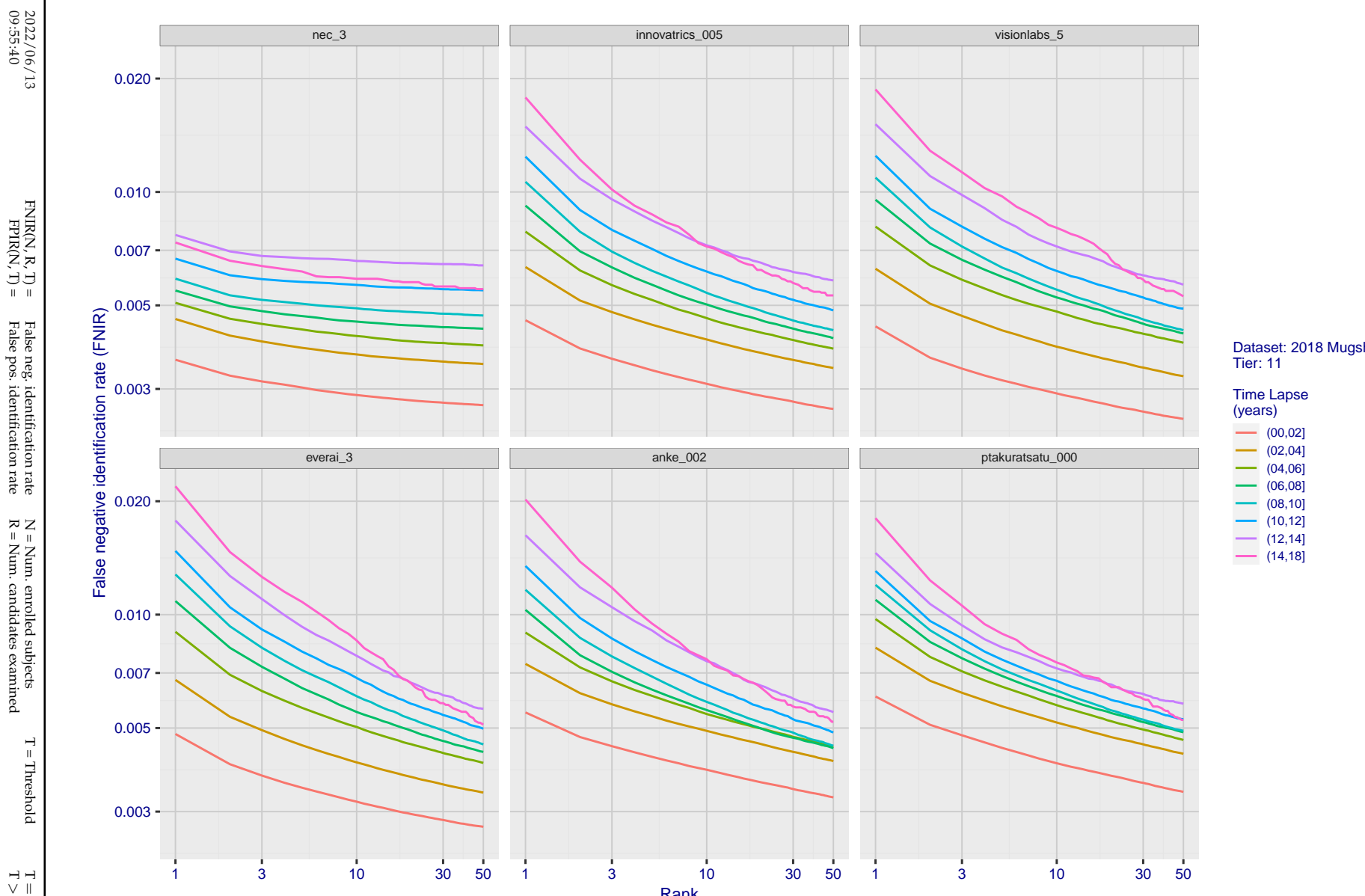


Figure 70: [FRVT-2018 Mugshot Ageing Dataset] Identification miss rates vs. rank by time-elapsed. The oldest image of each individual is enrolled. Thereafter, all more recent images are searched. Miss rates are computed over all searches noted in row 17 of Table 1 and binned by number of years between search and initial enrollment.

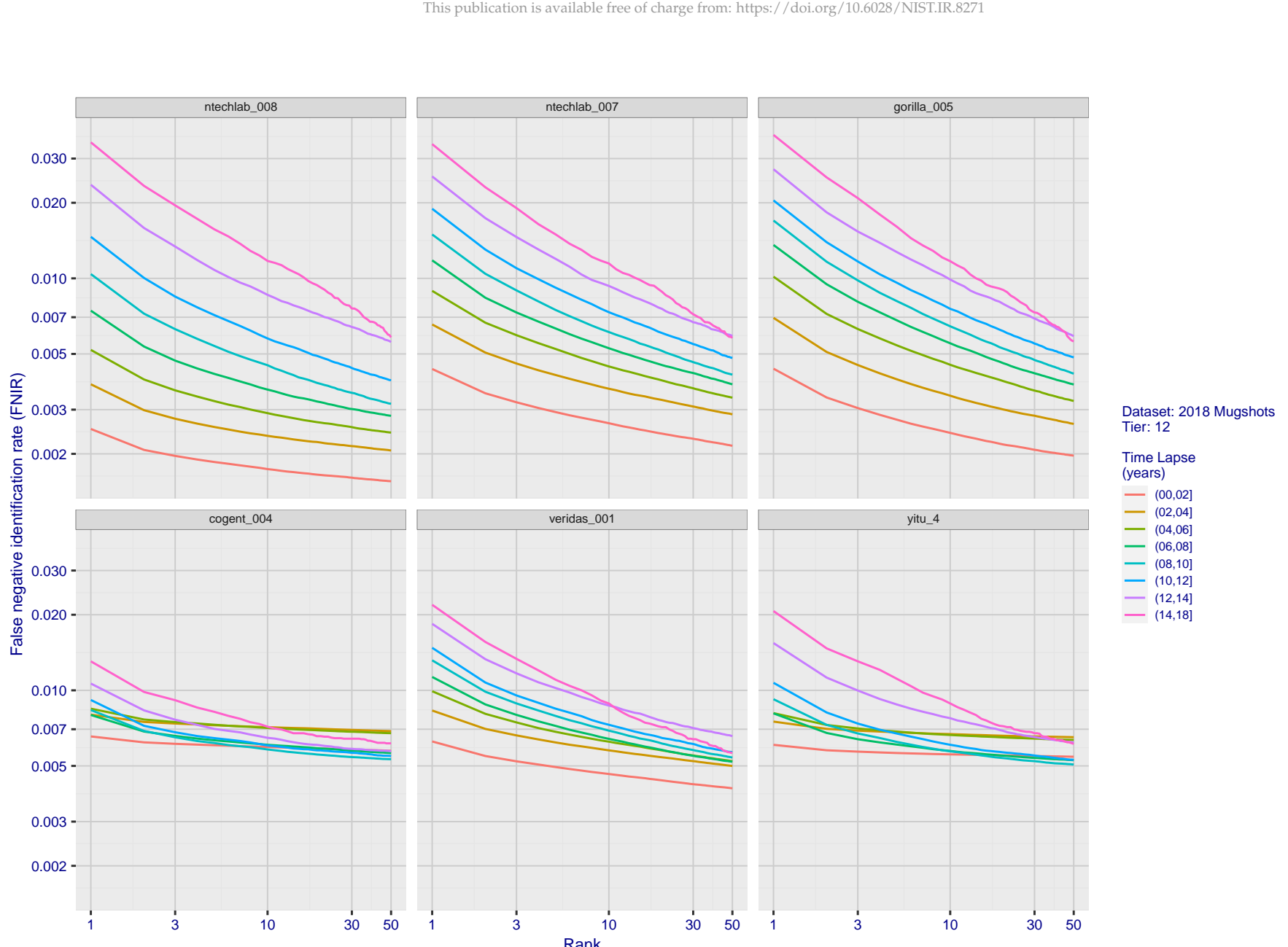
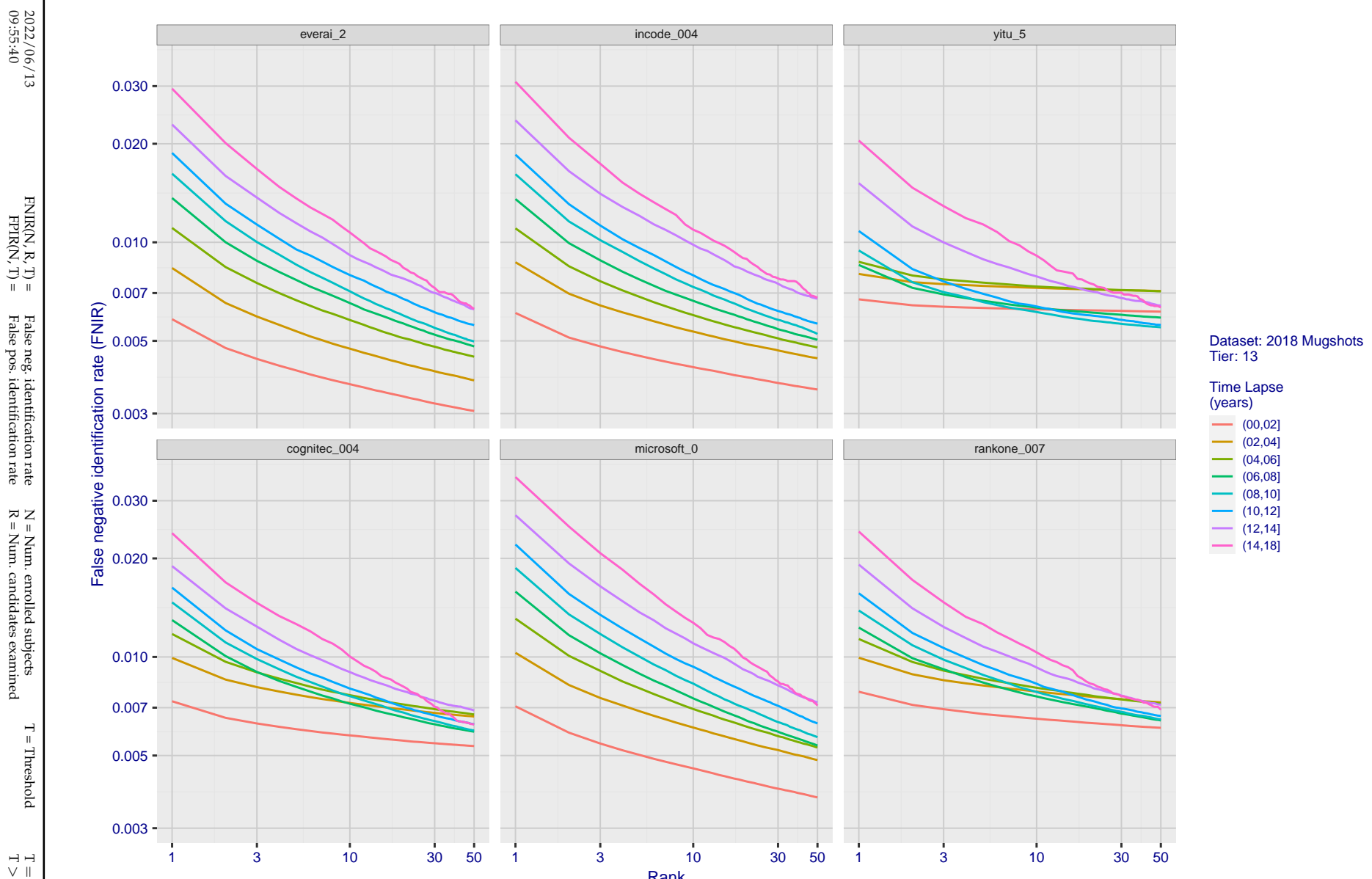


Figure 71: [FRVT-2018 Mugshot Ageing Dataset] Identification miss rates vs. rank by time-elapsed. The oldest image of each individual is enrolled. Thereafter, all more recent images are searched. Miss rates are computed over all searches noted in row 17 of Table 1 and binned by number of years between search and initial enrollment.



**Figure 72: [FRVT-2018 Mugshot Ageing Dataset] Identification miss rates vs. rank by time-elapsed.** The oldest image of each individual is enrolled. Thereafter, all more recent images are searched. Miss rates are computed over all searches noted in row 17 of Table 1 and binned by number of years between search and initial enrollment.

2022/06/13  
09:55:40FNIR(N, R, T) = False neg. identification rate  
FPIR(N, T) = False pos. identification rateN = Num. enrolled subjects  
R = Num. candidates examinedT = Threshold  
T = 0 → Investigation

T &gt; 0 → Identification

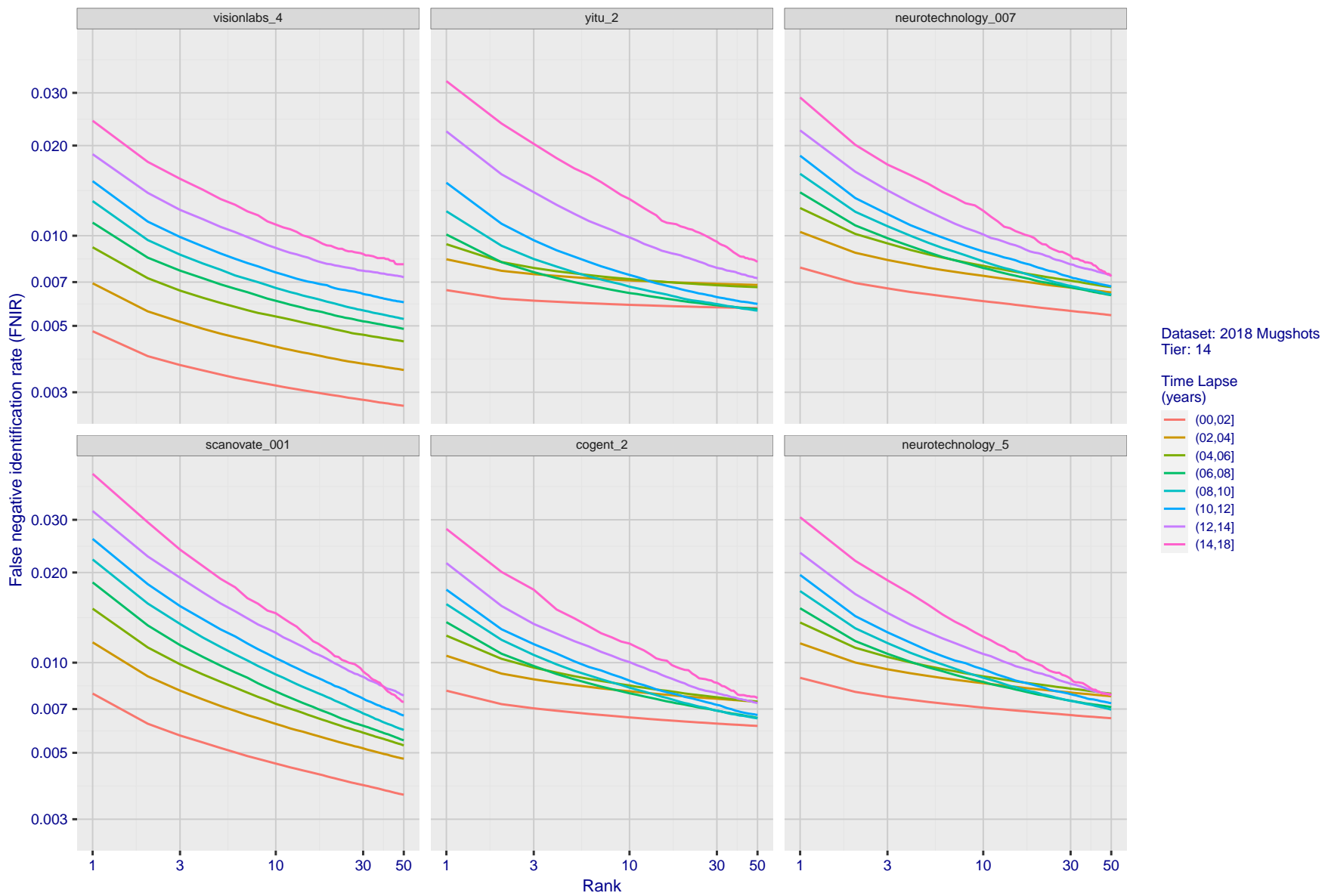


**Figure 73: [FRVT-2018 Mugshot Ageing Dataset] Identification miss rates vs. rank by time-elapsed.** The oldest image of each individual is enrolled. Thereafter, all more recent images are searched. Miss rates are computed over all searches noted in row 17 of Table 1 and binned by number of years between search and initial enrollment.

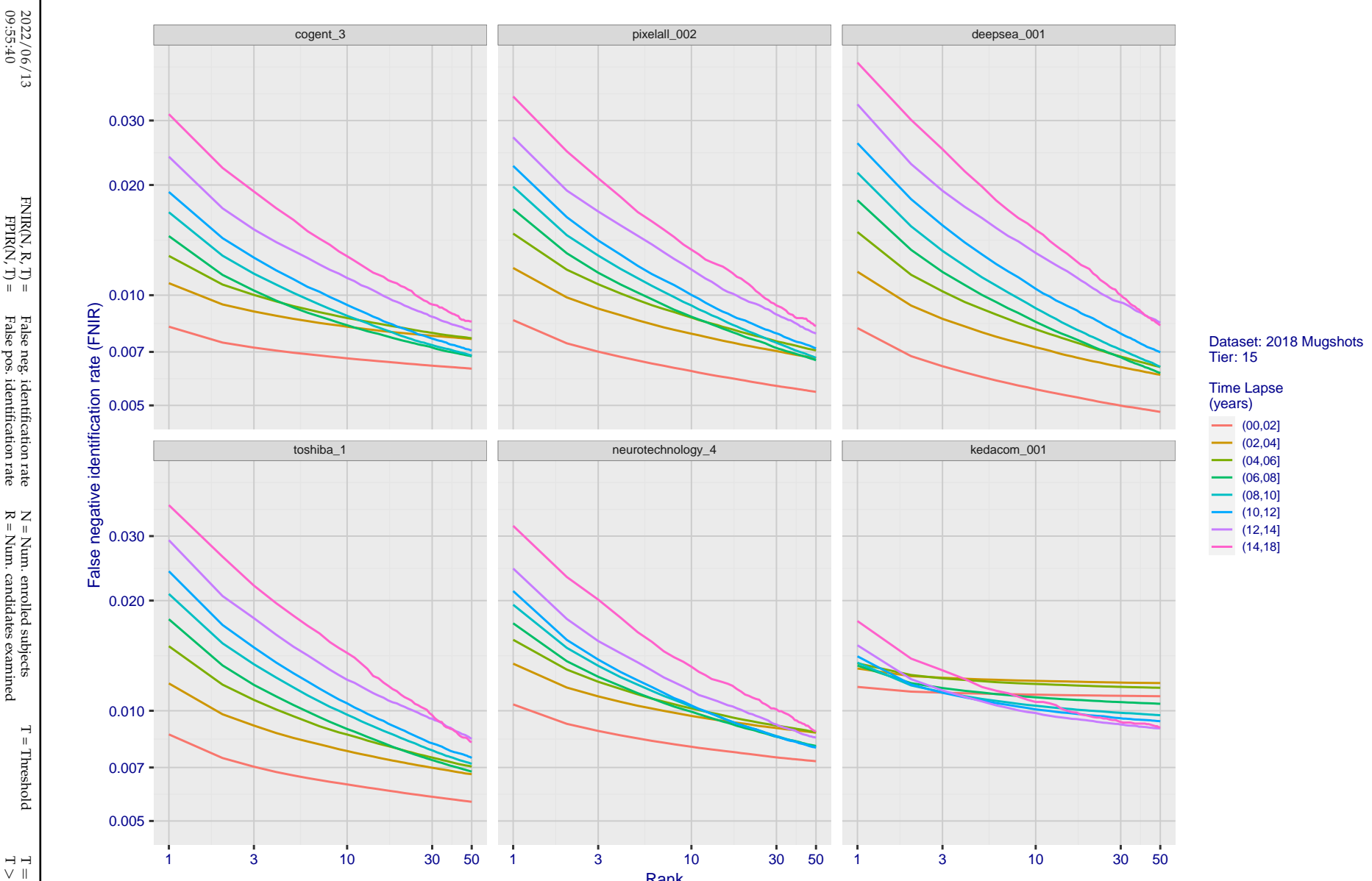


**Figure 74: [FRVT-2018 Mugshot Ageing Dataset] Identification miss rates vs. rank by time-elapsed.** The oldest image of each individual is enrolled. Thereafter, all more recent images are searched. Miss rates are computed over all searches noted in row 17 of Table 1 and binned by number of years between search and initial enrollment.

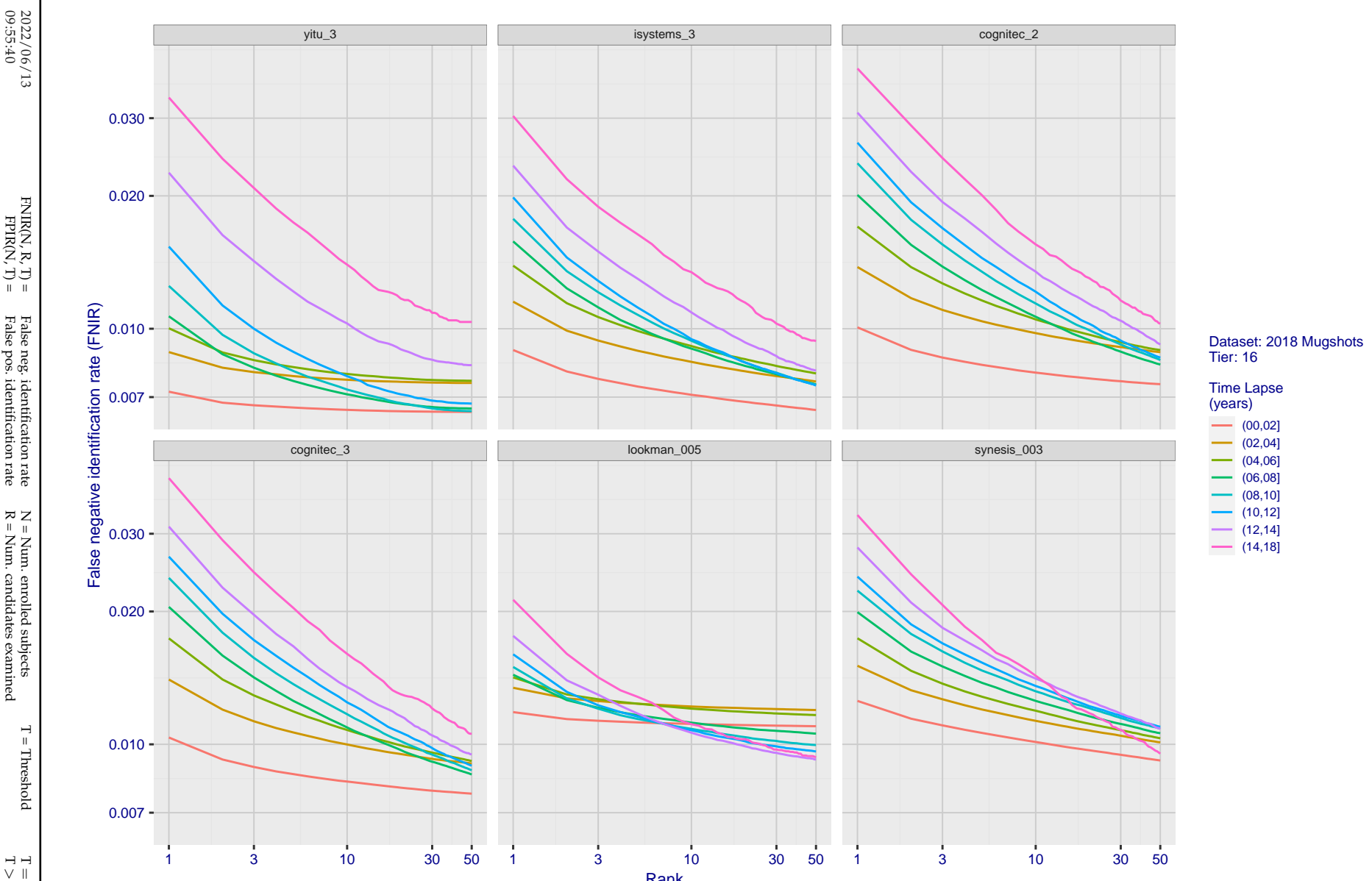


Figure 75: [FRVT-2018 Mugshot Ageing Dataset] Identification miss rates vs. rank by time-elapsed. The oldest image of each individual is enrolled. Thereafter, all more recent images are searched. Miss rates are computed over all searches noted in row 17 of Table 1 and binned by number of years between search and initial enrollment.

2022/06/13  
09:55:40  
  
 $\text{FNIR}(N, R, T) =$   
False neg. identification rate  
 $\text{FPIR}(N, T) =$   
False pos. identification rate  
 $N =$  Num. enrolled subjects  
 $R =$  Num. candidates examined  
 $T =$  Threshold  
 $T = 0 \rightarrow$  Investigation  
 $T > 0 \rightarrow$  Identification

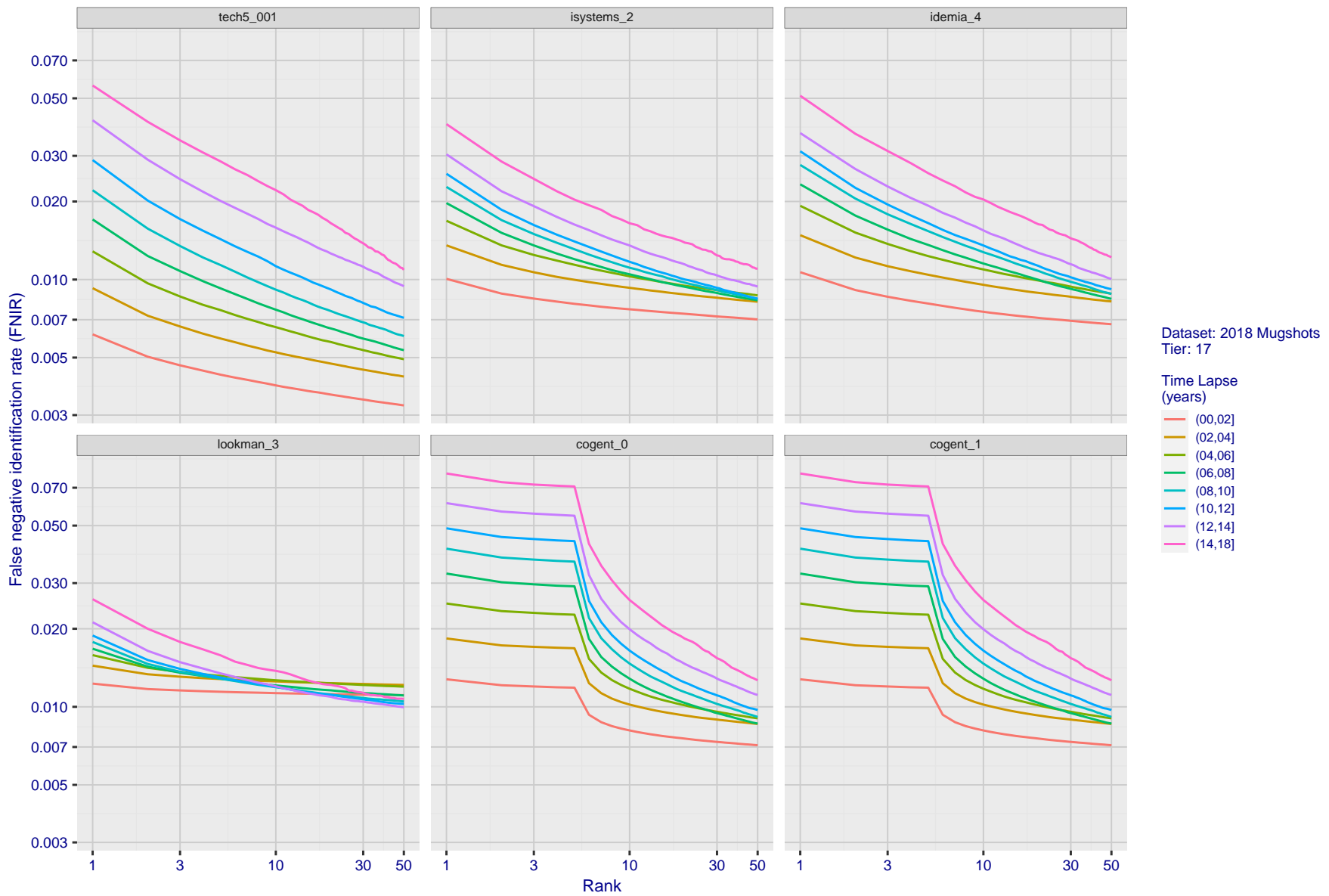


Figure 76: [FRVT-2018 Mugshot Ageing Dataset] Identification miss rates vs. rank by time-elapsed. The oldest image of each individual is enrolled. Thereafter, all more recent images are searched. Miss rates are computed over all searches noted in row 17 of Table 1 and binned by number of years between search and initial enrollment.

2022/06/13  
09:55:40  
  
 $\text{FNIR}(N, R, T) =$   
False neg. identification rate  
 $\text{FPIR}(N, T) =$   
False pos. identification rate  
 $N = \text{Num. enrolled subjects}$   
 $R = \text{Num. candidates examined}$   
 $T = \text{Threshold}$   
 $T = 0 \rightarrow \text{Investigation}$   
 $T > 0 \rightarrow \text{Identification}$

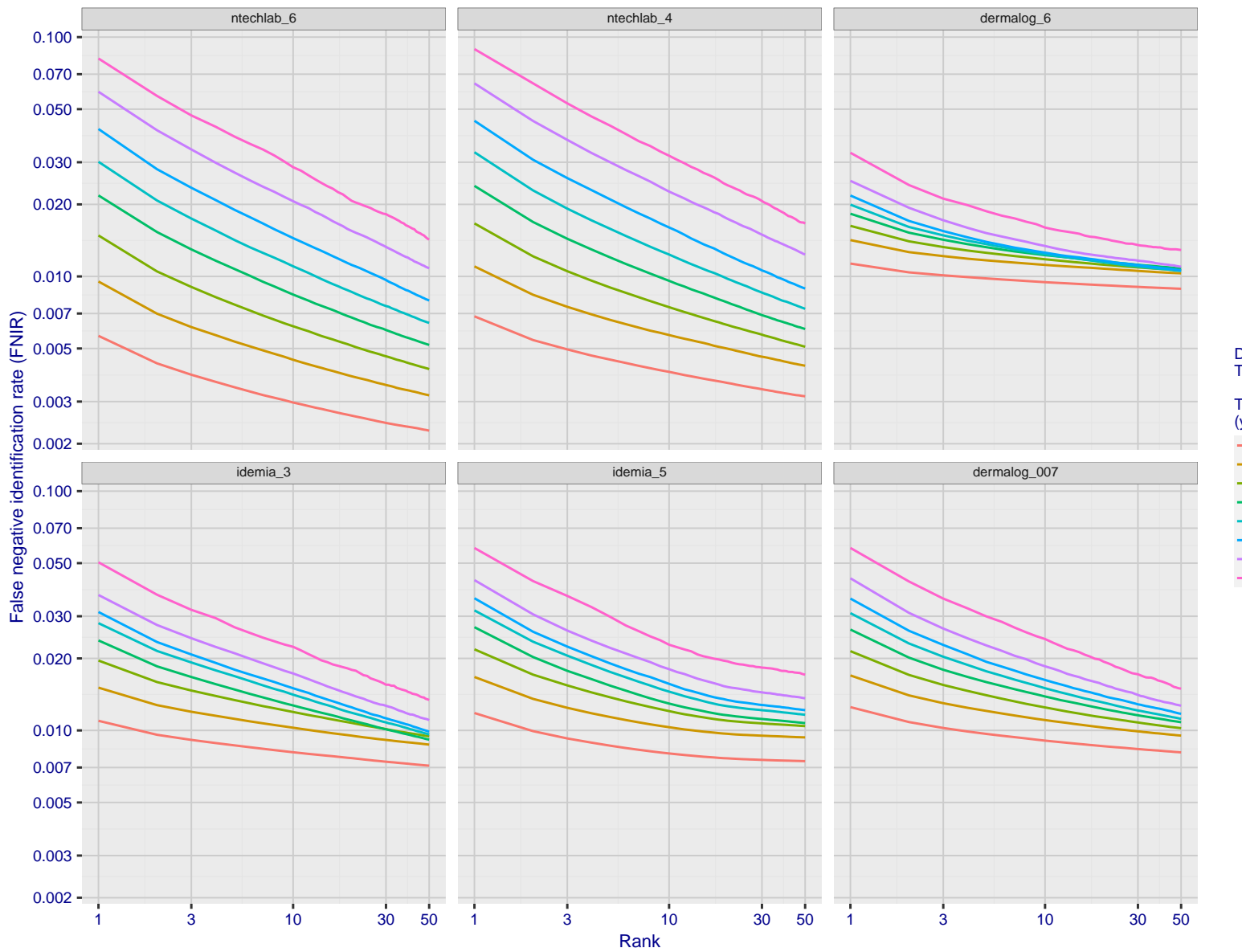


Figure 77: [FRVT-2018 Mugshot Ageing Dataset] Identification miss rates vs. rank by time-elapsed. The oldest image of each individual is enrolled. Thereafter, all more recent images are searched. Miss rates are computed over all searches noted in row 17 of Table 1 and binned by number of years between search and initial enrollment.

2022/06/13  
09:55:40FNIR(N, R, T) = False neg. identification rate  
FPIR(N, T) = False pos. identification rateN = Num. enrolled subjects  
R = Num. candidates examined

T = Threshold

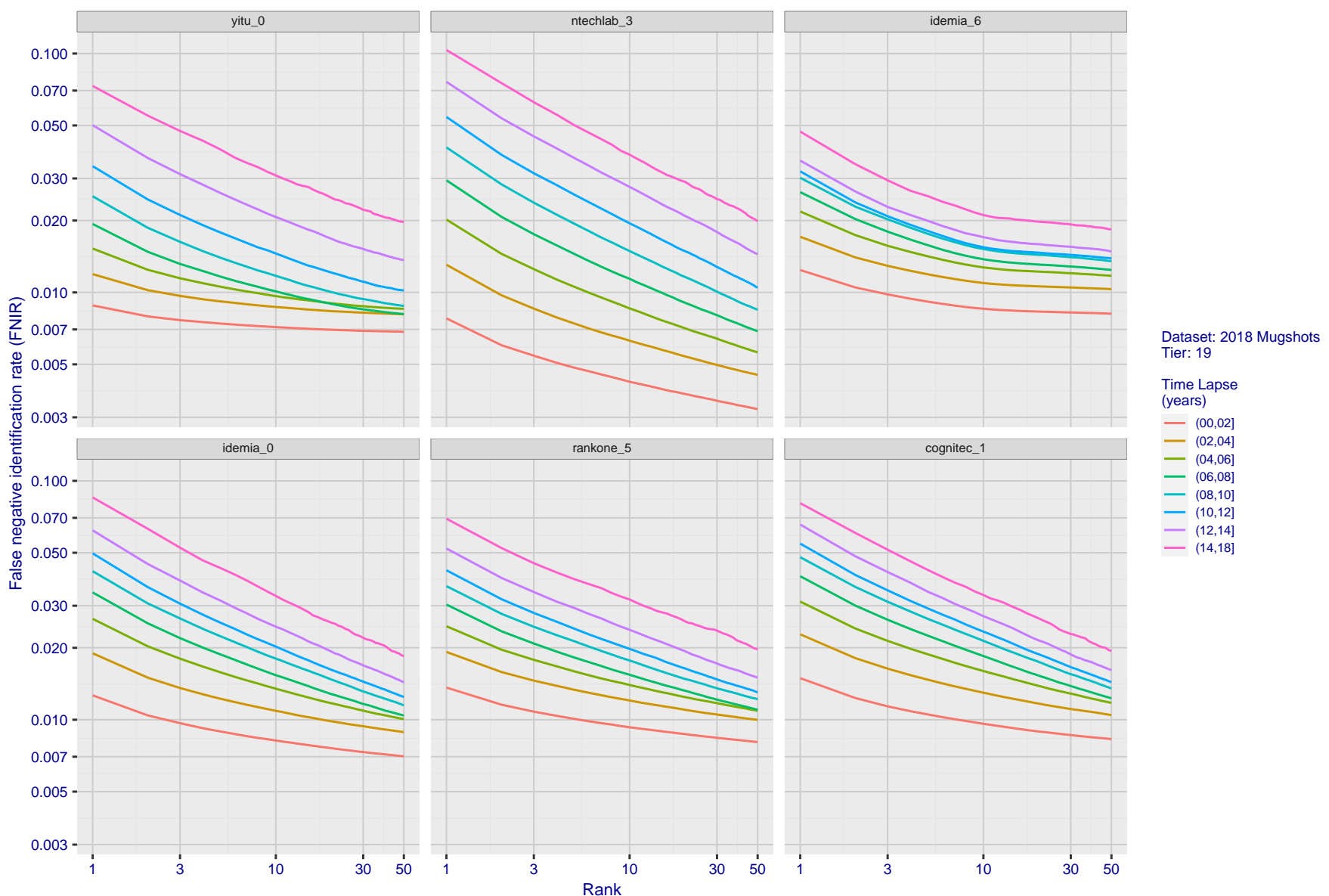
T = 0 → Investigation  
T > 0 → Identification

Figure 78: [FRVT-2018 Mugshot Ageing Dataset] Identification miss rates vs. rank by time elapsed. The oldest image of each individual is enrolled. Thereafter, all more recent images are searched. Miss rates are computed over all searches noted in row 17 of Table 1 and binned by number of years between search and initial enrollment.

2022/06/13  
09:55:40  
 $\text{FNIR}(N, R, T) =$   
 $\text{False neg. identification rate}$   
 $\text{FPFR}(N, T) =$   
 $\text{False pos. identification rate}$   
 $N = \text{Num. enrolled subjects}$   
 $R = \text{Num. candidates examined}$   
 $T = \text{Threshold}$   
 $T = 0 \rightarrow \text{Investigation}$   
 $T > 0 \rightarrow \text{Identification}$

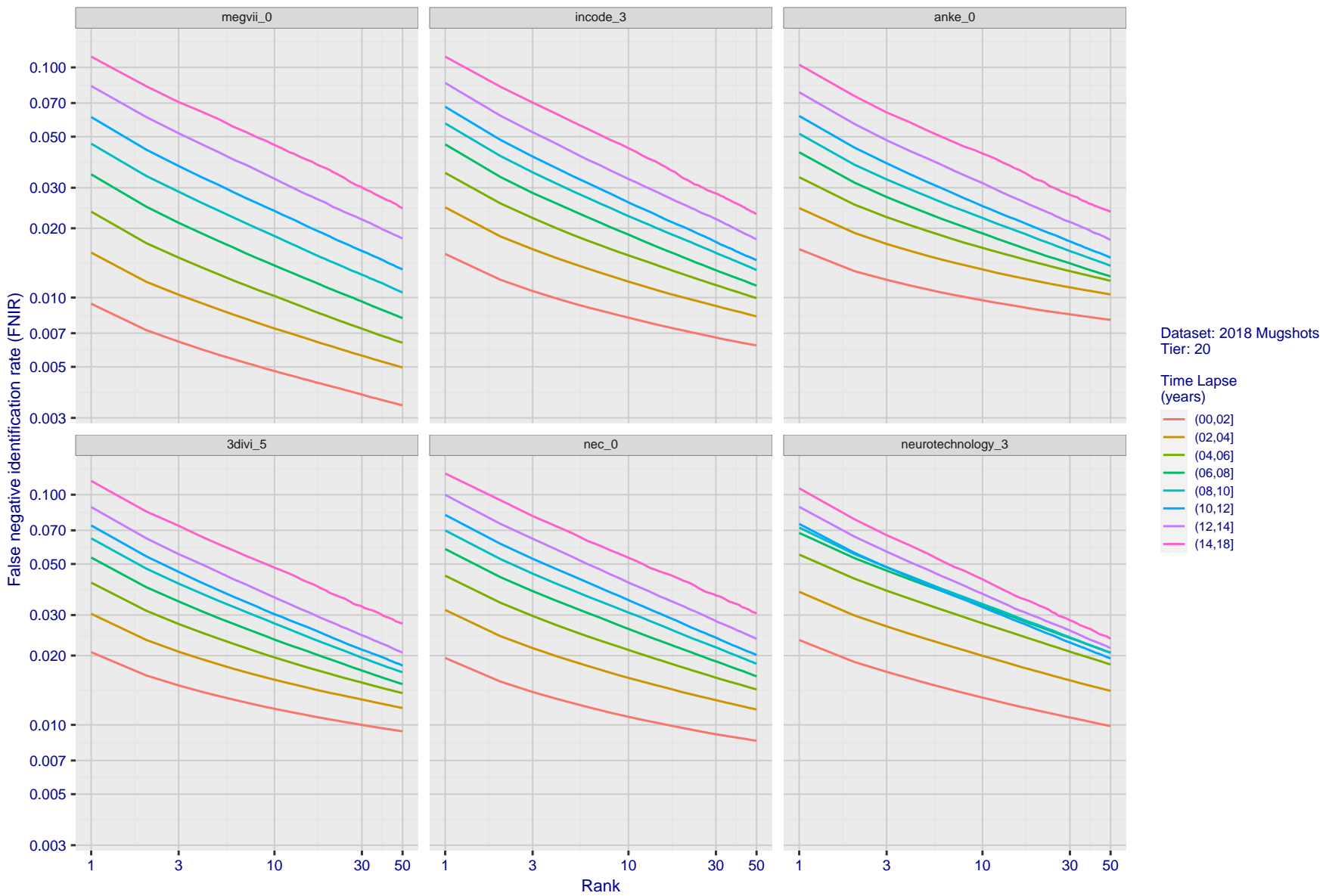


Figure 79: [FRVT-2018 Mugshot Ageing Dataset] Identification miss rates vs. rank by time-elapsed. The oldest image of each individual is enrolled. Thereafter, all more recent images are searched. Miss rates are computed over all searches noted in row 17 of Table 1 and binned by number of years between search and initial enrollment.

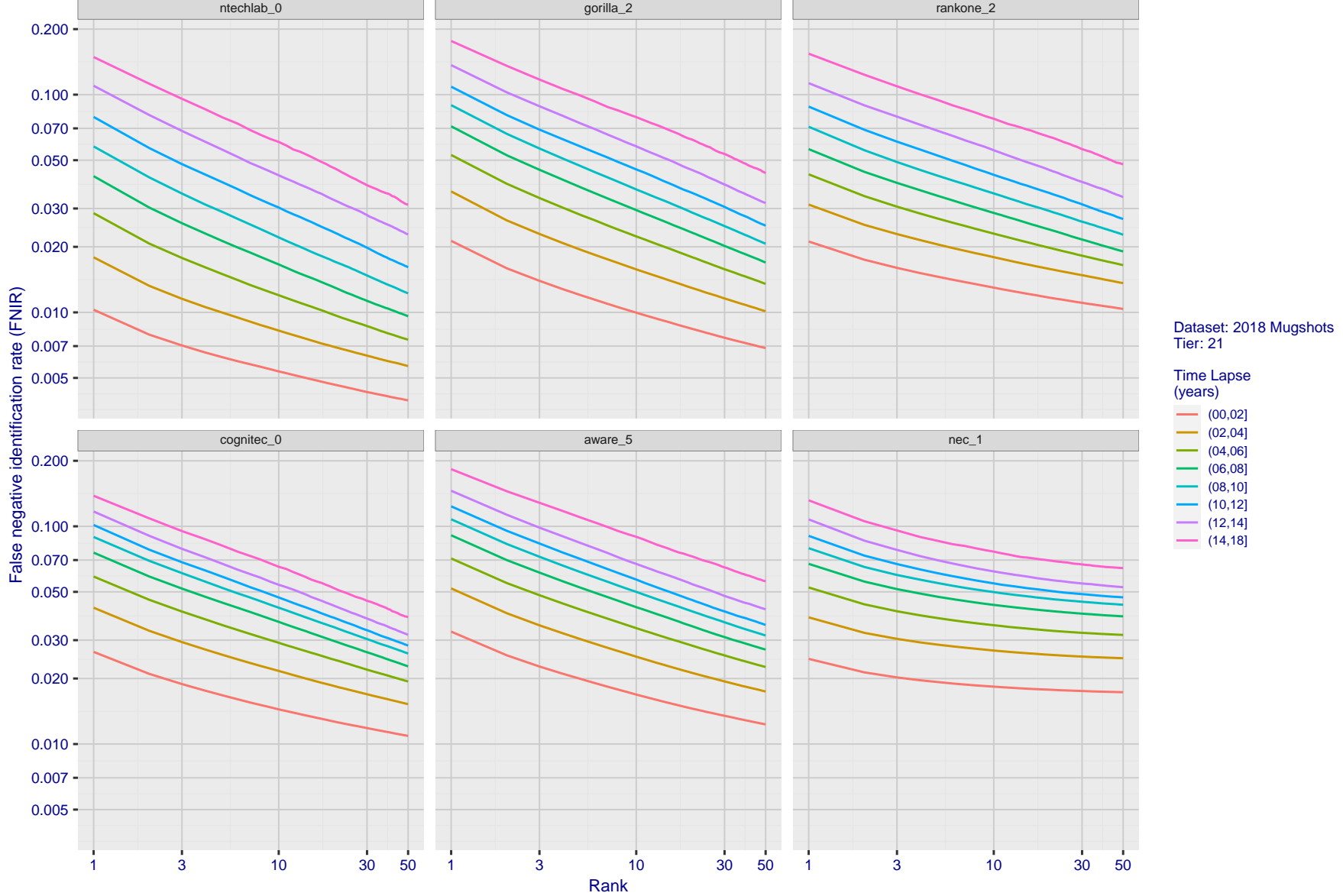


Figure 80: [FRVT-2018 Mugshot Ageing Dataset] Identification miss rates vs. rank by time-elapsed. The oldest image of each individual is enrolled. Thereafter, all more recent images are searched. Miss rates are computed over all searches noted in row 17 of Table 1 and binned by number of years between search and initial enrollment.

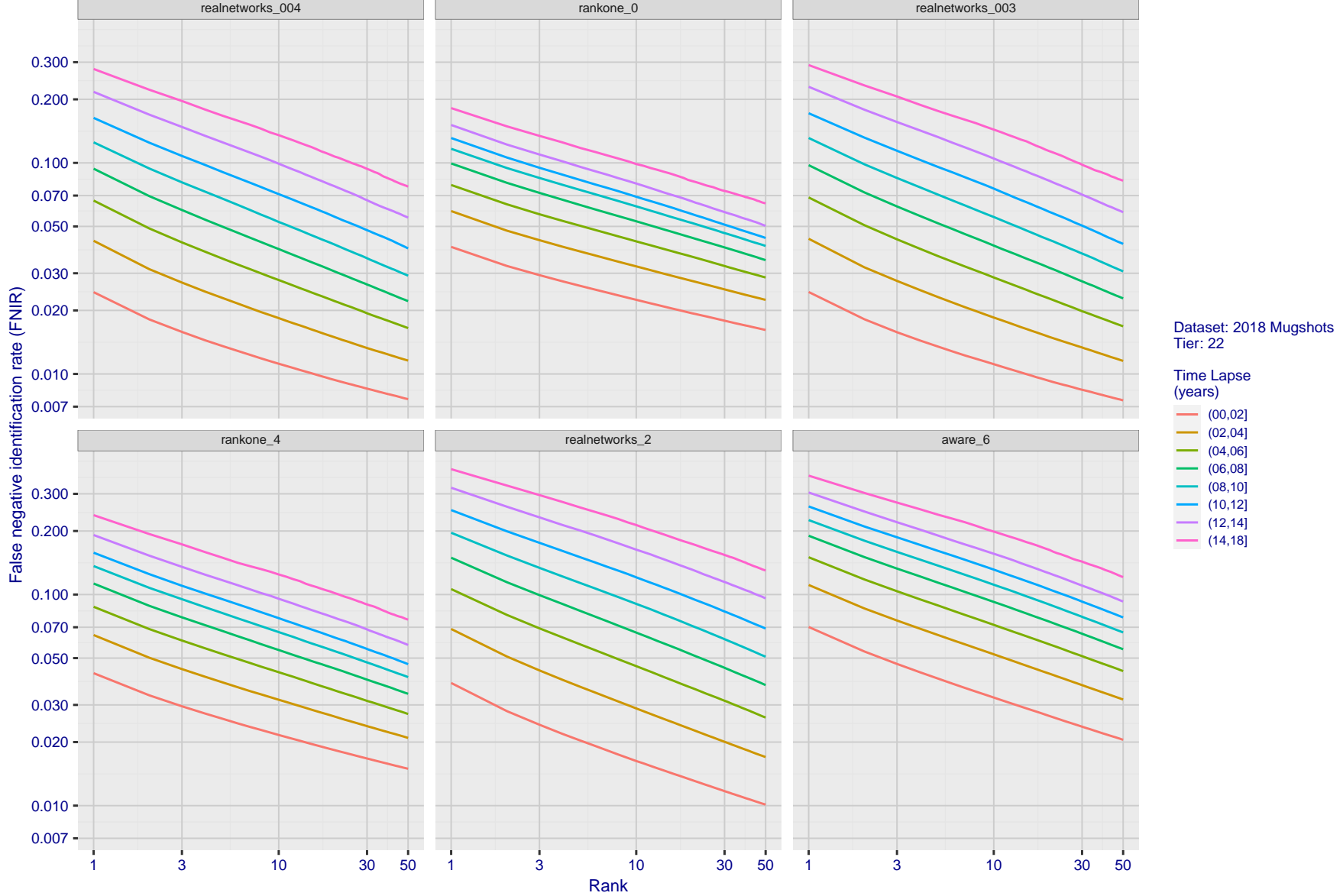


Figure 81: [FRVT-2018 Mugshot Ageing Dataset] Identification miss rates vs. rank by time-elapsed. The oldest image of each individual is enrolled. Thereafter, all more recent images are searched. Miss rates are computed over all searches noted in row 17 of Table 1 and binned by number of years between search and initial enrollment.

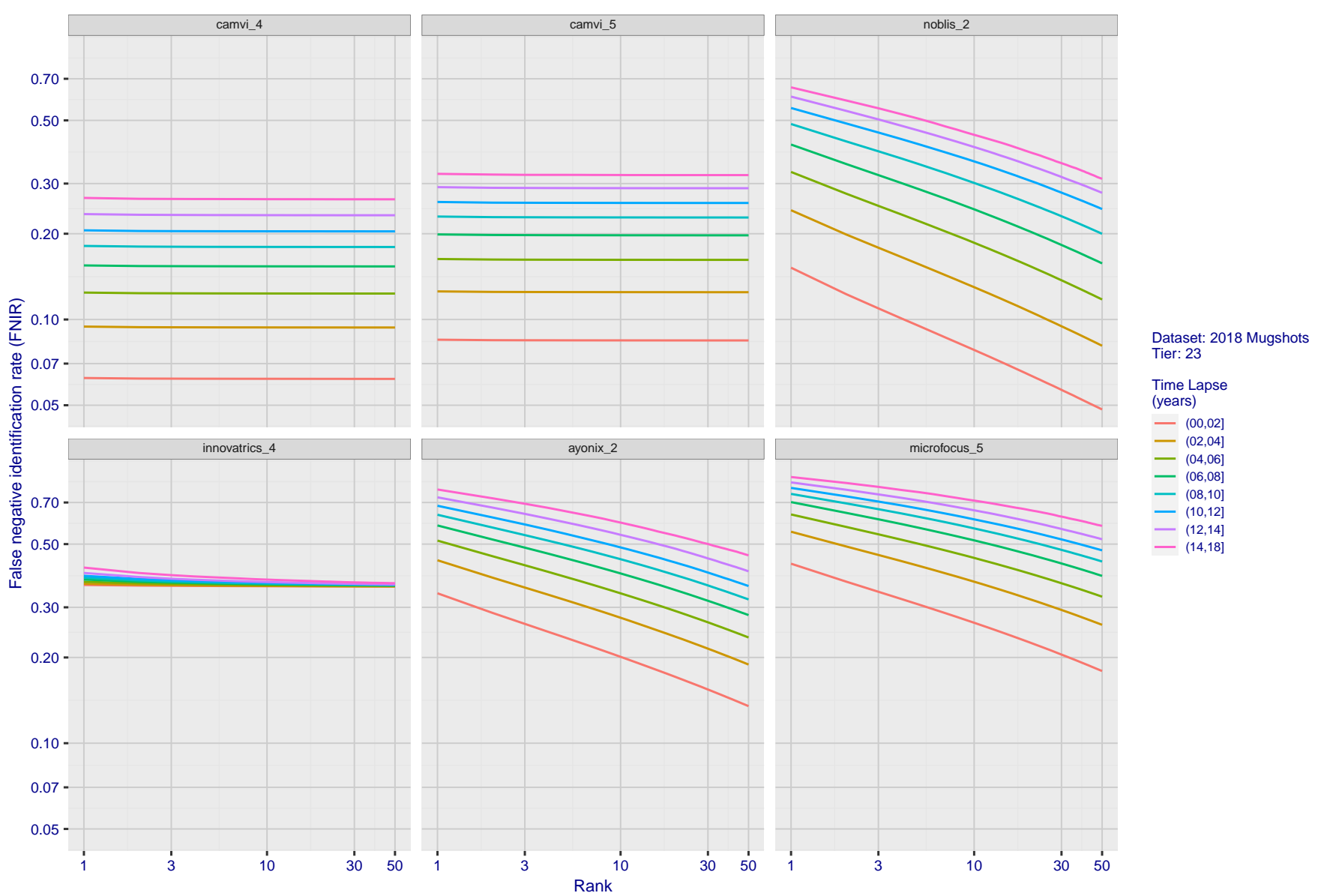


Figure 82: [FRVT-2018 Mugshot Ageing Dataset] Identification miss rates vs. rank by time-elapsed. The oldest image of each individual is enrolled. Thereafter, all more recent images are searched. Miss rates are computed over all searches noted in row 17 of Table 1 and binned by number of years between search and initial enrollment.

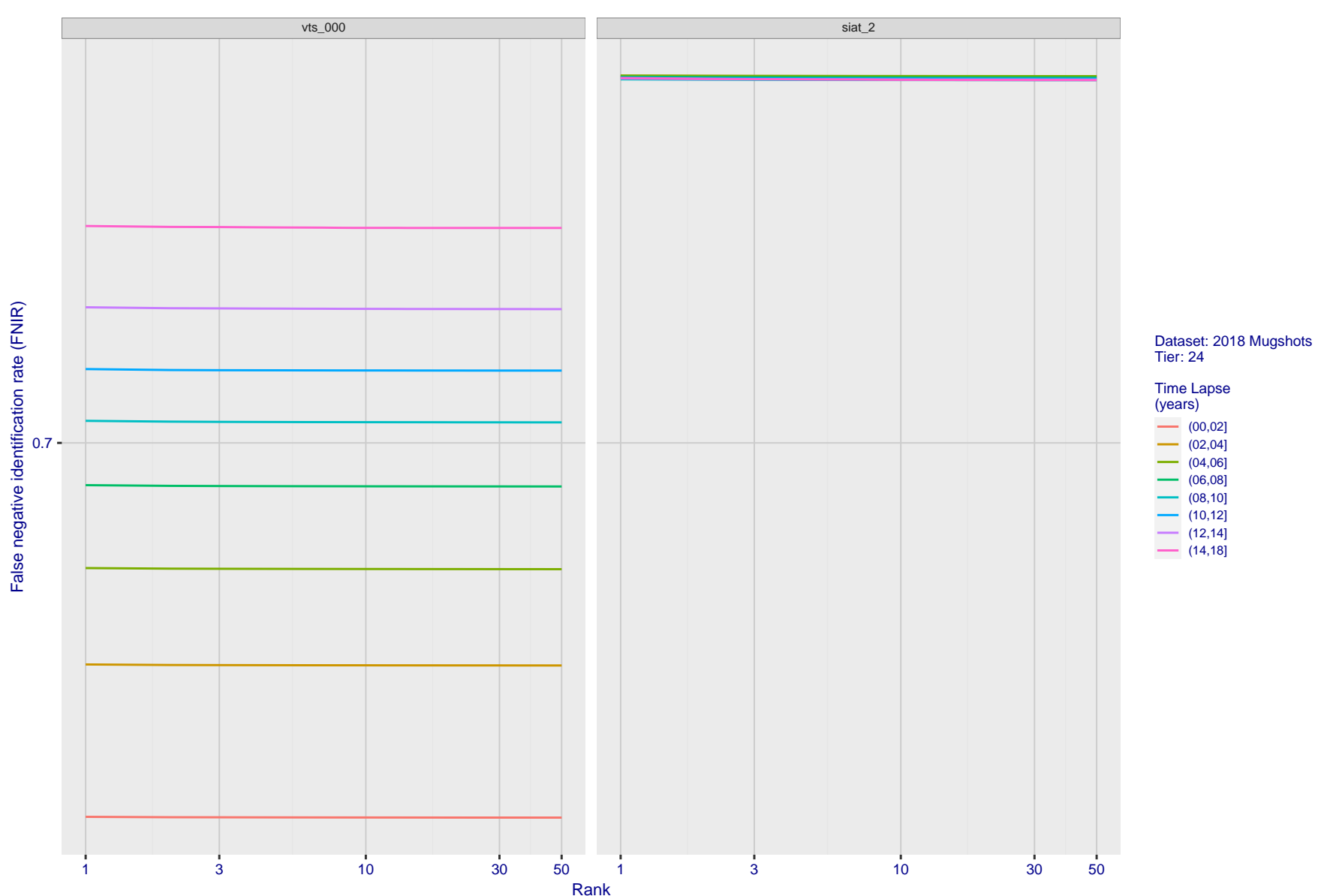
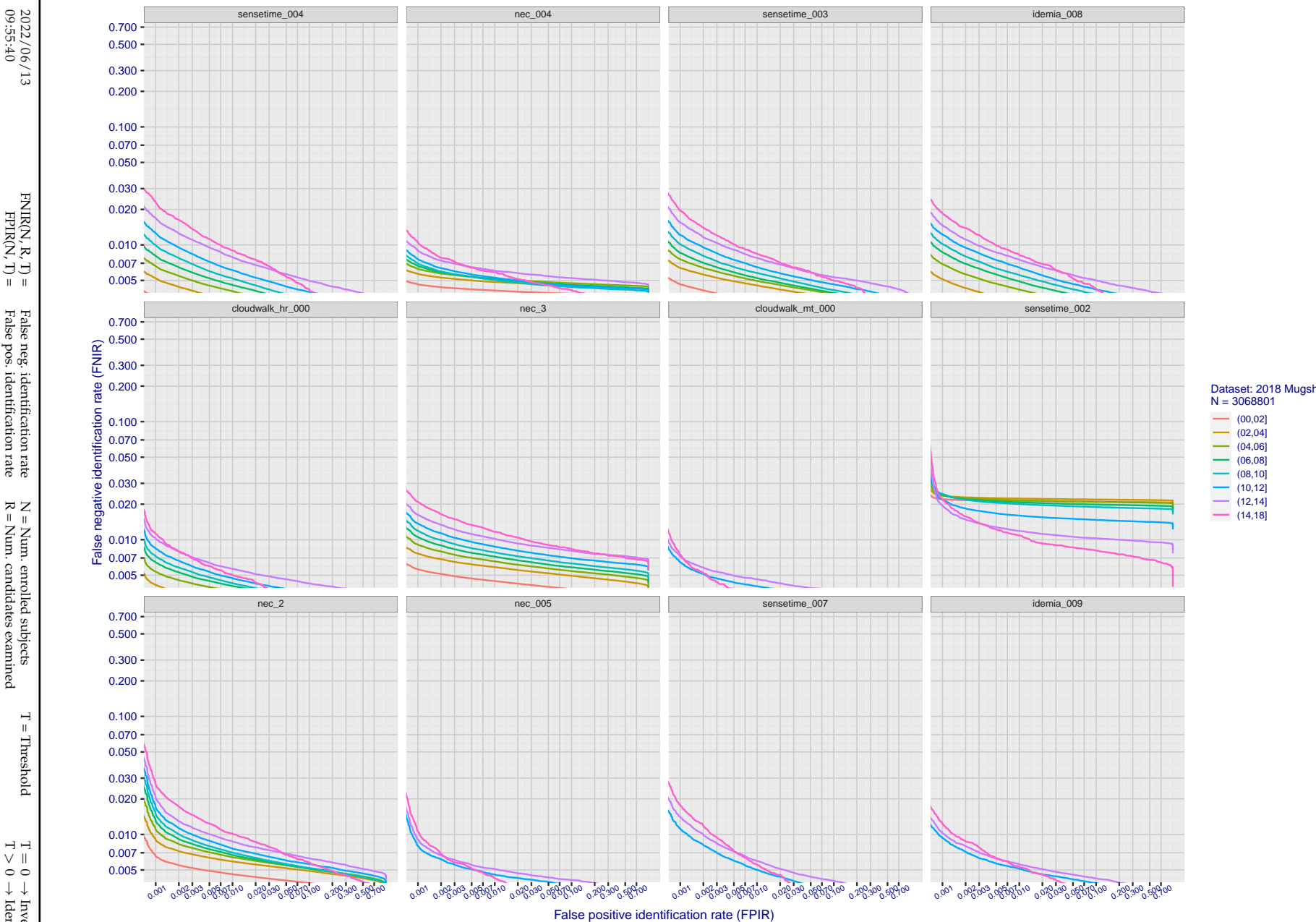


Figure 83: [FRVT-2018 Mugshot Ageing Dataset] Identification miss rates vs. rank by time-elapsed. The oldest image of each individual is enrolled. Thereafter, all more recent images are searched. Miss rates are computed over all searches noted in row 17 of Table 1 and binned by number of years between search and initial enrollment.

---

2022/06/13  
09:55:40      FNIR(N, R, T) = False neg. identification rate  
                  FPIR(N, T) = False pos. identification rate  
N = Num. enrolled subjects  
R = Num. candidates examined  
T = Threshold  
T = 0 → Investigation  
T > 0 → Identification



**Figure 84: [FRVT-2018 Mugshot Ageing Dataset] Identification miss rates vs. FPIR by time-elapsed.** The oldest image of each individual is enrolled. Thereafter, all more recent images are searched. Miss rates are computed over all searches noted in row 17 of Table 1 and binned by number of years between search and initial enrollment. FPIR is computed from the same FRVT 2018 non-mates noted in row 3 of Table 1 with  $N = 3000\,000$ .

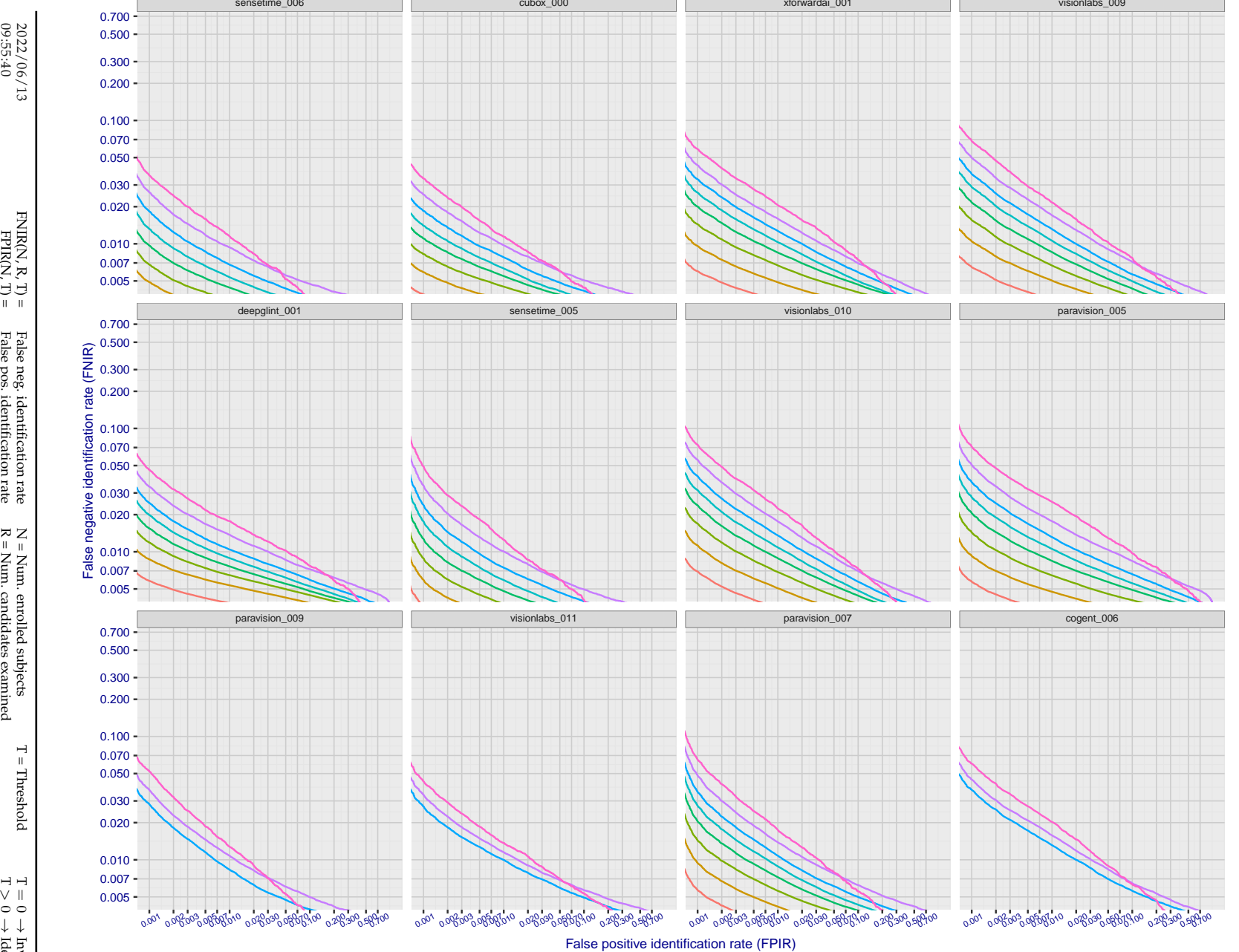


**Figure 85: [FRVT-2018 Mugshot Ageing Dataset] Identification miss rates vs. FPIR by time-elapsed.** The oldest image of each individual is enrolled. Thereafter, all more recent images are searched. Miss rates are computed over all searches noted in row 17 of Table 1 and binned by number of years between search and initial enrollment. FPIR is computed from the same FRVT 2018 non-mates noted in row 3 of Table 1 with  $N = 3\,000\,000$ .

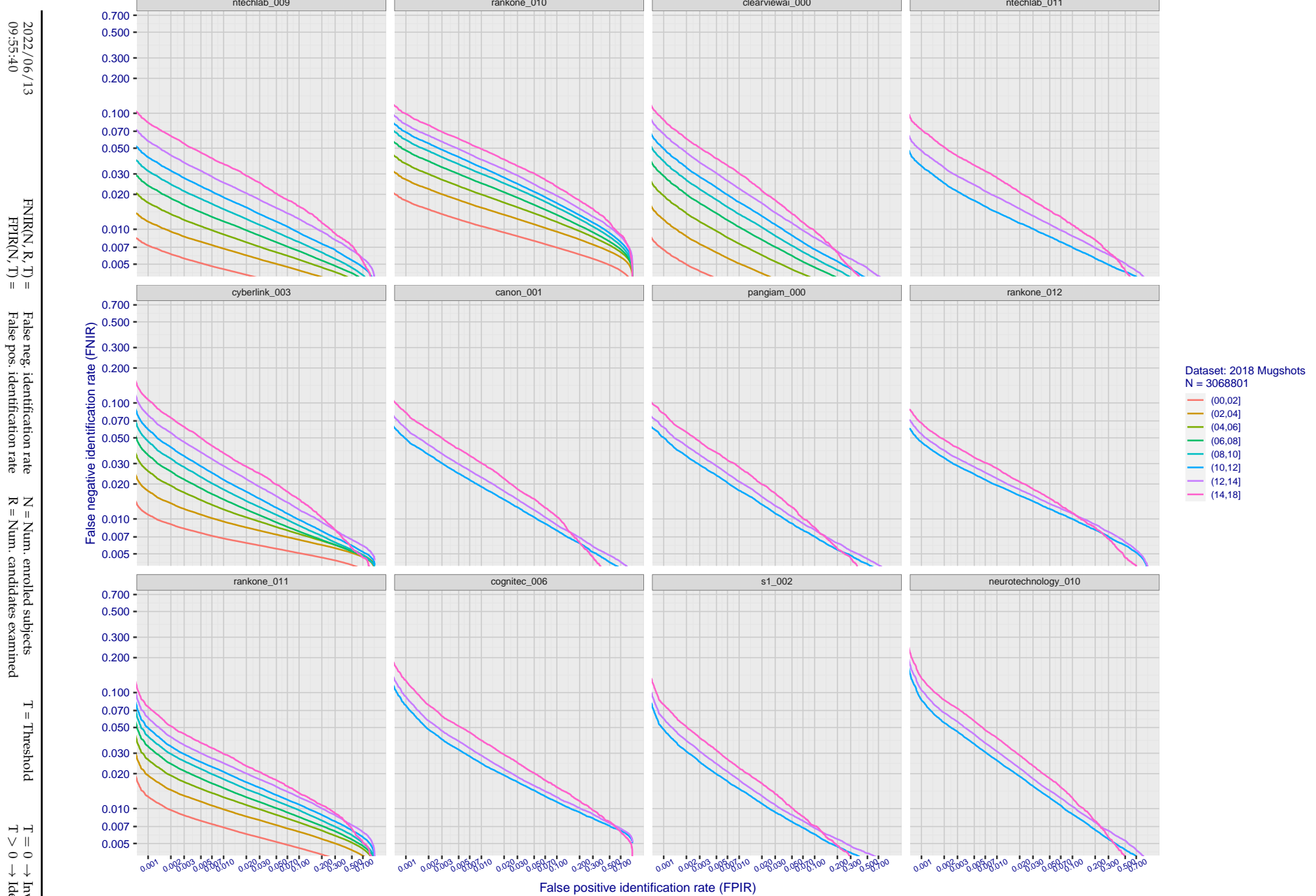


**Figure 86: [FRVT-2018 Mugshot Ageing Dataset] Identification miss rates vs. FPIR by time-elapsed.** The oldest image of each individual is enrolled. Thereafter, all more recent images are searched. Miss rates are computed over all searches noted in row 17 of Table 1 and binned by number of years between search and initial enrollment. FPIR is computed from the same FRVT 2018 non-mates noted in row 3 of Table 1 with N = 3 000 000.

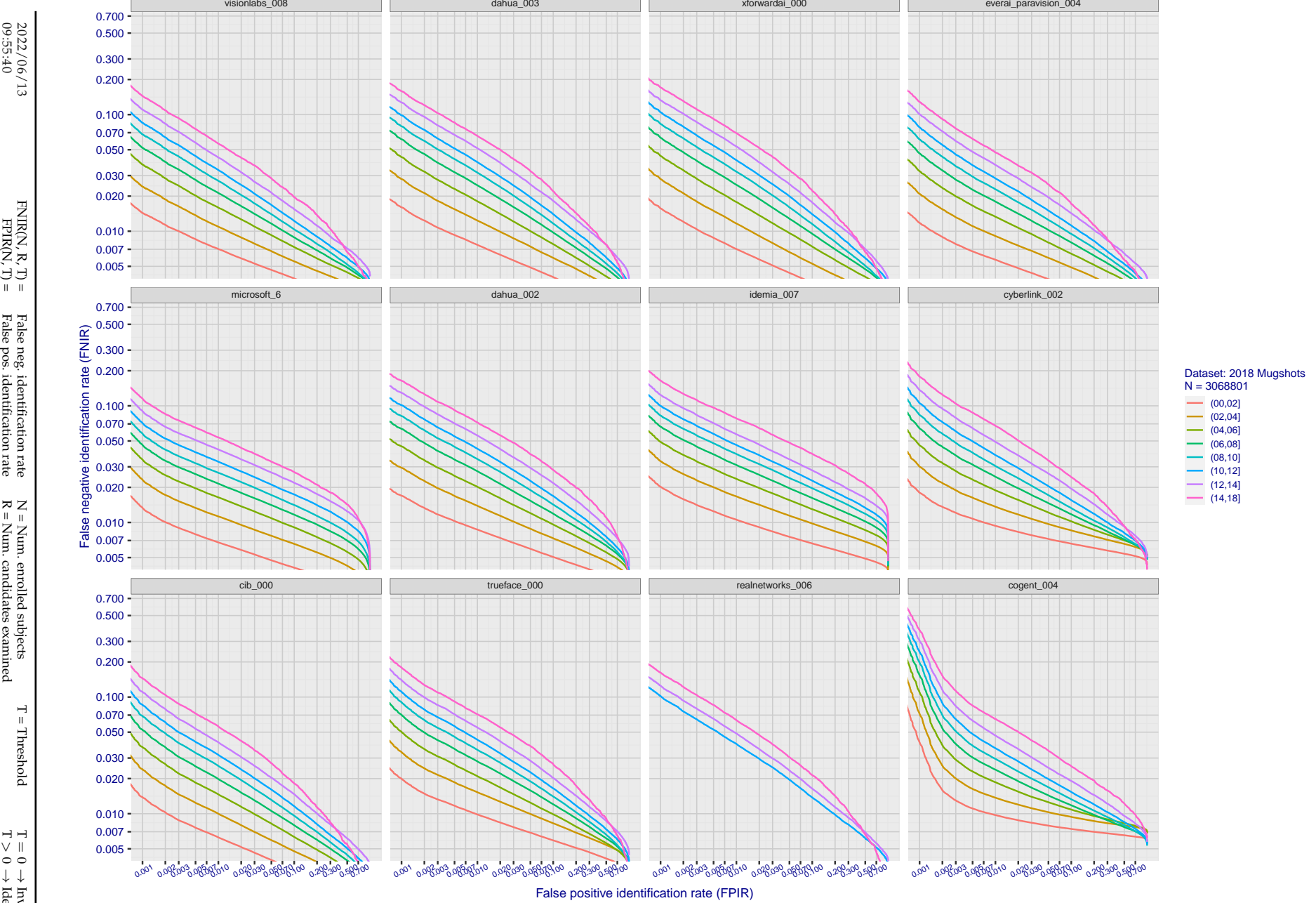


**Figure 87: [FRVT-2018 Mugshot Ageing Dataset] Identification miss rates vs. FPIR by time-elapsed.** The oldest image of each individual is enrolled. Thereafter, all more recent images are searched. Miss rates are computed over all searches noted in row 17 of Table 1 and binned by number of years between search and initial enrollment. FPIR is computed from the same FRVT 2018 non-mates noted in row 3 of Table 1 with N = 3 000 000.

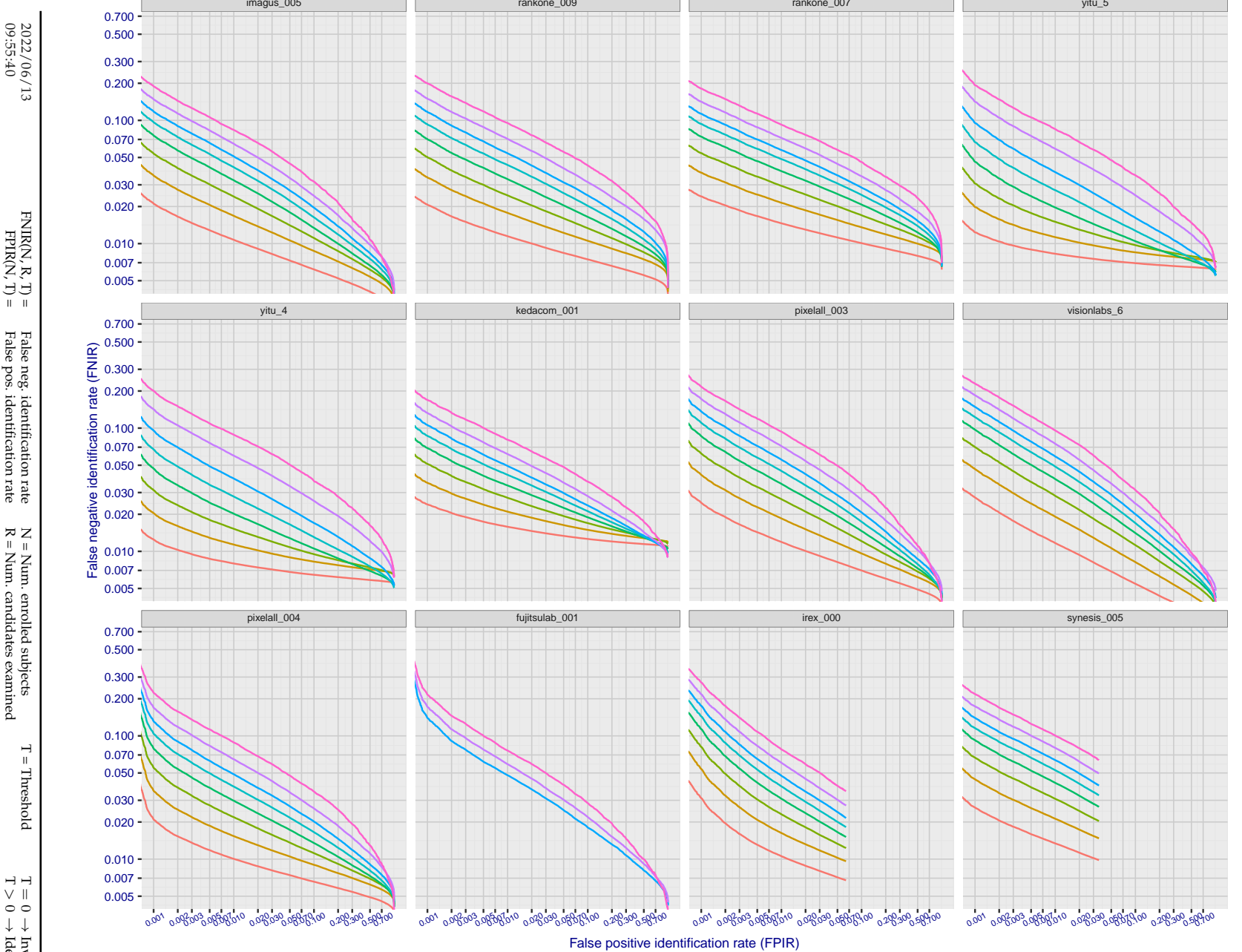


**Figure 88: [FRVT-2018 Mugshot Ageing Dataset] Identification miss rates vs. FPIR by time-elapsed.** The oldest image of each individual is enrolled. Thereafter, all more recent images are searched. Miss rates are computed over all searches noted in row 17 of Table 1 and binned by number of years between search and initial enrollment. FPIR is computed from the same FRVT 2018 non-mates noted in row 3 of Table 1 with  $N = 3\,000\,000$ .

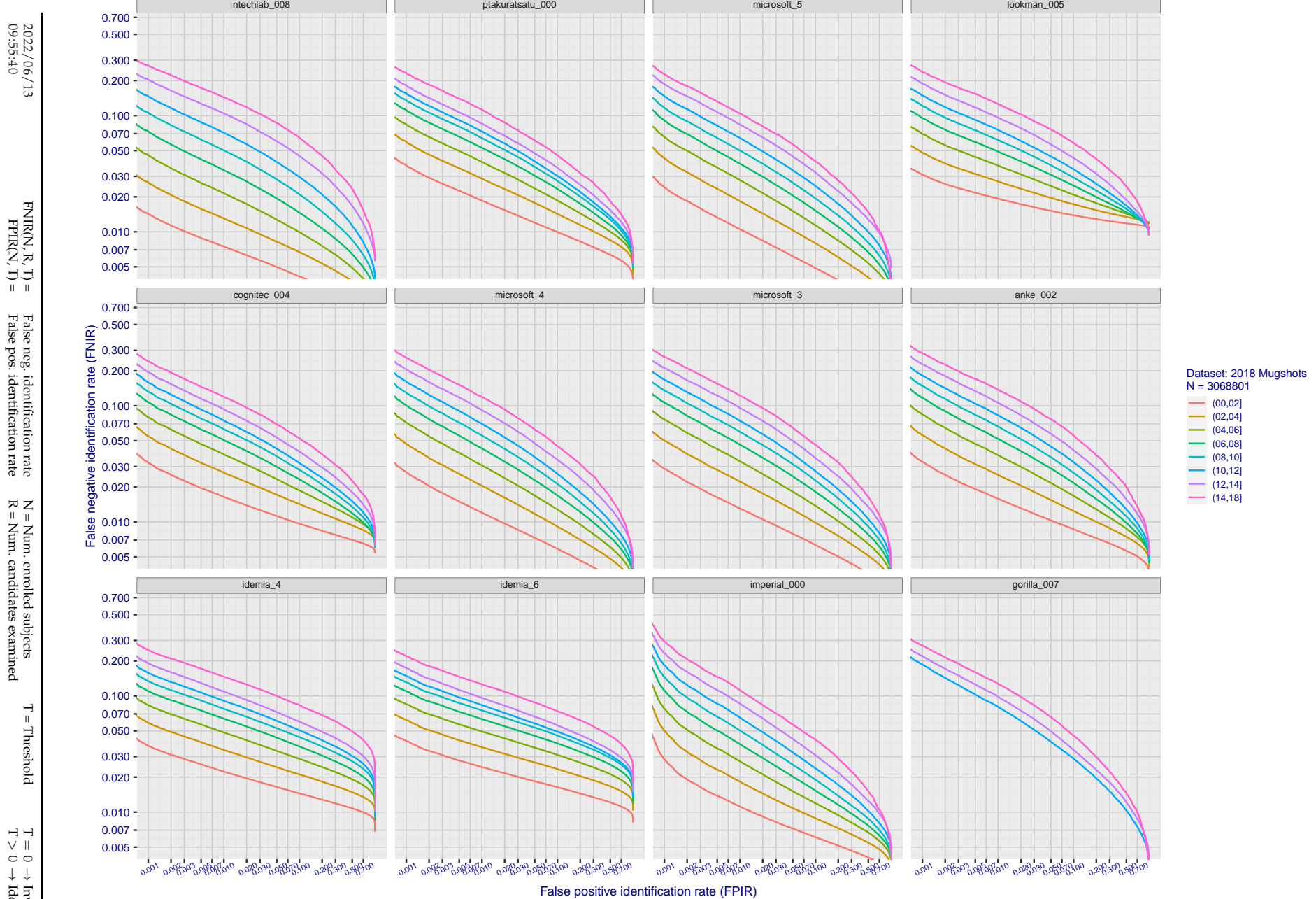


**Figure 89: [FRVT-2018 Mugshot Ageing Dataset] Identification miss rates vs. FPIR by time elapsed.** The oldest image of each individual is enrolled. Thereafter, all more recent images are searched. Miss rates are computed over all searches noted in row 17 of Table 1 and binned by number of years between search and initial enrollment. FPIR is computed from the same FRVT 2018 non-mates noted in row 3 of Table 1 with  $N = 3\,000\,000$ .

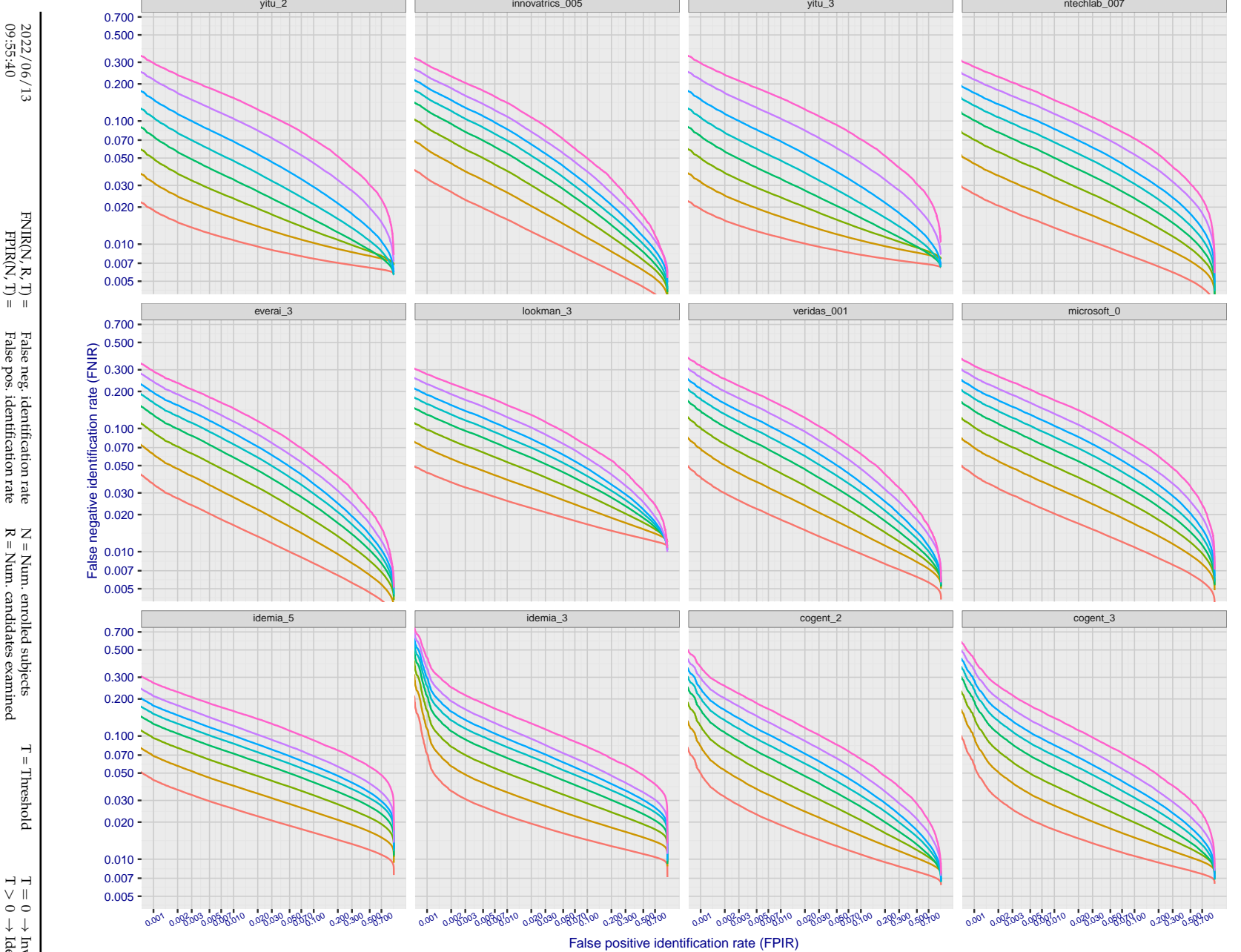


**Figure 90: [FRVT-2018 Mugshot Ageing Dataset] Identification miss rates vs. FPIR by time-elapsed.** The oldest image of each individual is enrolled. Thereafter, all more recent images are searched. Miss rates are computed over all searches noted in row 17 of Table 1 and binned by number of years between search and initial enrollment. FPIR is computed from the same FRVT 2018 non-mates noted in row 3 of Table 1 with  $N = 3\,000\,000$ .

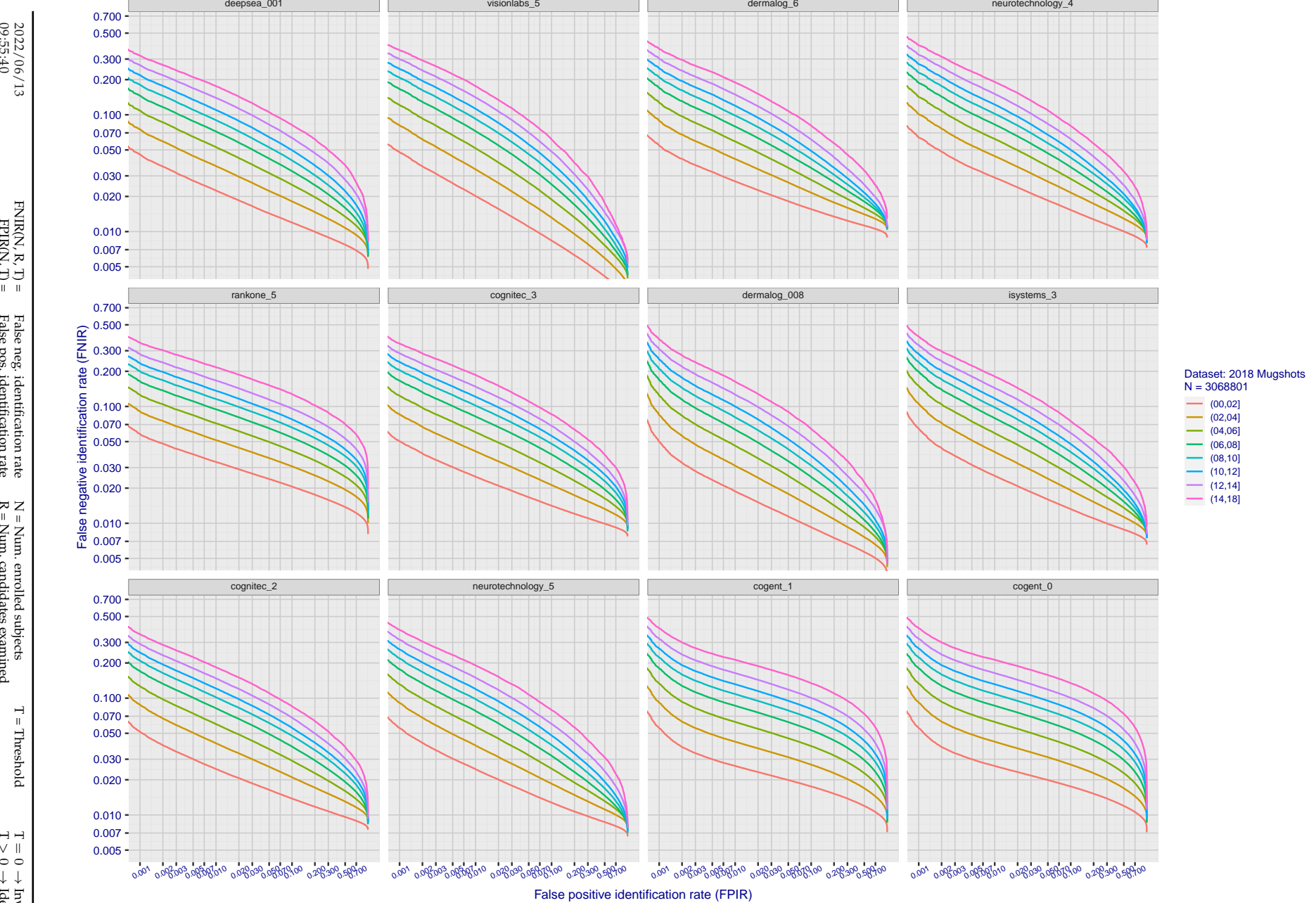


**Figure 91: [FRVT-2018 Mugshot Ageing Dataset] Identification miss rates vs. FPIR by time-elapsed.** The oldest image of each individual is enrolled. Thereafter, all more recent images are searched. Miss rates are computed over all searches noted in row 17 of Table 1 and binned by number of years between search and initial enrollment. FPIR is computed from the same FRVT 2018 non-mates noted in row 3 of Table 1 with  $N = 3\,000\,000$ .

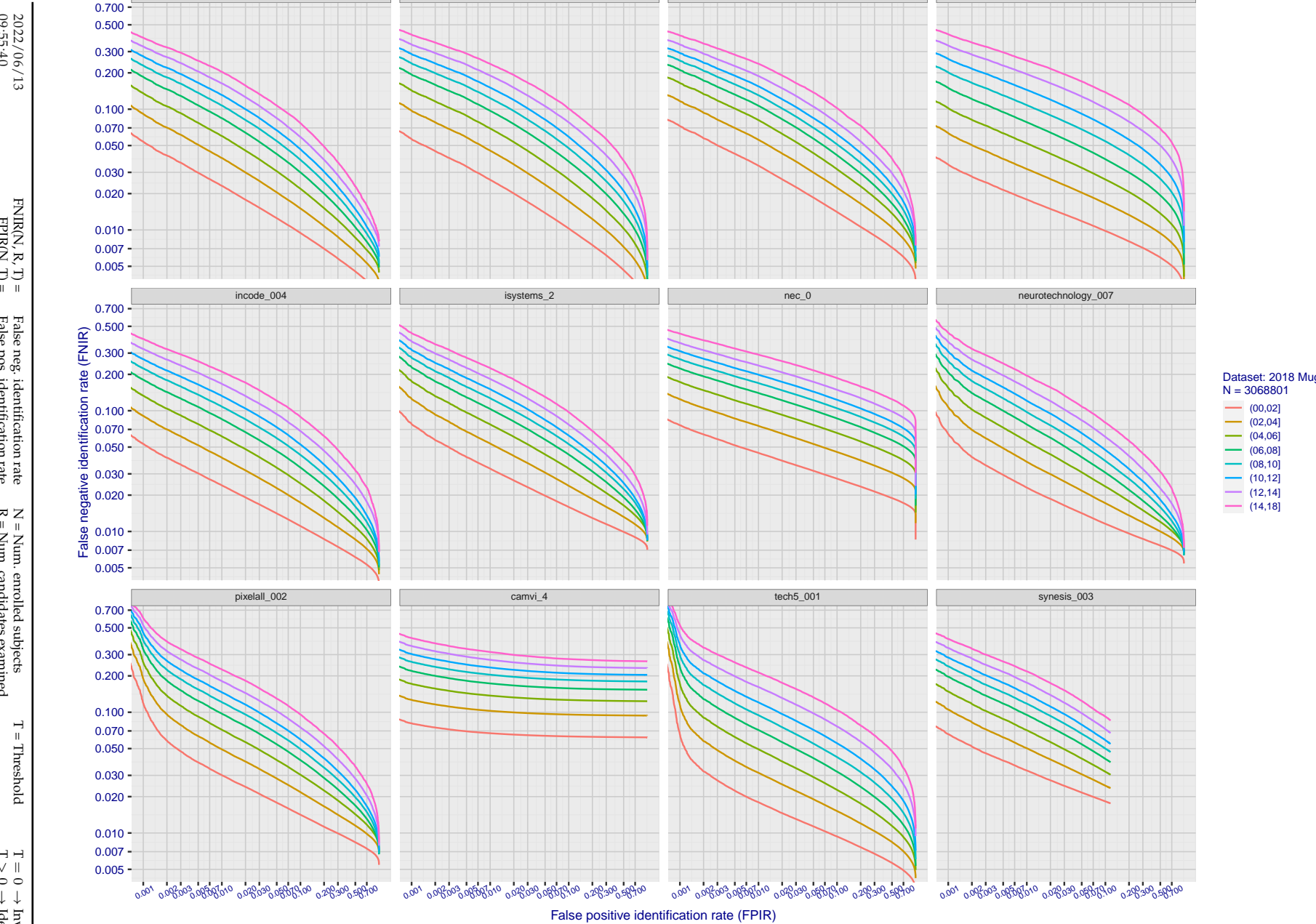


**Figure 92: [FRVT-2018 Mugshot Ageing Dataset] Identification miss rates vs. FPIR by time elapsed.** The oldest image of each individual is enrolled. Thereafter, all more recent images are searched. Miss rates are computed over all searches noted in row 17 of Table 1 and binned by number of years between search and initial enrollment. FPIR is computed from the same FRVT 2018 non-mates noted in row 3 of Table 1 with N = 3 000 000.

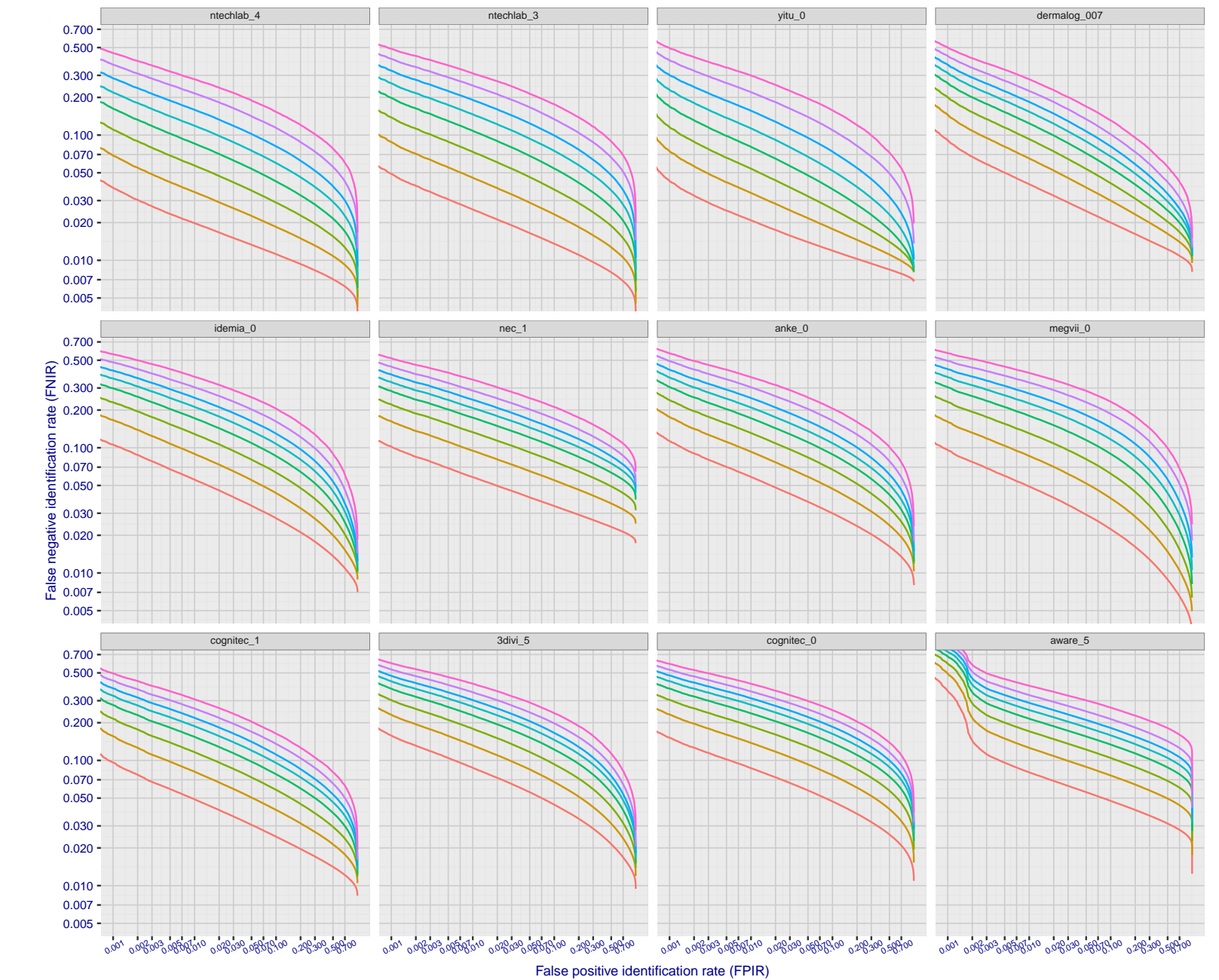


**Figure 93: [FRVT-2018 Mugshot Ageing Dataset] Identification miss rates vs. FPIR by time-elapsed.** The oldest image of each individual is enrolled. Thereafter, all more recent images are searched. Miss rates are computed over all searches noted in row 17 of Table 1 and binned by number of years between search and initial enrollment. FPIR is computed from the same FRVT 2018 non-mates noted in row 3 of Table 1 with  $N = 3\,000\,000$ .

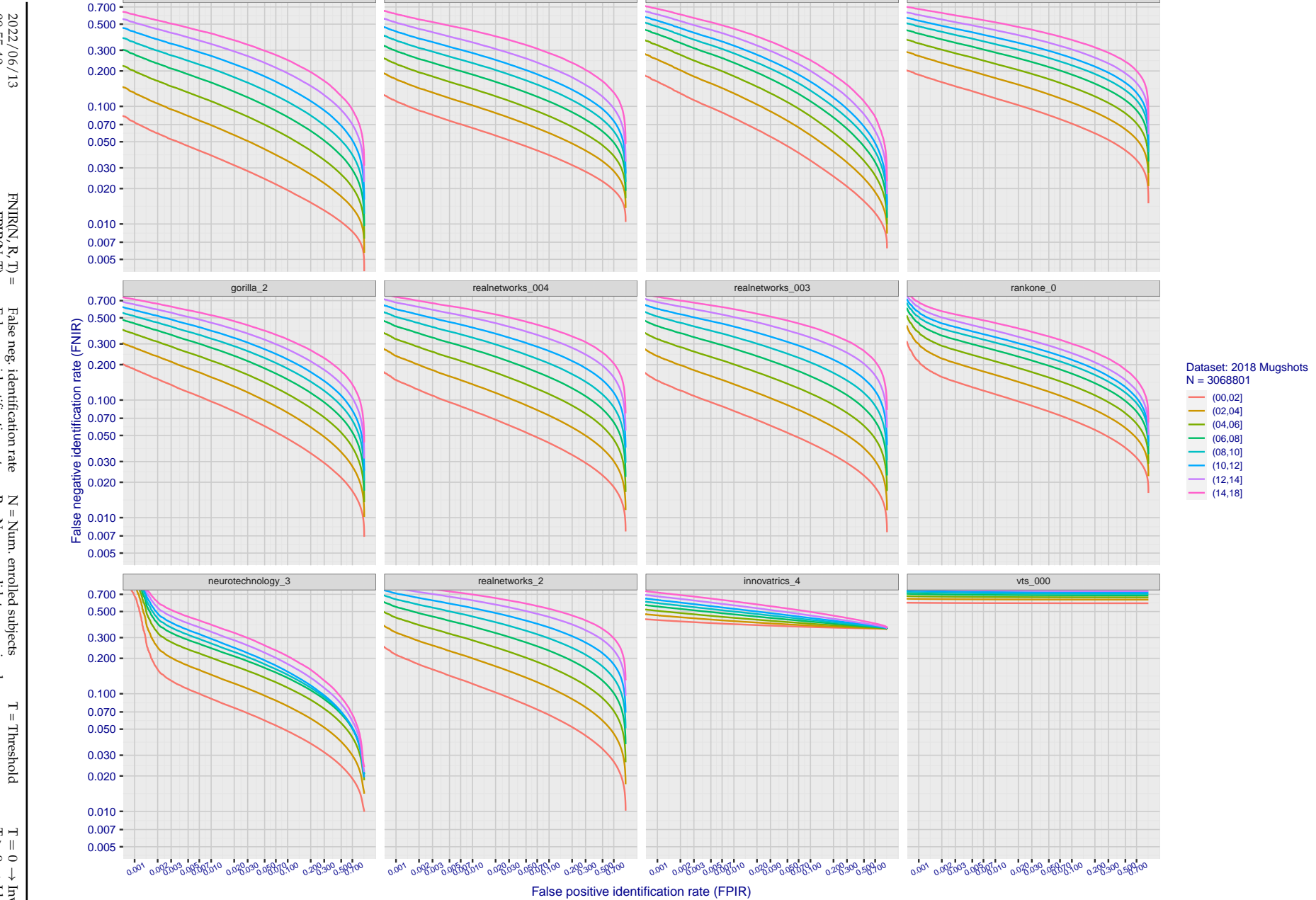


**Figure 94: [FRVT-2018 Mugshot Ageing Dataset] Identification miss rates vs. FPIR by time-elapsed.** The oldest image of each individual is enrolled. Thereafter, all more recent images are searched. Miss rates are computed over all searches noted in row 17 of Table 1 and binned by number of years between search and initial enrollment. FPIR is computed from the same FRVT 2018 non-mates noted in row 3 of Table 1 with  $N = 3\,000\,000$ .

2022/06/13  
09:55:40  
  
 $\text{FNIR}(N, R, T) =$   
False neg. identification rate  
 $\text{FPIR}(N, T) =$   
False pos. identification rate  
  
 $N = \text{Num. enrolled subjects}$   
 $R = \text{Num. candidates examined}$   
 $T = \text{Threshold}$   
 $T = 0 \rightarrow \text{Investigation}$   
 $T > 0 \rightarrow \text{Identification}$

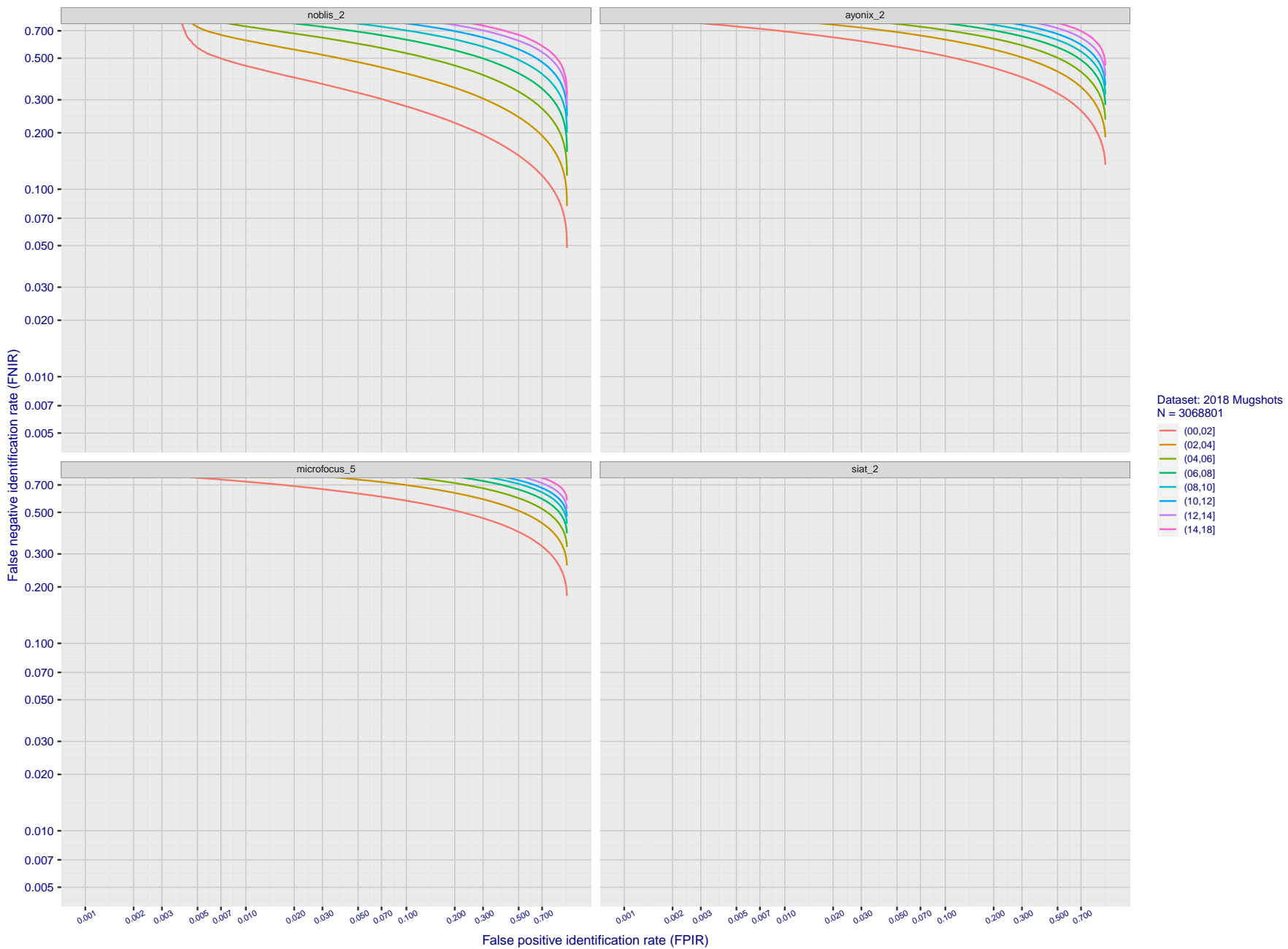


Figure 95: [FRVT-2018 Mugshot Ageing Dataset] Identification miss rates vs. FPIR by time elapsed. The oldest image of each individual is enrolled. Thereafter, all more recent images are searched. Miss rates are computed over all searches noted in row 17 of Table 1 and binned by number of years between search and initial enrollment. FPIR is computed from the same FRVT 2018 non-mates noted in row 3 of Table 1 with  $N = 3\,000\,000$ .

---

2022/06/13  
09:55:40      FNIR(N, R, T) = False neg. identification rate  
                  FPIR(N, T) = False pos. identification rate  
N = Num. enrolled subjects  
R = Num. candidates examined  
T = Threshold  
T = 0 → Investigation  
T > 0 → Identification

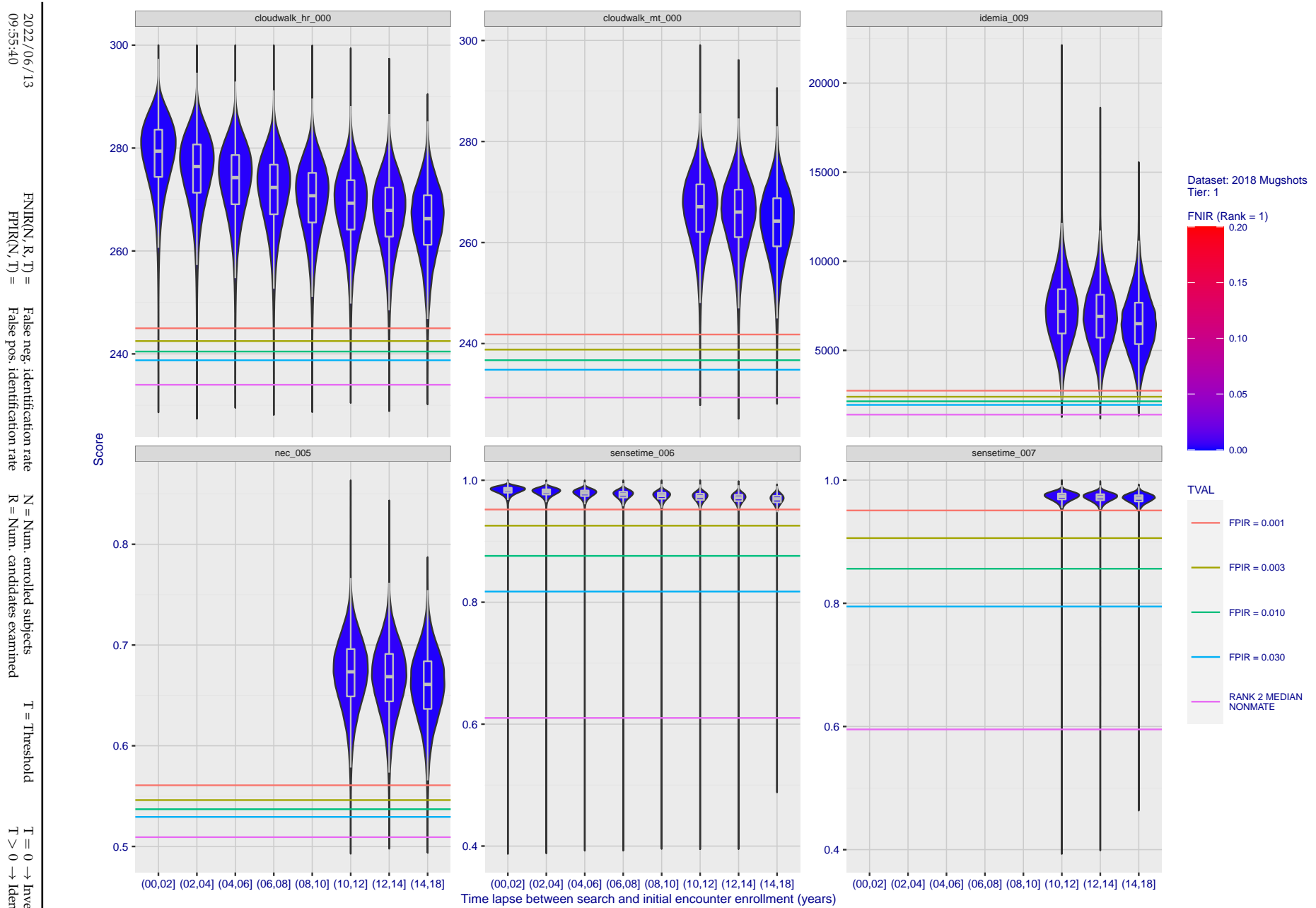


Figure 96: [FRVT-2018 Mugshot Ageing Dataset] Native mate scores vs. time-elapsed. The oldest image of each individual is enrolled. Thereafter, all more recent images are searched. Mated score distributions are computed over all searches noted in row 17 of Table 1 binned by number of years between search and initial enrollment.

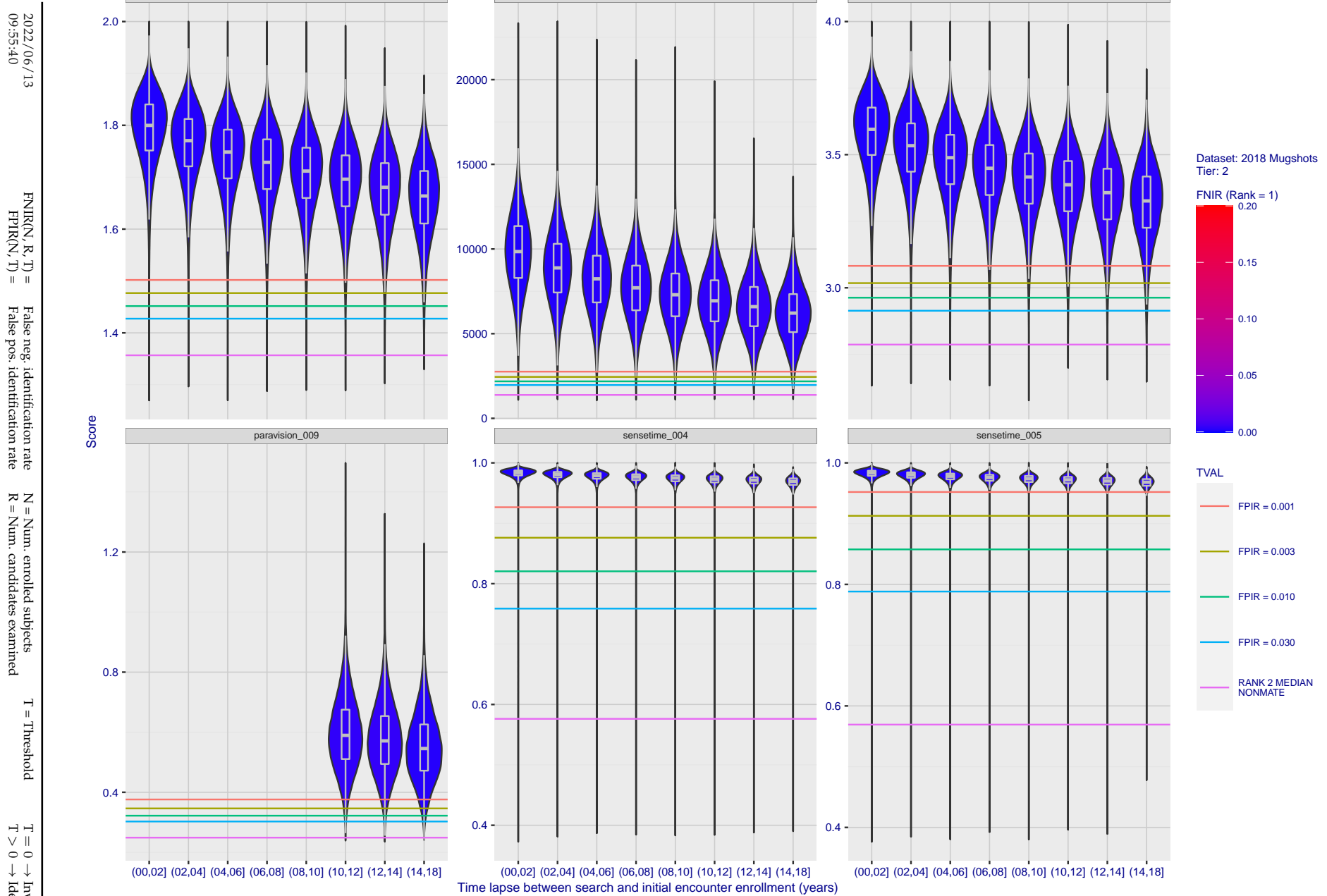
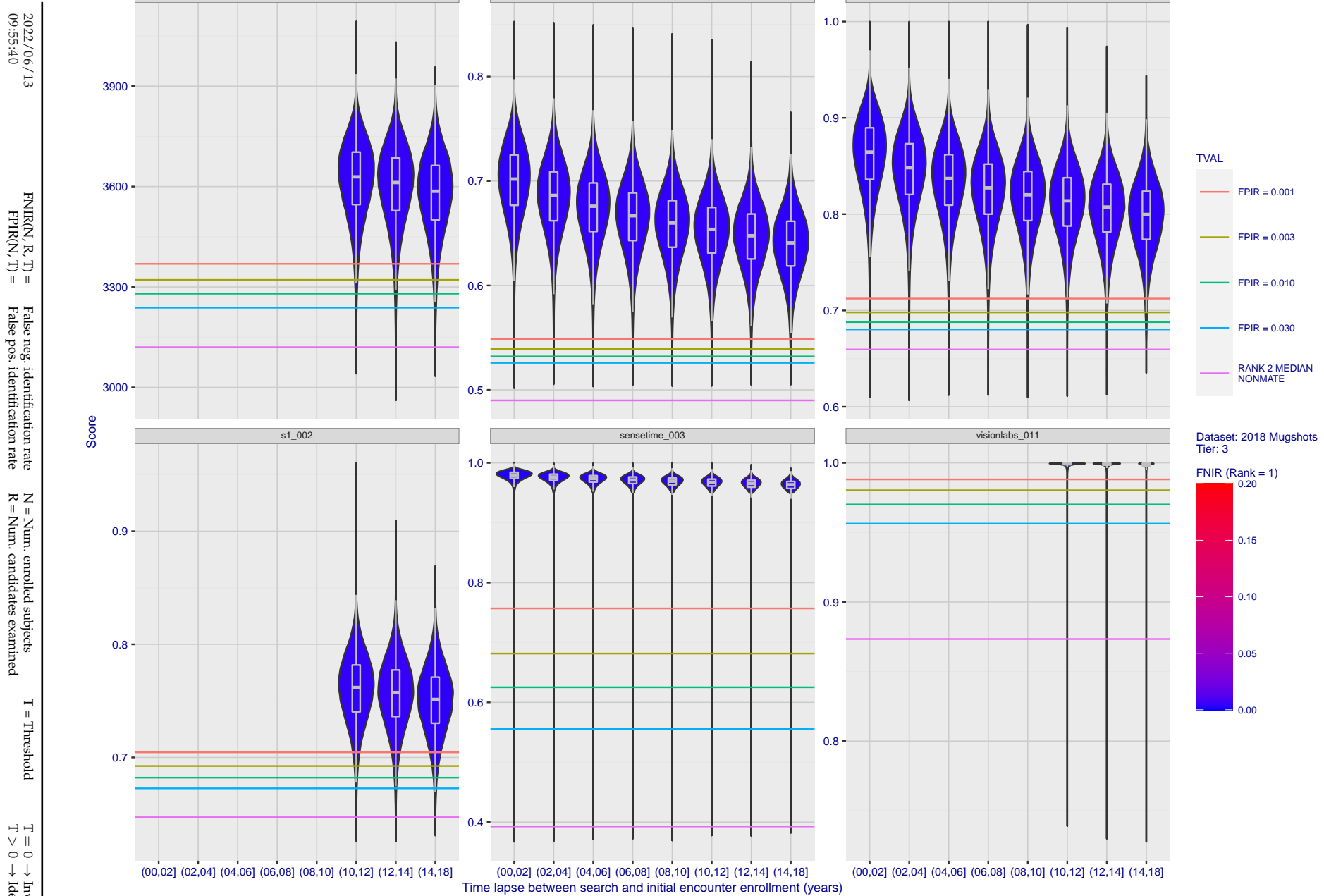


Figure 97: [FRVT-2018 Mugshot Ageing Dataset] Native mate scores vs. time-elapsed. The oldest image of each individual is enrolled. Thereafter, all more recent images are searched. Mated score distributions are computed over all searches noted in row 17 of Table 1 binned by number of years between search and initial enrollment.



**Figure 98: [FRVT-2018 Mugshot Ageing Dataset] Native mate scores vs. time-elapsed.** The oldest image of each individual is enrolled. Thereafter, all more recent images are searched. Mated score distributions are computed over all searches noted in row 17 of Table 1 binned by number of years between search and initial enrollment.

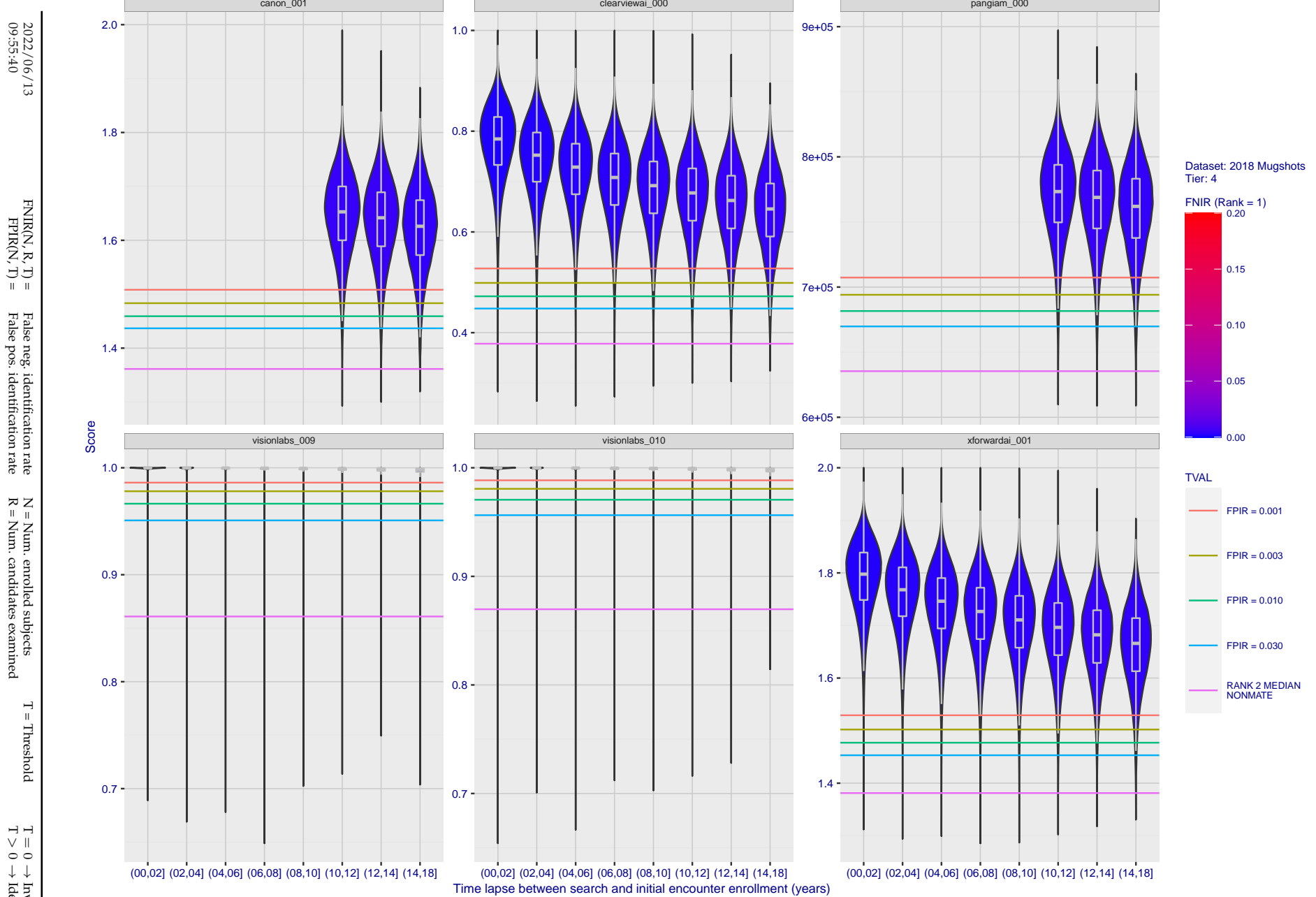
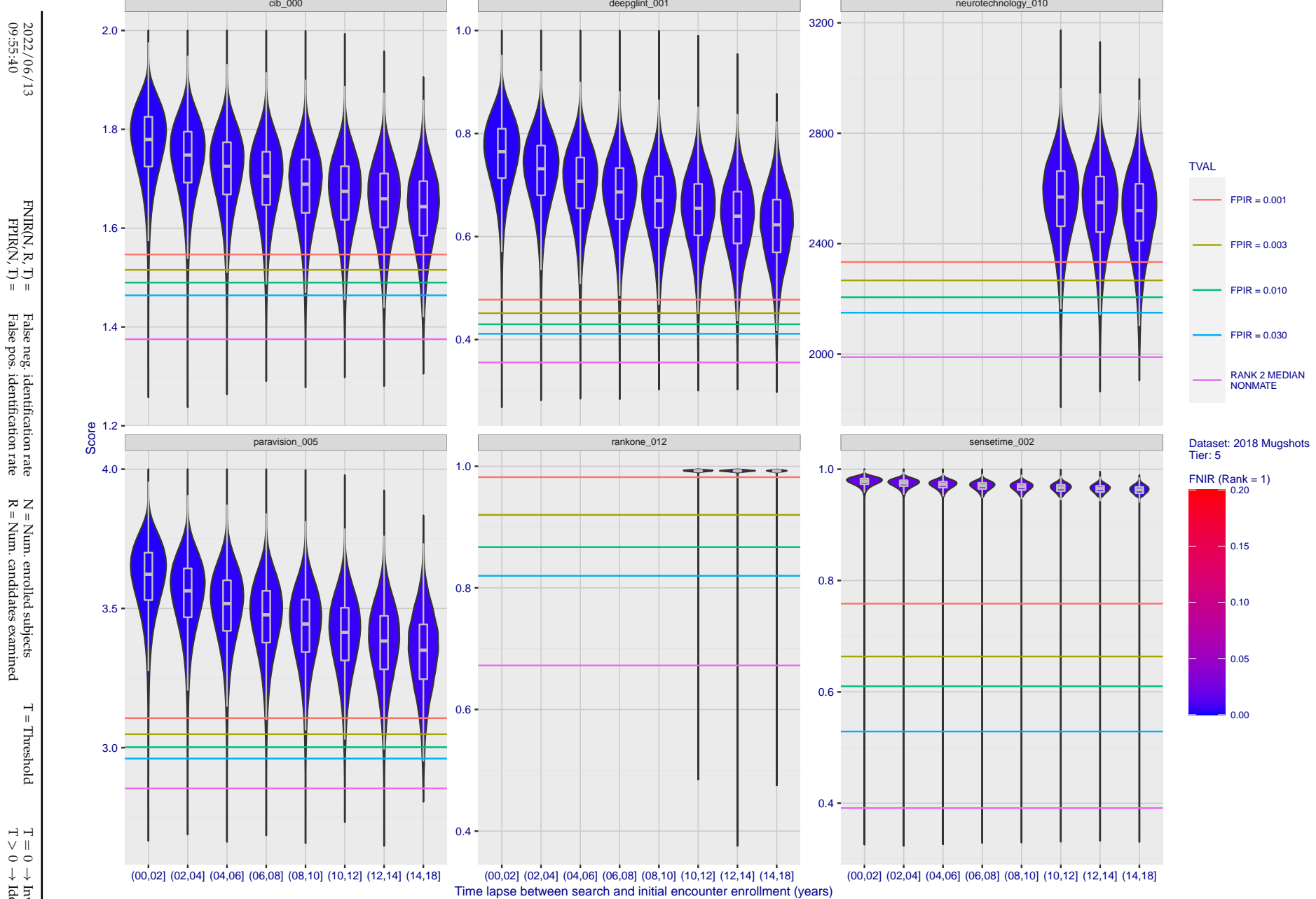


Figure 99: [FRVT-2018 Mugshot Ageing Dataset] Native mate scores vs. time-elapsed. The oldest image of each individual is enrolled. Thereafter, all more recent images are searched. Mated score distributions are computed over all searches noted in row 17 of Table 1 binned by number of years between search and initial enrollment.



**Figure 100: [FRVT-2018 Mugshot Ageing Dataset] Native mate scores vs. time-elapsed.** The oldest image of each individual is enrolled. Thereafter, all more recent images are searched. Mated score distributions are computed over all searches noted in row 17 of Table 1 binned by number of years between search and initial enrollment.

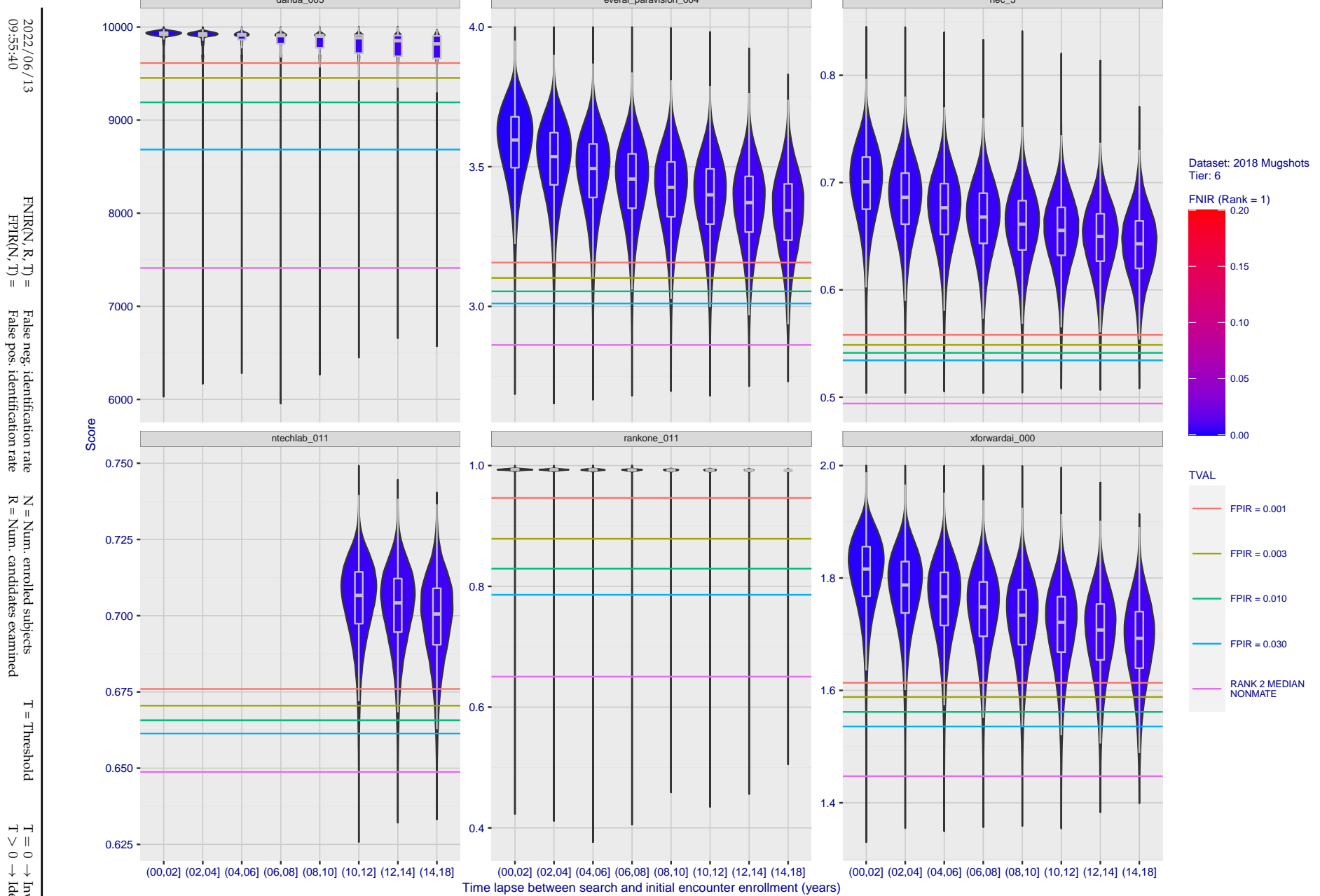
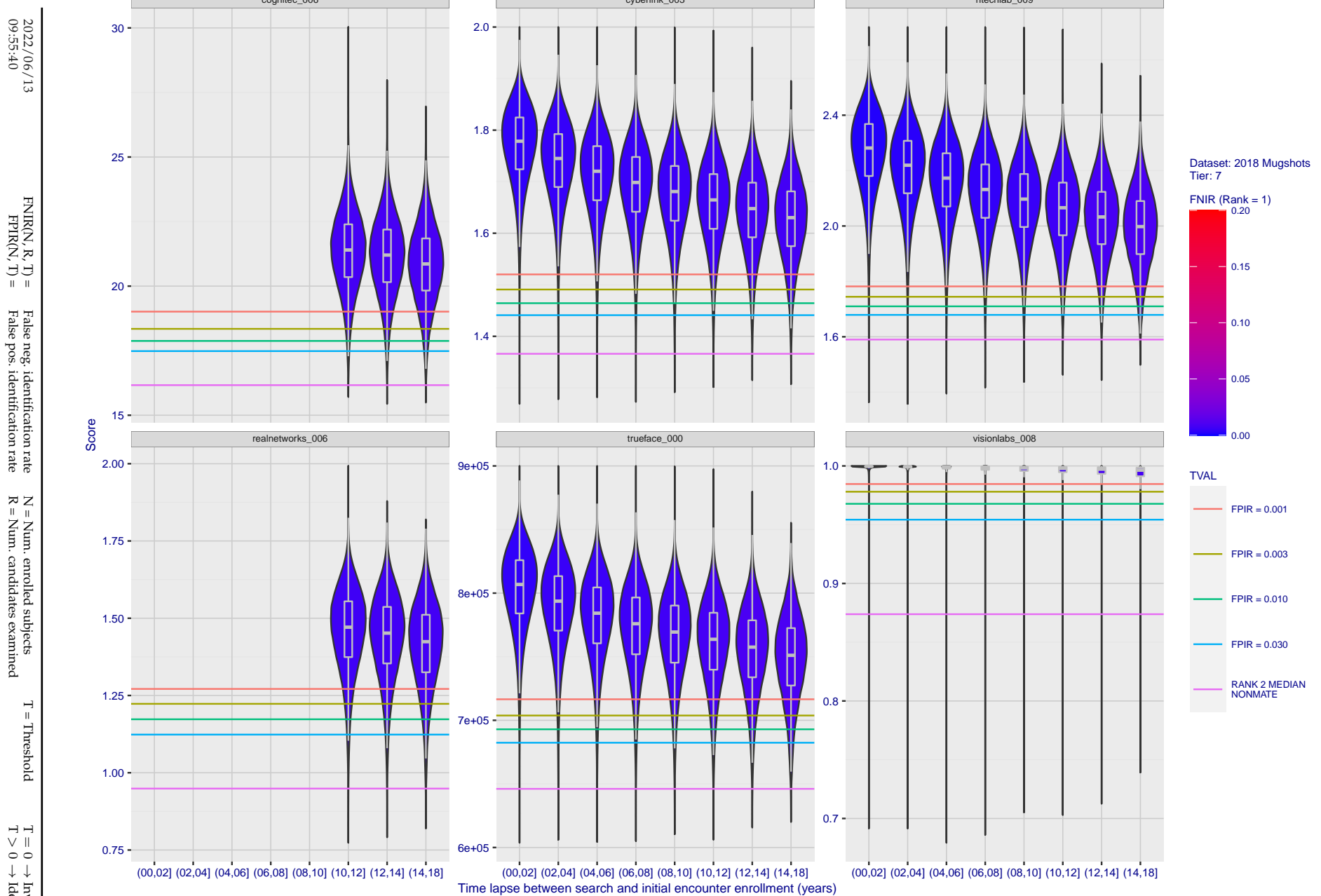
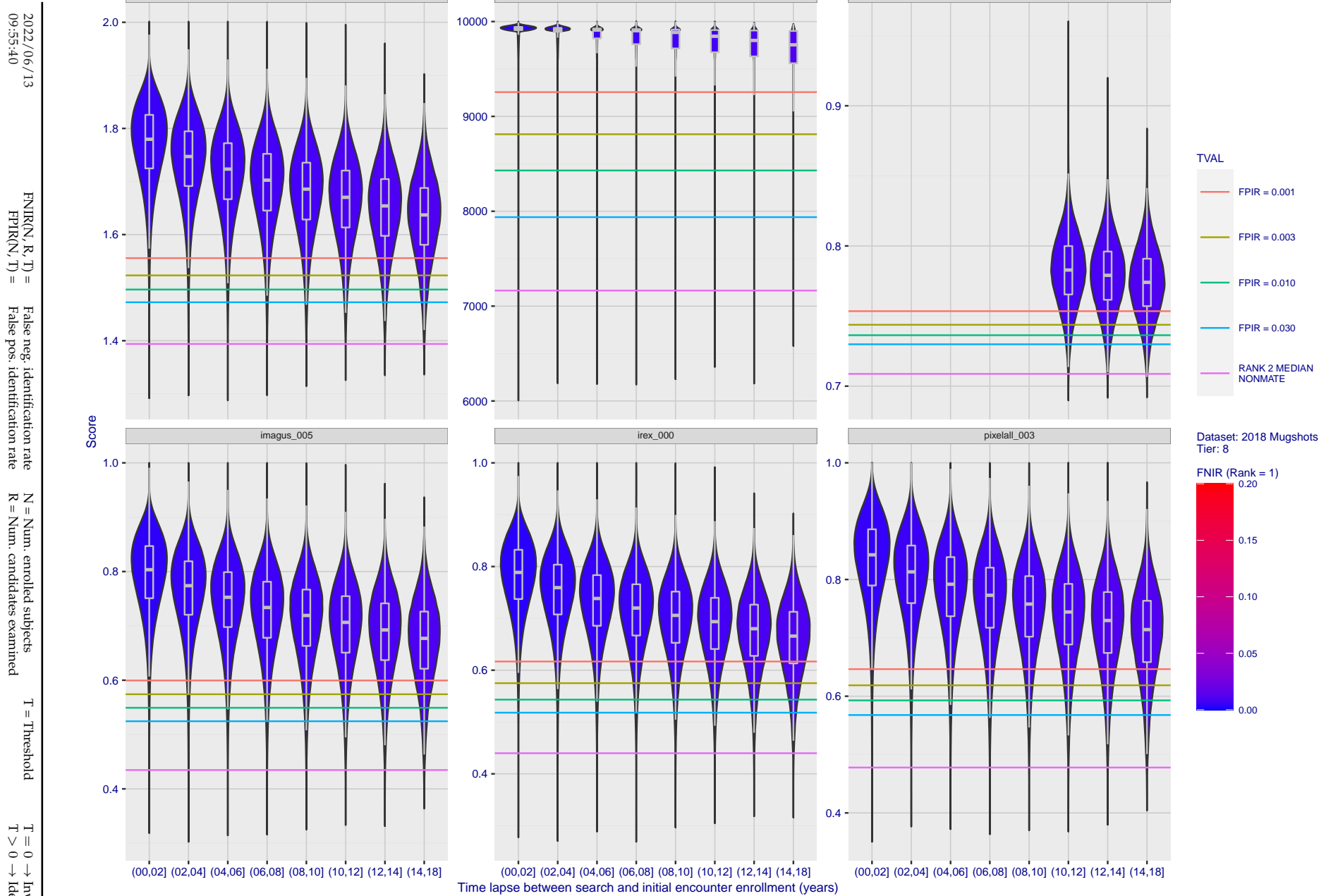


Figure 101: [FRVT-2018 Mugshot Ageing Dataset] Native mate scores vs. time-elapsed. The oldest image of each individual is enrolled. Thereafter, all more recent images are searched. Mated score distributions are computed over all searches noted in row 17 of Table 1 binned by number of years between search and initial enrollment.



**Figure 102: [FRVT-2018 Mugshot Ageing Dataset] Native mate scores vs. time-elapsed.** The oldest image of each individual is enrolled. Thereafter, all more recent images are searched. Mated score distributions are computed over all searches noted in row 17 of Table 1 binned by number of years between search and initial enrollment.



**Figure 103: [FRVT-2018 Mugshot Ageing Dataset] Native mate scores vs. time-elapsed.** The oldest image of each individual is enrolled. Thereafter, all more recent images are searched. Mated score distributions are computed over all searches noted in row 17 of Table 1 binned by number of years between search and initial enrollment.

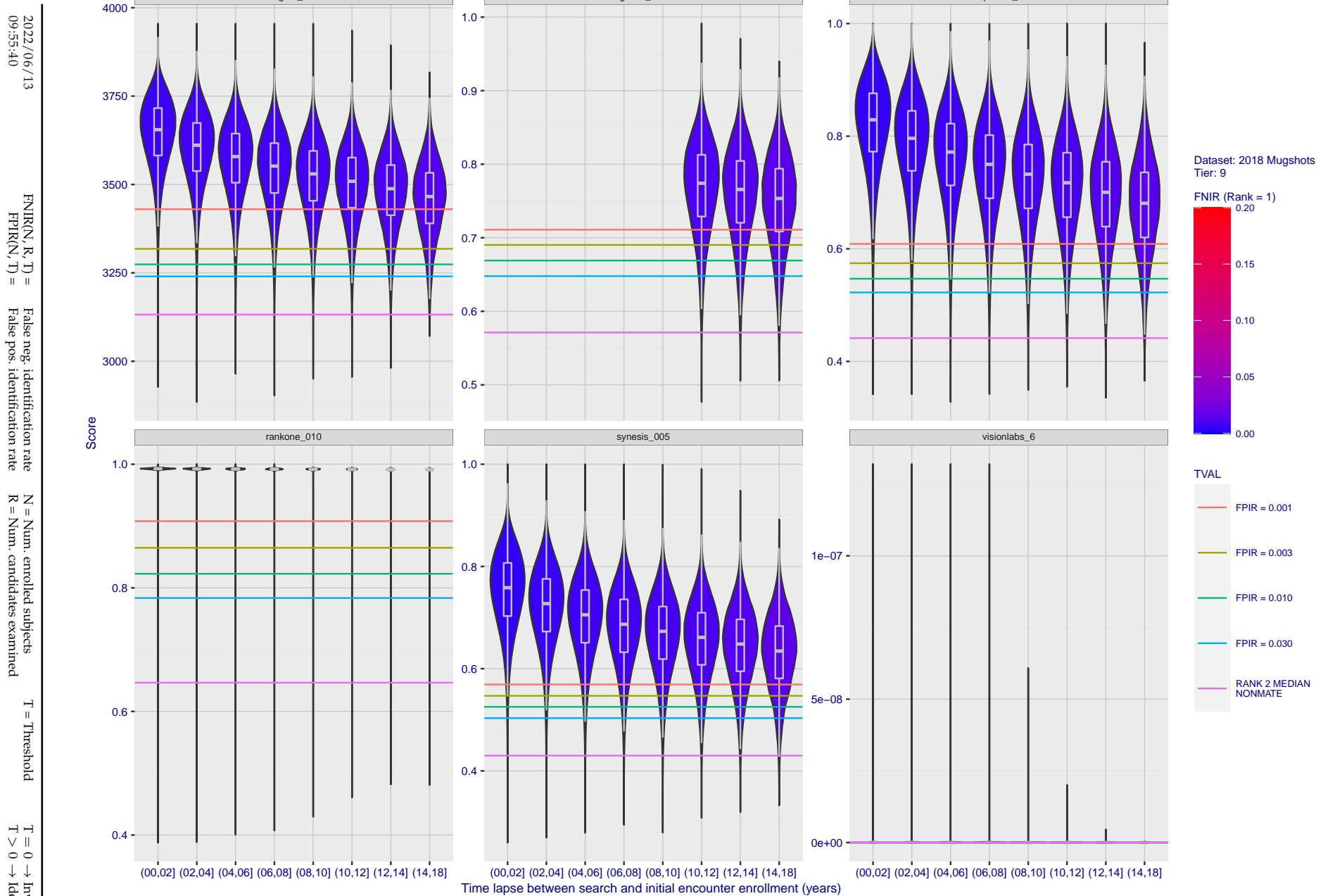
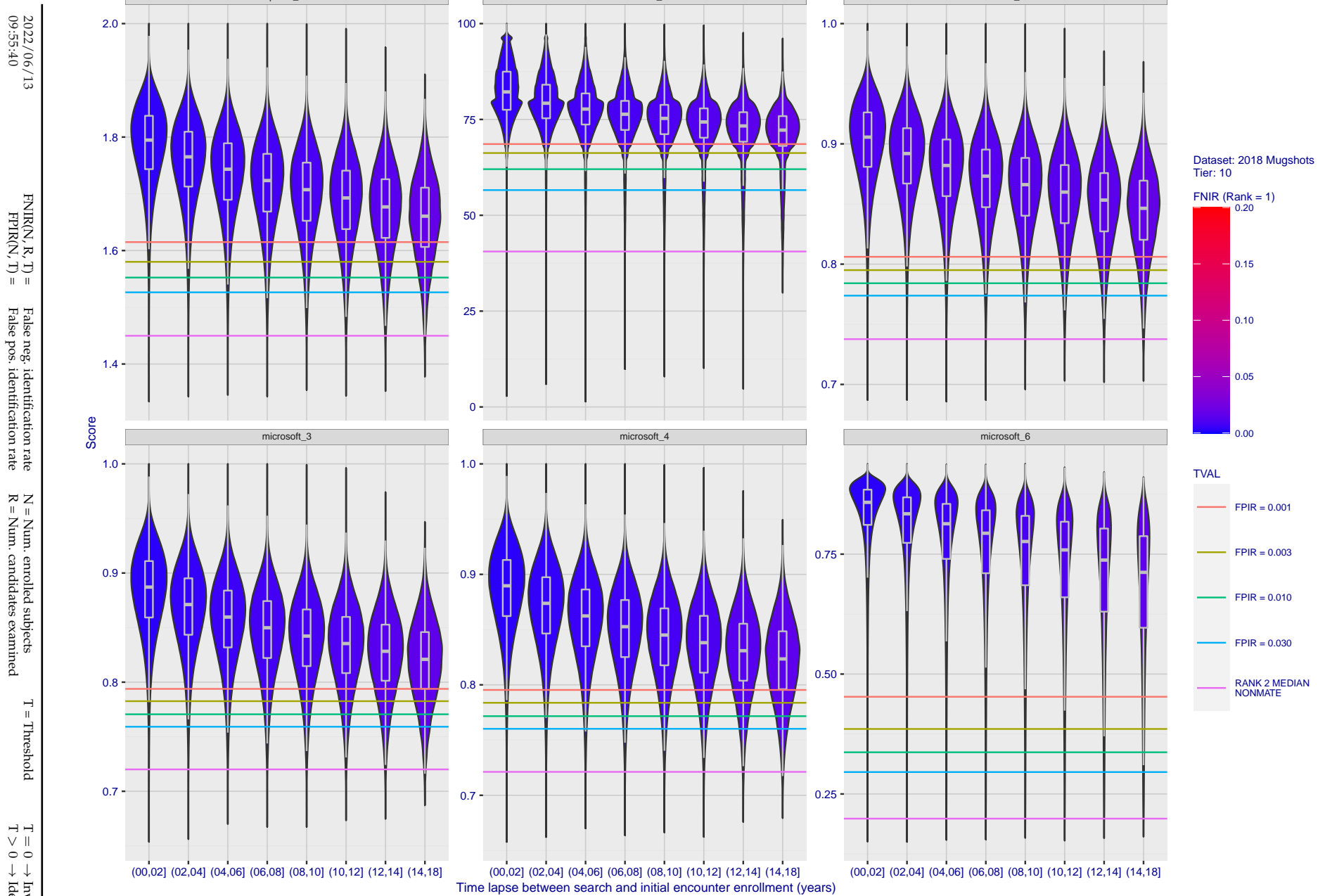
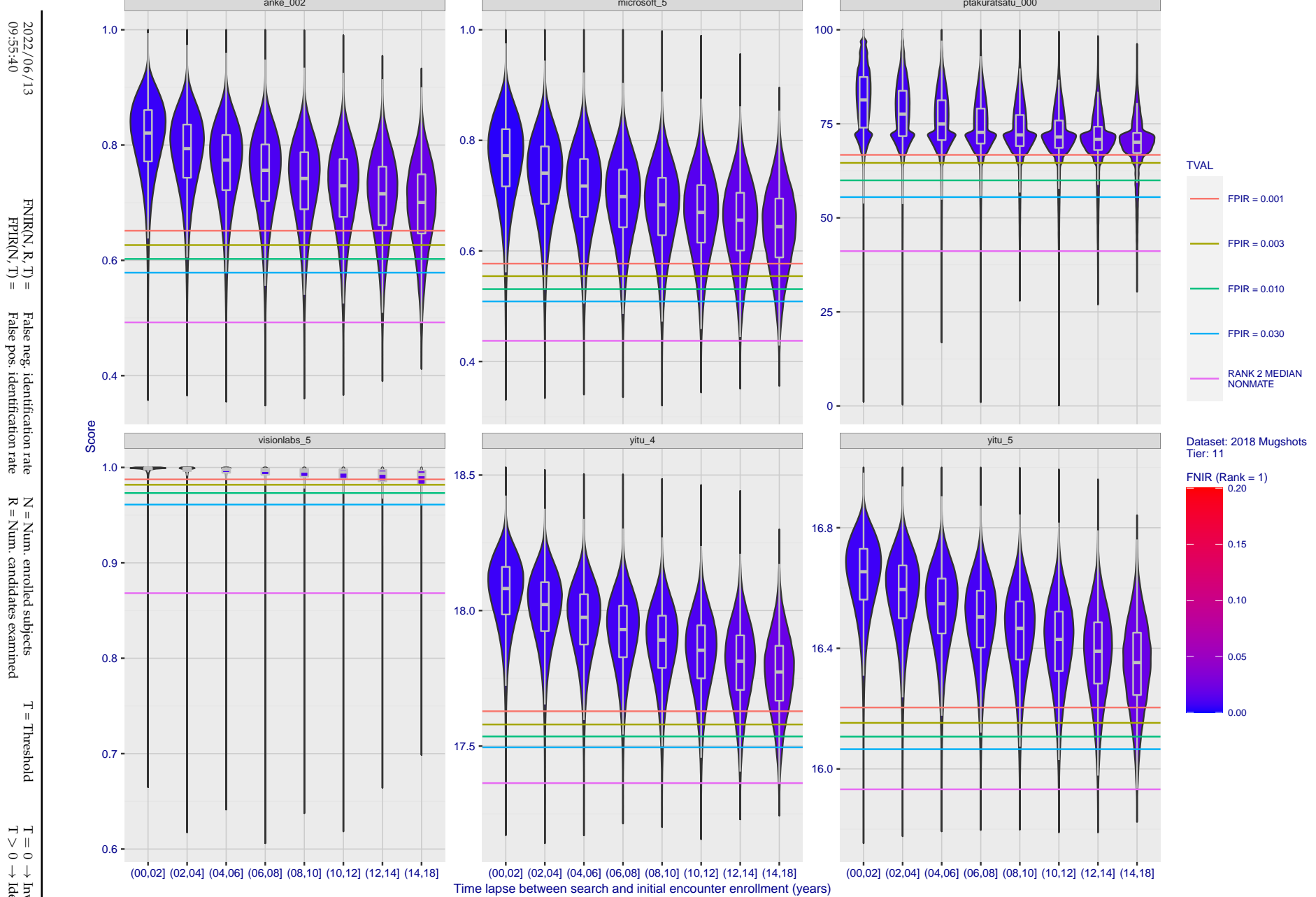


Figure 104: [FRVT-2018 Mugshot Ageing Dataset] Native mate scores vs. time-elapsed. The oldest image of each individual is enrolled. Thereafter, all more recent images are searched. Mated score distributions are computed over all searches noted in row 17 of Table 1 binned by number of years between search and initial enrollment.



**Figure 105: [FRVT-2018 Mugshot Ageing Dataset] Native mate scores vs. time-elapsed.** The oldest image of each individual is enrolled. Thereafter, all more recent images are searched. Mated score distributions are computed over all searches noted in row 17 of Table 1 binned by number of years between search and initial enrollment.



**Figure 106: [FRVT-2018 Mugshot Ageing Dataset] Native mate scores vs. time-elapsed.** The oldest image of each individual is enrolled. Thereafter, all more recent images are searched. Mated score distributions are computed over all searches noted in row 17 of Table 1 binned by number of years between search and initial enrollment.

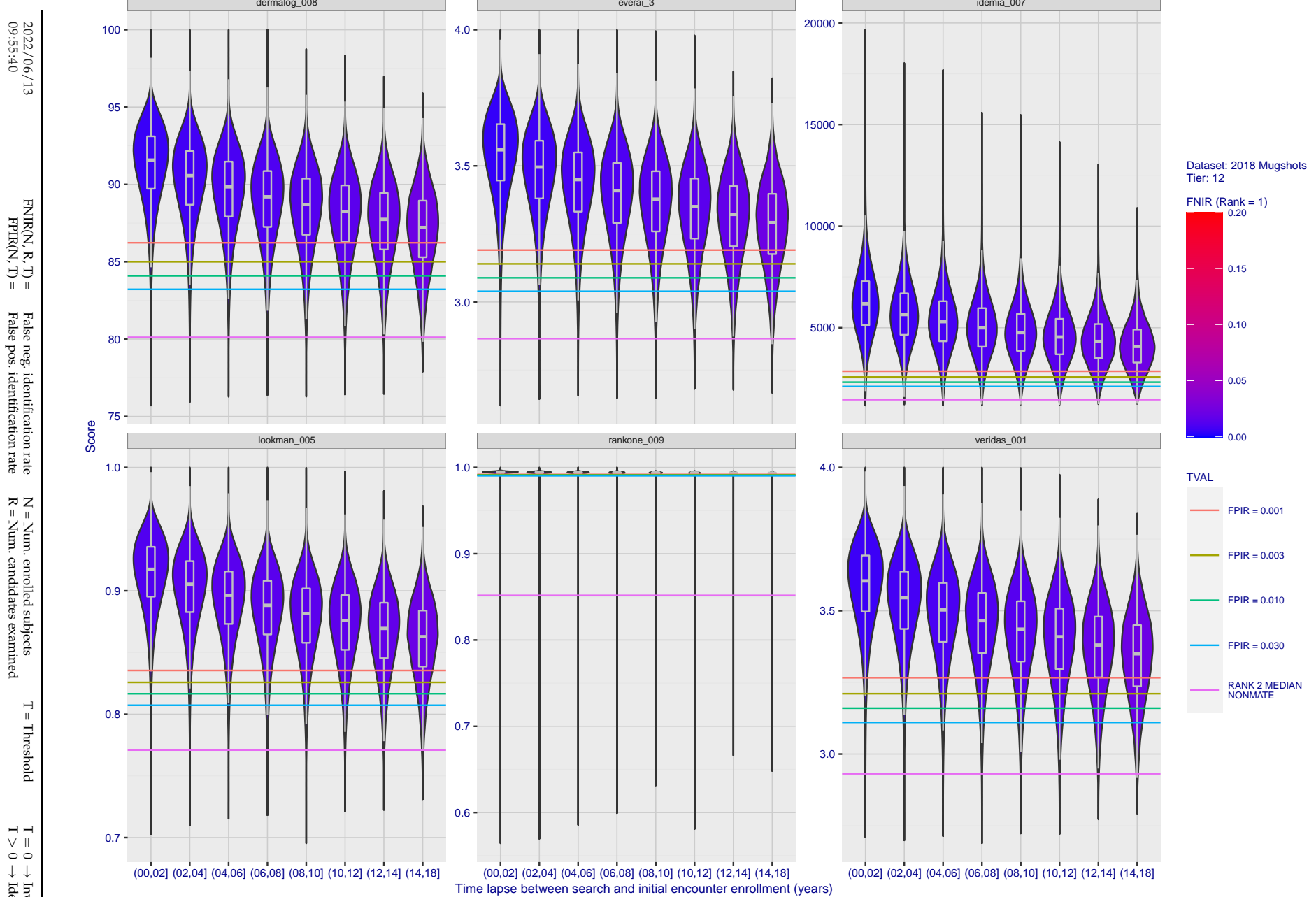


**Figure 107: [FRVT-2018 Mugshot Ageing Dataset] Native mate scores vs. time-elapsed.** The oldest image of each individual is enrolled. Thereafter, all more recent images are searched. Mated score distributions are computed over all searches noted in row 17 of Table 1 binned by number of years between search and initial enrollment.

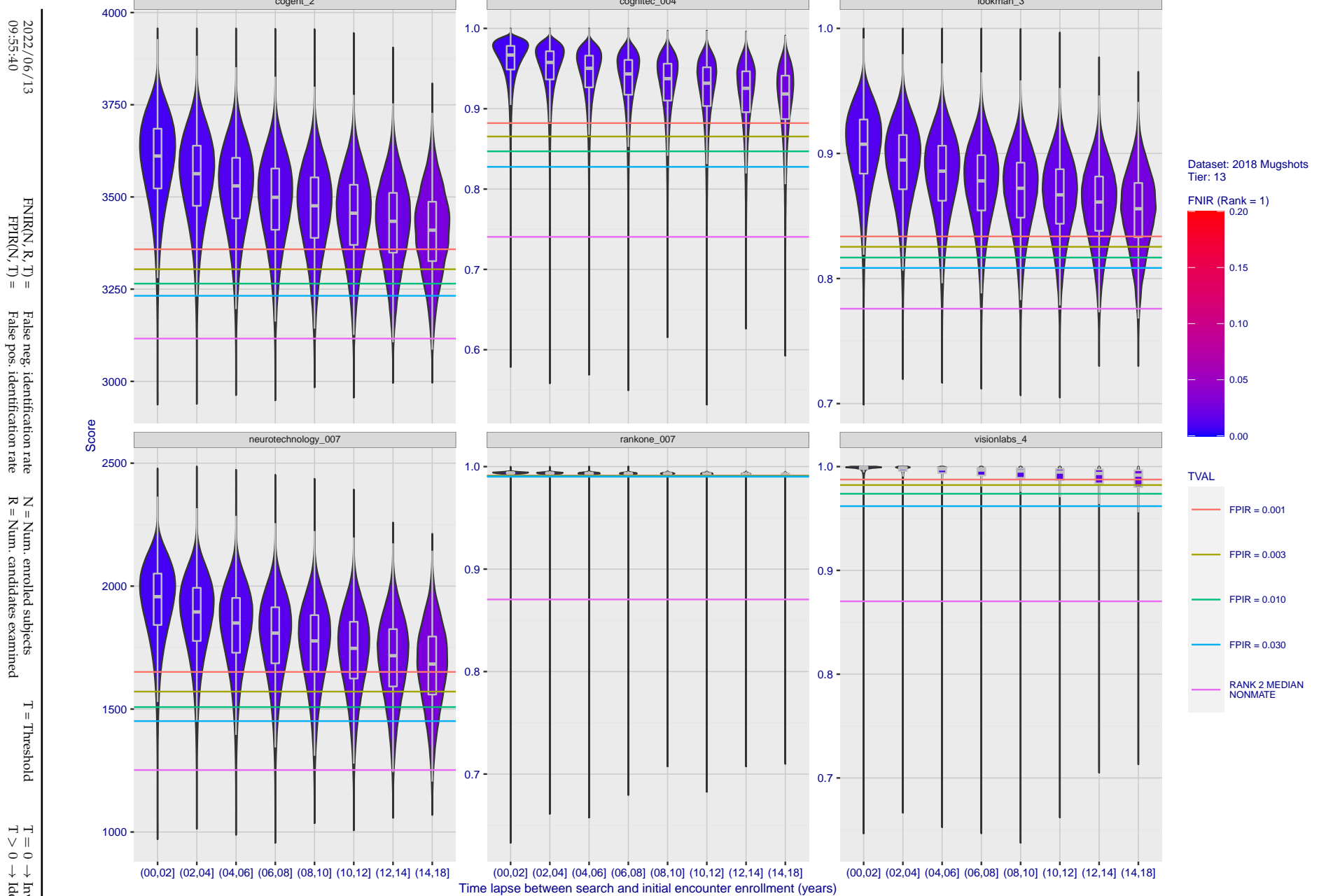


Figure 108: [FRVT-2018 Mugshot Ageing Dataset] Native mate scores vs. time-elapsed. The oldest image of each individual is enrolled. Thereafter, all more recent images are searched. Mated score distributions are computed over all searches noted in row 17 of Table 1 binned by number of years between search and initial enrollment.

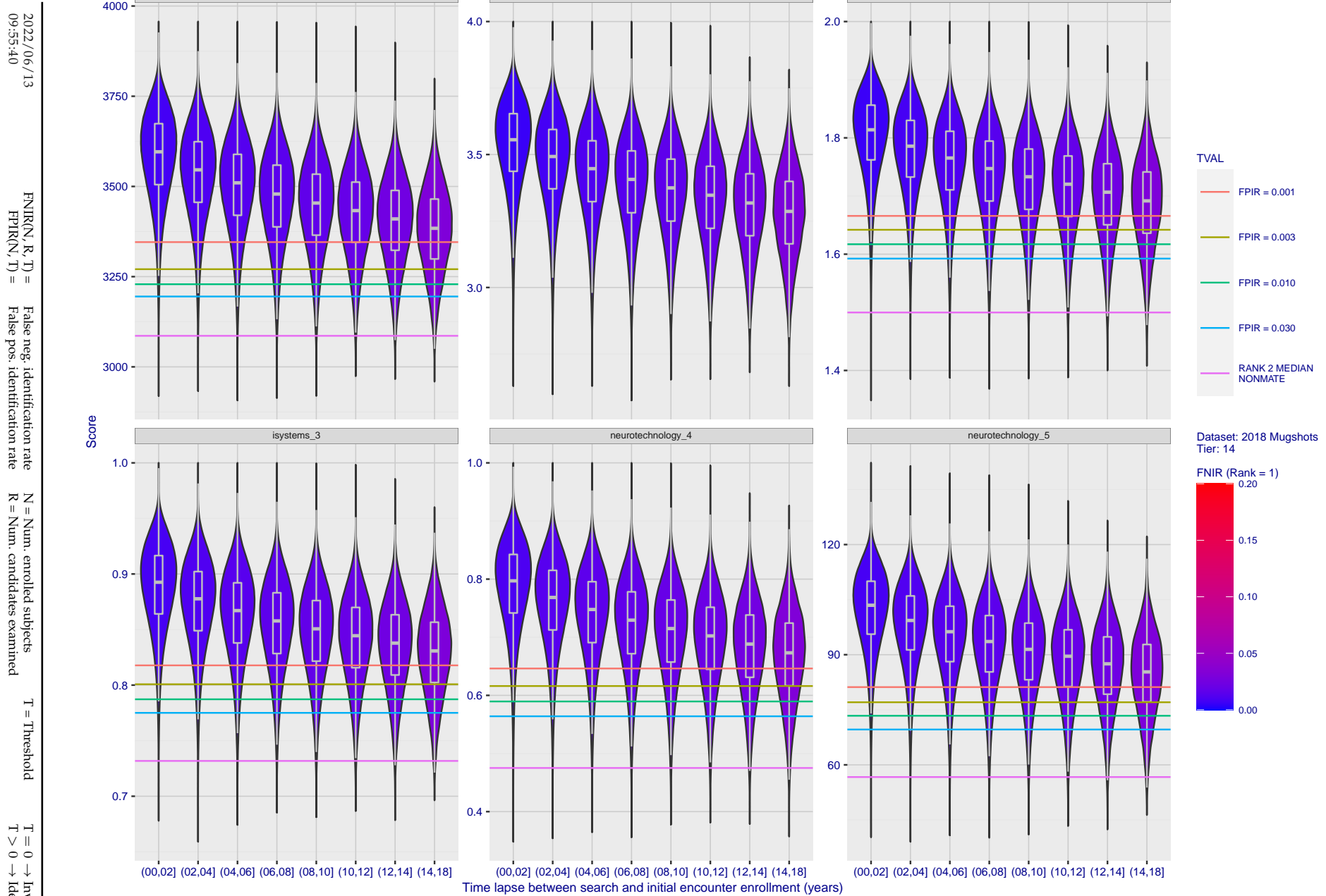


Figure 109: [FRVT-2018 Mugshot Ageing Dataset] Native mate scores vs. time-elapsed. The oldest image of each individual is enrolled. Thereafter, all more recent images are searched. Mated score distributions are computed over all searches noted in row 17 of Table 1 binned by number of years between search and initial enrollment.

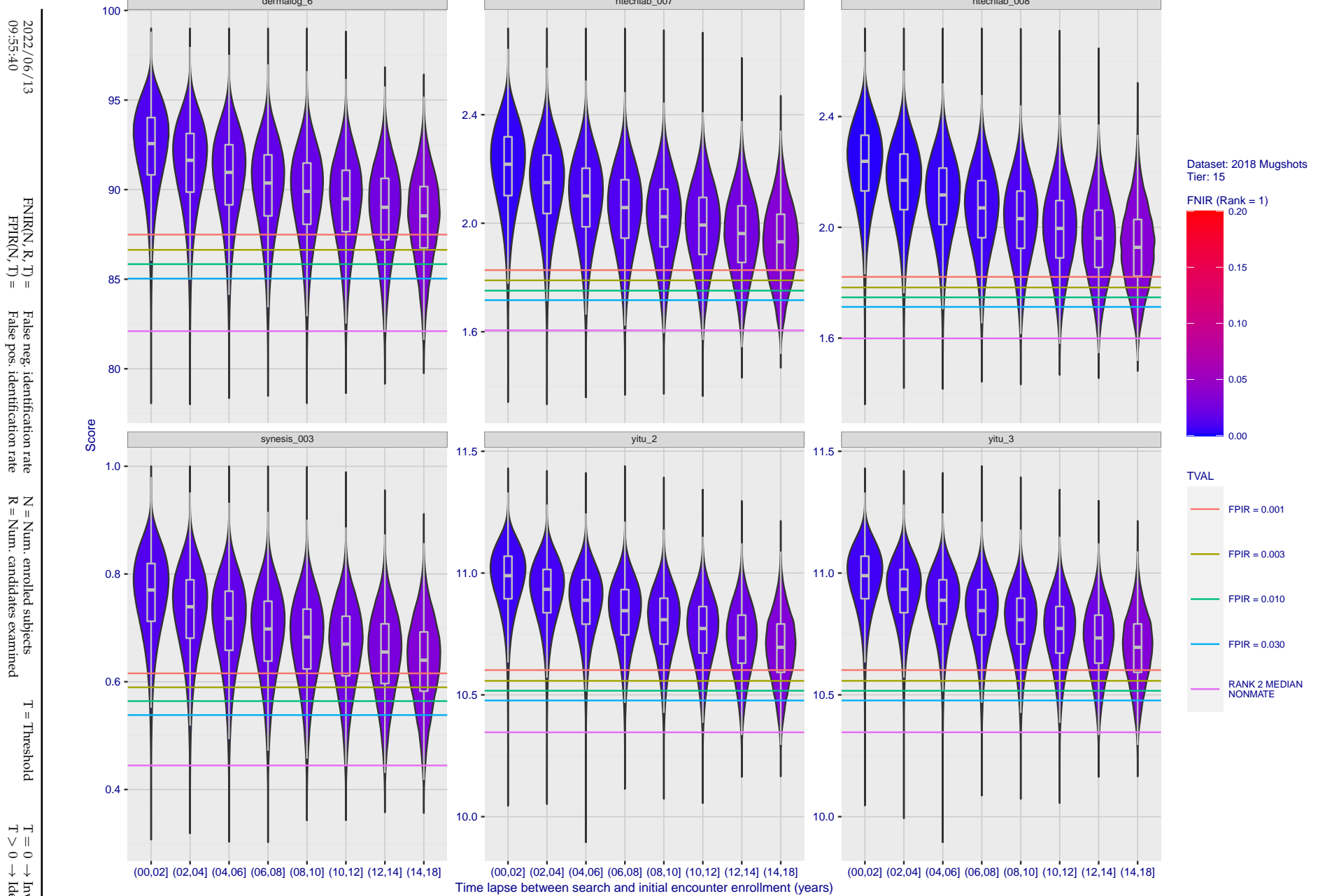
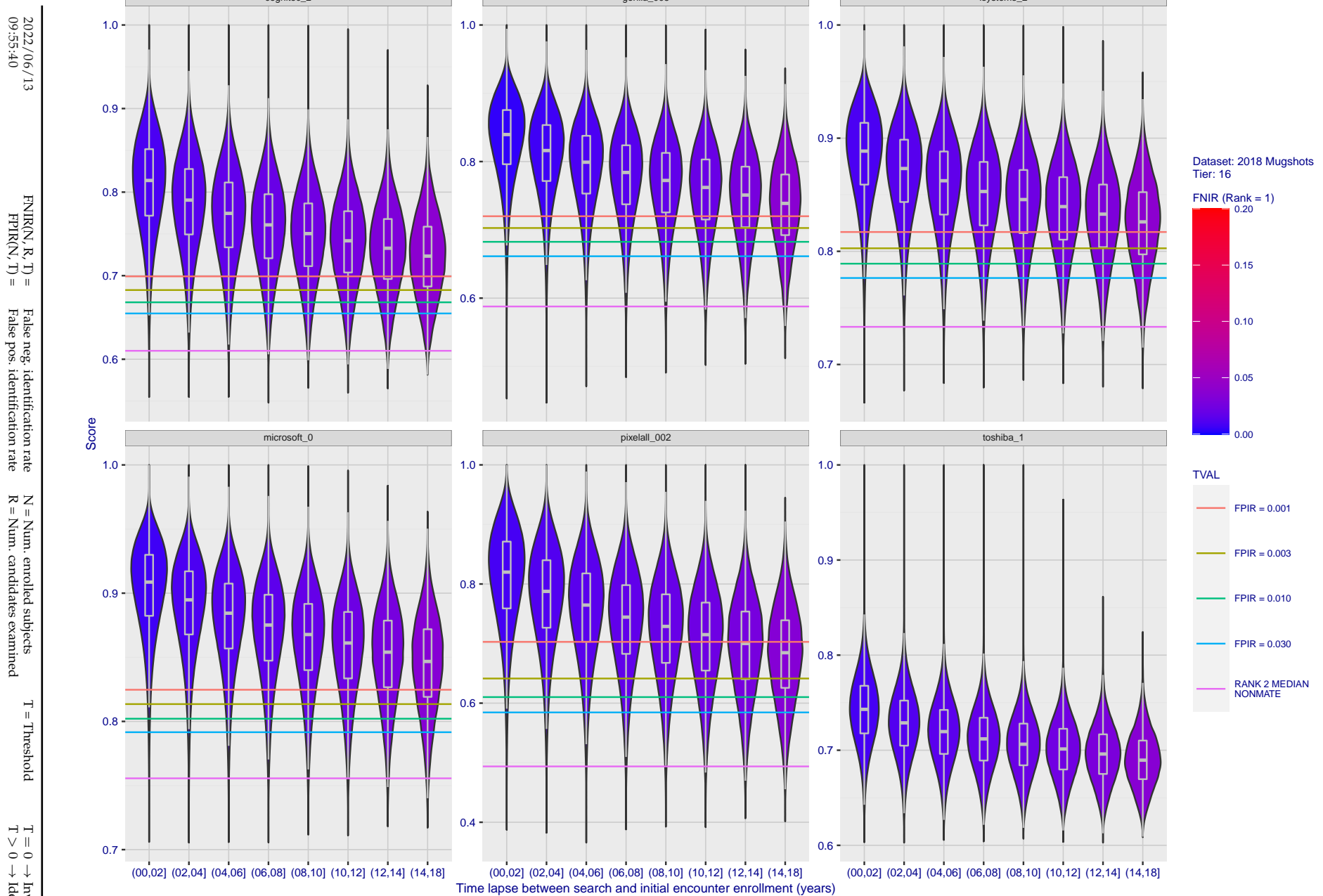


Figure 110: [FRVT-2018 Mugshot Ageing Dataset] Native mate scores vs. time-elapsed. The oldest image of each individual is enrolled. Thereafter, all more recent images are searched. Mated score distributions are computed over all searches noted in row 17 of Table 1 binned by number of years between search and initial enrollment.



**Figure 111: [FRVT-2018 Mugshot Ageing Dataset] Native mate scores vs. time-elapsed.** The oldest image of each individual is enrolled. Thereafter, all more recent images are searched. Mated score distributions are computed over all searches noted in row 17 of Table 1 binned by number of years between search and initial enrollment.

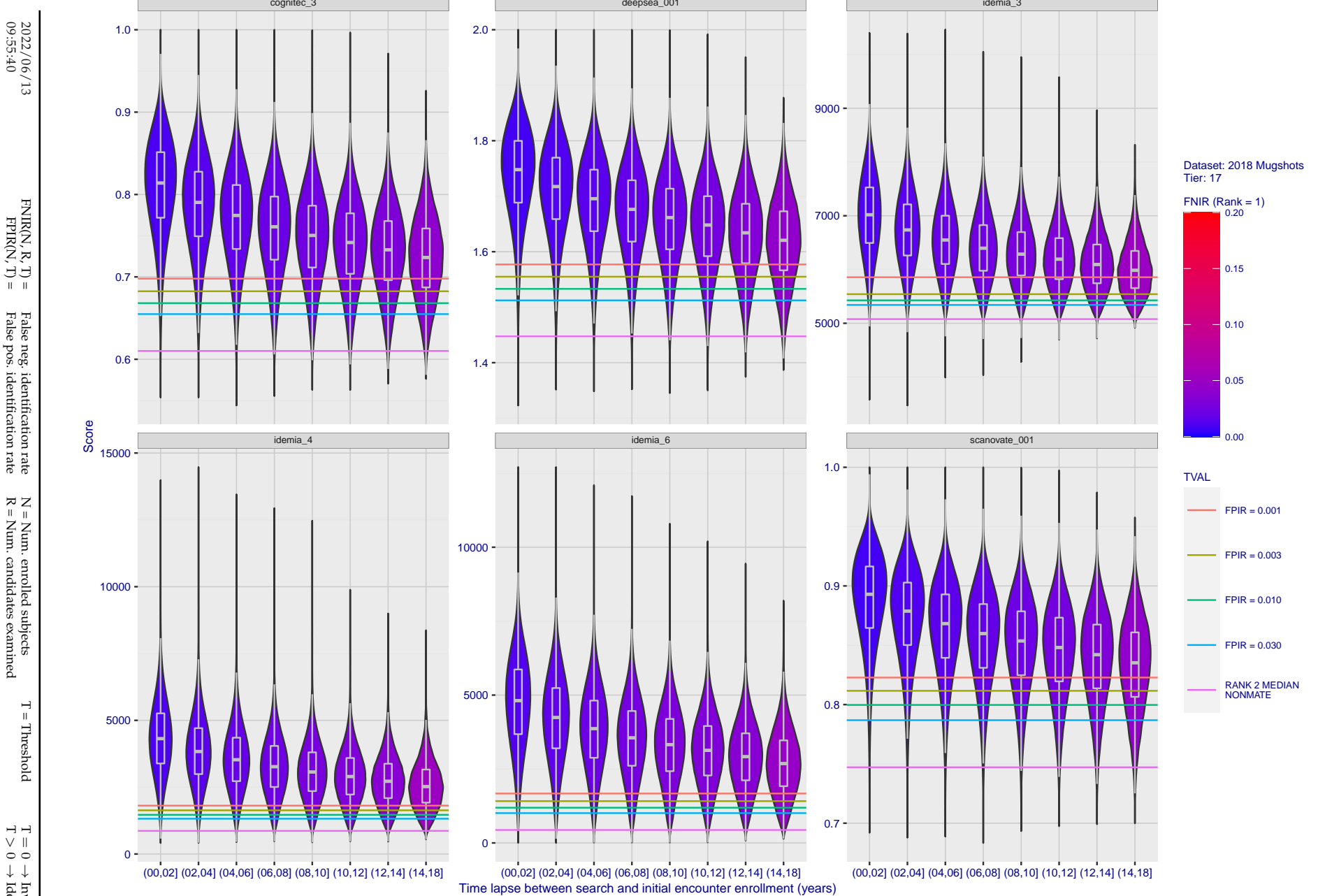
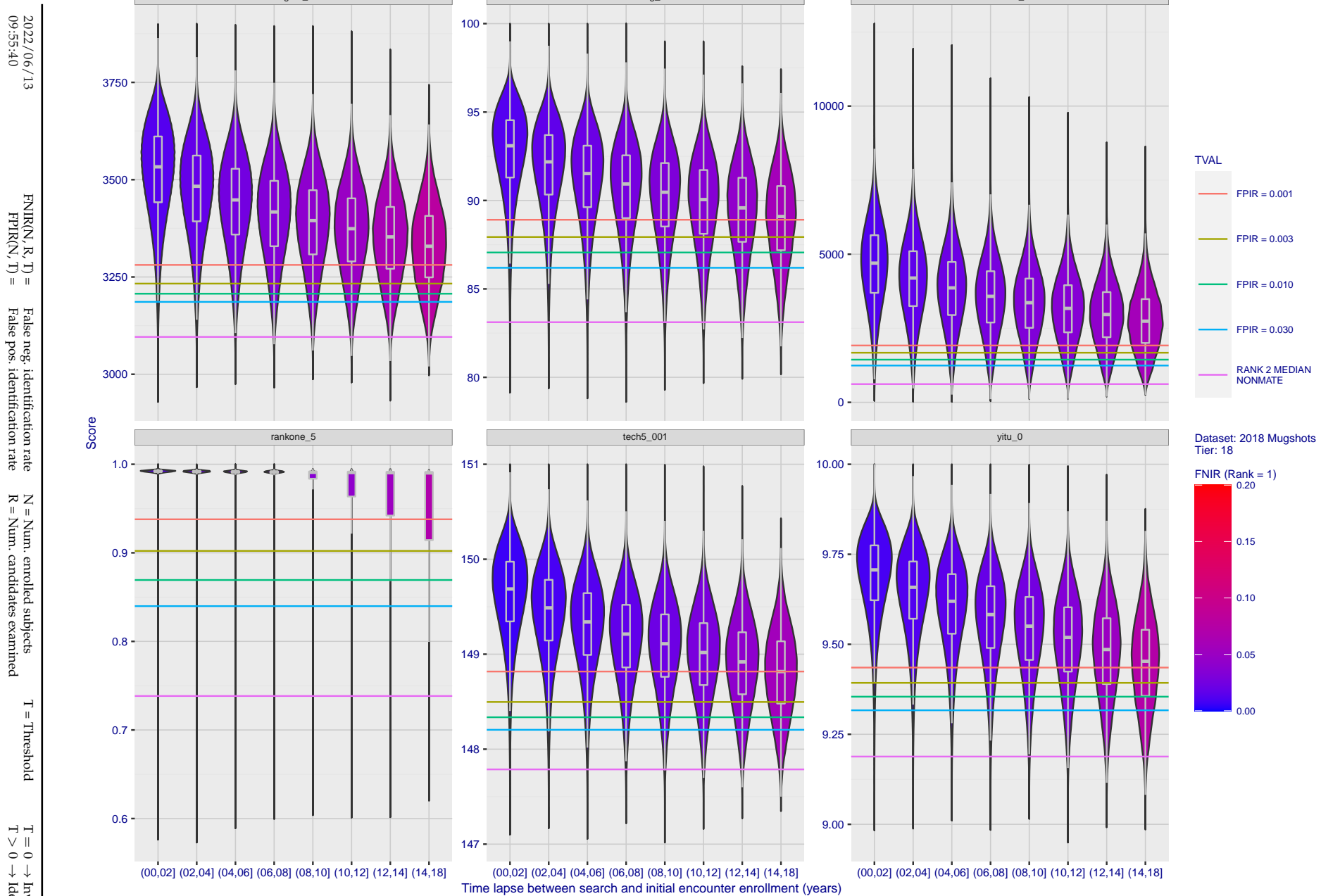


Figure 112: [FRVT-2018 Mugshot Ageing Dataset] Native mate scores vs. time-elapsed. The oldest image of each individual is enrolled. Thereafter, all more recent images are searched. Mated score distributions are computed over all searches noted in row 17 of Table 1 binned by number of years between search and initial enrollment.



**Figure 113: [FRVT-2018 Mugshot Ageing Dataset] Native mate scores vs. time-elapsed.** The oldest image of each individual is enrolled. Thereafter, all more recent images are searched. Mated score distributions are computed over all searches noted in row 17 of Table 1 binned by number of years between search and initial enrollment.

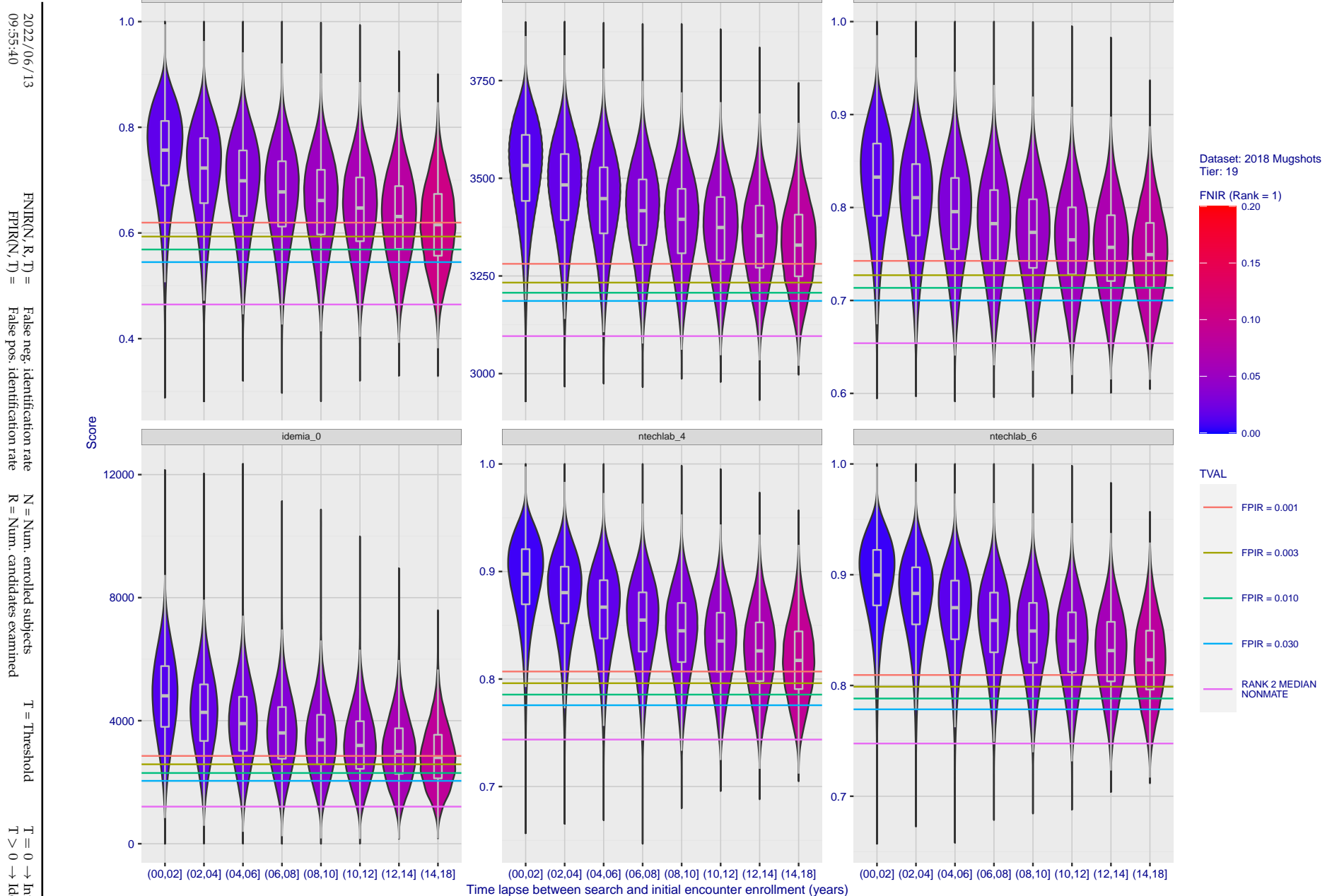
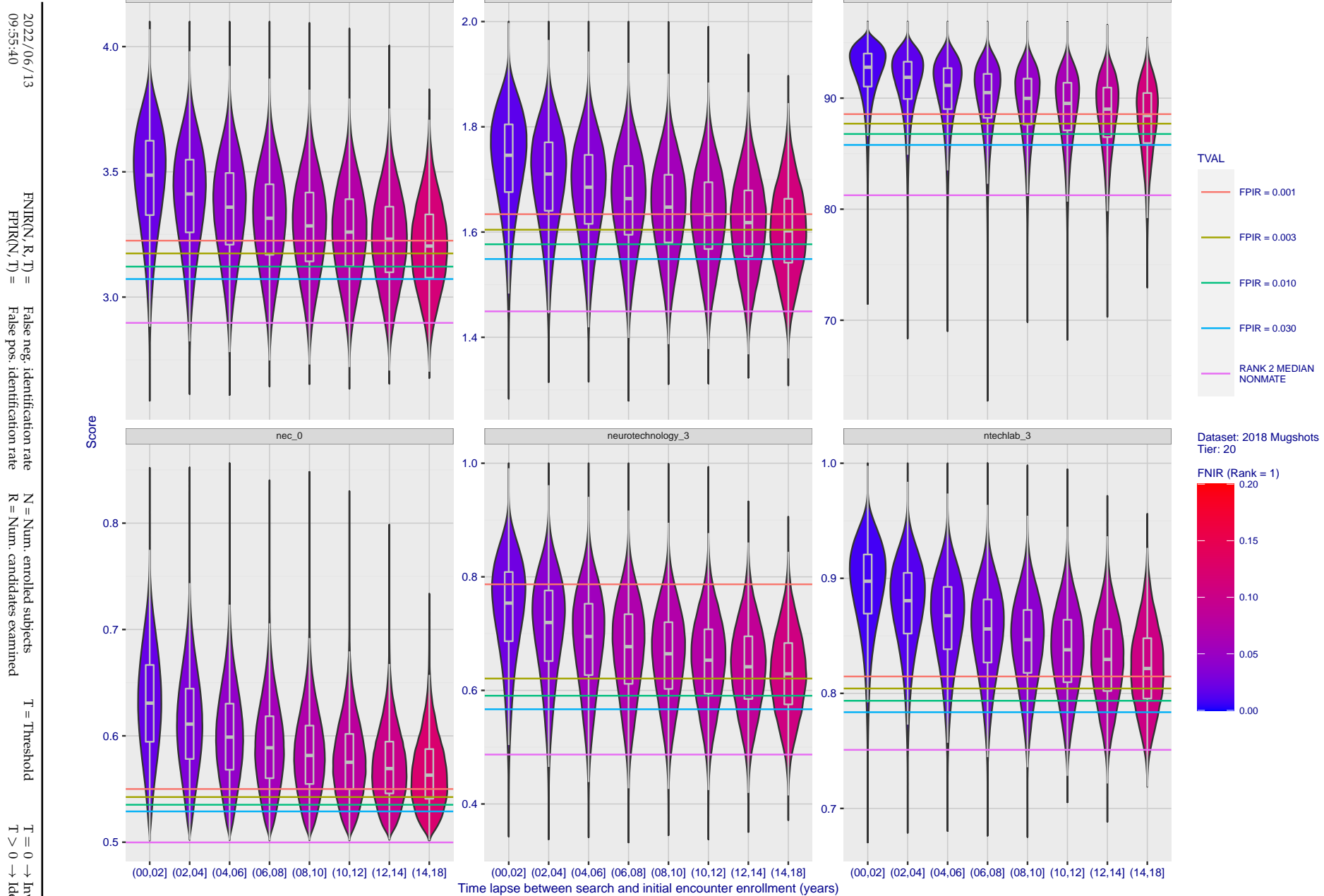


Figure 114: [FRVT-2018 Mugshot Ageing Dataset] Native mate scores vs. time-elapsed. The oldest image of each individual is enrolled. Thereafter, all more recent images are searched. Mated score distributions are computed over all searches noted in row 17 of Table 1 binned by number of years between search and initial enrollment.



**Figure 115: [FRVT-2018 Mugshot Ageing Dataset] Native mate scores vs. time-elapsed.** The oldest image of each individual is enrolled. Thereafter, all more recent images are searched. Mated score distributions are computed over all searches noted in row 17 of Table 1 binned by number of years between search and initial enrollment.

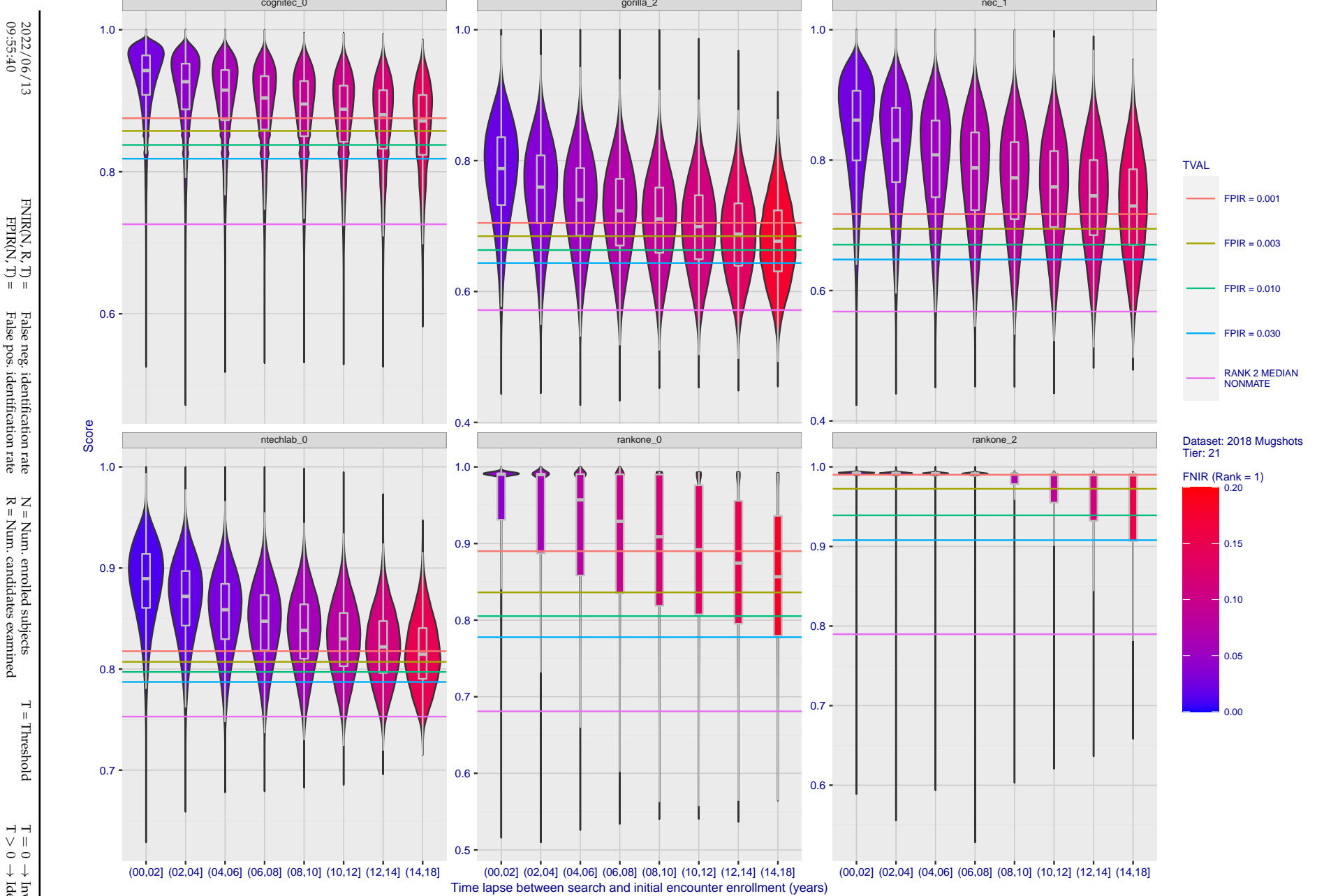
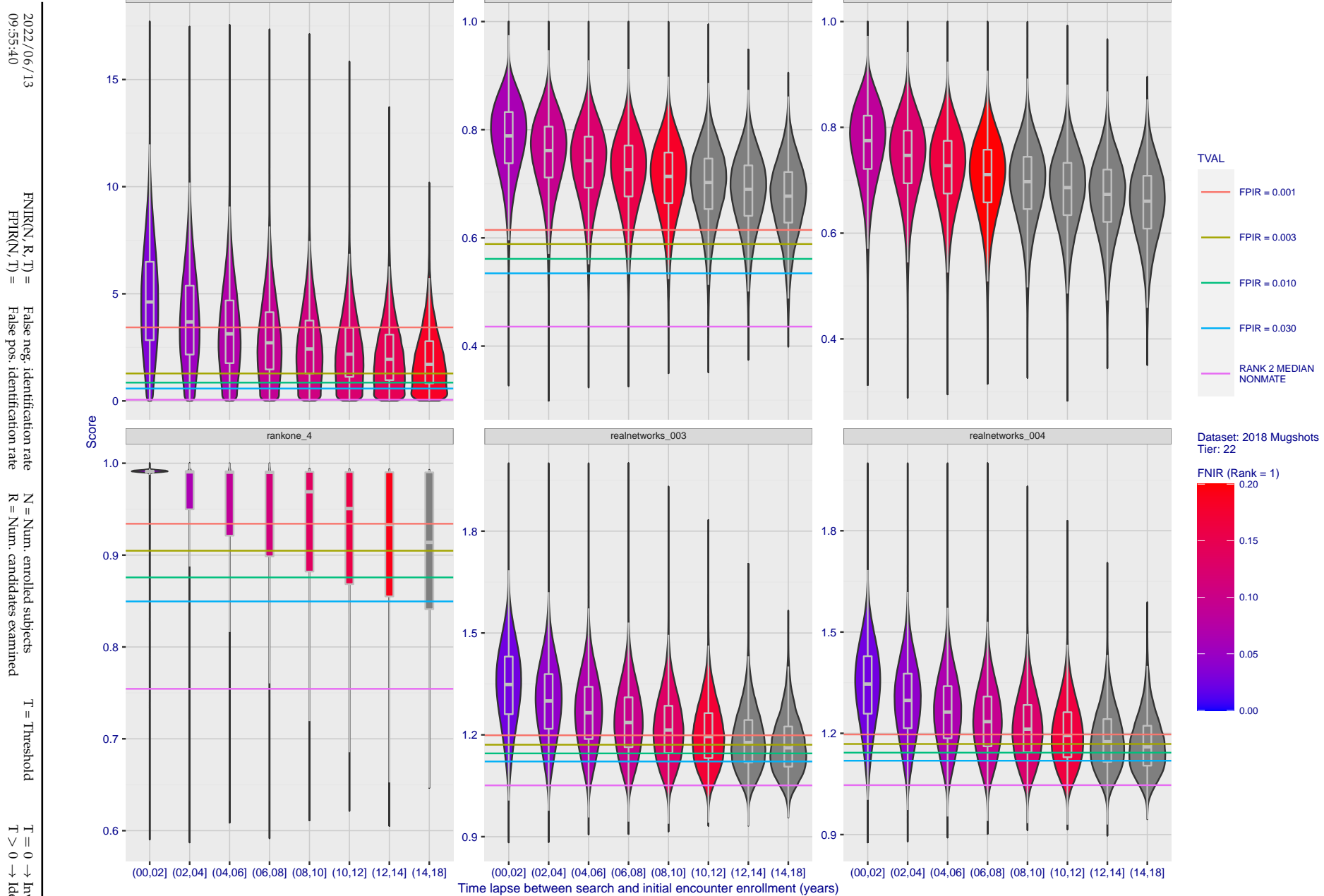


Figure 116: [FRVT-2018 Mugshot Ageing Dataset] Native mate scores vs. time-elapsed. The oldest image of each individual is enrolled. Thereafter, all more recent images are searched. Mated score distributions are computed over all searches noted in row 17 of Table 1 binned by number of years between search and initial enrollment.



**Figure 117: [FRVT-2018 Mugshot Ageing Dataset] Native mate scores vs. time-elapsed.** The oldest image of each individual is enrolled. Thereafter, all more recent images are searched. Mated score distributions are computed over all searches noted in row 17 of Table 1 binned by number of years between search and initial enrollment.

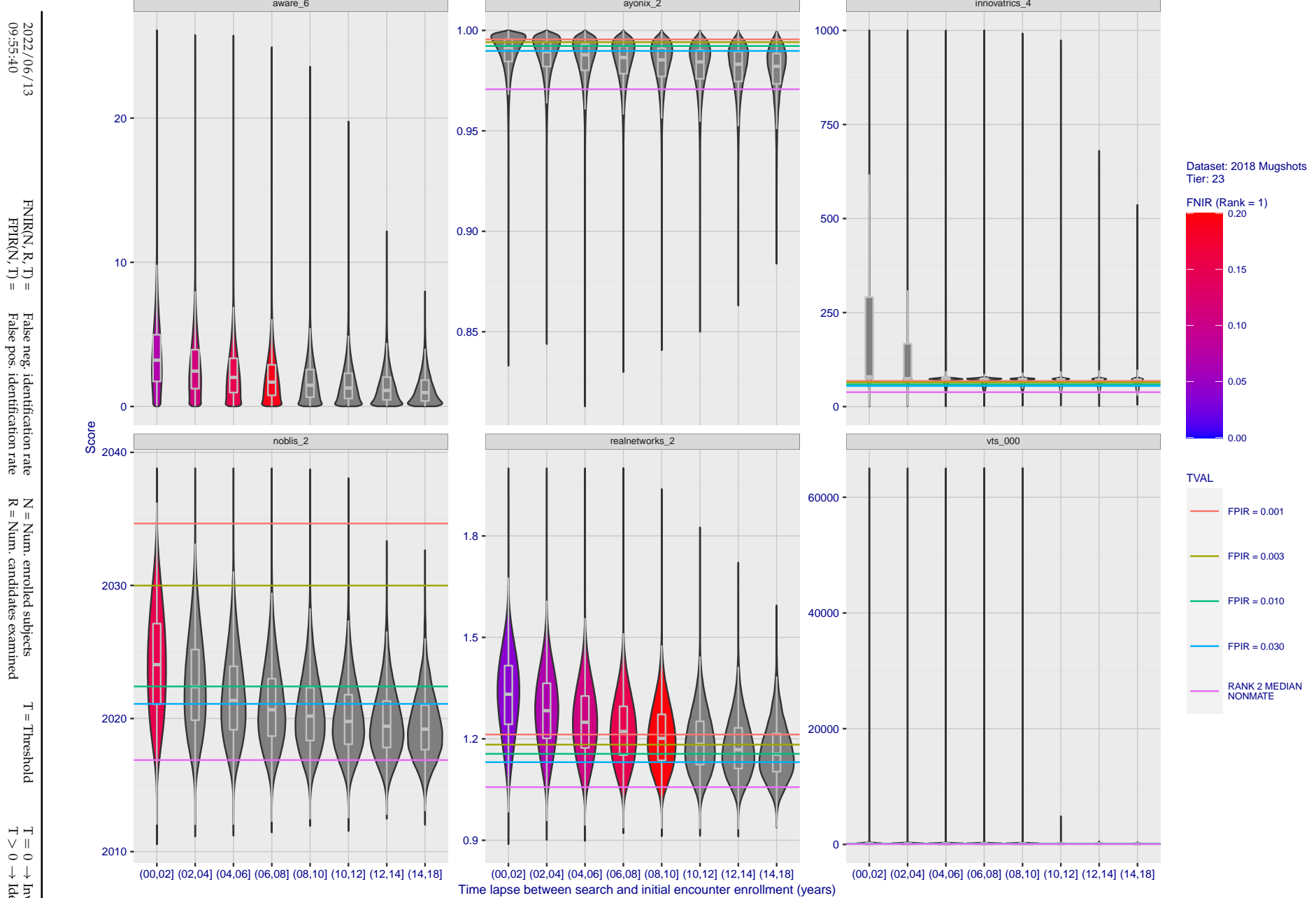
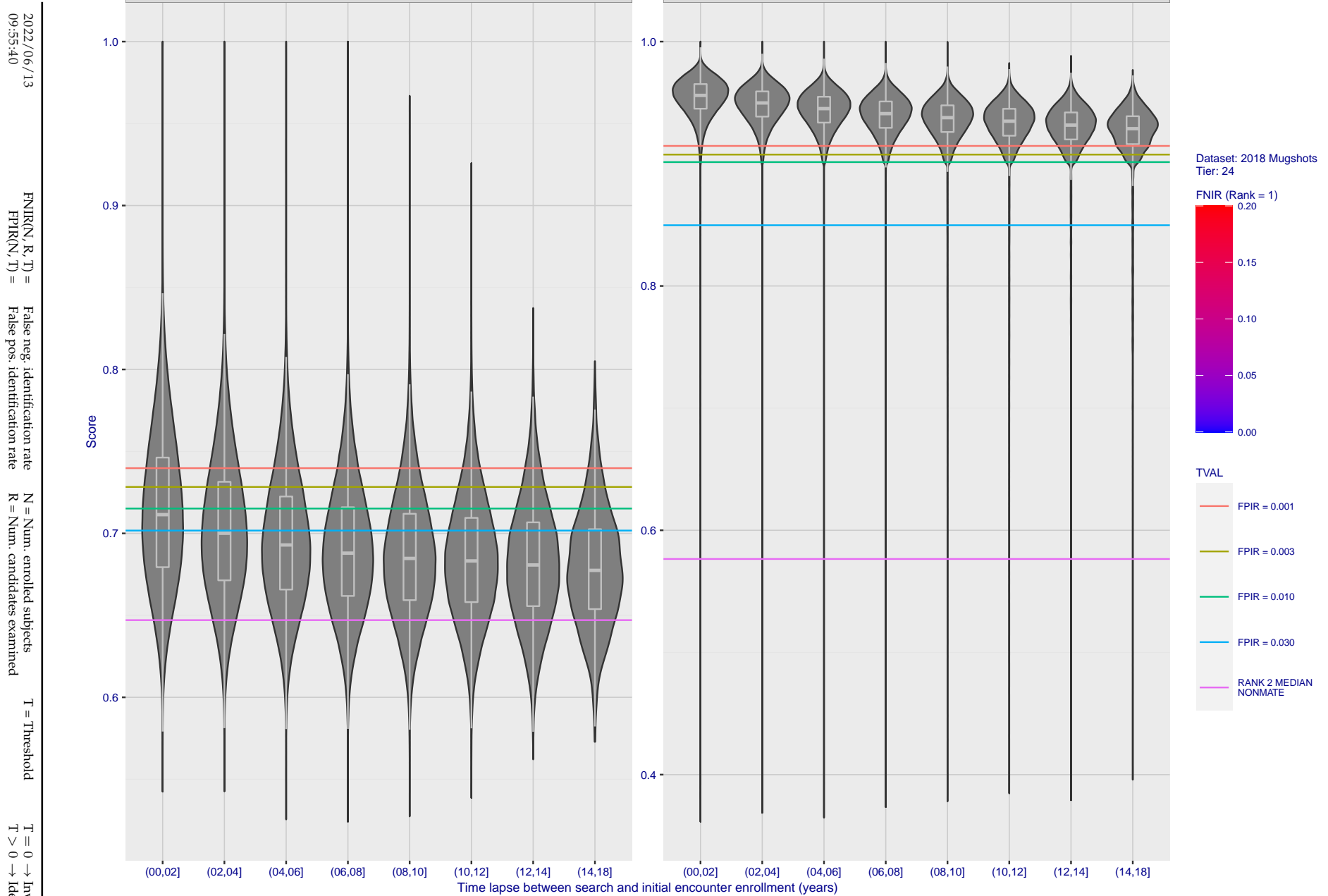


Figure 118: [FRVT-2018 Mugshot Ageing Dataset] Native mate scores vs. time-elapsed. The oldest image of each individual is enrolled. Thereafter, all more recent images are searched. Mated score distributions are computed over all searches noted in row 17 of Table 1 binned by number of years between search and initial enrollment.



**Figure 119: [FRVT-2018 Mugshot Ageing Dataset] Native mate scores vs. time-elapsed.** The oldest image of each individual is enrolled. Thereafter, all more recent images are searched. Mated score distributions are computed over all searches noted in row 17 of Table 1 binned by number of years between search and initial enrollment.

## Appendix C Effect of enrolling multiple images

2022/06/13  
09:55:40FNIR(N, R, T) = False neg. identification rate  
FPIR(N, T) = False pos. identification rateN = Num. enrolled subjects  
R = Num. candidates examined

T = Threshold

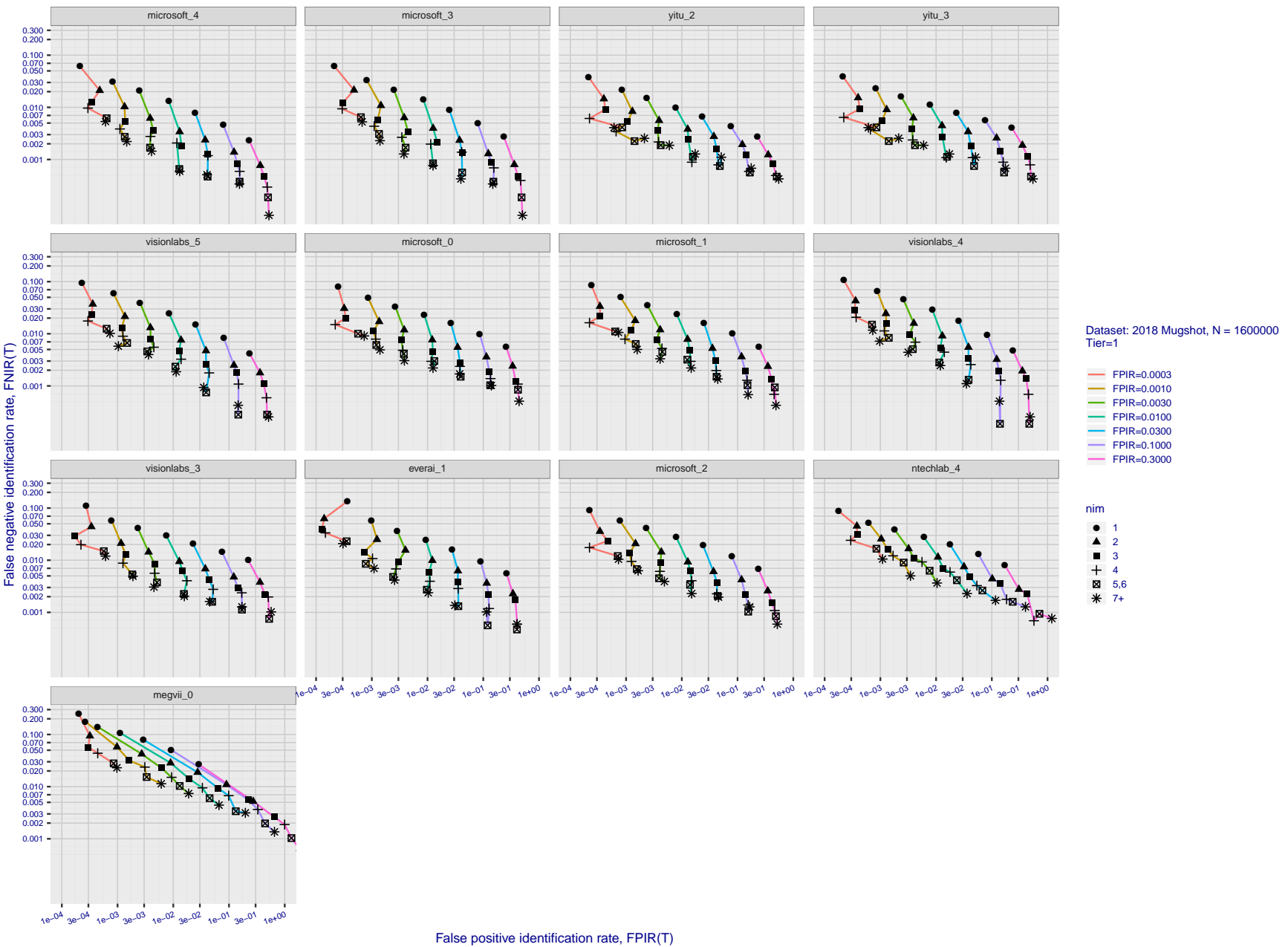
T = 0 → Investigation  
T > 0 → Identification

Figure 120: [FRVT-2018 Mugshot Dataset] Effect of enrolling multiple images for each identity. The plot shows an identification miss rates vs. false positive rates, at seven operating thresholds. The enrolled population size is fixed. The images are enrolled with lifetime-consolidation - see section 2.3.

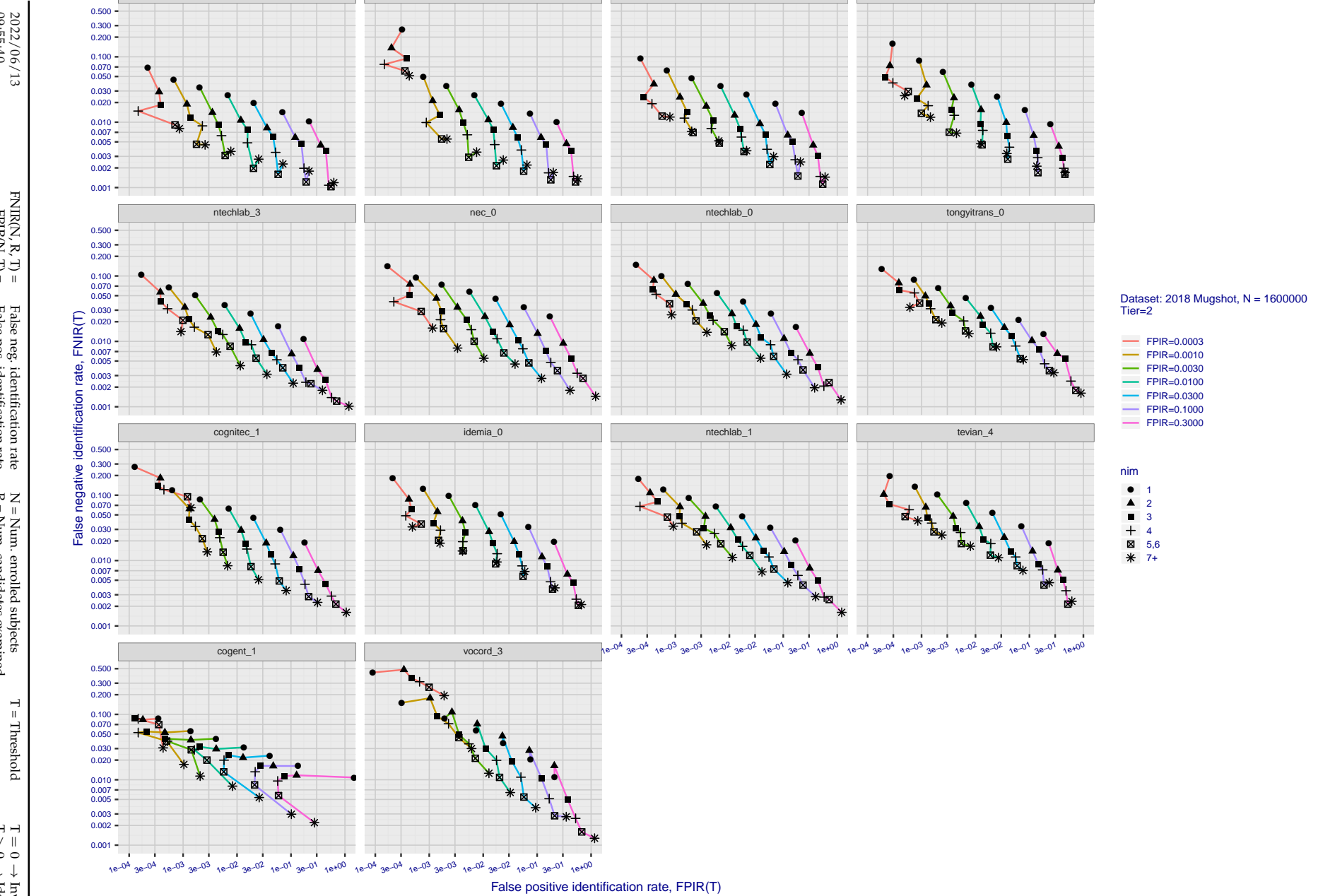


Figure 121: [FRVT-2018 Mugshot Dataset] Effect of enrolling multiple images for each identity. The plot shows an identification miss rates vs. false positive rates, at seven operating thresholds. The enrolled population size is fixed. The images are enrolled with lifetime-consolidation - see section 2.3.

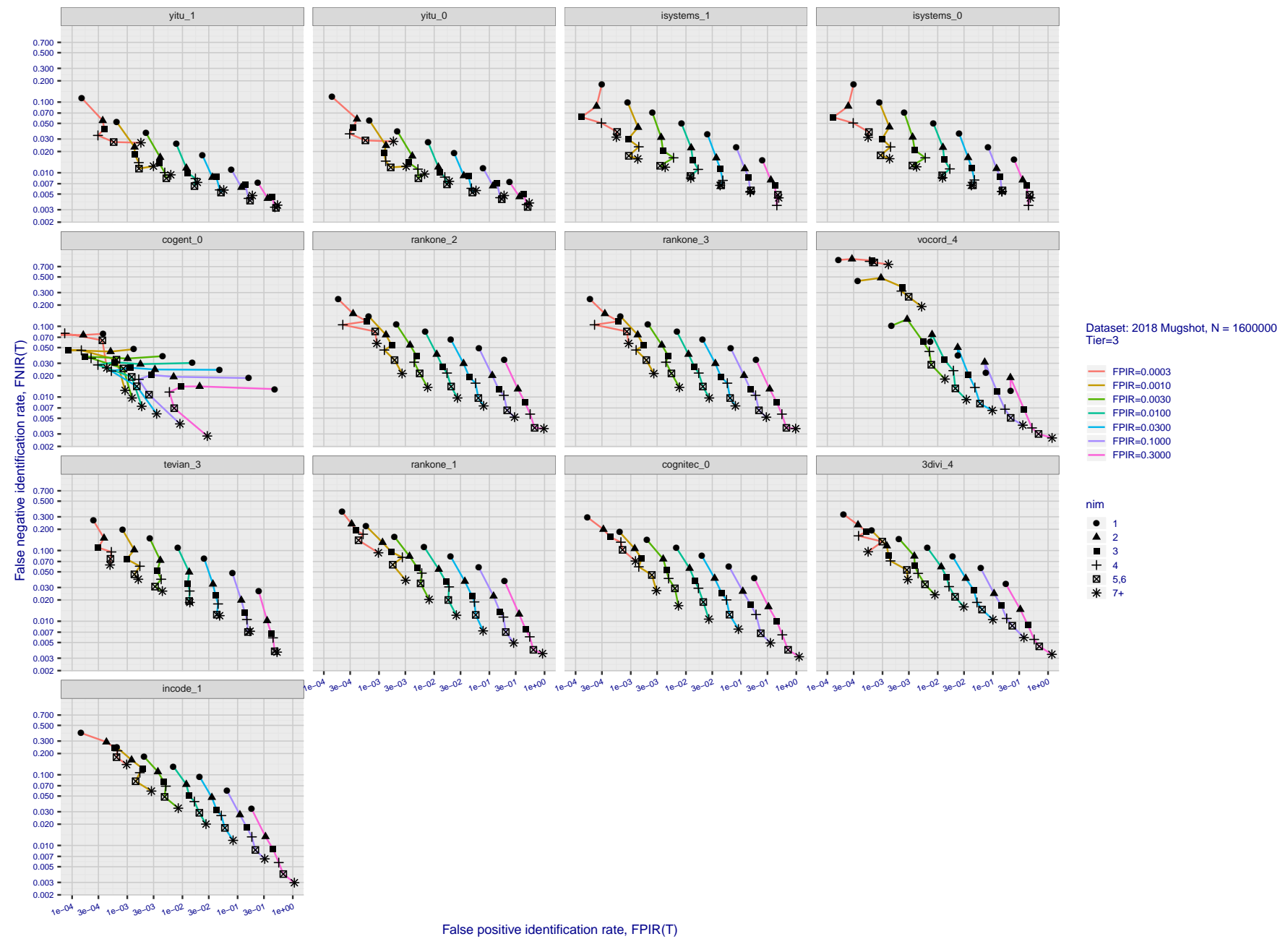


Figure 122: [FRVT-2018 Mugshot Dataset] Effect of enrolling multiple images for each identity. The plot shows an identification miss rates vs. false positive rates, at seven operating thresholds. The enrolled population size is fixed. The images are enrolled with lifetime-consolidation - see section 2.3.

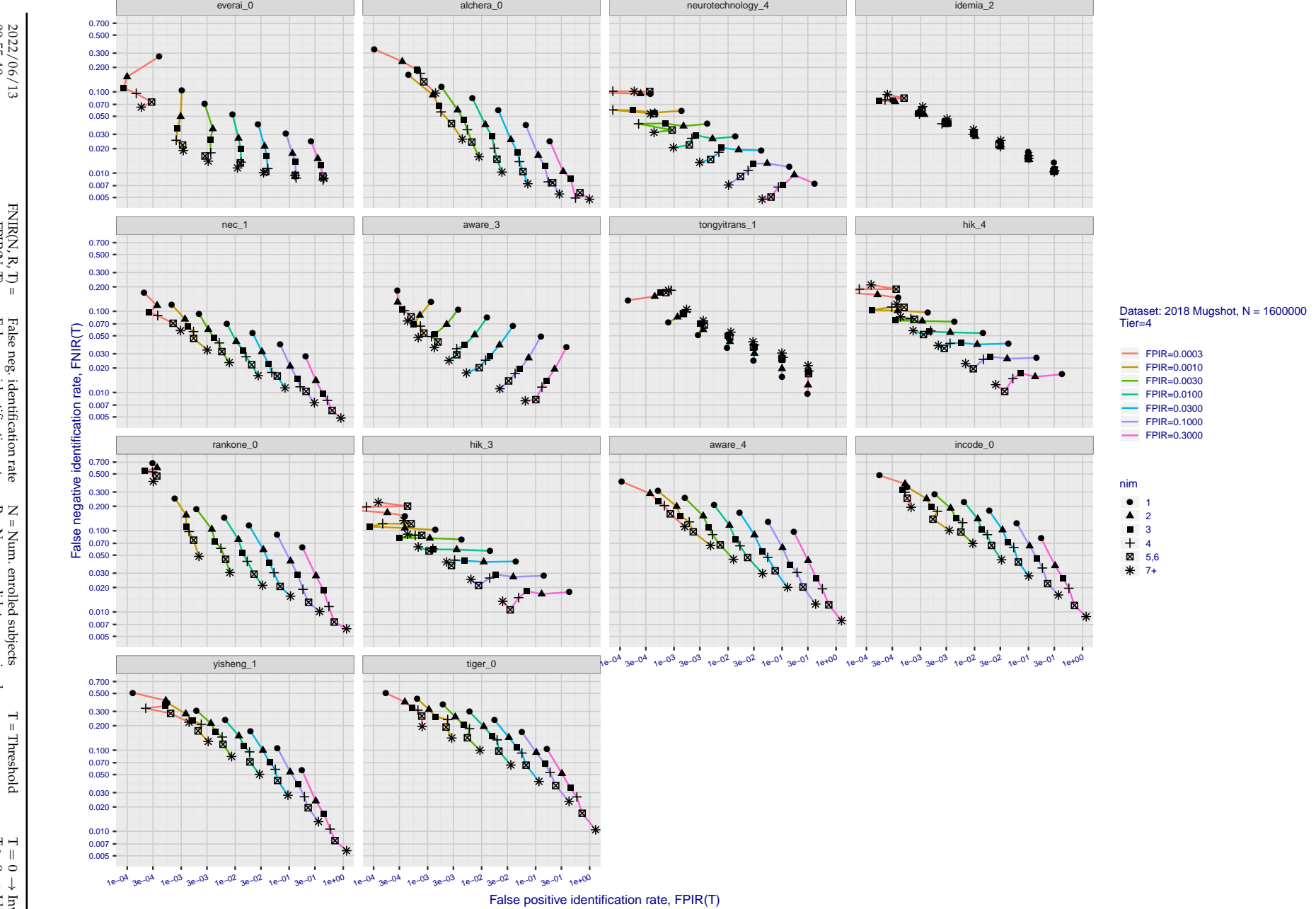


Figure 123: [FRVT-2018 Mugshot Dataset] Effect of enrolling multiple images for each identity. The plot shows an identification miss rates vs. false positive rates, at seven operating thresholds. The enrolled population size is fixed. The images are enrolled with lifetime-consolidation - see section 2.3.

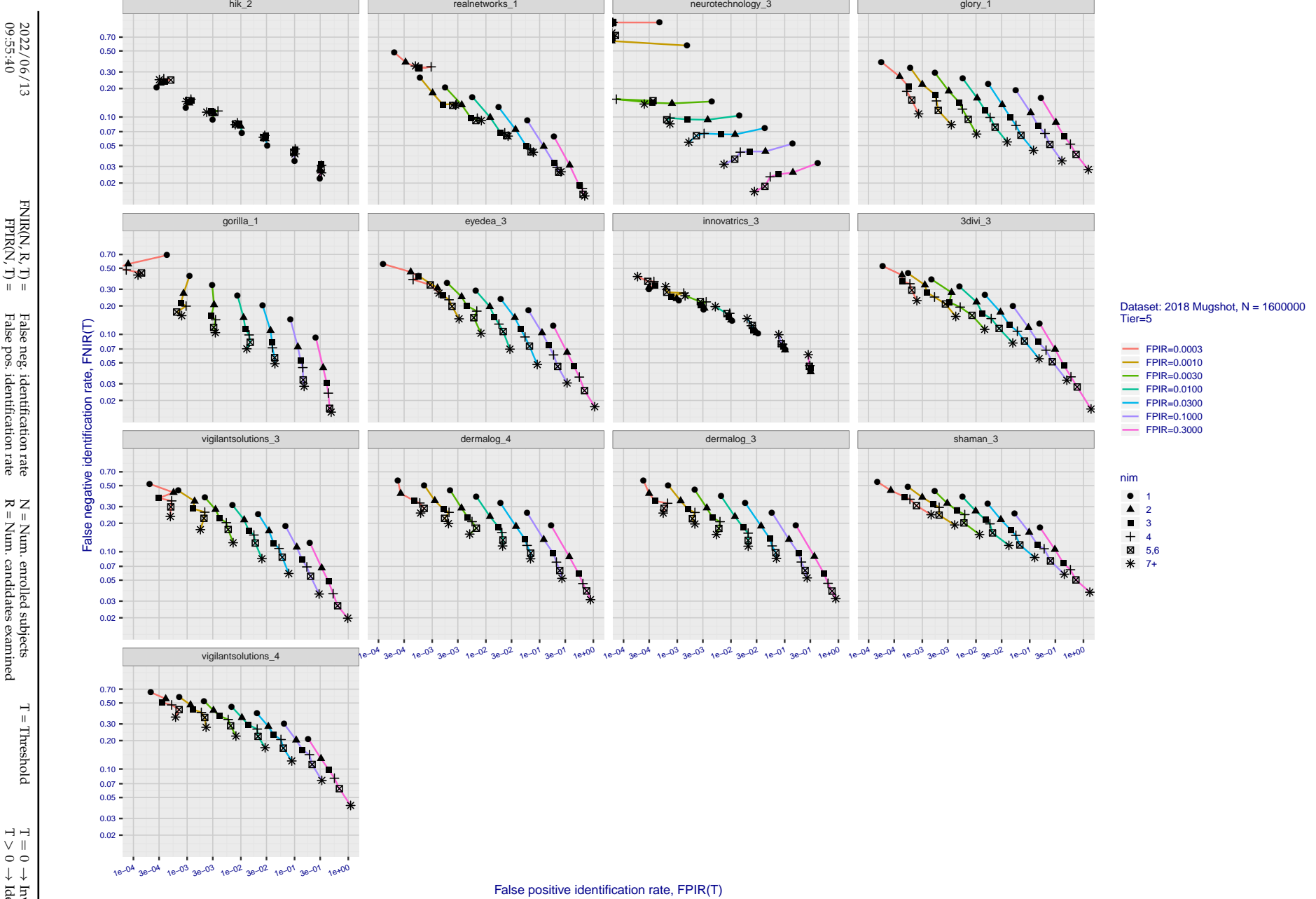


Figure 124: [FRVT-2018 Mugshot Dataset] Effect of enrolling multiple images for each identity. The plot shows an identification miss rates vs. false positive rates, at seven operating thresholds. The enrolled population size is fixed. The images are enrolled with lifetime-consolidation - see section 2.3.

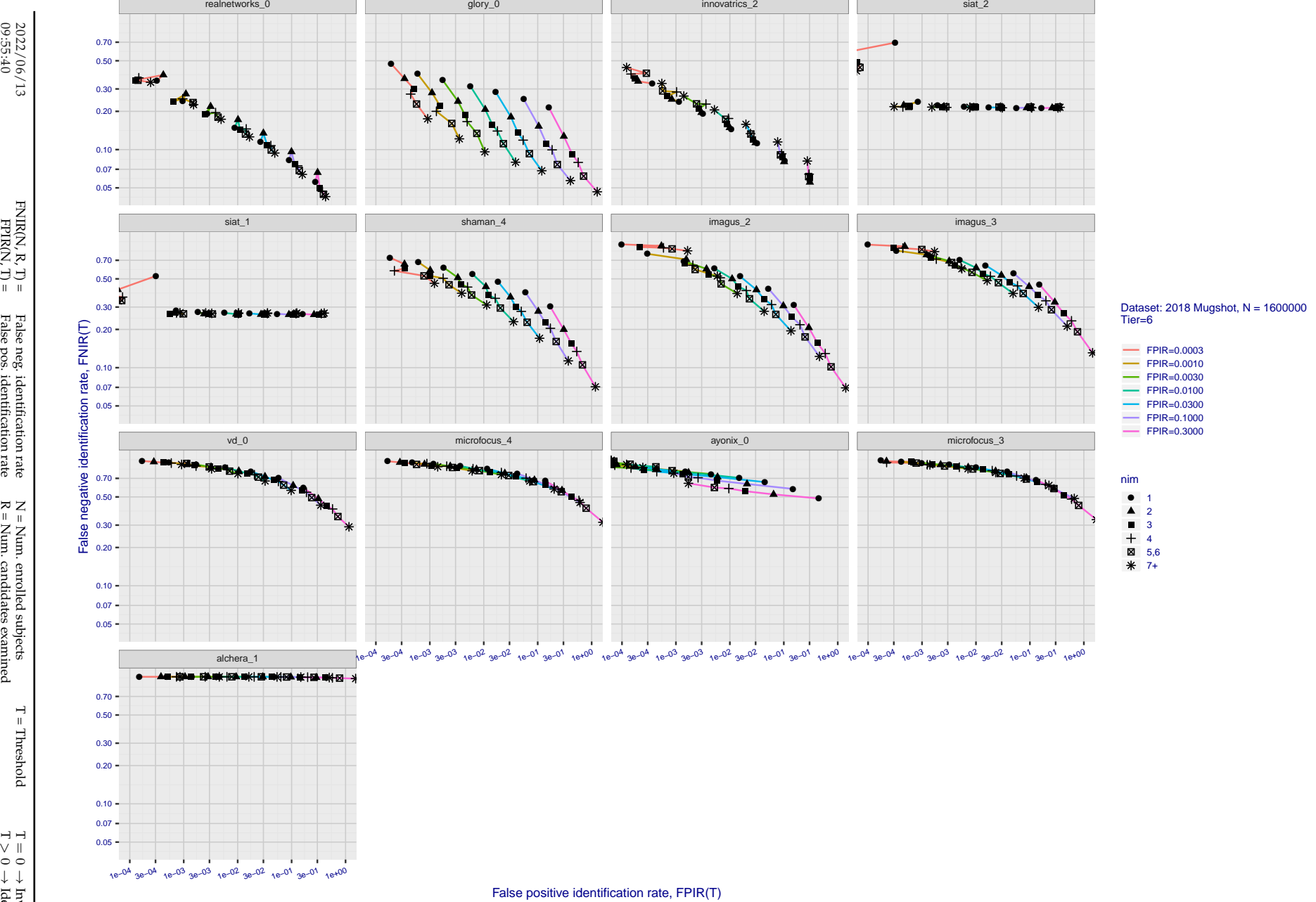


Figure 125: [FRVT-2018 Mugshot Dataset] Effect of enrolling multiple images for each identity. The plot shows an identification miss rates vs. false positive rates, at seven operating thresholds. The enrolled population size is fixed. The images are enrolled with lifetime-consolidation - see section 2.3.

## Appendix D Accuracy with poor quality webcam images

---

2022/06/13  
09:55:40      FNIR(N, R, T) = False neg. identification rate  
                  FPIR(N, T) = False pos. identification rate  
N = Num. enrolled subjects  
R = Num. candidates examined  
T = Threshold  
T = 0 → Investigation  
T > 0 → Identification

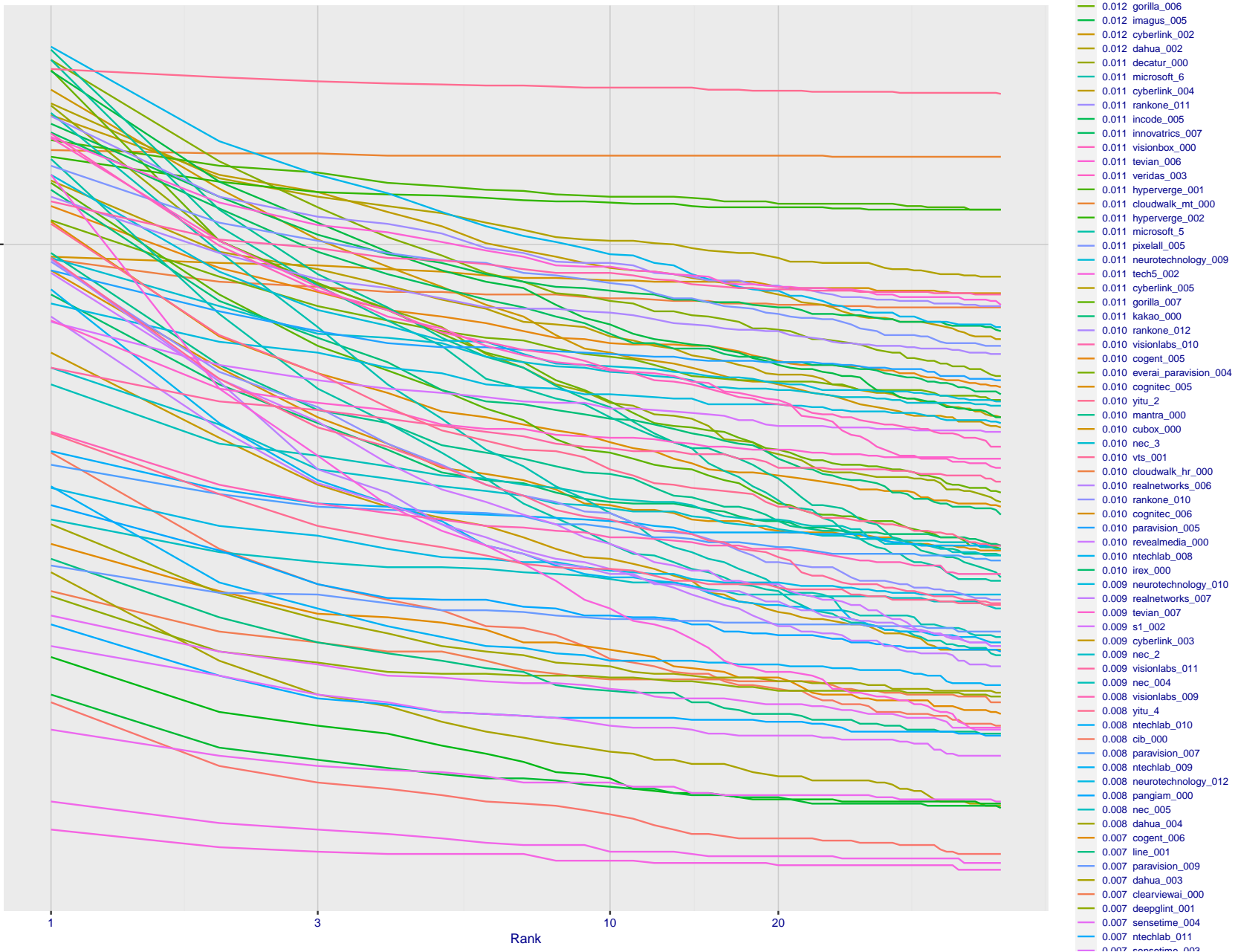


Figure 126: [Webcam Dataset] Identification miss rates vs. rank. The results apply to cross-domain recognition in which webcams are searched against enrolled mugshots. The FNIR values are higher than those for mugshot-mugshot identification due to low image resolution, lighting and less constrained subject pose in webcam images - see Figure 6.

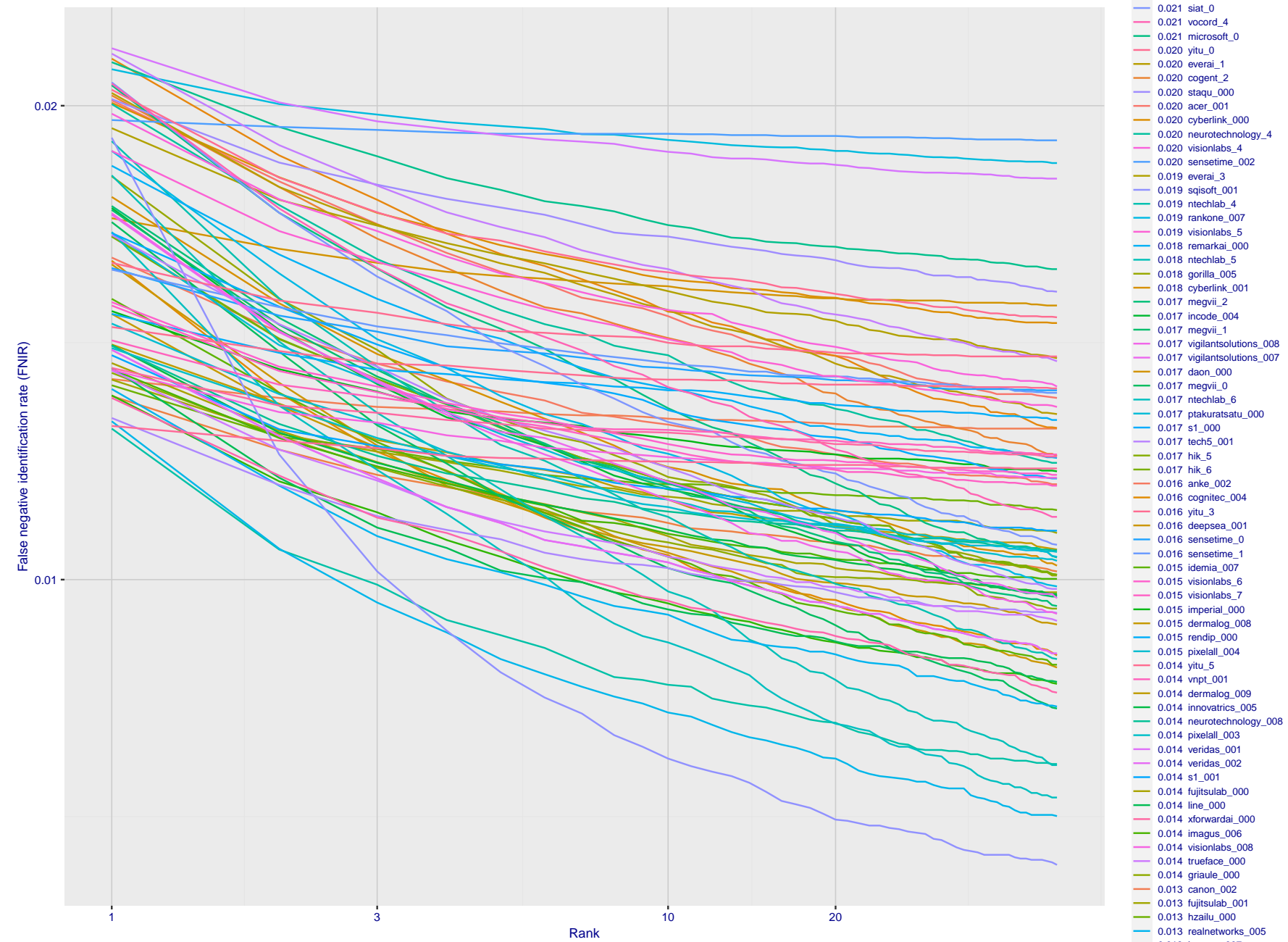


Figure 127: [Webcam Dataset] Identification miss rates vs. rank. The results apply to cross-domain recognition in which webcams are searched against enrolled mugshots. The FNIR values are higher than those for mugshot-mugshot identification due to low image resolution, lighting and less constrained subject pose in webcam images - see Figure 6.

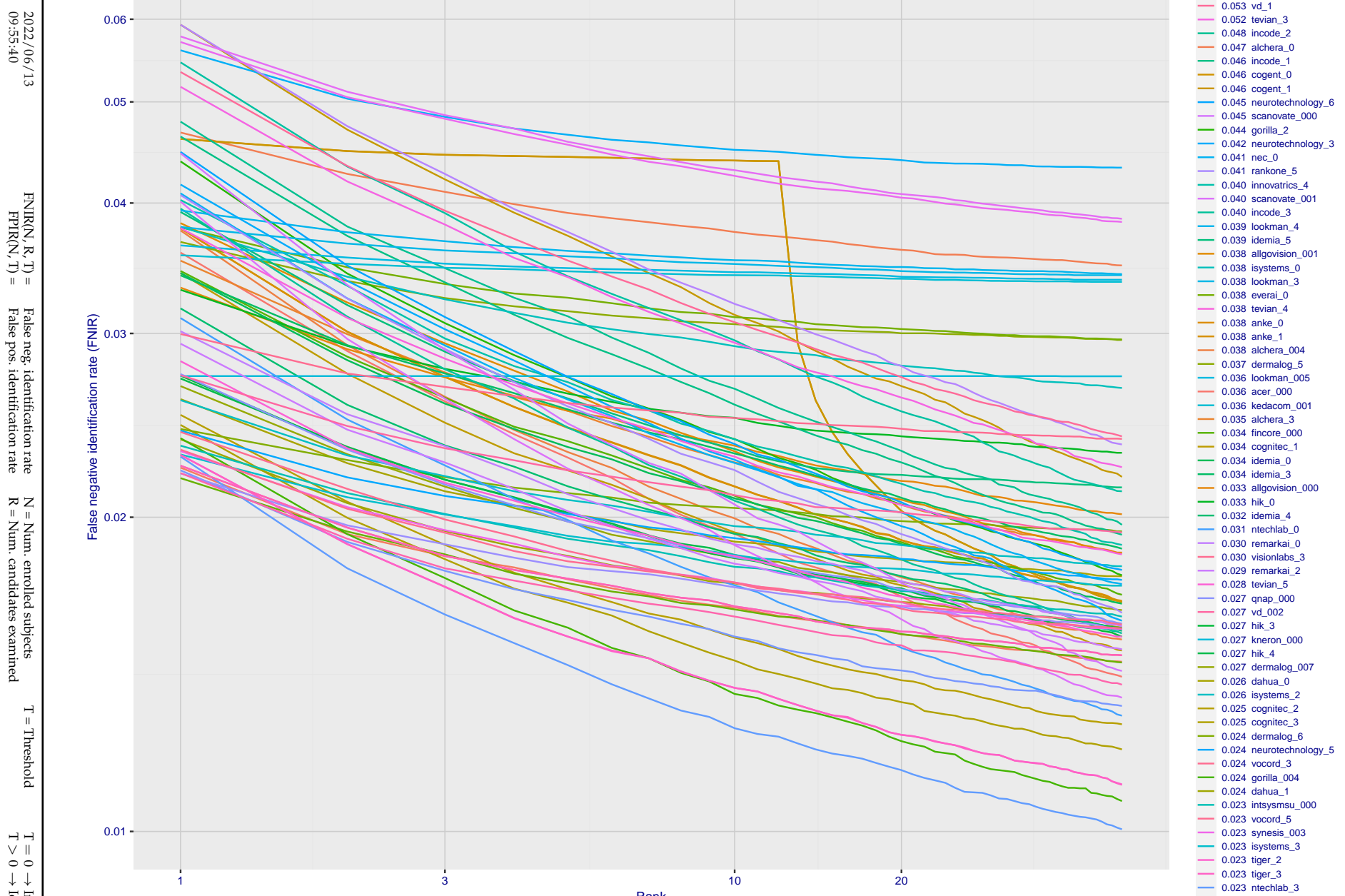


Figure 128: [Webcam Dataset] Identification miss rates vs. rank. The results apply to cross-domain recognition in which webcams are searched against enrolled mugshots. The FNIR values are higher than those for mugshot-mugshot identification due to low image resolution, lighting and less constrained subject pose in webcam images - see Figure 6.

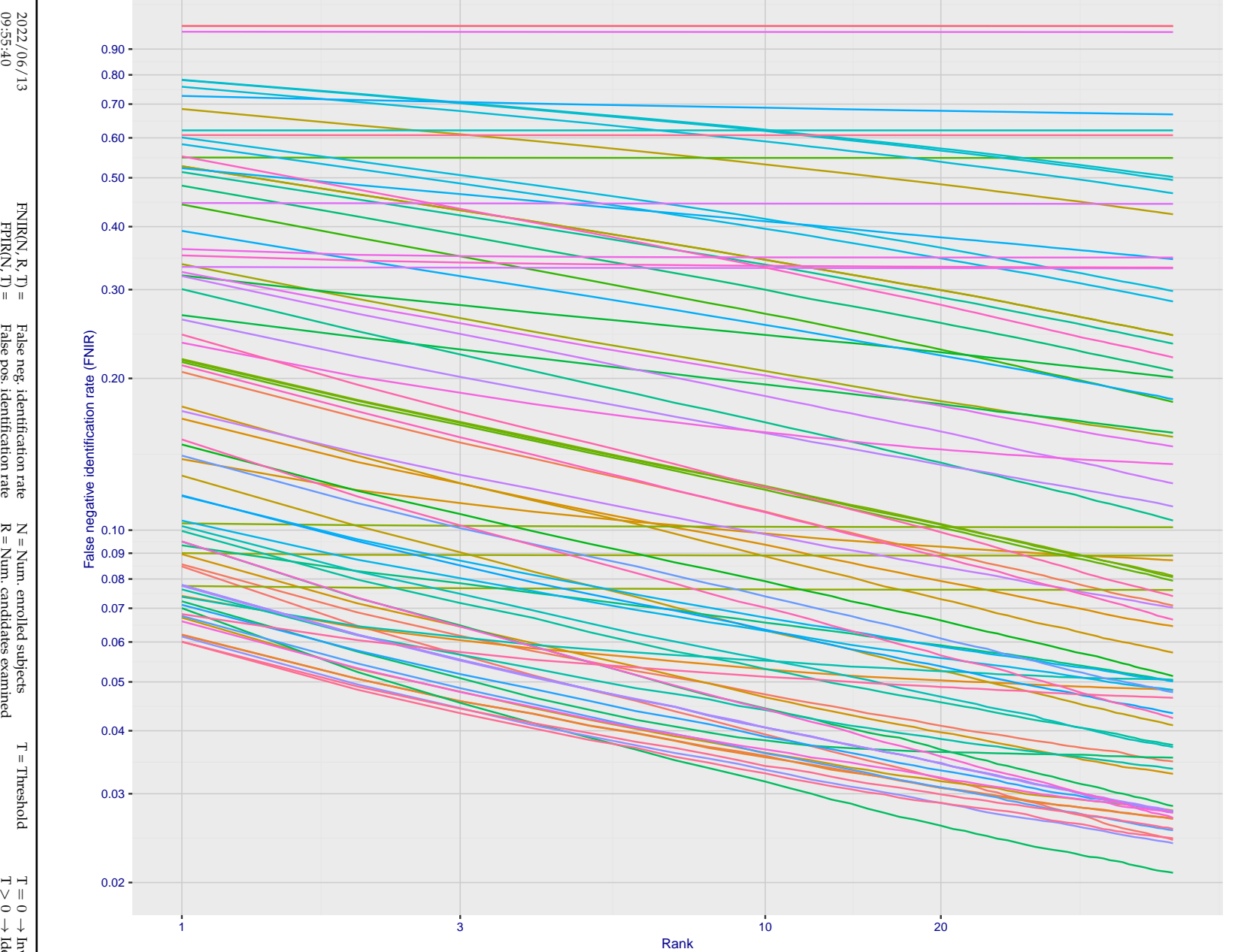


Figure 129: [Webcam Dataset] Identification miss rates vs. rank. The results apply to cross-domain recognition in which webcams are searched against enrolled mugshots. The FNIR values are higher than those for mugshot-mugshot identification due to low image resolution, lighting and less constrained subject pose in webcam images - see Figure 6.

2022/06/13  
09:55:40

---

$\text{FNIR}(N, R, T) =$	False neg. identification rate	$N = \text{Num. enrolled subjects}$	$T = \text{Threshold}$	$T = 0 \rightarrow \text{Investigation}$
$\text{FPIR}(N, T) =$	False pos. identification rate	$R = \text{Num. candidates examined}$		$T > 0 \rightarrow \text{Identification}$

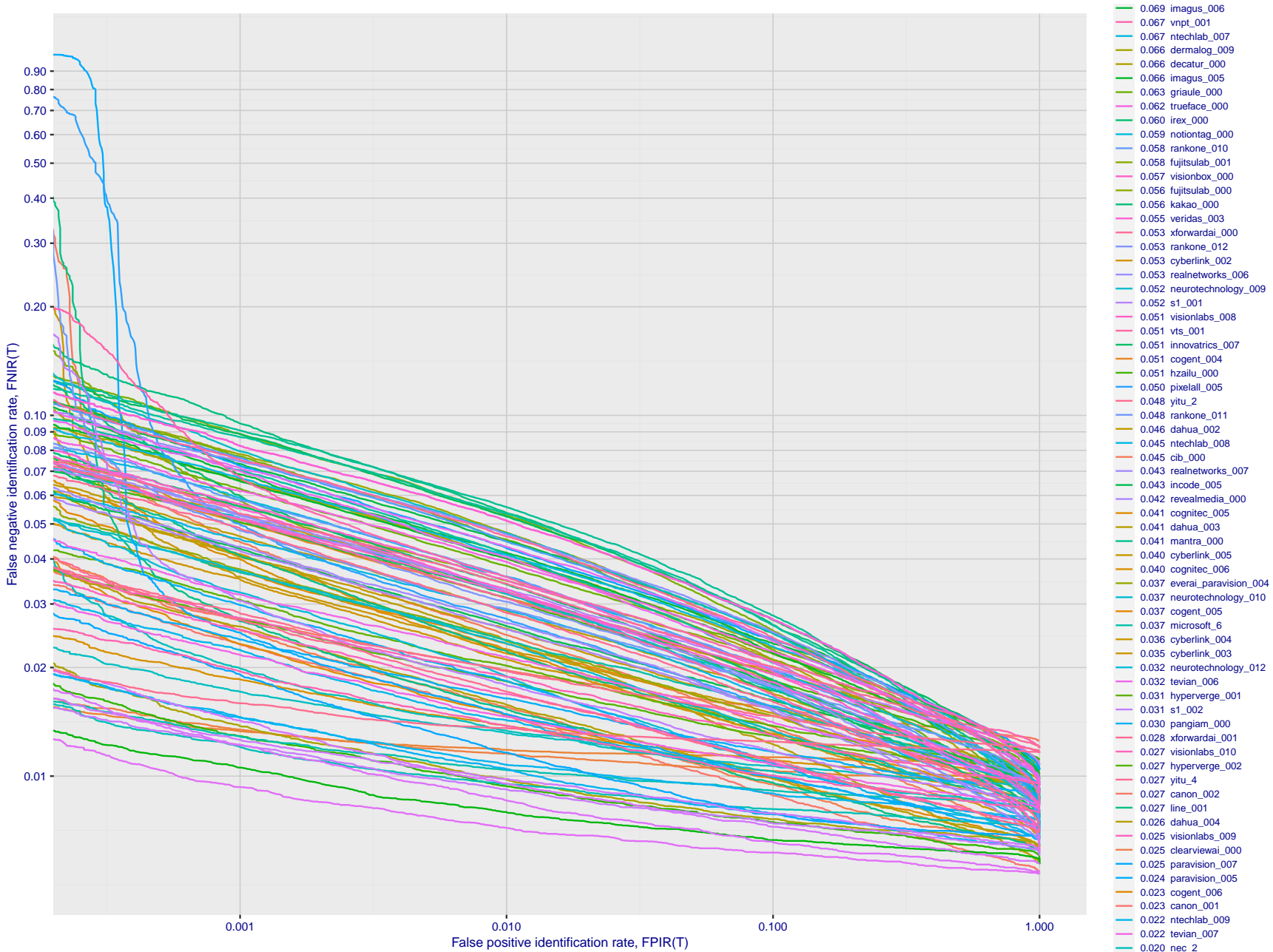
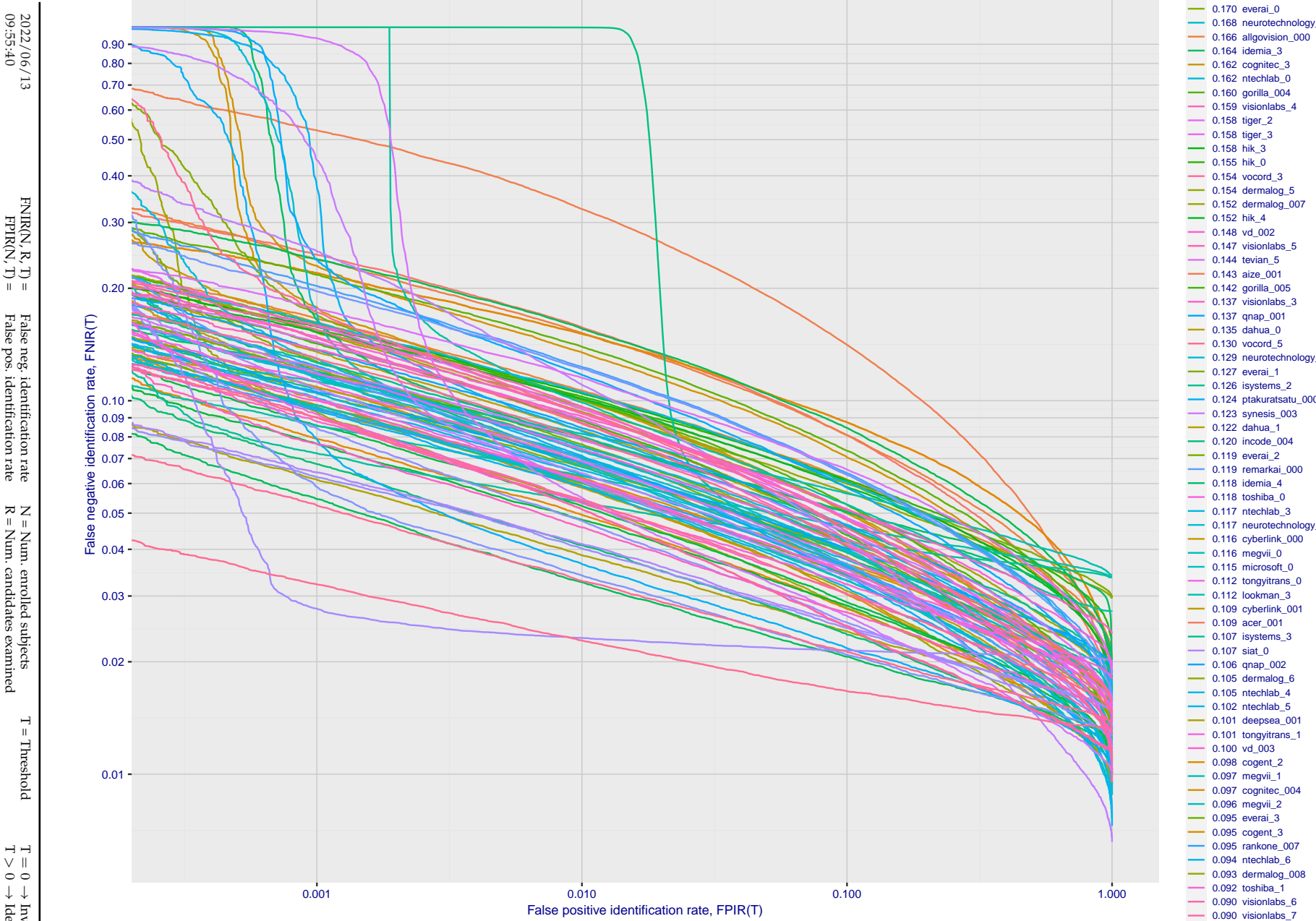
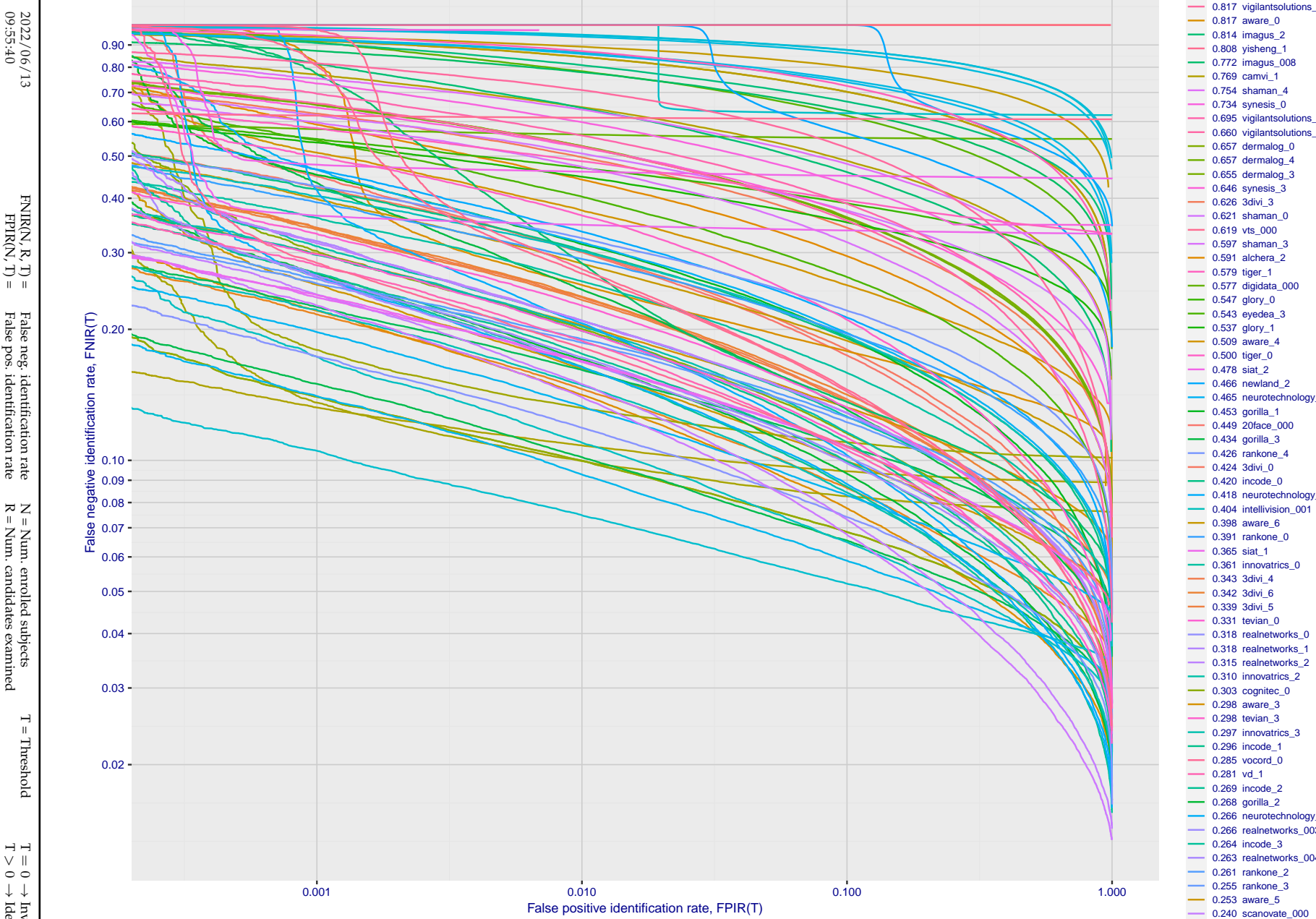


Figure 130: [Webcam Dataset] Identification miss rates vs. false positive rates. The results apply to cross-domain recognition in which webcams are searched against enrolled mugshots. The FNIR values are higher than those for mugshot-mugshot identification due to low image resolution, lighting and less constrained subject pose in webcam images - see Figure 6.



**Figure 131: [Webcam Dataset] Identification miss rates vs. false positive rates.** The results apply to cross-domain recognition in which webcams are searched against enrolled mugshots. The FNIR values are higher than those for mugshot-mugshot identification due to low image resolution, lighting and less constrained subject pose in webcam images - see Figure 6.



**Figure 132: [Webcam Dataset] Identification miss rates vs. false positive rates.** The results apply to cross-domain recognition in which webcams are searched against enrolled mugshots. The FNIR values are higher than those for mugshot-mugshot identification due to low image resolution, lighting and less constrained subject pose in webcam images - see Figure 6.

## Appendix E Accuracy for profile-view to frontal recognition

Figures 133 - 135 gives accuracy results for searching 100 000 mated and 100 000 non-mated profile-view images against the same FRVT 2018 frontal enrollment dataset,  $N = 1\,600\,000$ , used in the main mugshot trials. This experiment corresponds to row-13 of Table 1. An example of profile-view image is given in Figure 7.

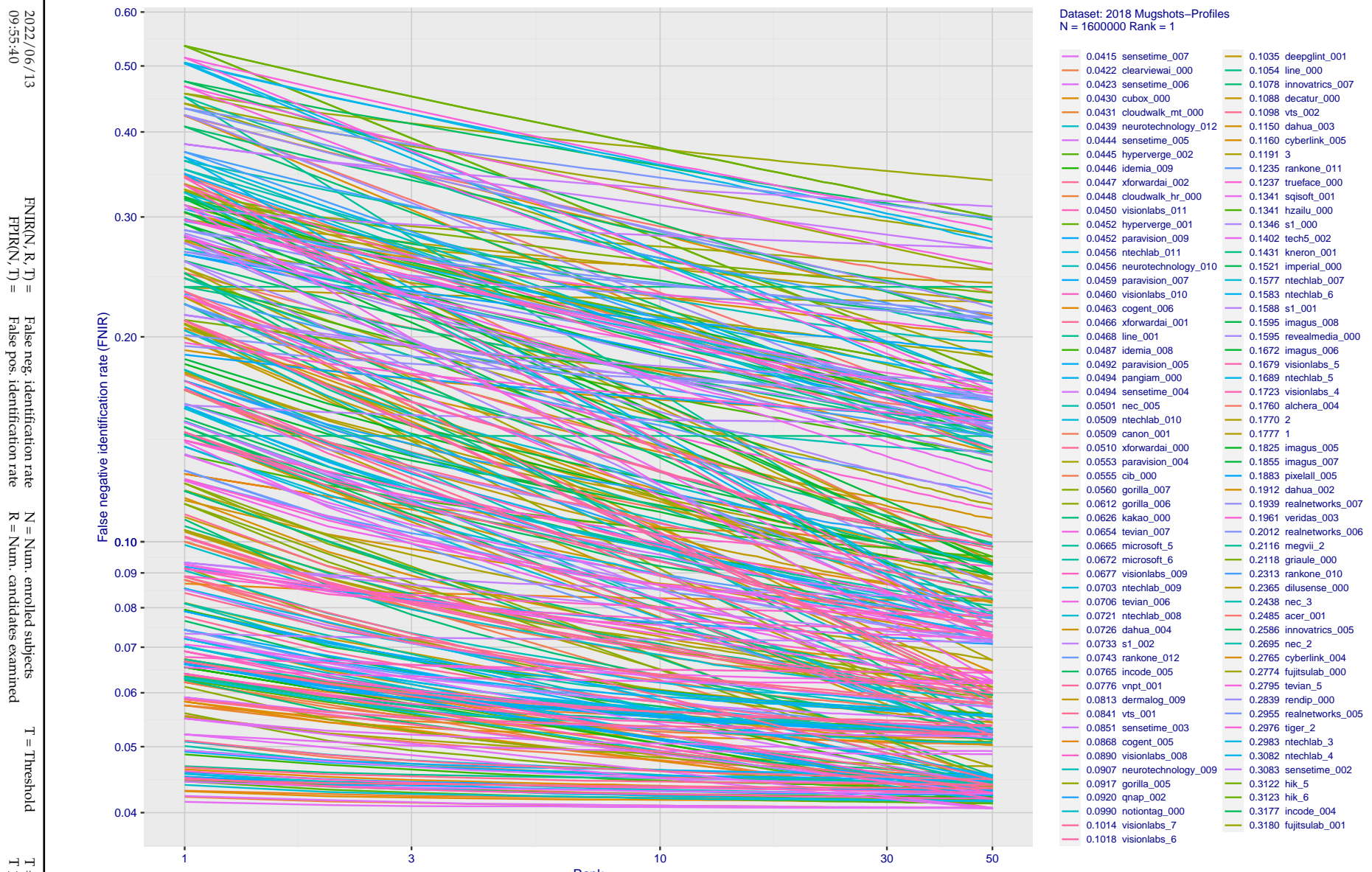


**Figure 133: [Mugshot and profile-view dataset] Rank-based accuracy.** For some of the more accurate Phase 3 algorithms the figure plots error tradeoff characteristics for frontal and profile-view searches into an enrolled set of  $N = 1600\,000$  frontal images. Note that some algorithms fail on profile-view images with  $\text{FNIR} \rightarrow 1$  - this evaluation did not ask developers to provide profile-view capability. Some algorithms, on the other hand, give  $\text{FNIR}$  approaching that for frontal-view searches using c. 2010 algorithms. The best result is that 91% of profile-view searches yield the correct mate at rank 1, and better than 94% in the top-50 candidates.

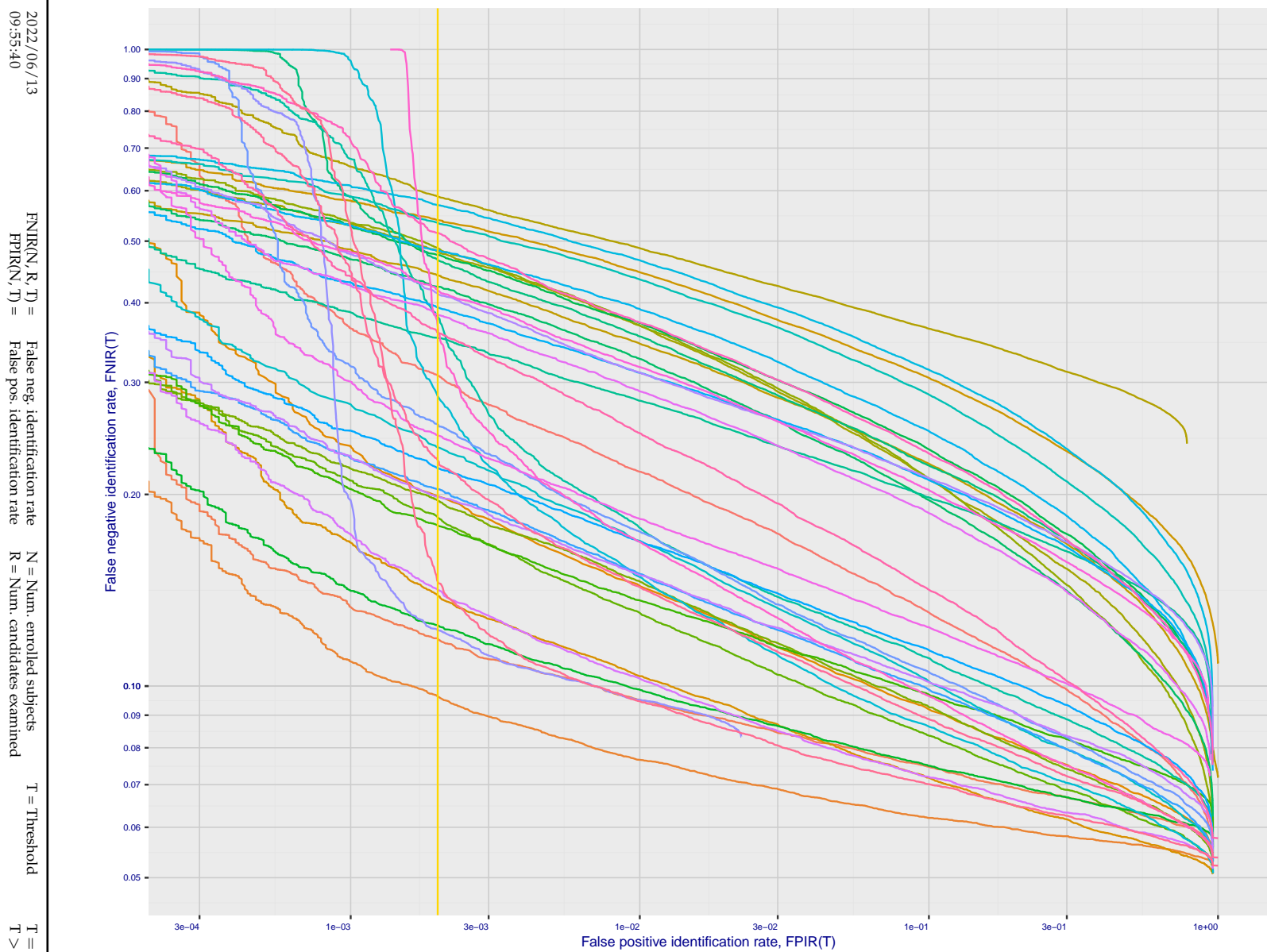
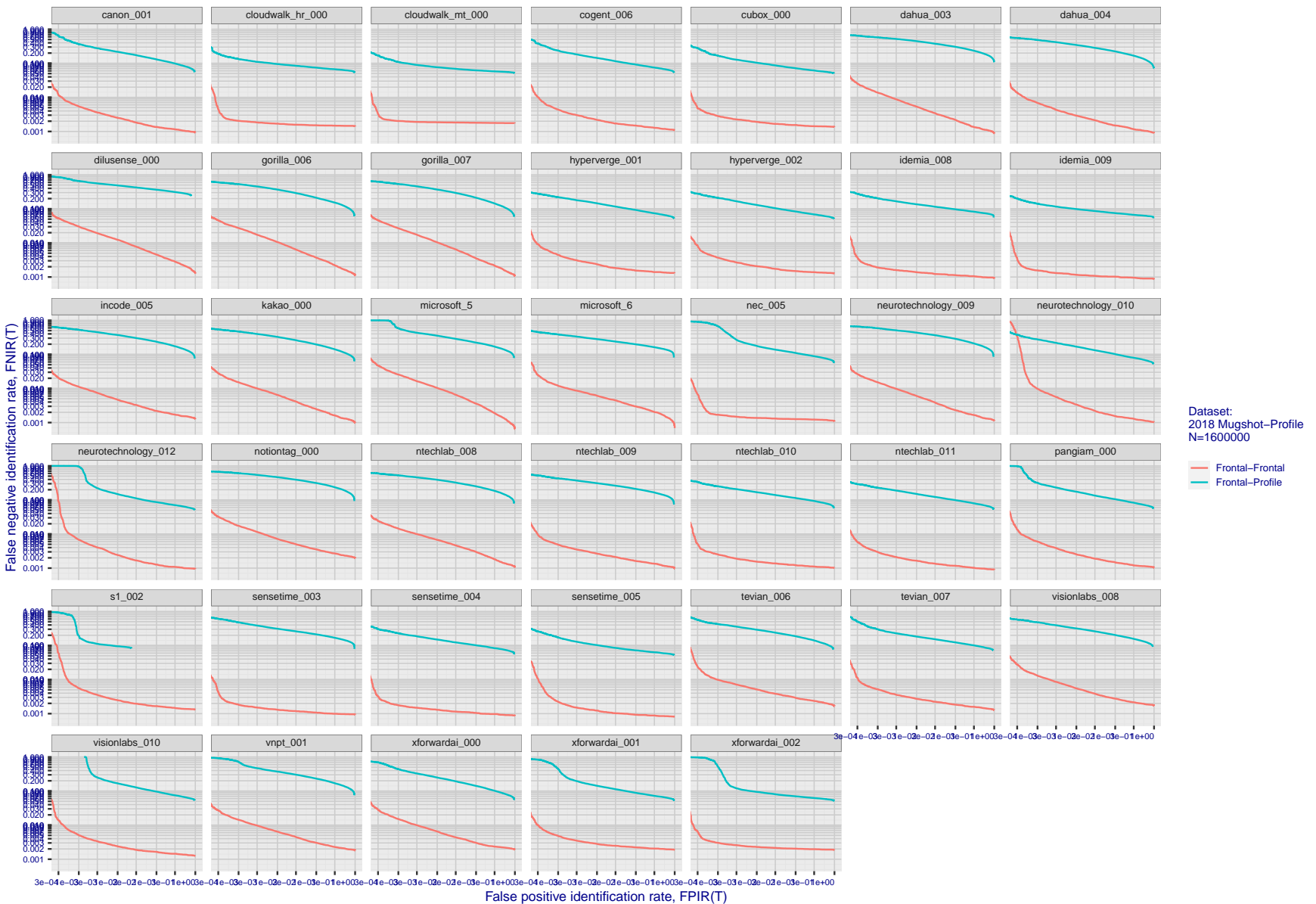


Figure 134: [Mugshot and profile-view dataset] Threshold-based accuracy. For some of the more accurate Phase 3 algorithms the figure plots error tradeoff characteristics for frontal and profile-view searches into an enrolled set of  $N = 1\,600\,000$  frontal images. Note that some algorithms fail on profile-view images with  $\text{FNIR} \rightarrow 1$  - this evaluation did not ask developers to provide profile-view capability. Some algorithms, on the other hand, give  $\text{FNIR}$  approaching that for frontal-view searches using c. 2010 algorithms.



**Figure 135: [Mugshot and profile-view dataset] Speed-accuracy tradeoff.** For some of the more accurate Phase 3 algorithms the figure plots error tradeoff characteristics for frontal and profile-view searches into an enrolled set of  $N = 1\,600\,000$  frontal images. Some algorithms fail on profile-view images with  $FNIR \rightarrow 1$  - this evaluation did not ask developers to provide profile-view capability. Some algorithms, on the other hand, give  $FNIR$  approaching that for frontal-view searches using c. 2010 algorithms. Blue lines connect points of equal threshold from which it is evident that some algorithms would give markedly higher false positive outcomes if profile-view images were searched in a system configured for frontal searches. This would be a vulnerability in an access control system.

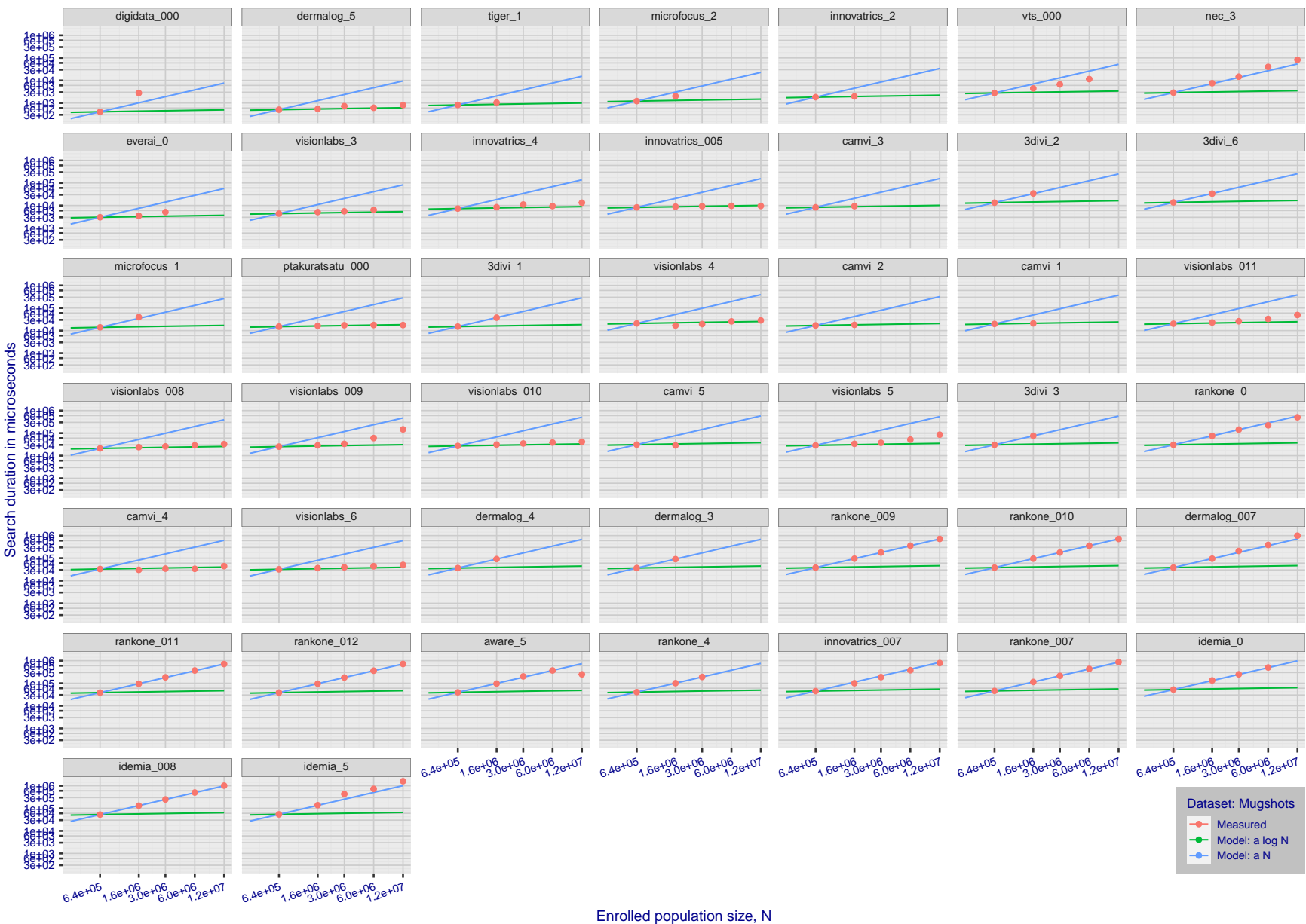
## Appendix F Search duration

As in and prior tests, this section documents search speeds spanning three orders of magnitude. In applications where search volumes are high enough, this will have implications for hardware requirements especially for large N or when search duration is appreciably larger than the time it takes to prepare a template from the search image(s). Further, given very large (and growing) operational databases, the scalability of algorithms is important. It has been reported previously [8] that search duration can scale sublinearly with enrolled population size N. Further there has been considerable recent research on indexing, exact [13] and approximate nearest neighbor search [1,13] and fast-search [14,16].

Figure 136 charts the search duration measurements presented earlier in Tables 2 - 4.

- ▷ Most algorithms scale linearly. For those in that category, there is a wide range in speed with search durations ranging from 82 milliseconds for a 12 million gallery (for NEC-3) to more than 40 seconds (for Yitu-3, Toshiba-2) and even higher for less accurate algorithms.
- ▷ Some developers (Camvi, Dermalog, EverAI, Innovatrics, and Visionlabs) provide algorithms whose template search durations grow approximately logarithmically i.e.  $T(N) \sim \log N$  with the constant  $a$  varying between implementations. In the figure this model is fit using the point  $T(1) = 0$ , and  $T(640\,000)$ . This very sublinear behaviour affords extremely fast search times in very large galleries. One caveat for the sublinear algorithms is that their fast-search data structures can require considerable computation time - on the order of hours - for N in the millions, and this scales mildly super-linearly, i.e.  $O(N^b)$ ,  $b > 1$ . There are exceptions: the Camvi algorithms take minutes; and Innovatrics' scale sublinearly.

2022/06/13 09:55:40	$\text{FNIR}(N, R, T) =$ $\text{FPTR}(N, T) =$	False neg. identification rate False pos. identification rate	$N =$ Num. enrolled subjects $R =$ Num. candidates examined	$T =$ Threshold $T > 0 \rightarrow$ Identification	$T = 0 \rightarrow$ Investigation
------------------------	---------------------------------------------------	------------------------------------------------------------------	----------------------------------------------------------------	-------------------------------------------------------	-----------------------------------

2022/06/13  
09:55:40FNIR(N, R, T) = False neg. identification rate  
FPFR(N, T) = False pos. identification rateN = Num. enrolled subjects  
R = Num. candidates examinedT = Threshold  
T = 0 → Investigation  
T > 0 → Identification

**Figure 136: [Mugshot Dataset] Search duration vs. enrolled population size.** In red are the actual point durations measured on a single c. 2016 core. The blue shows linear growth from  $N = 640\,000$ . The green line shows logarithmic growth from that point to  $N = 1\,600\,000$ . Note the sublinear growth from algorithms from Camvi, Dermalog, EverAI, Innovatrics, and Visionlabs. The tiger\_1 algorithm is also sublinear, but inaccurate and inoperable at  $N \geq 3000000$ . This capability sometimes comes at the additional expense of converting a linear gallery data structure into whatever fast-search data structure is used. Note that search times are sometimes dominated by the template generation times shown in Table 24.

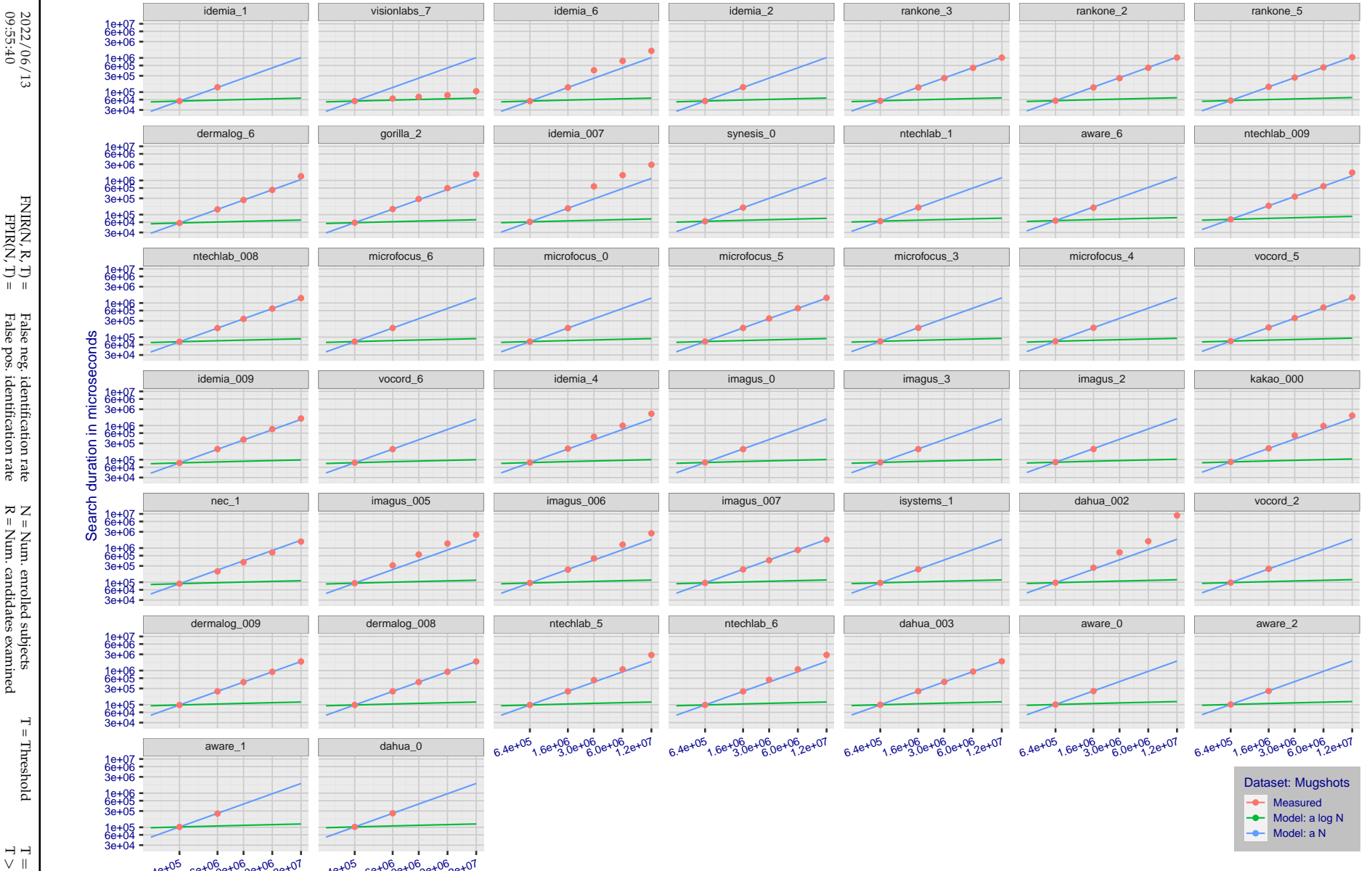


Figure 137: [Mugshot Dataset] Search duration vs. enrolled population size. In red are the actual point durations measured on a single c. 2016 core. The blue shows linear growth from  $N = 640\,000$ . The green line shows logarithmic growth from that point to  $N = 1\,600\,000$ . Note the sublinear growth from algorithms from Camvi, Dermalog, EverAI, Innovatrics, and Visionlabs. The tiger\_1 algorithm is also sublinear, but inaccurate and inoperable at  $N \geq 3000000$ . This capability sometimes comes at the additional expense of converting a linear gallery data structure into whatever fast-search data structure is used. Note that search times are sometimes dominated by the template generation times shown in Table 24.

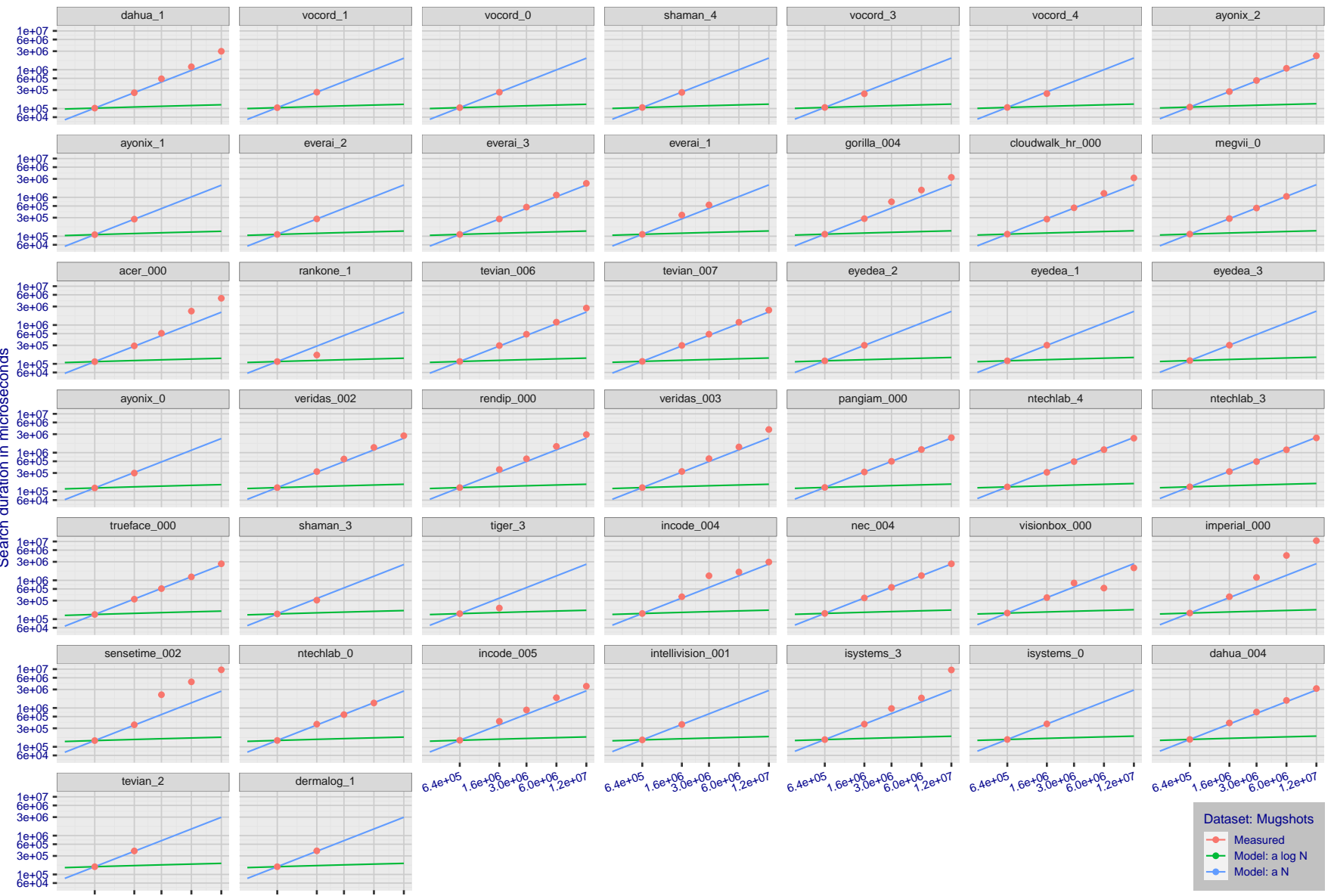
2022/06/13  
09:55:40FNIR(N, R, T) = False neg. identification rate  
FPFR(N, T) = False pos. identification rateN = Num. enrolled subjects  
R = Num. candidates examinedT = Threshold  
T = 0 → Investigation  
T > 0 → Identification

Figure 138: [Mugshot Dataset] Search duration vs. enrolled population size. In red are the actual point durations measured on a single c. 2016 core. The blue shows linear growth from  $N = 640\,000$ . The green line shows logarithmic growth from that point to  $N = 1\,600\,000$ . Note the sublinear growth from algorithms from Camvi, Dermalog, EverAI, Innovatrics, and Visionlabs. The tiger\_1 algorithm is also sublinear, but inaccurate and inoperable at  $N \geq 3000000$ . This capability sometimes comes at the additional expense of converting a linear gallery data structure into whatever fast-search data structure is used. Note that search times are sometimes dominated by the template generation times shown in Table 24.

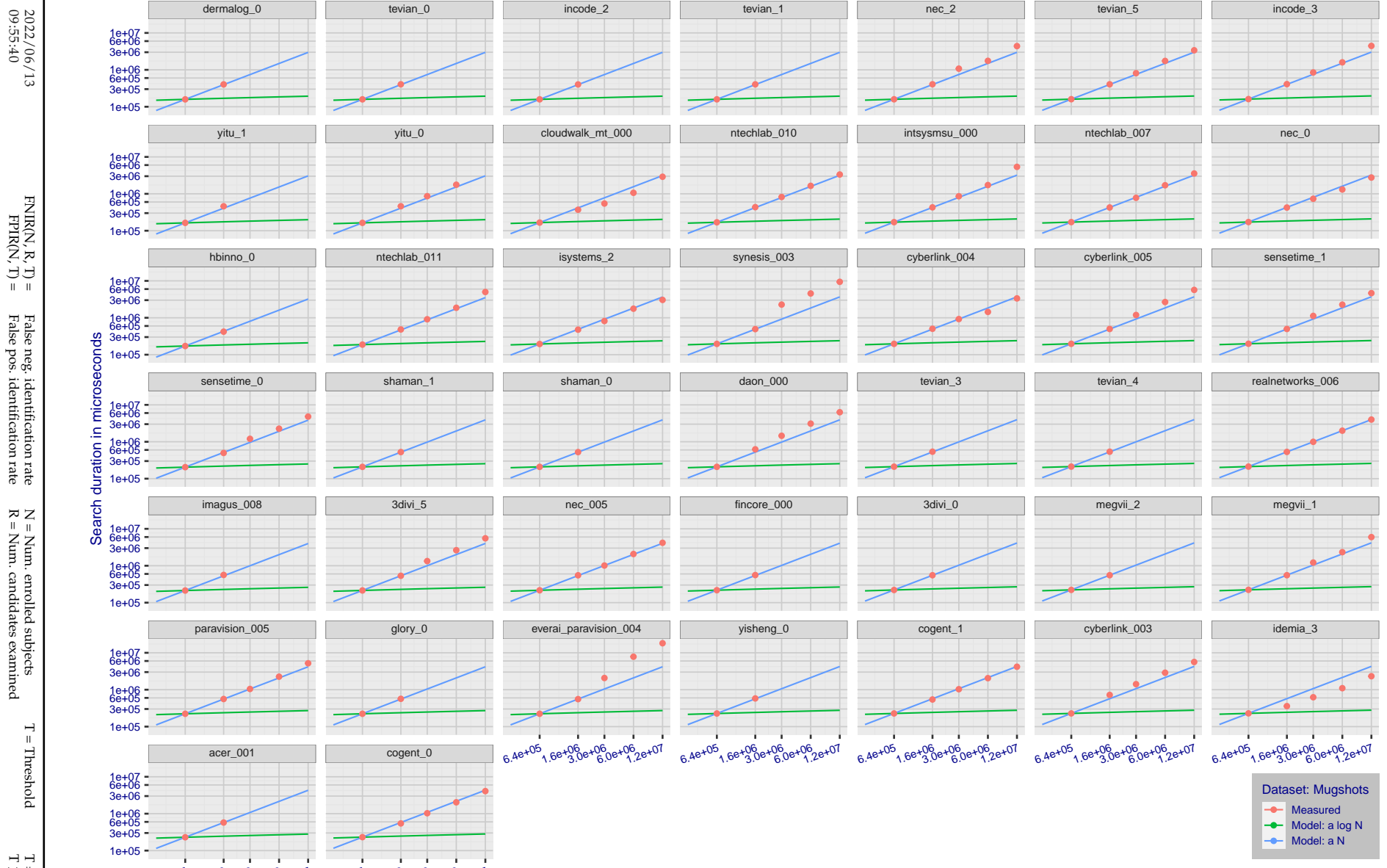


Figure 139: [Mugshot Dataset] Search duration vs. enrolled population size. In red are the actual point durations measured on a single c. 2016 core. The blue shows linear growth from  $N = 640\,000$ . The green line shows logarithmic growth from that point to  $N = 1\,600\,000$ . Note the sublinear growth from algorithms from Camvi, Dermalog, EverAI, Innovatrics, and Visionlabs. The tiger\_1 algorithm is also sublinear, but inaccurate and inoperable at  $N \geq 3000000$ . This capability sometimes comes at the additional expense of converting a linear gallery data structure into whatever fast-search data structure is used. Note that search times are sometimes dominated by the template generation times shown in Table 24.

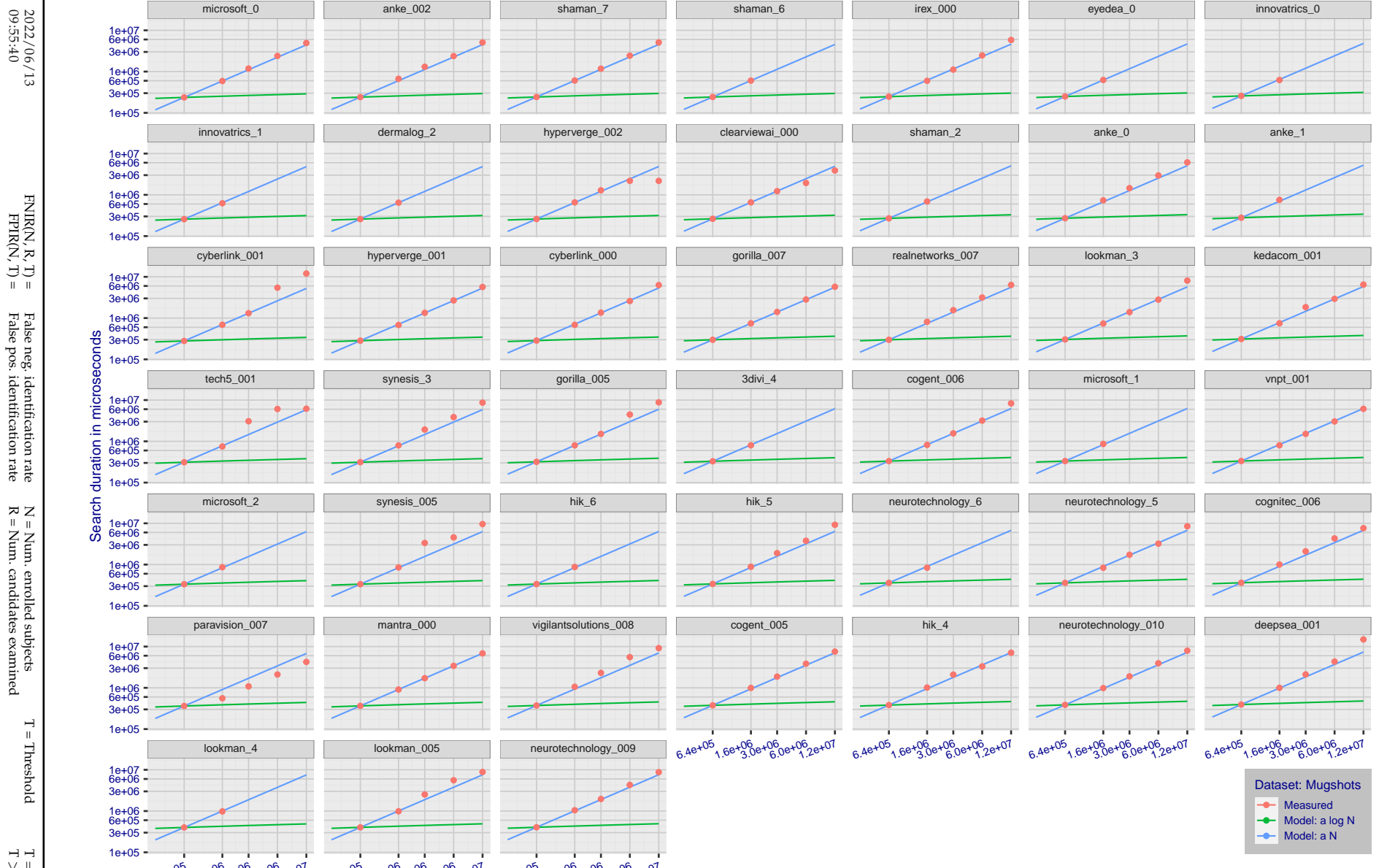


Figure 140: [Mugshot Dataset] Search duration vs. enrolled population size. In red are the actual point durations measured on a single c. 2016 core. The blue shows linear growth from  $N = 640\,000$ . The green line shows logarithmic growth from that point to  $N = 1\,600\,000$ . Note the sublinear growth from algorithms from Camvi, Dermalog, EverAI, Innovatrics, and Visionlabs. The tiger\_1 algorithm is also sublinear, but inaccurate and inoperable at  $N \geq 3000000$ . This capability sometimes comes at the additional expense of converting a linear gallery data structure into whatever fast-search data structure is used. Note that search times are sometimes dominated by the template generation times shown in Table 24.

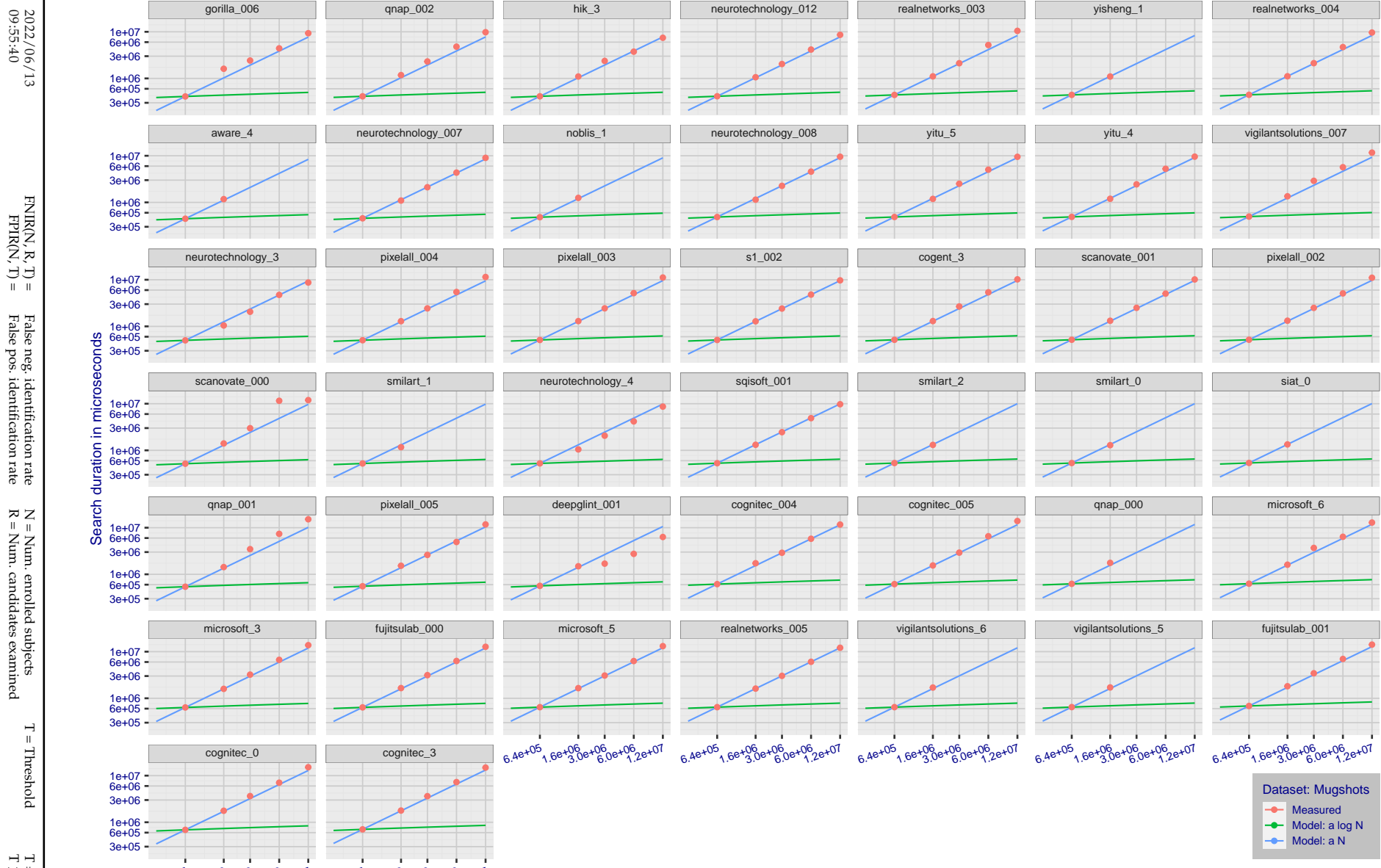


Figure 141: [Mugshot Dataset] Search duration vs. enrolled population size. In red are the actual point durations measured on a single c. 2016 core. The blue shows linear growth from  $N = 640\,000$ . The green line shows logarithmic growth from that point to  $N = 1\,600\,000$ . Note the sublinear growth from algorithms from Camvi, Dermalog, EverAI, Innovatrics, and Visionlabs. The tiger\_1 algorithm is also sublinear, but inaccurate and inoperable at  $N \geq 3000000$ . This capability sometimes comes at the additional expense of converting a linear gallery data structure into whatever fast-search data structure is used. Note that search times are sometimes dominated by the template generation times shown in Table 24.

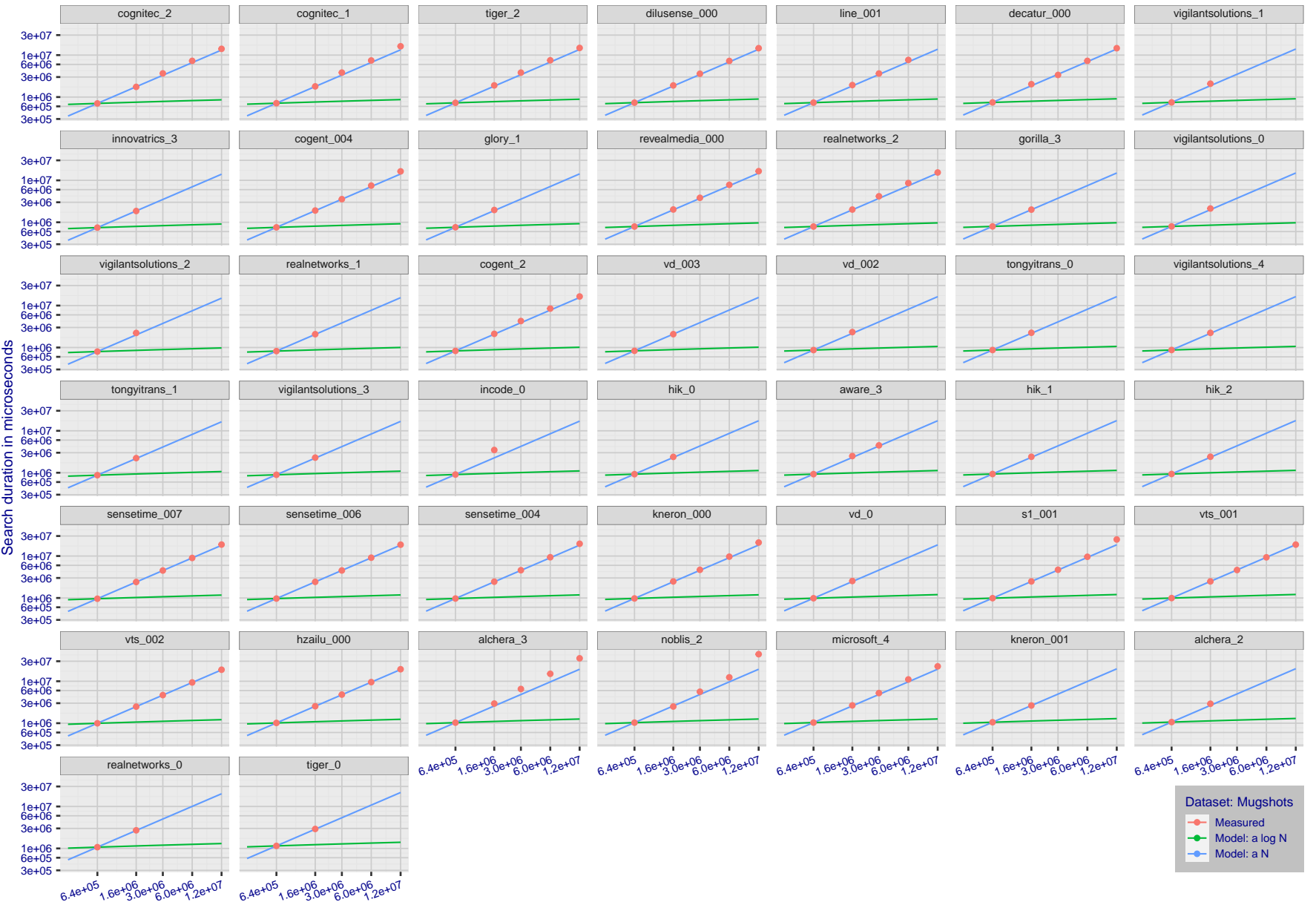


Figure 142: [Mugshot Dataset] Search duration vs. enrolled population size. In red are the actual point durations measured on a single c. 2016 core. The blue shows linear growth from  $N = 640\,000$ . The green line shows logarithmic growth from that point to  $N = 1\,600\,000$ . Note the sublinear growth from algorithms from Camvi, Dermalog, EverAI, Innovatrics, and Visionlabs. The tiger\_1 algorithm is also sublinear, but inaccurate and inoperable at  $N \geq 3000000$ . This capability sometimes comes at the additional expense of converting a linear gallery data structure into whatever fast-search data structure is used. Note that search times are sometimes dominated by the template generation times shown in Table 24.

2022/06/13 09:55:40

FNIR(N, R, T) = False neg. identification rate  
FPF(N, T) = False pos. identification rateN = Num. enrolled subjects  
R = Num. candidates examined

T = Threshold

T = 0 → Investigation  
 $T > 0 \rightarrow$  Identification

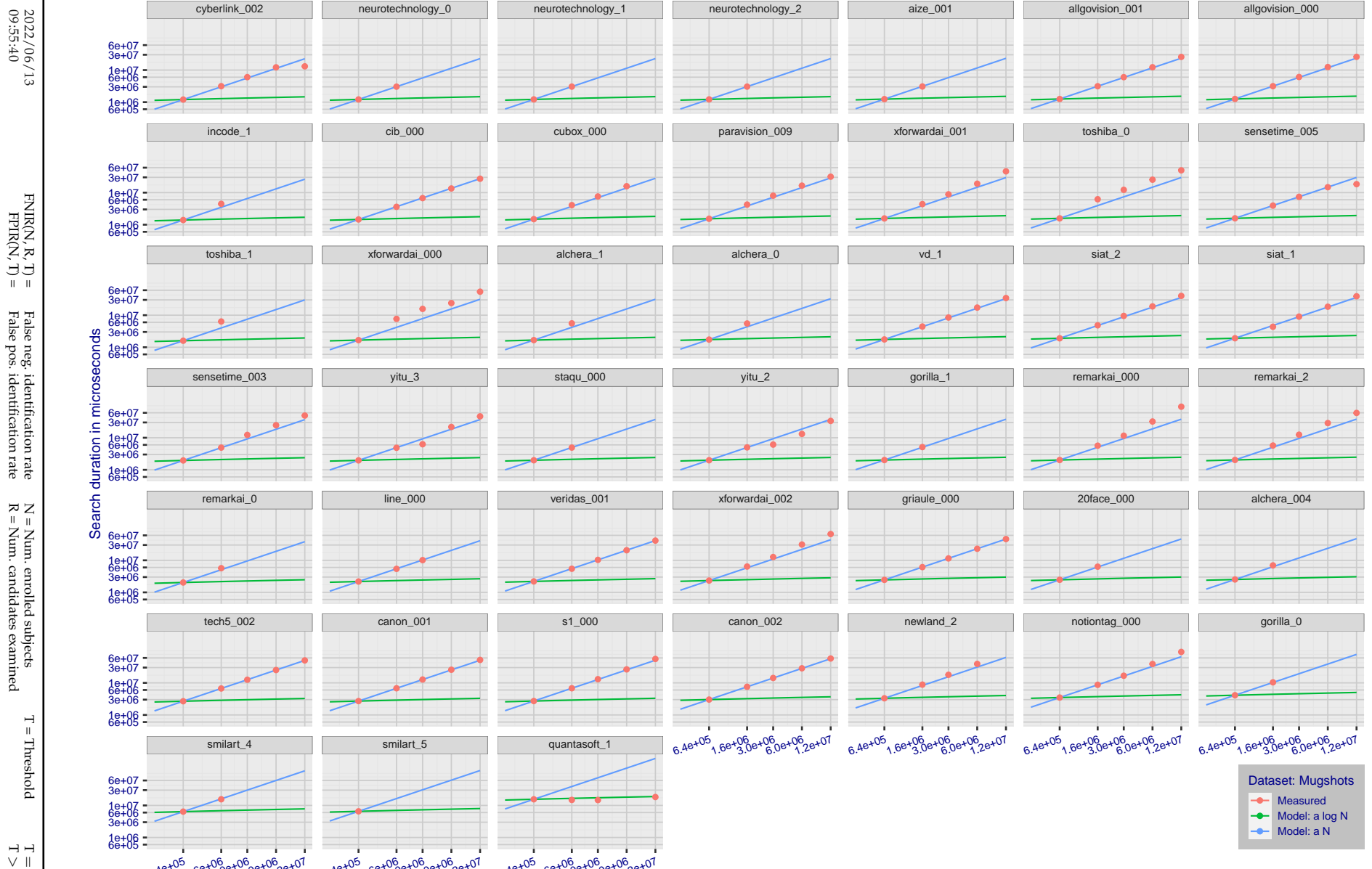
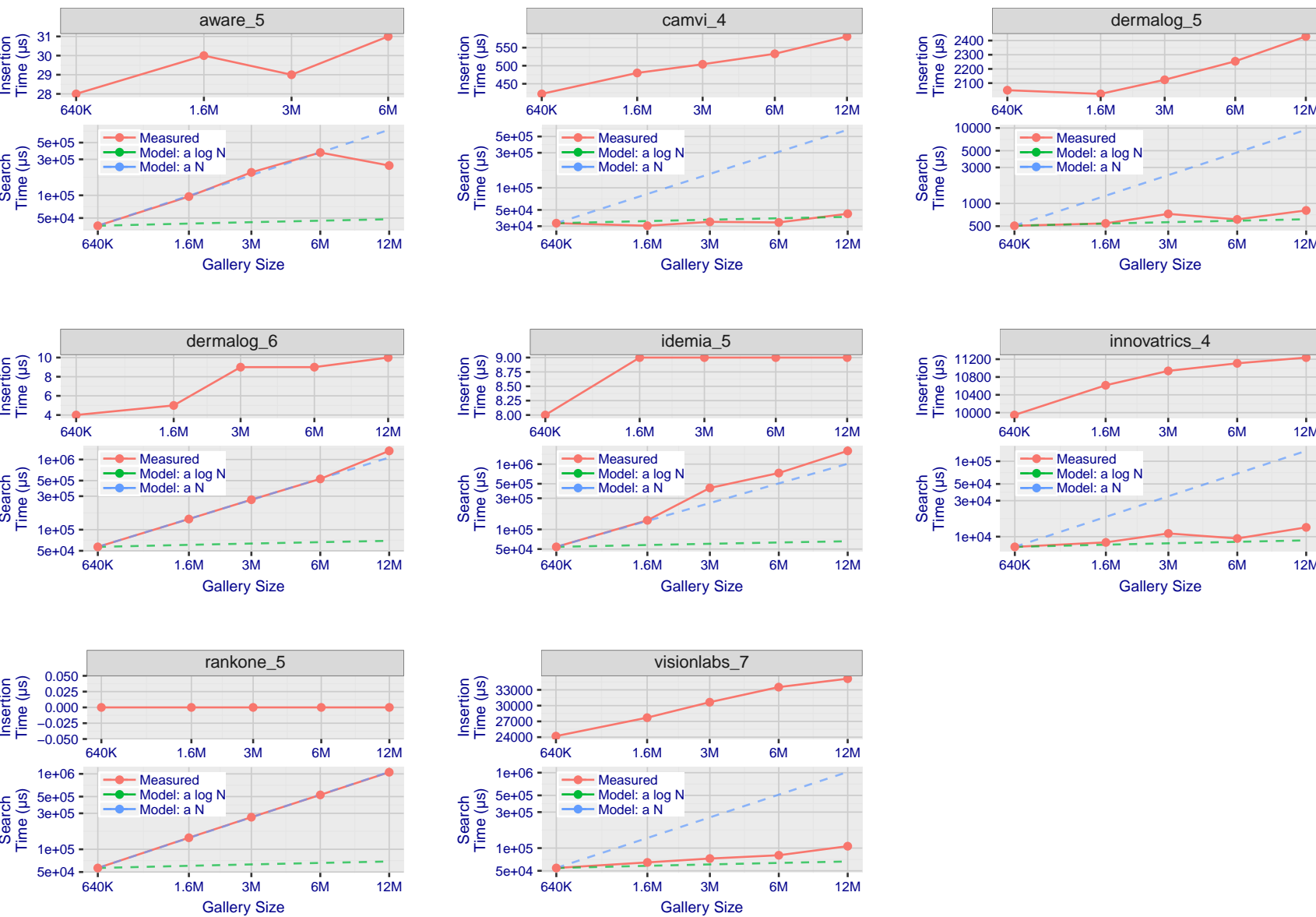


Figure 143: [Mugshot Dataset] Search duration vs. enrolled population size. In red are the actual point durations measured on a single c. 2016 core. The blue shows linear growth from  $N = 640\,000$ . The green line shows logarithmic growth from that point to  $N = 1\,600\,000$ . Note the sublinear growth from algorithms from Camvi, Dermalog, EverAI, Innovatrics, and Visionlabs. The tiger\_1 algorithm is also sublinear, but inaccurate and inoperable at  $N \geq 3000000$ . This capability sometimes comes at the additional expense of converting a linear gallery data structure into whatever fast-search data structure is used. Note that search times are sometimes dominated by the template generation times shown in Table 24.

## Appendix G Gallery Insertion Timing

2022/06/13  
09:55:40FNIR(N, R, T) = False neg. identification rate  
FPIR(N, T) = False pos. identification rateN = Num. enrolled subjects  
R = Num. candidates examined

T = Threshold

T = 0 → Investigation  
T > 0 → Identification

**Figure 144: [Mugshot Dataset] Gallery insertion duration vs. enrolled population size.** This chart plots the time it takes to insert a single template into a finalized gallery, illustrated over increasing gallery sizes. For reference, search times on finalized galleries of corresponding sizes are plotted right underneath. Gallery insertion time plots were generated on algorithms that 1) successfully implemented gallery insertion with no errors and 2) that were run on galleries with  $N$  up to 12 000 000. Generally, only the more accurate algorithms were run on galleries with  $N$  up to 12 000 000.

2022/06/13  
09:55:40FNIR(N, R, T) = False neg. identification rate  
FPFR(N, T) = False pos. identification rateN = Num. enrolled subjects  
R = Num. candidates examinedT = Threshold  
T = 0 → Investigation

T &gt; 0 → Identification

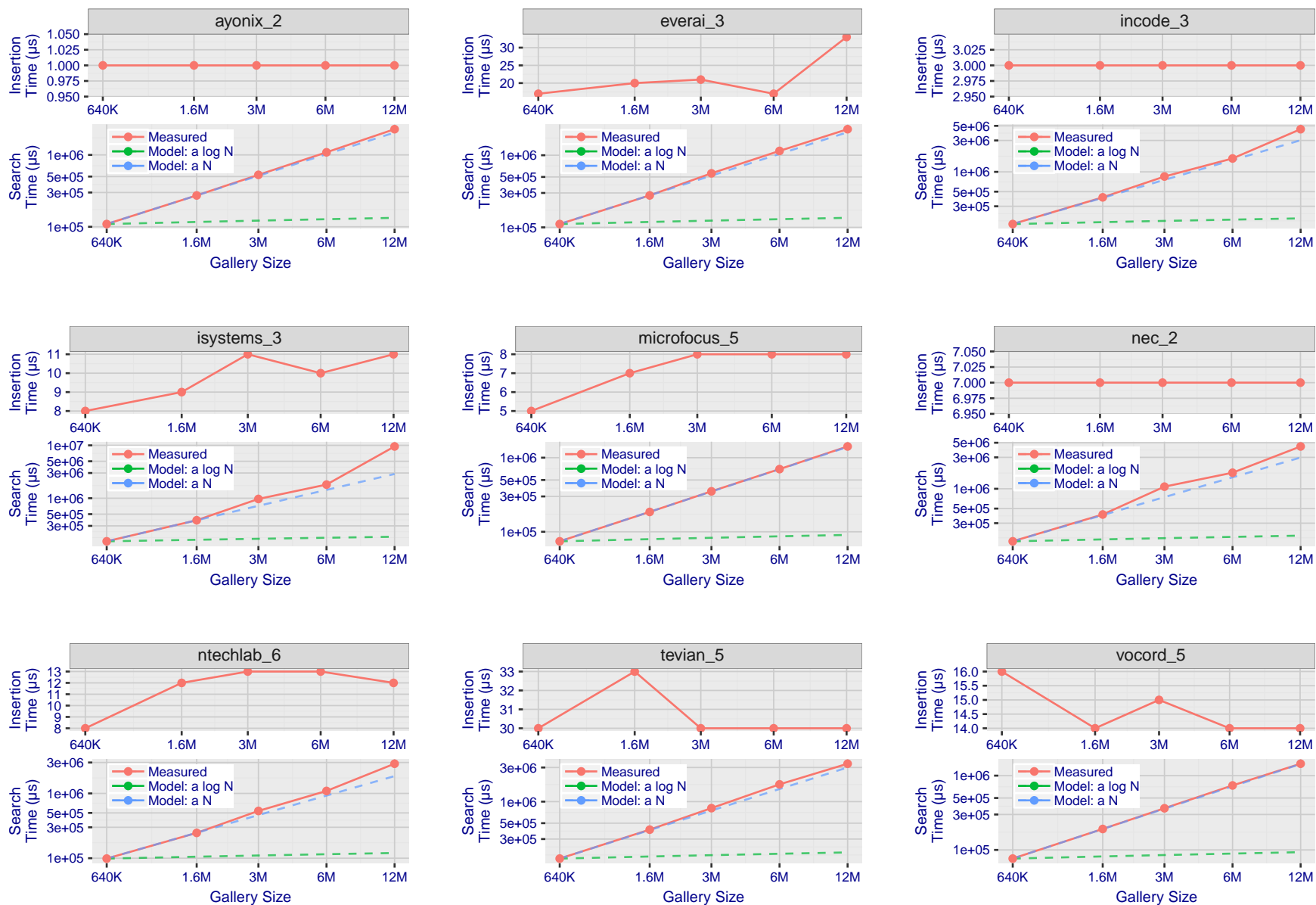


Figure 145: **[Mugshot Dataset] Gallery insertion duration vs. enrolled population size.** This chart plots the time it takes to insert a single template into a finalized gallery, illustrated over increasing gallery sizes. For reference, search times on finalized galleries of corresponding sizes are plotted right underneath. Gallery insertion time plots were generated on algorithms that 1) successfully implemented gallery insertion with no errors and 2) that were run on galleries with  $N$  up to 12 000 000. Generally, only the more accurate algorithms were run on galleries with  $N$  up to 12 000 000.

2022/06/13  
09:55:40FNIR(N, R, T) = False neg. identification rate  
FPTR(N, T) = False pos. identification rateN = Num. enrolled subjects  
R = Num. candidates examinedT = Threshold  
T = 0 → Investigation

T &gt; 0 → Identification

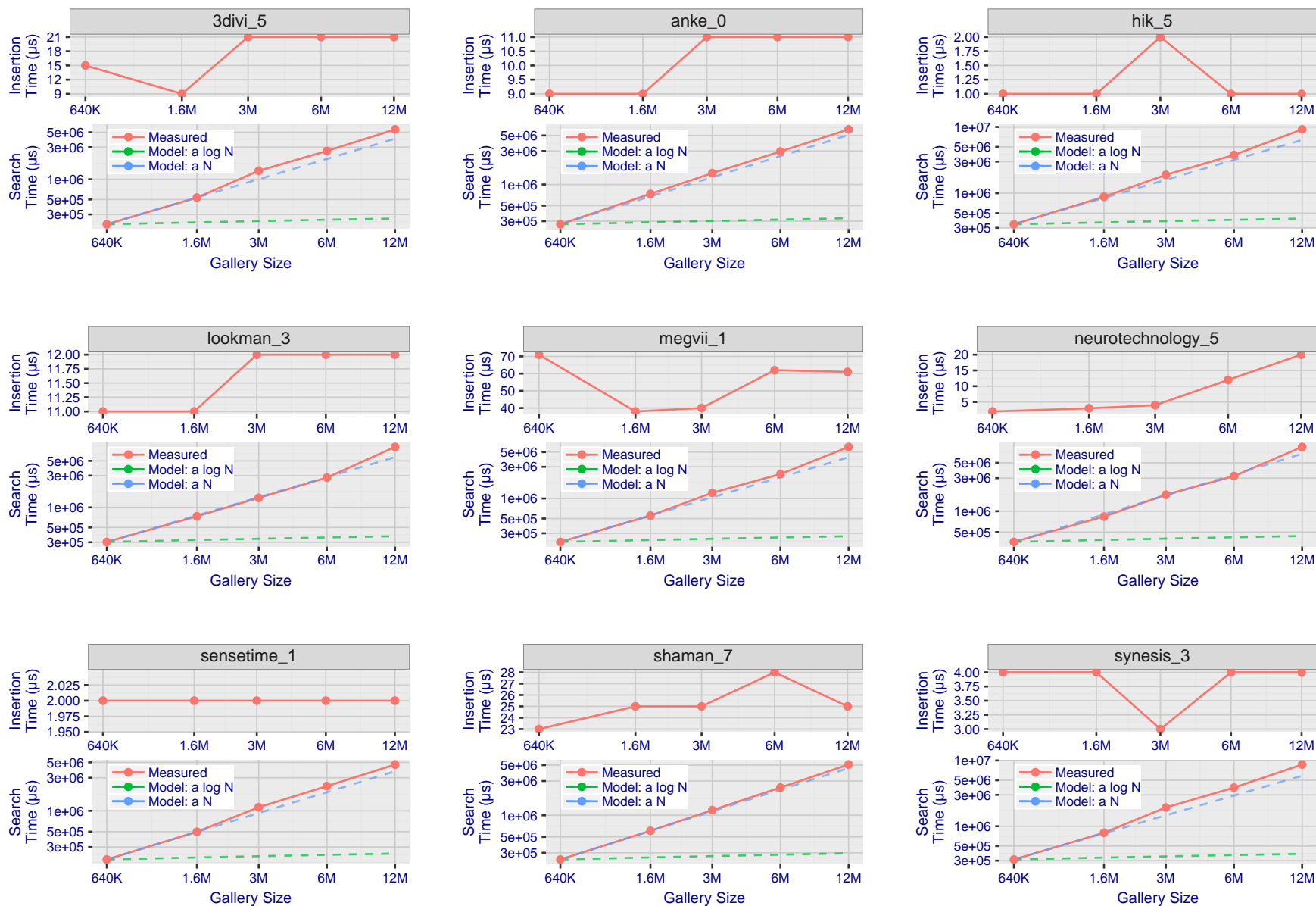


Figure 146: [Mugshot Dataset] Gallery insertion duration vs. enrolled population size. This chart plots the time it takes to insert a single template into a finalized gallery, illustrated over increasing gallery sizes. For reference, search times on finalized galleries of corresponding sizes are plotted right underneath. Gallery insertion time plots were generated on algorithms that 1) successfully implemented gallery insertion with no errors and 2) that were run on galleries with  $N$  up to 12 000 000. Generally, only the more accurate algorithms were run on galleries with  $N$  up to 12 000 000.

2022/06/13  
09:55:40FNIR(N, R, T) = False neg. identification rate  
FPTR(N, T) = False pos. identification rateN = Num. enrolled subjects  
R = Num. candidates examinedT = Threshold  
T = 0 → Investigation

T &gt; 0 → Identification

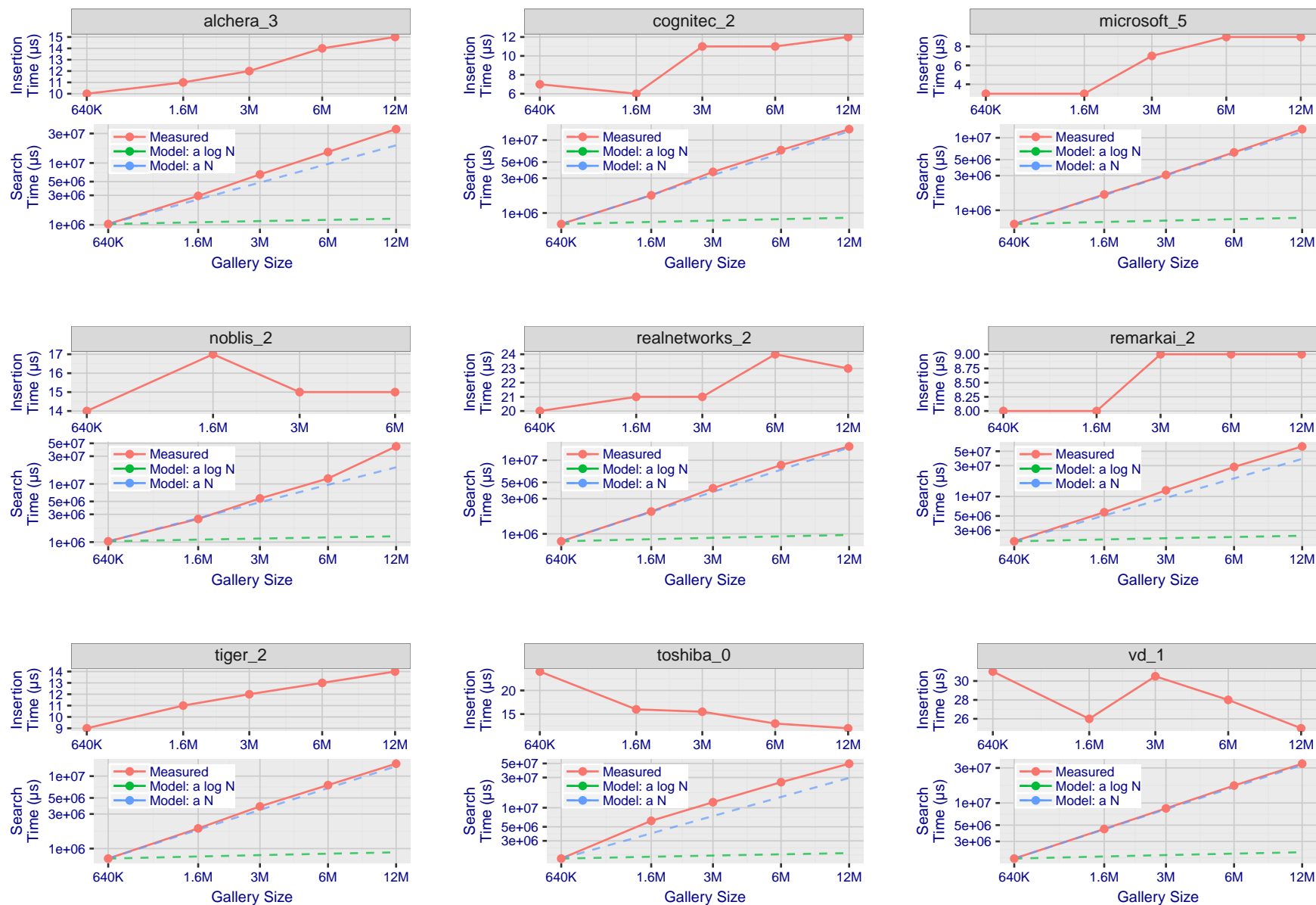


Figure 147: **[Mugshot Dataset] Gallery insertion duration vs. enrolled population size.** This chart plots the time it takes to insert a single template into a finalized gallery, illustrated over increasing gallery sizes. For reference, search times on finalized galleries of corresponding sizes are plotted right underneath. Gallery insertion time plots were generated on algorithms that 1) successfully implemented gallery insertion with no errors and 2) that were run on galleries with  $N$  up to 12 000 000. Generally, only the more accurate algorithms were run on galleries with  $N$  up to 12 000 000.

## References

- [1] Artem Babenko and Victor Lempitsky. Efficient indexing of billion-scale datasets of deep descriptors. In *The IEEE Conference on Computer Vision and Pattern Recognition (CVPR)*, June 2016.
- [2] L. Best-Rowden and A. K. Jain. Longitudinal study of automatic face recognition. *IEEE Transactions on Pattern Analysis and Machine Intelligence*, 40(1):148–162, Jan 2018.
- [3] Blumstein, Cohen, Roth, and Visher, editors. *Random parameter stochastic models of criminal careers*. National Academy of Sciences Press, 1986.
- [4] Thomas P. Bonczar and Lauren E. Glaze. Probation and parole in the united statesm 2007, statistical tables. Technical report, Bureau of Justice Statistics, December 2008.
- [5] White D., Kemp R. I., Jenkins R., Matheson M, and Burton A. M. Passport officers' errors in face matching. *PLoS ONE*, 9(8), 2014. e103510. doi:10.1371/journal.pone.0103510.
- [6] P. Grother, G. W. Quinn, and P. J. Phillips. Evaluation of 2d still-image face recognition algorithms. NIST Interagency Report 7709, National Institute of Standards and Technology, 8 2010. <http://face.nist.gov/mbe> as MBE2010 FRVT2010.
- [7] P. J. Grother, R. J. Micheals, and P. J. Phillips. Performance metrics for the frvt 2002 evaluation. In *Proceedings of Audio and Video Based Person Authentication Conference (AVBPA)*, June 2003.
- [8] Patrick Grother and Mei Ngan. Interagency report 8009, performance of face identification algorithms. *Face Recognition Vendor Test (FRVT)*, May 2014.
- [9] Patrick Grother, George Quinn, and Mei Ngan. Face in video evaluation (five) face recognition of non-cooperative subjects. Interagency Report 8173, National Institute of Standards and Technology, March 2017. <https://doi.org/10.6028/NIST.IR.8173>.
- [10] Patrick Grother, George W. Quinn, and Mei Ngan. Face recognition vendor test - still face image and video concept, evaluation plan and api. Technical report, National Institute of Standards and Technology, 7 2013. [http://biometrics.nist.gov/cs.links/face/frvt/frvt2012/NIST\\_FRVT2012.api\\_Aug15.pdf](http://biometrics.nist.gov/cs.links/face/frvt/frvt2012/NIST_FRVT2012.api_Aug15.pdf).
- [11] K. He, X. Zhang, S. Ren, and J. Sun. Deep residual learning for image recognition. In *2016 IEEE Conference on Computer Vision and Pattern Recognition (CVPR)*, pages 770–778, June 2016.
- [12] Gary B. Huang, Manu Ramesh, Tamara Berg, and Erik Learned-Miller. Labeled faces in the wild: A database for studying face recognition in unconstrained environments. Technical Report 07-49, University of Massachusetts, Amherst, October 2007.
- [13] Masato Ishii, Hitoshi Imaoka, and Atsushi Sato. Fast k-nearest neighbor search for face identification using bounds of residual score. In *2017 12th IEEE International Conference on Automatic Face & Gesture Recognition (FG 2017)*, pages 194–199, Los Alamitos, CA, USA, May 2017. IEEE Computer Society.
- [14] Jeff Johnson, Matthijs Douze, and Hervé Jégou. Billion-scale similarity search with gpus. *CoRR*, abs/1702.08734, 2017.

- [15] Ira Kemelmacher-Shlizerman, Steven M. Seitz, Daniel Miller, and Evan Brossard. The megaface benchmark: 1 million faces for recognition at scale. *CoRR*, abs/1512.00596, 2015.
- [16] Yury A. Malkov and D. A. Yashunin. Efficient and robust approximate nearest neighbor search using hierarchical navigable small world graphs. *CoRR*, abs/1603.09320, 2016.
- [17] Joyce A. Martin, Brady E. Hamilton, Michelle J.K. Osterman, Anne K. Driscoll, , and Patrick Drake. National vital statistics reports. Technical Report 8, Centers for Disease Control and Prevention, National Center for Health Statistics, National Vital Statistics System, Division of Vital Statistics, November 2018.
- [18] O. M. Parkhi, A. Vedaldi, and A. Zisserman. Deep face recognition. In *British Machine Vision Conference*, 2015.
- [19] P. Jonathon Phillips, Amy N. Yates, Ying Hu, Carina A. Hahn, Eilidh Noyes, Kelsey Jackson, Jacqueline G. Cava-zos, Géraldine Jeckeln, Rajeev Ranjan, Swami Sankaranarayanan, Jun-Cheng Chen, Carlos D. Castillo, Rama Chellappa, David White, and Alice J. O'Toole. Face recognition accuracy of forensic examiners, superrecognitioners, and face recognition algorithms. *Proceedings of the National Academy of Sciences*, 115(24):6171–6176, 2018.
- [20] Florian Schroff, Dmitry Kalenichenko, and James Philbin. Facenet: A unified embedding for face recognition and clustering. *CoRR*, abs/1503.03832, 2015.
- [21] Jeroen Smits and Christiaan Monden. Twinning across the developing world. *PLOS ONE*, 6(9):1–5, 09 2011.
- [22] Yaniv Taigman, Ming Yang, Marc'Aurelio Ranzato, and Lior Wolf. Deepface: Closing the gap to human-level performance in face verification. In *Proceedings of the 2014 IEEE Conference on Computer Vision and Pattern Recognition, CVPR '14*, pages 1701–1708, Washington, DC, USA, 2014. IEEE Computer Society.
- [23] A. Towler, R. I. Kemp, and D White. *Unfamiliar face matching systems in applied settings*. Nova Science, 2017.
- [24] Working Group 3. Ed. M. Werner. *ISO/IEC 19794-5 Information Technology - Biometric Data Interchange Formats - Part 5: Face image data*. JTC1 :: SC37, 2 edition, 2011. <http://webstore.ansi.org>.
- [25] David White, James D. Dunn, Alexandra C. Schmid, and Richard I. Kemp. Error rates in users of automatic face recognition software. *PLoS ONE*, 10:1–14, October 2015.
- [26] Bradford Wing and R. Michael McCabe. Special publication 500-271: American national standard for information systems data format for the interchange of fingerprint, facial, and other biometric information part 1. Technical report, NIST, September 2015. ANSI/NIST ITL 1-2015.
- [27] Andreas Wolf. Portrait quality - (reference facial images for mrtd). Technical report, ICAO, April 2018.
- [28] D. Yadav, N. Kohli, P. Pandey, R. Singh, M. Vatsa, and A. Noore. Effect of illicit drug abuse on face recognition. In *2016 IEEE Winter Conference on Applications of Computer Vision (WACV)*, pages 1–7, Los Alamitos, CA, USA, mar 2016. IEEE Computer Society.